THE PROGRESS OF RARE LESIONS OF THE SELLAR REGION

EDITED BY: Congxin Dai, Run Yu and Wang Haijun
PUBLISHED IN: Frontiers in Endocrinology

frontiers Research Topics

ISSN 1664-8714
ISBN 978-2-83250-156-6
DOI 10.3389/978-2-83250-156-6

About Frontiers

Frontiers is more than just an open-access publisher of scholarly articles: it is a pioneering approach to the world of academia, radically improving the way scholarly research is managed. The grand vision of Frontiers is a world where all people have an equal opportunity to seek, share and generate knowledge. Frontiers provides immediate and permanent online open access to all its publications, but this alone is not enough to realize our grand goals.

Frontiers Journal Series

The Frontiers Journal Series is a multi-tier and interdisciplinary set of open-access, online journals, promising a paradigm shift from the current review, selection and dissemination processes in academic publishing. All Frontiers journals are driven by researchers for researchers; therefore, they constitute a service to the scholarly community. At the same time, the Frontiers Journal Series operates on a revolutionary invention, the tiered publishing system, initially addressing specific communities of scholars, and gradually climbing up to broader public understanding, thus serving the interests of the lay society, too.

Dedication to Quality

Each Frontiers article is a landmark of the highest quality, thanks to genuinely collaborative interactions between authors and review editors, who include some of the world's best academicians. Research must be certified by peers before entering a stream of knowledge that may eventually reach the public - and shape society; therefore, Frontiers only applies the most rigorous and unbiased reviews.
Frontiers revolutionizes research publishing by freely delivering the most outstanding research, evaluated with no bias from both the academic and social point of view. By applying the most advanced information technologies, Frontiers is catapulting scholarly publishing into a new generation.

What are Frontiers Research Topics?

Frontiers Research Topics are very popular trademarks of the Frontiers Journals Series: they are collections of at least ten articles, all centered on a particular subject. With their unique mix of varied contributions from Original Research to Review Articles, Frontiers Research Topics unify the most influential researchers, the latest key findings and historical advances in a hot research area! Find out more on how to host your own Frontiers Research Topic or contribute to one as an author by contacting the Frontiers Editorial Office: frontiersin.org/about/contact

THE PROGRESS OF RARE LESIONS OF THE SELLAR REGION

Topic Editors:
Congxin Dai, Capital Medical University, China
Run Yu, University of California, Los Angeles, United States
Wang Haijun, The First Affiliated Hospital of Sun Yat-sen University, China

Citation: Dai, C., Yu, R., Haijun, W., eds. (2022). The Progress of Rare Lesions of the Sellar Region. Lausanne: Frontiers Media SA. doi: 10.3389/978-2-83250-156-6

Table of Contents

frontiers | Frontiers in Endocrinology

TYPE Editorial
PUBLISHED 24 August 2022
DOI 10.3389/fendo.2022.978284

OPEN ACCESS

EDITED AND REVIEWED BY
Nienke Biermasz,
Leiden University, Netherlands

*CORRESPONDENCE
Congxin Dai
daicongxin@163.com

SPECIALTY SECTION
This article was submitted to Pituitary Endocrinology, a section of the journal Frontiers in Endocrinology

RECEIVED 25 June 2022
ACCEPTED 05 August 2022
PUBLISHED 24 August 2022

CITATION
Dai C, Yu R, Wang H and Castaño JP (2022) Editorial: The progress of rare lesions of the sellar region. *Front. Endocrinol.* 13:978284. doi: 10.3389/fendo.2022.978284

Editorial: The progress of rare lesions of the sellar region

Congxin Dai[1]*, Run Yu[2], Haijun Wang[3] and Justo P. Castaño[4]

[1]Department of Neurosurgery, Beijing Tongren Hospital, Capital Medical University, Beijing, China, [2]David Geffen School of Medicine, University of California, Los Angeles, CA, United States, [3]Department of Neurosurgery, The First Affiliated Hospital of Sun Yat-sen University, Guangzhou, China, [4]Maimonides Biomedical Research Institute of Córdoba (IMIBIC), Reina Sofia University Hospital, CIBERobn, University of Córdoba, Córdoba, Spain

KEYWORDS

rare lesions of the sellar region, diagnostic molecular markers, pathogenesis, surgery, targeted therapies, radiotherapy, chemotherapy

Editorial on the Research Topic
The progress of rare lesions of the sellar region

Lesions of the sellar region are a heterogeneous group of diseases with complex clinical manifestations. The common lesions of the sellar region include pituitary adenomas (PAs), craniopharyngiomas (CPs), Rathke's Cleft Cysts (RCCs), germ cell tumors, etc. (1–3). Rare lesions of the sellar region include PAs associated with McCune-Albright syndrome (MAS), or multiple endocrine neoplasia type 1 (MEN1), pituitary carcinomas (PCs), clival chordoma, pituitary metastasis from other tumors, giant invasive PAs, giant CPs, etc. (4, 5). These rare lesions of the sellar region present with complex clinical and atypical imaging features. Precisely diagnosing these rare lesions of the sellar region before surgery is notoriously difficult (6, 7). Accordingly, the challenge of diagnosing and treating these rare lesions of the sellar region, prompted us to devise a Research Topic related to the current progress on rare lesions of the sellar region.

In the present Research Topic in Frontiers in Endocrinology, we collected 22 studies and case reports on rare lesions of the sellar region. This Research Topic consists of two parts, the first part included nine articles of case reports that described various rare lesions of the sellar region. (i) IgG4-related inflammatory pseudotumors are one of the rare lesions of the sellar region, which are often misdiagnosed as other diseases. Liu et al. reported a case of an IgG4-related inflammatory pseudotumor involving the clivus mimicking meningioma. A male presented with intermittent headache for 2 years, and sudden dysphagia and hoarseness for 1 week. The magnetic resonance imaging (MRI) revealed an enhanced lesion located at the middle of the upper clivus region, which was preoperatively diagnosed with meningioma. The lesion was partially resected by endoscopic transsphenoidal surgery (TSS), and was pathologically diagnosed as IgG4-related inflammatory pseudotumor. Glucocorticoid was used postoperatively, and the patient's symptoms including dysphagia and dysphonia were improved. Therefore, although the IgG4-related inflammatory pseudotumor is a rare lesion of the sellar region, it should also be considered a preoperative differential diagnosis. (ii) Primary

pituitary lymphoma (PPL) is an extremely rare lesion of the sellar region with poor prognosis. Zhang et al. presented two cases of PPL and guided treatment and predicted prognosis using genetic analysis. The TP53 mutation and BCL6-LPP fusion were identified in one case of PPL by genetic analysis of cerebrospinal fluid and tumor tissue, and may be used as a marker for prognosis of PPL. Genetic analysis thus should be considered as a novel approach for prognosis prediction and treatment for PPL. (iii) Pituitary metastasis is an unusual and very rare disease, which accounts for approximately 1% of all intracranial metastases. It is difficult to diagnose the asymptomatic pituitary metastasis especially for patients with unknown primary malignant origin. Liu et al. reported a case of a male patient with visual changes and diabetes insipidus, and PA was initially diagnosed according to the MRI results with an extensive mass in the sellar region. The lesion of sellar region was completely resected though TSS, and the pathological results suggested the resected tumor tissue was pituitary metastasis from lung neuroendocrine tumor. Chest CT scan confirmed a pulmonary mass consistent with the primary neoplasm. Preoperative differentiation of pituitary metastases from PAs is very challenging because their clinical and radiological features are very similar. This case highlights the importance of a preoperative differential diagnosis of invasive lesions of the sellar region. (iv) Mature Cystic Teratoma (MCT) is a subset of intracranial germ cell tumors, and rarely occurs in the suprasellar region. Jiang et al. presented a unique and rare case of suprasellar MCT mimicking RCC. A young female patient complained of intermittent headache and oligomenorrhea for 11 years, and MRI demonstrated an irregular suprasellar lesion with slight intrasellar extension without obvious gadolinium enhancement. Endoscopic TSS was performed to remove the suprasellar lesion. According to the clinical, radiological, and operative findings, RCC was initially considered. However, the postoperative pathological findings revealed a mature cystic teratoma. Because the suprasellar MCTs are extremely rare, and their clinical and imaging features usually lacks specificity, it difficult to distinguish MCT from other cystic lesions located in the suprasellar region, and the precise diagnosis of MCT often relies on histological diagnosis. This case highlights the importance of obtaining a histological diagnosis to differentiate MCT from other lesions. (v) Rhabdomyosarcoma (RMS) is a malignant skeletal muscle sarcoma that rarely occurs intracranially, especially within the sellar region. Lu and Chen reported a pituitary RMS arising from a pituitary macroadenoma and its molecular profiling. They described an elderly man with an incidental discovery of a pituitary macroadenoma by MRI and underwent radiotherapy. Three years after radiation treatment, the tumor size increased significantly and caused mass effect on the optic chiasm. Transnasal endoscopic resection of the pituitary mass was performed, and a pituitary adenoma along with a separate spindle-cell sarcomatous component was identified by histological studies. Molecular profiling of the tumor using NextGen Sequencing identified mutations in TP53, ATRX, LZTR1, and NF1. This is the first case to report molecular features of a pituitary RMS arising from PA, which will help better understand its pathogenesis and to provide precise treatment plans. (vi) Extraventricular neurocytoma (EVN) located in the sellar/suprasellar region is an extremely rare tumor, and its biological behavior is unclear. Zhang et al. retrospectively analyzed the clinicopathological and molecular features of 4 cases of EVN arising from the sellar/suprasellar region, and demonstrated that EVNs arising from the sellar/suprasellar region had similar morphological features and immunophenotypes to classic central neurocytoma. However, there was no amplification of MYCN or EGFR, or no alterations in IDH1, IDH2, BRAF V600E, 1p/19q, H3F3A or CDKN2A were found in these tumors by molecular genetic testing. (vii) Granular cell tumors (GCT) of the pituitary are extremely rare lesion of the sellar region that arise from the posterior pituitary gland. Hong et al. reported a case of GCT of the pituitary and its genomic analysis results. An elderly female underwent resection of an incidentally diagnosed pituitary mass causing radiographic compression of the optic nerves. Histopathological findings of the resected tumor demonstrated a granular cell tumor of the posterior pituitary gland. The genomic analysis revealed mutations in key oncogenes such as SETD2 and PAX8, which have been reported in other cancers. This is the first report on comprehensive genomic characterization of granular cell tumor of the posterior pituitary gland. These data revealed feasible molecular pathogenesis of GCT and provided potential targeted therapies. (viii) Sellar glomus tumors are extremely rare lesions, which may be easily misdiagnosed as PAs. Cheng et al. reported a case of sellar glomus tumor which was misdiagnosed as NFPA. An elderly man presented with sellar mass for over 5 years and visual deficits for about 3 months. MRI revealed a lesion with cystic structures in the sellar region that was heterogeneously enhancing, and macroadenoma was initially diagnosed. The sellar mass was resected via the TSS, and histopathological examination indicated a glomus tumor. This case suggests that glomus tumor should be considered as a differential diagnosis for sellar mass, and digital subtraction angiography examination is recommended before surgery. (ix) Although surgery is the first choice of treatment of CPs, it is associated with high long-term morbidity especially for CPs with hypothalamic involvement. Calvanese et al. reported that the BRAF/MEK inhibitor remarkably reduced tumor volume in two cases of papillary CP with confirmation of BRAFV600E mutation by biopsy. Therefore, BRAF/MEK inhibitor therapy may be a very useful and promising alternative treatment for giant and invasive CPs harboring the BRAFV600E mutation.

The second part included thirteen clinical studies that addressed the clinical characteristics and treatment outcome of

lesions of the sellar region. (i) MAS is a disorder characterized by fibrous dysplasia, hyperfunctioning endocrinopathies and café-au-lait-spot. The coexistence of precocious puberty (PP) and growth hormone (GH) excess in patients with MAS is extremely rare. Zhai et al. reviewed seven MAS patients with GH excess and PP and found that all patients have craniofacial fibrous dysplasia-induced optic and otologic complications, increased growth velocity and advanced skeletal age. Early control of GH excess and PP leads to a reduced growth velocity and stabilized bone age. (ii) Cushing's disease (CD) and ectopic ACTH syndrome (EAS) are two main causes of ACTH-dependent Cushing's syndrome (CS). How to differentiate CD from EAS remain challenging. Currently, the high-dose dexamethasone suppression test (HDDST) was used to differentiate CD and EAS, low-dose dexamethasone suppression test (LDDST) was used to determine the diagnosis of CS. To develop an optimized pathway for the differential diagnosis of CD and EAS based on LDDST, Chen et al. performed a retrospective study of 261 CD and 29 EAS patients who underwent consecutive low- and high-dose DST. They found that LDDST with specific cut-off and HDDST had similar value to in differentiating CD from EAS, and combined LDDST and BIPSS could accurately differentiate CD from EAS. (iii) Basal ganglia germ cell tumors (BGGCTs) with or without sellar involvement is a group of very rare diseases. Zhang et al. evaluated the independent prognostic risk factors of patients with BGGCTs using multivariate analysis, and demonstrated that delayed diagnosis, focal radiotherapy, and non-pure germinoma were the independent poor prognostic risk factors of patients with BGGCTs. (iv) Adolescent thyrotropin-secreting adenoma (TSH-oma) in is a very rare kind of functional PA. Yang et al. summarized the clinical and therapeutic characteristics of 20 adolescent patients with TSH-oma, and found that these patients had larger tumors, higher TSH and thyroid hormone levels, and worse treatment outcomes than adult patients. (v) Large or giant PAs are relative rare tumors of the sellar region and remain therapeutically challenging. Chen et al. explored the risk factors of recurrence or progression and predictors of prognosis of giant and large PAs after TSS, and indicated that partial resection, smoking, BMI $\geqq$25 kg/m^2, Ki-67 $\geq$3%, and Knosp classification grade 4 increase the risk of the recurrence or progression of large and giant PAs. (vi) RCCs is benign and cystic disease of the sellar region, which often cause pituitary dysfunction. The relationship between clinical characteristics of RCCs and pituitary gland function is not very clear. Zhang et al. retrospectively analyzed 221 patients with RCC, and found that although pituitary function was not related closely to size of RCC, endocrine functions need to be evaluated for patient with RCC. (vii) Clival chordoma is a locally aggressive tumor of the sellar region. Chen et al. retrospectively analyzed the clinicopathological features and surgical outcomes of 17 consecutive patients with clival chordoma, and showed that endoscopic transsphenoidal surgery (ETS) is a safe and reliable approach for clival chordoma with high resection rates and low morbidity rates. (viii) Intracranial aneurysms (IAs) located at sellar region account for 10% to 20% among all the IAs and the co-existence of IAs and sellar region lesions is very rare and easily overlooked. Yan et al. retrospectively reviewed 515 continuous patients diagnosed with sellar region lesions and found the overall prevalence of sellar region lesions co-existed with the IAs is 11.1%. The patients with sellar region lesions and IAs exhibit higher comorbidity rate of endoscopic endonasal approach (EEA). Moreover, they suggested computed tomography angiography (CTA) as a routine preoperative examination for patients with sellar region lesions before EEA to guarantee surgical safety. (ix) Repeat surgery for recurrent or residual PAs (rrPAs) is technically challenging. To evaluate the safety and outcomes of ETS in rrPAs, Gong et al. reviewed clinical and radiological characteristics of 73 patients with rrPAs and investigated the factors influencing gross total resection (GTR) and intraoperative cerebrospinal fluid (CSF) leakage using logistic regression analyses. This study demonstrated that Knosp grade is an independent predictor of GTR in repeat ETS, and previous transcranial surgery and non-functional PAs are significantly associated with intraoperative CSF leakage. (x) Gangliocytomas/mixed gangliocytoma-adenomas (GCs/MGAs) are extremely rare lesions in the sellar region. Zheng et al. retrospectively studied the histological features of 4 patients with mixed gangliocytoma PAs and found that MGAs are associated with endocrinopathies such as acromegaly. Furthermore, they indicated that PIT1-positive PAs may have neural differentiation potential, which suggests that the neuronal transdifferentiation of adenomatous cells maybe a possible mechanism for MGA pathogenesis. (xi) It is difficult to resect completely PAs in Knosp grade 4, which are generally associated with poor prognosis. Guan et al. retrospectively reviewed the surgical outcome of transcranial approaches in the large-to-giant pPAs in Knosp grade 4 and found that 26.2% of them achieve gross total resection. Moreover, frontotemporal approach is more appropriate for tumors with large size and extending into the lateral skull base. In contrast, the frontotemporal approach was associated with longer surgical time and more bleeding volume. (xii) Chen et al. also retrospectively analyzed surgical outcomes of TSS in 239 patients with giant PAs in a single-center cohort and indicated that maximum diameter and Knosp grade of giant PAs have a significant impact on the extent of tumor resection. In addition, they found that the incidence of CSF leaks in neuroendoscopy group is significantly higher than that in the microscopic group. (xiii) Postoperative central nervous system infection (PCNSI) is an uncommon but serious complication of patient with sellar region tumors who underwent surgical interventions. Wen et al. identified risk factors for PCNSI via univariate and multivariate analyses, and indicated that transcranial surgery, intraoperative CSF leakage, postoperative diabetes insipidus and adrenal insufficiency are risk factors for PCNSIs

In summary, lesions of the sellar region are very complex, and a subset of them lack specific clinical and imaging features. Therefore, it is challenging to accurately diagnose these diseases before surgery, especially int the case of rare lesions. This Research Topic included a group of rare lesions of the sellar region that are easily misdiagnosed as other diseases. In addition, studies of surgical outcomes, risk factor analysis and molecular genetic testing for some sellar lesions were also included. Moreover, new therapeutic concepts and strategies such as personalized and targeted therapy also were reported. Through this Research Topic, we aimed at attaining a better understanding of rare lesions of the sellar region, and to provide new tools to diagnose and treat these diseases more accurately. We expect future issues will collect more studies on basic and translational research on lesions of the sellar region, bringing a better understanding of their characteristics and pathogenetic mechanisms to improve the clinical outcomes for these patients.

Author contributions

CD and RY draft this manuscript. HW and JPC polished and revised the text. All authors contributed to the article and approved the submitted version.

Funding

Financial support for this study was provided by the Beijing Municipal Administration of Hospitals Incubating Program (grant number: PX2022004). The funding institutions had no role in the design of the study, data collection and analysis, decision to publish, or preparation of the manuscript.

Conflict of interest

The authors declare that the research was conducted in the absence of any commercial or financial relationships that could be construed as a potential conflict of interest.

Publisher's note

References

1. Daly AF, Beckers A. The epidemiology of pituitary adenomas. *Endocrinol Metab Clin North Am* (2020) 49(3):347–55. doi: 10.1016/j.ecl.2020.04.002

2. Gadelha MR, Wildemberg LE, Lamback EB, Barbosa MA, Kasuki L, Ventura N. Approach to the patient: Differential diagnosis of cystic sellar lesions. *J Clin Endocrinol Metab* (2022) 107(6):1751–8. doi: 10.1210/clinem/dgac033

3. Kirsch C. Imaging of sella and parasellar region. *Neuroimaging Clin N Am* (2021) 31(4):541–52. doi: 10.1016/j.nic.2021.05.010

4. Kameda-Smith MM, Zhang E, Lannon M, Algird A, Reddy K, Lu JQ. Pituitary metastasis: From pathology to clinical and radiological considerations. *J Clin Neurosci* (2021) 93:231–40. doi: 10.1016/j.jocn.2021.09.016

5. Dai C, Sun B, Kang J. Is seed and soil theory suitable for metastatic spread of pituitary carcinomas? *Front Endocrinol* (2021) 11:607405. doi: 10.3389/fendo.2020.607405

6. Zhao K, Nimchinsky E, Agarwalla PK. Differential diagnosis and radiographic imaging of pituitary lesions: An integrated approach. *Otolaryngol Clin North Am* (2022) 55(2):247–64. doi: 10.1016/j.otc.2021.12.002

7. Altshuler DB, Andrews CA, Parmar HA, Sullivan SE, Trobe JD. Imaging errors in distinguishing pituitary adenomas from other sellar lesions. *J Neuroophthalmol* (2021) 41(4):512–8. doi: 10.1097/WNO.0000000000001164

frontiers in Endocrinology

ORIGINAL RESEARCH
published: 04 January 2021
doi: 10.3389/fendo.2021.802426

Sellar Region Lesions and Intracranial Aneurysms in the Era of Endoscopic Endonasal Approach

Siyu Yan[1,2†], Yifan Liu[1†], Chang Liu[3], Li Yang[3], Yun Qin[3], Ran Liu[4], Shan Wang[5], Xue Li[5], Wenjie Yang[5], Lu Ma[1], Chao You[1], Liangxue Zhou[1] and Rui Tian[1*]*

[1] Department of Neurosurgery, West China Hospital, Sichuan University, Chengdu, China, [2] West China School of Medicine, West China Hospital, Sichuan University, Chengdu, China, [3] Department of Radiology, West China Hospital, Sichuan University, Chengdu, China, [4] 4Engineering Research Center of Medical Information Technology, Ministry of Education, West China Hospital, Sichuan University, Chengdu, China, [5] Department of Clinical Research Management, West China Hospital, Sichuan University, Chengdu, China

OPEN ACCESS

Edited by:
Congxin Dai,
Capital Medical University, China

Reviewed by:
Xiaohai Liu,
Capital Medical University, China
Changxiang Yan,
Capital Medical University, China

***Correspondence:**
Rui Tian
tianrui17419@wchscu.cn
Liangxue Zhou
zhlxlll@163.com

†These authors have contributed equally to this work and share first authorship

Specialty section:
This article was submitted to Pituitary Endocrinology, a section of the journal Frontiers in Endocrinology

Received: 26 October 2021
Accepted: 06 December 2021
Published: 04 January 2021

Citation:
Yan S, Liu Y, Liu C, Yang L, Qin Y, Liu R, Wang S, Li X, Yang W, Ma L, You C, Zhou L and Tian R (2021) Sellar Region Lesions and Intracranial Aneurysms in the Era of Endoscopic Endonasal Approach. Front. Endocrinol. 12:802426. doi: 10.3389/fendo.2021.802426

In the clinical practice of neurosurgery, the endoscopic endonasal approach (EEA) has been the mainstream approach in the management of sellar region diseases. However, clinicians have come to realize that EEA procedure is associated with intraoperative hemorrhage. Due to the limited surgical field and poor proximal control under endoscope, massive hemorrhage always leads to severe complication or even perioperative death. Previously, intraoperative hemorrhage used to be attributed to endoscopic intervention of cavernous sinus or internal carotid artery, but our recent understanding of EEA indicated that preoperatively complicated intracranial aneurysms (IAs) may play a role. In this article, we retrospectively reviewed the baseline characteristics, treatment strategy, pathology, intraoperative findings, as well as radiological profiles of sellar region lesions complicated with IAs. With the focus put on the high comorbidity rate of sellar region lesions and IAs, we did further statistical analysis to sketch the outline of this coexisting circumstance and to emphasize the importance of computed tomography angiography (CTA) as routine EEA preoperative examination. Thorough patient-surgeon communication should be proceeded before the formulation of an individualized treatment strategy.

Keywords: intracranial aneurysm, computed tomography angiography, endoscopic endonasal transsphenoidal surgery, sellar mass lesions, strategy

INTRODUCTION

Sellar region lesions are a group of rare diseases in the clinical practice of neurosurgery, with various pathological classifications including pituitary adenomas, craniopharyngioma, Rathke's cyst, meningioma, pituitary abscess, glioma, and so on. Patients usually presented with endocrinological dysfunctions and neurological manifestations such as headache, oculomotor nerve palsy, blurred vision, or even visual loss. Thus, primary diagnosis should be made based on endocrinological test and enhanced sellar magnetic resonance imaging (MRI), with or without visual field examination. Once confirmed, surgical resection should be the first-line treatment for most of the circumstances (1).

As for surgical modalities of sellar region lesions, there has been an evolution corridor in the history of neurosurgery, from open surgery to microscopic transoral surgery, then from microscopic transnasal transsphenoidal surgery to the endoscopic endonasal approach (EEA) (2–5). Until today, EEA has become an established treatment for sellar region lesions by the benefit of its minimal invasiveness and improved surgical field (6, 7). The common procedures involve pulling and dragging movements during the EEA could cause surgical damage of parasellar region structures and sometimes even result in massive hemorrhage, which is thought to be the most severe intraoperative complication. It is generally acknowledged that such an emergency is attributed to the damage of parasellar structures such as the internal carotid artery (ICA) or cavernous sinus in EEA (8). However, our recent understanding of the modality indicated that preoperatively complicated intracranial aneurysms (IAs) may also play a role with the stability of the IAs may be affected, as well as parasellar region around it, and the IAs which locate on the circle of Willis could in a greater risk.

According to literature, the prevalence of IAs can be as high as 3.2% (9), and the prevalence of sellar region lesions ranges from 10% to 20% among the general population. Thus, the co-existence of IAs and sellar region lesions used to be taken as a rare condition by inertial thinking and drawn little attention during preoperative evaluation. In the recent decades, a few studies focused on this coexisting circumstance and reported the prevalence varied between 0.9% and 8.3% (10–14),while the real-world prevalence data of sellar region lesions complicated with IAs among Chinese population is limited. Also, the therapy challenges of complicated occasional IAs in the era of EEA modality for sellar region lesions has not been well discussed. In this article, we presented a retrospective observational study to sketch the clinical and radiological characteristics of patients diagnosed with sellar region lesions co-existed with IAs, with the emphasis on the discussion of preoperative evaluation and individualized formulation of treatment strategy under the high comorbidity rate.

MATERIALS AND METHODS

Study Population

Continuous patients diagnosed with sellar region lesions from December 2016 to November 2020, in the Department of Neurosurgery, Shangjin branch of West China Hospital, Sichuan University, were retrospectively screened. On the basis of the electronic health records, the detailed inclusion criteria were as follows: (1) age ≥ 18 years; (2) sellar region lesions diagnosed with the composite of clinical presentations, laboratory tests, histological investigations, and enhanced sellar magnetic resonance imaging (MRI); (3) complicated with IAs diagnosed by computed tomography angiography (CTA), digital subtraction angiography (DSA), or intraoperative findings; (4) be capable to offer informed consent independently or with the help of relatives. While exclusion criteria were as follows: (1) patients with other systemic diseases contradict surgical intervention; (2) patients lack of valid radiological evidence of IA diagnosis.

Data Acquisition

This study was consistent with the 1964 Declaration of Helsinki and its later amendments or comparable ethical standards, and was reviewed and approved by the Institutional Review Board and Ethics Committee of West China Hospital, Sichuan University. Written informed consent to participate in this study was provided by the participants' legal guardian/next of kin.

Baseline characteristics including sex, age, tobacco use, alcohol intake, history of hypertension, history of subarachnoid hemorrhage (SAH), onset symptoms, preoperative and postoperative hormone load, and treatment strategies were collected from electronic health records of all included patients.

Based on the histological evidence or evaluated comprehensively by the laboratory results of endocrinology examination before surgeries and clinical symptoms, tumors of the sellar region were classified according to the 4th edition of the World Health Organization (WHO) classification of endocrine tumors (15, 16), among which including corticotroph adenoma, somatotroph adenoma, lactotroph adenoma, thyrotroph adenoma, gonadotroph adenoma, null-cell adenoma, craniopharyngioma, and chordoma. On the grounds of the preoperative enhanced sellar MRI, the invasiveness of cavernous sinus was evaluated and graded in line with the Knosp classification (17) independently by two neurosurgeons on the Picture Archiving and Communication System. Sellar region tumors graded from 0 to 2 were defined as noninvasive while from 3 to 4 were invasive ones. Elevation of the optic nerve was investigated as well.

Features of intracranial IAs were also reviewed by two neurosurgeons independently that relevant parameters were extracted from the outcome of multiplanar 3D reconstruction on the Picture Archiving and Communication System. IA was defined as an abnormal outpouching in the wall of cerebral blood vessels (18). The suspicious localized dilation judged by both reviewers was excluded. The number, location, size, neck width, and direction of detected IAs of patients were collected. The location of IAs was recognized as ICA and its segments in accordance with the Bouthillier classification (19), among which includes anterior cerebral artery (ACA), middle cerebral artery (MCA), posterior cerebral artery (PCA), anterior communicating artery (AoCA), and posterior communicating artery (PoCA). According to measured neck width, the dome-to-neck ratio was calculated for each scanned IAs, with the relatively high or low ruptures risks respectively during the EEA, then it would be divided into wide-neck (dome-to-neck ratio ≥ 2 or neck width < 4 mm) or narrow-neck (dome-to-neck ratio < 2 or neck width ≥ 4 mm) (20). At the same time, IAs were classified based on their direction to the cavernous sinus as well, which includes point to, in parallel with, or deviate from the cavernous sinus, presenting the fairly high, moderate, or mild rupture risks under the limited surgical field.

The prognosis was indicated by information compounding survival state, any newly emerging abnormalities, as well as any

improvement of symptoms before the surgery collected by telephone follow-up.

Statistical Analysis

A flowchart was applied to show the process of participants selection. SPSS software version 26.0 (IBM Corp., Armonk, New York, USA) was used to analyze the collected data in this study. Categorical variables were described with numbers and percentages, while continuous variables were described with means ± standard deviation.

RESULTS

A total of 515 continuous patients diagnosed with "sellar mass" by enhanced sellar MRI were reviewed through medical records. 110 of them were either endocrine-negative pituitary microadenomas with normal visual function or had surgical contradictions (such as systemic infection and recent heart attacks), 405 patients were further evaluated. By further review of radiological and intraoperative findings, we included 45 patients complicated with IAs diagnosed by CTA, DSA, or intraoperative findings. Patient recruitment flowchart was shown in **Figure 1**. The baseline information of included patients was shown in **Table 1**. The typical radiological profile of a sellar mass patient complicated IAs is shown in **Figure 2**.

Clinical characteristics of all the 45 included sellar region lesions were listed in **Table 2**, including histological and endocrinological subtype and tumor invasiveness. Thus, 38 out of 45 (84.4%) patients proved to be pituitary adenoma, and 34 out of 45 (75.6%) patients had noninvasive tumors (Knosp classification 0-2). The operation information among patients presenting different tumor invasiveness was shown in **Table 2-S1**, while the preoperative and postoperative hormone loads in different subtypes of functional pituitary adenomas was presented in **Table 2-S2**.

Clinical characteristics and radiological profiles of IAs of all the 45 included patients was shown in **Table 3**. Detailed information of IAs included number, location, size (maximal diameter), dome to neck ratio, as well as pointing direction. Thus, 35 out of 45 (77.8%) patients had only single aneurysm, 19 out of 58 (32.8%) IAs located on ICA C6 segment (ophthalmic segment), 30 out of 58 (51.7%) IAs were micro-aneurysms with diameter less than 3 mm, 39 out of 58 (67.2%) IAs were narrow-neck (dome to neck ratio < 2). As for the pointing direction of IAs, 23 out of 58 IAs (39.7%) pointed to the cavernous sinus, and 21 out of 58 (36.2%) IAs pointed deviated from the cavernous

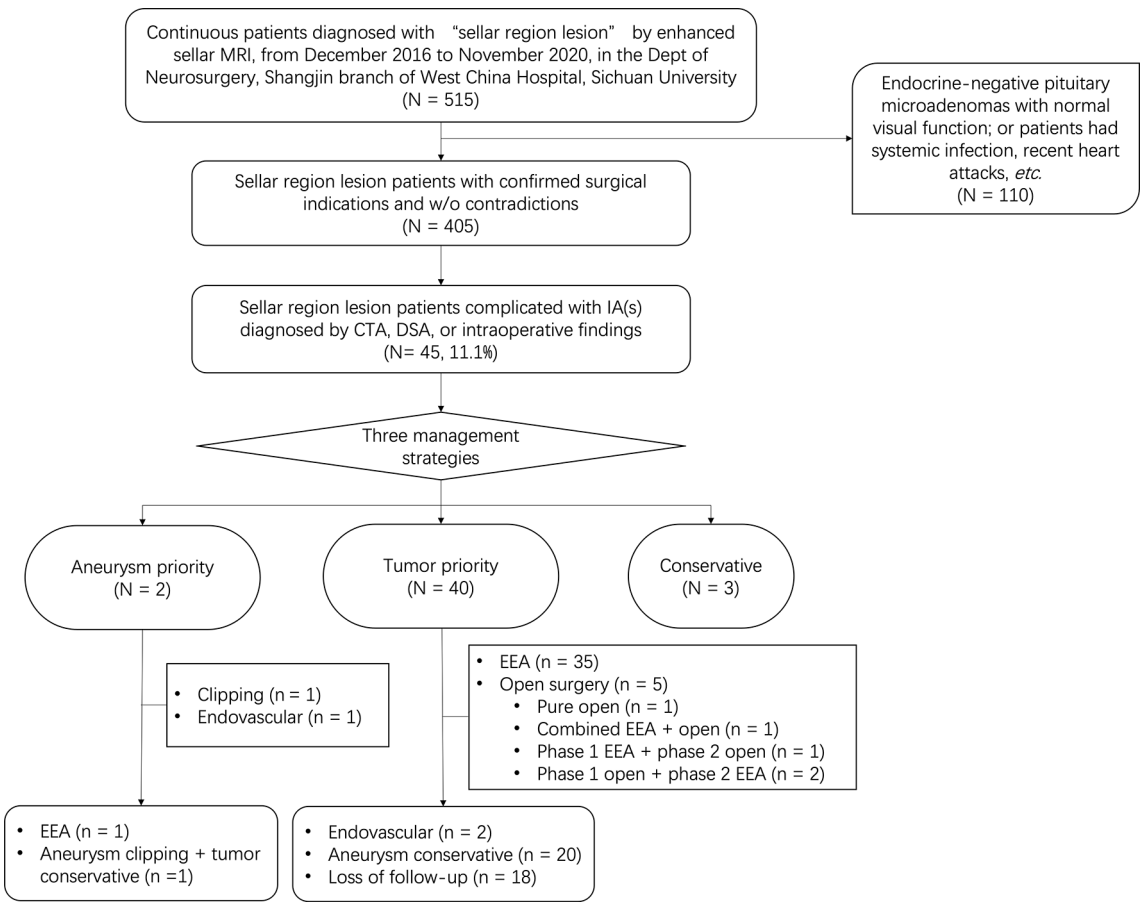

FIGURE 1 | Patient recruitment flowchart of sellar region lesions complicated with IAs.

TABLE 1 | Baseline characteristics of included patients.

Characteristic	n (%), mean ± SD, or description
Sex(M/F)	24/21
Age (years)	56.38 ± 11.21
Tobacco use	13/45 (28.9%)
Alcohol intake	9/45 (20.0%)
History of hypertension	16/45 (35.6%)
History of SAH	0/45 (0.0%)
Onset symptoms	
Dizziness or headache	26/45 (57.8%)
Acute visual loss	23/45 (51.1%)
Oculomotor nerve palsy	3/45 (6.7%)
Endocrinological symptoms	4/45 (8.9%)
Other symptoms	Nausea, vomiting, weakness or numbness of limbs, unilateral facial pain, and sexual dysfunction
Treatment strategies	
Underwent surgeries for tumor first and follow-up for IAs	40/45 (88.9%)
EEA	35/40 (87.5%)
Craniotomy	5/40 (12.5%)
Total tumor excision	21/40 (52.5%)
Subtotal tumor excision	19/40 (47.5%)
Underwent surgeries for IAs first	2/45 (4.4%)
Underwent surgeries for both tumor and IAs	0/45 (0.0%)
Conservative w/o any surgeries during follow-up	3/45 (6.7%)

NOTES: SAH, subarachnoid hemorrhage; IAs, unruptured intracranial aneurysms; EEA, endoscopic endonasal approach.

TABLE 2 | Clinical characteristics of sellar region lesions.

Characteristic	n (%) or mean ± SD
Histological and endocrinological subtype	
Pituitary adenoma	38/45 (84.4%)
Corticotroph adenoma	1/38 (2.6%)
Somatotroph adenoma	2/38 (5.3%)
Lactotroph adenoma	10/38 (26.3%)
Thyrotroph adenoma	1/38 (2.6%)
Gonadotroph adenoma	1/38 (2.6%)
Null-cell adenoma	23/38 (60.5%)
Craniopharyngioma	3/45 (6.7%)
Chordoma	4/45 (8.9%)
Tumor invasiveness	
Noninvasive tumors (Knosp classification 0-2)	34/45 (75.6%)
Invasive tumors (Knosp classification 3-4)	11/45 (24.4%)
Optic nerve elevation	34/45 (75.6%)

sinus or far away. And the operation information among patients with different IAs size, different dome-to-neck ratio of IAs, as well as different direction of IAs, were shown in **Tables 3-S1**–**3-S3**, respectively.

As for follow-up data of long-term prognosis, detailed information was presented in **Table 4**. Follow-up information included follow-up rate, survival state, newly emerging abnormalities, as well as improvement of symptoms. A total of 27 out of 45 (60%) patients were on follow-up, and 21 out of 27 (77.8%) patients reached complete improvement.

DISCUSSIONS

In this article, we retrospectively reviewed the baseline characteristics, treatment strategy, pathology, intraoperative findings, as well as radiological profiles of sellar region lesions complicated with IAs. Among 45 included patients (M/F, 24/21), the mean age is 56.38 ± 11.21 (± SD) years old. Dizziness, headache, and acute visual loss are the most common symptoms of onset, suggesting that atypical manifestations such as dizziness and headache should not be ignored in clinic practice.

Importantly, we found that the real-world comorbidity rate of sellar region lesions and IAs in the Chinese population is greater than the traditionally perceived data reported from 1978 to 2016 by foreign literature, which varied from 0.9% to 6.0% (10–13), as well as greater than that reported by another Chinese neurosurgical team (8.3%) (14). However, in our study, the overall prevalence of sellar region lesions co-existed with the IAs is as high as 11.1%. The difference can be attributed to the rapid development of radiological techniques. More advanced medical imaging equipment brings an increased detection rate compared to the autopsy-confirmed times in history (21, 22). By referring to the data distribution of the baseline demographic data, tumor

TABLE 3 | Clinical characteristics and radiological profiles of IAs.

Characteristic	n (%) or mean ± SD
Number	58
1	35/45 (77.8%)
2	7/45 (15.5%)
3	3/45 (6.7%)
Location	
ICA C1 (cervical segment)	1/58 (1.7%)
ICA C2 (petrous segment)	0 (0.0%)
ICA C3 (lacerum segment)	0 (0.0%)
ICA C4 (cavernous segment)	4/58 (6.9%)
ICA C5 (clinoid segment)	7/58 (12.1%)
I CA C6 (ophthalmic segment)	19/58 (32.8%)
I CA C7 (communicating segment)	14/58 (24.1%)
ACA	1/58 (1.7%)
MCA	4/58 (6.9%)
PCA	1/58 (1.7%)
AoCA	0/58 (0.0%)
PoCA	5/58 (8.6%)
Others	VA (1/58, 1.7%); ICA, segment unidentified (1/58, 1.7%)
Size (Maximal diameter)	
d≥10mm	3/58 (5.2%)
3mm≤d<10mm	22/58 (37.9%)
d<3mm	30/58 (51.7%)
Without description	3/58 (5.2%)
Dome to neck ratio	
Wide-neck(ratio≥2)	16/58 (27.6%)
Narrow-neck(ratio<2)	39/58 (67.2%)
Without description	3/58 (5.2%)
Pointing direction	
Point to the cavernous sinus	23/58 (39.7%)
In parallel with the cavernous sinus	8/58 (13.8%)
Deviate from the cavernous sinus or far away	21/58 (36.2%)
Cannot be identified	6/58 (10.3%)

NOTES: ICA, internal carotid artery; ACA, anterior cerebral artery; MCA, middle cerebral artery; PCA, posterior cerebral artery; AoCA, anterior communicating cerebral artery; PoCA, posterior communicating cerebral artery; VA, vertebral artery.

biology information, and radiological features of IAs, our reported data has been in accordance with clinical reality and proved reliable. Therefore, the 11.1% high prevalence of comorbidity brings out new challenges to neurosurgeons that cerebrovascular screening for occasional IAs should be taken into considerations before the surgery. Rupture of undetected IAs during EEA procedures can be catastrophic and always leads to patient death on operation table. CTA is a non-invasive imaging modality with greater availability and lower cost to detect IAs (23), which may benefit EEA patients for sellar region lesions. To decrease the risk of unprepared intraoperative IAs rupture during an EEA operation, which is impossible to achieve proximal control of ICA, we strongly suggested that CTA be written into related clinical guidelines as routine preoperative evaluation before EEA.

When there is known IAs complicated with sellar region lesions, the IAs circumstances must be treated with super cautiousness and individualized strategy of treatment must be formulated for safety concerns. By the statistical sketching of

TABLE 4 | Prognosis of included patients *via* follow-up.

Characteristics	n (%) or description
Follow-up rate	27/45 (60.0%)
Survival state	
Survival	27/27 (100.0%)
Disabled	3/27 (11.1%)
Dead	0/27 (0.0%)
Newly emerging abnormalities	3/27 (11.1%, including loss of vision, speech disorder, and paralysis)
Improvement of symptoms	
Complete improvement	21/27 (77.8%)
Partial improvement	6/27 (22.2%)
No improvement	0/27 (0.0%)
Impaired improvement	0/27 (0.0%)

outline of this coexisting circumstance, we found the major pathological classifications of patients were pituitary adenoma (84.4%), and more than half (60.5%) were null-cell adenoma, who barely have endocrinological discomforts and usually present with compression symptoms. So, the null-cell adenomas are usually moderate to huge in size, and tender to be invasive with greater Knosp classification. In this way, there might be more pulling movements with a higher risk of intraoperative interruption of the complicated IAs during EEA. The direction of the IAs also contributes to a certain risk of IAs rupture for their different accessibilities during the separation. **Table 3-S3** demonstrated that nearly two-thirds of IAs do not deviate from the cavernous sinus. These IAs are at greater risk of rupture during EEA operation.

An individualized treatment strategy needs to be formulated for patients who have sellar region lesions complicated with IAs. In the total of 45 included patients, there were 58 detected IAs. In **Table 3**, we found that 77.8% of patients had a single aneurysm instead of multiple IAs, and 67.2% of aneurysms were narrow-neck instead of wide-neck. This rendered equal priority between clipping surgery and intravascular therapy when considering aneurysm management. For aneurysm location, **Table 3** showed that 32.8% of IAs clustered on ICA C6 segment (ophthalmic segment), where clipping surgery encounters greater difficulties and risks. Hence, intravascular therapy should be privileged here for ophthalmic segment IA complicated with sellar region lesions. Other locations of complicated IAs were C7 (communicating segment, 24.1%), C5 (clinoid segment, 12.1%), PoCA (8.6%), C4 (cavernous segment, 6.9%), MCA (6.9%), C1 (cervical segment, 1.7%), ACA (1.7%), by the sequence of decreased frequency of occurrence. Above all, no matter EEA approach or open cranial approach, total or subtotal tumor excision, treatment strategy of such comorbidity should be comprehensively formulated based on both the features of sellar region lesions and the IAs. It was noted that 4 patients in our study had huge parasellar blood clots far from sellar lesions, indicating hemorrhage instead of tumor apoplexy before the operation. Among these 4 patients, 3 patients chose to deal with sellar lesions first (2 of 3 had subtotal tumor excision), and 1 patient chose conservative treatment without dealing with neither IAs nor sellar lesions.

One of the comforting results of **Table 3** was that 51.7% IAs were micro-aneurysms with a lower risk of rupture, and most patients are in the mild to moderate risk. Given the 0.87% to 1.6% annual rupture rate per IA patient in natural history (9, 24, 25) and aneurysm diameter > 7 mm is an independent risk factor of rupture (25), included patients were divided into three hierarchical subgroups representing different rupture risk. 36 out of 38 (94.7%) patients had IA diameter larger than 3 mm, therefore at middle to low risk. In most cases, it is not recommended to perform aggressive intervention for complicated IAs since they have a relatively low risk of

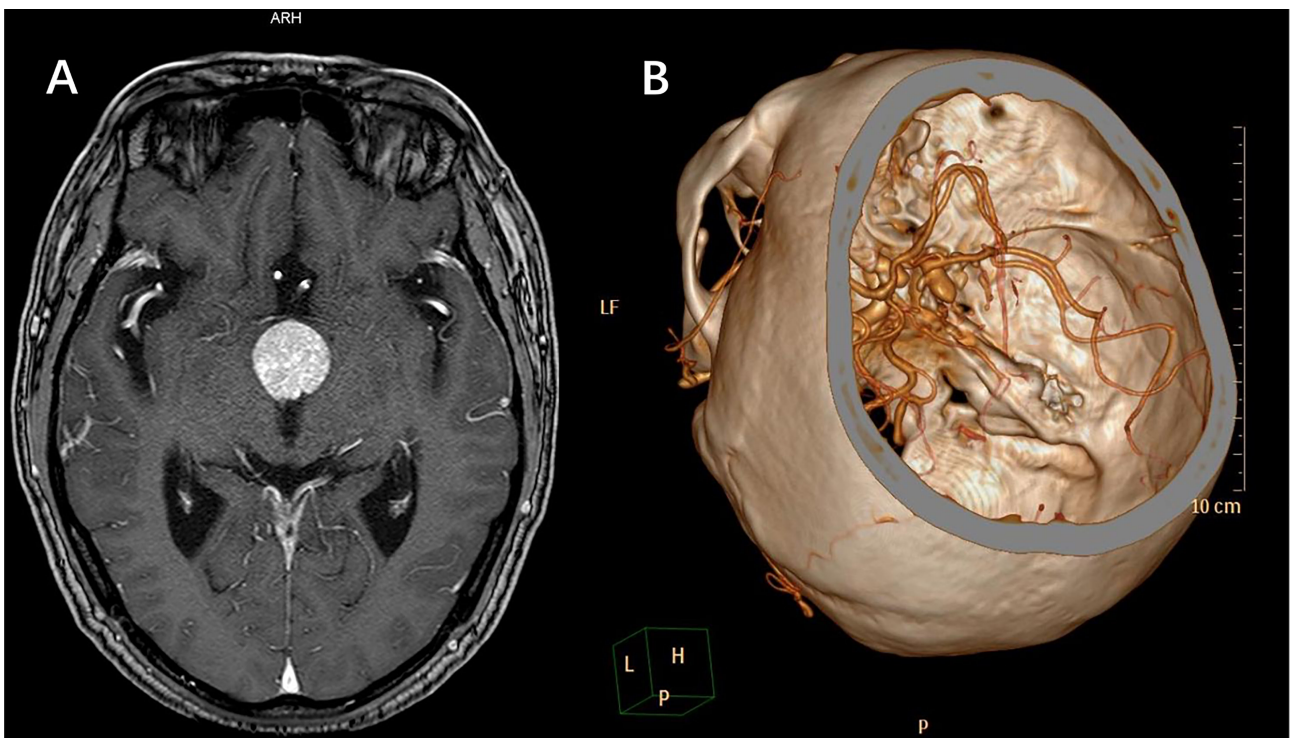

FIGURE 2 | A case of typical radiological profile of sellar region lesion complicated with IAs. **(A)** MRI indicated sellar region lesion. **(B)** Further CTA revealed a partially thrombotic pseudoaneurysm formed from ruptured IA, and the IA located close to the sellar region lesion. In such occasion, incomplete preoperative examinations without CTA can lead to intraoperative massive hemorrhage, even perioperative death.

rupture, especially those with a diameter less than 7 mm (9). But the clinical experience on aneurysm size and risk of rupture is established under the premise of the natural history of IAs, it may not work here under the intervention of EEA. Thus, even microaneurysms should arise enough attention during integrated management. Thorough patient-surgeon communication should proceeded before the formulation of an individualized treatment strategy.

In **Tables 3-S1**–**Table 3-S3**, we can find that EEA has been favored by more and more neurosurgeons for tumor resection in the sellar region in recent years due to its specific advantages including minimally invasive, less complication, lower morbidity as well as mortality rates over the conventional craniotomy (26–28). But the incidence of operation-associated massive hemorrhage during EEA could never be ignored. Once IA was found to be complicated with sellar region lesions by preoperative CTA screening, further treatment strategy must be formulated based on the features of IAs (such as number, location, and morphological characteristics) as well as its association with sellar region lesions (such as tumor invasiveness and pointing direction) (29).

The favorable outcome from follow-up highlighted the importance of CTA as a routine preoperative evaluation in the formulation of individualized treatment strategy. CTA is a non-invasive imaging modality with lower cost, faster acquisition, and great accessibility. A meta-analysis conducted by Menke J et al. revealed that the sensitivity and specificity for intracranial aneurysm detection were over 97% (30). Also, relevant yielded outcomes had a 96% sensitivity for IAs with maximal diameters ≥ 3 mm (31).

There are some limitations to our study. First, the sample size of 45 patients is relatively small, though already has been the largest cohort among literatures. Second, we didn't recruit a healthy population as control. Third, data was manually collected and analyzed so there might exist a certain bias. Fourth, this is a retrospective observational study, the further randomized evaluation may be acquired in a more generalized population.

CONCLUSIONS

The overall prevalence of sellar region lesions co-existed with the IAs is 11.1%. In the era of EEA for the sellar region lesions complicated with IAs, specific and individualized treatment strategy should be carried out during the clinical management. And we strongly recommend that CTA be considered as routine cerebrovascular screening before EEA to guarantee the safety of procedure.

DATA AVAILABILITY STATEMENT

The raw data supporting the conclusions of this article will be made available by the authors, without undue reservation.

ETHICS STATEMENT

The studies involving human participants were reviewed and approved by Institutional Review Board and Ethics Committee of West China Hospital, Sichuan University. Written informed consent to participate in this study was provided by the participants' legal guardian/next of kin. Written informed consent was obtained from the individual(s), and minor(s)' legal guardian/next of kin, for the publication of any potentially identifiable images or data included in this article.

AUTHOR CONTRIBUTIONS

SY and YL are co-first authors and contributed equally to this article. Correspondence addressed to RT (tianrui17419@wchscu.cn) and LZ (zhlxlll@163.com). All authors contributed to the article and approved the submitted version.

FUNDING

This research was funded by 1) National Key R&D Program of China, No. 2018YFA0108603; 2) National Key R&D Program of China, No. 2018YFA0108604; 3) 1·3·5 Project for Disciplines of Excellence, West China Hospital, Sichuan University, No. 2021HXFH014; 4) Clinical Research Innovation Project, West China Hospital, Sichuan University, No. 2019HXCX07.

SUPPLEMENTARY MATERIAL

The Supplementary Material for this article can be found online at: https://www.frontiersin.org/articles/10.3389/fendo.2021.802426/full#supplementary-material

REFERENCES

1. Sivakumar W, Chamoun R, Nguyen V, Couldwell WT. Incidental Pituitary Adenomas. *Neurosurg Focus* (2011) 31(6):E18. doi: 10.3171/2011.9.FOCUS11217
2. Schloffer H. Zur Frage Der Operationen an Der Hypophyse. *Beitr Klin Chir* (1906) 50:767–817.
3. Cushing H. The Pituitary Body and its Disorders: Clinical States Produced by Disorders of the Hypophysis Cerebri. *jB Lippincott* (1912) 296–03. doi: 10.1097/00000441-191212000-00019
4. Jho HD, Carrau RL. Endoscopic Endonasal Transsphenoidal Surgery: Experience With 50 Patients. *J Neurosurg* (1997) 87(1):44–51. doi: 10.3171/jns.1997.87.1.0044
5. Cappabianca P, Cavallo LM, Colao A, Del Basso De Caro M, Esposito F, Cirillo S, et al. Endoscopic Endonasal Transsphenoidal Approach: Outcome Analysis of 100 Consecutive Procedures. *Min-Minimally Invasive Neurosurg* (2002) 45(04):193–200. doi: 10.1055/s-2002-36197
6. Cavallo LM, Somma T, Solari D, Iannuzzo G, Frio F, Baiano C, et al. Endoscopic Endonasal Transsphenoidal Surgery: History and Evolution. *World Neurosurg* (2019) 127:686–94. doi: 10.1016/j.wneu.2019.03.048

7. Wang F, Zhou T, Wei S, Meng X, Zhang J, Hou Y, et al. Endoscopic Endonasal Transsphenoidal Surgery of 1,166 Pituitary Adenomas. *Surg Endoscopy* (2015) 29(6):1270–80. doi: 10.1007/s00464-014-3815-0
8. Lee CH, Chen SM, Lui TN. Posterior Cerebral Artery Pseudoaneurysm, a Rare Complication of Pituitary Tumor Transsphenoidal Surgery: Case Report and Literature Review. *World Neurosurg* (2015) 84(5):e1–1493.e3:1493. doi: 10.1016/j.wneu.2015.04.043
9. Thompson BG, Brown RD Jr, Amin-Hanjani S, Broderick JP, Cockroft KM, Connolly ES Jr, et al. Guidelines for the Management of Patients With Unruptured Intracranial Aneurysms: A Guideline for Healthcare Professionals From the American Heart Association/American Stroke Association. *Stroke* (2015) 46(8):2368–400. doi: 10.1161/STR.0000000000000070
10. Jakubowski J, Kendall B. Coincidental Aneurysms With Tumours of Pituitary Origin. *J Neurol Neurosurg Psychiatry* (1978) 41(11):972–9. doi: 10.1136/jnnp.41.11.972
11. Pant B, Arita K, Kurisu K, Tominaga A, Eguchi K, Uozumi T. Incidence of Intracranial Aneurysm Associated With Pituitary Adenoma. *Neurosurg Rev* (1997) 20(1):13–7. doi: 10.1007/BF01390519
12. Oh MC, Kim EH, Kim SH. Coexistence of Intracranial Aneurysm in 800 Patients With Surgically Confirmed Pituitary Adenoma. *J Neurosurg* (2012) 116(5):942–7. doi: 10.3171/2011.12.JNS11875
13. Raper DM, Ding D, Evans E, Starke RM, Crowley RW, Liu KC, et al. Clinical Features, Management Considerations and Outcomes in Case Series of Patients With Parasellar Intracranial Aneurysms Undergoing Anterior Skull Base Surgery. *World Neurosurg* (2017) 99:424–32. doi: 10.1016/j.wneu.2016.11.150
14. Hu J, Lin Z, Zhang Y, Zheng X, Ran Q, Zhang D, et al. Prevalence of Unruptured Intracranial Aneurysms Coexisting With Pituitary Adenomas. *World Neurosurg* (2019) 126:e526–33. doi: 10.1016/j.wneu.2019.02.084
15. Klöppel G, Couvelard A, Hruban R, Klimstra D, Komminoth P, Osamura R, et al. *WHO Classification of Tumours of Endocrine Organs*. Lyon, France: World Health Organization (2017).
16. Lopes MBS. The 2017 World Health Organization Classification of Tumors of the Pituitary Gland: A Summary. *Acta Neuropathologica* (2017) 134(4):521–35. doi: 10.1007/s00401-017-1769-8
17. Knosp E, Steiner E, Kitz K, Matula C. Pituitary Adenomas With Invasion of the Cavernous Sinus Space: A Magnetic Resonance Imaging Classification Compared With Surgical Findings. *Neurosurgery* (1993) 33(4):610–8. doi: 10.1227/00006123-199310000-00008
18. Adams RD, Victor M, Ropper AH, Daroff RB. Principles of Neurology. (New York, NY: McGraw-Hill Education) (1997) p. 841.
19. Bouthillier A, Van Loveren HR, Keller JT. Segments of the Internal Carotid Artery: A New Classification. *Neurosurgery* (1996) 38(3):425–33. doi: 10.1097/00006123-199603000-00001
20. Hendricks BK, Yoon JS, Yaeger K, Kellner CP, Mocco J, De Leacy RA, et al. Wide-Neck Aneurysms: Systematic Review of the Neurosurgical Literature With a Focus on Definition and Clinical Implications. *J Neurosurg* (2019) 133(1):159–65 doi: 10.3171/2019.3.JNS183160
21. Daly AF, Beckers A. The Epidemiology of Pituitary Adenomas. *Endocrinol Metab Clin North Am* (2020) 49(3):347–55. doi: 10.1016/j.ecl.2020.04.002
22. Lake MG, Krook LS, Cruz SV. Pituitary Adenomas: An Overview. *Am Family physician* (2013) 88(5):319–27.
23. Howard BM, Hu R, Barrow JW, Barrow DL. Comprehensive Review of Imaging of Intracranial Aneurysms and Angiographically Negative Subarachnoid Hemorrhage. *Neurosurg Focus* (2019) 47(6):E20. doi: 10.3171/2019.9.FOCUS19653
24. Müller TB, Sandvei MS, Kvistad KA, Rydland J, Haberg A, Vik A, et al. Unruptured Intracranial Aneurysms in the Norwegian Nord-Trøndelag Health Study (HUNT) Risk of Rupture Calculated From Data in a Population-Based Cohort Study. *Neurosurgery* (2013) 73(2):256–61. doi: 10.1227/01.neu.0000430295.23799.16
25. Korja M, Lehto H, Juvela S. Lifelong Rupture Risk of Intracranial Aneurysms Depends on Risk Factors: A Prospective Finnish Cohort Study. *Stroke* (2014) 45(7):1958–63. doi: 10.1161/STROKEAHA.114.005318
26. García-Garrigós E, Arenas-Jiménez JJ, Monjas-Cánovas I, Abarca-Olivas J, Cortes-Vela JJ, De La Hoz-Rosa J, et al. Transsphenoidal Approach in Endoscopic Endonasal Surgery for Skull Base Lesions: What Radiologists and Surgeons Need to Know. *Radiographics* (2015) 35(4):1170–85. doi: 10.1148/rg.2015140105
27. Cappabianca P, Cavallo LM, Colao A, de Divitiis E. Surgical Complications Associated With the Endoscopic Endonasal Transsphenoidal Approach for Pituitary Adenomas. *J Neurosurg* (2002) 97(2):293–8. doi: 10.3171/jns.2002.97.2.0293
28. White DR, Sonnenburg RE, Ewend MG, Senior BA. Safety of Minimally Invasive Pituitary Surgery (MIPS) Compared With a Traditional Approach. *Laryngoscope* (2004) 114(11):1945–8. doi: 10.1097/01.mlg.0000147925.04605.cc
29. Perondi GE, Isolan GR, de Aguiar PH, Stefani MA, Falcetta EF. Endoscopic Anatomy of Sellar Region. *Pituitary* (2013) 16(2):251–9. doi: 10.1007/s11102-012-0413-9
30. Menke J, Larsen J, Kallenberg K. Diagnosing Cerebral Aneurysms by Computed Tomographic Angiography: Meta-Analysis. *Ann Neurol* (2011) 69(4):646–54. doi: 10.1002/ana.22270
31. White PM, Wardlaw JM, Easton V. Can Noninvasive Imaging Accurately Depict Intracranial Aneurysms? A Systematic Review. *Radiology* (2000) 217(2):361–70. doi: 10.1148/radiology.217.2.r00nv06361

Conflict of Interest: The authors declare that the research was conducted in the absence of any commercial or financial relationships that could be construed as a potential conflict of interest.

Publisher's Note: All claims expressed in this article are solely those of the authors and do not necessarily represent those of their affiliated organizations, or those of the publisher, the editors and the reviewers. Any product that may be evaluated in this article, or claim that may be made by its manufacturer, is not guaranteed or endorsed by the publisher.

frontiers in Endocrinology

CASE REPORT
published: 30 April 2021
doi: 10.3389/fendo.2021.666791

IgG4-Related Inflammatory Pseudotumor Involving the Clivus: A Case Report and Literature Review

Xiaohai Liu[1,2], *Renzhi Wang*[2,3], *Mingchu Li*[1,2] *and Ge Chen*[1,2*]

[1] Department of Neurosurgery, Xuanwu Hospital Capital Medical University, Beijing, China, [2] Chinese Pituitary Specialists Congress, Beijing, China, [3] Department of Neurosurgery, Peking Union Medical College Hospital, Chinese Academy of Medical Sciences and Peking Union Medical College, Beijing, China

IgG4-related inflammatory pseudotumors are very uncommon and are characterized histologically by the presence of inflammatory swellings with increasing IgG4-positive plasma cells and lymphocytes infiltrating the tissues. As reports of intracranial IgG4-related pseudotumors are very rare, we report a case of an IgG4-related inflammatory pseudotumor involving the clivus mimicking meningioma. A 46-year-old male presented with intermittent headache for 2 years and a sudden onset of dysphagia and dysphonia of 7 days' duration along with lower limb weakness. Enhanced magnetic resonance imaging (MRI) of the skull base revealed an isointense signal on T1- and T2-weighted images from an enhanced mass located at the middle of the upper clivus region, for which a meningioma was highly suspected. Then, an endoscopic transsphenoidal approach was adopted and the lesion was partially resected, as the subdural extra-axial lesion was found to be very tough and firm, exhibiting fibrous scarring attaching to the brain stem and basal artery. After the surgery, brain stem and posterior cranial nerve decompression was achieved, and the patient's symptoms, such as dysphagia, dysphonia and lower limb weakness, improved. Pathological findings showed many IgG4-positive plasma cells and lymphocytes surrounded by collagen-rich fibers. The patient was sent to the rheumatology department for further glucocorticoids after the diagnosis of an IgG4-related inflammatory pseudotumor was made. This case highlights the importance of considering IgG4-related inflammatory pseudotumors as a differential diagnosis in patients with lesions involving the clivus presenting with a sudden onset of symptoms of dysphagia and dysphonia along with lower limb weakness when other more threatening causes have been excluded. IgG4-related inflammatory pseudotumors are etiologically enigmatic and unpredictable, and total resection might not be warranted. Glucocorticoids are usually the first line of treatment after diagnosis.

Keywords: IgG4-related disease, IgG4-related inflammatory pseudotumor, clivus, endoscopic transsphenoidal approach, case report

OPEN ACCESS

Edited by:
Run Yu,
UCLA David Geffen School of Medicine, United States

Reviewed by:
Odelia Cooper,
Cedars Sinai Medical Center, United States
Songbai Gui,
Capital Medical University, China

****Correspondence:***
Ge Chen
chengecn@139.com

Specialty section:
This article was submitted to Pituitary Endocrinology, a section of the journal Frontiers in Endocrinology

Received: *11 February 2021*
Accepted: *06 April 2021*
Published: *30 April 2021*

Citation:
Liu X, Wang R, Li M and Chen G (2021) IgG4-Related Inflammatory Pseudotumor Involving the Clivus: A Case Report and Literature Review. Front. Endocrinol. 12:666791. doi: 10.3389/fendo.2021.666791

INTRODUCTION

Although intracranial hypophysitis is well known and relatively common, IgG4-related disease (IgG4-RD) is very rare and characterized histologically by the presence of acute or chronic inflammatory swellings of involved organs with increasing IgG4-positive plasma cells and lymphocytes infiltrating the tissues (1). Although several cases of IgG4-related inflammatory pseudotumors have been reported, there are few reports of intracranial IgG4-related inflammatory pseudotumors (2–14). The preoperative diagnosis of the disease is very important as IgG4-related inflammatory pseudotumors are more likely sensitive to steroid therapy but not surgery. Here, we report a rare case of an IgG4-related inflammatory pseudotumor in the middle of the upper clivus region, mimicking meningioma, and review the literature on such cases (2–14). We hope to highlight the importance of considering IgG4-related inflammatory pseudotumors as a differential diagnosis in patients presenting with clivus lesions.

CASE PRESENTATION

Medical History

The patient was a 46-year-old male who presented with intermittent headache for 2 years and a sudden onset of dysphagia and dysphonia of 7 days' duration along with lower limb weakness upon physical examination. His visual acuity and fields for both eyes were relatively normal. He had no past history of autoimmune disease or other illness. Magnetic resonance imaging (MRI) of the skull base revealed a predominantly hypointense signal on T1- and T2-weighted images from a mass located in the middle of the upper clivus area, and it was homogenously enhanced after contrast MRI; meningioma was highly suspected (**Figures 1A–F**). Routine laboratory tests showed no abnormal data. The levels of pituitary hormones were all within normal limits. The study was approved by the Research Ethics Committee of our hospital and written informed consent was obtained from the patient according to institutional guidelines for publication of this case report and any accompanying images.

Surgical Details

On Dec. 30, 2020, the patient underwent endoscopic transsphenoidal surgery. During the operation, the extra-axial lesion was found to be subdural and was very tough and firm, exhibiting fibrous scarring attaching the mass to the brain stem (**Figures 2A, B**). Because the lesion did not resemble meningioma in texture, we sent some tumor tissue for intraoperative frozen tissue pathology, which showed many lymphoplasmacytes surrounded by collagen-rich fibers. As inflammatory lesions may be sensitive to glucocorticoids, the lesion was partially resected owing to its tenacious texture and close adhesion to the brain stem (**Figures 1G–I**). Postoperatively, brain stem and posterior cranial nerve decompression was achieved. Symptoms, such as dysphagia and dysphonia along with lower limb weakness, were improved, and the patient did not suffer from additional neurological deficits.

Postoperative Treatment

The histopathological findings revealed an inflammatory pseudotumor involving the clivus, with sclerosing fibrosis mixed with lymphocytes and IgG4-positive plasma cells infiltrating into the tissues (**Figure 3**). Hematoxylin and eosin (H&E) stain showed the lesion was composed of sclerosing fibrosis associated with dense lymphoplasmacytic infiltration (**Figures 3A, B**). Immunohistochemical analysis revealed over IgG4-positive cells per high-powered field and a high IgG4/IgG ratio (**Figures 3C, D**). Immunohistochemistry revealed positivity for vimentin, EMA, CD3, CD20, CD38, CD68, kappa, lambda and IgG4 but negativity for PAS and CD34. and the Ki-67 index was 10% (**Figures 3E, F**). The blood sample for further immune disease investigations showed no elevated levels of IgG (12.5 g/L; reference range 7.51-15.6 g/L), IgA (2.34 g/L; reference range 0.82-4.53 g/L), IgM (0.68 g/L; reference range 0.46-3.04 g/L) or IgE (131.0 IU/ml; reference range 5-165 g/L) in the serum. Subsequent ultrasonography and computed tomography (CT) for thorax and abdomen were performed, and no other lesions were detected. After a discussion of MDT (Multidisciplinary Team), the diagnosis of IgG4-related inflammatory pseudotumor was made, and the patient was sent to the rheumatology department for further glucocorticoid treatment.

DISCUSSION

IgG4-RD is a chronic inflammatory lesion involving many organs of unknown origin (15). An epidemiological study revealed an estimated prevalence in the Japanese population of 6 cases per 100,000 people (16). There are several alternative terms for IgG4-related inflammatory lesions, such as inflammatory pseudotumors, inflammatory myofibroblastic tumors, plasma cell granulomas or pseudotumors, xanthomatous disease, pseudosarcomatous myofibroblastic diffusion, and inflammatory myofibrohistiocytic myofibroblastoma (17). According to the consensus statement on the pathology of IgG4-related disease, the diagnosis of IgG4-RD is based on three histological criteria: dense lymphoplasmocytic infiltrate, fibrosis arranged at least focally in a storiform pattern and obliterative phlebitis (18). Interestingly, serum IgG4 levels are normal in approximately 40% of patients with biopsy-proven IgG4-RD. Therefore, increased serum IgG4 levels are not necessary for the diagnosis of IgG4-related inflammatory pseudotumors. In our case, the diagnosis of IgG4-related inflammatory pseudotumors was based on sclerosing fibrosis mixed with lymphocytes and IgG4-positive plasma cells infiltrating into the tissues, while the serum IgG4 level was normal in our case.

The most common organ affected by IgG4-related inflammatory pseudotumors is the pancreas, but it can also involve the biliary tract, salivary and lacrimal glands, kidneys, orbital tissues, lymph nodes, lungs and many others (18). IgG4-related inflammatory pseudotumors have been found to involve, in rare cases, the nervous system. For lesions in the nervous system, IgG4-RD is relatively common in the orbit and pituitary and is characterized by a variety of histological manifestations (19). Based on previous reports (2–14), MR of the lesion usually

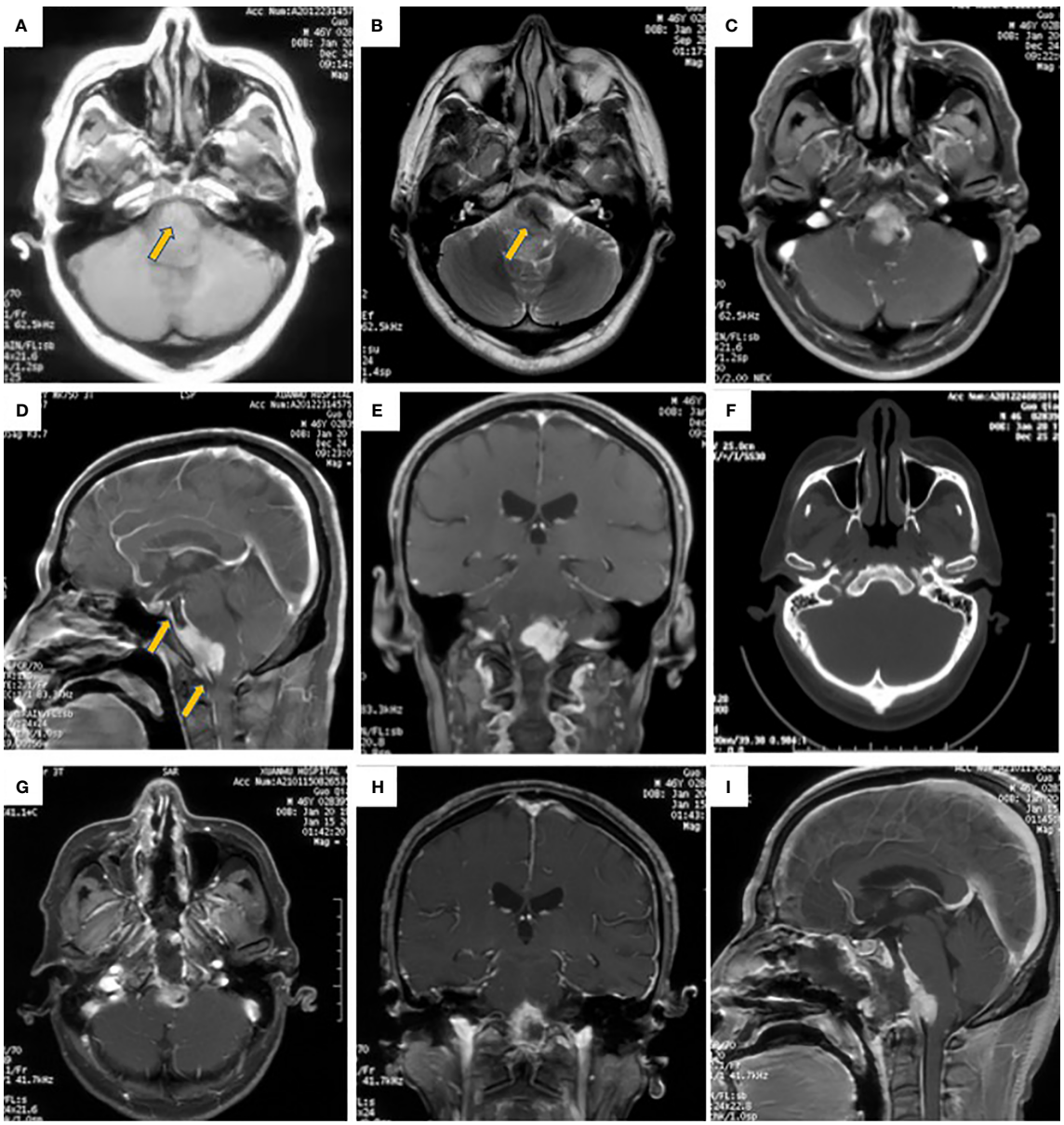

FIGURE 1 | Brain MRI images showed intracranial mass located at middle of upper clivus region. **(A, B)**. The lesion located at middle of upper clivus region presented with isointense signal in T1-weighted MRI image (**A**, the arrow), and hypointense signal in T2-weighted MRI image (**B**, the arrow); **(C, E)**: The mass was uniformly enhanced after contrast MRI scan, and the base of the tumor was extensively stick to the adjacent dura and brain stem, showing meningeal tail sign (the arrow in **D**), and meningioma was highly suspected. **(F)**. CT bone window showed no bone invasion. **(G, I)**. The MRI showed partial resection of the lesion.

demonstrated iso-signal intensity in T1-weighted imaging and low or iso-signal intensity in T2-weighted imaging, and intense enhancement was observed after gadolinium-enhanced T1-weighted imaging. Therefore, it is difficult to determine whether an infiltrating soft tissue mass is a IgG4-related inflammatory pseudotumor, a malignant tumor or a meningioma. For example, in our case, the tumor was initially thought to be a meningioma. In the absence of symptoms or signs of infection such as fever, the clinical manifestations varied based on the locations.

For our patients, the lesion was located in the middle of the upper clivus area. Based on the symptoms and MRI manifestation, a meningioma was highly suspected. Then, the endoscopic transsphenoidal approach was adopted, and the mass was partially resected, as the subdural extra-axial lesion was found to be very tough and firm, exhibiting fibrous scarring attaching the mass to the brain stem. Intraoperative frozen pathological findings showed many lymphoplasmacytes surrounded by collagen-rich fibers. The histopathological findings revealed an inflammatory

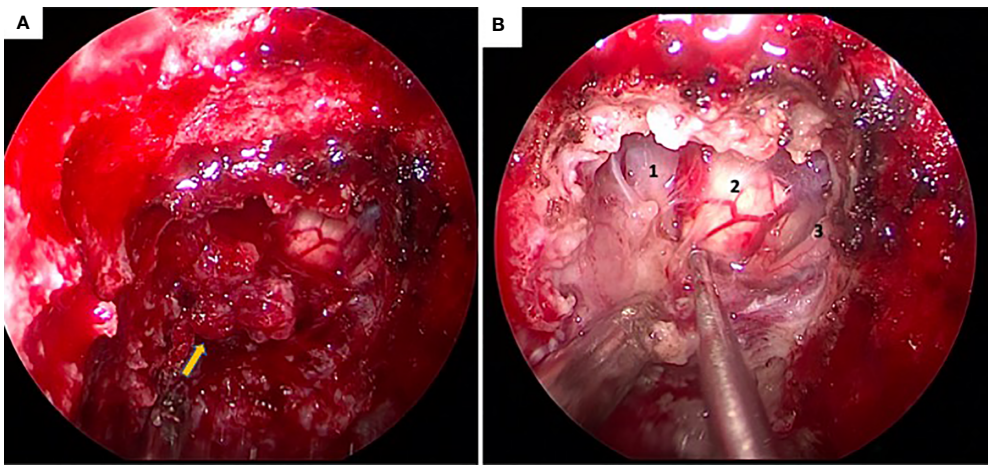

FIGURE 2 | Intra-operative condition of the lesion located at middle of upper clivus region. **(A)** the lesion was very tough and firm (the arrow); **(B)** the lesion was stick to the brain stem and basal artery (1: brain stem; 2: basal artery; 3: abducent nerve).

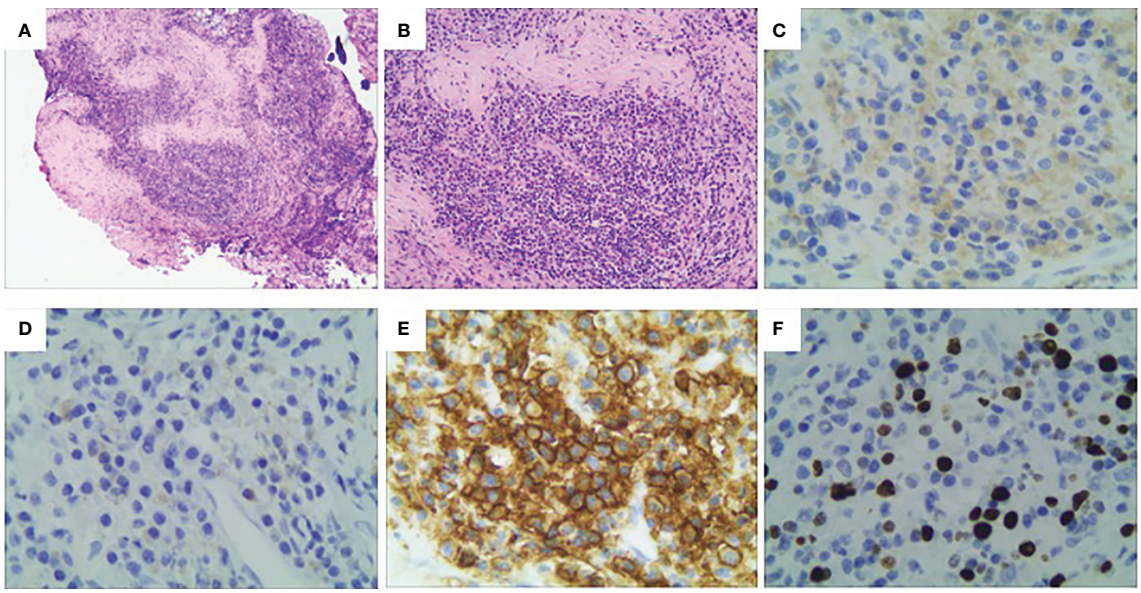

FIGURE 3 | Histological features of the lesion revealed an IgG4-related inflammatory pseudotumor. **(A, B)** Hematoxylin and eosin (H&E) stain showed the lesion was composed of sclerosing fibrosis associated with dense lymphoplasmacytic infiltration (A: ×40; B:×100); **(C, D)** Immunohistochemical analysis revealed over 400 IgG4-positive cells per high-powered field and a high IgG4/IgG ratio (C, IgG, ×200; D, IgG4, ×200). **(E)** Immunohistochemical staining of CD38; **(E)** Immunohistochemical staining of Ki-67. **(F)** Immunohistochemical staining of Ki-67.

pseudotumor involving the clivus, with sclerosing fibrosis mixed with lymphocytes and plasma cells in which the immunohistochemistry was positive for IgG4.

Although twenty-six cases of intracranial pseudotumors due to IgG4-RD have been described (**Table 1**) (2–14), the pathogenesis of IgG4-associated inflammatory pseudotumors is still unclear; nevertheless, multiorgan system conditions with pathological features that are largely consistent across a wide range of organ systems are recognized. The convex surface of the brain, the parasagittal falx, and the base of the skull (such as the sphenoid crest region) are common sites for meningiomas, but, as shown in this case, IgG4-related inflammatory pseudotumors are also possible, highlighting the importance of considering IgG4-related inflammatory pseudotumors as a differential diagnosis in these patients with lesions involving these structures.

In terms of treatment, glucocorticoids are the standard treatment once the diagnosis of IgG4-related inflammatory

TABLE 1 | Reported cases of IgG4-related intracranial pseudotumors.

	Author	Sex	Age	Lesion	Intracranial multiple lesions	Extracranial lesions	Tumor consistency	Encasing artery
1	Lui P.C (6).	F	52	rt. Lateral ventricle	–	–	n.d.	n.d.
2	Lui P.C (6).	M	45	dura at rt. frontal region	–	–	n.d.	n.d.
3	Lui P.C (6).	F	26	dura at lt. frontotemporal region	–	–	n.d.	n.d.
4	Okano (20)	M	62	rt. Meckle's cave and lt. foramen magnum	+	+	**hard**	n.d.
5	Lindstrom (7)	M	53	posterior fossa	–	–	n.d.	n.d.
6	Lindstrom (7)	F	54	dura at petrous apex	–	–	n.d.	n.d.
7	Lindstrom (7)	F	51	sella turcica	–	–	n.d.	n.d.
8	Kim (3)	M	43	lt. frontal area and near corpus callosum	+	–	**hard**	n.d.
9	Katsura (5)	F	59	along trigeminal nerve	–	–	n.d.	n.d.
10	Wong (21)	M	77	tumor at pituritory	–	+	**hard**	n.d.
11	Nishino (2)	M	67	dura-based mass in the Sylvian fissures, bilateral trigeminal nerves and pituitary stalk	+	+	non-surgery case	**attaching to bilateral ICA in MRI**
12	Noshiro (4)	M	39	optic nerve	–	+	n.d.	n.d.
13	Katsura (10)	M	64	orbital apex and cavernous sinus	–	+	n.d.	n.d.
14	Katsura (10)	F	61	cavernous sinus to pterygopalatine fossa, infraorbital canal	–	–	n.d.	n.d.
15	Katsura (10)	M	55	cavernous sinus to orbit	–	–	n.d.	n.d.
16	Katsura (10)	M	65	cavernous sinus to pterygopalatine fossa	–	+	n.d.	n.d.
17	Katsura (10)	M	62	anterior clinoid process and posterior fossa dura mater	–	+	n.d.	**VA penetrating the mass**
18	Moss (9)	F	36	middle cranial fossa, foramen magnum and superior frontal	+	–	n.d.	**involving cavernous sinus**
19	Moss (9)	F	50	middle and anterior cranial fossa	–	–	n.d.	**involving cavernous sinus**
20	Rice (11)	M	46	carotid canal, jugular foramen and foramen ovale	–	+	n.d.	n.d.
21	Goulam-Houssein (12)	M	70	anterior temporal lesion	–	–	n.d.	n.d.
22	Goulam-Houssein (12)	M	54	cavernous sinus and Meckel's cave	+	–	n.d.	**smooth narrowing cavernous ICA**
23	Goulam-Houssein (12)	F	28	suprasellar mass	–	–	n.d.	**occlusion of ICA**
24	Kuroda (13)	F	72	around medulla, cerebellum and middle fossa	+	–	hard	encasing VA
26	Tang (14)	F	50	right upper clivus area	–	–	soft	n.d.
27	**Our case**	F	50	**Middle upper clivus area**	–	–	**hard**	**attaching to BA**

Bold values represent our case.
n.d., not described.

pseudotumors is made (18). However, the diagnosis is based on the pathology from a biopsy or surgery. After diagnosis, glucocorticoids have been used in several cases of IgG4 intracranial pseudotumors, and nearly all the patients achieved remission or tumor reduction (2, 3, 9, 12, 13). Although recurrence despite after corticosteroid prescription has been reported in the literature, prognosis of the patients with IgG4-related related inflammatory pseudotumor was good. If patients are not steroid responsive, local radiation therapy has been shown to be effective in some cases (18). Therefore, our patient with residual pseudotumor was sent to the rheumatology department for further glucocorticoid treatment as soon as the diagnosis of IgG4-related inflammatory pseudotumor was made.

CONCLUSION

This case showed IgG4-related inflammatory pseudotumors involving the clivus, mimicking meningioma, highlighting the importance of considering IgG4-related inflammatory pseudotumors as a differential diagnosis in patients presenting with a sudden onset symptoms of dysphagia and dysphonia along with lower limb weakness when other more threatening causes were excluded. Inflammatory pseudotumors are etiologically enigmatic and unpredictable, and total resection might not be warranted. Glucocorticoids are usually the first line of treatment after diagnosis.

DATA AVAILABILITY STATEMENT

The original contributions presented in the study are included in the article/supplementary material. Further inquiries can be directed to the corresponding author.

ETHICS STATEMENT

The studies involving human participants were reviewed and approved by Research Ethics Committee of Xuanwu Hospital,

Capital Medical university. The patients/participants provided their written informed consent to participate in this study. Written informed consent was obtained from the individual(s) for the publication of any potentially identifiable images or data included in this article.

AUTHOR CONTRIBUTIONS

All these four authors were involved in patient treatment, data collection and analysis, and manuscript writing. All authors contributed to the article and approved the submitted version.

FUNDING

The financial support for this study was provided by the Scientific Research Project of Capital Health Development in 2018 (grant number: 2018-4-4018). The funding institutions played no role in the design of the study, data collection or analysis, decision to publish, or preparation of the manuscript.

REFERENCES

1. Della-Torre E, Lanzillotta M, Doglioni C. Immunology of IgG4-related Disease. *Clin Exp Immunol* (2015) 181:191–206. doi: 10.1111/cei.12641
2. Nishino T, Toda J, Nakatsuka T, Kimura T, Inaoka T, Terada H. IgG4-related Inflammatory Pseudotumors Mimicking Multiple Meningiomas. *Jpn J Radiol* (2013) 31:405–7. doi: 10.1007/s11604-013-0191-y
3. Kim EH, Kim SH, Cho JM, Ahn JY, Chang JH. Immunoglobulin G4-related Hypertrophic Pachymeningitis Involving Cerebral Parenchyma. *J Neurosurg* (2011) 115:1242–7. doi: 10.3171/2011.7.JNS1166
4. Noshiro S, Wanibuchi M, Akiyama Y, Okawa S, Ohtaki S, Sugino T, et al. IgG4-related Disease Initially Presented as an Orbital Mass Lesion Mimicking Optic Nerve Sheath Meningioma. *Brain Tumor Pathol* (2015) 32:286–90. doi: 10.1007/s10014-015-0223-7
5. Katsura M, Morita A, Horiuchi H, Ohtomo K, Machida T. IgG4-related Inflammatory Pseudotumor of the Trigeminal Nerve: Another Component of IgG4-related Sclerosing Disease? *AJNR Am J Neuroradiol* (2011) 32:E150–152. doi: 10.3174/ajnr.A2256
6. Lui PC, Fan YS, Wong SS, Chan AN, Wong G, Chau TK, et al. Inflammatory Pseudotumors of the Central Nervous System. *Hum Pathol* (2009) 40:1611–7. doi: 10.1016/j.humpath.2009.04.016
7. Lindstrom KM, Cousar JB, Lopes MB. IgG4-related Meningeal Disease: Clinico-Pathological Features and Proposal for Diagnostic Criteria. *Acta Neuropathol* (2010) 120:765–76. doi: 10.1007/s00401-010-0746-2
8. Hausler M, Schaade L, Ramaekers VT, Doenges M, Heimann G, Sellhaus B. Inflammatory Pseudotumors of the Central Nervous System: Report of 3 Cases and a Literature Review. *Hum Pathol* (2003) 34:253–62. doi: 10.1053/hupa.2003.35
9. Moss HE, Mejico LJ, de la Roza G, Coyne TM, Galetta SL, Liu GT. IgG4-related Inflammatory Pseudotumor of the Central Nervous System Responsive to Mycophenolate Mofetil. *J Neurol Sci* (2012) 318:31–5. doi: 10.1016/j.jns.2012.04.010
10. Katsura M, Mori H, Kunimatsu A, Sasaki H, Abe O, Machida T, et al. Radiological Features of IgG4-related Disease in the Head, Neck, and Brain. *Neuroradiology* (2012) 54:873–82. doi: 10.1007/s00234-012-1012-1
11. Rice CM, Spencer T, Bunea G, Scolding NJ, Sloan P, Nath U. Intracranial Spread of IgG4-related Disease *Via* Skull Base Foramina. *Pract Neurol* (2016) 16:240–2. doi: 10.1136/practneurol-2015-001315
12. Goulam-Houssein S, Grenville JL, Mastrocostas K, Munoz DG, Lin A, Bharatha A, et al. IgG4-related Intracranial Disease. *Neuroradiol J* (2019) 32:29–35. doi: 10.1177/1971400918806323
13. Kuroda N, Inenaga C, Arai Y, Otsuki Y, Tanaka T. Intracranial Multiple Pseudotumor Due to Immunoglobulin G4-related Disease Without Other Lesion: Case Report and Literature Review. *World Neurosurg* (2019) 132:69–74. doi: 10.1016/j.wneu.2019.08.127
14. Tang H, Ding G, Xiong J, Zhu H, Hua L, Xie Q, et al. Clivus Lesion Revealed Inflammatory Pseudotumor Associated With IgG4-related Disease: A Case Report. *World Neurosurg* (2018) 18:71–4. doi: 10.1016/j.wneu.2018.06.174
15. Guma M, Firestein GS. IgG4-related Diseases. *Best Pract Res Clin Rheumatol* (2012) 26:425–38. doi: 10.1016/j.berh.2012.07.001
16. Brito-Zeron P, Ramos-Casals M, Bosch X, Stone JH. The Clinical Spectrum of IgG4-related Disease. *Autoimmun Rev* (2014) 13:1203–10. doi: 10.1016/j.autrev.2014.08.013
17. Batsakis JG, Luna MA, El-Naggar AK, Goepfert H. "Inflammatory Pseudotumor": What is it? How Does it Behave? *Ann Otol Rhinol Laryngol* (1995) 104:329–32. doi: 10.1177/000348949510400415
18. Deshpande V, Zen Y, Chan JK, Yi EE, Sato Y, Yoshino T, et al. Consensus Statement on the Pathology of IgG4-related Disease. *Mod Pathol* (2012) 25 (9):1181–92.
19. Li Y, Gao H, Li Z, Zhang X, Ding Y, Li F. Clinical Characteristics of 76 Patients With IgG4-Related Hypophysitis: A Systematic Literature Review. *Int J Endocrinol* (2019). doi: 10.1155/2019/5382640
20. Okano A, Nakatomi H, Shibahara J, Tsuchiya T, Saito N. Intracranial Inflammatory Pseudotumors Associated with Immunoglobulin G4-Related Disease Mimicking Multiple Meningiomas: A Case Report and Review of the Literature. *World Neurosurg* (2015) 83:1181–4.
21. Wong S, Lam WY, Wong WK, Lee KC. Hypophysitis Presented as Inflammatory Pseudotumor in Immunoglobulin G4-Related Systemic Disease. *Hum Pathol* (2007) 38(11):1720–3.

Conflict of Interest: The authors declare that the research was conducted in the absence of any commercial or financial relationships that could be construed as a potential conflict of interest.

frontiers in Endocrinology

ORIGINAL RESEARCH
published: 30 April 2021
doi: 10.3389/fendo.2021.661305

Hypothalamus-Pituitary Dysfunction as an Independent Risk Factor for Postoperative Central Nervous System Infections in Patients With Sellar Region Tumors

Junxian Wen[1†], Rui Yin[1†], Yihao Chen[1], Jianbo Chang[1], Baitao Ma[2], Wei Zuo[3], Xiao Zhang[1], Xiaojun Ma[4], Ming Feng[1], Renzhi Wang[1], Wenbin Ma[1] and Junji Wei[1]*

[1] Departments of Neurosurgery, Peking Union Medical College Hospital, Peking Union Medical College, Chinese Academy of Medical Sciences, Beijing, China, [2] Departments of Vascular Surgery, Peking Union Medical College Hospital, Peking Union Medical College, Chinese Academy of Medical Sciences, Beijing, China, [3] Departments of Pharmacy, Peking Union Medical College Hospital, Peking Union Medical College, Chinese Academy of Medical Sciences, Beijing, China, [4] Departments of Infectious Disease, Peking Union Medical College Hospital, Peking Union Medical College, Chinese Academy of Medical Sciences, Beijing, China

Objective: The purpose of this study was to verify that hypothalamus-pituitary dysfunction is one of the risk factors for postoperative central nervous system infections (PCNSIs).

Method: We performed a retrospective analysis of all patients with sellar region lesions who underwent surgery between January 2016 and November 2019 at Peking Union Medical College Hospital. In total, 44 age– and sex-matched controls were enrolled. Univariate and multivariate analyses were performed to identify risk factors for PCNSIs.

Result: We enrolled 88 patients, 44 of whom had PCNSIs. Surgical approach (TCS) (P<0.001), previous surgery on the same site (P=0.001), intraoperative cerebral spinal fluid (CSF) leakage (P<0.001), postoperative adrenal insufficiency (P=0.017), postoperative DI (P=0.004) and the maximum Na^+ levels(<0.001) correlated significantly with PCNSIs. Multivariate analysis showed that Surgery approach (TCS)(OR: 77.588; 95%CI: 7.981-754.263; P<0.001), intraoperative CSF leakage (OR: 12.906; 95%CI: 3.499-47.602; P<0.001), postoperative DI (OR: 6.999; 95%CI:1.371-35.723; P=0.019) and postoperative adrenal insufficiency (OR: 6.115; 95%CI: 1.025-36.469; P=0.047) were independent influencing factors for PCNSIs.

Conclusion: TCS, intraoperative CSF leakage, postoperative DI and postoperative adrenal insufficiency are risk factors for PCNSIs in patients with sellar region tumors.

Keywords: hypothalamus-pituitary dysfunction, independent risk factor, central nervous system infections, sellar region tumors, endocrine

OPEN ACCESS

Edited by:
Run Yu,
UCLA David Geffen School of Medicine, United States

Reviewed by:
Hiroshi Nishioka,
Toranomon Hospital, Japan
Luiz Augusto Casulari,
University of Brasilia, Brazil

***Correspondence:**
Junji Wei
weijunji@pumch.cn

[†]These authors have contributed equally to this work and share first authorship

Specialty section:
This article was submitted to Pituitary Endocrinology, a section of the journal Frontiers in Endocrinology

Received: *30 January 2021*
Accepted: *09 March 2021*
Published: *30 April 2021*

Citation:
Wen J, Yin R, Chen Y, Chang J, Ma B, Zuo W, Zhang X, Ma X, Feng M, Wang R, Ma W and Wei J (2021) Hypothalamus-Pituitary Dysfunction as an Independent Risk Factor for Postoperative Central Nervous System Infections in Patients With Sellar Region Tumors. Front. Endocrinol. 12:661305. doi: 10.3389/fendo.2021.661305

INTRODUCTION

Central nervous system (CNS) infection is an uncommon but serious complication that can result in poor prognosis and even death. According to previous studies, the incidence of CNS infection after neurosurgical procedures is relatively variable and ranges from 0.3% to 10% (1–4). There are many causes of postoperative central nervous system infection (PCNSI), including the surgical technique, blood–brain barrier impairment, and postoperative management. Due to this urgent clinical situation, relevant predictors of PCNSI need to be identified, and prevention strategies need to be developed.

Although some studies have suggested that hypothalamus-with central nervous system infection remains unclear. A significant proportion of patients with meningitis have endocrine dysfunction (5); infection, such as sepsis, can also be caused by hypothalamus-pituitary dysfunction (6, 7). We propose that hypothalamus-pituitary dysfunction can induce PCNSI, and the purpose of this retrospective study was to test our hypothesis.

MATERIALS AND METHODS

Study Population

A retrospective observational study of all hospitalized patients diagnosed with sellar region lesions was conducted at the Department of Neurosurgery of PUMCH. From January 2016 to November 2019, the following inclusion criteria were applied: (1) pituitary hormone deficiency alone occurring before PCNSI was classified as hypothalamus-pituitary dysfunction; (2) no preoperative infectious disease, including systemic and local infections; (3) the ability to provide informed consent; (4) clinical and radiological evidence of sellar region tumors; and (5) clinical and laboratory evidence of central nervous system infections.

Patients were required to meet at least 1 of the following criteria for the diagnosis of central nervous system infection: 1. organisms cultured from cerebral spinal fluid (CSF); 2. at least 1 sign or symptom with no other recognized cause, including fever (>38°C), headache, stiff neck, meningeal signs, cranial nerve signs, or irritability, and at least 1 criterion, including a. increased white cells (>8*10^6), elevated protein (>0.45 g/L), and/or decreased glucose (<2.5 mmol/L) in CSF, b. organisms present based on Gram staining of CSF, c. organisms cultured from blood, d. positive antigen test using CSF, blood, or urine, e. diagnostic single-antibody titer (IgM) or 4-fold increase in paired sera (IgG) for pathogens (8).

Hypothalamus-pituitary dysfunction was defined as deficiency in one or more pituitary hormones and the presence of corresponding clinical symptoms. We collected all patients' blood at 8AM, The diagnosis of adrenal insufficiency was based on basal dosage of cortisol below 80 nmol/L and stimulated concentrations of cortisol less than 500 nmol/L in insulin tolerance test (9). Measurement of both serum TSH and thyroxine concentrations is needed to diagnose hypothyroidism. We defined hypothyroidism base on TSH or one of the thyroxine concentrations below the reference range of the PUMCH laboratory: thyrotropin (TSH) (<0.38 μIU/mL), free T3 (fT3) (<1.8 pg/mL), free T4 (fT4) (<0.81 pg/mL), total T3 (TT3) (<0.66 ng/mL), and total T4 (TT4) (<4.3 μg/dL). The diagnostic criteria of diabetes insipidus (DI) are a 24-h urinary volume exceeding 3 L (adults) or 2 L/m2/24 h (young children), urine osmolality less than 300 mOsm/kg H2O and urine specific gravity less than 1.005 (10, 11). All patients with hypothalamus-pituitary dysfunction enrolled in this study was revised promptly and properly. For patients with adrenal insufficiency, they will oral 15mg prednisone for a week, taking 10mg at 8AM and 5mg at 4PM. In the end, the total daily dose of prednisone will gradually be reduced to 5mg based on the level of cortisol. Moreover, we treat patients with suspected adrenal crisis due to secondary adrenal insufficiency with injection of 100 mg hydrocortisone for two days, twice a day.

Each PCNSI participant was matched to a noninfection control patient, conforming to 1:1 matching for sex and age and the closest matching principle. Controls were recruited from our hospital, underwent surgery for sellar region tumors and had no symptom or laboratory evidence of PCNSI. In total, 88 patients (44 PCNSI subjects, 44 controls) were enrolled in the study. Informed consent to participate was obtained from all patients. This retrospective study was performed under the authorization of the institutional ethics committee of PUMCH, Chinese Academy of Medical Sciences.

Data Collection

Basic information for all the patients was collected, including age, sex, and body mass index (BMI, calculated as weight in kilograms divided by the square of height in meters), signs and symptoms, white blood cell count and classification in blood and CSF, protein, glucose and chloride levels in CSF,CT and magnetic resonance imaging (MRI) examination, size of the tumor (the largest diameter of the tumor measured in the three orthogonal planes and reported by the imaging department of PUMCH), presence of underlying diseases (diabetes, hypertension), type of operative procedure, previous procedures or radiotherapy at the same location, presence of intraoperative CSF leakage, duration of hospitalization, duration of surgery, bleeding amount during the operation, presence of DI, Na^+ levels, Prognosis and preoperative and postoperative pituitary hormones levels, including adrenocorticotropin (ACTH), cortisol, TSH, fT4, fT3, TT3, and TT4.

Data Analysis

All data were analyzed using SPSS software version 26.0 (IBM Corp., Armonk, New York, USA). Continuous variables are described by means ± standard deviation; numbers and percentages are used for categorical variables. Univariate analyses for factors associated with central nervous system infections were performed using the chi-square test and Fisher's exact test for categorical variables. The Wilcoxon-Mann-Whitney test and Kruskal-Wallis test were employed for continuous variables that did not fit a normal distribution. A multivariate logistic regression model was applied to select factors significantly

associated with central nervous system infections. P values of 0.05 or less were considered statistically significant.

RESULTS

Patient Demographics

In total, 88 patients (44 with PCNSIs, 44 controls) were enrolled in this study. The demographic information is shown in **Table 1**. The mean age of patients, including 30 men and 58 women, was 44.4 ± 14.5 (± SD) years old. Average BMI was 24.9 ± 4.3(± SD) kg/m2. Most patients had undergone transsphenoidal surgery (TSS). Postoperative histological analysis revealed a large spectrum of sellar tumors, non-functioning tumors were the most common, followed by GH secretors, craniopharyngiomas and prolactinomas; with fewer numbers of cases were Rathke's cysts, ACTH and TSH-producing adenomas.

The characteristics of the PCNSI patients are shown in **Table 2**. Among them, the mean WBC count increased significantly. Neutrophils accounted for the majority, followed by lymphocytes. For CSF, the WBC count of all cell counts increased, as is the level of protein. Coenocytes were the most common cell type in WBCs. There is little different of the mean glucose and chloride in the CSF of PCNSI patients compared to healthy people. In addition, the mean levels of hypothalamus-pituitary hormones and the number of postoperative DI patients were recorded. Because most patients only have one or two pituitary hormones decreased, we didn't see a profound decrease of the mean pituitary hormone levels. There is one PCNSI patient died in our study. The direct reason of her death is Postoperative subarachnoid hemorrhage and uncontrollable Intracranial and pulmonary infections.

lumbar punctures were performed in all patients was suspected to have an intracranial infection. 9 patients are seen the presence of culture in CSF (**Table 3**) and 3 patients had polymicrobial infections. *Baumanii*(2/11) is common in the causative microorganisms of our study and the rest had the same frequency.

TABLE 1 | Patient characteristics and details.

Variables	n (%) or mean ± SD
Age (years)	44.4 ±14.5
BMI (kg/m2)	24.9 ± 4.3
Male	30 (34.1)
Surgery approach	
TSS	70(79.5)
TCS	18(20.5)
Pathology diagnosis	
Nonfunctioning adenomas	22 (25.0)
GH-secreting adenomas	14(15.9)
Craniopharyngioma	12(13.6)
Prolactinomas	11(12.5)
Rathke cleft cysts	10(11.4)
ACTH-producing adenomas	8(9.1)
TSH-producing adenomas	7(8.0)
Others	4 (4.5)

SD, standard deviation; TSS, transsphenoidal surgery; TCS, transcranial surgery.

TABLE 2 | Characteristics of PCNSI patients.

Variables	n (%) or mean ± SD
WBC (x109)	17.26 ± 7.36
neutrophil	86.99 ± 5.18
lymphocyte	8.65 ± 5.21
CSF	
Glucose (mmol/L)	3.43 ±1.69
Cl (mmol/L)	126.59 ± 8.35
Protein (g/L)	3.53 ± 2.80
Cell (X109)	48.76 ±10.85
WBC (X109)	2.61 ± 3.18
coenocyte (%)	83.59 ±11.85
monocyte (%)	16.54 ± 11.80
Hormone	
TSH (μIU/mL)	1.48 ± 1.47
TT3 (ng/mL)	0.89 ± 0.30
TT4 (μg/dL)	6.54 ± 3.19
FT3 (pg/mL)	2.48 ± 0.66
FT4 (ng/dL)	1.03 ± 0.33
Cortisol (μg/dL)	21.32 ± 34.04
DI	15(34.1)
Death	1(2.3)

SD, standard deviation; D, diabetes insipidus.

TABLE 3 | The presence of culture in the CSF.

Patients	Cerebrospinal Fluid Culture	
1	*Baumanii*	
2	*Bacillus pumilus*	
3	*Enterococcus faecalis*	*Staphylococcus epidermidis*
4	*Micrococcus*	*Corynebacterium*
5	*Aerococcus aeruginosa*	
6	*Baumanii*	
7	*Pseudomonas aeruginosa*	*Streptococcus pneumoniae*
8	*Enterobacter cloacae*	
9	*Streptococcus salivarius*	

Risk Factors for Postoperative Central Nervous System Infection

Through univariate analysis (**Table 4**), surgical approach (TCS) (P<0.001), previous surgery at the same site (P=0.001), intraoperative CSF leakage (P<0.001), postoperative adrenal insufficiency (P=0.017), postoperative DI (P=0.004) and the maximum Na^+ levels(<0.001)correlated significantly with PCNSIs. According to multivariate analysis (**Table 5**), Surgery approach (TCS)(OR: 77.588; 95%CI: 7.981-754.263; P<0.001), intraoperative CSF leakage (OR: 12.906; 95%CI: 3.499-47.602; P<0.001), postoperative DI (OR: 6.999; 95%CI:1.371-35.723; P=0.019) and postoperative adrenal insufficiency (OR: 6.115; 95%CI: 1.025-36.469; P=0.047) were independent factors influencing PCNSI.

DISCUSSION

The sellar region is a relatively common site for brain tumors (12, 13). Over the past 30 years, significant advances in neurosurgery, neuroimaging, and molecular biology have changed the evaluation and management of sellar tumors. Nevertheless,

TABLE 4 | Univariate analysis of the association between each factor and postoperative central nervous system infection.

Variable	PCNSI (n = 44)	Non-infection controls (n = 44)	P value
Age(±SD)	44.7±15.1	44.1±14.1	0.704
BMI	24.5 ± 4.2	25.2 ± 4.4	0.587
Sex			1.000
Male	15(17.0%)	15(17.0%)	
Female	29(33.0%)	29(33.0%)	
Hypertension	10(11.4%)	14(15.9%)	0.338
Diabetes	7(8.0%)	14(15.9%)	0.08
Surgery approach			<0.001
TCS	17(19.3%)	1(1.1%)	
TSS	27(30.7%)	43(48.9%)	
Previous surgery history	14(15.9%)	2(2.3%)	0.001
Previous radiotherapy	3(3.4%)	1(1.1%)	0,616*
Intraop. CSF leakage	19(27.1%)	9(12.9%)	<0.001
Postop. CSF leakage	7(15.9%)	1(2.3%)	0.058*
Postop. hypothyroidism	23(20.5%)	19(22.1%)	0.283
Postop. adrenal insufficiency	11(12.6%)	3(3.4%)	0.017
Postop. DI	15(17.0%)	4(4.5%)	0.004
Maximum Na^+ levels	150.4 ± 7.2	143.9 ± 4.4	<0.001
Minimum Na+ levels	136.8 ± 6.0	138.2 ± 2.6	0.409

*SD, standard deviation; Intraop, Intraoperative; Postop, Postoperative; *Fisher's exact test; TSS, transsphenoidal surgery; TCS, transcranial surgery.*

TABLE 5 | Multivariate analysis of factors associated with postoperative central nervous system infection.

Variable	Odd ratio	95% CI	P value
Surgery approach (TCS)	77.588	7.981-754.263	<0.001
Intraop. CSF leakage	12.906	3.499-47.602	<0.001
Postop. DI	6.999	1.371-35.723	0.019
Postop. adrenal insufficiency	6.115	1.025-36.469	0.047

TCS, transcranial surgery; CI, Confidence Interval; Intraop, Intraoperative; Postop, Postoperative.

changes in hypothalamus-pituitary function and CNS infection are still frequent postoperative complications and reasons for hospital readmissions (14–17). The incidence of hypothalamus-pituitary dysfunction is reported to be 4.2/100,000 per year, without sex differences; the prevalence is 45.5 per 100,000 people (18). The rate of PCNSIs in patients with sellar region tumors ranges from 0.5% to 14% (19). Some studies have shown the relationship between abnormal immune function and hypothalamus-pituitary dysfunction (9). Overall, it is generally recognized that patients with CNS infection might experience hypothalamus-pituitary hormone dysfunction.

In this study, we investigated pituitary hormone levels in patients with sellar region tumors and screened out those with hypothalamus-pituitary dysfunction before PCNSI. Ultimately, we found postoperative DI and postoperative adrenal insufficiency to be independent factors influencing PCNSI. Thus, we suggest that perioperative hypothalamus-pituitary dysfunction may be an underlying cause of PCNSI.

As our multivariate logistic regression analysis indicated, postoperative adrenal insufficiency significantly affected the occurrence of PCNSI (20, 21). According to a previous study, much of the excess mortality in patients with adrenal insufficiency is attributable to infectious diseases (22). Indeed, a functional hypothalamic-pituitary-adrenal (HPA) axis is essential for normal health and life expectancy. Furthermore, central adrenal insufficiency is a life-threatening disorder associated with increased morbidity and mortality (21). The possible infection-related pathogenesis pathways may involve dysregulated systemic inflammation resulting from inadequate intracellular glucocorticoid-mediated anti-inflammatory activity (23).

In addition, postoperative DI is a risk factor for PCNSI, and we speculate that the reason is impairment of plasma sodium homeostasis. Postoperative hyponatremia and hypernatremia in neurosurgical patients are typically caused by the development of DI (24). Based on inconsistencies in the definition of DI across the literature, the reported incidence of postsurgical central DI varies from 1 to 67% (25–28). The course of postoperative DI may be transient, persistent, or triphasic. In the typical triphasic response, a polyuric phase of DI is followed by an oliguric phase of SIADH and then by a third and final phase of persistent DI. When water deficits occur due to inadequate water intake to compensate for polyuria, symptoms of dehydration and/or hyperosmolality develop. Patients may present with hypernatremia in the first and third phases of DI (16, 29, 30). In addition, a hyponatremic state may result in severe metabolic derangement, myocardial depression and injury, neurologic impairment, venous thromboembolism, and poor wound healing (31). Moreover, patients with dehydration and hyperosmolality might experience a range of neurological symptoms, including irritability, cognitive decline, disorientation, and confusion, with decreased levels of consciousness, seizure and coma. Various focal neurological deficits may also develop in this context (32). In general, deterioration of the patient's basic conditions may explain the increased risk of PCNSI that we observed.

Hyponatremia often follow after pituitary surgery. It is produced by the syndrome of SIADH and the cerebral salt-wasting syndrome (33). We don't see the minimum Na+ levels significantly correlated to PCNSI, but Some evidence suggests that sodium is a significant promoter of immune function. Sodium acts by enhancing the function of macrophages and T lymphocytes (34, 35). A hypernatremic environment may serve as an immunological defense mechanism in inflammatory states, and sodium levels can act in concert with tissue infection as a danger signal, enhancing proinflammatory macrophage and T cell function while dampening anti-inflammatory immune responses (35). Thus, patients with hyponatremia may show decreased immune function, which may provide an explanation for the frequency of infection among patients with DI. Nevertheless, these studies generally focused on the skin and kidney, and the regulatory circuits that drive salt accumulation in the infected brain are unknown.

Postoperative hypothyroidism is not correlated significantly with PCNSI in our study. However, some evidences showed hypothalamic pituitary dysfunction could present as normal or modest increases in TSH. Moreover, in cases of chronic liver disease and chronic kidney disease patients, TSH serum

concentrations could be higher than TSH biological activity (36). We didn't measure the TSH bioactivity of patients, Consequently,it's possible that we missed some potential patients with Postoperative hypothyroidism. The association between postoperative hypothyroidism and PCNSI need further study.

PCNSIs occurred more frequently in the TCS cohort than in the TSS cohort in our study. This result is consistent with some previous studies (3, 37). Currently, transcranial procedures are only applied in special situations, such as for a dumb bell-shaped tumor or one with irregular extensions into the frontal or temporal lobes or when TSS has failed to achieve complete tumor resection (38). This may result in an increased operation time, an increased risk of postoperative swelling or bleeding of the residual mass and the need for nonbiodegradable materials left at the completion of the TCS. These conditions may lead to an increase in the infection rate. In addition, TCS may also lead to more vigorous dissection of hypothalamus and normal pituitaries which may compromise post-operative pituitary dysfunction and bring out PCNSI.

Multivariate logistic regression analysis showed a very strong association of PCNSI development for intraoperative CSF leakage, which is already known. In fact, the risk of postoperative CSF leakage is a major impediment to the use of TSS for resection of sellar lesions, and there are clear correlations between the cranial cavity and the external environment in the event of CSF leakage. Thus, bacteria may more easily enter the cranial cavity from the external environment through the gap and cause a postoperative infection. However, skull base closure techniques have recently evolved, such that CSF leakage is no longer a significant issue following TSS.

As mentioned above, there are many causes associated with PCNSI, yet most of these factors are difficult to correct. A second operation may even be required. In contrast, hypothalamus-pituitary dysfunction can be easily identified and rectified. We believe that the results presented here will help physicians reduce the rate of PCNSI in patients with sellar region tumors.

Because of the retrospective nature of our study, our findings depend on the accuracy of the data recorded in clinical charts, which might have resulted in selection bias. It is hoped that the study findings will prompt future research.

CONCLUSION

We found that TCS, postoperative DI and postoperative adrenal insufficiency are independent risk factors for PCNSI, as is intraoperative CSF leakage. Overall, awareness of hypothalamus-pituitary dysfunction may be effective to prevent PCNSIs in the future. The exact nature of the association between postoperative hypothalamus-pituitary dysfunction and PCNSI deserves further study.

DATA AVAILABILITY STATEMENT

The original contributions presented in the study are included in the article/supplementary material. Further inquiries can be directed to the corresponding author.

ETHICS STATEMENT

This study was approved by the Ethics Committee of Peking Union Medical College Hospital (PUMCH) and written informed consent to participate was granted from all patients.

AUTHOR CONTRIBUTIONS

JXW and RY performed the analysis and co-wrote the manuscript. YC, JC, and BM collected the patient information. WZ, XZ, XM, and MF revised paper. RW, WM and JJW supervised the project, conceived the study, and guided the editing of the manuscript. JXW and RY contributed equally to the manuscript. All authors contributed to the article and approved the submitted version.

FUNDING

This research received a grant from Beijing Tianjin Hebei basic research cooperation project [19JCZDJC64600(Z)], which support the design of the study and collection, analysis, and interpretation of data. There was no other grant from funding agencies in the public, commercial, or not-for-profit sectors.

ACKNOWLEDGMENTS

The authors thank all the patients for their help.

REFERENCES

1. Chen C, Zhang B, Yu S, Sun F, Ruan Q, Zhang W, et al. The incidence and risk factors of meningitis after major craniotomy in China: a retrospective cohort study. *PloS One* (2014) 9(7):e101961. doi: 10.1371/journal.pone.0101961
2. Federico G, Tumbarello M, Spanu T, Rosell R, Iacoangeli M, Scerrati M, et al. Risk factors and prognostic indicators of bacterial meningitis in a cohort of 3580 postneurosurgical patients. *Scand J Infect Dis* (2001) 33(7):533–7. doi: 10.1080/00365540110026557
3. Ivan ME, Iorgulescu JB, El-Sayed I, McDermott MW, Parsa AT, Pletcher SD, et al. Risk factors for postoperative cerebrospinal fluid leak and meningitis after expanded endoscopic endonasal surgery. *J Clin Neurosci* (2015) 22 (1):48–54. doi: 10.1016/j.jocn.2014.08.009
4. Borg A, Kirkman MA, Choi D. Endoscopic Endonasal Anterior Skull Base Surgery: A Systematic Review of Complications During the Past 65 Years. *World Neurosurg* (2016) 95:383–91. doi: 10.1016/j.wneu.2015.12.105
5. Karadag-Oncel E, Cakir M, Kara A, Gonc N, Cengiz A, Ozon A, et al. Evaluation of hypothalamic-pituitary function in children following acute

bacterial meningitis. *Pituitary* (2015) 18(1):1–7. doi: 10.1007/s11102-013-0547-4
6. Annane D, Bellissant E, Bollaert P, Briegel J, Confalonieri M, De Gaudio R, et al. Corticosteroids in the treatment of severe sepsis and septic shock in adults: a systematic review. *JAMA* (2009) 301(22):2362–75. doi: 10.1001/jama.2009.815
7. Alavi S, Tan C, Menon D, Simpson H, Hutchinson P. Incidence of pituitary dysfunction following traumatic brain injury: A prospective study from a regional neurosurgical centre. *Br J Neurosurg* (2016) 30(3):302–6. doi: 10.3109/02688697.2015.1109060
8. Horan TC, Andrus M, Dudeck MA. CDC/NHSN surveillance definition of health care-associated infection and criteria for specific types of infections in the acute care setting. *Am J Infect Control* (2008) 36(5):309–32. doi: 10.1016/j.ajic.2008.03.002
9. Higham C, Johannsson G, Shalet S. Hypopituitarism. *Lancet* (2016) 388 (10058):2403–15. doi: 10.1016/s0140-6736(16)30053-8
10. Lu HA. Diabetes Insipidus. *Adv Exp Med Biol* (2017) 969:213–25. doi: 10.1007/978-94-024-1057-0_14
11. GL R. Diabetes insipidus: Differential diagnosis and management. *Best Pract Res Clin Endocrinol Metab* (2016) 30(2):205–18. doi: 10.1016/j.beem.2016.02.007
12. Saeger W, Lüdecke DK, Buchfelder M, Fahlbusch R, Quabbe HJ, Petersenn S. Pathohistological classification of pituitary tumors: 10 years of experience with the German Pituitary Tumor Registry. *Eur J Endocrinol* (2007) 156 (2):203–16. doi: 10.1530/eje.1.02326
13. Jagannathan J, Kanter AS, Sheehan JP, Jane JA, Laws ER. Benign brain tumors: sellar/parasellar tumors. *Neurologic Clin* (2007) 25(4):1231–49, xi. doi: 10.1016/j.ncl.2007.07.003
14. Bohl MA, Ahmad S, Jahnke H, Shepherd D, Knecht L, White WL, et al. Delayed Hyponatremia Is the Most Common Cause of 30-Day Unplanned Readmission After Transsphenoidal Surgery for Pituitary Tumors. *Neurosurgery* (2016) 78(1):84–90. doi: 10.1227/neu.0000000000001003
15. Krogh J, Kistorp CN, Jafar-Mohammadi B, Pal A, Cudlip S, Grossman A. Transsphenoidal surgery for pituitary tumours: frequency and predictors of delayed hyponatraemia and their relationship to early readmission. *Eur J Endocrinol* (2018) 178(3):247–53. doi: 10.1530/eje-17-0879
16. Yuen KCJ, Ajmal A, Correa R, Little AS. Sodium Perturbations After Pituitary Surgery. *Neurosurg Clinics North Am* (2019) 30(4):515–24. doi: 10.1016/j.nec.2019.05.011
17. Chen S, Cui A, Yu K, Huang C, Zhu M, Chen M. Risk factors associated with meningitis after neurosurgery operation: a retrospective cohort study in a Chinese hospital. *World Neurosurg* (2017), S187887501732226X. doi: 10.1016/j.wneu.2017.12.110
18. Regal M, Páramo C, Sierra S, Garcia-Mayor R. Prevalence and incidence of hypopituitarism in an adult Caucasian population in northwestern Spain. *Clin Endocrinol* (2001) 55(6):735–40. doi: 10.1046/j.1365-2265.2001.01406.x
19. Shibao S, Toda M, Tomita T, Ogawa K, Yoshida K. Analysis of the Bacterial Flora in the Nasal Cavity and the Sphenoid Sinus Mucosa in Patients Operated on with an Endoscopic Endonasal Transsphenoidal Approach. *Neurol Med Chir* (2014) 54(12):1009–13. doi: 10.2176/nmc.oa.2014-0129
20. Jahangiri A, Wagner J, Han S, Tran M, Miller L, Tom M, et al. Rate and time course of improvement in endocrine function after more than 1000 pituitary operations. *Neurosurgery* (2014), 163–6. doi: 10.1227/neu.0000000000000405
21. Ceccato F, Scaroni C. Central adrenal insufficiency: open issues regarding diagnosis and glucocorticoid treatment. *Clin Chem Lab Med* (2019) 57 (8):1125–35. doi: 10.1515/cclm-2018-0824
22. Bergthorsdottir R, Leonsson-Zachrisson M, Odén A, Johannsson G. Premature mortality in patients with Addison's disease: a population-based study. *J Clin Endocrinol Metab* (2006) 91(12):4849–53. doi: 10.1210/jc.2006-0076
23. Annane D, Pastores S, Rochwerg B, Arlt W, Balk R, Beishuizen A, et al. Guidelines for the diagnosis and management of critical illness-related corticosteroid insufficiency (CIRCI) in critically ill patients (Part I): Society of Critical Care Medicine (SCCM) and European Society of Intensive Care Medicine (ESICM) 2017. *Intensive Care Med* (2017) 43(12):1751–63. doi: 10.1007/s00134-017-4919-5
24. JM S, JP S, GL D, RB P. DDAVP use in patients undergoing transsphenoidal surgery for pituitary adenomas. *Acta Neurochir* (2006) 148(3):287–91; discussion 91. doi: 10.1007/s00701-005-0686-0
25. Nemergut EC, Zuo Z, Jane JA, Laws ER. Predictors of diabetes insipidus after transsphenoidal surgery: a review of 881 patients. *J Neurosurg* (2005) 103 (3):448–54. doi: 10.3171/jns.2005.103.3.0448
26. Kristof RA, Rother M, Neuloh G, Klingmüller D. Incidence, clinical manifestations, and course of water and electrolyte metabolism disturbances following transsphenoidal pituitary adenoma surgery: a prospective observational study. *J Neurosurg* (2009) 111(3):555–62. doi: 10.3171/2008.9.Jns08191
27. Staiger RD, Sarnthein J, Wiesli P, Schmid C, Bernays RL. Prognostic factors for impaired plasma sodium homeostasis after transsphenoidal surgery. *Br J Neurosurg* (2013) 27(1):63–8. doi: 10.3109/02688697.2012.714013
28. Schreckinger M, Szerlip N, Mittal S. Diabetes insipidus following resection of pituitary tumors. *Clin Neurol Neurosurg* (2013) 115(2):121–6. doi: 10.1016/j.clineuro.2012.08.009
29. Hannon MJ, Finucane FM, Sherlock M, Agha A, Thompson CJ. Clinical review: Disorders of water homeostasis in neurosurgical patients. *J Clin Endocrinol Metab* (2012) 97(5):1423–33. doi: 10.1210/jc.2011-3201
30. Simon SK, Pavithran PV, Asirvatham AR, Ayyadurai R, Parasuram A. Disorders of Water Balance Following Sellar and Suprasellar Surgeries: Patterns, Determinants and Utility of Quantitative Analysis. *Indian J Endocrinol Metab* (2018) 22(2):191–5. doi: 10.4103/ijem.IJEM_647_17
31. Leung AA, McAlister FA, Finlayson SR, Bates DW. Preoperative hypernatremia predicts increased perioperative morbidity and mortality. *Am J Med* (2013) 126(10):877–86. doi: 10.1016/j.amjmed.2013.02.039
32. Alharfi I, Stewart T, Kelly S, Morrison G, Fraser D. Hypernatremia is associated with increased risk of mortality in pediatric severe traumatic brain injury. *J Neurotrauma* (2013) 30(5):361–6. doi: 10.1089/neu.2012.2410
33. Casulari L, Costa K, Albuquerque R, Naves L, Suzuki K, Domingues L. Differential diagnosis and treatment of hyponatremia following pituitary surgery. *J Neurosurg Sci* (2004) 48(1):11–8.
34. Jantsch J, Schatz V, Friedrich D, Schröder A, Kopp C, Siegert I, et al. Cutaneous Na+ storage strengthens the antimicrobial barrier function of the skin and boosts macrophage-driven host defense. *Cell Metab* (2015) 21 (3):493–501. doi: 10.1016/j.cmet.2015.02.003
35. Schatz V, Neubert P, Schröder A, Binger K, Gebhard M, Müller DN, et al. Elementary immunology: Na as a regulator of immunity. *Pediatr Nephrol (Berlin Germany)* (2017) 32(2):201–10. doi: 10.1007/s00467-016-3349-x
36. Estrada J, Soldin D, Buckey T, Burman K, Soldin O. Thyrotropin isoforms: implications for thyrotropin analysis and clinical practice. *Thyroid* (2014) 24 (3):411–23. doi: 10.1089/thy.2013.0119
37. Komotar RJ, Starke RM, Raper DM, Anand VK, Schwartz TH. Endoscopic endonasal compared with microscopic transsphenoidal and open transcranial resection of craniopharyngiomas. *World Neurosurg* (2012) 77(2):329–41. doi: 10.1016/j.wneu.2011.07.011
38. Mortini P, Barzaghi R, Losa M, Boari N, Giovanelli M. Surgical treatment of giant pituitary adenomas: strategies and results in a series of 95 consecutive patients. *Neurosurgery* (2007) 60(6):993–1002; discussion 3-4. doi: 10.1227/01.Neu.0000255459.14764.Ba

Conflict of Interest: The authors declare that the research was conducted in the absence of any commercial or financial relationships that could be construed as a potential conflict of interest.

frontiers in Endocrinology

CASE REPORT
published: 14 July 2021
doi: 10.3389/fendo.2021.678947

Pituitary Metastasis of Lung Neuroendocrine Carcinoma Mimicking Pituitary Adenoma: Case Report and Literature Review

Xiaohai Liu[1,2], *Renzhi Wang*[2,3], *Mingchu Li*[1,2] *and Ge Chen*[1,2*]

[1] *Department of Neurosurgery, Xuanwu Hospital Capital Medical University, Beijing, China,* [2] *Chinese Pituitary Specialists Congress, Beijing, China,* [3] *Department of Neurosurgery, Peking Union Medical College Hospital, Chinese Academy of Medical Sciences and Peking Union Medical College, Beijing, China*

OPEN ACCESS

Edited by:
Wang Haijun,
The First Affiliated Hospital of Sun Yat-Sen University, China

Reviewed by:
Moises Mercado,
Mexican Social Security Institute (IMSS), Mexico
Mauro Antonio Czepielewski,
Federal University of Rio Grande do Sul, Brazil

***Correspondence:**
Ge Chen
chengecn@139.com

Specialty section:
This article was submitted to Pituitary Endocrinology, a section of the journal Frontiers in Endocrinology

Received: *10 March 2021*
Accepted: *15 June 2021*
Published: *14 July 2021*

Citation:
Liu X, Wang R, Li M and Chen G (2021) Pituitary Metastasis of Lung Neuroendocrine Carcinoma Mimicking Pituitary Adenoma: Case Report and Literature Review. Front. Endocrinol. 12:678947. doi: 10.3389/fendo.2021.678947

Pituitary metastasis is an unusual situation in clinical practice, while the incidence is increasing with age. Breast cancer for women and lung cancer for men were the most frequent primary origins of pituitary metastasis. Diagnosing asymptomatic patients with unknown primary malignant origin is difficult, thus pituitary metastasis may be diagnosed as primary pituitary adenoma. Here, we report a case of a 65-year-old patient with visual changes and diabetes insipidus, showing an extensive mass in the sellar region which was initially thought to be a primary pituitary adenoma. Patient corticotropic deficits were corrected, and transnasal transsphenoidal surgery was adopted, leading to total tumor resection. Tumor texture during surgical procedure was similar to that of pituitary adenoma. However, the histopathological and immunohistochemistry results suggested it as a pituitary metastasis from lung neuroendocrine tumor. Postoperative chest CT scan confirmed a pulmonary mass consistent with primary neoplasm. Abdominal CT further detected multiple metastases in liver, pancreas, and colon. Despite intensive treatment, the patient continued to show decreased level of consciousness due to cachexia, resulting in death 1 week after surgery. This case highlights the importance of differential diagnosis of invasive lesions of the sellar region, especially in individuals over 60 years of age with diabetes insipidus.

Keywords: pituitary metastasis, lung neuroendocrine carcinoma, pituitary adenoma, case report, diabetes insipidus

Abbreviations: ACTH, adrenocorticotropic hormone; CgA, chromogranin; CK, cytokeratin; CT, computed tomography; DI, diabetes insipidus; H&E, Hematoxylin and eosin; IGF-1, insulin like growth factor-1; LCA, leukocyte common antigen; MRI, magnetic resonance imaging; PRL, prolactin; T4, thyroxine; Syn, synaptophysin; TSH, thyroid stimulating hormone; TSS, trans-sphenoidal surgery; TTF1, thyroid transcription factor 1.

INTRODUCTION

The incidence of pituitary metastasis is very low, accounting for approximately 1% of all intracranial metastases (1). As clinical symptoms of pituitary metastasis are similar to those of other sellar tumors and Magnetic resonance imaging (MRI) is nonspecific, pituitary metastases are easily misdiagnosed. Here, we report a 65-year-old patient harboring pituitary metastasis derived from lung neuroendocrine carcinoma, was misdiagnosed and died of cachexia after surgery. We hope our case report will highlight the importance of differential diagnosis for invasive lesions of the sellar region, especially in individuals over 60 years of age with diabetes insipidus. It is possible that invasive pituitary lesions could be metastasized from unknown primary neoplasm, although the incidence is extremely low.

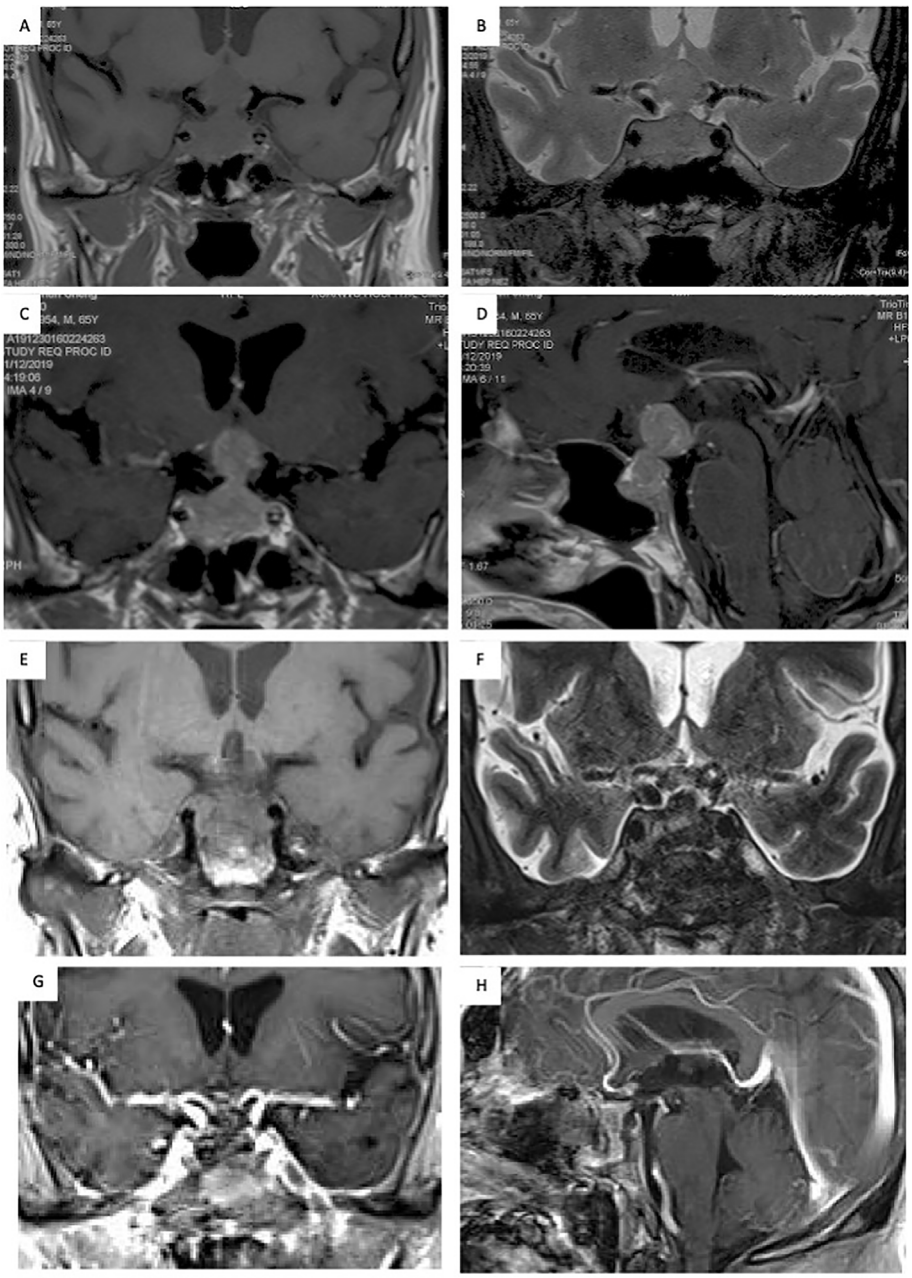

FIGURE 1 | Seller MRI scans showed a sellar lesion with suprasellar extension and compression of the optic chiasm. **(A, B)** The lesion located in the sellar region presented with an isointense signal on T1- and T2-weighted MRI; **(C, D)** The mass was uniformly enhanced on MRI after contrast enhancement, and a pituitary adenoma was highly suspected. **(E–H)** The postoperative MRI showed total resection of the lesion.

CASE PRESENTATION

The patient was a 65-year-old male who presented with progressive impaired vision and diabetes insipidus (DI) for 2 months. Visual fields of both eyes were relatively normal, and no past cancer history was reported. MRI indicated a sellar lesion with isointense signal on T1- and T2-weighted images which was homogenously enhanced after contrast MRI. The lesion was approximately 36 mm × 24 mm × 17 mm (Knosp grade 3) with suprasellar extension and compression of the optic chiasm. A pituitary adenoma was highly suspected (**Figures 1A–D**). Hormonal evaluation revealed hypoadrenocorticism and hypogonadism (**Table 1**). Other routine laboratory tests did not show abnormality.

Subsequently, the patient underwent an endoscopic transsphenoidal surgery. During the surgical operation, the lesion was found to be soft, mimicking pituitary adenoma in texture (**Figures 2A–C**). The lesion was totally resected (**Figure 2D**). Postoperatively, the patient's impaired vision was improved, but diabetes insipidus persisted. And the postoperative MRI showed total resection of the lesion (**Figures 1E–H**).

POSTOPERATIVE TREATMENT

Hematoxylin and eosin (H&E) staining showed a solid tumor involving the pituitary gland, and characterized by small cells with high-grade nuclear atypia and fibrosis (**Figure 3A**). Immunohistochemistry revealed positivity for CK (**Figure 3B**), TTF-1 (**Figure 3C**), Syn (**Figure 3D**), and CgA (**Figure 3E**) and negativity for vimentin and LCA. The Ki-67 index was 90%, indicating a neuroendocrine carcinoma (**Figure 3F**). Postoperative chest CT scan confirmed a pulmonary mass consistent with the primary neoplasm and abdominal CT indicated multiple metastases in liver, pancreas, and colon. Although immunostain for all these markers may be positive in primary pituitary neuroendocrine carcinoma, pituitary metastasis from lung neuroendocrine carcinoma is far more likely than a primary pituitary neuroendocrine carcinoma with liver and lung metastasis. Despite intensive treatment, the patient continued to show decreased level of consciousness due to cachexia, resulting in death 1 week after surgery.

TABLE 1 | Initial hormonal evaluation, indicating hypoadrenocorticism and hypogonadism of the patient.

Hormone	Result	Reference
Testosterone (ng/ml)	26.93	175.0-781.0
PRL (ng/ml)	6.55	0-22.0
TSH (uIU/ml)	0.05	0.34-5.6
FT4 (ng/dl)	0.92	0.89-1.76
Cortisol (ug/dl)	1.88	5.0-25.0
ACTH (pg/ml)	5.13	7.2-63.3
IGF-1 (ng/ml)	25	75-212

DISCUSSION

Pituitary adenoma is the most common sellar lesion, constituting approximately 15% of all intracranial neoplasms (2), while pituitary metastasis accounts for only approximately 1% of all pituitary adenomas in previous serial studies (1). With the aging population, the occurrence of pituitary metastasis is increasing in clinical practice. Tumors originating from multiple organs can metastasize to the sellar region, such as liver cancer, renal cell carcinoma, thyroid cancer, and prostate cancer, among which the most common primary malignancies are breast cancer in female and lung cancer in male, and these two cancers account for approximately two-thirds of all cases (3).

It is often difficult to distinguish pituitary metastasis from primary pituitary adenomas, as the clinical and radiological features of pituitary metastases are usually nonspecific (4). Most pituitary metastases are clinically silent, and only 6.8% of cases are symptomatic (5). The most common clinical manifestations include DI, visual field defects and hypopituitarism. As DI is very race and occurs only in less than 1% of patients with pituitary adenomas, the possibility of pituitary metastasis could be increased in patients with DI (6). According to Siqueira, et al., it could be a differential diagnosis of invasive lesions in the sellar region, mainly in patients over 50 years of age and/or associated with diabetes insipidus. Therefore, the presence of DI is a useful distinguishing factor, which is more common in pituitary metastasis than in PA. Radiological findings of pituitary metastasis are not specific (7), although some authors mentioned that the most typical radiographic features of metastatic pituitary tumors were enlargement or enhancement of the pituitary stalk with a pituitary mass (8). In our case, the patient presented with clinical visual changes and diabetes insipidus, which is not common in PA. However, the radiological findings of the patient showed typical snowman-shaped appearance of a pituitary adenoma. As there was no previous history of malignancy reported, clinical suspicion of pituitary metastases was low, and diagnosis of nonfunctional PA was made.

Neuroendocrine carcinomas metastasizing to the pituitary gland are extremely rare (9). In a recent review, 15 cases of pituitary metastases were reported, most of which were from neuroendocrine carcinomas (10). The treatment of pituitary metastasis requires to be individualized. Appropriate treatment should be taken based on the patient's primary tumor situation, clinical symptoms, and physical conditions (11). The main therapeutic methods include surgery, radiotherapy and chemotherapy. Patient survival was generally determined by the type of primary tumor, while the overall prognosis was poor, with a median survival of only 12.9 months (12, 13). Surgical treatment is typically suitable for symptomatic patients with pituitary metastasis, as this approach is designed for symptom relief and provides a pathological diagnosis for subsequent treatment. Unfortunately, surgery cannot extend the overall survival of patients (14, 15). Although tumor resection of pituitary metastasis by transsphenoidal surgery or craniotomy is safe and effective, pituitary metastasis, which is highly aggressive, often destroys the dura of the sellar base and diaphragm; tough texture of pituitary metastases, tight adhesions to surrounding tissues,

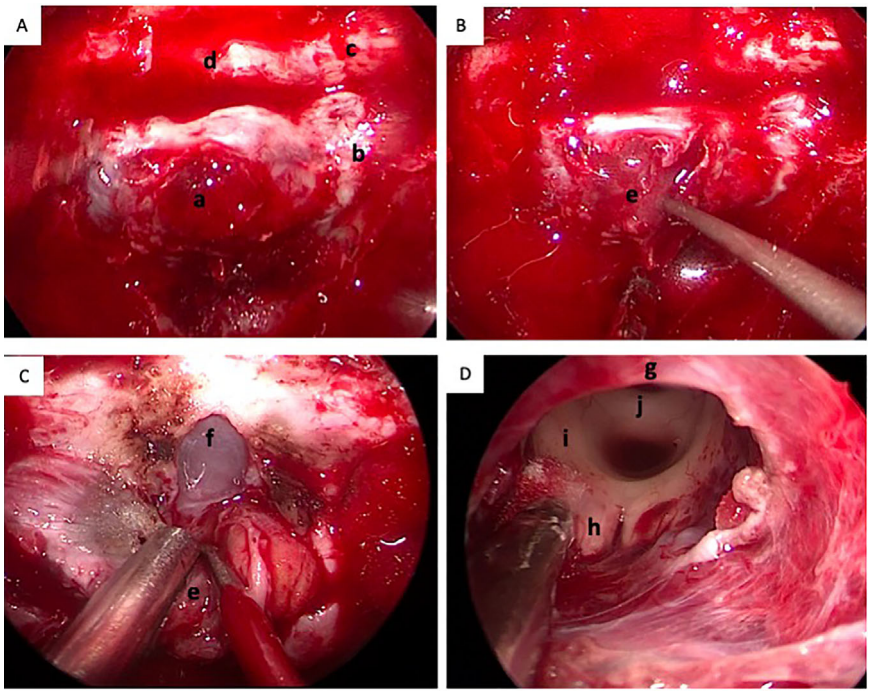

FIGURE 2 | Intra-operative conditions of the lesion. **(A)** The dura of sellar floor was invaded by the tumor; **(B)** The lesion was soft, mimicking pituitary adenoma in texture (the arrow); **(C)** The dura of sphenoid platform was opened; **(D)** The lesion was totally resected and the third ventricle was revealed. a, the invaded dura of the sellar floor; b, the cavernous sinus; c, the optic nerve; d, the sphenoid platform; e, the tumor; f, the arachnoid membrane of sphenoid platform; g, the optic chiasm; h, the mamillary body; i, posterior commissure.

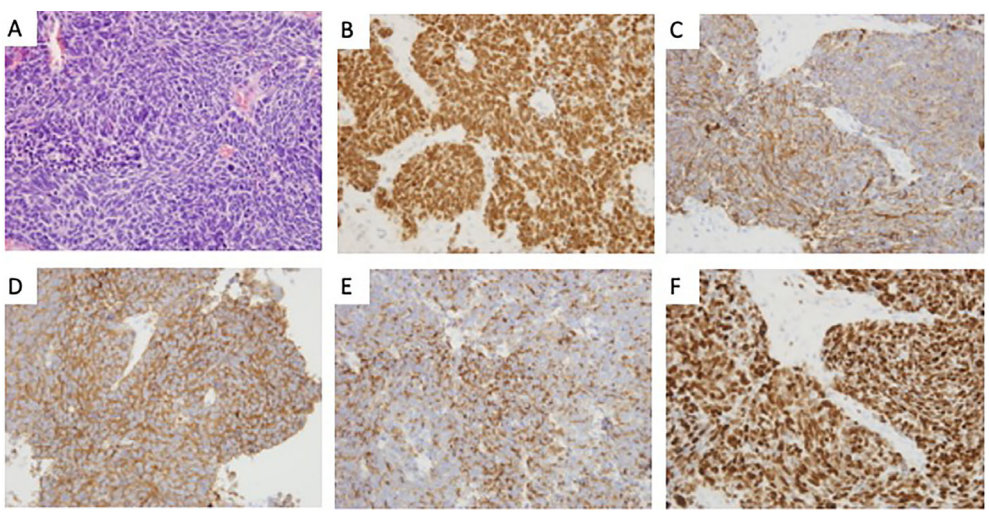

FIGURE 3 | The histological features of the lesion revealed pituitary metastasis of lung neuroendocrine. **(A)** Hematoxylin and eosin (H&E) staining revealed a solid tumor involving the pituitary gland, characterized by small cells with high-grade nuclear atypia and fibrosis (×400); **(B–E)** Immunohistochemistry revealed positivity for TTF-1(B), CK(C), Syn(D), and CgA(E) (×400); **(F)** Immunohistochemical staining of Ki-67 (×400).

and abundant blood supply make it difficult to achieve total resection (15). Therefore, systemic chemotherapy and targeted therapy should be adopted according to the type of primary tumor, which is the most important factor affecting the overall prognosis and progression-free survival of patients (16). In our case, despite intensive treatment, the patient continued to show a decreased level of consciousness due to cachexia, resulting in death one week after surgery.

A small but accumulating numbers of literature described clinical and histopathological correlations with pituitary metastases derived from neuroendocrine tumors, however, genetic basis underlying this presentation remains poorly characterized. Christopher, et al. reported a case of a 68-year-old with a history of lung carcinoid tumor who developed a suprasellar lesion, in which key mutations in PTCH1 and BCOR that have been previously implicated in both systemic neuroendocrine and primary pituitary tumors with potentially actionable therapeutic targets (17).

CONCLUSION

Although the incidence of pituitary metastasis is very low and its clinical symptoms and MRI findings are similar to those of other sellar tumors, its progression is fast and prognosis is poor. Our case highlights the importance of a differential diagnosis of invasive lesions of the sellar region, mainly in individuals over 60 years of age with diabetes insipidus.

DATA AVAILABILITY STATEMENT

The raw data supporting the conclusions of this article will be made available by the authors, without undue reservation.

ETHICS STATEMENT

The studies involving human participants were reviewed and approved by Research Ethics Committee of Xuanwu Hospital. The patients/participants provided their written informed consent to participate in this study. Written informed consent was obtained from the individual(s) for the publication of any potentially identifiable images or data included in this article.

AUTHOR CONTRIBUTIONS

All four authors were involved in patient treatment, data collection and analysis, and manuscript writing. All authors contributed to the article and approved the submitted version.

FUNDING

Financial support for this study was provided by the Scientific Research Project of Capital Health Development in 2018 (grant number: 2018-4-4018). The funding institutions played no role in the design of the study, data collection or analysis, decision to publish, or preparation of the manuscript.

REFERENCES

1. He W, Chen F, Dalm B, Kirby PA, Greenlee JD. Metastatic Involvement of the Pituitary Gland: A Systematic Review With Pooled Individual Patient Data Analysis. *Pituitary* (2015) 18:159–68. doi: 10.1007/s11102-014-0552-2
2. Kobalka PJ, Huntoon K, Becker AP. Neuropathology Of Pituitary Adenomas and Sellar Lesions. *Neurosurgery* (2021) 20:nyaa548. doi: 10.1093/neuros/nyaa548
3. Al-Aridi R, El Sibai K, Fu P, Khan M, Selman WR, Arafah BM. Clinical and Biochemical Characteristic Features of Metastatic Cancer to the Sella Turcica: An Analytical Review. *Pituitary* (2014) 17:575–87. doi: 10.1007/s11102-013-0542-9
4. Fassett DR, Couldwell WT. Metastases to the Pituitary Gland. *Neurosurg Focus* (2004) 16:E8.
5. Teears RJ, Silverman EM. Clinicopathologic Review of 88 Cases of Carcinoma Metastatic to the Pituitary Gland. *Cancer* (1975) 36:216–20. doi: 10.1002/1097-0142(197507)36:1<216::aid-cncr2820360123>3.0.co;2-e
6. Leães CG, Silva LA, Pereira-Lima JF, Kramer J, Oliveira Mda C. Pituitary Metastasis From Adenocarcinoma. *Arq Neuropsiquiatr* (2011) 69:845–6. doi: 10.1590/s0004-282x2011000600026
7. Uzum AK, Kartal I, Gonca T, Mert M, Colak N, Aral F. Pituitary Metastasis of Breast Carcinoma. *Neurosurg Q* (2013) 23:53–4.
8. Morita A, Meyer FB, Laws ERJr. Symptomatic Pituitary Metastases. *J Neurosurg* (1998) 89:69–73. doi: 10.3171/jns.1998.89.1.0069
9. Goglia U, Ferone D, Sidoti M, Spaziante R, Dadati P, Ravetti JL, et al. Treatment of a Pituitary Metastasis From a Neuroendocrine Tumour: Case Report and Literature Review. *Pituitary* (2008) 11:93–102. doi: 10.1007/s11102-007-0038-6
10. Moshkin O, Rotondo F, Scheithauer BW, Soares M, Coire C, Smyth HS, et al. Bronchial Carcinoid Tumors Metastatic to the Sella Turcica and Review of the Literature. *Pituitary* (2012) 15:160–5. doi: 10.1007/s11102-012-0388-6
11. Kano H, Niranjan A, Kondziolka D, Flickinger JC, Lunsford LD. Stereotactic Radiosurgery for Pituitary Metastases. *Surg Neurol* (2009) 72:248–56. doi: 10.1016/j.surneu.2008.06.003
12. de Siqueira PF, Gomes Mathez AL, Pedretti DB, Abucham J. Pituitary Metastasis of Lung Neuroendocrine Carcinoma: Case Report and Literature Review. *Arch Endocrinol Metab* (2015) 59(6):548–53. doi: 10.1590/2359-3997000000139
13. Habu M, Tokimura H, Hirano H, Yasuda S, Nagatomo Y, Iwai Y, et al. Pituitary Metastases: Current Practice in Japan. *J Neurosurg* (2015) 123:998–1007. doi: 10.3171/2014.12.JNS14870
14. Gilard V, Alexandru C, Proust F, Derrey S, Hannequin P, Langlois O. Pituitary Metastasis: Is There Still a Place for Neurosurgical Treatment? *J Neurooncol* (2016) 126:219–24. doi: 10.1007/s11060-015-1967-y
15. Burkhardt T, Henze M, Kluth LA, Westphal M, Schmidt NO, Flitsch J. Surgical Management of Pituitary Metastases. *Pituitary* (2016) 19:11–8. doi: 10.1007/s11102-015-0676-z
16. Park Y, Kim H, Kim EH, Suh CO, Lee S. Effective Treatment of Solitary Pituitary Metastasis With Panhypopituitarism in HER2-Positive Breast Cancer by Lapatinib. *Cancer Res Treat* (2016) 48:403–8. doi: 10.4143/crt.2014.165
17. Hong CS, Kundishora AJ, Elsamadicy AA, Koo AB, Beckta JM, McGuone D, et al. Genetic Characterization of a Case of Sellar Metastasis From Bronchial Carcinoid Neuroendocrine Tumor. *Surg Neurol Int* (2020) 25:11:303. doi: 10.25259/SNI_265_2020

Conflict of Interest: The authors declare that the research was conducted in the absence of any commercial or financial relationships that could be construed as a potential conflict of interest.

frontiers in Endocrinology

CASE REPORT
published: 26 July 2021
doi: 10.3389/fendo.2021.673908

Case Report: Identification of Potential Prognosis-Related *TP53* Mutation and *BCL6-LPP* Fusion in Primary Pituitary Lymphoma by Next Generation Sequencing: Two Cases

Yi Zhang[1†], Liyuan Ma[2†], Jie Liu[1†], Huijuan Zhu[2], Lin Lu[2], Kan Deng[1], Wenbin Ma[1], Hui Pan[2], Renzhi Wang[1] and Yong Yao[1]*

[1] Department of Neurosurgery, Peking Union Medical College Hospital, Beijing, China, [2] Department of Endocrinology, Peking Union Medical College Hospital, Beijing, China

OPEN ACCESS

Edited by:
Congxin Dai,
Capital Medical University, China

Reviewed by:
Sergei I. Bannykh,
Cedars Sinai Medical Center, United States
Murat Aydin Sav,
Yeditepe University, Turkey

***Correspondence:**
Yong Yao
tigerfreeyy@126.com

[†]These authors have contributed equally to this work

Specialty section:
This article was submitted to Pituitary Endocrinology, a section of the journal Frontiers in Endocrinology

Received: 28 February 2021
Accepted: 20 May 2021
Published: 26 July 2021

Citation:
Zhang Y, Ma L, Liu J, Zhu H, Lu L, Deng K, Ma W, Pan H, Wang R and Yao Y (2021) Case Report: Identification of Potential Prognosis-Related TP53 Mutation and BCL6-LPP Fusion in Primary Pituitary Lymphoma by Next Generation Sequencing: Two Cases. Front. Endocrinol. 12:673908. doi: 10.3389/fendo.2021.673908

Background: Primary pituitary lymphoma (PPL) is an extremely rare disease with poor prognosis. Although PPL has been shown to be different from classical primary central nervous system lymphoma because of the embryological origin of structures, individual and precise treatment of PPL remains unknown.

Methods: A 61-year-old man and a 65-year-old woman both diagnosed with primary pituitary diffuse large B cell lymphoma underwent genetic analysis of cerebrospinal fluid and tumor tissue by next generation sequencing.

Results: In the first case, partial remission was achieved following R²-MTX chemotherapy. In the other case with *TP53* mutation and *BCL6-LPP* fusion, disease progressed although different chemotherapy regimens were given.

Conclusion: The gene mutation of *TP53* and *BCL6* may be identified as a marker responsible for prognostic difference in patients with PPL. Genetic analysis may provide a novel approach for precise management and prognosis prediction.

Keywords: primary pituitary lymphoma, *TP53*, *BCL6*, high-dose methotrexate, diffuse large B cell lymphoma, next generating sequencing

INTRODUCTION

Primary pituitary lymphoma (PPL) is an extremely rare clinical entity with much poorer prognosis, while it has an emerging trend these years (1, 2). It is commonly limited in the sellar and parasellar areas without systematic involvement. Histologically, B-cell lymphoma is the most common cell type, followed by T cell type and NK/T cell type (1). The diagnosis of PPL usually can only be determined by pathological analysis since the clinical history, radiological findings and physical examinations do not show significant distinctions with other intracranial neoplasms (1). Although previous studies tend to consider PPL as different primary central nervous system lymphoma (PCNSL) because of embryological origin, the treatment of PPL often follows the management protocol of PCNSL. However, we noticed that the sensitivity and effectiveness of treatment varied in

the patients of PPL (3–5). Genetic analysis might provide a novel approach to selecting the most appropriate regimen and predicting the prognosis of PPL patients. Here we reported two cases of PPL undergoing genetic analysis of cerebrospinal fluid (CSF) and tumor tissue by next generation sequencing (NGS). We firstly found that the gene mutation of *TP53* and *BCL6* might be responsible for prognostic difference in patients with PPL.

MATERIAL AND METHODS

CSF was collected in Streck tubes (Streck, Omaha, NE, USA) from each patient for lymphoma gene detection. Tumor tissue samples and peripheral blood as controls were collected for Whole Exome Sequencing (WES). Library construction was performed using protocols of the Illumina TruSeq DNA library preparation kit (Illumina, San Diego, CA), and then hybridized to custom-designed biotinylated oligonucleotide probes (Roche NimbleGen, Madison, WI, USA). Targeted sequencing was carried out using Illumina HiSeq 3000 platform (Geneplus, Beijing, China). Reads were further aligned to human genome (hg19) using Burrows–Wheeler Aligner (BWA, version 0.7.12-r1039). Somatic single nucleotide variants (SNVs), small insertions and deletions (InDels) and fussion were detected using GATK toolkit (version 3.4). CNV(copy number variation) were identified by CNVKit (version: 0.9.2.dev0).

Case Presentation

Case 1

A 61-year-old man suffered from increasing right-side headache and blurred vision for 10 months and right eye lid ptosis for 4 months. Laboratory tests, including blood routine and biochemistry, immunological indices, thorax, abdominal and pelvis CT and lumbar puncture were normal. Endocrine investigation disclosed multiple anterior pituitary hypofunction: adrenocorticotrophic hormone of 21.34 pg/ml, morning cortisol of 40.6 nmol/L (NR: 166–507 nmol/L); Thyroid function: FT3 3.09 ng/L, FT4 0.31 ng/dL, TSH 0.11 μIU/ml; Gonadal hormone: LH 1.0 mIU/ml, FSH 2.5 IU/ml, E <18 pmol/L, P <0.159 nmol/L, testosterone <0.087 nmol/L, DHEA 0.1 μmol/L, prolactin of 792 mIU/L (NR: 166–507 nmol/L); GH 1.2 ng/ml. Pituitary magnetic resonance imaging (MRI) 10 and 5 months ago both demonstrated suspected "pituitary microadenoma" on the right side (**Figures 1A, B**). The patient was twice diagnosed with "autoimmune hypophysitis" and treated with hydrocortisone or prednisone together with azathioprine, and twice diagnosed with "viral encephalitis" and received pulsed methylprednisolone in different local hospitals in these 10 months. However, his symptoms didn't improve but worsened. The MRI three months ago showed the mass in sella turcica enlarged to 1.3 × 0.9 cm, involving the right cavernous sinus and internal carotid artery (**Figure 1C**). The remaining past medical, personal and family history was unremarkable.

Last month, the patient visited our hospital. Blood test work up showed hypothalamus–pituitary dysfunction similar with before. The pituitary MRI showed the mass might be "pituitary macroadenoma" (12.7 × 6.7 × 11.1 mm, demonstrating equal T1 and equal T2 signal with slightly homogeneous enhancement) in the sellar region with the right cavernous sinus invasion (Knosp IV) (**Figure 1D**). Physical examination after admission revealed right third cranial nerve palsy and classic signs of Cushing's syndrome resulting from glucocorticoids treatment.

A presumptive diagnosis of nonsecretory pituitary macroadenoma was made, and the mass caused anterior pituitary hypofunction. Endoscopic endonasal transsphenoidal surgery was performed for biopsy in our hospital. Pathological examination confirmed diffuse large B cell lymphoma (DLBCL) (germinal center-like). Immunohistochemical staining showed the tumor cells to be immunoreactive for B-cell marker CD20 and negative for the T-cell marker CD3. Further marker studies showed the tumor cells to be positive for Bcl-2, Bcl-6, CD5, CD20, C-MYC (index 60%) and P53. Markers Mum-1, CD10, CD23, CD3, Cyclin D1, CD30 (Ki-1), AE1/AE3, CAM5.2, ER, PIT-1, T-PIT were negative. Cell proliferation index Ki-67 was 70%. *In situ* hybridization showed EBER ISH (−).

A total body PET/CT, bone marrow biopsy and CSF analysis confirmed the absence of systemic involvement. Testing for the HIV were negative.

Thus, the diagnose of primary central nervous system lymphoma (DLBCL, GCB type, double positive expression, Ann Arbor stage IE A) was made. Further genetic testing for lymphoma by NGS of CSF sample showed the patient contained *MYD88* (c.794T>C), *TNFRSF14* (c.95C>T), *ETV6* (c.26G>A) and *ETV6* (c.33+1G>A) mutations (**Table 1**). NGS result of tumor tissue was similar to it.

Pituitary MRI reexamination half months after biopsy surgery showed the mass enlarged compared with before, involving bilateral cavernous sinus (**Figure 1E**). Three courses of R^2-MTX chemotherapy (800 mg iv d1 of Rituximab, 7 g iv d2 of methotrexate, and 25 mg d1–14 of lenalidomide) were administrated in the next three months. MRI scan showed marked reduction of the tumor size (**Figures 1F, G**). The symptom of eyelids ptosis, blurred vision and headache gradually improved. He is considered to be in partial remission.

Case 2

A 65-year-old woman had paroxysmal headache with no obvious inducement from 2 months ago, accompanied with nausea, denying vomiting, blurred vision or slurred speech. The patient also had dry mouth, polydipsia and polyuria with loss of appetite and fatigue. For past medical history, she received an operation of right adnexectomy and total hysterectomy because of mucinous cystadenoma of right ovary 10 years ago.

Last month in local hospital, endocrines test showed hypopituitarism: FT4 8 pmol/L, TSH 0.11 mIU/ml; LH <0.01 mIU/ml, FSH 1.16 mIU/ml; 0 ACTH 1.88 pmol/L, serum cortisol 0.506, 8 ACTH 1.91 pmol/L, serum cortisol 0.536; GH 0.803 ng/ml, IGF-1 150 ng/ml. The tumor marker NSE was of 21.77 ng/ml (0–16.3), while AFP and CEA were normal. IgG4 was of 0.47 g/L. Pituitary MRI showed a mass appeared as soft tissue density in sellar area with a size of about 1.5 × 1.3 × 2.2 cm, and partial of it had no clear boundary between optic chiasma. PET-CT showed the mass (2.3 × 2.0 cm) in pituitary gland with increased FDG uptake and SUVmax of 75.7 (**Figure 2**). The patient was treated

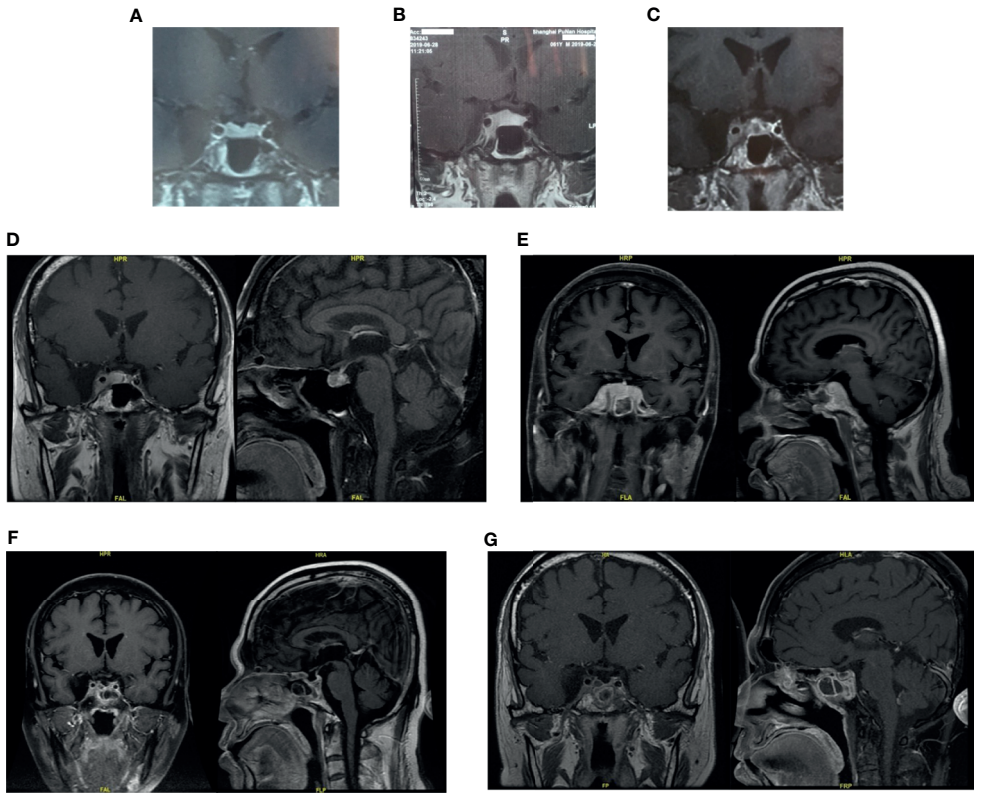

FIGURE 1 | The pituitary images in different period of Case 1. **(A, B)** Pituitary magnetic resonance imaging (MRI) 10 and 5 months ago both demonstrated suspected "pituitary microadenoma" on the right side. **(C)** Three months ago, enhanced MRI showed the mass in sella turcica enlarged to 1.3 × 0.9 cm, involving the right cavernous sinus and internal carotid artery. **(D)** One months ago, the pituitary MRI showed the mass might be "pituitary macroadenoma" (12.7 × 6.7 × 11.1 mm, demonstrating equal T1 and equal T2 signal with slightly homogeneous enhancement) in the sellar region with the right cavernous sinus invasion (Knosp IV). **(E)** Pituitary MRI reexamination half months after biopsy surgery showed the mass enlarged compared with before, involving bilateral cavernous sinus. **(F, G)** Enhanced head MRI + DWI and Pituitary gland plain scan + enhanced MRI showed the mass was significantly smaller than before after three months' chemotherapy.

orally with desmopressin 0.05 mg bid, prednisone acetate 5 mg qd, and euthyrox 25 μg qd. The symptoms of thirst and polyuria were obviously relieved, but headache and nausea were not relieved.

Two weeks ago, the headache worsened with persistent pain, accompanied by nausea and vomiting. She went to the department of emergency in our hospital with a blood pressure of 85/66 mmHg. After symptomatic treatment, the patient was admitted to the department of neurosurgery. Physical examination revealed normal vision and visual field. Further examination was finished, which showed: TSH 30.014 μIU/ml, FT3 1.55 pg/ml; Tumor markers: CEA 2.3 ng/ml, CA 125 10.9 μ/ml; IgG4 506 mg/L, ESR 44 mm/h.

Mass in sellar area which might be metastatic pituitary cancer was considered and endoscopic endonasal transsphenoidal surgery was performed for biopsy. Pathological examination showed the tumor was consistent with DLBCL (B cell derived from germinal center). The immunohistochemical staining showed: CD20(++), Bcl-2(+), Mum-1(10%+), Bcl-6(95%+), C-MYC(80%+), P53(+), CD3(scattered+), CD5(scattered+), CD15 (−), CD10(−), CD30(Ki-1)(−), PAX-5(+), AE1/AE3(−), CgA(−), NUT(−), HMB45(−), Syn(−), S-100(−), Ki-67(index 90%). *In situ* hybridization showed EBER ISH (−).

NGS testing for lymphoma-related genes of CSF sample showed the patient contained point mutations of *MYD88* (c.794T>C), *TP53* (c.401T>G), *CD79B* (c.68-1G>C), *PCLO* (c.6632C>T) and *JAK2* (c.678G>T), amplification of gene *JAK2*, *CD274*, *PDCD1LG2* and fusion of gene *BCL6-LPP* (**Table 1**). **Figures 3** and **4** schematically display two mutations closely related to poor prognosis of lymphoma, *TP53* (c.401T>G) mutation and *BCL6-LPP* fusion, which existed in patient 2 but not in patient 1. Result of WES of tumor tissue was consistent with CSF.

CT of the chest, abdomen, and pelvis as well as bone marrow biopsy were negative for dissemination. Then the patient received chemotherapy in local hospital, including one course of R-HDMTX (rituximab and high-dose methotrexate) chemotherapy regimen, one course of rituximab associated to temozolomide and one course of R-MT protocol (580 mg d0 of rituximab, 2.0 g d1 of methotrexate, and 200 mg d2-5 of temozolomide). A pituitary MRI at two months from the

TABLE 1 | Gene mutations of cerebrospinal fluid sample in two patients.

Gene	Transcript	Mutation	Amino acid	Function Zones	Variation frequency
Case 1					
MYD88	NM_002468.4	c.794T>C	p.L265P	EX5	5.0%
TNFRSF14	NM_003820.2	c.95C>T	p.A32V	EX2	4.7%
ETV6	NM_001987.4	c.26G>A	p.S9N	EX1	1.6%
ETV6	NM_001987.4	c.33+1G>A	–	IVS1	1.6%
Case 2					
MYD88	NM_002468.4	c.794T>C	p.L265P	EX5	55.8%
TP53	NM_000546.5	c.401T>G	p.F134C	EX5	39.0%
CD79B	NM_000626.2	c.68-1G>C	–	IVS1	23.7%
PCLO	NM_033026.5	c.6632C>T	p.T2211I	EX5	11.7%
JAK2	NM_004972.3	c.678G>T	p.R226S	EX7	3.6%
JAK2	NM_004972.3	Amplification	–	9p24.1	14.2
CD274	NM_014143.3	Amplification	–	9p24.1	13.6
PDCD1LG2	NM_025239.3	Amplification	–	9p24.1	7.1
BCL6-LPP	NM_001706.4 /NM_001167672.1	Fusion	–	3q27.3/3q28	38.4%

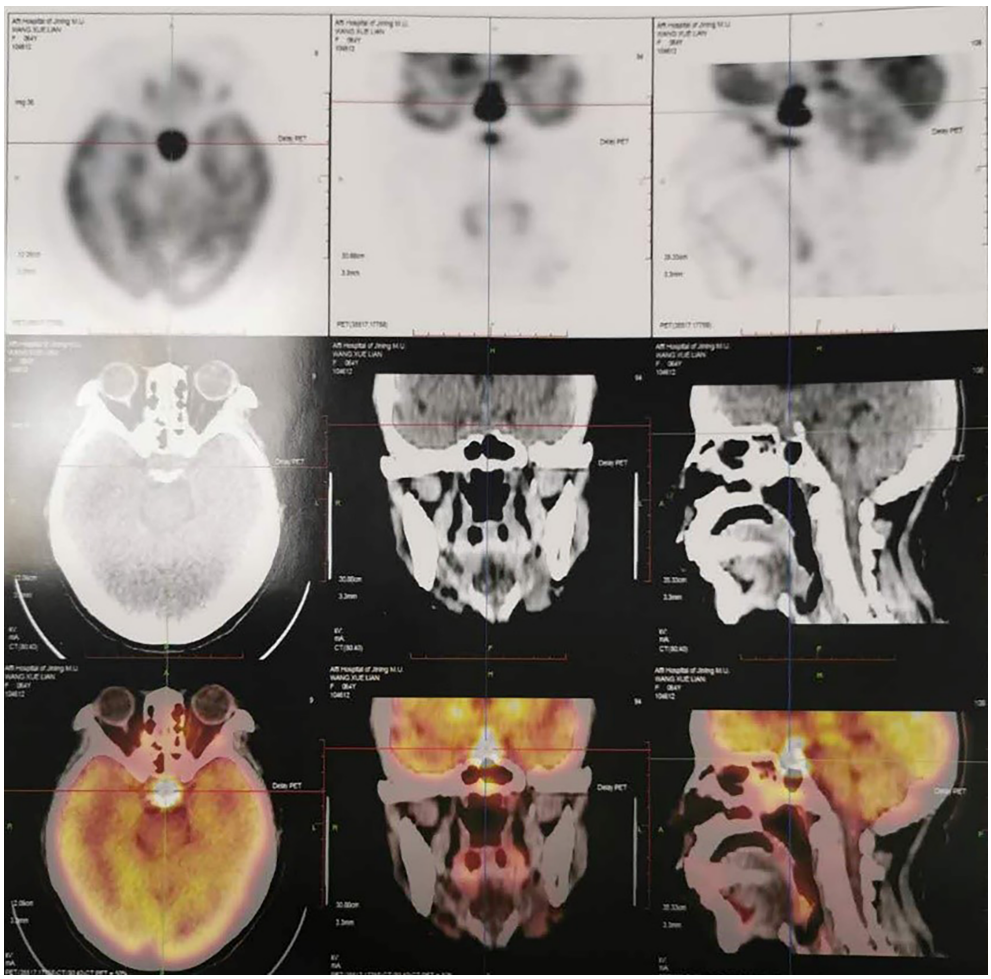

FIGURE 2 | PET-CT one month ago showed the mass (2.3 × 2.0 cm) in pituitary gland with increased FDG uptake and SUVmax of 75.7 in Case 2.

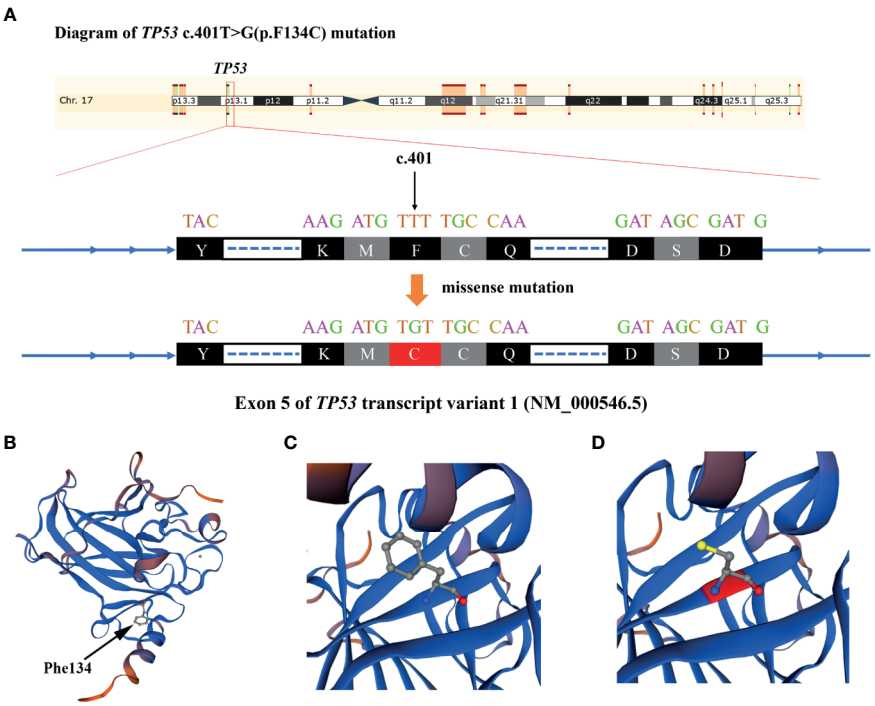

FIGURE 3 | Diagram of *TP53* c.401T>G (p.F134C) alteration in Case 2. **(A)** The base of c.401 mutated from T to G and amino acid changed from phenylalanine to cysteine. **(B)** The 3-dimentional model structure of TP53 wild-type analyzed by SWISSMODEL. **(C)** The Phe134 of TP53. **(D)** The Cys134 of mutated TP53.

beginning of chemotherapy demonstrated the tumor (size of about 2 × 1.5 × 3.2 cm) was larger than before without cavernous sinus involving (**Figure 5**). Thus, the treatment of chemotherapy continued.

DISCUSSION

We present two cases of PPL using genetic analysis to guide treatment and predict prognosis. To the best of our knowledge, this is the first attempt to distinguish PPL from PCNSL genetically and manage PPL based on gene sequencing and we administered different treatment modality of chemotherapy and targeted therapy accordingly. We also identified that gene mutation of *TP53* and *BCL6* was responsible for prognostic difference. Normally, the treatment of PPL often follows the management protocol of PCNSL consisting of surgery, chemotherapy and/or radiotherapy (6). However, it is said that surgical intervention suggests no obvious benefits in the outcome of PCNSL and the neurotoxic effects of radiotherapy should be noted (3, 5). Therefore, the therapeutic regimen consisting of HD-MTX combined with rituximab and other cytostatic drugs that penetrate the blood–brain barrier is highly recommended (3, 4). Both of our patients initiated chemotherapy immediately after the diagnosis of PPL was confirmed pathologically, but one patient seemed not to be sensitive to such regimen. Genetic analysis was thus performed to predict prognosis and adjust treatment modality. Since the two patients showed different prognosis, we identified gene mutation of *TP53* and *BCL6* as a distinct characteristic after genetic comparison was made. Some other typical gene mutations of PPL are also investigated here which we believe are highly likely to make a difference.

TP53 is mutated in 20–25% of aggressive B-cell lymphoma. The negative prognostic impact of *TP53* mutations in DLBCL has been reported in a number of studies (7). Mutation and copy loss of *TP53* are independent negative prognostic factors in DLBCL (8), while recent studies indicated that the prognostic role should be validated when combined with other indexes (9). For instance, Dobashi et al. found that *TP53* mutations and *TP53* deletions were confirmed to be poor prognostic factors for overall survival (OS) and progression-free survival (PFS) only when both aberrations co-existed (10). In the patients of DLBCL treated with R-CHOP, *TP53* mutation significantly correlate with worse survival in either ABC- or GCB-DLBCL (11). Such a negative correlation could also be seen in chemotherapy ± rituximab (CCT-treated) PCNSL patients, with hotspot/direct DNA contact *MUT-TP53* being predictive of poor outcome (12). Todorovic et al. investigated that *TP53* was the only gene harboring mutations in all surveyed PCNSL patients, which showed a more frequent mutation incidence than DLBCL (13). Therefore, we believe the unfavorable prognostic effect of *TP53* mutation is more likely to be employed in PCNSL and PPL patients. *TP53* alterations can either give rise to a loss-of-function or a gain-of-function phenotype (14). In the cases of *TP53* loss-of-function, they

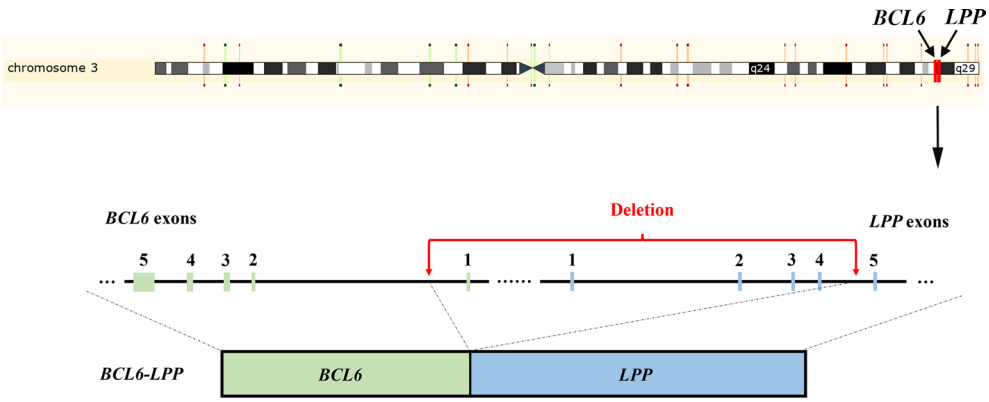

FIGURE 4 | Schematic representation of the *BCL6-LPP* fusion in Case 2. An 838 kb-sized deletion of chromosome 3q27.3–3q28 (base 187461439 on chromosome 3q27 to base 188299507 on chromosome 3q28), resulting in a fusion of the *BCL6* with the *LPP* gene.

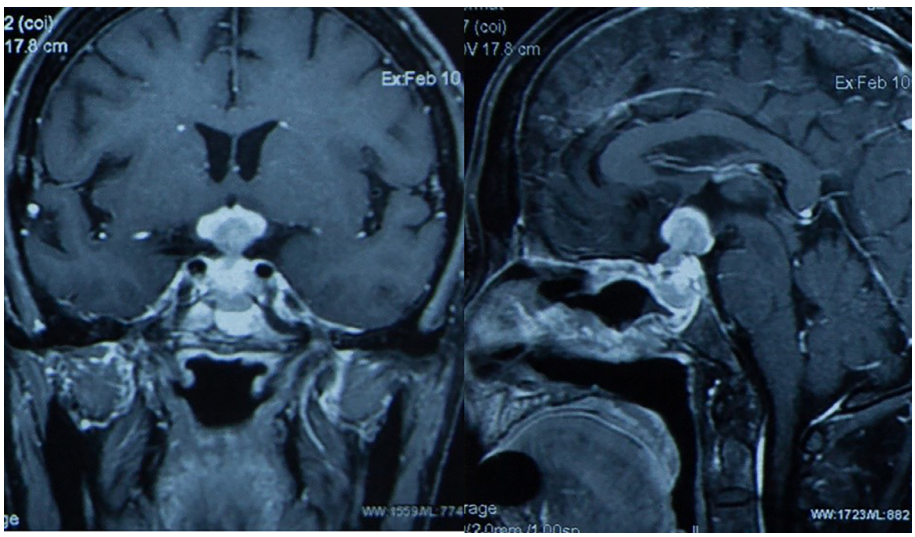

FIGURE 5 | Pituitary MRI at two months from the beginning of chemotherapy demonstrated the tumor (size of about 2 × 1.5 × 3.2 cm) was larger than before without cavernous sinus involving in Case 2.

might undergo two sequential events. The first event is mutation or methylation of the *TP53* promoter, leading to appearance of a cell with increased risk of malignant transformation. The second event is the loss of an intact allele of the gene; this change is necessary for tumorigenesis (15). The gain-of-function mutations could partly account for the observation of *TP53* overexpression in haematological malignancies and resistance to conventional chemotherapeutic agents, leading to poor survival (14). The drug resistance could be seen in studies pointing out that response to both CHOP and R-CHOP treatments was significantly inferior in patients with *TP53* mutation and that the Hodgkin Reed-Sternberg cell lines with drug resistance all contained *TP53* defects (7, 14). One of our patients showed *TP53* mutation without sufficient drug effect and prognosis was not well, which might indicate a potentially predictive role of *TP53* in the prognosis of PPL.

In DLBCL, The *BCL6* locus can fuse with different partner genes. Ueda et al. found that non-immunoglobulin/*BCL6* gene fusion in DLBCL is a poor prognostic indicator and plays a pathogenetic role in a proportion of DLBCL (16). In PCNSLs, the *BCL6* gene fusion with its partner genes such as lipoma-preferred partner (*LPP*) in band 3q27, may contribute to aberrant expression of *BCL6* protein (17). A deletion in 3q leads to loss of an 837-kb fragment extending from the first intron of *BCL6* to the third intron of the *LPP* gene, which may bring the *BCL6* gene under the control of regulatory elements of the *LPP* gene or the miRNA-28 gene located in intron 4 of *LPP* (17). One of our patients showed *BCL6-LPP* gene fusion and the prognosis was

not good. Whether BCL6 can be considered as a prognostic factor of PCNSL is still controversial. Cady et al. investigated that *BCL6* was associated with inferior OS alone or concomitant with del (6) (q22) (18). However, the expression of *BCL6* was paradoxically correlated with the prognosis of PCNSL. Kreher et al. found that *BCL6* expression was associated with shorter Progression-free survival (PFS) (19), while Lossos et al. found *BCL6* expression had improved survival (20) and Niparuck et al. found that *BCL6* expression showed no significant predictive effect in PFS and OS (21). Considering the high relative expression of *BCL6* can be detected in the majority of PCNSL cases, a potential role for *BCL6* antagonists in the next generation of therapies for PCNSL could be explored (22).

CONCLUSION

Generally, we presented two extremely rare cases of PPL and developed genetic analysis as a novel approach for prognosis prediction and treatment adaption where gene mutation of *TP53* and *BCL6* were identified as a marker for prognostic difference of PPL. We believe such an attempt will inspire clinicians to yield more precise and effective management approaches of PPL and more details about genetic analysis in PPL should be validated in larger prospective studies.

DATA AVAILABILITY STATEMENT

The data presented in the study are deposited in the NCBI Sequence Read Archive (SRA) repository, accession numbers (SRR14774001, SRR14774002, SRR14783994, SRR14783995, SRR14783996).

ETHICS STATEMENT

The ethical approvals for this study were granted by the PUMCH Institutional Review Board. The patients/participants provided their written informed consent to participate in this study.

AUTHOR CONTRIBUTIONS

Conception and design: YY, RW, and YZ. Development of methodology: HP, WM, and YZ. Acquisition and analysis of data: YZ, LM, JL, and KD. Writing, review and revision of manuscript: YZ, LM, and JL. Technical and material support: HJZ and LL. Study supervision: YY, RW, and HJZ. All authors contributed to the article and approved the submitted version.

FUNDING

This study was supported by Chinese Academy of Medical Sciences Innovation Fund for Medical Sciences (No. 2016-I2M-1-002) from YY: providing conception and design and supervision. Youth Science Foundation of Peking Union Medical College Hospital (No. pumch201911867) from YZ: analysis of data and writing manuscript.

REFERENCES

1. Tarabay A, Cossu G, Berhouma M, Levivier M, Daniel RT, Messerer M. Primary Pituitary Lymphoma: An Update of the Literature. *J Neurooncol* (2016) 130:383–95. doi: 10.1007/s11060-016-2249-z
2. Giustina A, Gola M, Doga M, Rosei EA. Clinical Review 136: Primary Lymphoma of the Pituitary: An Emerging Clinical Entity. *J Clin Endocrinol Metab* (2001) 86:4567–75. doi: 10.1210/jcem.86.10.7909
3. Batchelor TT. Primary Central Nervous System Lymphoma: A Curable Disease. *Hematol Oncol* (2019) 37 Suppl 1:15–8. doi: 10.1002/hon.2598
4. von Baumgarten L, Illerhaus G, Korfel A, Schlegel U, Deckert M, Dreyling M. The Diagnosis and Treatment of Primary Cns Lymphoma. *Dtsch Arztebl Int* (2018) 115:419–26. doi: 10.3238/arztebl.2018.0419
5. Hoang-Xuan K, Bessell E, Bromberg J, Hottinger AF, Preusser M, Rudà R, et al. Diagnosis and Treatment of Primary CNS Lymphoma in Immunocompetent Patients: Guidelines From the European Association for Neuro-Oncology. *Lancet Oncol* (2015) 16:e322–32. doi: 10.1016/S1470-2045(15)00076-5
6. Li Y, Zhang Y, Xu J, Chen N. Primary Pituitary Lymphoma in an Immunocompetent Patient: A Rare Clinical Entity. *J Neurol* (2012) 259:297–305. doi: 10.1007/s00415-011-6179-6
7. Zenz T, Kreuz M, Fuge M, Klapper W, Horn H, Staiger AM, et al. TP53 Mutation and Survival in Aggressive B Cell Lymphoma. *Int J Cancer* (2017) 141:1381–8. doi: 10.1002/ijc.30838
8. Cao Y, Zhu T, Zhang P, Xiao M, Yi S, Yang Y, et al. Mutations or Copy Number Losses of CD58 and TP53 Genes in Diffuse Large B Cell Lymphoma Are Independent Unfavorable Prognostic Factors. *Oncotarget* (2016) 7:83294–307. doi: 10.18632/oncotarget.13065
9. Chan A, Dogan A. Prognostic and Predictive Biomarkers in Diffuse Large B-Cell Lymphoma. *Surg Pathol Clin* (2019) 12:699–707. doi: 10.1016/j.path.2019.03.012
10. Dobashi A, Togashi Y, Tanaka N, Yokoyama M, Tsuyama N, Baba S, et al. TP53 and OSBPL10 Alterations in Diffuse Large B-Cell Lymphoma: Prognostic Markers Identified Via Exome Analysis of Cases With Extreme Prognosis. *Oncotarget* (2018) 9:19555–68. doi: 10.18632/oncotarget.24656
11. Xu-Monette ZY, Wu L, Visco C, Tai YC, Tzankov A, Liu WM, et al. Mutational Profile and Prognostic Significance of TP53 in Diffuse Large B-Cell Lymphoma Patients Treated With R-CHOP: Report From an International Dlbcl Rituximab-CHOP Consortium Program Study. *Blood* (2012) 120:3986–96. doi: 10.1182/blood-2012-05-433334
12. Munch-Petersen HD, Asmar F, Dimopoulos K, Areškevičiūtė A, Brown P, Girkov MS, et al. TP53 Hotspot Mutations Are Predictive of Survival in Primary Central Nervous System Lymphoma Patients Treated With Combination Chemotherapy. *Acta Neuropathol Commun* (2016) 4:40. doi: 10.1186/s40478-016-0307-6
13. Todorovic Balint M, Jelicic J, Mihaljevic B, Kostic J, Stanic B, Balint B, et al. Gene Mutation Profiles in Primary Diffuse Large B Cell Lymphoma of Central Nervous System: Next Generation Sequencing Analyses. *Int J Mol Sci* (2016) 17(5). doi: 10.3390/ijms17050683
14. Cheung KJ, Horsman DE, Gascoyne RD. The Significance of TP53 in Lymphoid Malignancies: Mutation Prevalence, Regulation, Prognostic Impact and Potential as a Therapeutic Target. *Br J Haematol* (2009) 146:257–69. doi: 10.1111/j.1365-2141.2009.07739.x
15. Voropaeva EN, Pospelova TI, Voevoda MI, Maksimov VN, Orlov YL, Seregina OB. Clinical Aspects of TP53 Gene Inactivation in Diffuse Large B-Cell Lymphoma. *BMC Med Genomics* (2019) 12:35. doi: 10.1186/s12920-019-0484-9

16. Ueda C, Akasaka T, Ohno H. Non-Immunoglobulin/BCL6 Gene Fusion in Diffuse Large B-Cell Lymphoma: Prognostic Implications. *Leuk Lymphoma* (2002) 43:1375–81. doi: 10.1080/10428190290033305
17. Schwindt H, Akasaka T, Zühlke-Jenisch R, Hans V, Schaller C, Klapper W, et al. Chromosomal Translocations Fusing the BCL6 Gene to Different Partner Loci Are Recurrent in Primary Central Nervous System Lymphoma and May Be Associated With Aberrant Somatic Hypermutation or Defective Class Switch Recombination. *J Neuropathol Exp Neurol* (2006) 65:776–82. doi: 10.1097/01.jnen.0000229988.48042.ae
18. Cady FM, O'Neill BP, Law ME, Decker PA, Kurtz DM, Giannini C, et al. Del (6)(q22) and BCL6 Rearrangements in Primary CNS Lymphoma Are Indicators of an Aggressive Clinical Course. *J Clin Oncol* (2008) 26:4814–9. doi: 10.1200/jco.2008.16.1455
19. Kreher S, Jöhrens K, Strehlow F, Martus P, Borowiec K, Radke J, et al. Prognostic Impact of B-Cell Lymphoma 6 in Primary CNS Lymphoma. *Neuro Oncol* (2015) 17:1016–21. doi: 10.1093/neuonc/nov046
20. Lossos C, Bayraktar S, Weinzierl E, Younes SF, Hosein PJ, Tibshirani RJ, et al. LMO2 and BCL6 Are Associated With Improved Survival in Primary Central Nervous System Lymphoma. *Br J Haematol* (2014) 165:640–8. doi: 10.1111/bjh.12801
21. Niparuck P, Boonsakan P, Sutthippingkiat T, Pukiat S, Chantrathammachart P, Phusanti S, et al. Treatment Outcome and Prognostic Factors in PCNSL. *Diagn Pathol* (2019) 14:56. doi: 10.1186/s13000-019-0833-1
22. Ponzoni M, Issa S, Batchelor TT, Rubenstein JL. Beyond High-Dose Methotrexate and Brain Radiotherapy: Novel Targets and Agents for Primary CNS Lymphoma. *Ann Oncol* (2014) 25:316–22. doi: 10.1093/annonc/mdt385

Conflict of Interest: The authors declare that the research was conducted in the absence of any commercial or financial relationships that could be construed as a potential conflict of interest.

GLOSSARY

ABC-DLBCL	activated B-cell-like lymphoma-DLBCL
ACTH	adrenocorticotropic hormone
AFP	alpha-fetoprotein
Bcl-2	B-cell lymphoma 2 protein
BCL6	B-cell lymphoma 6 gene
CA125	carbohydrate antigen 125
CD79B	Cluster of Differentiation 79B gene
CEA	carcinoembryonic antigen
CgA	chromogranin-A
CNV	copy number variation
CSF	cerebrospinal fluid
DHEA	Dehydroepiandrosterone
DLBCL	diffuse large B cell lymphoma
E	estrogen
EBER ISH	*in situ* hybridization of EBV-encoded RNA
ER	Estrogen receptor
ESR	erythrocyte sedimentation rate
ETV6	translocation-Ets-leukemia virus 6 gene
FDG	fluorodeoxyglucose
FSH	follicle-stimulating hormone
FT3	free triiodothyronine
FT4	free thyroxine
GCB	germinal center B-cell-like lymphoma
GH	growth hormone
HIV	Human Immunodeficiency Virus
HMB45	Human Melanoma Black 45
IGF-1	insulin-like growth factor 1
IgG4	immunoglobin G4
InDel	Insertion and Deletion
JAK2	Janus kinase 2 gene
LH	luteinizing hormone
LPP	lipoma-preferred partner gene
MRI	magnetic resonance imaging
Mum-1	Multiple myeloma antigen 1
MYD88	Myeloid differentiation primary response 88 gene
NGS	next generation sequencing
NR	normal range
NSE	neuron-specific enolase
NUT	nuclear protein in testis
OS	overall survival
P	progesterone
PAX-5	paired-box domain 5
PCLO	Piccolo gene
PCNSL	primary central nervous system lymphoma
PDCD1LG2	Programmed cell death 1 ligand 2 gene
PET-CT	positron emission tomography-computed tomography
PFS	progression-free survival
PPL	primary pituitary lymphoma
R^2-MTX	Rituximab and methotrexate
R-CHOP	Rituximab-Cyclophosphamide
Hydroxyldaunorubicin	Oncovin and Prednisone
S-100	S-100 protein
SNV	single nucleotide variant
SUV	standard uptake value
Syn	synaptophysin
TNFRSF14	tumor necrosis factor receptor superfamily member 14 gene
TP53	tumor protein p53 gene
TSH	thyroid stimulating hormone
WES	Whole Exome Sequencing

frontiers in Endocrinology

ORIGINAL RESEARCH
published: 02 September 2021
doi: 10.3389/fendo.2021.720823

An Optimized Pathway for the Differential Diagnosis of ACTH-Dependent Cushing's Syndrome Based on Low-Dose Dexamethasone Suppression Test

Kang Chen[1,2], Shi Chen[1], Lin Lu[1]*, Huijuan Zhu[1], Xiaobo Zhang[3], Anli Tong[1], Hui Pan[1,4], Renzhi Wang[5] and Zhaolin Lu[1]*

[1] Department of Endocrinology, Key Laboratory of Endocrinology of National Health Commission, Translation Medicine Centre, Peking Union Medical College Hospital, Peking Union Medical College, Chinese Academy of Medical Sciences, Beijing, China, [2] Eight-Year Program of Clinical Medicine, Peking Union Medical College Hospital, Peking Union Medical College, Chinese Academy of Medical Sciences, Beijing, China, [3] Department of Radiology, Peking Union Medical College Hospital, Peking Union Medical College, Chinese Academy of Medical Sciences, Beijing, China, [4] State Key Laboratory of Complex Severe and Rare Diseases, Peking Union Medical College Hospital, Chinese Academy of Medical Science and Peking Union Medical College, Beijing, China, [5] Department of Neurosurgery, Peking Union Medical College Hospital, Peking Union Medical College, Chinese Academy of Medical Sciences, Beijing, China

OPEN ACCESS

Edited by:
Run Yu,
UCLA David Geffen School of Medicine, United States

Reviewed by:
Przemyslaw Witek,
Warsaw Medical University, Poland
Luiz Augusto Casulari,
University of Brasilia, Brazil

***Correspondence:**
Shi Chen
cs0083@126.com
Lin Lu
lulin88@sina.com

Specialty section:
This article was submitted to Pituitary Endocrinology, a section of the journal Frontiers in Endocrinology

Received: *05 June 2021*
Accepted: *10 August 2021*
Published: *02 September 2021*

Citation:
Chen K, Chen S, Lu L, Zhu H, Zhang X, Tong A, Pan H, Wang R and Lu Z (2021) An Optimized Pathway for the Differential Diagnosis of ACTH-Dependent Cushing's Syndrome Based on Low-Dose Dexamethasone Suppression Test. Front. Endocrinol. 12:720823. doi: 10.3389/fendo.2021.720823

Context: Traditionally, low-dose dexamethasone suppression test (LDDST) was used to confirm the diagnosis of Cushing's syndrome (CS), and high-dose dexamethasone suppression test (HDDST) was used to differentiate Cushing's disease (CD) and ectopic adrenocorticotropin (ACTH) syndrome (EAS), but some studies suggested that HDDST might be replaced by LDDST. For the differential diagnosis of CS, dexamethasone suppression test was usually combined with other tests such as bilateral petrosal sinus sampling (BIPSS) and pituitary magnetic resonance imaging, but the optimal pathway to incorporate these tests is still controversial.

Objectives: To develop an optimized pathway for the differential diagnosis of CD and EAS based on LDDST.

Design and Setting: Single-center retrospective study (2011–2019).

Patients: Two hundred sixty-nine CD and 29 EAS patients with pathological diagnosis who underwent consecutive low- and high-dose DST.

Results: For the differential diagnosis of CD and EAS, the area under curve (AUC) of LDDST using urine free cortisol (0.881) was higher than that using serum cortisol (0.685) ($p < 0.001$) in head-to-head comparison among a subgroup of 108 CD and 10 EAS. The AUC of LDDST (0.883) was higher than that of HDDST (0.834) among all the included patients. With the cutoff of <26%, the sensitivity and specificity of LDDST were 39.4% and 100%. We designed a new pathway in which BIPSS was only reserved for those patients with unsuppressed LDDST and adenoma <6mm, yielding an overall sensitivity of 97.7% and specificity of 86.7%.

Conclusion: LDDST had similar value to HDDST in differentiating CD and EAS using the specific cutoff point. The pathway that combined LDDST and BIPSS could differentiate CD and EAS accurately.

Keywords: Cushing's disease, ectopic ACTH syndrome, dexamethasone suppression test, petrosal sinus sampling, ROC curve

INTRODUCTION

Cushing's disease (CD) and ectopic ACTH syndrome (EAS) are two main causes of ACTH-dependent Cushing's syndrome (CS) (1). Their clinical manifestations are similar, but the treatments for them are quite different, so the differential diagnosis of CD and EAS is a crucial but challenging task.

Dexamethasone suppression test was first introduced by Liddle in 1960 (2). While normal hypothalamus–pituitary–adrenal axis was regulated by negative feedback, the cortisol secretion in CS was partly resistant to excess glucocorticoid, and it was believed that the ectopic tumor has higher autonomy of ACTH secretion compared with the pituitary tumor (1, 3). Based on these characteristics, low-dose dexamethasone suppression test (LDDST) was designed to diagnose CS and high-dose dexamethasone suppression test (HDDST) to differentiate CD and EAS (4). In standard HDDST, 24-h urine before and after a 2-day administration of dexamethasone (5) is time consuming and usually needs hospitalization. Modifications was made to simplify the procedure, such as the measurement of morning cortisol instead of 24-h urine free cortisol (UFC) or the overnight administration of 8-mg dexamethasone (4, 6). The sensitivity and specificity were highly variable among studies, both ranging from 60% to 100% (3, 4). Some sophisticated criteria to interpret the HDDST results was developed to improve its accuracy, but their reproducibility seemed to be poor (4, 7). Some studies found that HDDST provided little information for the differential diagnosis of CD and EAS and even suggested that it might be abandoned (8, 9). Moreover, the administration of high-dose dexamethasone in CS patients with already high cortisol level may lead to some side effects, exacerbating their hypertension and glucose metabolism disorder. Thus, the necessity of HDDST should be questioned. Meanwhile, it was proposed that LDDST per se may be an alternative for the differential diagnosis of ACTH-dependent Cushing's syndrome (7, 10, 11), but such viewpoint has not been widely accepted.

Dexamethasone suppression test alone was not accurate enough to discriminate CD and EAS, so a diagnostic pathway that incorporate several diagnostic tests was necessary (3). In the commonly used pathway, corticotropin-releasing hormone (CRH) test, HDDST, pituitary MRI, and bilateral petrosal sinus sampling (BIPSS) were combined to establish the cause of ACTH-dependent CS (1, 12). It was reported that HDDST combined with CRH stimulation test could yield satisfactory accuracy, but CRH is not available in many districts, and the interpretation of CRH test was confusing (1, 12–14). BIPSS is another powerful diagnostic tool with high sensitivity and specificity, but its invasiveness and high cost limit its wide application, and the indication for BIPSS was still controversial (15–17). Besides, the traditional pathway was time consuming, mainly due to the HDDST.

The aim of the present study is to develop an optimized pathway for the differential diagnosis of CD and EAS based on the available tests. In this study, we analyze the data of consecutive low- and high-dose dexamethasone suppression test and BIPSS in a large series, and compared the accuracy of the traditional pathway and our new pathway.

MATERIALS AND METHODS

Patients

Data were retrospectively collected from patients who were evaluated in Peking Union Medical College Hospital from 2011 to 2019. All of the included patients underwent consecutive low- and high-dose dexamethasone suppression test, and their final diagnosis of CD or EAS were pathologically confirmed after surgery or biopsy. The Institutional Review Board of Peking Union Medical College Hospital, Chinese Academy of Medical Sciences approved this study (approval number ZS-1083), and all the patients gave their informed consent for the use of their data.

For patients with suspected CS, serum cortisol, 24-h UFC, and LDDST were routinely conducted to confirm or exclude the diagnosis of CS. Patients were diagnosed as CS if the 24-h UFC after LDDST was not suppressed to below the lower limit of reference interval (12.3 μg). Experienced endocrinologists evaluate the history of the patients, and the onset of symptoms related to hypercortisolism was used to calculated the duration of the disease. After that, ACTH measurement, HDDST, pituitary dynamic enhanced MRI, and BIPSS were conducted as needed to establish the cause of CS. While overnight LDDST can be conducted for outpatients, "standard" 2-day LDDST was usually repeated after hospitalization, most of which were follow by HDDST immediately (see below) in our center. To avoid potential influence from the fluctuation of cortisol secretion, patients who underwent LDDST and HDDST separately were not included in this study.

Dexamethasone Suppression Test

Consecutive low- and high-dose dexamethasone suppression test was conducted according to the protocol by Flack et al. (5). Twenty-four-hour urine on days 1 and 2 was collected, and their average UFC was the baseline. On days 3 and 4, 0.5 mg dexamethasone was administered every 6 h (low-dose), and 24-h UFC was measured on day 4. On days 5 and 6, 2 mg dexamethasone was administered every 6 h (high-dose), and

24-h UFC was measured on day 6. The ratio of 24-h UFC of day 4 and baseline was the result of LDDST, and the ratio of day 6 and baseline was the result of HDDST. In part of the patients, serum cortisol was measured in the morning of days 1, 2, 5, and 7, and the results of LDDST and HDDST were also calculated according to the serum cortisol. Their cutoff values are discussed in detail in the following text.

MRI

Dynamic contrast-enhanced MRI of pituitary was conducted routinely. When distinct hypoenhanced lesion was detected (18), the MRI result was considered to be positive, and the maximum dimension of the lesion was recorded.

BIPSS

The BIPSS procedures were all conducted by the same team of experienced radiologist according to the protocol described by Doppman et al. (19). In brief, catheters were guided into inferior petrosal sinus (IPS) through bilateral femoral veins, and blood samples were collected from peripheral vein and bilateral IPS simultaneously at baseline and 3, 5, and 10 min after desmopressin (10 μg iv) stimulation. There was no major complication among all the patients in this series. The IPS to peripheral ACTH ratio (IPS:P) was calculated. An IPS:P of more than 2 before stimulation or more than 3 at any time after stimulation supports the diagnosis of CD.

Hormone Assay

Serum and urine cortisol was measured by direct chemiluminescence immunoassay (Siemens ADVIA Centaur). ACTH samples were delivered on ice and measured by chemiluminescence immunoassay (Siemens IMMULITE 2000).

Comparison of Diagnostic Pathways

A subgroup were selected from the above-mentioned patients for the comparison of our new diagnostic pathway and the traditional pathway. The inclusion criteria were as follows: (i) the patient underwent BIPSS with desmopressin stimulation and (ii) the size of pituitary adenoma as measured by MRI were available. The accuracy of each pathway were retrospectively calculated according to these data. The traditional pathway was based on those reviewed by Lacroix et al. (1) and Sharma et al. (12), but the CRH stimulation test was omitted since it was unavailable in our center. In accordance with the recent guideline, BIPSS was not indicated among patients with tumor ≥6 mm on pituitary MRI in both the new and the traditional pathway in our study (16).

Statistical Analysis

Normal variables decided by Shapiro–Wilk test were presented as average ± standard deviation and non-normal variables as median (first quartile, third quartile), and they were analyzed by t-test or non-parametric test, respectively. Chi-square test or Fisher's exact test was used to analyzed categorical data. A $p < 0.05$ was considered statistically significant. Receiver operating characteristic (ROC) analysis was conducted, and the area under curve (AUC) was calculated to compare the diagnostic efficacy of different tests. For each diagnostic test, the cutoff to maximize the Youden index (sensitivity + specificity − 1) was calculated (20), and the cutoff to maximize the specificity. These analyses were performed using SPSS 25.0 and MedCalc 19.6.1.

RESULTS

Characteristics of Patients

A total of 269 CD patients and 29 EAS patients were included in our study. The average age of all the included patients was 35.6 ± 12.7 years (range, 10–75 years). CD patients were predominantly female (84.4%), while 48.3% of the EAS patients were female ($p < 0.001$). Compared with the EAS patients, the CD patients had a longer duration of disease and lower morning cortisol, ACTH and 24-h UFC (all $p < 0.001$). Besides, the serum potassium level was significantly lower among the EAS patients ($p = 0.003$). Pituitary MRI results were positive among 88.4% (237/268) of the CD patients, while 25.0% (7/28) of the EAS patients also had positive MRI findings ($p < 0.001$). Their detailed clinical characteristics are presented in **Table 1**.

For the 29 EAS patients, the ectopic tumor was mainly located at lung (15 patients, 51.7%) or mediastinum (10 patients, 34.5%). Three EAS cases were caused by pheochromocytoma, medullary thyroid carcinoma, and pelvic primitive neuroectodermal tumor, respectively (one patient for each type). The remaining one patient underwent biopsy of bone metastasis to establish the diagnosis of EAS, but the primary lesion was not pathologically confirmed.

UFC and Serum Cortisol in DST

The data of both UFC and serum cortisol during DST were available among 108 CD patients and 10 EAS patients, and the diagnostic accuracy of LDDST and HDDST were compared among these patients (**Figure 1**). The LDDST calculated by UFC yielded an AUC of 0.881 (95%CI, 0.808–0.933), while that of LDDST by serum cortisol was 0.685 (95%CI, 0.593–0.768), the difference of which was significant ($p < 0.001$). The difference of HDDST by UFC or serum cortisol (0.847; 95%CI, 769–0.907 *vs.* 0.785, 95% CI, 0.700–0.855) was not significant ($p = 0.210$). Subsequent analyses on DST in this research were based on the results calculated by UFC.

LDDST and HDDST

After LDDST, the median 24-h UFC was 117.9 (59.2, 299.8) μg for CD and 1,053.4 (572.9, 2,450.0) μg for EAS (**Figure 2A**).

TABLE 1 | Clinical characteristics of patients with CD and EAS.

	CD (n = 269)	EAS (n = 29)	p-value
Age (years)	35.6 ± 12.6	35.8 ± 13.8	0.951
Sex (male/female)	42:227 (0.19:1)	15:14 (1.07:1)	<0.001
BMI (kg/m^2)	26.6 ± 4.2	25.7 ± 3.2	0.278
Duration of disease (months)	36 (24, 72)	12 (4, 25)	<0.001
Serum K+ (mmol/L)	3.8 ± 0.6	3.2 ± 0.8	0.003
Morning cortisol (μg/dl)	26.7 (21.7, 32.9)	35.4 (27.6, 52.0)	<0.001
ACTH (ng/L)	65.6 (45.9, 98.3)	135.0 (82.4, 238.0)	<0.001
24-h UFC (μg)	423.8 (279.0, 680.6)	1,280.9 (396.4, 2,299.8)	<0.001
Positive pituitary MRI	88.4% (237/268)	25.0% (7/28)	<0.001

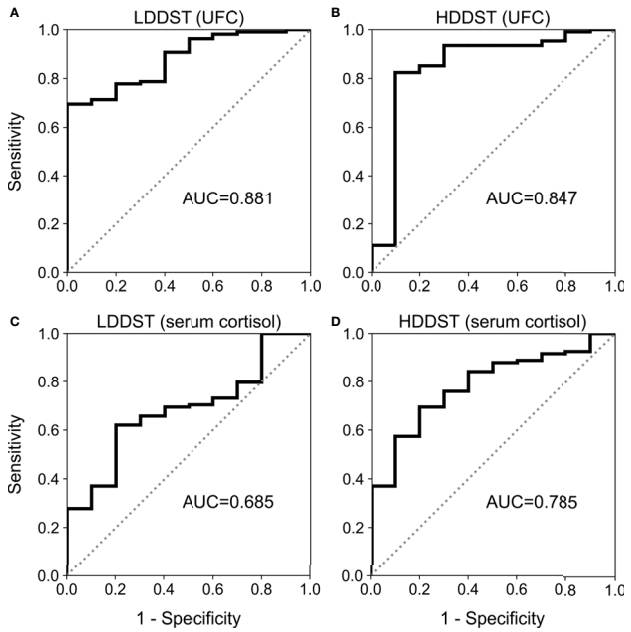

FIGURE 1 | Receiver operating characteristic (ROC) curve for low-dose dexamethasone suppression test (LDDST) or high-dose dexamethasone suppression test (HDDST) using urine-free cortisol (UFC) **(A, B)** or serum cortisol **(C, D)** among 108 CD and 10 EAS patients with both serum and urine cortisol measurement during dexamethasone suppression test.

The 24-h UFC were suppressed to a median of 33.9% (20.0%, 55.3%) of baseline among the CD patients and 97.0% (65.2%, 123.6%) of baseline among the EAS patients (**Figure 2B**). The greatest suppression among the EAS patients was 26.1% of baseline, while the greatest suppression among the CD patients was 2.7% of baseline.

After HDDST, the median 24-h UFC was 36.5 (20.4, 122.8) μg for the CD patients, and 1,123.7 (350.8, 1,856.4) μg for the EAS patients (**Figure 2A**). The 24-h UFC were suppressed to a median of 10.7% (4.9%, 25.0%) of baseline for the CD patients and 66.1% (43.2%, 114.0%) of baseline for the EAS patients (**Figure 2B**). Thirteen CD patients were suppressed to undetectable level, while the lowest 24-h UFC after HDDST among the EAS patients was 3.5 μg (1.8% of baseline).

ROC Analysis and Diagnostic Accuracy

The results of ROC analysis are demonstrated in **Figure 3**. The area under curve (AUC) for LDDST was 0.883 (95%CI, 0.840–0.916). The AUC for HDDST was 0.834 (95%CI, 0.787–0.874).

The cutoff to maximize the Youden index was suppressed to <52.3% of baseline for LDDST, and was <37.6% of baseline for HDDST. The cutoff to maximize the specificity was suppressed to <26.0% of baseline for LDDST and was <1.7% of baseline for HDDST. The corresponding values of sensitivity and specificity are listed in **Table 2**. While retaining 100% specificity, the highest sensitivity was reached when the cutoff of <26% of baseline after LDDST was used, which yield a sensitivity of 39.4%. On the contrary, the sensitivity of HDDST was only 7.8% when the cutoff to retain 100% specificity (<1.7% of baseline) was used. The commonly used cutoff for HDDST (<50% of baseline) yielded a sensitivity of 90.0% and a specificity of only 62.1%.

Comparison of CD Patients who Were Suppressed or Unsuppressed During LDDST

When the cutoff of <26% of baseline was adopted during LDDST, 106 CD patients were suppressed while 163 CD patients were not

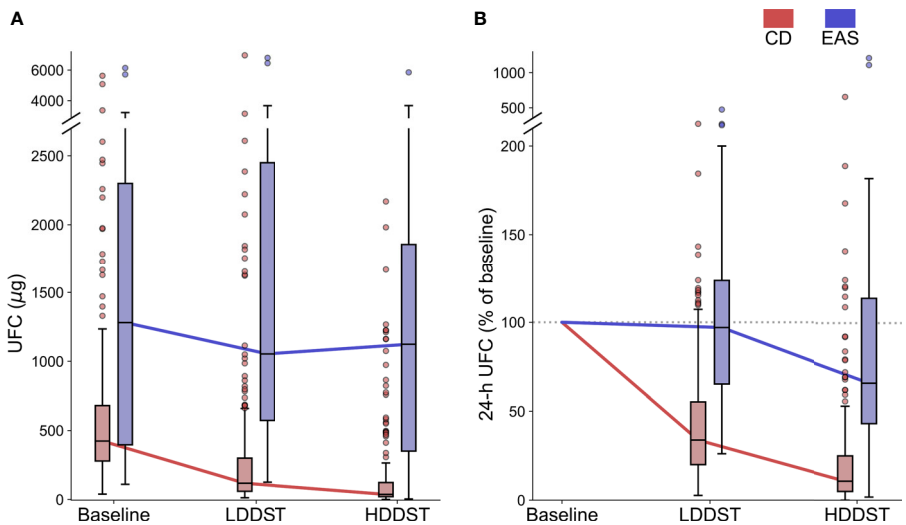

FIGURE 2 | Change of UFC during consecutive low-dose dexamethasone suppression test (LDDST) and high-dose dexamethasone suppression test (HDDST) for CD (red) and EAS (blue) patients. **(A)** 24-h UFC at baseline, after LDDST, and after HDDST. **(B)** The ratio of 24-h UFC after dexamethasone suppression test and baseline. Box: interquartile range (IQR). Horizontal line inside each box: median. Whisker: maximum and minimum within median ± 1.5 × IQR. Circle: outlier outside 1.5 IQR.

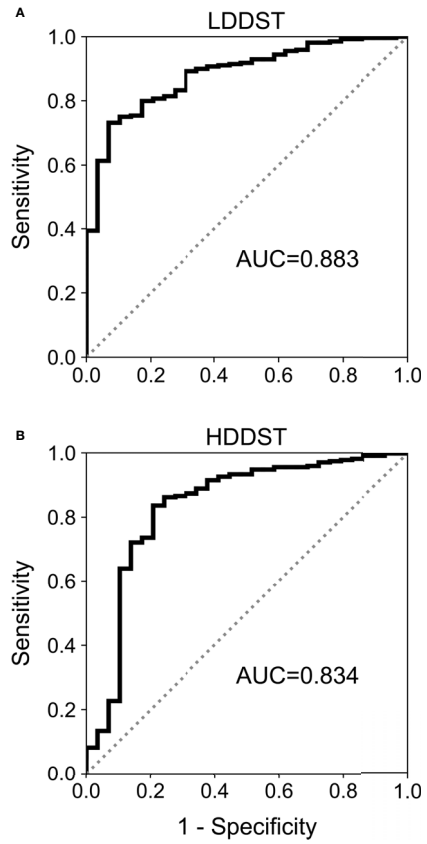

FIGURE 3 | Receiver operating characteristic (ROC) curves for **(A)** low-dose dexamethasone suppression test (LDDST) and **(B)** high-dose dexamethasone suppression test (HDDST) among all the included patients.

suppressed, and the comparisons of their clinical characteristics along with EAS patients are shown in **Figure 4** (significance of difference was only calculated for suppressed and unsuppressed CD patients). The body mass index (BMI) ($p = 0.257$), duration of disease ($p = 0.722$), and 24-h UFC ($p = 0.063$) of suppressed and unsuppressed CD patients were not significant different. Among the CD patients who cannot be suppressed during LDDST, the serum potassium level ($p = 0.006$) were significantly lower. In contrast, their age ($p = 0.001$), morning cortisol ($p = 0.008$), ACTH level ($p < 0.001$), and 24-h UFC after HDDST ($p < 0.001$) were significantly higher than those who were suppressed during LDDST. Besides, 13.2% (14/106) of the suppressed patients were male, while 17.2% (28/163) of the unsuppressed patients were male ($p = 0.397$).

Comparison of New and Traditional Diagnostic Pathway

A subgroup of 146 patients were selected for the comparison of the two diagnostic pathway, including 131 CD patients and 15 EAS patients. The age, BMI, duration of disease, morning cortisol, ACTH, and 24-h UFC were not significantly different between the selected and the excluded patients (data not shown).

Our new diagnostic pathway that incorporated LDDST and BIPSS was illustrated in **Figure 5A**. The overall sensitivity for this pathway was 97.7% (128/131), which was comparable to the sensitivity of the traditional pathway (100%, 131/131) (**Figure 5B**). The specificity of the new pathway was 86.7% (13/15), which was much higher than that of the traditional pathway (33.3%, 5/15). In the new pathway, BIPSS was needed in 65 (44.5%) patients, while 18 (12.3%) patients needed BIPSS in the traditional pathway.

DISCUSSION

To the best of our knowledge, this is the largest series to compare the value of LDDST and HDDST in discriminating CD and EAS among pathologically confirmed cases. We found that LDDST could not only differentiate CD and EAS with higher efficacy than HDDST but also reached a relatively high sensitivity when the specificity retained 100%. Based on this feature, a simplified pathway that incorporated LDDST could be designed for the differential diagnosis of ACTH-dependent CS, and HDDST might be abandoned to avoid potential side effects.

Before further discussion about LDDST and HDDST, the measures in these tests, that is, UFC or serum cortisol, should be clarified first. Although it was recommended to use serum cortisol in LDDST in diagnosis of CS (21), our study found that UFC performed better in LDDST for the differential

TABLE 2 | Utility of low- and high-dose dexamethasone suppression test for the differential diagnosis of CD and EAS.

Criteria for suppression	CD, suppressed (TP)	EAS, not suppressed (TN)	EAS, suppressed (FP)	CD, not suppressed (FN)	Sensitivity % (95%CI)	Specificity % (95%CI)
LDDST <52.3%	197	27	2	72	73.2 (67.5, 78.4)	93.1 (77.2, 99.2)
LDDST <26.0%	106	29	0	163	39.4 (33.5, 45.5)	100 (88.1, 100)
HDDST <37.6%	225	23	6	44	83.6 (78.7, 87.9)	79.3 (60.3, 92)
HDDST <50%	242	18	11	27	90.0 (85.7, 93.3)	62.1 (42.3, 79.3)
HDDST <1.7%	21	29	0	248	7.8 (4.9, 11.7)	100 (88.1, 100)

TP, true positive; TN, true negative; FP, false positive; FN, false negative.

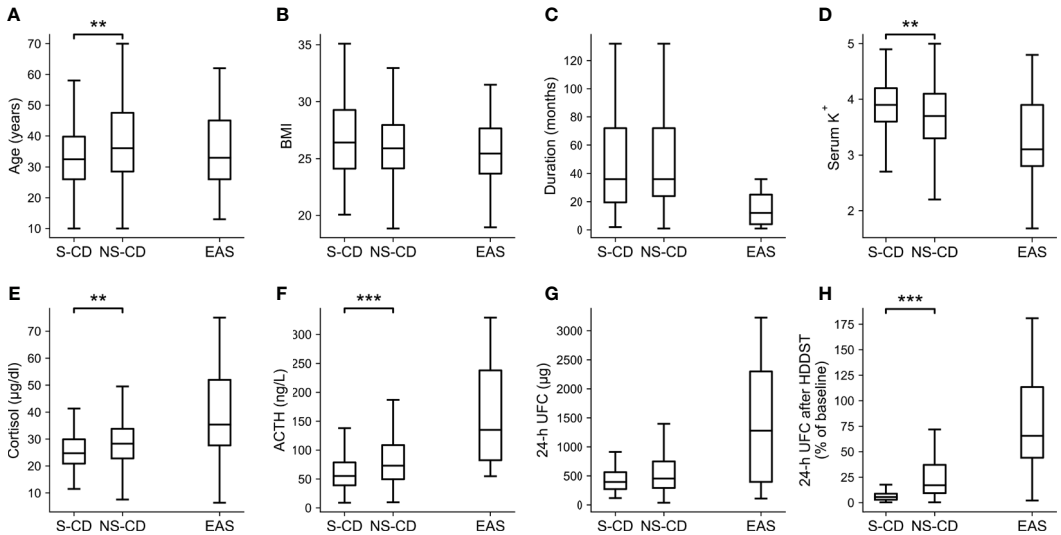

FIGURE 4 | Clinical characteristics of the CD patients whose UFC was suppressed (S-CD) or cannot be suppressed (NS-CD) to <26% of baseline during LDDST and the EAS patients. **(A)** Age. **(B)** Body mass index (BMI). **(C)** Duration of disease. **(D)** Serum potassium level. **(E)** Morning cortisol. **(F)** ACTH. **(G)** 24-hour urine free cortisol (UFC). **(H)** 24-h UFC after high-dose dexamethasone suppression test. Box: interquartile range (IQR). Line inside the box: median. Whisker: maximum and minimum within median ± 1.5 × IQR. Outliers outside 1.5 IQR were not shown. Comparisons were only made between S-CD and US-CD but not EAS. *p < 0.05. **p < 0.01. ***p < 0.001.

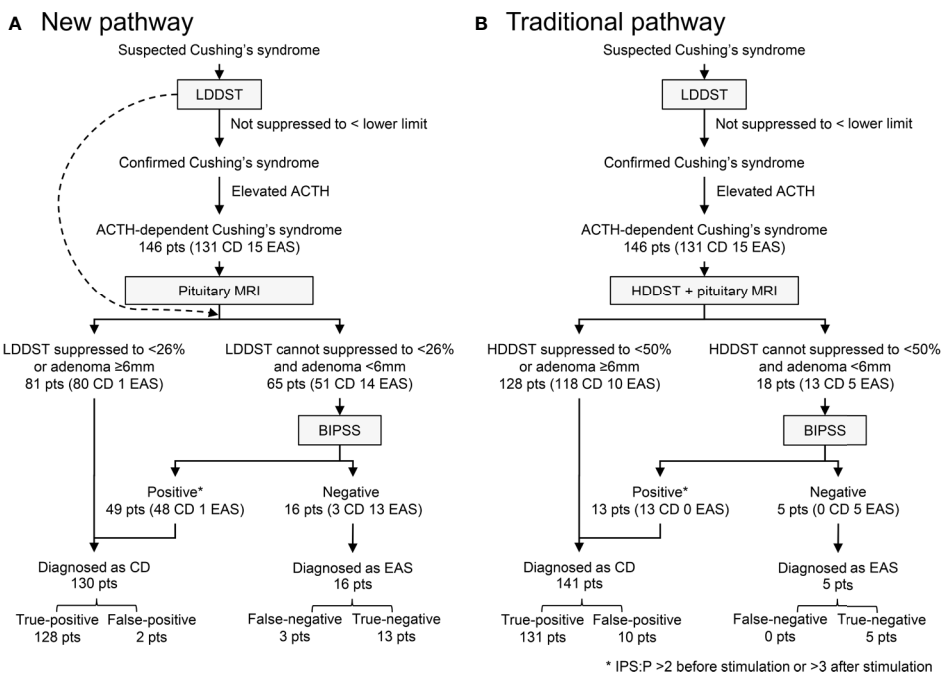

FIGURE 5 | Diagnostic utility of new **(A)** and traditional **(B)** pathway. IPS:P refers to inferior petrosal sinus to peripheral ACTH gradient.

diagnosis of CD and EAS. As for HDDST, our head-to-head comparison showed that serum cortisol and UFC had similar efficacy, which was consistent with previous studies that different measures were used in different patients or centers (22, 23). As a result, UFC was used in LDDST in this study and also in HDDST to ensure comparability.

The prevalence of CD is much higher than EAS (1), and conducting pituitary surgery in EAS patients due to misdiagnosis

is more unacceptable than delaying the diagnosis of CD. Thus, an ideal test to distinguish CD from EAS should have a high specificity even with a compromised sensitivity. In this sense, HDDST might not be competent due to its unsatisfactory specificity. The difference in response to dexamethasone in CD and EAS was in a quantitative rather than a qualitative manner, and the cortisol secretion in some EAS patients can actually be suppressed to a very low level after HDDST in our study, which greatly reduced its specificity. Similarly, previous studies also reported that HDDST could hardly reach a high specificity with an acceptable sensitivity (3, 4, 9). On the contrary, EAS patients only showed minimal suppression during LDDST, while quite a few CD patients was greatly suppressed. In fact, LDDST not only had higher AUC but also better specificity with enough sensitivity in our study when an appropriate cutoff was selected, which was in concordance with the study by Isidori et al. (7). With a high specificity, patients with suppressed LDDST could be diagnosed as CD almost without exception.

After LDDST with our high-specificity cutoff, only a part of the CD patients along with all the EAS patients needed further tests to establish their causes of CS, but this is a more difficult task since this subgroup of patients were quite similar. According to our observations, the pituitary tumors in these CD patients with unsuppressed LDDST might be more active and autonomous than those that can be suppressed. They produced more ACTH and responded less to the negative feedback from glucocorticoid, mimicking the behavior of ectopic tumors to some extent. Thus, conducting HDDST after LDDST could hardly produce additional information for the differential diagnosis.

Based on the combination of LDDST, pituitary MRI, and BIPSS, we designed a new pathway for the differential diagnosis of CD and EAS. After establishing the diagnosis of ACTH-dependent CS, LDDST should be the first test to schedule. Patients whose 24-h UFC can be suppressed to <26% of baseline during LDDST are considered as "typical" CD, and further diagnostic tests are unnecessary for them. Otherwise, patients with unsuppressed LDDST should consider BIPSS. Further selection was made according to the recent guideline (16), so BIPSS was only indicated for patients with unsuppressed LDDST and tumor below 6 mm. If BIPSS is not available or the patients refuse such invasive test, LDDST can also be a substitute for HDDST since LDDST has higher AUC. In this scenario, the cutoff with maximal Youden index can be adopted to balance the sensitivity and the specificity.

Compared with the traditional pathway, this new pathway could discriminate CD and EAS with a similar sensitivity but much higher specificity. The time to establish the diagnosis was much shorter, and most of the tests could even be finished in outpatient. Moreover, the side effect of glucocorticoid such as fluctuation in blood pressure or blood glucose could be minimized, since only a small dose of dexamethasone was administered during LDDST.

The combination of multiple tests is necessary for the accurate and robust differential diagnosis of CD and EAS. The most valuable tests include biochemical test like DST and CRH stimulation test, imaging studies such as pituitary dynamic enhanced MRI and radioisotope studies, and BIPSS (24). BIPSS was a reliable test for the differential diagnosis of CD and EAS with an excellent sensitivity and a specificity of near 100% (17, 25). However, BIPSS is invasive and expensive, and currently, it is not widely available. Thus, identifying those who need BIPSS most is a critical step in the diagnostic pathway. A well-established strategy is to waive BIPSS among those patients with adenoma over 6 mm on MRI plus concordant HDDST and CRH stimulation test (1, 12). However, CRH test is also not widely available, and HDDST is time consuming and complicated. Luckily, the current study found that LDDST in combination with pituitary MRI might serve as a filter to ruled out those "typical" CD who could be correctly diagnosed without BIPSS, which was more accurate and convenient than the traditional pathway based on the combination of HDDST and MRI in the absence of CRH test.

It should be noticed that the new pathway in this study may not be the optimal one. On the one hand, a pituitary adenoma over 6 mm was observed in some EAS patients in the current series, so this cutoff may need optimization. On the other hand, it was regrettable that CRH test was not included in our pathway. CRH test is more convenient than BIPSS, and the combination of CRH test and HDDST was reported to be highly accurate (12–14). However, CRH stimulation test was not carried out since CRH was not available in our area. We believe that the incorporation of CRH test in our pathway might further improve the accuracy and reduce the reliance on BIPSS. The combination of LDDST and CRH test can be validated in centers where CRH is available.

Our study had some limitations. Some patients, especially EAS patients, underwent LDDST and HDDST separately in our center. These patients were not included in this study, and it is unclear whether they had major difference with the included patients. The comparison of pathways was also conducted retrospectively, and some "typical" patients did not undergo BIPSS. These factors might introduce selection bias. Besides, this is a single-center study, and the cutoff should be validated in other centers.

In conclusion, the optimized pathway that combined LDDST, pituitary MRI, and BIPSS could differentiate CD and EAS accurately. LDDST could effectively identify the cases who were difficult to differentiate and really needed advanced tests such as BIPSS, and thus, it might replace HDDST to save several days of examination and to prevent risks due to elevated cortisol, making the pathway simpler.

DATA AVAILABILITY STATEMENT

The raw data supporting the conclusions of this article will be made available by the authors, without undue reservation.

ETHICS STATEMENT

The studies involving human participants were reviewed and approved by Institutional Review Board of Peking Union

Medical College Hospital, Chinese Academy of Medical Sciences. Written informed consent to participate in this study was provided by the participants' legal guardian/next of kin.

AUTHOR CONTRIBUTIONS

KC collected and analyzed the data and prepared the manuscript. SC and LL conceptualized the study and revised the manuscript. HZ, XZ, AT, and RW managed the patients and revised the manuscript. HP and ZL supervised the study. All authors contributed to the article and approved the submitted version.

FUNDING

This work was supported by the CAMS Innovation Fund for Medical Science (grant number CAMS-2017-I2M-1-011) and the National Key Research and Development Program of China (grant number 2016YFC0901500).

REFERENCES

1. Lacroix A, Feelders RA, Stratakis CA, Nieman LK. Cushing's Syndrome. *Lancet* (2015) 386(9996):913–27. doi: 10.1016/S0140-6736(14)61375-1
2. Liddle GW. Tests of Pituitary-Adrenal Suppressibility in the Diagnosis of Cushing's Syndrome. *J Clin Endocrinol Metab* (1960) 20(12):1539–60. doi: 10.1210/jcem-20-12-1539
3. Arnaldi G, Angeli A, Atkinson AB, Bertagna X, Cavagnini F, Chrousos GP, et al. Diagnosis and Complications of Cushing's Syndrome: A Consensus Statement. *J Clin Endocrinol Metab* (2003) 88(12):5593–602. doi: 10.1210/jc.2003-030871
4. Newell-Price J, Trainer P, Besser M, Grossman A. The Diagnosis and Differential Diagnosis of Cushing's Syndrome and Pseudo-Cushing's States. *Endocr Rev* (1998) 19(5):647–72. doi: 10.1210/edrv.19.5.0346
5. Flack MR, Oldfield EH, Cutler GBJr., Zweig MH, Malley JD, Chrousos GP, et al. Urine Free Cortisol in the High-Dose Dexamethasone Suppression Test for the Differential Diagnosis of the Cushing Syndrome. *Ann Intern Med* (1992) 116(3):211–7. doi: 10.7326/0003-4819-116-3-211
6. Dichek HL, Nieman LK, Oldfield EH, Pass HI, Malley JD, Cutler GBJr. A Comparison of the Standard High Dose Dexamethasone Suppression Test and the Overnight 8-Mg Dexamethasone Suppression Test for the Differential Diagnosis of Adrenocorticotropin-Dependent Cushing's Syndrome. *J Clin Endocrinol Metab* (1994) 78(2):418–22. doi: 10.1210/jcem.78.2.8106630
7. Isidori AM, Kaltsas GA, Mohammed S, Morris DG, Jenkins P, Chew SL, et al. Discriminatory Value of the Low-Dose Dexamethasone Suppression Test in Establishing the Diagnosis and Differential Diagnosis of Cushing's Syndrome. *J Clin Endocrinol Metab* (2003) 88(11):5299–306. doi: 10.1210/jc.2003-030510
8. Findling JW, Kehoe ME, Shaker JL, Raff H. Routine Inferior Petrosal Sinus Sampling in the Differential Diagnosis of Adrenocorticotropin (ACTH)-Dependent Cushing's Syndrome: Early Recognition of the Occult Ectopic ACTH Syndrome. *J Clin Endocrinol Metab* (1991) 73(2):408–13. doi: 10.1210/jcem-73-2-408
9. Aron DC, Raff H, Findling JW. Effectiveness *Versus* Efficacy: The Limited Value in Clinical Practice of High Dose Dexamethasone Suppression Testing in the Differential Diagnosis of Adrenocorticotropin-Dependent Cushing's Syndrome. *J Clin Endocrinol Metab* (1997) 82(6):1780–5. doi: 10.1210/jcem.82.6.3991
10. Dias R, Storr HL, Perry LA, Isidori AM, Grossman AB, Savage MO. The Discriminatory Value of the Low-Dose Dexamethasone Suppression Test in the Investigation of Paediatric Cushing's Syndrome. *Horm Res* (2006) 65 (3):159–62. doi: 10.1159/000091830
11. Savage MO, Chan LF, Grossman AB, Storr HL. Work-Up and Management of Paediatric Cushing's Syndrome. *Curr Opin Endocrinol Diabetes Obes* (2008) 15(4):346–51. doi: 10.1097/MED.0b013e328305082f
12. Sharma ST, Committee AAS. An Individualized Approach to the Evaluation of Cushing Syndrome. *Endocr Pract* (2017) 23(6):726–37. doi: 10.4158/EP161721.RA
13. Hermus AR, Pieters GF, Pesman GJ, Smals AG, Benraad TJ, Kloppenborg PW. The Corticotropin-Releasing-Hormone Test *Versus* the High-Dose Dexamethasone Test in the Differential Diagnosis of Cushing's Syndrome. *Lancet* (1986) 2(8506):540–4. doi: 10.1016/s0140-6736(86)90113-3
14. Barbot M, Trementino L, Zilio M, Ceccato F, Albiger N, Daniele A, et al. Second-Line Tests in the Differential Diagnosis of ACTH-Dependent Cushing's Syndrome. *Pituitary* (2016) 19(5):488–95. doi: 10.1007/s11102-016-0729-y
15. Oldfield EH, Doppman JL, Nieman LK, Chrousos GP, Miller DL, Katz DA, et al. Petrosal Sinus Sampling With and Without Corticotropin-Releasing Hormone for the Differential Diagnosis of Cushing's Syndrome. *N Engl J Med* (1991) 325(13):897–905. doi: 10.1056/NEJM199109263251301
16. Nieman LK, Biller BM, Findling JW, Murad MH, Newell-Price J, Savage MO, et al. Treatment of Cushing's Syndrome: An Endocrine Society Clinical Practice Guideline. *J Clin Endocrinol Metab* (2015) 100(8):2807–31. doi: 10.1210/jc.2015-1818
17. Chen S, Chen K, Wang S, Zhu H, Lu L, Zhang X, et al. The Optimal Cut-Off of BIPSS in Differential Diagnosis of ACTH-Dependent Cushing's Syndrome: Is Stimulation Necessary? *J Clin Endocrinol Metab* (2020) 105(4):e1673–85. doi: 10.1210/clinem/dgz194
18. Kanou Y, Arita K, Kurisu K, Tomohide A, Iida K. Clinical Implications of Dynamic MRI for Pituitary Adenomas: Clinical and Histologic Analysis. *J Clin Neurosci* (2002) 9(6):659–63. doi: 10.1054/jocn.2002.1141
19. Doppman JL, Oldfield E, Krudy AG, Chrousos GP, Schulte HM, Schaaf M, et al. Petrosal Sinus Sampling for Cushing Syndrome: Anatomical and Technical Considerations. Work in Progress. *Radiology* (1984) 150(1):99–103. doi: 10.1148/radiology.150.1.6316418
20. Youden WJ. Index for Rating Diagnostic Tests. *Cancer* (1950) 3(1):32–5. doi: 10.1002/1097-0142(1950)3:1<32::aid-cncr2820030106>3.0.co;2-3
21. Nieman LK, Biller BM, Findling JW, Newell-Price J, Savage MO, Stewart PM, et al. The Diagnosis of Cushing's Syndrome: An Endocrine Society Clinical Practice Guideline. *J Clin Endocrinol Metab* (2008) 93(5):1526–40. doi: 10.1210/jc.2008-0125
22. Invitti C, Giraldi FP, De Martin M, Cavagnini F, Angeli A, Terzolo M, et al. Diagnosis and Management of Cushing's Syndrome: Results of an Italian Multicentre Study. *J Clin Endocrinol Metab* (1999) 84(2):440–8. doi: 10.1210/jc.84.2.440
23. Valassi E, Franz H, Brue T, Feelders RA, Netea-Maier R, Tsagarakis S, et al. Diagnostic Tests for Cushing's Syndrome Differ From Published Guidelines: Data From ERCUSYN. *Eur J Endocrinol* (2017) 176(5):613–24. doi: 10.1530/eje-16-0967
24. Witek P, Witek J, Zieliński G, Podgajny Z, Kamiński G. Ectopic Cushing's Syndrome in Light of Modern Diagnostic Techniques and Treatment Options. *Neuro Endocrinol Lett* (2015) 36(3):201–8.
25. Pecori Giraldi F, Cavallo LM, Tortora F, Pivonello R, Colao A, Cappabianca P, et al. The Role of Inferior Petrosal Sinus Sampling in ACTH-Dependent Cushing's Syndrome: Review and Joint Opinion Statement by Members of the Italian Society for Endocrinology, Italian Society for Neurosurgery, and Italian Society for Neuroradiology. *Neurosurg Focus* (2015) 38(2):E5. doi: 10.3171/2014.11.FOCUS14766

Conflict of Interest: The authors declare that the research was conducted in the absence of any commercial or financial relationships that could be construed as a potential conflict of interest.

Publisher's Note: All claims expressed in this article are solely those of the authors and do not necessarily represent those of their affiliated organizations, or those of the publisher, the editors and the reviewers. Any product that may be evaluated in this article, or claim that may be made by its manufacturer, is not guaranteed or endorsed by the publisher.

frontiers in Endocrinology

ORIGINAL RESEARCH
published: 29 September 2021
doi: 10.3389/fendo.2021.752361

Molecular Profile of a Pituitary Rhabdomyosarcoma Arising From a Pituitary Macroadenoma: A Case Report

*Jinci Lu and Liam Chen**

Department of Laboratory Medicine and Pathology, University of Minnesota Medical School, Minneapolis, MN, United States

OPEN ACCESS

Edited by:
Run Yu,
UCLA David Geffen School of Medicine, United States

Reviewed by:
Xiaohai Liu,
Capital Medical University, China
Akira Sugawara,
Tohoku University, Japan

***Correspondence:**
Liam Chen
llchen@umn.edu

Specialty section:
This article was submitted to Pituitary Endocrinology, a section of the journal Frontiers in Endocrinology

Received: *02 August 2021*
Accepted: *13 September 2021*
Published: *29 September 2021*

Citation:
Lu J and Chen L (2021) Molecular Profile of a Pituitary Rhabdomyosarcoma Arising From a Pituitary Macroadenoma: A Case Report. Front. Endocrinol. 12:752361. doi: 10.3389/fendo.2021.752361

Pituitary sarcoma arising in association with pituitary adenoma is an uncommon finding. Most cases of secondary sarcoma have been noted to arise with a median interval of 10.5 years post radiation. In this case report, we describe a 77-year-old man with an incidental discovery of a pituitary macroadenoma on magnetic resonance imaging (MRI) and underwent radiotherapy. Three years after radiation treatment, there was an acute change in clinical symptoms and increase in tumor size and mass effect on the optic chiasm which prompted surgical resection. A pituitary adenoma along with a separate spindle-cell sarcomatous component was identified in histology. Immunohistochemical stain for muscle markers confirmed a development of pituitary rhabdomyosarcoma (RMS). Molecular profiling of the tumor identified mutations in TP53, ATRX, LZTR1, and NF1. Despite its rarity, characterization of pituitary RMS with immunohistochemistry and molecular studies may provide an insight to its pathophysiological relationship with pituitary adenoma.

Keywords: pituitary adenoma, rhabdomyosarcoma, TP53, ATRX, LZTR1, NF1

INTRODUCTION

RMS is a malignant skeletal muscle sarcoma that commonly occurs in children and rarely in adults. It is uncommon for RMS to arise intracranially, especially within the sellar region. Sellar RMS have been mostly reported in association with radiation for pituitary tumors (1, 2). Though rare, there are a few reported cases of pituitary RMS arising from pituitary adenoma without any prior therapy (3–6). It has been suggested in the literature that the median latency period between radiotherapy and tumor occurrence is 10.5 years (7). In this case report, we present the first molecular characterization of a pituitary RMS arising from a pituitary macroadenoma, three years post radiotherapy.

CASE REPORT

A 77-year-old man with a history of Waldenstrom macroglobulinemia and prostate cancer initially presented to the emergency department complaining of fall. In MRI, an incidental finding of a heterogeneously enhancing and T2 signaling sellar mass with extension to suprasellar cistern measuring 2 x 2.7 x 2 cm^3 (TR x AP x CC) was identified (**Figures 1A–D**). Additionally, the lesion encased two-thirds of the left cavernous carotid artery along with significant mass effect on the optic chiasm. The patient was referred to follow up with Neurosurgery and Endocrinology, and it was diagnosed as a pituitary macroadenoma. At the time of diagnosis, the patient had minimal visual field deficits, specifically left-side blurriness. The patient also had secondary hypopituitarism which was replaced with levothyroxine, prednisone, and elected not to take testosterone. Given the patient's age and comorbidities, it was decided that medical management is the best course of action. The patient underwent 28 fractions of volumetric modulated arc therapy with a total dosage of 5040 cGy.

Over the course of three years, the size of the pituitary mass was relatively stable until early 2021. The mass then was measuring 3.3 x 3.0 x 2.6 cm^3 with a significant increase in mass effect on adjacent structures (**Figures 1E–H**). The patient was also experiencing acute change in his vision, especially on their left eye. To preserve the patient's vision, stealth-guided transnasal endoscopic resection of the pituitary macroadenoma was performed, and specimens were sent for microscopic examination.

Histological studies of the resected tumor revealed pituitary adenoma with the loss of acinar architecture and ribbon-like arrays (**Figure 2A**). In addition, there was a presence of spindle-like cells with necrosis and brisk mitotic activity (**Figure 2B**). Immunohistochemical stain for synaptophysin, adrenocorticotropic (ACTH) and growth hormone (GH) was positive for the pituitary adenoma but not the sarcomatous component (**Figures 2C–E**). Instead, the sarcomatous component was positive for desmin, myogenin, and p53, confirming the diagnosis of a pituitary RMS arising from the pituitary adenoma (**Figures 2F–H**). NextGen Sequencing (NGS) was also performed on the RMS part, and the following pathological mutations were identified: *TP53* (c.503A>G, p.H168R), *ATRX* (c.5406dup, p.R1803Tfs*7), *LZTR1* (c.791+1G>A), and *NF1* (c.2998del, p.R1000Vfs*12).

DISCUSSION

Pituitary sarcoma arising from pituitary adenoma are extremely rare, and most cases have been reported to be associated with prior radiation. Although our patient had prior radiation, it was only three years prior compared to the median interval of 10.5 years between radiation and tumor occurrence (7). Thus, it is more likely of a pituitary sarcoma arising from the adenoma rather than a radiation-induced tumor. As proposed by de Silva et al., this may potentially be a metaplastic transformation from the pituitary adenoma or two independent lesions, with the RMS

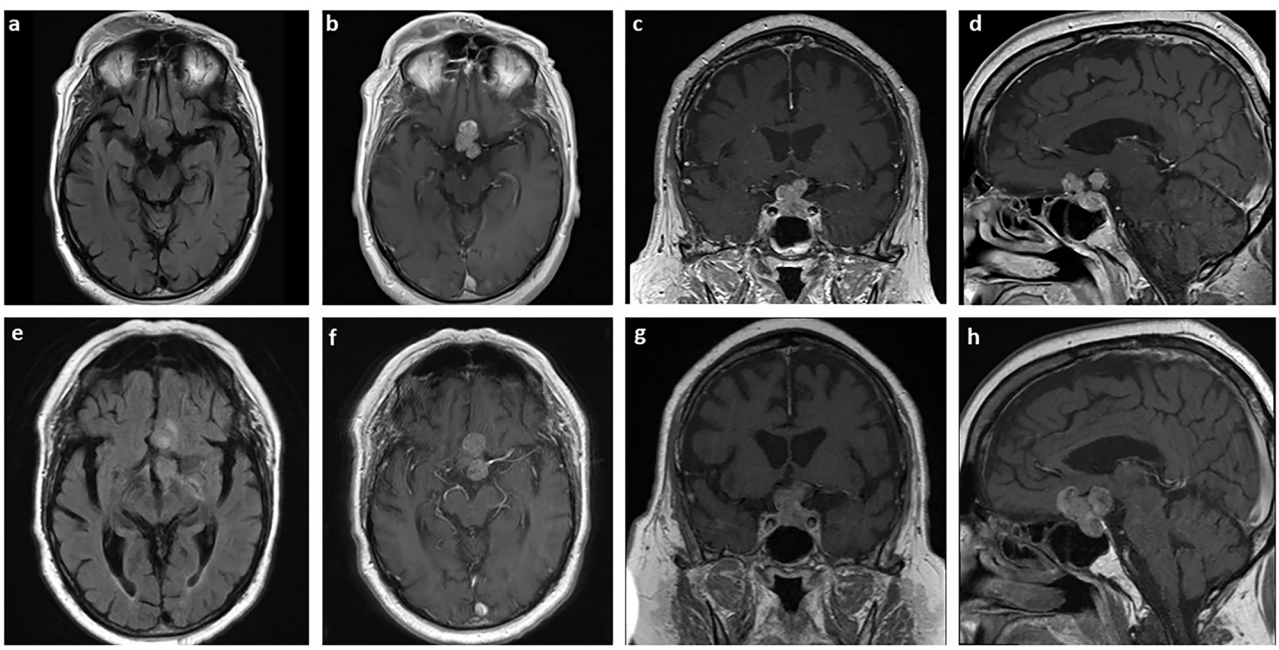

FIGURE 1 | MRI of the pituitary sarcoma arising from a pituitary adenoma. Axial T2 FLAIR **(A)** and axial **(B)**, coronal **(C)**, and sagittal **(D)** T1-weighted with contrast MRI of tumor measuring 2 x 2.7 x 2 cm^3 at the time of diagnosis. The same sections are shown for the tumor three years later, prior to surgical resection, measuring 3.3 x 3.0 x 2.6 cm^3 **(E–H)**.

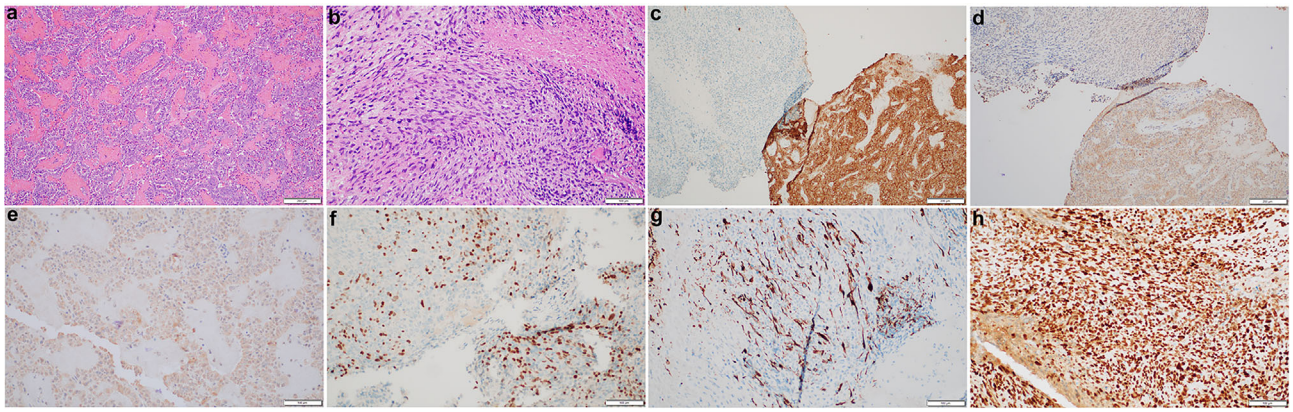

FIGURE 2 | Histopathological and immunohistochemical characterization of the pituitary sarcoma arising from a pituitary adenoma. H&E stains of the pituitary adenoma **(A)** and a concurrent sarcoma which has brisk mitotic activity and necrosis **(B)**. The adenoma is immunoreactive for synaptophysin **(C)**, ACTH **(D)** and GH **(E)** whereas the sarcomatous component has lost synaptophysin stain **(C)**, but become patchy positive for myogenin **(F)**, desmin **(G)**, and diffusely positive for p53 **(H)**.

originating from primitive mesenchymal in the dura mater of the sellar floor or in pericapillary space of the pituitary gland (5, 6). Another interesting finding is the presence of multiple genetic mutations in the tumor. *TP53* mutations are common in sarcomas, including leiomyosarcoma, liposarcomas, and RMS (8–12). Loss of *ATRX* is highly associated with alternative lengthening of telomeres, and it is frequently found in complex sarcomas (8, 13–15). Though the mechanism has yet to be elucidated in sarcomas, mutations or deletions of *LZTR1* disrupt RAS regulations by *LZTR1*-mediated ubiquitination and allow glioblastoma to retain its proliferative features (16, 17). Lastly, *NF1* mutations can also be present in sarcomas along with other mutations. Specifically, a study has shown that of 22 primary intracranial spindle cell sarcoma with RMS features, 22% have mutations or deletions of NF1 and 55% have TP53 mutations (11). To our knowledge, this is the first case to report molecular characterizations of a pituitary RMS arising from a pituitary adenoma. Understanding the molecular profile of pituitary sarcoma will help to better understand its etiology and refine treatment plan.

DATA AVAILABILITY STATEMENT

The original contributions presented in the study are included in the article/supplementary material. Further inquiries can be directed to the corresponding author.

ETHICS STATEMENT

The studies involving human participants were reviewed and approved by University of Minnesota Institutional Review Board. The patients/participants provided their written informed consent to participate in this study.

AUTHOR CONTRIBUTIONS

JL collected the history and drafted the manuscript. LC performed the pathological examination and edited the manuscript. All authors contributed to the article and approved the submitted version.

REFERENCES

1. Sedney CL, Morris JM, Giannini C, Link MJ, Swetz KM. Radiation-Associated Sarcoma of the Skull Base After Irradiation for Pituitary Adenoma. *Rare Tumors* (2012) 4(1):e7. doi: 10.4081/rt.2012.e7
2. Berkmann S, Tolnay M, Hänggi D, Ghaffari A, Gratzl O. Sarcoma of the Sella After Radiotherapy for Pituitary Adenoma. *Acta Neurochir (Wien)* (2010) 152 (10):1725–35. doi: 10.1007/s00701-010-0694-6
3. Stein TD, Chae YS, Won N, Lee JH. Hedley-Whyte ET. A 34-Year-Old Man With Bitemporal Hemianopsia. *Brain Pathol* (2014) 24:107–10. doi: 10.1111/bpa.12108
4. Duncan VE, Nabors LB, Warren PP, Conry RM, Willey CD, Perry A, et al. Primary Sellar Rhabdomyosarcoma Arising in Association With a Pituitary Adenoma. *Int J Surg Pathol* (2016) 24(8):753–6. doi: 10.1177/1066896916658955
5. de Silva AC, Rodriguez FJ, Aldecoa I, McDonald W, Ribalta T. Compound Gonadotrophic Pituitary Adenoma and Rhabdomyosarcoma. *Histopathology* (2016) 68(7):1111–4. doi: 10.1111/his.12890
6. Arita K, Sugiyama K, Tominaga A, Yamasaki F. Intrasellar Rhabdomyosarcoma: Case Report. *Neurosurgery* (2001) 48(3):677–80. doi: 10.1097/00006123-200103000-00048
7. Guerrero-Pérez F, Vidal N, López-Vázquez M, Sánchez-Barrera R, Sánchez-Fernández JJ, Torres-Díaz A, et al. Sarcomas of the Sellar Region: A Systematic Review. *Pituitary* (2021) 24(1):117–29. doi: 10.1007/s11102-020-01073-9
8. Yang CY, Liau JY, Huang WJ, Chang YT, Chang MC, et al. Targeted Next-Generation Sequencing of Cancer Genes Identified Frequent TP53 and ATRX Mutations in Leiomyosarcoma. *Am J Transl Res* (2015) 7(10):2072–81.
9. Gonin-Laurent N, Gibaud A, Huygue M, Lefèvre SH, Le Bras M, Chauveinc L, et al. Specific TP53 Mutation Pattern in Radiation-Induced Sarcomas. *Carcinogenesis* (2006) 27(6):1266–72. doi: 10.1093/carcin/bgi356
10. Casey DL, Pitter KL, Wexler LH, Slotkin EK, Gupta GP, Wolden SL. TP53 Mutations Increase Radioresistance in Rhabdomyosarcoma and Ewing Sarcoma. *Br J Cancer* (2021) 125(4):576–81. doi: 10.1038/s41416-021-01438-2

11. Koelsche C, Mynarek M, Schrimpf D, Bertero L, Serrano J, Sahm F, et al. Primary Intracranial Spindle Cell Sarcoma With Rhabdomyosarcoma-Like Features Share a Highly Distinct Methylation Profile and DICER1 Mutations. *Acta Neuropathol* (2018) 136(2):327–37. doi: 10.1007/s00401-018-1871-6
12. Barretina J, Taylor BS, Banerji S, Ramos AH, Lagos-Quintana M, et al. Subtype-Specific Genomic Alterations Define New Targets for Soft-Tissue Sarcoma Therapy. *Nat Genet* (2010) 42(8):715–21. doi: 10.1038/ng.619
13. Liau JY, Lee JC, Tsai JH, Yang CY, Liu TL, Ke ZL, et al. Comprehensive Screening of Alternative Lengthening of Telomeres Phenotype and Loss of ATRX Expression in Sarcomas. *Mod Pathol* (2015) 28(12):1545–54. doi: 10.1038/modpathol.2015.114
14. Liau JY, Tsai JH, Jeng YM, Lee JC, Hsu HH, Yang CY. Leiomyosarcoma With Alternative Lengthening of Telomeres Is Associated With Aggressive Histologic Features, Loss of ATRX Expression, and Poor Clinical Outcome. *Am J Surg Pathol* (2015) 39(2):236–44. doi: 10.1097/PAS.0000000000000324
15. Koelsche C, Renner M, Johann P, Leiss I, Sahm F, Schimmack S, et al. Differential Nuclear ATRX Expression in Sarcomas. *Histopathology* (2016) 68 (5):738–45. doi: 10.1111/his.12812
16. Frattini V, Trifonov V, Chan JM, Castano A, Lia M, et al. The Integrated Landscape of Driver Genomic Alterations in Glioblastoma. *Nat Genet* (2013) 45(10):1141–9. doi: 10.1038/ng.2734
17. Steklov M, Pandolfi S, Baietti MF, Batiuk A, Carai P, Najm P, et al. Mutations in LZTR1 Drive Human Disease by Dysreg ulating RAS Ubiquitination. *Science* (2018) 362(6419):1177–82. doi: 10.1126/science.aap7607

Conflict of Interest: The authors declare that the research was conducted in the absence of any commercial or financial relationships that could be construed as a potential conflict of interest.

Publisher's Note: All claims expressed in this article are solely those of the authors and do not necessarily represent those of their affiliated organizations, or those of the publisher, the editors and the reviewers. Any product that may be evaluated in this article, or claim that may be made by its manufacturer, is not guaranteed or endorsed by the publisher.

frontiers in Endocrinology

ORIGINAL RESEARCH
published: 30 September 2021
doi: 10.3389/fendo.2021.731088

Suprasellar Mature Cystic Teratoma Mimicking Rathke's Cleft Cyst: A Case Report and Systematic Review of the Literature

Shenzhong Jiang[1], Zhaojian Wang[1], Yan You[2], Renzhi Wang[1] and Xinjie Bao[1]**

[1] Department of Neurosurgery, Peking Union Medical College Hospital, Chinese Academy of Medical Sciences and Peking Union Medical College, Beijing, China, [2] Department of Pathology, Peking Union Medical College Hospital, Chinese Academy of Medical Sciences and Peking Union Medical College, Beijing, China

OPEN ACCESS

Edited by:
Maria Fleseriu, Oregon Health and Science University, United States

Reviewed by:
Akira Sugawara, Tohoku University, Japan
Hidetaka Suga, Nagoya University Hospital, Japan

***Correspondence:**
Xinjie Bao
baoxinjie1@pumch.cn
Renzhi Wang
wangrz@126.com

Specialty section:
This article was submitted to Pituitary Endocrinology, a section of the journal Frontiers in Endocrinology

Received: *26 June 2021*
Accepted: *09 September 2021*
Published: *30 September 2021*

Citation:
Jiang S, Wang Z, You Y, Wang R and Bao X (2021) Suprasellar Mature Cystic Teratoma Mimicking Rathke's Cleft Cyst: A Case Report and Systematic Review of the Literature. Front. Endocrinol. 12:731088. doi: 10.3389/fendo.2021.731088

In this article, we present a 31-year-old female who presented with intermittent headache and oligomenorrhea of over 10 years' duration. Imaging revealed a large suprasellar mass with sellar extension. The patient underwent an endoscopic endonasal trans-sphenoidal surgery to resection of the mass. Clinical, radiological, and operative findings from this patient were initially considered to be Rathke's cleft cyst (RCC). However, postoperative histological examinations revealed a mature cystic teratoma. No radiotherapy was performed after surgery. At the most recent follow-up, approximately 1 year later, the patient is doing well with no headache and no recurrence of the teratoma.

Keywords: mature cystic teratomas, sellar region, rare lesion, neuropathology, case

INTRODUCTION

Teratomas are a type of germ cell tumor (GCT) differentiating from three germ layers. Central nervous system teratomas are very rare, accounting for 0.2%–0.9% of all intracranial tumors (1). According to *The 2016 WHO Classification of Tumors of the Central Nervous System*, teratomas can be classified into three types: mature, immature, and teratomas with malignant transformation (2). Mature teratomas are benign tumors that contain well-differentiated tissues from at least two germinal layers which can be divided into two subtypes: mature solid teratomas and mature cystic teratomas (MCT); the former is exceedingly rare. The latter accounts for about 0.04% to 0.7% of all intracranial tumors (3, 4). Mature teratoma recurrence rate is extremely low in cases of complete resection and usually occurs within 1 year after treatment (5), and the 10-year survival rate is 93% (6). Most of the intracranial MCTs have been found to occur in the midline structures, and the pineal area is the most frequent site (7, 8). Suprasellar MCTs have rarely been reported. Here, we describe an unusual case of a large suprasellar MCT mimicking Rathke's cleft cyst, and conduct a systematic review of eight cases of MCTs in the sellar region (**Tables 2–4**). We hope to shed new light for physicians on the diagnosis and treatment of this rare disease.

CASE PRESENTATION

History and Examination

A 31-year-old female was admitted to our hospital complaining of oligomenorrhea and increasing headaches. She reported an 11-year history of intermittent headache (visual analog scale, with 10 as the worst pain, of 4/10 points), which used to be precipitated by fatigue and were alleviated by rest or non-steroidal anti-inflammatory drugs (NSAIDs). When the headaches increased in frequency and intensity and were accompanied by mild nausea, culminating in a headache lasting for 1 week with no relief from NSAIDs, the patient sought medical attention. She denied vision loss, visual field defects, polyuria, lactation, central obesity, or acromegaly during the course. The general physical examination was completely normal, and the neurologic examination showed no focal signs. A brain magnetic resonance imaging (MRI) scan with contrast was performed, demonstrating a 19 mm × 24 mm × 23 mm irregular suprasellar lesion with slight intrasellar extension. The lesion signal characteristics were isointense on T1-weighted imaging and hyperintense on T2-weighted imaging. No obvious gadolinium enhancement was noted (**Figures 1A–C**). Endocrine workup showed that the levels of pituitary hormones were within normal limits (**Table 1**).

Surgical Biopsy and Histological Findings

Endoscopic trans-sphenoidal surgery was performed. In the procedure, the cyst was observed to be predominantly suprasellar in location. It contained ivory-whitish viscous material and was resected. Hematoxylin–eosin staining is as follows: on a background of abundant myxoid stroma, we can see the following components: fibrous cyst walls lined with simple cuboidal and short columnar epithelium (H&E ×100, **Figure 1D**), a mass of mucous acinous cells (**Figure 1E**), and some chondroid tissue (**Figure 1F**).

Postoperative Course

The postoperative course was uneventful, with the headaches completely resolving after surgery. During the 1-year follow-up, our patient is well and there is no evidence of recurrence.

DISCUSSION

In the case report, we present a unique and rare case of MCT mimicking Rathke's cleft cyst (RCC) of the sellar region in terms of clinical manifestations and neuroimaging.

According to *The 2016 WHO Classification of Tumors of the Central Nervous System* (2), teratomas are a subset of intracranial germ cell tumors and rarely present as pure teratomas (rather than mixed germ cell tumors). Teratomas can be classified into three types: mature, immature, and teratomas with malignant transformation. Intracranial teratomas are rare space-occupying lesions that account for about 0.5% of all intracranial tumors. MCTs are a subset of these neoplasms, and their occurrence in the brain is even rarer. They are benign tumors that contain well-differentiated tissues from at least two germinal layers. MCTs occur more frequently during the first or second decade of life, and there is a clear male predominance (4:1). Most intracranial MCTs occur in midline structures, most frequently in the pineal region (7).

MRI is the first choice of neuroimaging in the diagnosis of RCC. On MRI, RCCs often appear as well-demarcated, centrally located spherical or ovoid lesions of the sellar region with

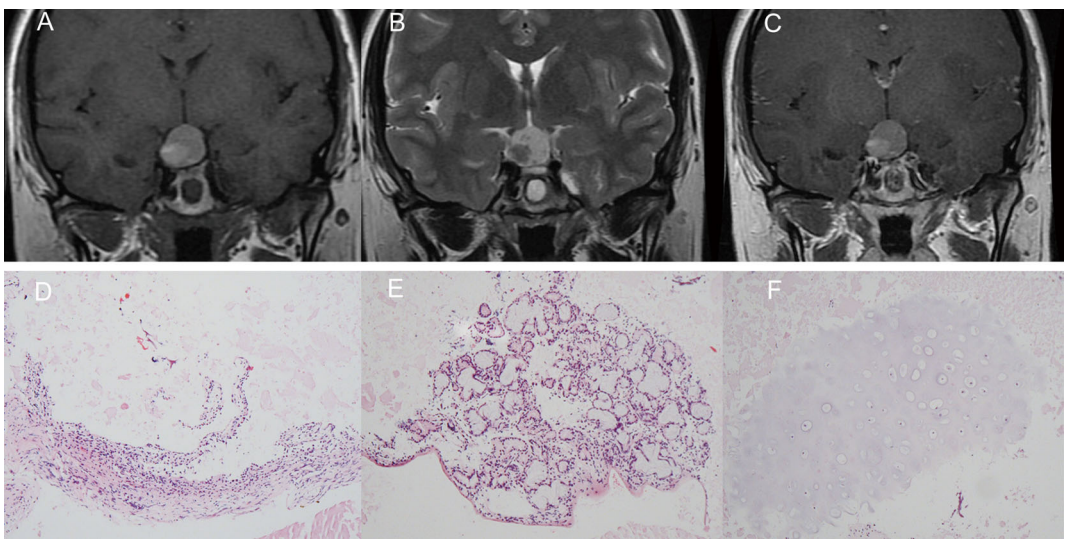

FIGURE 1 | The lesion signal characteristics on magnetic resonance imaging were isointense on T1-weighted imaging and hyperintense on T2-weighted imaging. No obvious gadolinium enhancement was noted **(A–C)**. Pathological findings: on a background of abundant myxoid stroma, we can see fibrous cyst walls lined with simple cuboidal and short columnar epithelium (H&E ×100, **D**), a mass of mucous acinous cells **(E)**, and some chondroid tissue **(F)**.

TABLE 1 | Results of endocrine examinations before and after surgery.

Test	Reference range	Before surgery Value	3 months after surgery Value
Sex hormone			
LH	1.20–103.03 IU/L	10.08	19.36
FSH	<30.34 IU/L	6.57	10.33
E2	27–433 pg/ml	60	130
P	0.38–29.26 ng/ml	0.21↓	1.73
PRL	<30 ng/ml	16.72	4.92
ACTH related			
ACTH	0–46 pg/ml	18.9	10.5
F	4.0–22.3 μg/dl	17.28	12.35
Thyroid function			
FT3	1.80–4.10 pg/ml	3.17	2.67
FT4	0.81–1.89 ng/dl	1.081	1.222
T3	0.66–1.92 ng/ml	1.179	0.824
T4	4.30–12.50 μg/dl	7.6	8.06
TSH	0.38–4.34 μIU/ml	3.154	2.335

LH, luteinizing hormone; FSH, follicle-stimulating hormone; E2, estradiol; P, progesterone; PRL, prolactin; β-HCG, β-human chorionic gonadotropin; ACTH, adrenocorticotropic hormone; F, cortisol; FT3, free triiodothyronine; FT4, free thyroxine; T3, triiodothyronine; T4, thyroxine; TSH, thyroid-stimulating hormone.

nodules inside the cyst occasionally. The majority of these smooth contoured cysts are unilobar with a diameter ranging between 5 and 40 mm (mean approximately 17 mm) (9). MRI signal intensity varies and is highly dependent on the biochemical nature of intracystic contents, which can range from clear, CSF-like fluid to thick, mucoid material (10, 11).

In the present case, RCC was suspected prior to the histological examinations of the tumor because the gender, age, clinical presentations, and neuroimaging characteristics aligned with a diagnosis of RCC.

Suprasellar MCTs are relatively rare. MCTs occur more frequently during the first or second decade of life. Rarely, reported cases have occurred on the third or fourth decade of life (5). Overall, these tumors appear to be more common in men, with a finding of 79.7% in men versus 20.3% in women (6). Moreover, the tumor mimicking RCC is a further peculiarity of the case.

The published case reports and series written in English that focus on suprasellar MCTs are limited. Therefore, we performed a comprehensive literature review of related articles and identified eight patients with a diagnosis of MCT, summarizing the data of clinical manifestations (**Table 2**), pituitary function (**Table 3**), MRI signal features (**Table 3**), and treatment (**Table 4**) of this lesion.

The most prominent symptoms at diagnosis are neurological defects (six of eight patients), particularly visual disturbance (five of eight). Headache (three of eight) and diabetes insipidus (three of eight) were also commonly seen. One patient reported amenorrhea. Regarding MRI appearance, signal intensities on T1WI and T2WI vary from case to case. In some cases, inclusions like teeth, fat, and calcification can be detected (13, 15). Variable enhancement with contrast was reported in three patients. Liu et al. (19) suggest that mature teratoma on MRI is an ovoid or irregular mass with or without multilocularity and has mixed signals derived from different tissues. The presence of fatty tissue or multilocularity is a characteristic feature of teratoma. The tumor usually presents with heterogeneous hyperintensity on T1W images and non-enhanced or moderate

TABLE 2 | Demographic data and clinical presentation from published reports.

Patient	Author	Year	Country	Age/sex	Presentation	Other manifestation
1 (12)	Li et al.	2015	China	13/F	Polyuria, polydipsia, and amenorrhea	Headache, blurred vision, short stature
2 (8)	Sweiss et al.	2013	USA	57/M	Vision impairment	Left-sided facial weakness, ataxia, and short-term memory loss, seizure
3 (13)	Vendrell et al.	2010	France	18 months/M	Bilateral decreased visual acuity and hyperphagia	
4 (14)	Kim et al.	2010	Korea	17/M	Polyuria and polydipsia with severe thirst, headache, and diplopia	
5 (15)	Muzumdar et al.	2001	India	26/M	Headache, vision impairment	Short stature, weight gain
6 (16)	Araki et al.	2000	Japan	3 months/M	Fontanelle bossing	Accelerated deep tendon reflexes, incomplete head control
7 (17)	Narayanam et al.	2012	India	7/F	Seizures, precocious puberty, headache, and vomiting	Irritable
8 (18)	Tobo et al.	1981	Japan	14/M	Diabetes insipidus/panhypopituitarism	
9	Current case	2021	China	31/F	Headache, oligomenorrhea	

F, female; M, male.

TABLE 3 | Pituitary function and pituitary magnetic resonance imaging data from published reports.

Patient	Pituitary function	Size	Location	T1	T2	T1 contrast	CT
1	T4↓, TSH↑, PRL↑	Large	Sellar and suprasellar	Cystic: hypointense	Heterogeneous hyperintense	Cystic: rim enhancement; solid: evidently enhanced	Hypodense
2	FSH↑, LH↑	Large	Intra- and suprasellar	NA	NA	NA	NA
3	PRL↑, TSH↑, T3↑	Large	Endosuprasellar	Mixed intensity	Mixed intensity	Intense enhancement	Hyperdense due to calcification
4	ADH↓	Large	Sellar and suprasellar	NA	NA	Partial enhancement	NA
5	Panhypopituitarism	Large	Suprasellar	Hyperintense	NA	NA	Hypodense with peripheral rim of calcification
6	Normal	Large	Suprasellar	Hypointense	NA	NA	NA
7	Normal	Large	Suprasellar	Isointense	Isointense	No enhancement	Hypodense
8	Panhypopituitarism	NA	Sellar and suprasellar region	NA	NA	NA	A mass in the suprasellar region with contrast enhancement
9	Normal	Large	Sellar and suprasellar	Iso/ hyperintensity	Hyperintensity with a hypointense nodule	No enhancement	–

Size: large = large tumor size (>1 cm).

T3, triiodothyronine; T4, thyroxine; TSH, thyroid-stimulating hormone; LH, luteinizing hormone; FSH, follicle-stimulating hormone; PRL, prolactin; ADH, anti-diuretic hormone; NA, not available.

enhanced multilocularity on T1W images with contrast. However, Chiloiro et al. (5) suggest that teratomas appear as low-intensity heterogeneous mass in T1- and T2-weighted magnetic resonance imaging, with variable enhancement after contrast administration. Surgery was performed in all patients, two of which were followed by radiotherapy or chemotherapy. Only one patient reported hydrocephalus and blindness during follow-up.

Neuroimaging characteristics of teratomas are not of high specificity, which make it difficult to distinguish mature teratomas from other intracranial neoplasms located in the suprasellar region that include other GCTs (germinoma, choriocarcinoma, embryonal carcinoma, and endodermal sinus tumor), craniopharyngioma, and RCC. Therefore, our case highlights the importance of obtaining a histological diagnosis to differentiate teratomas from other lesions.

TABLE 4 | Treatment and outcome of patients from published reports.

Patient	Surgery	Tumor contents	Pathology	Outcome	Complication
1	Right pterional approach	Dark yellow fluid; hair and whitish fat material	Mature teratoma	Total resection/vision improved	Transient DI
2	Right pterional craniotomy/ trans-sylvian approach	Thick and yellow oil-like fluid, yellow clumps of hair embedded within fatty deposit	Mature cystic teratoma	Incomplete resection followed by external beam radiotherapy and stereotactic radiosurgery/significantly improved neurological status and vision	No
3	TSS	Teeth	Mature teratoma	Normal neurological examination except loss of visual acuity in the left eye	No
4	TSS		Mature teratoma	Followed by chemotherapy and radiotherapy	NA
5	Sublabial trans-sphenoidal approach	Fat, bony septation, keratinaceous flakes	Mature teratoma	Total resection/vision improved, normal visual field, headache gone	No
6	Surgery	NA	Mature teratoma	Total resection/panhypopituitarism and diabetes insipidus	Hydrocephalus/ complete blindness
7	Left pterional approach	Whitish structure	Mature teratoma	Total resection/headache gone, seizure-free, regression of precocious puberty	No
8	Craniotomy	Bone, cartilage, and several hairs	Mature teratoma	NA	NA
9	TSS	Ivory-whitish viscous materials	Mature cystic teratoma	Total resection/headache resolved	No

TSS, trans-sphenoidal surgery; NA, not available.

Histologically, MCTs are commonly multicystic, contain sebaceous fluid, and are identified by the presence of differentiated ectodermal (skin, hair, brain), mesodermal (muscle, fat, teeth, bone, cartilage), and/or endodermal elements (mucinous and ciliated epithelium). All three layers may not be seen in every case of teratoma. The differential diagnosis includes dermoid cysts, epidermoid cysts, colloid cysts, immature teratomas, and teratomas with malignant transformation.

For this case, our preoperative diagnosis was Rathke's cleft cyst, and given the absence of hair, skin, or teeth, the intraoperative findings seemed to confirm our primary diagnosis. However, MCTs were confirmed by the histological examination of the specimen when cyst walls lined with simple cuboidal and columnar epithelium, a mass of mucous acinous cells (salivary glands), and cartilage were identified. Our case highlights the importance of obtaining a histological diagnosis to differentiate MCTs from other lesions. It would also be important to exclude the presence of additional germ cell components, which would require additional treatment postresection.

The typical treatment for mature teratomas is neurosurgical excision because of their benign behavior (20), which was successfully done in this case. It is well advised to perform radical excision as the long-term outcome is excellent. Mature teratoma recurrence rate is extremely low in cases of complete resection and usually occurs within 1 year after treatment (5). Sano (6) reported that the 10-year survival rate for mature teratomas is 93%. Whether to perform radiotherapy for mature teratomas after surgery remains controversial. Sano (6) points out that radiotherapy should be conducted after surgery to suppress further growth of tumor cells. Jakacki (21) suggests that it is advocated to perform radiotherapy to immature teratomas and teratomas with malignant transformation; while mature teratomas are not typically responsive to radiation therapy, surgery is the only proven treatment modality. Therefore, the clinical experience from physicians really matters in the postoperative treatment choices for patients with mature teratomas.

CONCLUSION

MCTs in the sellar region are extremely rare, and their imaging usually lacks specificity. Therefore, it is important to obtain a thorough histological diagnosis. MCTs are benign, and complete surgical excision is the first-line treatment. In selected cases, radiation therapy was conducted in some cases but is not recommended as routine treatment. Whether to perform radiotherapy depends on the physician as there is a lack of evidence on this aspect. Close follow-up is indispensable for patients with MCTs.

DATA AVAILABILITY STATEMENT

The raw data supporting the conclusions of this article will be made available by the authors, without undue reservation.

ETHICS STATEMENT

Written informed consent was obtained from the participant for the publication of any potentially identifiable images or data included in this article. The authors are accountable for all aspects of the work in ensuring that questions related to the accuracy or integrity of any part of the work are appropriately investigated and resolved.

AUTHOR CONTRIBUTIONS

SJ drafted the manuscript. SJ and ZW analyzed the data. YY made the pathological diagnosis and drafted the article of pathological findings. All authors contributed to the article and approved the submitted version.

FUNDING

This work was supported by the National Key Research and Development Program of China (2018YFA0108600), the Natural Science Foundation of Beijing Municipality (7182134), the CAMS Initiative for Innovative Medicine (2016-I2M-1-017), Beijing Nova Program (Z181100006218003), and the National Natural Science Foundation of China (82170799).

ACKNOWLEDGMENTS

We express many thanks to the patient for generously authorizing us to share her rare case.

REFERENCES

1. Li Q, You C, Zan X, Chen N, Zhou L, Xu J. Mature Cystic Teratoma (Dermoid Cyst) in the Sylvian Fissure: A Case Report and Review of the Literature. *J Child Neurol* (2012) 27(2):211–7. doi: 10.1177/0883073811415681
2. Louis DN, Perry A, Reifenberger G, von Deimling D, Figarella-Branger D, Cavenee WK, et al. The 2016 World Health Organization Classification of Tumors of the Central Nervous System: A Summary. *Acta Neuropathol* (2016) 131(6):803–20. doi: 10.1007/s00401-016-1545-1
3. Abderrahmen K, Bouhoula A, Aouidj L, Jemel H. Temporal Dermoid Cyst With Unusual Imaging Appearance: Case Report. *Turk Neurosurg* (2016) 26 (1):176–9. doi: 10.5137/1019-5149.JTN.12624-14.1
4. Amelot A, Borha A, Calmon R, Barbet P, Puget S. Child Dermoid Cyst Mimicking a Craniopharyngioma: The Benefit of MRI T2-Weighted Diffusion Sequence. *Child's Nervous Syst* (2018) 34(2):359–62. doi: 10.1007/s00381-017-3602-z
5. Chiloiro S, Giampietro A, Bianchi A, De Marinis L. Clinical Management of Teratoma, a Rare Hypothalamic-Pituitary Neoplasia. *Endocrine* (2016) 53 (3):636–42. doi: 10.1007/s12020-015-0814-4

6. Sano K. Pathogenesis of Intracranial Germ Cell Tumors Reconsidered. *J Neurosurg* (1999) 90(2):258–64. doi: 10.3171/jns.1999.90.2.0258
7. Bohara M, Yonezawa H, Karki P, Bakhtiar Y, Hirano H, Kitazono I, et al. Mature Posterior Fossa Teratoma Mimicking Dermoid Cyst. *Brain Tumor Pathol* (2013) 30(4):262–5. doi: 10.1007/s10014-012-0129-6
8. Sweiss RB, Shweikeh F, Sweiss FB, Zyck S, Dalvin L, Siddiqi J. Suprasellar Mature Cystic Teratoma: An Unusual Location for an Uncommon Tumor. *Case Rep Neurol Med* (2013) 2013:180497. doi: 10.1155/2013/180497
9. Zada G, Lin N, Ojerholm E, Ramkissoon S, Laws ER. Craniopharyngioma and Other Cystic Epithelial Lesions of the Sellar Region: A Review of Clinical, Imaging, and Histopathological Relationships. *Neurosurg Focus* (2010) 28(4): E4. doi: 10.3171/2010.2.FOCUS09318
10. Nishioka H, Haraoka J, Izawa H, Ikeda Y. Magnetic Resonance Imaging, Clinical Manifestations, and Management of Rathke's Cleft Cyst. *Clin Endocrinol (Oxf)* (2006) 64(2):184–8. doi: 10.1111/j.1365-2265.2006.02446.x
11. Larkin S, Karavitaki N, Ansorge O. Rathke's Cleft Cyst. *Handb Clin Neurol* (2014) 124:255–69. doi: 10.1016/B978-0-444-59602-4.00017-4
12. Li Y, Zhang Y, Xu J, Chen N. Successful Surgical Treatment of Mature Teratoma Arising From the Sella. *J Clin Med Res* (2015) 7(2):122–5. doi: 10.14740/jocmr1998w
13. Vendrell JF, Hoa D, Gahide G. Mature Teratoma Arising From the Sella. *Lancet* (2010) 375(9725):1556–6. doi: 10.1016/S0140-6736(09)60300-7
14. Kim YS, Kang SG, Kim YO. Pituitary Teratoma Presenting as Central Diabetes Insipidus With a Normal MRI Finding. *Yonsei Med J* (2010) 51 (2):293–4. doi: 10.3349/ymj.2010.51.2.293
15. Muzumdar D, Goel A, Desai K, Shenoy A. Mature Teratoma Arising From the Sella - Case Report. *Neurol Med-Chir* (2001) 41(7):356–9. doi: 10.2176/nmc.41.356
16. Araki K, Koga M, Okada T, Kurashige T, Naruse K, Hiroi M. A Boy With Normal Growth in Spite of Growth Hormone Deficiency After Resection of a Suprasellar Teratoma. *Endocrine J* (2000) 47(Suppl):S101–4. doi: 10.1507/endocrj.47.SupplMarch_S101
17. Sai Kiran NA, Ghosal N, Thakar S, Hegde AS. Synchronous Occurrence of a Hemorrhagic Hypothalamic Hamartoma and a Suprasellar Teratoma. *Pediatr Neurosurg* (2011) 47(6):430–5. doi: 10.1159/000338896
18. Tobo M, Sumiyoshi A, Yamakawa Y. Sellar Teratoma With Melanotic Progonoma. A Case Report. *Acta Neuropathol* (1981) 55(1):71–3. doi: 10.1007/BF00691534
19. Liu Z, Lv X, Wang W, An J, Duan F, Feng X, et al. Imaging Characteristics of Primary Intracranial Teratoma. *Acta Radiol* (2014) 55(7):874–81. doi: 10.1177/0284185113507824
20. Nishio S, Inamura T, Takeshita I, Fukui M, Kamikaseda K. Germ Cell Tumor in the Hypothalamo-Neurohypophysial Region: Clinical Features and Treatment. *Neurosurg Rev* (1993) 16(3):221–7. doi: 10.1007/BF00304332
21. Jakacki R. Central Nervous System Germ Cell Tumors. *Curr Treat Options Neurol* (2002) 4(2):139–45. doi: 10.1007/s11940-002-0022-4

Conflict of Interest: The authors declare that the research was conducted in the absence of any commercial or financial relationships that could be construed as a potential conflict of interest.

Publisher's Note: All claims expressed in this article are solely those of the authors and do not necessarily represent those of their affiliated organizations, or those of the publisher, the editors and the reviewers. Any product that may be evaluated in this article, or claim that may be made by its manufacturer, is not guaranteed or endorsed by the publisher.

frontiers in Endocrinology

ORIGINAL RESEARCH
published: 29 October 2021
doi: 10.3389/fendo.2021.672394

Clinical Characteristics and Management of Patients With McCune-Albright Syndrome With GH Excess and Precocious Puberty: A Case Series and Literature Review

*Xiao Zhai[1,2], Lian Duan[1,2], Yong Yao[3], Bing Xing[3], Kan Deng[3], Linjie Wang[1,2], Feng Feng[4], Zhiyong Liang[5], Hui You[4], Hongbo Yang[1,2], Lin Lu[1,2], Shi Chen[1,2], Renzhi Wang[3], Hui Pan[1,2] and Huijuan Zhu[1,2]**

[1] Key Laboratory of Endocrinology of National Health Commission, Department of Endocrinology, State Key Laboratory of Complex Severe and Rare Diseases Peking Union Medical College Hospital, Chinese Academy of Medical Science and Peking Union Medical College, Beijing, China, [2] Department of Endocrinology, Peking Union Medical College Hospital, Chinese Academy of Medical Science (CAMS), Beijing, China, [3] Department of Neurosurgery, Peking Union Medical College Hospital, Chinese Academy of Medical Science and Peking Union Medical College, Beijing, China, [4] Department of Radiology, Peking Union Medical College Hospital, Chinese Academy of Medical Science and Peking Union Medical College, Beijing, China, [5] Department of Pathology, Peking Union Medical College Hospital, Chinese Academy of Medical Science and Peking Union Medical College, Beijing, China

OPEN ACCESS

Edited by:
Run Yu,
UCLA David Geffen School of Medicine, United States

Reviewed by:
Domenico Corica,
University of Messina, Italy
Fu Qiong Chen,
Huazhong University of Science and Technology, China

***Correspondence:**
Huijuan Zhu
shengxin2004@163.com

Specialty section:
This article was submitted to Pituitary Endocrinology, a section of the journal Frontiers in Endocrinology

Received: *25 February 2021*
Accepted: *11 October 2021*
Published: *29 October 2021*

Citation:
Zhai X, Duan L, Yao Y, Xing B, Deng K, Wang L, Feng F, Liang Z, You H, Yang H, Lu L, Chen S, Wang R, Pan H and Zhu H (2021) Clinical Characteristics and Management of Patients With McCune-Albright Syndrome With GH Excess and Precocious Puberty: A Case Series and Literature Review. Front. Endocrinol. 12:672394. doi: 10.3389/fendo.2021.672394

Background: McCune-Albright syndrome is a rare disorder characterized by fibrous dysplasia, café au lait skin spots, and hyperfunctioning endocrinopathies. The coexistence of precocious puberty and growth hormone excess in McCune-Albright syndrome is rare. Both conditions can manifest as accelerated growth, and treatments can be more challenging for such patients. This study aimed to describe the clinical manifestations of combined GH excess and PP in the context of McCune-Albright syndrome and analyze the clinical features and treatments of these patients.

Method: Clinical data from 60 McCune-Albright syndrome patients from Peking Union Medical College Hospital were obtained. The demographic characteristics, growth hormone, insulin-like growth factor-1, prolactin, alkaline phosphatase, and sex hormone levels; growth velocity; and bone age data were obtained. The growth velocity Z-score, bone age over chronological age ratio, and predicted adult height Z-score were calculated before and after treatment. Published studies and case reports were systemically searched, and data on demographic, clinical, and biochemical characteristics and treatment outcomes were obtained.

Results: We reviewed seven patients among 60 McCune-Albright syndrome patients at Peking Union Medical College Hospital (5 female) and 39 patients (25 female) from the published literature. Six of the seven patients from Peking Union Medical College Hospital and half of the patients from the published studies were pediatric patients. These patients

had increased growth velocity Z-scores and bone age over chronological age ratios. After good control of both conditions, the growth velocity Z-score and bone age over chronological age ratio decreased significantly, and the predicted adult height Z-score increased. The final heights and predicted adult height Z-scores were not impaired in patients with gigantism. All the patients had craniofacial fibrous dysplasia associated with optic and otologic complications.

Conclusion: McCune-Albright syndrome with growth hormone excess and precocious puberty is more common in girls. Patients have accelerated linear growth and advanced skeletal age, and early and good control of both conditions leads to a reduced growth velocity and stabilized bone age. The predicted adult and final heights are not negatively affected when growth hormone excess is diagnosed in pediatric patients.

Keywords: McCune-Albright syndrome, GH excess, precocious puberty (PP), gigantism, acromegaly

BACKGROUND

McCune-Albright syndrome (MAS) is a sporadic disease caused by somatic activating mutations of the *GNAS1* gene encoding the α subunit of guanine nucleotide-binding protein (1), which lead to constitutive receptor activation and dysregulated production of cAMP (2). MAS is characterized by the triad of monostotic/polyostotic fibrous dysplasia (FD), café au lait skin pigmentation, and hyperfunctioning endocrinopathies, including gonadotropin-independent precocious puberty (PP), thyrotoxicosis, growth hormone (GH) excess, hyperprolactinemia, or neonatal hypercortisolism (2–6).

MAS is a rare disease, and the estimated prevalence is between 1/100,000 and 1/1,000,000 (7). Gonadotropin-independent sexual puberty is the most common endocrinopathy in MAS (4), affecting 50% of girls, and is far more common in girls than in boys with MAS (8). MAS-associated precocious puberty (PP) is a rare cause of PP, and the estimated prevalence of PP (including gonadotropin-dependent and gonadotropin-independent PP) in the general population from a Danish national registry was 0.2% in female patients and less than 0.05% in males (9). Progression to gonadotropin-dependent PP over time has also been documented in some patients (10, 11). MAS-associated PP in girls is caused by recurrent, unilateral autonomously functioning ovarian cysts, which leads to episodic estrogen production with suppressed gonadotropins (12). Girls typically present with breast development and painless vaginal bleeding. PP in boys with MAS is associated with a premature penile growth and bilateral testicular enlargement, secondary to Leydig cell hyperplasia and elevated testosterone production (5). Additionally, PP causes growth acceleration and skeletal advancement (13), leading to impaired adult height. GH excess, which is present in 20~30% of patients with MAS (8, 14–16), presents with increased growth velocity in children and adolescents, and facial and acral dysmorphia in adults. GH excess is usually accompanied by serious craniofacial FD complications—e.g., visual, hearing, and olfactory injuries (16–22).

The co-occurrence of PP and GH excess in MAS is rare. To date, only a few case reports regarding GH excess and PP in MAS have been reported. The diagnosis and treatment of GH excess may become challenging when PP is also present. GH excess and PP both present with accelerated linear growth, and facial dysmorphia is often difficult to assess because of craniofacial fibrous dysplasia (CFFD). Therefore, it is easy to miss the diagnosis of GH excess because of the coexistence of PP and CFFD. Additionally, choosing the appropriate treatment of GH excess and PP is essential for children and adolescents to achieve normal adult height.

This study aimed to retrospectively analyze the clinical manifestations, treatments, and outcomes of combined GH excess and PP in MAS patients from Peking Union Medical College Hospital (PUMCH), review all reported cases, and analyze the clinical features and treatments of these patients.

SUBJECTS AND METHODS

Patients

This study was conducted in accordance with the rules of the hospital medical ethics committee, and informed consent was obtained. A retrospective study was performed on seven MAS patients who had a combined diagnosis of GH excess (including gigantism and acromegaly) and PP over 10 years (2010~2020) at PUMCH. The inclusion and exclusion process is shown in **Figure 1**.

Literature Review

All the studies and case reports of GH excess and PP with MAS (GH excess, acromegaly, gigantism, precocious puberty, and McCune-Albright syndrome were the keywords) were systematically sought in the world literature up to September 2020. Studies and case reports were identified in the PubMed, Embase, Google Scholar, and Chinese Biomedical (CBM) databases, and those with an English abstract were included in the analysis.

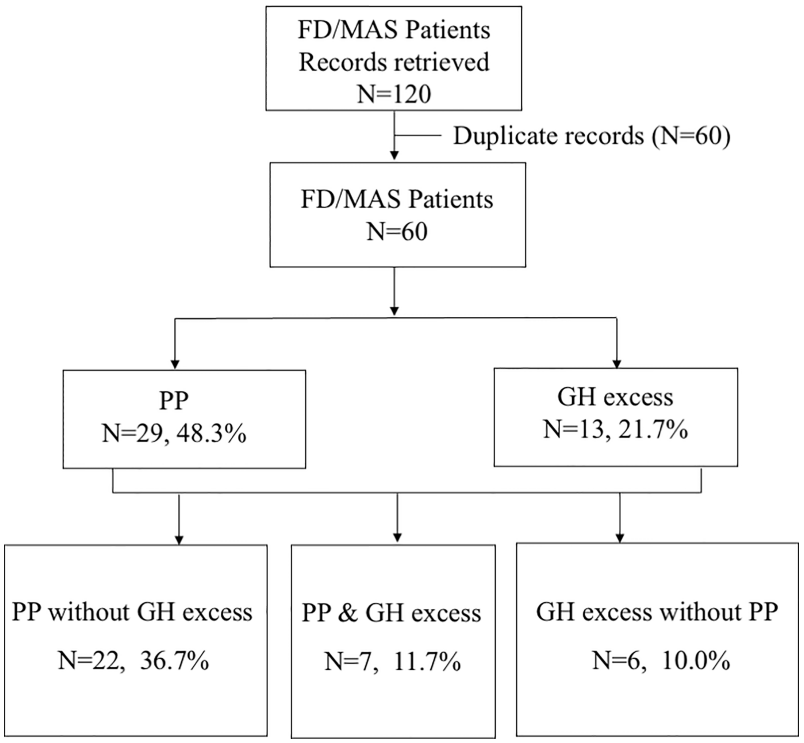

FIGURE 1 | Flowchart of the study population.

Data Extraction

We extracted data from medical records in PUMCH and published studies and analyzed each patient in case reports and case series. Pretreatment data were routinely collected before the initiation of treatment, and posttreatment data were collected at the last consultation for patients under therapy. The following data were extracted (1): demographic characteristics (2); age at MAS, GH excess, and PP diagnosis (3); type of fibrous dysplasia: craniofacial fibrous dysplasia (CFFD) *versus* polyostotic FD (4); pituitary imaging findings (5); GH, insulin-like growth factor (IGF-1), and prolactin (PRL) levels, bone age (BA) before and after treatment (6); alkaline phosphatase (ALP) levels before and after treatment (7); transabdominal pelvic (females) or testicular ultrasounds (males) (ovarian and testicular volumes were calculated using the formula volume = length × width × thickness × 0.52) (8); treatment for GH excess (9); treatment for PP; and (10) final heights and his/her parents' heights.

Diagnosis and Treatment of MAS, GH Excess, and PP

A diagnosis of MAS was made when at least two of the following major features existed: fibrous dysplasia of bone, café au lait skin pigmentation, and hyperfunctioning endocrinopathies.

The diagnosis of GH excess was based on the presence of typical clinical manifestations (accelerated linear growth, facial dysmorphia, shoe size modification, visual defects, and/or headaches), elevated IGF-1 levels (as assessed using the IMMULITE 2000 IGF-1 analyzer; Siemens Healthcare Diagnostic Inc.), and GH nadir ≥1 μg/L following documented hyperglycemia during an oral glucose load. The IGF-1 Z-scores were calculated according to the normal values of serum IGF-1 (5th and 95th percentiles) with adjustment for age and sex (15, 23, 24), and Z-scores greater than 2.0 were considered elevated. Gigantism is defined when GH excess leads to linear growth acceleration before the end of puberty and epiphyseal closure, while acromegaly is determined when GH excess is present in individuals after epiphyseal closure. Complete remission of GH excess is defined as a normal IGF-1 level for age and sex (Z score<2.0), and GH nadir<1 μg/L after the oral glucose tolerance test (OGTT).

Gonadotropin-independent PP is defined as the onset of secondary sexual characteristics before the age of 8 years in girls and 9 years in boys (25), with excess secretion of sex hormones (estrogens or androgens) and suppressed production of gonadotropins. The gonadotropin-releasing hormone (GnRH) stimulation test was performed to exclude gonadotropin-dependent PP. Girls typically present with painless vaginal bleeding with breast development in early childhood, and boys present with a premature increase in penile size and mild bilateral testicular enlargement (13).

Height and Skeletal Measurements

Height measurements were taken at PUMCH using a stadiometer and reported as the average of three consecutive morning values. BAs were determined using the Greulich and

Pyle atlas reading method (26). The predicted adult height (PAH) was calculated according to the Bayley-Pinneau method (27). The baseline BA and height measurements were obtained before the initiation of treatment. Height and growth velocity (GV) Z-scores were determined based on normative reference data for children and adolescents in China (28, 29). Height Z-scores from the literature review were based on normative reference data for children and adolescents of the World Health Organization (30). Posttreatment data were obtained at the time of treatment discontinuation or last evaluation for those remaining on treatment. Additionally, the predicted height was calculated as the mean parental height plus 6.5 cm for male patients and minus 6.5 cm for female patients. The ALP Z-scores were based on the reported distributions of ALP levels in the Chinese population (31).

Statistical Analysis

Statistical analyses were performed using SPSS 23.0, and figures were prepared using GraphPad Prism, version 6 (GraphPad Software Inc.). The data are presented as the means (minimal, max) or medians (minimal, max) as appropriate depending on the normality of the distribution. Paired samples t-tests were performed to compare patients before and after treatment. Independent sample t-tests were performed to make comparisons between GH excess patients diagnosed with MAS with or without PP. P values <0.05 were considered statistically significant.

RESULTS

Clinical Characteristics and Treatment Outcomes in PUMCH

Baseline Demographic and Clinical Features

Seven MAS patients from PUMCH who had been diagnosed with GH excess and PP were included in this study; five were female (71.4%), and the mean age was 5.4 years (min,max 2.1, 8.9 years) of the diagnosis of MAS (**Table 1**). Café au lait spots were present in five individuals (71.4%). The mean age of the individuals at the initial development of signs of PP was 4.3 years (1.0, 7.0 years). In girls, the symptoms prompting evaluation were vaginal bleeding in three subjects (patients 1, 4, and 7) and breast development in two subjects (patients 3 and 5). Pelvic ultrasound showed unilateral (patients 1, 5, and 7) or bilateral (patient 3) ovarian cysts. In boys, the diagnosis was suggested by acne, scrotum enlargement, and erection. Testicular ultrasound showed bilateral testicular enlargement in patients 2 and 6 and focal hyperechoic lesions in patient 6. Subjects showed advanced skeletal maturation [median BA over chronological age (BA/CA) ratio: 1.44; 1.39, 1.98]. Six of the seven patients had gigantism, and the mean age at diagnosis was 6.5 years (4.7, 8.9 years). The presenting sign of the patients was accelerated linear growth. Patient 4 had experienced intermittent vaginal bleeding and focal bone dysplasia since the age of 7 years, and she was diagnosed with acromegaly at the age of 27 years in routine assessment during follow-up for MAS. CFFD was present in all the patients from PUMCH, among whom three patients (42.9%) had visual field deficits, two patients (28.6%) had conductive hearing loss, and one patient (14.3%) had olfactory dysfunction. The clinical characteristics of the patients from PUMCH are listed in **Table 1**.

Hormone Measurements and Imaging Findings

For hormone measurements, the mean random GH level, GH nadir after OGTT, and IGF-1 Z-score at the diagnosis of GH excess at PUMCH were 14.1 μg/L (4.9, 33.6), 13.2 μg/L (5.2, 35.3), and 6.4 (2.0, 10.2), respectively. Hyperprolactinemia was present in four patients (57.1%, mean 70.5 ng/ml; 47.7, 204.4), and a value greater than 200 ng/ml was only observed in patient 1. Magnetic resonance imaging (MRI) data were available for six individuals (**Figure 2**), revealing three macroadenomas and one microadenoma; patient 5 had multiple microadenomas, and patient 7 had normal MRI imaging findings. MRI imaging of patient 1 before and after surgery and pharmacological treatment is illustrated in **Figure 3**. Regarding other endocrinopathies, hyperthyroidism was present in one patient from PUMCH who had endocrinopathies accompanied by GH excess and PP in MAS (1/7; 14.3%).

Treatment of PP and GH Excess

The treatment for PP varied at PUMCH (the clinical characteristics and treatment outcomes of PP at PUMCH are listed in **Table 2**).

TABLE 1 | Demographic and clinical characteristics of PUMCH patients.

Patient ID	Sex	Age at dx of MAS (y)	Age at sx of PP (y)	Age at dx ofGH excess (y)	Café au lait	Polyostotic FD	CFFD	Height Z-score	Other endocrinopathies	Hearing or olfactory deficits	Visual Deficits
1	F	6.3	5.0	6.3	+	+	+	3.3	None	Unilateral hyposmia	Bilateral temporal hemianopia
2	M	8.9	7.0	8.9	+	+	+	2.1	None	Hyposmia	Unilateral visual field defect
3	F	4.7	1.0	4.7	+	+	+	4.0	None	None	None
4	F	7.0	7.0	27	–	+	+	-0.7	None	None	Diplopia
5	F	4.3	4.0	6.6	–	+	+	4.1	None	CHL	None
6	M	6.3	5.0	6.3	+	+	+	4.53	None	CHL	Unilateral visual field defect
7	F	2.1	1.0	6.4	+	+	+	1.9	Hyperthyroidism	None	None

CHL, conductive hearing loss; Dx, diagnosis; Sx, symptom and sign; FD, fibrous dysplasia; CFFD, craniofacial fibrous dysplasia; PP, precocious puberty. Height Z-score was recorded at the first visit.

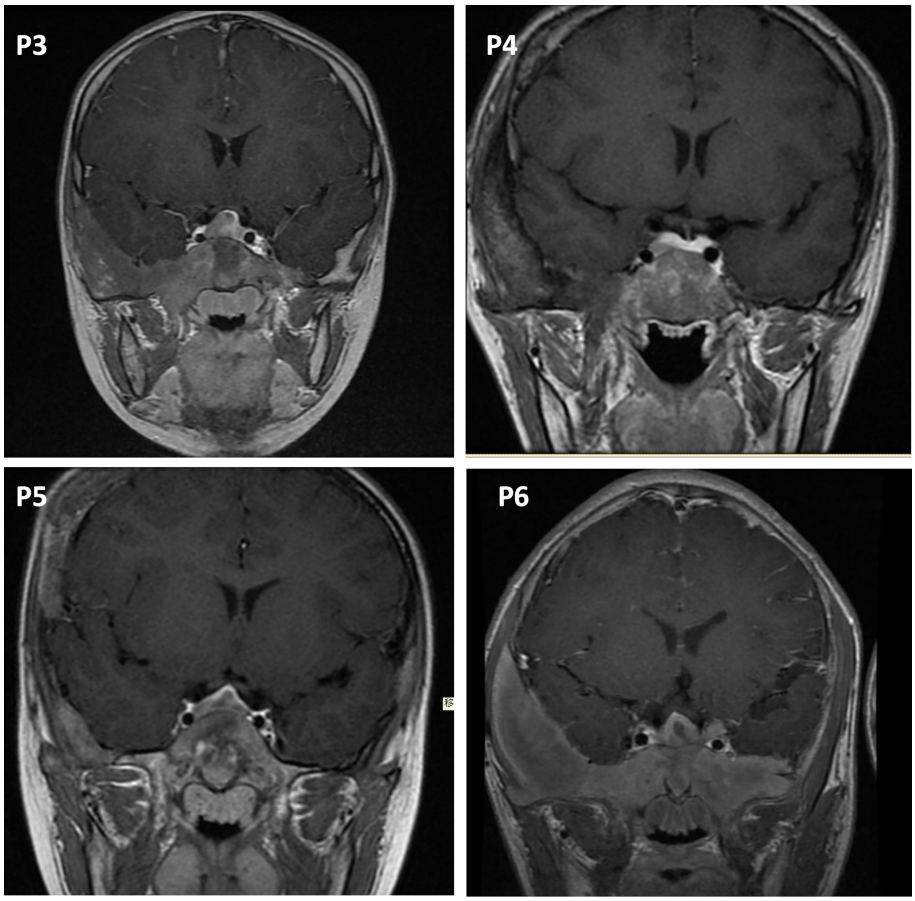

FIGURE 2 | Pituitary MRI in the coronal view. P3, patient 3, macroadenoma. P4, patient 4, microadenoma. P5, patient 5, multiple microadenomas. P6, patient 6, macroadenoma with a cystic zone.

Letrozole was used in two of seven patients, either alone (patient 6) or in combination with medroxyprogesterone (patient 7). Patient 5 was treated with tamoxifen. Patient 2 was treated with a GnRH agonist (GnRHa) because of central PP secondary to peripheral PP. However, after 3 months of treatment, patient 2 discontinued GnRHa because of financial restriction. Patients 1 and 3 were closely monitored without medical treatment. Their symptoms were relatively stable, and their BA/CA ratios were close to the normal range.

Five patients (71.4%) from PUMCH had undergone navigation-assisted transsphenoidal pituitary tumor resection, and two patients achieved complete remission (the clinical characteristics and treatment outcomes of patients with GH excess are listed in **Table 3**). Three patients (patients 1, 3, and 6) had partial remission after surgery and continued pharmacological treatment. Patient 1 then received treatment with dopamine agonist (DA) bromocriptine and long-acting somatostatin analog (LAR) octreotide (Sandostatin LAR, Novartis). The random GH level fell to 3.7 ng/ml, and the IGF-1 level was 601 ng/ml (IGF-1 Z-score 0.3). LAR was also effective in further lowering the IGF-1 levels after surgery in patient 3, but she had a partial response. Patient 6 was treated with bromocriptine alone after surgery, and the patient's GH excess was partially controlled. Patient 7 was closely followed up without surgical or pharmacological treatment because her IGF-1 Z-score was slightly elevated and her GV was within the normal range. Visual and auditory complications remained stable after treatment. The ALP Z-score decreased significantly after successful treatment with GH excess and PP (P=0.04, **Figure 4A**).

Growth Outcome

For patients diagnosed before the age of 16 years at PUMCH (patients 1, 3, 5, 6, and 7 were included; patient 2 was not included in the analysis because of a relatively short follow-up time), there was accelerated linear growth (mean GV Z-score: 11.5; 9.0, 13.4) and overall advanced skeletal maturation (mean BA/CA ratio: 1.53; 1.39, 1.98). After good control of GH excess and PP, the mean GV Z-score decreased from 11.49 to 0.12, which was statistically significant (P <0.001) (**Figure 4B**). The median BA/CA ratio also decreased significantly (1.44 to 1.24; P =0.005) (**Figure 4C**). The posttreatment PAH or final height Z-score (mean PAH or final height Z-score 1.8) was higher than the predicted height Z score (mean predicted height Z-score 0.1; P=0.03) (**Figure 4E**). The PAH Z-scores were normal (−2 to +2) in four of six patients (66.7%;

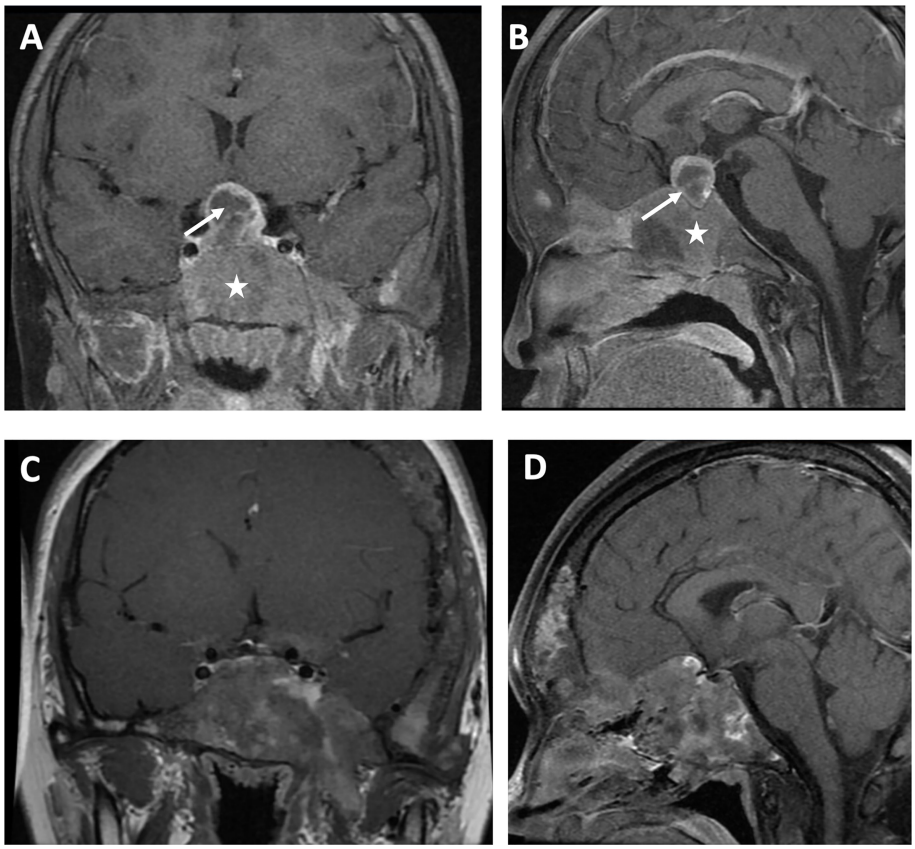

FIGURE 3 | Visualization by MRI in the coronal view **(A)** and sagittal view **(B)** of a macroadenoma (arrow) surrounded by cranial fibrous dysplasia (star) in a patient with MAS and GH excess before surgery and pharmacologic treatment. Coronal view **(C)** and sagittal view **(D)** after surgery and pharmacologic treatment.

patients 2, 5, 6, and 7), and patients 1 and 3 had increased PAH Z-scores. Most of the patients had PAH Z-scores that increased after treatment except for patient 1. The mean PAH Z-score increased from 1.46 to 2.2 after treatment, with no statistical significance (**Figure 4D**). The GV Z-score of patient 1 decreased from 8.99 to −2.1 after surgical and pharmacological treatment. Patient 4, diagnosed with acromegaly at the age of 27, had a final height of 156 cm (Z-score −0.7) and a predicted height of 159 cm (Z-score −0.3).

Six patients were diagnosed with GH excess without PP in our cohort (the clinical characteristics and final height of these patients are illustrated in **Table 4**), four of six had symptoms of gigantism before the age of 16 (without a diagnosis or treatment until adulthood), and two of six were diagnosed in adulthood. The final height Z-score of gigantic patients without PP (mean final height Z-score: 3.6; 2.2, 4.9) was higher than the final height Z-score or posttreatment PAH Z-score of patients codiagnosed with gigantism and PP (mean Z-score: 1.8; −0.3, 3.3; P=0.064) (**Figure 4F**).

Clinical Characteristics and Treatment Outcomes From the Literature Review

The clinical characteristics, treatment, and outcomes of patients with MAS with GH excess and PP from previous case series and reports are summarized in **Tables 5** and **6**. Thirty-nine (25 females, 64.1%) patients were analyzed. Regarding GH excess, 13 patients were diagnosed before the age of 16 years old (mean age: 7.7 years; 4, 13), and 13 patients (50%) were diagnosed in adulthood, with an average age of 27.1 years (17.8, 38). The mean random GH level and IGF-1 Z-score were 39.0 μg/L (2.8, 290) and 5.9 (−0.2, 17.7), respectively. MRI data were available for 27 of 39 cases (69.2%), and CT and X-ray scans were performed for eight patients, revealing 14 macroadenomas (51.9%) and 7 (25.9%) microadenomas. For craniofacial FD complications, 11 patients had various degrees of visual impairment, and five patients had olfactory impairment. Five patients received treatment for PP among the 19 patients with available data. Aromatase inhibitors, tamoxifen, GnRHas, testolactone, anastrozole, and medroxyprogesterone acetate were administered (cases 3, 15, 16, 27, and 34). Syptoms of PP were well controlled in cases 15 and 16, and partially controlled in case 34. The response to treatment of PP was not mentioned in case 3 or 27. Eight (36.4%) out of 22 patients for whom data were available achieved complete remission, 10 (45.5%) individuals had partial remission, GH excess was not controlled in 4 (18.2%) individuals, and 1 (4.5%) patient died after surgery from postoperative hemorrhage. Among the patients with complete

TABLE 2 | Clinical and biochemical characteristics and treatment outcomes of patients with PP from PUMCH.

Patient ID	Pretreatment										Tx for PP	Tx duration (y)	Posttreatment								
	BA/CA	PAHZ-score	GV (cm/y) Z-score	LH (IU/L)	Peak LH (IU/L)	FSH (IU/L)	E2 (pg/ml)	T (ng/ml)	Mean testicular or ovarian volumn(mm^3)				BA/CA	PAHZ-score	Predicted Ht (cm)	Predicted HtZ-score	Final HtZ-score	GV (cm/y) Z-score	LH (IU/L)	FSH (IU/L)	E2 (pg/ml)	T (ng/ml)	Mean testicular or ovarian volumn(mm^3)
1	1.44	+4.9	+8.99	0.21	2.2	2.10	10.2	<0.1	1.6	None			1.0		157.5	−0.5	+3.3	−2.10					
2	1.43	−0.2	NA	2.60	25.6	8.40	21.1	1.39	4.2	GnRHa	0.25		NA	NA	171.0	−0.2	−0.3	NA	0.40	0.46	26.30	0.21	NA
3	1.39	+2.1	+12.40	<0.2	1.15	0.25	216.0	<0.1	1.8	None			1.02	+2.6	161.5	0.1		−0.6	<0.2	0.25	11.05	<0.1	2.6
5	1.53	+0.41	+13.38	<0.2	0.98	0.78	165.0	0.31	7.5	Tamoxifen 5 mg bid	5.25		1.24	+2.1	162.5	0.3		+1.91	<0.2	0.31	33.00	0.22	1.7
6	1.98	−0.3	+11.72	1.14	1.20	0.78	21.0	1.65	3.3	Letrozole 2.5 mg qod Medroxyprogesterone 4 mg bid	2.25		1.53	+2.1	174.5	0.3		−0.94	<0.2	0.32	<5	1.12	4.4
7	1.40	+0.2	+10.97	<0.2	3.76	0.11	57.73	<0.1	2.3	Letrozole 1.25 mg qd	0.5		1.27	+0.9	163	0.4		2.35	0.26	3.36	11.06	<0.1	1.3

BA/CA, bone age over chronological age; PAH, predicted adult height; GV, growth velocity; LH, luteinizing hormone; FSH, follicle-stimulating hormone; Tx, treatment; E2, estradiol; T, testosterone; Y, year; Ht, height; NA, not available. Peak LH was LH level after GnRH stimulation test. The posttreatment sex hormones and average ovarian measurements for patient 1 are not listed because she was sexually mature at the last follow-up at age 17.

disease resolution, one patient was cured by surgery; one patient was treated with a DA alone; one patient was cured by an LAR and DA; and the remaining five patients received combination treatment with either pegvisomant, an LAR and DA or pegvisomant and fractioned radiotherapy.

In the literature review, for patients who had been diagnosed with gigantism, for whom the final height was thoroughly documented, the final heights were 180 cm, 183 cm, and 169 cm, and the height Z-scores were 2.2, 2.6, and −0.9 for cases 9, 11, and 15, respectively. Additionally, the predicted heights were 172.5 and 175 cm for cases 11 and 15, respectively (the parental height was not mentioned in case 9). For patients who had been diagnosed with acromegaly, three of six patients (cases 1, 12, 14, 32, 38, and 39) had short stature (139 cm, Z-score= −3.2 in case 14; 147.5 cm, Z-score= −2.1 in case 32; and 140 cm, Z-score= −3.1 in case 39).

DISCUSSION

This study is the first case series to illustrate the clinical manifestations, treatment, and predicted or final height and the status of FD of combined GH excess and PP in the context of MAS patients. We found that the proportion of women with GH excess and PP of MAS was higher, whereas GH excess in MAS (14, 16) and "classic" acromegaly (59) affected almost equal proportions of women and men. This difference is likely due to PP affecting more female patients than male patients with MAS (8). In this case series, the number of MAS patients from PUMCH with gigantism was higher than the number with acromegaly, while approximately half of the literature review patients had gigantism. The average age at the acromegaly diagnosis in patients with MAS and PP in the literature review was 27.1 years, which is slightly lower than 30.1 years, the mean age of patients with acromegaly and MAS reported in a previous study (9); however, both of these ages were much younger than the median age of 40~50 years observed in "classic" acromegaly (60–62).

The data from PUMCH demonstrated that patients with a diagnosis of gigantism and PP have growth rate acceleration and skeletal maturation, and good control of both conditions leads to normalized GV and stabilized bone age. However, the data from PUMCH and a literature review showed that these patients had unaffected final heights. For those who were diagnosed with gigantism, the PAH Z-scores or final height Z-scores were higher than the predicted adult height Z-score. For patients diagnosed with acromegaly, one patient from PUMCH and approximately half of the patients reviewed in the literature had a short stature. Previous findings (15, 16) indicated that patients with a history of gigantism and PP achieve normal adult height despite early epiphyseal fusion, while those diagnosed with PP and acromegaly can end up with a significantly shorter adult height (63). The growth outcome in our cohort was that the height of MAS patients with PP and gigantism was higher than their predicted heights. This is probably because, in our cohort, PP was well controlled, while gigantism was partially relieved in

TABLE 3 | Clinical and biochemical characteristics and treatment outcomes of patients with GH excess and PP from PUMCH.

Patient ID	Pretreatment						Posttreatment					Outcome
	GH nadir (μg/L)	IGF-1Z-score	PRL (μg/L)	ALPZ-score	MRI (largest diameter; mm)	Treatment for GH excess	IHC postivity	GH nadir (μg/L)	IGF-1Z-score	PRL (μg/L)	ALPZ-score	
1	35.3	10.2	204.4	+5.25	Macro (24)	Surgery+LAR+DA	GH,PRL	3.1	0.3	24.4	+1.48	PR
2	8.3	7.8	21.0	+9.97	NA	None		–	–	–	–	NA
3	NA	10.0	143.4	+5.54	Macro (14)	LAR + Surgery	GH,PRL	2.52	2.64	21.1	+4.85	PR
4	5.9	2.2	13.7	+17.50	Micro (7)	Surgery	GH	0.1	−0.6	7.8	+16.39	CR
5	5.2	6.9	51.8	+6.22	Multiple micro	Surgery	GH	0.748	−0.9	22.1	+5.32	CR
6	21.4	5.7	47.7	+14.24	Macro (19)	Surgery+DA	GH	6.4	5.0	4.7	+11.02	PR
7	3.0	2.0	11.19	+21.28	Absence	None		–	–	–	–	–

GH, growth hormone; IGF-1, insulin-like growth factor-1; PRL, prolactin; ALP, alkaline phosphatase; Macro, macroadenoma; Micro, microadenoma; LAR, long-acting somatostatin analogue octreotide; DA, dopamine agonist; NA, not available. The reference value for GH nadir is less than 1 μg/L. The reference value of prolactin for females is less than 30 μg/L in female patients, and 2.6~13.1 μg/L in male patients.

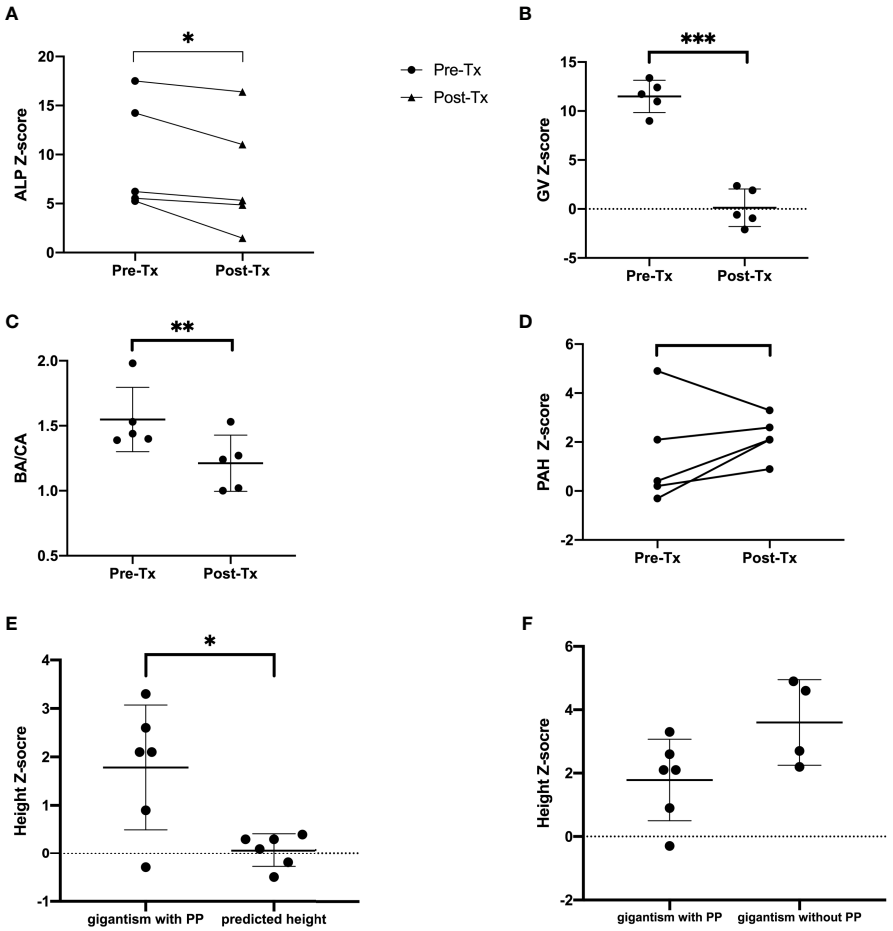

FIGURE 4 | ALP-Z score **(A)**, GV Z-score **(B)**, BA/CA ratio **(C)**, PAH Z-score **(D)** before and after treatment. The post-Tx data were collected at the last consultation for patients under therapy. **(E)** Final height or PAH Z-scores of patients diagnosed with gigantism and PP of MAS *versus* their predicted adult height. **(F)** Final height Z-scores of patients diagnosed with gigantism and PP *versus* final height or PAH Z-scores of patients diagnosed with gigantism without PP. Tx, treatment; Pre-Tx, pretreatment; Post-Tx,posttreatment; ALP, alkaline phosphatase; GV, growth velocity; BA/CA, bone age over chronological age; PAH, predicted adult height. ***P < 0.001, **P < 0.01, *P < 0.05.

TABLE 4 | Clinical characteristics and final height of patients diagnosed with GH excess without PP from PUMCH.

Patient ID	Sex	Café au lait	Age of Dx of MAS (y)	Age of Sx of GH excess (y)	CFFD	Polyostotic FD	Final Ht (cm)	Final Ht Z-score	Predicated Ht (cm)	Predicated HtZ-score
1	M	Y	26	15	Y	Y	188	2.2	179	0.9
2	M	Y	9	9	Y	Y	204	4.6	NA	NA
3	F	N	24	10	Y	Y	191f	4.9	164.5	0.6
4	M	Y	34	15	Y	Y	191.3	2.7	181.5	1.3
5	M	Y	11	45	Y	Y	173	0.0	NA	NA
6	M	Y	16	23	Y	Y	183.5	1.6	181.5	1.3

Dx, diagnosis; Sx, symptom and sign; FD, fibrous dysplasia; CFFD, craniofacial fibrous dysplasia; Ht, height; NA, not available.

some patients. This phenomenon indicates that sex hormones and GH have cumulative effects on the growth plate, and the time point at which GH excess appears is related to the final adult height.

The diagnosis and treatment of the coexistence of GH excess and PP is challenging. Under these circumstances, BA can better indicate the degree of sexual maturity. When height and BA are not parallel, we should consider comorbid gigantism. Laboratory screening for GH excess helps confirm the diagnosis. Good control of GH excess and PP is essential to reduce the growth rate and stabilize bone maturity.

Although patients with gigantism and PP in both our cohort and the literature review have unaffected final heights, early detection and treatment are still important because uncontrolled gigantism worsens CFFD. Bone turnover is increased in patients with GH excess, and they have increased levels of markers of bone formation and resorption (64). These biomarkers, particularly ALP, are usually related to the scope and intensity of bone involvement in MAS (65). Previous studies have already shown that uncontrolled gigantism is associated with the aggravation of CFFD and an increased risk of optic neuropathy (16–18) and hearing loss (19). Studies have also shown that early treatment during the pediatric period decreases the risk of these morbidities (15, 18) and results in lower serum ALP levels (14). In the present study, CFFD lesions were present in all patients from PUMCH, and polyostotic FD lesions were present in most patients, suggesting that they may be correlated with excess GH. Additionally, after effective treatment of GH excess, the visual field, hearing, and olfactory functions remained stable, and the ALP Z-score decreased after treatment. These results indicate that early successful treatment of GH excess might help ameliorate FD.

In addition to aggravating FD, GH excess is also related to impaired glucose tolerance, hypertension, cardiomyopathy, and an increased risk of tumors (22). Therefore, choosing the proper treatment is critical. Conventional treatments for GH excess include surgery, medications (somatostatin receptor ligands, Das, and the GH receptor antagonist pegvisomant), and radiotherapy. According to previous studies, medical therapy is considered the first-line treatment because pituitary surgery is technically difficult in patients with MAS because of the massive thickening of the skull base with FD (16, 35). However, technological progress has been made in this field in recent years, and we suggest that transphenoidal tumor resection under the guidance of neuronavigation might be feasible. An earlier cohort study from PUMCH revealed that transsphenoidal complete tumor excision with neuronavigational guidance is effective in patients with MAS with GH excess. In the present study, five of seven patients from PUMCH had undergone navigation-assisted transsphenoidal pituitary surgery, and two out of the five patients achieved full recovery. The remaining three patients had a partial response and then continued to receive long-acting somatostatin and bromocriptine. None of our patients had hypopituitarism after surgery. Therefore, from the experience of our center, navigation-assisted transsphenoidal pituitary surgery could be an effective and relatively safe choice for patients with MAS diagnosed with GH excess and PP. Radiotherapy is generally not advised because of the risk of fatal malignant transformation of CFFD in bones (66–68).

Uncontrolled PP can also cause psychological problems in children, and long-term exposure to high levels of estrogen elevates the risk of breast cancer and endometrial cancer. It has already been demonstrated that letrozole, a 3rd-generation aromatase inhibitor, and tamoxifen, an estrogen receptor modulator, are the most evidenced treatments (69). Medroxyprogesterone is also effective for controlling vaginal bleeding and breast development in the short term (13, 70). When secondary central PP develops, GnRHa is beneficial for blocking the hypothalamus-pituitary-gonadal (HPG) axis (71). In this study, the treatments for PP ranged from observation only to combinations of two medications. Letrozole and tamoxifen were the most frequently used. One patient developed secondary central PP and was treated with GnRHa for 3 months. Medroxyprogesterone was also used in combination with letrozole in one 6-year-old boy. During follow-up, we need to focus on changes in BA or the BA/CA ratio, not only changes in the growth rate, because the decline in the growth rate may only benefit from controlling excessive GH.

The co-occurrence of GH excess and PP in MAS is extremely rare. This study is the first to analyze the clinical features of this condition, and the diagnosis and treatment of both conditions pose considerable challenges. First, the diagnosis of gigantism may be overlooked because PP can also cause accelerated linear growth and atypical facial dysmorphia due to CFFD. Additionally, when evaluating the effectiveness of PP treatment in these patients, attention should be given to not only changes in GV but also changes in BA. A comprehensive consideration of GV, BA, and IGF-1 levels may lead to an accurate diagnosis and smooth follow-up.

However, this study still had several limitations. First, the sample size from PUMCH was small because the prevalence of this condition was extremely low, and patient 2 was lost of follow-up because of financial problem. We added 39 cases from the literature as supplementation. Additionally, when analyzing the association of GH excess with FD, we did not include a control group, and the severity of bone lesions and incidence of

TABLE 5 | Clinical characteristics of patients from the literature review.

Patient No.	First author, year	Type of study	Sex	Age at Dx (y)	Age at dx of GH excess (y)	Age at dx of PP (y)	CAL	CFFD	Polyostotic FD	Other endocrinopathies	Imaging	Type of lesion on imaging (largest diameter; mm)	Treatment for PP	Ovarian or testicular ultrasound
1	Rajan, 2019 (32)	Case report	F	24	24	NA, menarche at 7	+	+	+	Hyperthyroidism	MRI	Macro (40)	None	NA
2	Franco, 2019 (33)	Case report	F	26	26	9	+	+	+		MRI	Macro	None	NA
3	Wong, 2017 (34)	Cohort study	M	2	8	NA	+	+	+	Hyperthyroidism	MRI	Absence	Aromatase inhibitor and tamoxifen, GnRHa	Heterogeneous changes Echogenic lesions Microlithiasis
4	Wong, 2017 (34)	Cohort study	M	3	NA	6	+	+	+	Hyperthyroidism	MRI	Micro (4)	None	Echogenic lesions Microlithiasis
5	Wong, 2017 (34)	Cohort study	F	36	36	NA	+	+	+	Hyperthyroidism	MRI	Adenoma	None	NA
6	Akintoye, 2006 (35)	Randomized controlled crossover study	F	13	NA	NA	+	+	+	Hyperthyroidism	MRI	Abnormal enhancement	NA	NA
7	Vortmeyer, 2012 (36)	Case series	F	29	NA	NA	+	+	+		MRI	Micro	NA	NA
8	Vortmeyer, 2012 (36)	Case series	M	19	NA	NA	+	+	+		MRI	Macro	NA	NA
9	Classen, 2012 (37)	Case report	F	3	11	NA	–	+	NA		MRI	Micro	None	NA
10	Nozieres, 2011 (38)	Cohort study	M	6.5	6	NA	+	+	+		MRI	Hyperplasia	NA	NA
11	Madsen, 2010 (39)	Case series	F	8.2	8.2	5	–	+	+		MRI	Micro	None	NA
12	Almeida, 2009 (40)	Case report	F	29	29	NA	+	+	+		MRI	Macro (19)	None	NA
13	Imanaka, 2007 (41)	Case report	F	5	21	4	+	+	–	Hyperthyroidism	MRI	Macro (15)	NA	NA
14	Galland, 2006 (42)	Cohort study	F	27	27	NA	+	+	+	Hyperthyroidism	MRI	Macro	NA	NA
15	Papadopoulou, 2006 (43)	Case report	M	9	9	9	+	+	+		MRI	Micro (9)	testolactone	Microlithiasis
16	Zacharin, 2005 (44)	Case report	M	2.5	8.5	5	+	+	+		MRI	Hyperplasia	Testolactone→anastrozole	NA
17	Akintoye, 2002 (15)	Cohort study	M	7	NA	NA	+	+	+	Hyperthyroidism	MRI	Abnormal enhancement	NA	NA
18	Akintoye, 2002 (15)	Cohort study	M	30	NA	NA	+	+	+		MRI	Macro (17)	NA	NA
19	Akintoye, 2002 (15)	Cohort study	F	34	NA	NA	+	+	+		MRI	Macro (17)	NA	NA
20	Akintoye, 2002 (15)	Cohort study	F	5	NA	NA	+	+	+	Hyperthyroidism	MRI	Absence	NA	NA

(Continued)

TABLE 5 | Continued

Patient No.	First author, year	Type of study	Sex	Age at Dx (y)	Age at dx of GH excess (y)	Age at dx of PP (y)	CAL	CFFD	Polyostotic FD	Other endocrinopathies	Imaging	Type of lesion on imaging (largest diameter; mm)	Treatment for PP	Ovarian or testicular ultrasound
21	Akintoye, 2002 (15)	Cohort study	F	26	NA	NA	+	+	+		MRI	Micro (9)	NA	NA
22	Akintoye, 2002 (15)	Cohort study	F	11	NA	NA	+	+	+	Hyperthyroidism	MRI	Absence	NA	NA
23	Akintoye, 2002 (15)	Cohort study	F	4	NA	NA	+	+	+		MRI	Absence	NA	NA
24	Akintoye, 2002 (15)	Cohort study	F	13	NA	NA	+	+	+	Hyperthyroidism	MRI	Adenoma	NA	NA
25	Zumkeller, 2001 (45)	Case report	M	8	8	7	+	+	+	Hyperthyroidism	MRI	Micro (4)	NA	NA
26	Dotsch, 1996 (46)	Case report	M	6.5	6.5	6.5	–	+	+		MRI	Macro (18)	NA	NA
27	Feuillan, 1995 (47)	Case report	F	6 months	7.3	6 months	+	+	+	Hyperthyroidism	MRI	Absence	Testolactone	NA
28	Premawardhana, 1992 (48)	Case report	F	26	26	3	+	+	+	Adrenal insufficiency	CT	Macro	None	NA
29	Abs, 1990 (49)	Case report	F	36	36	8	–	+	+	Hyperthyroidism	MRI	Macro (15)	None	NA
30	Laughlin, 1989 (50)	Case report	F	9	13	9	+	+	+		MRI	Macro (36)	NA	NA
31	Cuttler, 1989 (51)	Case series	M	9.5	NA	NA	+	+	+		NA	NA	None	NA
32	Geffner, 1987 (52)	Case report	F	8 months	17.8	8 months	+	+	+	Hyperthyroidism	CT	Macro (21)	none	NA
33	Mauras, 1986 (53)	Case report	M	4	4	NA	+	+	+	Hyperthyroidism, CS	CT	NA	NA	NA
34	Kovacs, 1984 (54)	Case report	F	4	6	4	+	+	+		CT	NA	Medroxyprogesterone acetate	NA
35	Albin, 1981 (55)	Case series	F	19	19	NA	+	+	+		XR	NA	None	NA
36	Albin, 1981 (55)	Case series	M	23	23	NA	+	+	+		XR	Absence	None	NA
37	Lightner, 1975 (56)	Case report	M	4	4	4	+	+	+		XR	Macro (15)	NA	NA
38	Scurry, 1964 (57)	Case report	F	22	38	5	+	+	+		NA	NA	NA	NA
39	Carr, 1979 (58)	Case report	F	30	30	19 months	+	+	+		XR		None	NA

Dx, diagnosis; FD, fibrous dysplasia; CFFD, craniofacial fibrous dysplasia; PP, precocious puberty; GH, growth hormone; CAL, Café au lait; CS, Cushing's syndrome. The number in brackets of type of lesion is the largest diameter of the pituitary tumor. NA, not available.

TABLE 6 | Biochemical characteristics and treatment outcomes of patients with GH excess from the literature review.

Patient No.	Pretreatment				Tx for GH excess	Posttreatment			Visual defect	Hearing and olfactory defects
	GH nadir (μg/L)	IGF-1Z-score	PRL (μg/L)	ALP (IU/L)		IGF-1Z-score	ALP (IU/L)	GH excesscontrolled		
1	8.21	8.1	3,218	216	DA	NA	NA	NA	Bitemporal hemianopia	NA
2	NA	14.8	155.8	2,259	LAR+PEG	NA	NA	NA	Left eye dystopia	NA
3	NA	2.0	24.9	NA	LAR+DA	NA	NA	No	NA	NA
4	NA	2.0	20	NA	LAR+DA	NA	NA	Yes	NA	NA
5	NA	4.5	4.43	NA	LAR+DA	NA	NA	No	NA	NA
6	NA	1.8	NA	715	LAR+DA+PEG	−2.8	515	Yes	NA	NA
7	40.5	6.2	26	NA	Surgery	1	NA	PR	Unilateral blindness	Deafness
8	127	8.8	17	NA	Surgery	−2.4	NA	Yes	NA	NA
9	NA	6.0	285.3	690	DA	NA	417	Yes	Mild left-sided hemianopia	NA
10	NA	3.0	NA	NA	LAR+DA+PEG	−1	NA	Yes	NA	NA
11	NA	17.7	38.5	NA	2 surgeries + LAR + DA	3.6	NA	PR	NA	NA
12	3.4	3.0	177	537.9	Surgery + LAR + DA	2.3	NA	PR	NA	NA
13	NA	2.3	18.9	8721	LAR	−0.3	6,870	PR	Bitemporal upper quarter blindness	NA
14	NA	8.3	18	NA	RT+PEG	0.7	NA	Yes	NA	NA
15	12.5	NA	NA	NA	LAR	NA	NA	NA	Normal	Normal
16	26	NA	NA	812	LAR		NA	PR	Binasal visual field loss	NA
17	1.2	1.8	20	1224	LAR+DA+PEG	−2.5	970	Yes	Normal	Normal
18	60.2	8.2	81.5	474	LAR+DA/PEG	3	366	PR	Blindness	Hearing loss
19	14.3	4.6	98	871	LAR+DA/PEG	1.1	833	Yes	Normal	Normal
20	16.2	3.2	27	NA	LAR	NA	NA	NA	Normal	Normal
21	29	>5	53	NA	DA	NA	NA	NA	Normal	Normal
22	2.3	−0.2	36	NA	None	NA	NA	NA	Normal	Normal
23	5.3	2.5	17	NA	LAR	NA	NA	NA	Normal	Hearing loss
24	16.3	>5	68	NA	DA+LAR	NA	NA	NA	Normal	Hearing loss
25	NA	3.9	206.7	256	LAR	1.4	NA	PR	NA	NA
26	37	12.1	62.1	NA	Surgery+LAR	4.6	NA	PR	NA	NA
27	11	8.1	35	1,105	LAR	NA	NA	NA	NA	NA
28	4.9	9.4	14.6	NA	RT+LAR	NA	NA	PR	Normal	NA
29	NA	NA	27–33	NA	Sandostatin+DA		NA	No	NA	NA
30	NA	NA	NA	NA	Surgery	NA	NA	NA	Bitemporal hemianopsia	NA
31	10.4	NA	46.1	NA	DA	–	No	NA	NA	
32	NA	NA	66	NA	Sandostatin+DA	NA	NA	NA	Normal	NA
33	5.4	NA	NA	NA	NA	NA	NA	NA	NA	NA
34	NA	NA	>200	NA	Surgery+DA	NA	NA	No	NA	NA
35	170	NA	190	2,500	Surgery	–	–	Dead	Visual defect	Hearing loss
36	5	NA	45.6	285	NA	NA	NA	NA	Right eye optic atrophy	Normal
37	98	NA	NA	NA	NA	NA	NA	NA	Normal	NA
38	NA	NA	NA	NA	Fractionated radiotherapy	NA	NA	NA	Left temporal hemianopsia	NA
39	5.3	NA	86.9	NA	DA	NA	NA	PR	Normal	Normal

GH, growth hormone; IGF-1, insulin-like growth factor-1; PRL, prolactin; ALP, alkaline phosphatase; Macro, macroadenoma; Micro, microadenoma; LAR, long-acting somatostatin analogue octreotide; DA, dopamine agonist; PEG, pegvisomant.

optic, hearing, and olfactory complications could not be compared with those in patients without GH excess.

CONCLUSION

MAS with GH excess and PP is rare, and these patients present with increased growth velocity and advanced bone age. Early diagnosis and proper treatments are essential. The predicated or final height of patients with gigantism is not impaired, while the final height of patients with acromegaly is shorter.

DATA AVAILABILITY STATEMENT

The original contributions presented in the study are included in the article/supplementary material. Further inquiries can be directed to the corresponding author.

ETHICS STATEMENT

This study is in compliance with the Helsinki Declaration, and the parents signed the informed consent form, with the approval

of the Ethics Committee of Peking Union Medical College Hospital (Reference number: JS-1663). Written informed consent to participate in this study was provided by the participants' legal guardian/next of kin.

AUTHOR CONTRIBUTIONS

XZ, LD, and HZ participated in the design of the study. XZ carried out the study and collected important background information. LW and HYa carried out literature research. LL, SC, and HP provided assistance for statistical analysis. YY, BX, KD, and RW provided assistance for surgical clinical data collection. FF and HYo helped with radiologic data collection. ZL participated in pathology data collection. All authors contributed to the article and approved the submitted version.

FUNDING

This work was supported by a grant from the National Key Research and Development Program of China (No. 2016YFC0901501) and CAMS Innovation Fund for Medical Science (CAMS-2016-I2M-1-002).

REFERENCES

1. Boyce AM, Collins MT. Fibrous Dysplasia/McCune-Albright Syndrome: A Rare, Mosaic Disease of Gαs Activation. *Endocr Rev* (2020) 41(2):345–70. doi: 10.1210/endrev/bnz011
2. Weinstein LS, Shenker A, Gejman PV, Merino MJ, Friedman E, Spiegel AM. Activating Mutations of the Stimulatory G Protein in the McCune–Albright Syndrome. *New Engl J Med* (1991) 325(24):1688–95. doi: 10.1056/NEJM199112123252403
3. Albright F, Butler AM, Hampton AO, Smith P. Syndrome Characterized by Osteitis Fibrosa Disseminata, Areas of Pigmentation and Endocrine Dysfunction, With Precocious Puberty in Females: Report of Five Cases. *New Engl J Med* (1937) 216(17):727–46. doi: 10.1056/NEJM193704292161701
4. Boyce AM, Florenzano P, de Castro LF, Collins MT. *Fibrous Dysplasia/Mccune-Albright Syndrome*. University of Washington, Seattle: GeneReviews (2019).
5. Tufano M, Ciofi D, Amendolea A, Stagi S. Auxological and Endocrinological Features in Children With McCune Albright Syndrome: A Review. *Front Endocrinol (Lausanne)* (2020) 11:522. doi: 10.3389/fendo.2020.00522
6. Holbrook L, Brady R. *McCune Albright Syndrome. StatPearls*. Treasure Island (FL: StatPearls Publishing LLC (2021). StatPearls Publishing Copyright © 2021.
7. Dumitrescu CE, Collins MT. McCune-Albright Syndrome. *Orphanet J Rare Dis* (2008) 3(1):12. doi: 10.1186/1750-1172-3-12
8. Collins MT, Singer FR, Eugster E. McCune-Albright Syndrome and the Extraskeletal Manifestations of Fibrous Dysplasia. *Orphanet J rare Dis* (2012) 7(Suppl 1):S4. BioMed Central. doi: 10.1186/1750-1172-7-S1-S4
9. Teilmann G, Pedersen CB, Jensen TK, Skakkebaek NE, Juul A. Prevalence and Incidence of Precocious Pubertal Development in Denmark: An Epidemiologic Study Based on National Registries. *Pediatrics* (2005) 116 (6):1323–8. doi: 10.1542/peds.2005-0012
10. Schmidt H, Kiess W. Secondary Central Precocious Puberty in a Girl With McCune-Albright Syndrome Responds to Treatment With GnRH Analogue. *J Pediatr Endocrinol Metab* (1998) 11(1):77–81. doi: 10.1515/jpem.1998.11.1.77
11. Pasquino AM, Tebaldi L, Cives C, Maciocci M, Boscherini B. Precocious Puberty in the McCune-Albright Syndrome. Progression From Gonadotrophin-Independent to Gonadotrophin-Dependent Puberty in a Girl. *Acta Paediatr Scand* (1987) 76(5):841–3. doi: 10.1111/j.1651-2227.1987.tb10576.x
12. Corica D, Aversa T, Pepe G, De Luca F, Wasniewska M. Peculiarities of Precocious Puberty in Boys and Girls With McCune-Albright Syndrome. *Front Endocrinol (Lausanne)* (2018) 9:337. doi: 10.3389/fendo.2018.00337
13. Schoelwer M, Eugster EA. *Treatment of Peripheral Precocious Puberty. Puberty From Bench to Clinic* Vol. 29. Basel: Karger Publishers (2016) p. 230–9.
14. Yao Y, Liu Y, Wang L, Deng K, Yang H, Lu L, et al. Clinical Characteristics and Management of Growth Hormone Excess in Patients With McCune-Albright Syndrome. *Eur J Endocrinol* (2017) 176(3):295–303. doi: 10.1530/EJE-16-0715
15. Akintoye SO, Chebli C, Booher S, Feuillan P, Kushner H, Leroith D, et al. Characterization of Gsp-Mediated Growth Hormone Excess in the Context of McCune-Albright Syndrome. *J Clin Endocrinol Metab* (2002) 87(11):5104–12. doi: 10.1210/jc.2001-012022
16. Salenave S, Boyce AM, Collins MT, Chanson P. Acromegaly and McCune-Albright Syndrome. *J Clin Endocrinol Metab* (2014) 99(6):1955–69. doi: 10.1210/jc.2013-3826
17. Boyce AM, Glover M, Kelly MH, Brillante BA, Butman JA, Fitzgibbon EJ, et al. Optic Neuropathy in McCune-Albright Syndrome: Effects of Early Diagnosis and Treatment of Growth Hormone Excess. *J Clin Endocrinol Metab* (2013) 98(1):E126–34. doi: 10.1210/jc.2012-2111
18. Tessaris D, Boyce AM, Zacharin M, Matarazzo P, Lala R, De Sanctis L, et al. Growth Hormone—Insulin-Like Growth Factor 1 Axis Hyperactivity on Bone Fibrous Dysplasia in McCune-Albright Syndrome. *Clin Endocrinol* (2018) 89 (1):56–64. doi: 10.1111/cen.13722
19. Boyce AM, Brewer C, DeKlotz TR, Zalewski CK, King KA, Collins MT, et al. Association of Hearing Loss and Otologic Outcomes With Fibrous Dysplasia. *JAMA Otolaryngol–Head Neck Surg* (2018) 144(2):102–7. doi: 10.1001/jamaoto.2017.2407
20. Burke AB, Collins MT, Boyce AM. Fibrous Dysplasia of Bone: Craniofacial and Dental Implications. *Oral Dis* (2017) 23(6):697–708. doi: 10.1111/odi.12563
21. Özcan İ, Ünsal G, Koca RB, Orhan K. Craniofacial Fibrous Dysplasia Involvements of Mccune-Albright Syndrome: A Review With an Additional Case. *Curr Med Imaging* (2020) 17(7):864–70. doi: 10.2174/1573405616666201209102418
22. Raborn LN, Pan KS, FitzGibbon EJ, Collins MT, Boyce AM. Optic Disc Edema in Fibrous Dysplasia/McCune-Albright Syndrome: Prevalence, Etiologies, and Clinical Implications. *Bone* (2021) 143:115661. doi: 10.1016/j.bone.2020.115661
23. Zhu H, Xu Y, Gong F, Shan G, Yang H, Xu K, et al. Reference Ranges for Serum Insulin-Like Growth Factor I (IGF-I) in Healthy Chinese Adults. *PloS One* (2017) 12(10):e0185561. doi: 10.1371/journal.pone.0185561
24. Xu S, Gu X, Pan H, Zhu H, Gong F, Li Y, et al. Reference Ranges for Serum IGF-1 and IGFBP-3 Levels in Chinese Children During Childhood and Adolescence. *Endocr J* (2010) 57(3):221–8. doi: 10.1507/endocrj.K09E-200
25. Adashi EY, Rock JA, Rosenwaks Z. *Reproductive Endocrinology, Surgery, and Technology*. Philadelphia: Lippincott-Raven (1996).
26. Greulich WW, Pyle SI. *Radiographic Atlas of Skeletal Development of the Hand and Wrist*. Redwood City: Stanford University Press (1959).
27. Bayley N, Pinneau SR. Tables for Predicting Adult Height From Skeletal Age. Revised for Use With the Greulich-Pyle Hand Standards. *J Pediatr* (1952) 40 (4):423–41. doi: 10.1016/S0022-3476(52)80205-7
28. Li H, Ji C, Zong X, Zhang Y. Height and Weight Standardized Growth Charts for Chinese Children and Adolescents Aged 0 to 18 Years. *Zhonghua er ke za zhi= Chin J Pediatr* (2009) 47(7):487–92. doi: 10.3760/cma.j.issn.0578-1310.2009.07.003
29. Zong X, Li H. General Growth Patterns and Simple Mathematic Models of Height and Weight of Chinese Children. *Zhonghua er ke za zhi= Chin J Pediatr* (2009) 47(5):371–5. doi: 10.3760/cma.j.issn.0578-1310.2009.05.017
30. de Onis M, Onyango AW, Borghi E, Siyam A, Nishida C, Siekmann J. Development of a WHO Growth Reference for School-Aged Children and Adolescents. *Bull World Health Organ* (2007) 85(9):660–7. doi: 10.2471/BLT.07.043497
31. Lu Q, Jia Z. Reference Values of Serum Alkaline Phosphatase for Chinese Children and Adolescents Aged 0 to 18 Years. *Clinics Lab Med* (2009) 6:1069–70. doi: 10.3969/j.issn.1672-9455.2009.13.026

32. Rajan R, Cherian KE, Asha HS, Paul TV. McCune Albright Syndrome: An Endocrine Medley. *BMJ Case Rep CP* (2019) 12(7):e229141. doi: 10.1136/bcr-2018-229141
33. Franco JMPL, Rêgo RD, Gomes GMF, da Silveira Santos DF, Santos ES. Surgical Treatment of Polyostotic Craniomaxillofacial Fibrous Dysplasia Associated With Acromegalia: The McCune–Albright Syndrome. *J Craniofacial Surg* (2019) 30(6):1806–8. doi: 10.1097/SCS.0000000000005498
34. Wong SC, Zacharin M. Long-Term Health Outcomes of Adults With McCune-Albright Syndrome. *Clin Endocrinol* (2017) 87(5):627–34. doi: 10.1111/cen.13419
35. Akintoye SO, Kelly MH, Brillante B, Cherman N, Turner S, Butman JA, et al. Pegvisomant for the Treatment of Gsp-Mediated Growth Hormone Excess in Patients With McCune-Albright Syndrome. *J Clin Endocrinol Metab* (2006) 91(8):2960–6. doi: 10.1210/jc.2005-2661
36. Vortmeyer AO, Gläsker S, Mehta GU, Abu-Asab MS, Smith JH, Zhuang Z, et al. Somatic GNAS Mutation Causes Widespread and Diffuse Pituitary Disease in Acromegalic Patients With McCune-Albright Syndrome. *J Clin Endocrinol Metab* (2012) 97(7):2404–13. doi: 10.1210/jc.2012-1274
37. Classen CF, Mix M, Kyank U, Hauenstein C, Haffner D. Pamidronic Acid and Cabergoline as Effective Long-Term Therapy in a 12-Year-Old Girl With Extended Facial Polyostotic Fibrous Dysplasia, Prolactinoma and Acromegaly in McCune-Albright Syndrome: A Case Report. *J Med Case Rep* (2012) 6 (1):32. doi: 10.1186/1752-1947-6-32
38. Nozières C, Berlier P, Dupuis C, Raynaud-Ravni C, Morel Y, Chazot FB, et al. Sporadic and Genetic Forms of Paediatric Somatotropinoma: A Retrospective Analysis of Seven Cases and a Review of the Literature. *Orphanet J Rare Dis* (2011) 6(1):67. doi: 10.1186/1750-1172-6-67
39. Madsen H, Borges MT, Kerr JM, Lillehei KO, Kleinschmidt-Demasters B. McCune–Albright Syndrome: Surgical and Therapeutic Challenges in GH-Secreting Pituitary Adenomas. *J Neuro-Oncol* (2011) 104(1):215–24. doi: 10.1007/s11060-010-0461-9
40. Almeida JPC, Albuquerque LAF, Ferraz CL, Mota Í, Gondim J, Ferraz TM. McCune-Albright Syndrome and Acromegaly: Hormonal Control With Use of Cabergoline and Long-Acting Somatostatin-Case Report. *Arquivos Brasileiros Endocrinologia Metabologia* (2009) 53(1):102–6. doi: 10.1590/S0004-27302009000100015
41. Imanaka M, Iida K, Nishizawa H, Fukuoka H, Takeno R, Takahashi K, et al. McCune-Albright Syndrome With Acromegaly and Fibrous Dysplasia Associated With the GNAS Gene Mutation Identified by Sensitive PNA-Clamping Method. *Internal Med* (2007) 46(18):1577–83. doi: 10.2169/internalmedicine.46.0048
42. Galland F, Kamenicky P, Affres H, Reznik Y, Pontvert D, Le Bouc Y, et al. McCune-Albright Syndrome and Acromegaly: Effects of Hypothalamopituitary Radiotherapy and/or Pegvisomant in Somatostatin Analog-Resistant Patients. *J Clin Endocrinol Metab* (2006) 91(12):4957–61. doi: 10.1210/jc.2006-0561
43. Papadopoulou M, Doula S, Kitsios K, Kaltsas T, Kosta K. A Boy With McCune-Albright Syndrome Associated With GH Secreting Pituitary Microadenoma. Clinical Findings and Response to Treatment. *Hormones-Athens-* (2006) 5(3):205. doi: 10.14310/horm.2002.11186
44. Zacharin M. Paediatric Management of Endocrine Complications in McCune-Albright Syndrome. *J Pediatr Endocrinol Metab* (2005) 18(1):33–42. doi: 10.1515/JPEM.2005.18.1.33
45. Zumkeller W, Jassoy A, Lebek S, Nagel M. Clinical, Endocrinological and Radiological Features in a Child With McCune-Albright Syndrome and Pituitary Adenoma. *J Pediatr Endocrinol Metab* (2001) 14(5):553–60. doi: 10.1515/JPEM.2001.14.5.553
46. Dötsch J, Kiess W, Hänze J, Repp R, Lüdecke D, Blum W, et al. Gs Alpha Mutation at Codon 201 in Pituitary Adenoma Causing Gigantism in a 6-Year-Old Boy With McCune-Albright Syndrome. *J Clin Endocrinol Metab* (1996) 81(11):3839–42. doi: 10.1210/jcem.81.11.8923825
47. Feuillan PP, Jones J, Ross JL. Growth Hormone Hypersecretion in a Girl With McCune-Albright Syndrome: Comparison With Controls and Response to a Dose of Long-Acting Somatostatin Analog. *J Clin Endocrinol Metab* (1995) 80 (4):1357–60. doi: 10.1210/jcem.80.4.7714111
48. Premawardhana L, Vora J, Mills R, Scanion M. Acromegaly and Its Treatment in the McCune-Albright Syndrome. *Clin Endocrinol* (1992) 36(6):605–8. doi: 10.1111/j.1365-2265.1992.tb02272.x
49. Abs R, Beckers A, Van de Vyver F, De Schepper A, Stevenaert A, Hennen G. Acromegaly, Multinodular Goiter and Silent Polyostotic Fibrous Dysplasia, A Variant of the McCune—Albright Syndrome. *J Endocrinological Invest* (1990) 13(8):671–5. doi: 10.1007/BF03349592
50. O'Laughlin RL, Selinger SE, Moriarty PE. Pituitary Adenoma in McCune-Albright Syndrome: MR Demonstration. *J Comput Assisted Tomography* (1989) 13(4):685–8. doi: 10.1097/00004728-198907000-00026
51. Cuttler L, Jackson JA, Uz-Zafar MS, Levitsky LL, Mellinger RC, Frohman LA. Hypersecretion of Growth Hormone and Prolactin in McCune-Albright Syndrome. *J Clin Endocrinol Metab* (1989) 68(6):1148–54. doi: 10.1210/jcem-68-6-1148
52. Geffner ME, Nagel RA, Dietrich RB, Kaplan SA. Treatment of Acromegaly With a Somatostatin Analog in a Patient With McCune-Albright Syndrome. *J Pediatr* (1987) 111(5):740–3. doi: 10.1016/S0022-3476(87)80258-5
53. Mauras N, Blizzard RM. The McCune-Albright Syndrome. *Eur J Endocrinol* (1986) 113(4_Suppl):S207–17. doi: 10.1530/acta.0.112S207
54. Kovacs K, Horvath E, Thorner MO, Rogol AD. Mammosomatotroph Hyperplasia Associated With Acromegaly and Hyperprolactinemia in a Patient With the McCune-Albright Syndrome. *Virchows Archiv A* (1984) 403(1):77–86. doi: 10.1007/BF00689340
55. Albin J, Wu R. Abnormal Hypothalamic-Pituitary Function in Polyostotic Fibrous Dysplasia. *Clin Endocrinol* (1981) 14(5):435–43. doi: 10.1111/j.1365-2265.1981.tb00632.x
56. Lightner ES, Penny R, Frasier SD. Growth Hormone Excess and Sexual Precocity in Polyostotic Fibrous Dysplasia (McCune-Albright Syndrome): Evidence for Abnormal Hypothalamic Function. *J Pediatr* (1975) 87(6):922–7. doi: 10.1016/S0022-3476(75)80906-1
57. Scurry MT, Bicknell JM, Fajans SS. Polyostotic Fibrous Dysplasia and Acromegaly. *Arch Internal Med* (1964) 114(1):40–5. doi: 10.1001/archinte.1964.03860070086008
58. Carr D, Mathie I, Manners A, Colman C. Hyperprolactinaemia In A Patient With The Mccune-Albright Syndrome. *BJOG: Int J Obstetrics Gynaecol* (1979) 86(4):330–1. doi: 10.1111/j.1471-0528.1979.tb11264.x
59. Colao A, Grasso LF, Giustina A, Melmed S, Chanson P, Pereira AM, et al. Acromegaly. *Nat Rev Dis Primers* (2019) 5(1):1–17. doi: 10.1038/s41572-019-0071-6
60. Gruppetta M, Mercieca C, Vassallo J. Prevalence and Incidence of Pituitary Adenomas: A Population Based Study in Malta. *Pituitary* (2013) 16(4):545–53. doi: 10.1007/s11102-012-0454-0
61. Dal J, Feldt-Rasmussen U, Andersen M, Kristensen LO, Laurberg P, Pedersen L, et al. Acromegaly Incidence, Prevalence, Complications and Long-Term Prognosis: A Nationwide Cohort Study. *Eur J Endocrinol* (2016) 175(3):181–90. doi: 10.1530/EJE-16-0117
62. Fernandez A, Karavitaki N, Wass JA. Prevalence of Pituitary Adenomas: A Community-Based, Cross-Sectional Study in Banbury (Oxfordshire, Uk). *Clin Endocrinol* (2010) 72(3):377–82. doi: 10.1111/j.1365-2265.2009.03667.x
63. Haddad N, Eugster E. An Update on the Treatment of Precocious Puberty in McCune-Albright Syndrome and Testotoxicosis. *J Pediatr Endocrinol Metab* (2007) 20(6):653–62. doi: 10.1515/JPEM.2007.20.6.653
64. Scillitani A, Chiodini I, Carnevale V, Giannatempo GM, Frusciante V, Villella M, et al. Skeletal Involvement in Female Acromegalic Subjects: The Effects of Growth Hormone Excess in Amenorrheal and Menstruating Patients. *J Bone Miner Res* (1997) 12(10):1729–36. doi: 10.1359/jbmr.1997.12.10.1729
65. Collins MT, Kushner H, Reynolds JC, Chebli C, Kelly MH, Gupta A, et al. An Instrument to Measure Skeletal Burden and Predict Functional Outcome in Fibrous Dysplasia of Bone. *J Bone Miner Res* (2005) 20(2):219–26. doi: 10.1359/JBMR.041111
66. Ruggieri P, Sim FH, Bond JR, Krishnan Unni K. Malignancies in Fibrous Dysplasia. *Cancer* (1994) 73(5):1411–24. doi: 10.1002/1097-0142(19940301)73:5<1411::AID-CNCR2820730516>3.0.CO;2-T
67. Hansen MR, Moffat JC. Osteosarcoma of the Skull Base After Radiation Therapy in a Patient With McCune-Albright Syndrome: Case Report. *Skull Base* (2003) 13(02):079–84. doi: 10.1055/s-2003-40597
68. Fuyi L, Wenting L, Yong Y, Guilin L, Yi Y, Wanchen D, et al. A Case of McCune-Albright Syndrome Associated With Pituitary GH Adenoma: Therapeutic Process and Autopsy. *J Pediatr Endocrinol Metab* (2011) 24(5-6):283–7. doi: 10.1515/jpem.2011.178
69. Neyman A, Eugster EA. Treatment of Girls and Boys With McCune-Albright Syndrome With Precocious Puberty–Update 2017. *Pediatr Endocrinol reviews: PER* (2017) 15(2):136. doi: 10.17458/per.vol15.2017.nau.treatmentgirlsboys
70. Holland FJ. Gonadotropin-Lndependent Precocious Puberty. *Endocrinol Metab Clinics North Am* (1991) 20(1):191–210. doi: 10.1016/S0889-8529(18)30288-3

71. Schmidt H, Kiess W. Central Precocious Puberty in a Girl With McCune-Albright Syndrome Responds to Treatment With GnRH Analogue. *J Pediatr Endocrinol Metab* (1998) 11(1):77–82. doi: 10.1515/JPEM.1998.11.1.77

Conflict of Interest: The authors declare that the research was conducted in the absence of any commercial or financial relationships that could be construed as a potential conflict of interest.

Publisher's Note: All claims expressed in this article are solely those of the authors and do not necessarily represent those of their affiliated organizations, or those of the publisher, the editors and the reviewers. Any product that may be evaluated in this article, or claim that may be made by its manufacturer, is not guaranteed or endorsed by the publisher.

frontiers in Endocrinology

ORIGINAL RESEARCH
published: 10 November 2021
doi: 10.3389/fendo.2021.763609

Basal Ganglia Germ Cell Tumors With or Without Sellar Involvement: A Long-Term Follow-Up in a Single Medical Center and a Systematic Literature Review

Yi Zhang[1†], Li Wang[1†], Wenbin Ma[1], Hui Pan[2], Renzhi Wang[1], Huijuan Zhu[2] and Yong Yao[1*]*

[1] Department of Neurosurgery, Peking Union Medical College Hospital, Chinese Academy of Medical Science and Peking Union Medical College, Beijing, China, [2] Department of Endocrinology, Peking Union Medical College Hospital, Chinese Academy of Medical Science and Peking Union Medical College, Beijing, China

OPEN ACCESS

Edited by:
Run Yu,
UCLA David Geffen School of Medicine, United States

Reviewed by:
Xingfu Wang,
First Affiliated Hospital of Fujian Medical University, China
Akira Sugawara,
Tohoku University, Japan

****Correspondence:***
Yong Yao
tigerfreeyy@126.com
Huijuan Zhu
shengxin2004@163.com

[†]These authors have contributed equally to this work and share first authorship

Specialty section:
This article was submitted to Pituitary Endocrinology, a section of the journal Frontiers in Endocrinology

Received: *24 August 2021*
Accepted: *27 September 2021*
Published: *10 November 2021*

Citation:
Zhang Y, Wang L, Ma W, Pan H, Wang R, Zhu H and Yao Y (2021) Basal Ganglia Germ Cell Tumors With or Without Sellar Involvement: A Long-Term Follow-Up in a Single Medical Center and a Systematic Literature Review. Front. Endocrinol. 12:763609. doi: 10.3389/fendo.2021.763609

Background: Basal ganglia germ cell tumors (BGGCTs) represent an extremely rare subset of tumors about which little is known. Some patients suffer from tumor dissemination, such as sellar involvement. This study aimed to evaluate the independent prognostic risk factors of patients with BGGCTs with or without sellar involvement.

Methods: Sixteen patients were diagnosed with BGGCTs at Peking Union Medical College Hospital from January 2000 to December 2020. A literature review was performed on the online databases Medline and PubMed, and 76 cases in the 19 retrieved articles were identified at the same time. The data regarding biochemical tests, radiological examinations, and outcomes during follow-up were analyzed.

Results: Of 92 patients in this study, seven patients were clinically diagnosed as germinomas, with the remaining 85 patients receiving surgery. Fifty-two patients suffered from multifocal lesions or tumor dissemination. The patients with BGGCTs demonstrated a significant male predilection. The patients with delayed diagnosis more likely had cognitive disturbance ($p = 0.028$), mental disturbance ($p = 0.047$), and diabetes insipidus ($p = 0.02$). Multivariate analysis demonstrated that the independent poor prognostic risk factors of patients with BGGCTs were delayed diagnosis [odd ratio (OR) 2.33; 95% CI 1.02–5.31], focal radiotherapy (OR 4.00; 95% CI 1.69–9.49), and non-pure germinoma (OR 4.64; 95% CI 1.76–12.22).

Conclusions: The delayed diagnosis, focal radiotherapy, and non-pure germinoma were associated with a poorer prognosis for patients with BGGCTs with or without sellar involvement.

Keywords: basal ganglia germ cell tumors, sellar involvement, delayed diagnosis, independent prognostic risk factors, surgical therapy

INTRODUCTION

Intracranial germ cell tumors (GCTs) are rare, heterogeneous, and management challenging, with a geographically variable incidence of 0.6–2.7 per million (1, 2). GCTs usually develop in the region of the third ventricle along the midline axis, including sellar region, pineal region, or both regions involved (3, 4). In rare circumstances, GCTs also originate off the midline in the basal ganglionic region, thalamus, or other ventricular sites. It is reported that GCTs in basal ganglionic region are more likely to be germinomas, which are prone to delayed diagnosis for their insidious onset and atypical clinical presentation (3, 5, 6).

Basal ganglia consist of subcortical nuclei embedded in the deep brain hemispheres responsible for control of movement, behavior, cognition, and emotions (7). Slowly progressive hemiparesis and cognitive decline are frequent in patients with GCTs in the basal ganglia (8, 9). In this study, we define basal ganglia area based on the imaging, including internal capsule and peripheral white matter in addition to anatomical BG (striatum, claustrum, and amygdaloid body).

Due to the rarity of basal ganglia germ cell tumors (BGGCTs), there is a paucity of research on it and a lack of study on large populations. Our study aims to determine the demographic and clinical characteristics, associated factors, and impact of delayed diagnosis and treatment on outcome of BGGCTs with or without sellar involvement. We reviewed 92 BGGCT patients with complete clinical information and follow-up data since 2000, including 16 patients diagnosed with BGGCTs at our institution and 76 cases from other published studies. To the best of our knowledge, this study included the largest population so far.

MATERIALS AND METHODS

Patient Selection

Between January 2000 and December 2020, 16 patients were diagnosed with BGGCTs at Peking Union Medical College Hospital (PUMCH). Medical information was collected, including patients' demographics, symptoms and physical examination, clinical course, endocrine tests, radiological examinations, treatment modalities, and outcomes during follow-up. All patients underwent magnetic resonance imaging (MRI), including T1-weighted imaging (T1WI), T2-weighted imaging (T2WI), and contrast-enhancement T1WI (CE-T1WI). The tumor size, locations, calcification, cyst, hemorrhage, parenchymal atrophy, and hydrocephalus were recorded. The alpha-fetoprotein (AFP) (normal value range at PUMCH, 0–20 ng/ml) and β-human chorionic gonadotropin (β-HCG) (normal value range at PUMCH, 0–5 IU/L) in serum level were examined routinely.

Literature Review

The online database Medline and PubMed were searched for the phrases "basal ganglia" and "germ cell tumors" from January 2000 to December 2020. Forty results were totally returned. Furthermore, 11 articles were obtained by reviewing citations in the retrieved data. Cases were excluded if (1) articles were not published in English (2), case reports overlapped in two or more papers (3), individual basic data were not included in the articles, and (4) the follow-up time was less than 1 year. Finally, 76 cases in the 19 retrieved articles were identified.

Definition

Tumor size was recorded as the measured maximum diameter in MRI scans. Delayed diagnosis was defined as an interval of more than 6 months from the onset of symptoms to the date of diagnosis. Overall survival (OS) was defined as the length of time from the date of initial treatment to that of death or last follow-up. Progression-free survival (PFS) was defined as the length of time during and after the treatment that a patient lives without progression of disease. Odds ratio (OR) is a measure of association between an exposure and an outcome, representing the odds that an outcome will occur given a particular exposure, compared to the odds of the outcome occurring in the absence of that exposure. Confidence interval (CI) is a type of estimate computed from the observed data, giving a range of values for an unknown parameter.

Statistical Analysis

Quantitative data were described as mean ± SD or median (25 and 75th percentiles). Pearson chi-square test, Continuity correction chi-square test, or Fisher's exact test was used to assess the statistical significance in 2 × 2 table. The significant difference of R × C cross-table was evaluated by Wilcoxon rank test, Kruskal–Wallis test, or Spearman rank correlation. The survival curve was generated by Kaplan–Meier method. Multivariate logistic regression was used to identify the risk factors. The data were analyzed using SPSS 13.0 (IBM, NY, USA) and GraphPad Prism 6 (GraphPad Software, CA, USA).

RESULTS

Demographics

A total of 92 cases were diagnosed with BGGCTs, including 16 cases from our medical center. The male/female was 7.36:1, demonstrating a significant male predilection of BGGCTs. The median age at diagnosis was 12.5 years (interquartile range, 9.75–14 years). The age data showed that patients with BGGCTs tended to be diagnosed in the 5–15 years (**Figure 1**).

Clinical Features

The clinical features of patients with BGGCTs are shown in **Table 1**. The most frequent symptom was hemiparesis (67%), followed by cognitive disturbance (24.2%), nausea/vomiting (22%), and headache (16.5%). In addition, 18 patients suffered from diabetes insipidus. The other neurologic signs included dystonia (15.4%), positive pathologic reflex (15.4%), and gait abnormality (15.4%). The median duration of symptoms was 7 months (interquartile range, 1.5–23.1 months).

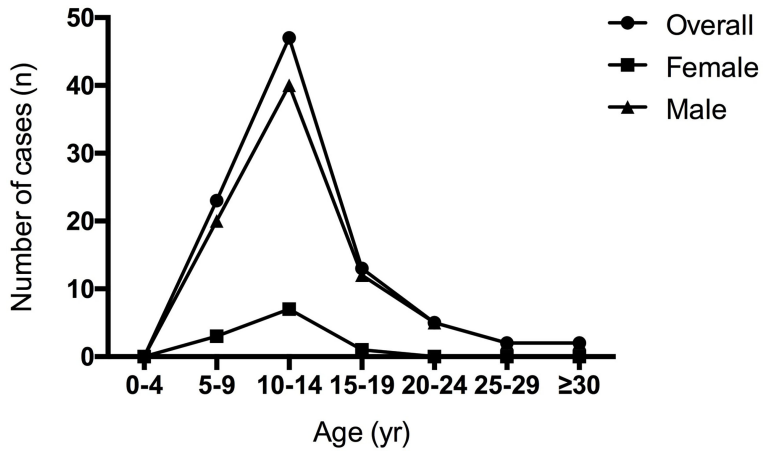

FIGURE 1 | Age of 92 patients with basal germ cell tumors.

TABLE 1 | Clinical features of patients with germ cell tumors with or without sellar involvement.

Presenting Symptom or Sign	Overall (n = 92)		Delayed (n = 53)		Undelayed (n = 39)		X^2	p
Hemiparesis	61	67.0%	35	67.3%	26	66.7%	0.004	0.949
Dystonia	14	15.4%	8	15.4%	6	15.4%	0	1
Positive pathologic reflex	14	15.4%	8	15.4%	6	15.4%	0	1
Gait abnormality	14	15.4%	10	19.2%	4	10.3%	1.379	0.24
Cognitive disturbance	22	24.2%	17	32.7%	5	12.8%	4.801	0.028#
Paresthesia	6	6.6%	5	9.6%	1	2.6%	0.836	0.36
Syncope	3	3.3%	2	3.8%	1	2.6%	0	1
Seizure	6	6.6%	4	7.7%	2	5.1%	0.04	0.951
Impulsive behavior/fluctuating emotional control	9	9.9%	6	11.5%	3	7.7%	0.064	0.8
Mental disturbance	8	8.7%	8	15.1%	0	0.0%	3.95	0.047#
Headache	15	16.5%	6	11.5%	9	23.1%	2.155	0.142
Nausea/vomiting	20	22.0%	10	19.2%	10	25.6%	0.534	0.465
Visual changes	7	7.7%	5	9.6%	2	5.1%	0.158	0.691
Slow growth	6	6.6%	4	7.7%	2	5.1%	0.004	0.951
Menstrual changes	2	2.2%	2	3.8%	0	0.0%	0.266	0.606
Decreased libido	3	3.3%	3	5.8%	0	0.0%	0.869	0.351
Precocious puberty	10	11.0%	7	13.5%	3	7.7%	0.283	0.595
Dry skin and mucosa	6	6.6%	6	11.5%	0	0.0%	3.126	0.077
Anorexia	5	5.5%	4	7.7%	1	2.6%	0.357	0.55
Fatigue	8	8.8%	7	13.5%	1	2.6%	2.081	0.149
Diabetes insipidus	18	19.6%	15	28.3%	3	7.7%	5.425	0.02#
Consciousness disturbance	3	3.3%	1	1.9%	2	5.1%	–	1
Pigmentation	4	4.4%	3	5.8%	1	2.6%	0.049	0.825

#$p < 0.05$.

Tumor Markers

All patients received the alpha-fetoprotein (AFP) and β-human chorionic gonadotropin (β-HCG) test in serum. Elevated β-HCG was observed in 29 patients, with elevated AFP occurring in seven patients. Among them, three patients were identified with both increased β-HCG and increased AFP levels.

Radiologic Features

All patients underwent at least one cranial MRI. The GCT mass was only in basal ganglia in 40 patients. And 52 patients suffered from multifocal lesions or tumor dissemination. Ten patients had only a subtle patchy lesion visible mainly in T2WI. The maximum of tumor size was 65 mm. On MRI, the tumors in 61 patients (66.3%) demonstrated hypo- to iso-intensity on T1-wighted sequences, with 89 patients (96.7%) showing hyper-intensity on T2-wighted sequences. The most typical enhancement patterns were heterogeneous (81.5%) after administration of intravenous contrast material. The presence of cystic formation was observed in 30 cases (32.6%), with calcification in 18 cases (19.6%), obstructive hydrocephalus in 11 cases (12.0%), and intratumor hemorrhage in 11 cases (12.0%), respectively. Notably, parenchymal atrophy was identified in 42 cases (46.7%), which mainly presented with cerebral peduncle.

Delayed diagnosis

Fifty-three of 92 patients with BGGCTs had a clinical course longer than 6 months. The clinical manifestation of patients with BGGCTs with or without delayed diagnosis is shown in **Table 1**. The three most common symptoms in patients with delayed diagnosis were hemiparesis (67.3%), cognitive disturbance (32.7%), and diabetes insipidus (28.35). The patients with delayed diagnosis more likely had cognitive disturbance ($p = 0.028$), mental disturbance ($p = 0.047$) and diabetes insipidus ($p = 0.02$).

The characteristics of patients with BGGCTs with delayed diagnosis are shown in **Table 2**. The male/female ratio of patients with delayed diagnosis is 9.6:1. The patients with delayed diagnosis more likely had multifocal lesions/tumor dissemination ($p = 0.003$). There were no statistically significant differences in tumor size and histological type ($p > 0.05$).

Diagnosis and Treatment

Seven patients with elevated β-HCG and normal AFP were clinically diagnosed as germinomas. The remaining 85 patients received surgery, including biopsy in 63 patients and debulking surgery in 22 patients. Twelve patients were pathologically diagnosed as non-germinomatous germ cell tumors (NGGCTs), with 65 patients as germinomas pathologically. Histological examination confirmed choriocarcinoma in two patients, teratoma in one patient, yolk sac tumor in one patient, and mixed GCT in eight patients.

Fifty-five patients received a combination of chemotherapy (CT) and radiotherapy (RT), while 21 patients received RT alone and 10 patients received CT alone. The irradiation fields were craniospinal irradiation (CSI) in 37, whole-brain irradiation (WBI) in 17, whole-ventricle irradiation (WVI) in 12, and only primary boost (PB) in 10. The CT protocols included cisplatin–etoposide (PE), carboplatin–etoposide (CE), ifosfamide–cisplatin–etoposide (ICE), bleomycin–etoposide–cisplatin (BEP), cisplatin–vincristine–bleomycin (PVB), and so on.

TABLE 2 | Characteristics of BGGCT patients with and without a delay in diagnosis.

	Delayed diagnosis (n = 53)	Undelayed diagnosis (n = 39)	p-value
Age (Mean ± SD)	13.8 ± 6.0	12.4 ± 3.2	
Sex (n)			0.78
Male	48	33	
Female	5	6	
Tumor size (mm)			0.38
≥30	25	22	
<30	28	17	
Tumor location (n)			**0.003**[#]
Solitary lesion	16	24	
Multifocal lesions/ Tumor dissemination	37	15	
Histological type(n)			0.57
Germinoma	47	33	
NGGCT	6	6	

Data were presented as mean ± SD or N.
p-values in bold font indicate statistical significance. [#]$p < 0.01$.
NGGCT, non-germinomatous germ-cell tumors; GCTs, germ cell tumors; BGGCTs, basal ganglia germ cell tumors.

Clinical Outcomes

All patients underwent follow-up without loss (**Table 3**). The follow-up time ranged from 0.5 to 205 months. At the time of the latest follow-up, 38 patients showed complete remission, 17 patients showed partial remission, 12 patients were alive with tumor size stable after the completion of all planned treatments, and 25 patients had progressive disease or were dead. The 1-, 3-, and 5-year OS rate was 97.9%, 93.0%, and 87.5%, respectively. The 1-, 3-, and 5-year PFS rate was 90.2%, 83.0%, and 83.0%, respectively (**Figure 2**). Considering the histological type, the mean survival time and PFS time of patients with pure germinoma were much longer than the ones with non-pure germinomas, 59.64 ± 5.05 months vs. 40.91 ± 10.78 months ($p = 0.003$) and 52.77 ± 5.17 months vs. 38.41 ± 11.74 months ($p = 0.001$), respectively (**Figure 3**).

For patients with non-pure germinoma, there were no statistically significant differences in the mean survival time between non-focal RT and focal RT ($p = 0.66$), neither did mean PFS time ($p = 0.16$). However, for patients with pure germinoma, non-focal RT was associated with a better PFS time than focal RT ($p = 0.001$) (**Figure 4**).

Given the tumor size and histological type over surgical resection, there were no statistically significant differences in mean OS and PFS time between patients with debulking and biopsy ($p > 0.05$) (**Figure 5**).

Prognostic Factors

Some demographic features, clinical manifestations, histological features, radiological features, and different treatment protocols were used for risk stratification (**Table 3**). The diagnosis time (with delayed diagnosis vs. without delayed diagnosis, $p = 0.017$), the RT field (non-focal RT vs. focal RT, $p = 0.001$), and histological type (pure germinoma vs. non-pure germinoma, $p = 0.002$) were significantly related to survival. Sex, presentation time, cognitive disturbance, diabetes insipidus, tumor size, tumor location, operation type, and combination of RT and CT were not significantly related to survival ($p > 0.05$).

The previous three statistically significant factors were analyzed by multivariate logistic regression analysis (**Table 4**). On the premise that regression model had good-fitness and statistical significance, the diagnosis time, RT field, and histological type were the independent risk factors associated with BGGCT prognosis. Patients with delayed diagnosis (OR 2.33; 95% CI 1.02–5.31), focal RT (OR 4.00; 95% CI 1.69–9.49), and non-pure germinoma (OR 4.64; 95% CI 1.76–12.22) had worse prognosis.

DISCUSSION

The interquartile range of age at diagnosis is from 9.75 to 14 years, with a median age of 12.5 years and a peak between 10 and 14 years. As shown in **Figure 1**, it is noticeable that males are more likely to have BGGCTs with or without sellar involvement in all age groups. Young-age onset and male predominance are two remarkable features of BGGCTs, which is consistent with previous studies (6, 10).

TABLE 3 | Univariate analysis of risk factors of patients with BGGCT.

	CR (n = 38)	PR (n = 17)	NC (n = 12)	PD (n = 25)	p-value
Sex (n)					0.630
Male	34	16	9	22	
Female	4	1	3	3	
Age at presentation (n)					0.567
<18	33	15	11	20	
≥18	5	2	1	5	
Delayed diagnosis (n)					0.017*
Yes	17	10	7	19	
No	21	7	5	6	
Cognitive disturbance (n)					0.245
Yes	6	6	3	7	
No	32	11	9	18	
Diabetes insipidus (n)					0.356
Yes	4	6	4	4	
No	34	11	8	21	
Tumor size (n)					0.675
≥30 mm	18	7	11	11	
<30 mm	20	10	1	14	
Tumor location (n)					0.366
Solitary	20	5	4	11	
Multifocal/Disseminated	18	12	8	14	
Operation types[a] (n)					0.628
Debulking	11	3	2	6	
Biopsy	23	13	10	17	
None	4	1	0	2	
Combined CT and RT (n)					0.481
Yes	22	13	9	11	
No	16	4	3	14	
RT field (n)					0.001#
CSI or WVI or WBI	32	10	11	8	
Focal PB or others[b]	6	7	1	17	
Histological type (n)					0.002#
Pure germinoma	34	14	9	13	
Others[c]	4	3	3	12	

#*p < 0.01.*

**p < 0.05.*

Operation types[a] were calculated by Kruskal–Wallis test.

Others[b] including non-radiotherapy and other types.

Others[c] including germinoma with STGC and NGGCT.

NGGCT, non-germinomatous germ-cell tumor; GCT, germ cell tumor; STGC, syncytiotrophoblastic giant cell; CR, complete remission; PR, partial remission; NC, no change; PD, progressive disease; CSI, craniospinal irradiation; WBI, whole-brain irradiation; WVI, whole-ventricle irradiation; PB, primary boost; CT, chemotherapy; RT, radiotherapy; BGGCTs, basal ganglia germ cell tumors.

Basal ganglia are a group of evolutionarily conserved deep forebrain nuclei, which form multiple parallel loops and reentering circuits and are involved in motor, cognition, and affective control (7, 11). Abnormalities in the basal ganglia area can lead to movement disorders, alterations of mood, and cognitive disorders. Distinctive clinical features can lead to early diagnosis and optimize the treatment. However, patients with BGGCTs with or without sellar involvement present with a variety of nonspecific clinical manifestations. Slowly progressive hemiparesis has been recognized as the initial and most common symptoms (12, 13), indicating the progressive lesions of the basal ganglia and internal capsule area (8). In this study, hemiparesis (67.0%) is also the most common initial complaint, and many previous studies have also reported the same finding (6, 13–15). Cognitive disturbance (24.2%) follows behind, indicating an abnormality in the basal ganglia area. Signs of increased intracranial pressure, like nausea/vomiting (22.0%) and headache (16.5%), are relatively frequent symptoms. Diabetes insipidus (19.6%) is observed and may indicate tumor involvement of the sellar area.

Magnetic resonance imaging (MRI) is highly sensitive in detecting intracranial GCTs, though it is limited in distinguishing GCTs with different pathological types (3). Brain MRI is routinely performed on all patients at the first time of evaluation. Abnormalities on MRI in patients with BGGCTs involve hemiatrophy, cystic components, mass effect, intratumoral hemorrhage, and peritumoral edema (13–15). Cerebral hemiatrophy or hemorrhagic or cystic formation is highly suggestive of BGGCTs (13). Hyperintensity in T2WI and heterogeneous enhancement seem more likely to be observed. Hemiatrophy, usually presenting as ipsilateral peduncle and hemispheric atrophy, is the most common radiologic feature.

In one study, five patients, among eight cases observed with hemiatrophy on MRI, present with hemiparesis (14), which may imply an association between hemiparesis and hemiatrophy. Atrophy of the basal ganglia, even before the development of

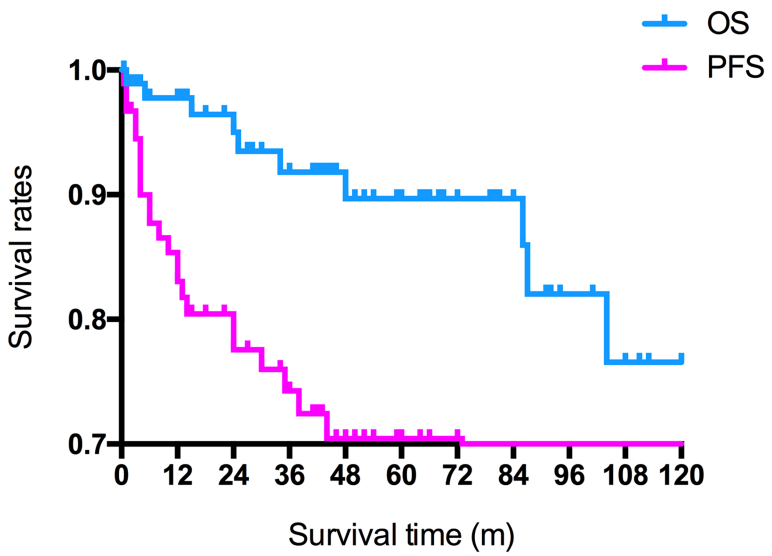

FIGURE 2 | Overall and progression-free survival rates of all patients. OS, overall survival; PFS, progression-free survival.

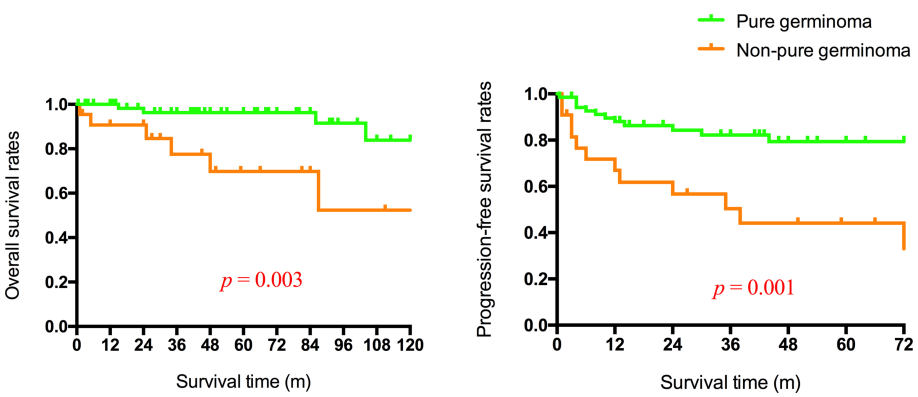

FIGURE 3 | Overall and progression-free survival rates of patients with germinoma or non-pure germinoma.

hemiparesis, was considered the earliest and most characteristic diagnostic feature in patients with BGGCTs (16).

BGGCTs can be classified as different types by the MRI features, but there is a lack of consensus on the universal standard. In the current study, we adopt a method of categorizing BGGCTs into four distinct patterns: a subtle lesion with faint or no enhancement (type 1), a small lesion <3 cm with enhancement (type 2), type 2 combined with subependymal seeding (type 3), and a large lesion ≥3 cm (type 4), among which type 1 lesions are easily misdiagnosed with non-tumorous conditions and have a longer delay in taking a biopsy (6).

Delayed diagnosis, which is defined as an interval of ≥6 months (from the onset of symptoms to the date of diagnostic MRI) (5), has been a topic of great concern in intracranial GCTs. It was considered that a longer diagnostic delay increased the risk of disseminated disease, negatively influenced treatment outcomes, left the occult lesions with enough time to develop into a full-blown disease, and significantly shorten OS (5, 6, 17). Compared with GCTs in other regions, GCTs in basal ganglia had a longer delay in diagnosis (15). In this study, delayed diagnosis was identified as a significant independent prognostic factor (OR 2.33, p = 0.045) for BGGCTs with or without sellar involvement, consistent with previous studies (6, 17). Besides, we observed that patients with BGGCTs and delayed diagnosis were more likely presenting with cognitive disturbance, mental disturbance, and diabetes insipidus (**Table 1**). In terms of clinical characteristics, delayed diagnosis was more likely in patients with multifocal lesions or tumor dissemination than that with a solitary lesion (**Table 2**). Although there is no definite cause and effect between clinical features/characteristics mentioned above and delayed diagnosis, it is recommended to

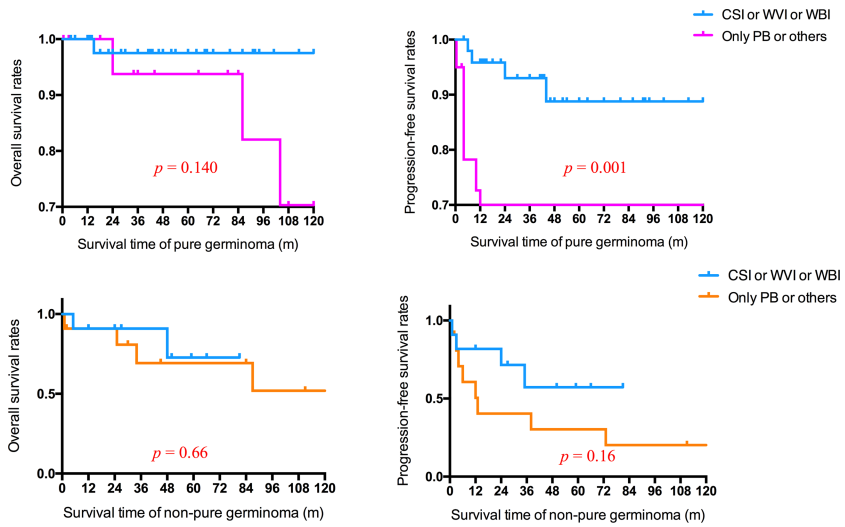

FIGURE 4 | Overall and progression-free survival rates of patients with pure germinoma or non-pure germinoma in different radiotherapy fields. CSI, craniospinal irradiation; WVI, whole-ventricle irradiation; WBI, whole-brain irradiation; PB, primary boost.

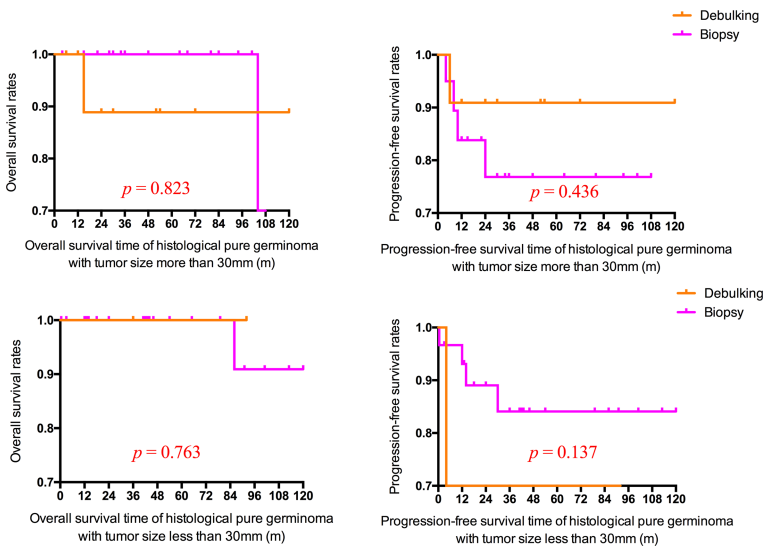

FIGURE 5 | Overall and progression-free survival rates of patients with histologically confirmed pure germinoma with different tumor sizes in different operation types.

carry out active diagnostic procedures in patients with high suspicion.

Different classification systems of intracranial GCTs were proposed based on histopathology, prognosis, and immunohistochemical markers. Germinoma GCT (GGCT) and NGGCTs are two main tumor patterns divided by pathological features, with the latter one further subdivided into embryonal carcinoma, endodermal sinus tumor/yolk sac tumor, choriocarcinoma, mixed GCT, and teratomas based on histology, tumor markers, and protein markers secreted by the tumor cells (18, 19). Diverse treatment outcomes and prognosis were observed in different histological subtypes, categorizing intracranial GCTs into three therapeutic groups with good, intermediate, and poor prognosis (20). Pure germinoma and mature teratoma were classified into the good prognosis group. In this study, patients with basal ganglia pure germinoma were more likely to achieve complete remission (p = 0.002) and had significantly higher OS rates and PFS rates (p = 0.003 and p = 0.001; **Figure 3**). Pure germinoma was revealed as a significant independent prognostic factor (OR 4.64, p = 0.002) for basal GCTs. Pure germinoma in basal ganglia showed similar prognostic characteristics to intracranial pure germinoma.

TABLE 4 | Multivariate logistic regression of parameters associated with prognosis of BGGCTs.

Variable	OR	95% CI	p-value
Delayed diagnosis	2.33	1.02–5.31	**0.045***
RT field	4.00	1.69–9.49	**0.002#**
Histological type	4.64	1.76–12.22	**0.002#**

Results were obtained in ordinal logistic regressions, adjusting for sex (male vs. female), age (≥18 vs. <18), cognitive disturbance (yes vs. no), diabetes insipidus (yes vs. no), tumor size (≥30 mm vs. <30 mm), tumor location (solitary vs. multifocal/disseminated), operation type (debulking vs. biopsy), and RT and CT (yes vs. no).
*p-values in bold font indicate statistical significance. #p < 0.01, *p < 0.05.*
OR, odds ratio; CI, confidence interval; CT, chemotherapy; RT, radiotherapy; GCT, germ cell tumor; BGGCTs, basal ganglia germ cell tumors.

It was considered that distinct therapeutic modalities should be applied to fit the patients in different prognosis groups (20, 21). Germinomas, making up over half of all intracranial GCTs, are extremely sensitive to RT and CT. All patients with intracranial germinoma were recommended to receive RT (2). It was reported that more than 90% of patients with intracranial germinomas were cured with CSI, and the long-term OS was from 90% to 100% after RT alone with a total cranial dose of 40–50 Gy (22). CT was considered an effective way to reduce the dose and volume of RT without weakening the survival rates (2, 19, 21, 23, 24). CT alone was not recommended for its significantly inferior outcomes in patients with intracranial GCTs compared with CT combined with RT (21, 23, 25). Following neoadjuvant CT, WVI was necessary and sufficient for patients with localized germinoma, minimizing adverse effects of RT without affecting outcome (2, 19, 21, 22, 26). For patients with spinal dissemination, craniospinal irradiation was required. In terms of NGGCTs, multidisciplinary therapy, including tumor resection, radiation, and CT, was established (2, 19, 24, 27). Patients with BGGCTs displayed significantly worse intelligent performance and health-related quality of life than those with tumors in sellar and pineal regions (26, 28). WBI rather than WVI was suggested in patients with basal ganglia germinoma, since the WVI was likely not sufficient for the deep brain lesions (14, 28). This study observed a statistically significant difference in PFS rates (p = 0.001; **Figure 4**) between patients with basal ganglia pure germinoma receiving CSI or WVI or WBI and those receiving only PB or others. For patients with non-pure germinoma, survival analysis revealed a higher PFS rate in CSI or WVI or WBI treatment group and was not significant.

A consensus emerged that surgical biopsy was required for intracranial germ-cell tumor diagnosis without elevated AFP or HCG, regardless of radiological imaging findings (2). Despite many disadvantages, the surgical biopsy was critical to obtain an accurate pathological subtype, which predicted treatment regimens and prognosis (29, 30). The extent of surgical resection for BGGCTs is still unproven. As the evolution of neurosurgical techniques and the reduction of surgery-related morbidities, benefits may be received from more aggressive resection (14, 23). In this study, we investigated the impact of surgical debulking on clinical outcomes compared with surgical biopsy. The survival analysis of the relationship between operation types and survival was shown in **Figure 5**. Although without statistical significance, a trend was observed that the PFS rate of surgical debulking was higher than surgical biopsy in patients with basal ganglia pure germinoma ≥3 cm (p = 0.436; **Figure 5**). However, in terms of tumor size <3 cm, the surgical biopsy revealed a trend to have a better prognosis (p = 0.137; **Figure 5**). The result suggested that surgical debulking for basal ganglia pure germinoma with tumor size more than 30 mm may provide some benefits. Further studies with a large sample size are needed to check the hypothesis on surgical debulking.

There are several limitations in our study. This study is a retrospective study whose data were retrieved from electronic medical records in our institution and collected from previously published studies. Consequently, selection bias, missing data, and inaccurate information are inevitable. Patients included in this study were heterogeneous, leading to selection bias and additional confounders. For example, a higher proportion of patients in our institute presented with a combined sellar region involved, but the stratified analysis was not performed because of the small sample size. Moreover, analysis related to complications was limited in this study as a lack of adequate clinical and prognostic information. Finally, the small sample size of this study was not sufficient to give more reliable and precisive results, suggesting more patients involved in future studies.

CONCLUSIONS

In conclusion, we discussed the clinical presentations, MRI features, delayed diagnosis, prognosis, and treatment of BGGCTs with or without sellar involvement. Young-age onset and male predominance are two outstanding features. Atrophy of the basal ganglia and hemiatrophy on MRI act as diagnostic characteristics in patients with BGGCTs, responsible for hemiparesis and cognitive disturbance. Delayed diagnosis, RT field (CSI or WVI or WBI), and pure germinoma were identified as significant independent prognostic factors. Pure germinoma in basal ganglia shows similar prognostic features to pure intracranial germinoma. RT keeps playing a pivotal role. The extent of surgical resection for BGGCTs is not yet clear. This study finds potential benefits from surgical debulking for basal ganglia pure germinoma ≥3 cm. Further studies with a large sample size are suggested to check the hypothesis on surgical debulking.

DATA AVAILABILITY STATEMENT

The raw data supporting the conclusions of this article will be made available by the authors without undue reservation.

ETHICS STATEMENT

The studies involving human participants were reviewed and approved by the Ethics Committee of Peking Union Medical

College Hospital. Written informed consent to participate in this study was provided by the participants' legal guardian/next of kin.

AUTHOR CONTRIBUTIONS

Conceptualization, HZ and YY. Data curation, YZ. Formal analysis, YZ, LW. Funding acquisition, YY and YZ. Writing—original draft, YZ and LW. Writing—review and editing, LW, WM, HP, and RW. All authors contributed to the article and approved the submitted version.

FUNDING

This study was supported by the Chinese Academy of Medical Sciences Innovation Fund for Medical Sciences (No. 2016-I2M-1-002) for YY and Youth Science Foundation of Peking Union Medical College Hospital (No. pumch201911867) for YZ.

REFERENCES

1. Mufti ST, Jamal A. Primary Intracranial Germ Cell Tumors. *Asian J Neurosurg* (2012) 7(4):197–202. doi: 10.4103/1793-5482.106652
2. Murray MJ, Bartels U, Nishikawa R, Fangusaro J, Matsutani M, Nicholson JC. Consensus on the Management of Intracranial Germ-Cell Tumours. *Lancet Oncol* (2015) 16(9):e470–7. doi: 10.1016/S1470-2045(15)00244-2
3. Packer RJ, Cohen BH, Cooney K. Intracranial Germ Cell Tumors. *Oncologist* (2000) 5(4):312–20. doi: 10.1634/theoncologist.2000-0312
4. Jennings MT, Gelman R, Hochberg F. Intracranial Germ-Cell Tumors: Natural History and Pathogenesis. *J Neurosurg* (1985) 63(2):155–67. doi: 10.3171/jns.1985.63.2.0155
5. Sethi RV, Marino R, Niemierko A, Tarbell NJ, Yock TI, MacDonald SM. Delayed Diagnosis in Children With Intracranial Germ Cell Tumors. *J Pediatr* (2013) 163(5):1448–53. doi: 10.1016/j.jpeds.2013.06.024
6. Phi JH, Cho BK, Kim SK, Paeng JC, Kim IO, Kim IH, et al. Germinomas in the Basal Ganglia: Magnetic Resonance Imaging Classification and the Prognosis. *J Neurooncol* (2010) 99(2):227–36. doi: 10.1007/s11060-010-0119-7
7. Lanciego JL, Luquin N, Obeso JA. Functional Neuroanatomy of the Basal Ganglia. *Cold Spring Harb Perspect Med* (2012) 2(12):a009621–a. doi: 10.1101/cshperspect.a009621
8. Crawford JR, Santi MR, Vezina G, Myseros JS, Keating RF, LaFond DA, et al. CNS Germ Cell Tumor (CNSGCT) of Childhood: Presentation and Delayed Diagnosis. *Neurology* (2007) 68(20):1668–73. doi: 10.1212/01.wnl.0000261908.36803.ac
9. Lee SM, Kim IO, Choi YH, Cheon JE, Kim WS, Cho HH, et al. Early Imaging Findings in Germ Cell Tumors Arising From the Basal Ganglia. *Pediatr Radiol* (2016) 46(5):719–26. doi: 10.1007/s00247-016-3542-x
10. Hao S, Liu B, Tang J, Jia G, Zhang Y, Ma Z, et al. Germinoma of Basal Ganglia in Female: Case Report and Review of the Literature. *Childs Nerv Syst* (2009) 25(5):613–7. doi: 10.1007/s00381-008-0769-3
11. Nelson AB, Kreitzer AC. Reassessing Models of Basal Ganglia Function and Dysfunction. *Annu Rev Neurosci* (2014) 37:117–35. doi: 10.1146/annurev-neuro-071013-013916
12. Wong T-T, Chen YW, Guo W-Y, Chang K-P, Ho DM, Yen S-H. Germinoma Involving the Basal Ganglia in Children. *Child's Nervous System* (2008) 24(1):71–8. doi: 10.1007/s00381-007-0495-2
13. Kumar N, Kotagal S, Parisi JE, Westmoreland BF. Cerebral Hemiatrophy With Superficial Siderosis and PLEDs Due to a Germ Cell Tumor of the Basal Ganglia. *Eur J Neurol* (2006) 13(8):904–7. doi: 10.1111/j.1468-1331.2006.01316.x
14. Zhang S, Liang G, Ju Y, You C. Clinical and Radiologic Features of Pediatric Basal Ganglia Germ Cell Tumors. *World Neurosurg* (2016) 95:516–24.e1. doi: 10.1016/j.wneu.2016.08.072
15. Sonoda Y, Kumabe T, Sugiyama S-I, Kanamori M, Yamashita Y, Saito R, et al. Germ Cell Tumors in the Basal Ganglia: Problems of Early Diagnosis and Treatment. *J Neurosurg: Pediatr PED* (2008) 2(2):118. doi: 10.3171/PED/2008/2/8/118
16. Okamoto K, Ito J, Ishikawa K, Morii K, Yamada M, Takahashi N, et al. Atrophy of the Basal Ganglia as the Initial Diagnostic Sign of Germinoma in the Basal Ganglia. *Neuroradiology* (2002) 44(5):389–94. doi: 10.1007/s00234-001-0735-1
17. Phi JH, Kim SK, Lee YA, Shin CH, Cheon JE, Kim IO, et al. Latency of Intracranial Germ Cell Tumors and Diagnosis Delay. *Childs Nerv Syst* (2013) 29(10):1871–81. doi: 10.1007/s00381-013-2164-y
18. Louis DN, Ohgaki H, Wiestler OD, Cavenee WK, Burger PC, Jouvet A, et al. The 2007 WHO Classification of Tumours of the Central Nervous System. *Acta Neuropathol* (2007) 114(2):97–109. doi: 10.1007/s00401-007-0243-4
19. Thakkar JP, Chew L, Villano JL. Primary CNS Germ Cell Tumors: Current Epidemiology and Update on Treatment. *Med Oncol* (2013) 30(2):496. doi: 10.1007/s12032-013-0496-9
20. Matsutani M, Sano K, Takakura K, Fujimaki T, Nakamura O, Funata N, et al. Primary Intracranial Germ Cell Tumors: A Clinical Analysis of 153 Histologically Verified Cases. *J Neurosurg* (1997) 86(3):446–55. doi: 10.3171/jns.1997.86.3.0446
21. Matsutani M. Combined Chemotherapy and Radiation Therapy for CNS Germ Cell Tumors–the Japanese Experience. *J Neurooncol* (2001) 54(3):311–6. doi: 10.1023/A:1012743707883
22. Kenjo M, Yamasaki F, Takayasu T, Nosaka R, Murakami Y, Kimura T, et al. Results of Sequential Chemoradiotherapy for Intracranial Germinoma. *Jpn J Radiol* (2015) 33(6):336–43. doi: 10.1007/s11604-015-0424-3
23. Millard NE, Dunkel IJ. Advances in the Management of Central Nervous System Germ Cell Tumors. *Curr Oncol Rep* (2014) 16(7):393. doi: 10.1007/s11912-014-0393-1
24. Lo AC, Hodgson D, Dang J, Tyldesley S, Bouffet E, Bartels U, et al. Intracranial Germ Cell Tumors in Adolescents and Young Adults: A 40-Year Multi-Institutional Review of Outcomes. *Int J Radiat Oncol Biol Phys* (2020) 106(2):269–78. doi: 10.1016/j.ijrobp.2019.10.020
25. da Silva NS, Cappellano AM, Diez B, Cavalheiro S, Gardner S, Wisoff J, et al. Primary Chemotherapy for Intracranial Germ Cell Tumors: Results of the Third International CNS Germ Cell Tumor Study. *Pediatr Blood Cancer* (2010) 54(3):377–83. doi: 10.1002/pbc.22381
26. Liang SY, Yang TF, Chen YW, Liang ML, Chen HH, Chang KP, et al. Neuropsychological Functions and Quality of Life in Survived Patients With Intracranial Germ Cell Tumors After Treatment. *Neuro Oncol* (2013) 15(11):1543–51. doi: 10.1093/neuonc/not127
27. Calaminus G, Frappaz D, Kortmann RD, Krefeld B, Saran F, Pietsch T, et al. Outcome of Patients With Intracranial Non-Germinomatous Germ Cell Tumors-Lessons From the SIOP-CNS-GCT-96 Trial. *Neuro Oncol* (2017) 19(12):1661–72. doi: 10.1093/neuonc/nox122
28. Li B, Lv W, Li C, Yang J, Chen J, Feng J, et al. Comparison Between Craniospinal Irradiation and Limited-Field Radiation in Patients With Non-Metastatic Bifocal Germinoma. *Cancer Res Treat* (2020) 52(4):1050–8. doi: 10.4143/crt.2020.437
29. Chiba K, Aihara Y, Kawamata T. Precise Detection of the Germinomatous Component of Intracranial Germ Cell Tumors of the Basal Ganglia and Thalamus Using Placental Alkaline Phosphatase in Cerebrospinal Fluid. *J Neurooncol* (2021) 152(2):405–13. doi: 10.1007/s11060-021-03715-9
30. Kong Z, Wang Y, Dai C, Yao Y, Ma W, Wang Y. Central Nervous System Germ Cell Tumors: A Review of the Literature. *J Child Neurol* (2018) 33(9):610–20. doi: 10.1177/0883073818772470

Conflict of Interest: The authors declare that the research was conducted in the absence of any commercial or financial relationships that could be construed as a potential conflict of interest.

Publisher's Note: All claims expressed in this article are solely those of the authors and do not necessarily represent those of their affiliated organizations, or those of the publisher, the editors and the reviewers. Any product that may be evaluated in

this article, or claim that may be made by its manufacturer, is not guaranteed or endorsed by the publisher.

frontiers in Endocrinology

CASE REPORT
published: 01 December 2021
doi: 10.3389/fendo.2021.762095

Comprehensive Genomic Characterization of A Case of Granular Cell Tumor of the Posterior Pituitary Gland: A Case Report

Christopher S. Hong[1], Aladine A. Elsamadicy[1], Adeniyi Fisayo[2], Silvio E. Inzucchi[3], Pallavi P. Gopal[4], Eugenia M. Vining[5], E. Zeynep Erson-Omay[1] and Sacit Bulent Omay[1]**

[1] Department of Neurosurgery, Yale School of Medicine, New Haven, CT, United States, [2] Department of Ophthalmology and Visual Science, Yale School of Medicine, New Haven, CT, United States, [3] Section of Endocrinology, Department of Medicine, Yale School of Medicine, New Haven, CT, United States, [4] Department of Pathology, Yale School of Medicine, New Haven, CT, United States, [5] Division of Otolaryngology, Department of Surgery, Yale School of Medicine, New Haven, CT, United States

OPEN ACCESS

Edited by:
Wang Haijun,
The First Affiliated Hospital of Sun Yat-Sen University, China

Reviewed by:
Sergei I. Bannykh,
Cedars Sinai Medical Center, United States
Linjie Wang,
Peking Union Medical College Hospital (CAMS), China
Changzhen Jiang,
First Affiliated Hospital of Fujian Medical University, China

***Correspondence:**
E. Zeynep Erson-Omay
zeynep.erson@yale.edu
Sacit Bulent Omay
sacit.omay@yale.edu

Specialty section:
This article was submitted to Cancer Endocrinology, a section of the journal Frontiers in Endocrinology

Received: 20 August 2021
Accepted: 25 October 2021
Published: 01 December 2021

Citation:
Hong CS, Elsamadicy AA, Fisayo A, Inzucchi SE, Gopal PP, Vining EM, Erson-Omay EZ and Bulent Omay S (2021) Comprehensive Genomic Characterization of A Case of Granular Cell Tumor of the Posterior Pituitary Gland: A Case Report. Front. Endocrinol. 12:762095. doi: 10.3389/fendo.2021.762095

Granular cell tumors of the pituitary belong to a rare family of neoplasms, arising from the posterior pituitary gland. Although considered benign, they may cause significant morbidity and residual disease after resection can lead to poor clinical outcomes. Currently, there is no known medical therapy for any posterior pituitary gland tumor, in part due to sparse molecular characterization of these lesions. We report data from whole exome sequencing of a case of granular cell tumor of the pituitary, performed under an institutional review board approved protocol. A 77 year-old female underwent resection of an incidentally diagnosed pituitary mass that was causing radiographic compression of the optic nerves with a subclinical temporal field defect and central hypothyroidism. The pathology of the resected specimen demonstrated a granular cell tumor of the posterior pituitary gland. Whole-exome sequencing revealed mutations predicted to be deleterious in key oncogenes, *SETD2* and *PAX8*, both of which have been described in other cancers and could potentially be amenable to targeted therapies with existing approved drugs, including immune checkpoint inhibitors and histone deacetylase inhibitors, respectively. To our knowledge, this is the first comprehensive genomic characterization of granular cell tumor of the posterior pituitary gland. We report mutations in oncogenes predicted to be deleterious and reported in other cancers with potential for therapeutic targeting with existing pharmacologic agents. These data provide new insights into the molecular pathogenesis of GCT of the pituitary and may warrant further investigation.

Keywords: pituitary, granular cell, sequencing, SETD2, PAX8, case report

INTRODUCTION

Granular cell tumors (GCT) of the pituitary are rare, benign WHO I tumors. They, alongside pituicytomas, spindle cell oncocytomas, and sellar ependymomas comprise a family of tumors of the posterior pituitary gland (1). According to the latest edition of the WHO Classification of CNS Tumors, these pathologies may represent morphological variants of the same tumor with shared

nuclear thyroid transcription factor-1 (TTF-1) expression and a lack of expression of pituitary hormones (2). Clinically, these tumors may cause symptoms related to local mass effect, including optic chiasm compression leading to visual field deficits, stalk compression with resultant hyperprolactinemia, and partial or even panhypopituitarism. Like pituitary adenomas, surgical resection of GCTs and other posterior pituitary tumors remains the mainstay of treatment (3). While considered benign, GCTs can be quite vascular (4–6), making complete surgical resection more difficult, and may lead to higher rates of tumor recurrence after subtotal resection and poorer survival outcomes (7, 8). The success of radiation therapy for residual tumors remains unclear, and likewise, there remain no known medical therapies for surgically refractory cases (7, 9, 10). As such, a better molecular understanding of these tumors is needed in order to develop potential novel targeted therapies.

To date, the molecular characterization of posterior pituitary tumors remain sparse and genomic sequencing have been comprised of only limited targeted sequencing panels (2, 11). To date, no genetic studies of GCTs of the pituitary have been performed. In this study, we report results from whole exome sequencing of a case of a GCT and discuss the relevant findings.

MATERIALS AND METHODS

This study was conducted under an institutional review board approved protocol at Yale University. The patient's blood and tumor tissue were collected after obtaining written informed consent. Histopathology, including immunohistochemical studies, were evaluated by a board-certified neuropathologist.

Whole exome sequencing and analysis was performed in accordance with our previously described methods at the Yale Cancer for Genome Analysis (YCGA) (12). Briefly, genomic DNA from the tumor and blood were isolated and coding regions were captured with IDT xGen Exome Research Panel v1 (Integrated DNA Technologies, Coralville, IA) with the additional spike-in of ~2,500 regions totaling ~620 kb of RefGene coding regions together with custom spikes designed specifically for cancer by Genomic Oncology Academic Laboratory (GOAL) Consortium. The captured regions were then sequenced on the Illumina NovaSeq6000 whole-exome sequencing platform with 2x100 base pair reads. Downstream analysis of raw reads, including alignment, duplicate marking, realignment, and base quality recalibration was performed according to "GATK Best Practice" recommendations (GATK v4.1.9). Somatic single nucleotide variant (SNV), insertion/deletions (INDEL) and, and copy number variations (CNV) were identified as previously described (12). Mean coverage of 130.1x was achieved for blood and 265.8x for tumor tissue.

RESULTS

Case Presentation

A 77 year-old female with a recent diagnosis of ductal carcinoma of the breast in-situ with subsequent radiation and no radiographic evidence of recurrence was incidentally found to have a pituitary mass, measuring 1.6x1.5x2.6 cm on magnetic resonance imaging (MRI) of the brain, performed for a work-up of worsening hearing loss (**Figures 1A–C**). Review of systems was unremarkable and she was neurologically intact without any other complaints. Endocrine evaluation was notable for a mildly elevated prolactin of 51.1 ng/ml (normal range: 4.8-23.3 ng/mL), felt to be due to stalk effect, and decreased free T4 of 0.63 ng/dL (normal range: 0.80-1.70 ng/dL), the latter suggesting central hypothyroidism. She also demonstrated inappropriately low levels of LH and FSH gonadotropins for her menopausal status but of no clinical significance. The extent of pre-operative endocrine testing is outlined in **Table 1**.

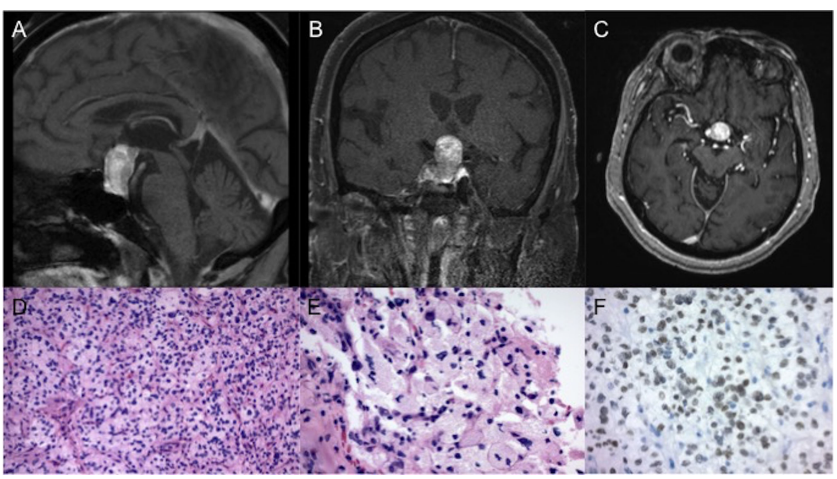

FIGURE 1 | Imaging and pathology of the tumor. Representative **(A)** sagittal **(B)** coronal and **(C)** axial slices of a T1-weighted post-contrast MRI, obtained prior to surgery, showed a pituitary mass, measuring 1.6x1.5x2.6 cm. Final pathology of the resected tumor revealed a low grade neoplasm of polygonal cells with mild nuclear pleomorphism and granular cytoplasm on routine hematoxylin and eosin staining at **(D)** 200x and **(E)** 400x magnification. **(F)** Immunohistochemical stains revealed strong positivity for TTF-1 (magnification 400x).

TABLE 1 | Pre-operative endocrine testing of index patient.

Hormone	Value	Normal range
LH	<1.0	7.7 - 58.5 mIU/mL
FSH	2.2	25.8 - 134.8 mIU/mL
IGF-1	44	34 - 245 ng/mL
Cortisol	7.7	6.0 - 18.4 ug/dL
Prolactin	51.1	4.8 - 23.3 ng/mL
TSH	2.91	0.270-4.200 µIU/mL
Free T4	0.63	0.80-1.70 ng/dL

Neuro-ophthalmology testing revealed a temporal defect in the right eye, while left eye testing was limited given congenital vision loss on this side due to a macular scar. Given her visual deficit and radiographic compression of the optic nerves on MRI, surgical resection was recommended. The tumor was removed *via* an endoscopic endonasal approach and was noted intra-operatively to be well-encapsulated and originating from the posterior pituitary. The patient's post-operative course was only remarkable for continued mildly reduced free T4 of 0.47 ng/dL and for a new low-normal morning cortisol level of 6.3 ug/dL (normal range: 6.0-18.4 ug/dL) for which she remained asymptomatic. She was started on levothyroxine and a prednisone taper, respectively. She was monitored for diabetes insipidus with serial sodium levels and urine output measurements but did not develop the condition. She also reported subjectively improved vision.

Final pathology revealed a low grade neoplasm composed of polygonal cells with discrete cell borders, mild nuclear pleomorphism, and ample granular to foamy cytoplasm (**Figures 1D, E**). PAS and PAS with diastase stains showed scattered tumor cells with diastase resistant granules. Immunohistochemical stains revealed strong positivity for S100 and TTF-1 (**Figure 1F**) with focal positivity for CD68. Tumor cells were negative for GFAP, synaptophysin, keratins (Cam5.2, pancytokeratin), inhibin, carbonic anhydrase, PAX8, and D2-40. The Ki-67 index was low at 1-2%. Taken together, given positive TTF-1 staining in the absence of cytokeratin expression, the immunoprofile of the surgical specimen was consistent with a diagnosis of GCT of the pituitary.

Genomic Analysis

Whole-exome sequencing (WES) was performed on the resected surgical specimen and matched blood in accordance with an institutional review board-approved protocol and utilizing previously described methods (13). No germline variants of potential pathological significance were identified. The analysis of somatic SNV/INDEL data revealed two somatic missense mutations in *SETD2* (c.T2081C:p.V694A) and *PAX8* (c.T527A:p.L176Q) with variant allele frequency (VAF) of 22.1% and 25.5%, respectively. Both variants are considered pathogenic by FATHMM algorithm (14). Detailed data are provided in **Table 2**. Chromosomal analysis revealed deletions in chromosomes 9, 10, and 13. Additionally, there was focal amplification on chromosome 12, involving *PIK3C2G*, a member of the class II PI3K kinase family, whose dysregulation may be involved in human metabolic diseases but its role in cancer remains unclear (15).

DISCUSSION

Outside of the posterior pituitary gland, GCTs have been described in many anatomic locations, most commonly in skin/subcutaneous soft tissues and the gastrointestinal tract and are thought to arise from Schwann cell origin (16). All GCTs stain positive for S100 and histologically show cells with granular eosinophilic cytoplasm, as demonstrated in our case. WES of GCTs remain limited, but recent hallmark studies have demonstrated loss-of-function mutations in vacuolar ATPase subunits, leading to aberrant lysosomal pH regulation and accumulation of intracytoplasmic granules, as observed histologically in GCTs (17–19). While these ATPase mutations may occur in up to 72% of GCTs (18), it is not known if they represent true driver mutations in tumorigenesis. We did not observe genomic alterations in ATPases or other genes integral to endosomal/lysosomal networks in our patient (17). It remains unclear whether GCTs of the posterior pituitary are true GCTs of similar Schwann cell origin. Alternatively, they have been proposed to belong to a morphologic spectrum of posterior pituitary tumors, all derived from pituicyte origin (20). Further genomic characterization of GCTs of the posterior pituitary may help elucidate this distinction.

Genomic characterization of posterior pituitary tumors have been limited to a handful of cases, given the rarity of these pathologies and limited sample sizes taken at time of surgery (11). For spindle cell oncocytomas and pituicytomas, individual mutations affecting the MAPK signaling pathway (*SND1, FAT1, HRAS*), as well as in other oncogenes (i.e. *MEN1, TSC1, CBL, FZD7, PIK3GC, SBK1, CDKN2A/B, SKT11, SMARCA4, CIC, SMARCB1, NF1, NF2*) have been reported in case reports or limited case series (11, 21, 22). Interestingly, *BRAF* mutations have been identified in two cases of spindle cell oncocytomas, which responded to targeted therapy with BRAF inhibitors (23, 24). However, to date, a comprehensive genetic study of GCTs of the pituitary has not been reported in the literature.

In this study, we found somatic mutations in *SETD2* and *PAX8*, which are known tumor-related genes but not reported in tumors of the posterior pituitary. *SETD2* is a histone methyltransferase whose normal function is critical for genomic stability and DNA damage repair (25). Clinically, *SETD2* mutations are most prevalent in clear cell renal carcinomas but are also less commonly seen in hematopoietic cancers, high-grade glioma, melanoma, and adenocarcinomas of

TABLE 2 | Somatic genetic findings of index patient.

Gene	Chromosome	Position	Ref	Alt	HGVS (RefGene)	dbSNP
SETD2	3	47164045	A	G	NM_014159:exon3:c.T2081C:p.V694A	rs786201856
PAX8	2	47164045	A	T	NM_003466:exon6:c.T527A:p.L176Q	rs587779780

the lung and gastrointestinal system (25). *SETD2* mutations have been correlated with shorter progression-free and overall survivals in metastatic renal cell carcinoma and breast cancers (26). Interestingly, SETD2 depletion *in vitro* led to microsatellite instability and increased mutational burden, characteristic of the mismatch repair deficient phenotype that may be amenable to immunotherapies (27). Indeed, in an analysis of The Cancer Genome Atlas (TCGA) pan-cancer cohort found that patients with tumors harboring *SETD2* mutations responded favorably to treatment with immune checkpoint inhibitors, raising the possibility for targeted therapies in *SETD2*-mutated cancers (28).

PAX8 is a member of the paired box family of transcription factors, which encode proteins important in embryogenesis, particularly for thyroid and urogenital system development. In cancer, mutations in *PAX8* have multiple downstream consequences affecting cell proliferation, adhesion, and angiogenesis (29). Clinically, positive immunohistochemical staining for PAX8 is widely used to diagnose primary renal cell tumors and mutations are also frequently seen in thyroid, ovarian, bladder, prostate, endometrial, cervical, and uterine cancers (29). In our case, the tumor did not stain for PAX8, as well as carbonic anhydrase and keratins, effectively ruling out a diagnosis of renal cell carcinoma. Although cases of pituitary metastasis have been reported from *PAX8*-mutated renal cell carcinoma (30), *PAX8* mutations have not been reported in primary pituitary pathologies. In addition, PAX8 is a promising therapeutic target as its expression is restricted in normal tissues, compared to its role in cancer (31). Several preclinical studies have demonstrated suppression of cancer growth with genetic knockdown or pharmacologic inhibition of PAX8 (32, 33), including histone deacetylases (HDAC) inhibitors, which may epigenetically downregulate PAX8 transcripts and are a class of small molecule drugs now approved for cancer therapy (34).

This study reports comprehensive genomic characterization of a case of GCT of the pituitary. We found mutations predicted to be deleterious in known oncogenes, *SETD2* and *PAX8*, previously not described in this pathology but have potential for therapeutic targeting with existing pharmacologic agents. The significance of these findings is limited by being a single case report, but genomic characterization of this rare tumor entity remains severely lacking. Further gene sequencing studies and mechanistic preclinical data are needed to better understand the pathophysiology and potential for molecularly based targeted therapies for GCTs of the pituitary.

DATA AVAILABILITY STATEMENT

The data used to support the findings of this study are available from the corresponding author upon request.

ETHICS STATEMENT

The studies involving human participants were reviewed and approved by Yale University Institutional Review Board. The patients/participants provided their written informed consent to participate in this study.

AUTHOR CONTRIBUTIONS

CH, ZE-O, and SB designed the study. All authors provided medical care to the patient. CH and ZE-O performed the genetic analysis. CH, ZE-O, and SB wrote the manuscript. All authors contributed to the article and approved the submitted version.

FUNDING

Funding for performing genomic sequencing and analysis of the data was provided by the Yale School of Medicine, Department of Neurosurgery Clinical Sequencing Funds.

REFERENCES

1. Mete O, Lopes MB. Overview of the 2017 WHO Classification of Pituitary Tumors. *Endocr Pathol* (2017) 28(3):228–43. doi: 10.1007/s12022-017-9498-z
2. Mete O, Lopes MB, Asa SL. Spindle Cell Oncocytomas and Granular Cell Tumors of the Pituitary Are Variants of Pituicytoma. *Am J Surg Pathol* (2013) 37(11):1694–9. doi: 10.1097/PAS.0b013e31829723e7
3. Ahmed AK, Dawood HY, Cote DJ, Bale TA, De Girolami U, Laws ERJr., et al. Surgical Resection of Granular Cell Tumor of the Sellar Region: Three Indications. *Pituitary* (2019) 22(6):633–9. doi: 10.1007/s11102-019-00999-z
4. Aquilina K, Kamel M, Kalimuthu SG, Marks JC, Keohane C. Granular Cell Tumour of the Neurohypophysis: A Rare Sellar Tumour With Specific Radiological and Operative Features. *Br J Neurosurg* (2006) 20(1):51–4. doi: 10.1080/02688690600600996
5. Covington MF, Chin SS, Osborn AG. Pituicytoma, Spindle Cell Oncocytoma, and Granular Cell Tumor: Clarification and Meta-Analysis of the World Literature Since 1893. *AJNR Am J Neuroradiol* (2011) 32(11):2067–72. doi: 10.3174/ajnr.A2717
6. Gagliardi F, Spina A, Barzaghi LR, Bailo M, Losa M, Terreni MR, et al. Suprasellar Granular Cell Tumor of the Neurohypophysis: Surgical Outcome of a Very Rare Tumor. *Pituitary* (2016) 19(3):277–85. doi: 10.1007/s11102-016-0704-7
7. Ahmed AK, Dawood HY, Penn DL, Smith TR. Extent of Surgical Resection and Tumor Size Predicts Prognosis in Granular Cell Tumor of the Sellar Region. *Acta Neurochir (Wien)* (2017) 159(11):2209–16. doi: 10.1007/s00701-017-3337-3
8. Kleinschmidt-DeMasters BK, Lopes MB. Update on Hypophysitis and TTF-1 Expressing Sellar Region Masses. *Brain Pathol* (2013) 23(5):495–514. doi: 10.1111/bpa.12068
9. Guerrero-Perez F, Marengo AP, Vidal N, Iglesias P, Villabona C. Primary Tumors of the Posterior Pituitary: A Systematic Review. *Rev Endocr Metab Disord* (2019) 20(2):219–38. doi: 10.1007/s11154-019-09484-1
10. Osman M, Wild A. Spindle Cell Oncocytoma of the Anterior Pituitary Presenting With an Acute Clinical Course Due To Intraventricular Hemorrhage. A Case Report and Review of Literature. *Am J Case Rep* (2017) 18:894–901. doi: 10.12659/AJCR.903702
11. Barresi V, Simbolo M, Gessi M, Rossi S, Caffo M, Eccher A, et al. Clinical-Pathological, Immunohistochemical, and Genetic Characterization of a Series of Posterior Pituitary Tumors. *J Neuropathol Exp Neurol* (2021) 80(1):45–51. doi: 10.1093/jnen/nlaa139

12. Fomchenko EI, Erson-Omay EZ, Zhao A, Bindra RS, Huttner A, Fulbright RK, et al. DNMT3A Co-Mutation in an IDH1-Mutant Glioblastoma. *Cold Spring Harb Mol Case Stud* (2019) 5(4). doi: 10.1101/mcs.a004119
13. Hong CS, Kuzmik GA, Kundishora AJ, Elsamadicy AA, Koo AB, McGuone D, et al. Hypermutated Phenotype in Gliosarcoma of the Spinal Cord. *NPJ Precis Oncol* (2021) 5(1):8. doi: 10.1038/s41698-021-00143-w
14. Rogers MF, Shihab HA, Mort M, Cooper DN, Gaunt TR, Campbell C. FATHMM-XF: Accurate Prediction of Pathogenic Point Mutations *via* Extended Features. *Bioinformatics* (2018) 34(3):511–3. doi: 10.1093/bioinformatics/btx536
15. Gulluni F, De Santis MC, Margaria JP, Martini M, Hirsch E. Class II PI3K Functions in Cell Biology and Disease. *Trends Cell Biol* (2019) 29(4):339–59. doi: 10.1016/j.tcb.2019.01.001
16. Mobarki M, Dumollard JM, Dal Col P, Camy F, Peoc'h M, Karpathiou G. Granular Cell Tumor a Study of 42 Cases and Systemic Review of the Literature. *Pathol Res Pract* (2020) 216(4):152865. doi: 10.1016/j.prp.2020.152865
17. Franca JA, Gayden T, Bareke E, Santos JN, de Sousa SF, Bastos-Rodrigues L, et al. Whole-Exome Sequencing Reveals Novel Vacuolar ATPase Genes' Variants and Variants in Genes Involved in Lysosomal Biology and Autophagosomal Formation in Oral Granular Cell Tumors. *J Oral Pathol Med* (2021) 50(4):410–7. doi: 10.1111/jop.13148
18. Pareja F, Brandes AH, Basili T, Selenica P, Geyer FC, Fan D, et al. Loss-Of-Function Mutations in ATP6AP1 and ATP6AP2 in Granular Cell Tumors. *Nat Commun* (2018) 9(1):3533. doi: 10.1038/s41467-018-05886-y
19. Sekimizu M, Yoshida A, Mitani S, Asano N, Hirata M, Kubo T, et al. Frequent Mutations of Genes Encoding Vacuolar H(+) -ATPase Components in Granular Cell Tumors. *Genes Chromosomes Cancer* (2019) 58(6):373–80. doi: 10.1002/gcc.22727
20. Whipple SG, Savardekar AR, Rao S, Mahadevan A, Guthikonda B, Kosty JA. Primary Tumors of the Posterior Pituitary Gland: A Systematic Review of the Literature in Light of the New 2017 World Health Organization Classification of Pituitary Tumors. *World Neurosurg* (2021) 145:148–58. doi: 10.1016/j.wneu.2020.09.023
21. Miller MB, Bi WL, Ramkissoon LA, Kang YJ, Abedalthagafi M, Knoff DS, et al. MAPK Activation and HRAS Mutation Identified in Pituitary Spindle Cell Oncocytoma. *Oncotarget* (2016) 7(24):37054–63. doi: 10.18632/oncotarget.9244
22. Viaene AN, Lee EB, Rosenbaum JN, Nasrallah IM, Nasrallah MP. Histologic, Immunohistochemical, and Molecular Features of Pituicytomas and Atypical Pituicytomas. *Acta Neuropathol Commun* (2019) 7(1):69. doi: 10.1186/s40478-019-0722-6
23. Dawoud FM, Naylor RM, Giannini C, Swanson AA, Meyer FB, Uhm JH. TTF-1 Positive Posterior Pituitary Tumor: Limitations of Current Treatment and Potential New Hope in BRAF V600E Mutation Variants. *Clin Neurol Neurosurg* (2020) 196:106059. doi: 10.1016/j.clineuro.2020.106059
24. Sollfrank L, Lettmaier S, Erdmann M, Uslu U. Panniculitis Under Successful Targeted Inhibition of the MAPK/ERK Signaling Pathway in a Patient With BRAF V600E-Mutated Spindle Cell Oncocytoma of the Pituitary Gland. *Anticancer Res* (2019) 39(7):3955–9. doi: 10.21873/anticanres.13549
25. Fahey CC, Davis IJ. SETting the Stage for Cancer Development: SETD2 and the Consequences of Lost Methylation. *Cold Spring Harb Perspect Med* (2017) 7(5). doi: 10.1101/cshperspect.a026468
26. Newbold RF, Mokbel K. Evidence for a Tumour Suppressor Function of SETD2 in Human Breast Cancer: A New Hypothesis. *Anticancer Res* (2010) 30(9):3309–11.
27. Li F, Mao G, Tong D, Huang J, Gu L, Yang W, et al. The Histone Mark H3K36me3 Regulates Human DNA Mismatch Repair Through Its Interaction With MutSalpha. *Cell* (2013) 153(3):590–600. doi: 10.1016/j.cell.2013.03.025
28. Lu M, Zhao B, Liu M, Wu L, Li Y, Zhai Y, et al. Pan-Cancer Analysis of SETD2 Mutation and Its Association With the Efficacy of Immunotherapy. *NPJ Precis Oncol* (2021) 5(1):51. doi: 10.1038/s41698-021-00193-0
29. Fernandez LP, Lopez-Marquez A, Santisteban P. Thyroid Transcription Factors in Development, Differentiation and Disease. *Nat Rev Endocrinol* (2015) 11(1):29–42. doi: 10.1038/nrendo.2014.186
30. Gandhi GY, Fung R, Natter PE, Makary R, Balaji KC. Symptomatic Pituitary Metastasis as Initial Manifestation of Renal Cell Carcinoma: Case Report and Review of Literature. *Case Rep Endocrinol* (2020) 2020:8883864. doi: 10.1155/2020/8883864
31. Chaves-Moreira D, Morin PJ, Drapkin R. Unraveling the Mysteries of PAX8 in Reproductive Tract Cancers. *Cancer Res* (2021) 81(4):806–10. doi: 10.1158/0008-5472.CAN-20-3173
32. Hardy LR, Pergande MR, Esparza K, Heath KN, Onyuksel H, Cologna SM, et al. Proteomic Analysis Reveals a Role for PAX8 in Peritoneal Colonization of High Grade Serous Ovarian Cancer That can be Targeted With Micelle Encapsulated Thiostrepton. *Oncogene* (2019) 38(32):6003–16. doi: 10.1038/s41388-019-0842-2
33. Shi K, Yin X, Cai MC, Yan Y, Jia C, Ma P, et al. PAX8 Regulon in Human Ovarian Cancer Links Lineage Dependency With Epigenetic Vulnerability to HDAC Inhibitors. *Elife* (2019) 8. doi: 10.7554/eLife.44306
34. Suraweera A, O'Byrne KJ, Richard DJ. Combination Therapy With Histone Deacetylase Inhibitors (HDACi) for the Treatment of Cancer: Achieving the Full Therapeutic Potential of HDACi. *Front Oncol* (2018) 8:92. doi: 10.3389/fonc.2018.00092

Conflict of Interest: The authors declare that the research was conducted in the absence of any commercial or financial relationships that could be construed as a potential conflict of interest.

Publisher's Note: All claims expressed in this article are solely those of the authors and do not necessarily represent those of their affiliated organizations, or those of the publisher, the editors and the reviewers. Any product that may be evaluated in this article, or claim that may be made by its manufacturer, is not guaranteed or endorsed by the publisher.

frontiers in Endocrinology

ORIGINAL RESEARCH
published: 14 December 2021
doi: 10.3389/fendo.2021.793337

Analysis of Related Factors of Tumor Recurrence or Progression After Transnasal Sphenoidal Surgical Treatment of Large and Giant Pituitary Adenomas and Establish a Nomogram to Predict Tumor Prognosis

Yike Chen[1†], Feng Cai[1†], Jing Cao[2], Feng Gao[3], Yao Lv[4], Yajuan Tang[1], Anke Zhang[1], Wei Yan[1], Yongjie Wang[1], Xinben Hu[1], Sheng Chen[1], Xiao Dong[1], Jianmin Zhang[1] and Qun Wu[1*]*

[1] Department of Neurosurgery, Second Affiliated Hospital, School of Medicine, Zhejiang University, Hangzhou, China, [2] Department of Statistical Office, The Affiliated Changsha Central Hospital, Hengyang Medical School, University of South China, Changsha, China, [3] Department of Neurosurgery, The Affiliated People's Hospital of Ningbo University, Ningbo, China, [4] Department of Neurosurgery, The Affiliated Quzhou People's Hospital of Wenzhou University, Quzhou, China

Background: Pituitary adenoma (PA) is a benign neuroendocrine tumor caused by adenohypophysial cells, and accounts for 10%-20% of all primary intracranial tumors. The surgical outcomes and prognosis of giant pituitary adenomas measuring ≥3 cm in diameter differ significantly due to the influence of multiple factors such as tumor morphology, invasion site, pathological characteristics and so on. The aim of this study was to explore the risk factors related to the recurrence or progression of giant and large PAs after transnasal sphenoidal surgery, and develop a predictive model for tumor prognosis.

Methods: The clinical and follow-up data of 172 patients with large or giant PA who underwent sphenoidal surgery at the Second Affiliated Hospital of Zhejiang University School of Medicine from January 2011 to December 2017 were retrospectively analyzed. The basic clinical information (age, gender, past medical history etc.), imaging features (tumor size, invasion characteristics, extent of resection etc.), and histopathological characteristics (pathological results, Ki-67, P53 etc.) were retrieved. SPSS 21.0 software was used for statistical analysis, and the R software was used to establish the predictive nomogram.

Results: Seventy out of the 172 examined cases (40.7%) had tumor recurrence or progression. The overall progress free survival (PFS) rates of the patients at 1, 3 and 5 years after surgery were 90.70%, 79.65% and 59.30% respectively. Log-rank test indicated that BMI ($P < 0.001$), Knosp classification ($P < 0.001$), extent of resection

OPEN ACCESS

Edited by:
Congxin Dai,
Capital Medical University, China

Reviewed by:
Zhu Huijuan,
Peking Union Medical College Hospital (CAMS), China
Changxiang Yan,
Capital Medical University, China

****Correspondence:***
Qun Wu
2192010@zju.edu.cn
Jianmin Zhang
zjm135@zju.edu.cn

†These authors have contributed equally to this work and share first authorship

Specialty section:
This article was submitted to Pituitary Endocrinology, a section of the journal Frontiers in Endocrinology

Received: *12 October 2021*
Accepted: *23 November 2021*
Published: *14 December 2021*

Citation:
Chen Y, Cai F, Cao J, Gao F, Lv Y, Tang Y, Zhang A, Yan W, Wang Y, Hu X, Chen S, Dong X, Zhang J and Wu Q (2021) Analysis of Related Factors of Tumor Recurrence or Progression After Transnasal Sphenoidal Surgical Treatment of Large and Giant Pituitary Adenomas and Establish a Nomogram to Predict Tumor Prognosis. Front. Endocrinol. 12:793337. doi: 10.3389/fendo.2021.793337

(P < 0.001), Ki-67 (P < 0.001), sphenoidal sinus invasion (P = 0.001), Hardy classification (P = 0.003) and smoking history (P = 0.018) were significantly associated with post-surgery recurrence or progression. Cox regression analysis further indicated that smoking history, BMI ≥25 kg/m^2, Knosp classification grade 4, partial resection and ≥3% Ki-67 positive rate were independent risk factors of tumor recurrence or progression (P < 0.05). In addition, the nomogram and ROC curve based on the above results indicated significant clinical value.

Conclusion: The postoperative recurrence or progression of large and giant PAs is related to multiple factors and a prognostic nomogram based on BMI (≥25 kg/m^2), Knosp classification (grade 4), extent of resection (partial resection) and Ki-67 (≥3%) can predict the recurrence or progression of large and giant PAs after transnasal sphenoidal surgery.

Keywords: pituitary adenoma, tumor recurrence, transnasal sphenoidal surgery, Cox regression model, nomogram

INTRODUCTION

Pituitary adenoma (PA) is a benign neuroendocrine tumor that originates from adenohypophysial cells, and accounts for 10%-20% of all primary intracranial tumors (1, 2). The global prevalence of PA ranges from 80 to 100 cases per 100,000 (3). Pituitary adenomas disrupt the endocrine function of the pituitary gland, and the growing tumor mass can lead to headaches, vision problems and visual field changes. Giant PA is defined as tumors with the largest diameter ≥4 cm (4–6), and some investigators have defined tumors with the largest diameter ≥3 cm as large PA (5, 7, 8). Large and giant PAs tend to invade the region surrounding the saddle, starting from the bone of saddle bottom and then progressing to the sphenoid sinus. Tumor growth through the diaphragm sella compresses the optic chiasm and third ventricle, and involvement of the cavernous sinus leads to encasement of the internal carotid artery. Therefore, the internal carotid artery and peripheral nerves can be easily damaged during the operation. In addition, some lesions are tough in texture or accompanied by spontaneous stroke, which further increases the difficulty of surgery and increases the risk of recurrence or progression.

Surgical removal is the first-line treatment for most large and giant PAs, except for prolactinoma (9, 10). Since craniotomy causes greater damage to normal brain tissues and results in more postoperative complications, it is now gradually being replaced with the transnasal sphenoidal approach (11). Jankowski et al. were the first to successfully perform neuroendoscopy-guided transsphenoidal resection of PA (12). Nevertheless, regardless of whether the surgery is performed using neuroendoscopy or microscopy, or *via* the transnasal sphenoidal or transcranial approach, the surgical outcomes are still not satisfactory. Over 50%-72% of the cases have postoperative residual (13–16), and the recurrence rates at 5- and 10 years after surgery are 40% and 50% respectively (17). Even with gross total resection, at least 10-20% of the patients relapse within 5 to 10 years (2, 14), which greatly affects their quality of life.

Apart from postoperative residual, the recurrence of PA also depends on the tumor size and cavernous sinus invasion, which are risk factors for poor prognosis (14, 18, 19). In addition, the pathological subtype is also a factor influencing tumor recurrence and progression (20). It was reported that sparsely granulated GH adenomas and prolactin PAs in male patients are highly aggressive and have poor prognosis (21, 22).

Recurrence and progression of residual PA lesions impair the function of the pituitary gland. Therefore, long-term hormone replacement therapy is often required after surgery, which greatly reduces the quality of life of patients. In addition, surgical resection of the recurrent or evolved tumors increases the risk of vascular rupture, nerve injury and other adverse complications, which further worsens patient prognosis. In this study, we retrospectively analyzed the clinical, pathological, surgical and imaging data of 172 patients with large or giant PA to identify the risk factors of tumor recurrence and progression. In addition, we developed a nomogram to predict tumor recurrence or progression and assess postoperative prognosis.

MATERIALS AND METHODS

Study Population

After obtaining institutional review board approval, the clinical data of 172 patients with large (>3 cm) or giant (>4 cm) PA that underwent surgery at The Second Affiliated Hospital Zhejiang University School of Medicine between January 2011 and December 2017 were retrospectively analyzed. The inclusion criteria were as follows: 1) histologically confirmed PAs with maximal diameter >3–4 cm (large) or >4 cm (giant), 2) underwent tumor resection through transnasal sphenoidal surgery, 3) no radiotherapy during the period of treatment, and 4) regular follow-up for a minimum of 6 months. Patients with serious intraoperative complications (such as internal carotid artery rupture or anesthesia accident), severe cardiopulmonary insufficiency, organ failure or other serious underlying diseases, anatomical variation or complicated with vascular disease (such as aneurysm), and those who underwent

craniotomy for PA were excluded. The patients were re-examined 3-, 6- and 12 months after surgery, and yearly thereafter. Images of the pituitary were assessed by a neurosurgeon and a neuroradiologist during the follow-up period. Recurrence or progression was defined as significant enlargement (>2 mm in any direction) of the tumor remnants or the appearance of new masses detected by MRI during the follow-up (14).

Data Collection

The patient data was divided into basic, radiological and pathological categories. Basic information included gender, age, history of hypertension, diabetes, smoking [patients who have smoked more than 100 cigarettes in lifetime were defined as having smoking history (23)], drinking, body mass index (overweight≥25kg/m^2, not overweight<25kg/m^2), function and operation methods (microscopy or neuroendoscopy). Radiological characteristics included cavernous sinus invasion, sphenoid sinus invasion, sella invasion, Hardy classification, Knosp classification, extent of resection [gross total resection (GTR), the extent of resection is greater than 95%; near total resection, NTR, the extent of resection is between 90% and 95%; subtotal resection, STR, the extent of resection is between 70%-90%; partial resection, PR, the extent of resection is less than 70% (8)]. The pathological classification, and P53 and Ki-67 positive rates were also collected.

Data Analysis

Differences between subgroups were analyzed using Student's t-test for the measurement data and the X^2 test was used for categorical variables. The Kaplan-Meier survival curves were plotted and compared by log-rank tests using SPSS 21.0. Multivariate Cox regression analysis was performed to assess the independent predictive risk factors for tumor relapse, and a nomogram model was established with the R software version 4.0.3 (https://www.r-project.org, R package "rms", "survival".) to predict outcomes at the 1-, 3-, and 5-year follow-up. The performance of the nomogram was determined with ROC curve and calibration curve. Two-sided P values below 0.05 were considered statistically significant.

RESULTS

General Characteristics

A total of 172 patients (83 females and 89 males) with pathologically confirmed PA were included. The mean age was 53.7 ± 12.7 years (range, 18-83 years), of which 109 patients (63.4%) were younger than 60 years and 63 patients (36.6%) were older than 60 years. Non-functional PA was detected in 150 patients (87.2%) and 22 patients (12.8%) had functional PAs. In addition, 101 patients (58.7%) had a BMI<25 kg/m^2 and 71 patients (41.3%) had BMI≥25 kg/m^2, 53 patients (30.8%) had a history of smoking, 60 patients (34.9%) had a history of alcohol consumption, 51 patients (29.7%) had a history of hypertension, and 17 patients (9.9%) had a history of diabetes. Based on the preoperative results of MRI and intraoperative observation, there were 150 cases of cavernous sinus invasion, 65 of sphenoid sinus invasion, and 152 cases of sella invasion. Due to the low number of patients in each group, the subgroups made on the basis of Knosp and Hardy classifications were pooled into several larger groups. For instance, the patients were divided into Knosp classification 0-1 (15 patients, 8.7%), 2-3 (92 patients, 53.5%) and 4 (65 patients, 37.8%), Hardy classification 1-2 (61 patients, 8.7%), 3 (77 patients, 55.3%) and 4-5 (34 patients, 37.8%). All patients underwent transnasal sphenoidal surgery, of which 112 patients (65.1%) were treated with neuroendoscopy and 60 (34.9%) with microscopy. GTR was performed in 28 cases (16.3%), NTR in 62 cases (36%), STR in 54 cases (31.4%) and PR in 28 cases (16.3%). According to the 2017 WHO classification of PA (some patients were not classified according to this standard, so this part of the results could not be included in the study), there was 1 case of somatotroph adenoma, 1 of lactotroph adenoma, 5 corticotroph adenoma (sparsely granulated corticotroph adenoma in 2 cases), 4 gonadotroph adenoma, 5 null cell adenoma, and 3 plurihormonal adenoma. Furthermore, 47 cases (27.3%) were P53 positive and 44 cases (25.6%) were Ki-67≥3% (**Table 1**).

Tumor Recurrence and Progression

Seventy patients (40.7%) had recurrence or progression, and the overall progress free survival (PFS) rates 1-, 3-, and 5 years after surgery was 90.70%, 79.65% and 59.30% respectively (**Figure 1**).

TABLE 1 | General characteristics.

Clinical Features	Groups	N of Patients (%)
Age	<60	109(63.4%)
	≥60	63(36.6%)
Clinical status	Non-functional PA	150(87.2%)
	Functional PA	22(12.8%)
BMI	<25 kg/m^2	101(58.7%)
	≥25 kg/m^2	71(41.3%)
Dietary Habit	Smoking	53(30.8%)
	Drinking	60(34.9%)
Past Medical History	Diabetes	17(9.9%)
	Hypertension	51(29.7%)
Hardy Classification	Grade 1~2	61(35.4%)
	Grade 3	77(44.8%)
	Grade 4~5	34(19.8%)
Knosp Classification	Grade 0~1	15(8.7%)
	Grade 2-3	92(53.5%)
	Grade 4	65(37.8%)
Structure of Tumor Invasion	Cavernous Sinus	150(87.2%)
	Sphenoid Sinus	65(37.7%)
	Sella	152(88.3%)
Operation Methods	Microscope	60(34.9%)
	Endoscope	112(65.1%)
Extent of resection	GTR	28(16.3%)
	NTR	62(36.0%)
	STR	54(41.4%)
	PR	28(16.3%)
Pathologic Results	P53+	47(27.3%)
	Ki-67≥3%	44(25.6%)

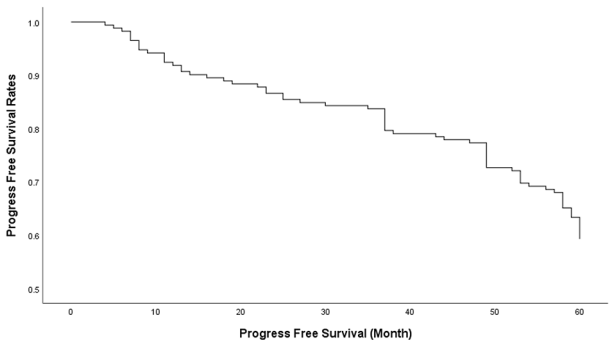

FIGURE 1 | The overall progress free survival (PFS) rates of 1, 3 and 5 years after transnasal sphenoidal surgery was 90.70%, 79.65% and 59.30% respectively.

Univariate Analysis of Potential Risk Factors

The following factors were subjected to univariate analysis to identify those significantly associated with postoperative recurrence or progression of large and giant PAs: age, gender, history of hypertension and diabetes, smoking history, drinking history, BMI (<25 kg/m^2/≧25 kg/m^2), clinical function, surgical method (endoscopic/microscope), cavernous sinus invasion, spinous sinus invasion, suprasellar invasion, Hardy classification, Knosp classification, extent of resection (GTR >95%, NTR 90%-95%, STR 70%-90% and PR <70%), P53 and Ki-67 (<3%/≥3%). BMI (P <0.001), Knosp classification (P <0.001), extent of resection (P <0.001), Ki-67 (P <0.001), sphenoid sinus invasion (P =0.001), Hardy classification (P =0.003) and smoking history (P =0.018) were the significant risk factors of tumor recurrence or progression (**Table 2**).

Studies show that tumor size and the extent of invasion into the sphenoid sinus significantly affect post-operative recurrence or progression of PA (14, 24, 25). The mean PFS duration (**Table 2**) and survival rate (**Figure 2**) of patients with Grade 4 Knosp classification were significantly less compared to that of the other groups (P < 0.001). Likewise, the mean PFS of Grade 4-5 Hardy classification was only 41 months, and the survival rate was significantly lower compared to that of grades 1-2 and 3 (P = 0.003). The mean PFS of patients with sphenoid sinus invasion was 45.26 months compared to 52.59 months in patients without sphenoid sinus invasion (P = 0.001), and the survival rates were significantly different (**Figure 2**). Ki-67 expression is an indicator of tumor cell proliferation and invasion (26). The mean PFS of patients with highly proliferative tumors (Ki-67 ≥3%) was only 38.64 months compared to the 53.97 months in patients with less active tumors (Ki-67 <3%) (P < 0.001). The extent of surgical resection was determined on the basis of surgical records and postoperative imaging results, and the patients were divided into GTR, NTR, STR and PR groups. The shortest mean PFS and survival rate was seen in the PR group (P < 0.001 versus all).

Although body mass index (BMI) and smoking history are not directly related to PA, univariate analysis suggested that both factors have a significant impact on postoperative recurrence or progression of large and giant PAs. Based on the pre-operative BMI, the patients were divided into overweight (BMI≧25 kg/m^2) and non-overweight (BMI < 25 kg/m^2) groups. The mean PFS of the overweight patients was 44.99 months as opposed to 53.6 in patients with healthy BMI (P< 0.001). Furthermore, patients with a history of smoking had a shorter mean PFS compared to the non-smokers (40.38 months vs 54.35 months). As shown in **Figure 2**, there was a significant difference in PFS between the two groups (P = 0.018).

Independent Risk Factors for Postoperative Recurrence or Progression of Large and Giant Pas

The factors identified in the univariate analysis were incorporated into the multivariate Cox regression model. Smoking history (HR=3.103, 95% CI: 1.812-5.314), BMI (≧25 kg/m^2) (HR=1.997, 95% CI:1.206-3.306), Knosp classification (grade 4) (HR=4.093, 95% CI:1.144-14.649), extent of resection (PR) (HR=3.723, 95% CI:1.152-12.033) and Ki-67 positivity (≥3%) (HR=4.639, 95% CI:2.686-8.013) were identified as the independent risk factors (**Table 3**).

Establishment and Validation of Predictive Nomogram

We next established a nomogram based on the extent of resection, BMI, Ki-67, Knosp classification and smoking to predict the 1-, 3-, and 5-year prognosis of patients (**Figure 3**). Each risk factor was designated a score, and the sum of the five scores in the individual patients corresponded to the probability of PFS 1, 3 and 5 years after surgery. The calibration curve and ROC were used to confirm the clinical value of this model, and indicated good agreement between the predicted and observed values (**Figure 4A**). As shown in **Figure 4B**, the area under the ROC curves (AUC) for 1-, 2-, and 3-year survival were 0.889, 0.885 and 0.832 respectively, indicating satisfactory accuracy.

DISCUSSION

In this study, we retrospectively analyzed the clinical data of 172 patients with large or giant PA, and identified multiple risk factors for postoperative recurrence or progression. A prognostic nomogram was established based on these factors, which could predict survival with satisfactory accuracy.

The extent of surgical resection is the main factor influencing tumor recurrence or progression. In this study, we defined GTR (>95%), NTR (90%-95%), STR (70%-90%) and PR (<70%) on the basis of postoperative imaging results and surgical records. PR was significantly associated with tumor recurrence or progression (HR: 3.302; *P*=0.048). The transsphenoidal approach with neuroendoscopy can improve the extent of surgical resection (19, 27). Fathalla et al. reviewed 65 patients with acromegaly, and found that the extent of resection was significantly greater in patients who underwent endoscopy as opposed to the microscopy group (61% vs 42%, P=0.05).

TABLE 2 | Univariate analysis results and mean PFS for each group.

Clinical Features	Groups	N	PFS	95%CI	X^2	*P*
Age						
	<60	109	49.32	(46.04,52.61)	0.016	0.899
	≥60	63	51.30	(47.14,55.46)		
Gender						
	Female	78	56.73	(52.20,61.26)	3.413	0.065
	Male	94	50.59	(46.82,54.35)		
Hypertension						
	N	121	48.98	(45.67,52.30)	0.170	0.68
	Y	51	52.57	(48.90,56.24)		
Diabetes						
	N	155	49.57	(46.75,52.39)	0.414	0.52
	Y	17	54.41	(50.13,58.69)		
Smoking						
	N	119	54.35	(52.30,56.40)	5.588	0.018
	Y	53	40.38	(34.11,46.65)		
Drinking						
	N	112	49.30	(46.09,52.5)	2.889	0.089
	Y	60	51.45	(47.1,55.81)		
BMI						
	<25 kg/m^2	101	53.60	(50.88,56.33)	13.708	<0.001
	≧25 kg/m^2	71	44.99	(40.31,49.66)		
Clinical status						
	N	150	55.35	47.64,53.06	0.282	0.596
	Y	22	57.96	39.85,56.06		
Operation Methods						
	Endoscope	112	50.50	(47.43,53.57)	0.072	0.788
	Microscope	60	49.20	(44.53,53.88)		
Cavernous Sinus Invasion						
	N	22	47.32	(39.58,55.06)	0.924	0.336
	Y	150	50.45	(47.72,53.18)		
Sphenoid Sinus Invasion						
	N	107	52.95	(50.22,55.69)	10.816	0.001
	Y	65	45.26	(40.34,50.19)		
Sella Invasion						
	N	51	48.02	(43.39,52.65)	3.229	0.072
	Y	152	50.90	(47.80,54.00)		
Hardy Classification						
	Grade 1~2	61	53.26	(49.98,56.54)	11.579	0.003
	Grade 3	77	51.49	(47.72,55.27)		
	Grade 4~5	34	41.00	(33.83,48.17)		
Knosp Classification						
	Grade 0~1	15	59.07	(57.56,60.57)	24.018	<0.001
	Grade 2~3	92	52.71	(49.52,55.90)		
	Grade 4	65	44.20	(39.46,48.94)		
Extent of resection						
	GTR	28	57.82	(55.02,60.62)	37.748	<0.001
	NTR	62	52.73	(49.02,56.44)		
	STR	54	50.26	(45.50,55.02)		
	PR	28	35.93	(28.55,43.31)		
P53						
	Negative	125	51.41	(48.56,54.25)	1.561	0.211
	Positive	47	46.43	(40.89,51.96)		
Ki-67						
	<3%	128	53.97	(51.58,56.36)	39.916	<0.001
	≥3%	44	38.64	(32.44,44.83)		

Furthermore, endoscopy also improved the extent of resection (48% vs 14.2%, P=0.09) when the tumor invaded the cavernous sinus (27). In our cohort however, the mean PFS of patients who were treated with neuroendoscopy and microscopy were 50.50 and 49.2 months respectively, indicating that the surgical method did not have any impact on the postoperative recurrence and progression.

The invasiveness of PA is also a risk factor for postoperative recurrence or progression. Similar to the diaphragm sella, the wall of the cavernous sinus is a thin dural bag (28), and most patients in our cohort had cavernous sinus invasion (87.2%) and/or suprasellar invasion (88.4%). However, only sphenoid sinus invasion was identified as a risk factor of postoperative tumor recurrence or progression. This is consistent with the views of

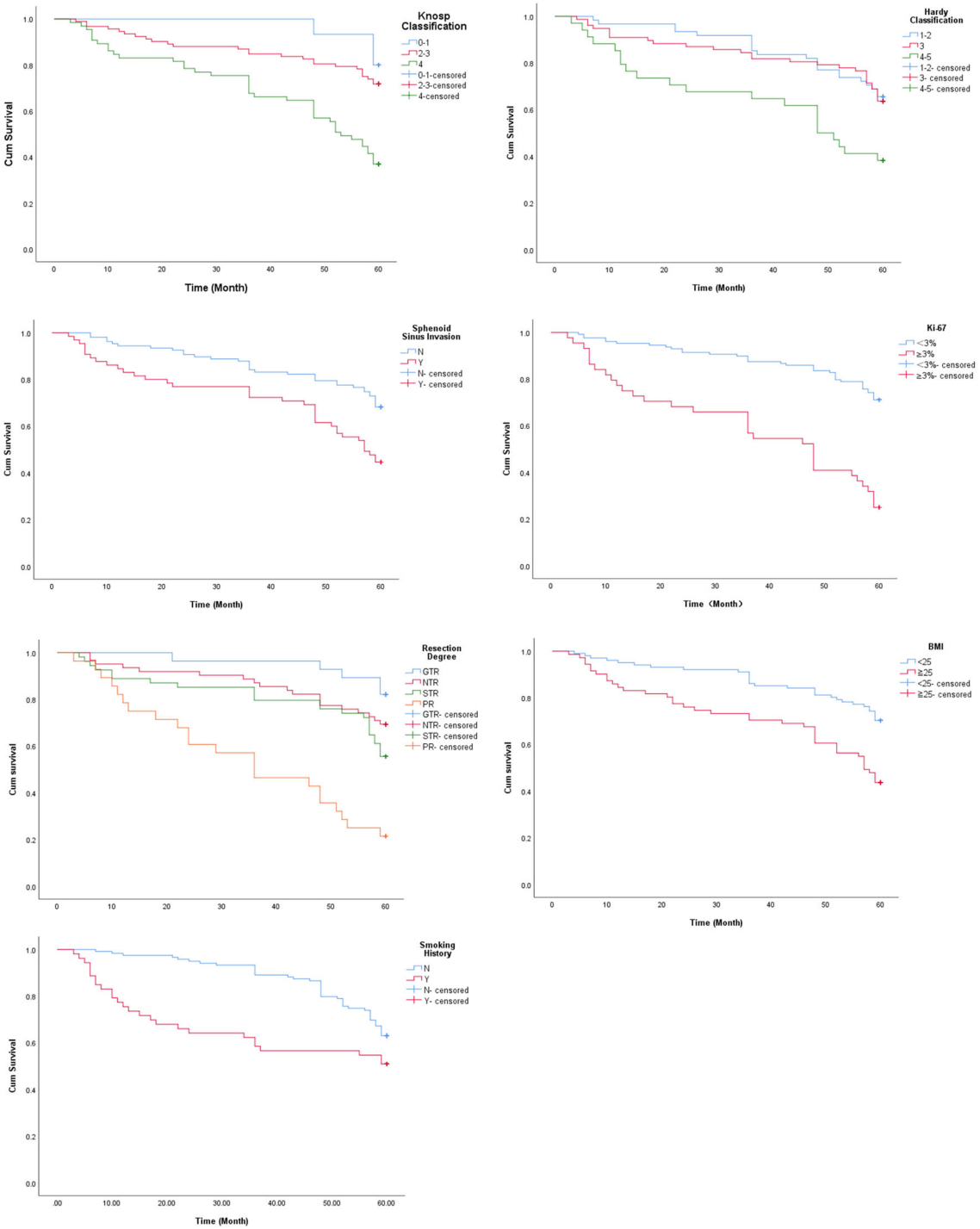

FIGURE 2 | Survival curves of patients stratified on the basis of Knosp classification, Hardy classification, sphenoid sinus invasion, Ki-67, extent of resection, BMI and smoking history.

some researchers that sphenoid sinus invasion rather than cavernous sinus invasion is a more indicative of "invasiveness" (29, 30). In one case of a particularly aggressive tumor, the growing mass passed through the bone of sellar floor to invade the sphenoid sinus in a cathepsin K-dependent manner (31). The size and invasion of PA are graded by Knosp classification and Hardy classification that are based on preoperative imaging data, and are used by neurosurgeons in preoperative evaluation and

TABLE 3 | Multivariate analysis results.

Variables	B	SE	Wald	*P*	HR	95.0% CI for HR
Smoking History	1.132	0.274	17.017	<0.001	3.103	1.812-5.314
BMI(≧25 kg/m^2)	0.691	0.257	7.222	0.007	1.997	1.206-3.306
Sphenoid Sinus Invasion	0.403	0.262	2.354	0.125	1.496	0.894-2.501
Hardy Classification						
Grade 1-2					1.000	
Grade 3	0.064	0.299	0.045	0.831	1.066	0.593-1.914
Grade 4-5	0.599	0.362	2.739	0.098	1.821	0.895-3.703
Knosp Classification						
Grade 0-1					1.000	
Grade 2-3	0.678	0.629	1.160	0.282	1.970	0.574-6.763
Grade 4	1.409	0.651	4.692	0.030	4.093	1.144-14.649
Extent of resection						
GTR					1.000	
NTR	0.503	0.520	0.936	0.333	1.653	0.597-4.579
STR	0.692	0.519	1.779	0.182	1.997	0.723-5.519
PT	1.315	0.598	4.825	0.028	3.723	1.152-12.033
P53 (-)	-0.259	0.298	0.754	0.385	0.772	0.430-1.385
Ki-67 (≥3%)	1.535	0.279	30.290	<0.001	4.639	2.686-8.013

prediction of surgical. We found that both were significantly associated with the recurrence or progression of large and giant PAs after surgery, and Knosp 4 was an independent risk factor, which is highly associated with tumor recurrence. Thus, Knosp classification may play an important role in predicting tumor recurrence as reported in previous studies (32–34).

The invasiveness of adenomas and other tumors is also evaluated in terms of pathological parameters, such as mitotic figures, Ki-67 index (35, 36) and p53 expression in the malignant tissues (26). Petry et al. conducted a retrospective analysis of 52 patients with PA and divided them into Ki-67 ≥3% and Ki-67 <3% groups, and found that high Ki-67 expression was correlated with more aggressive tumor growth and higher recurrence rate (67%vs 17%, P=0.03) (37). Consistent with this, we found that the mean PFS of patients with higher Ki-67 index tumors (≥3%) was significantly lower compared to those with

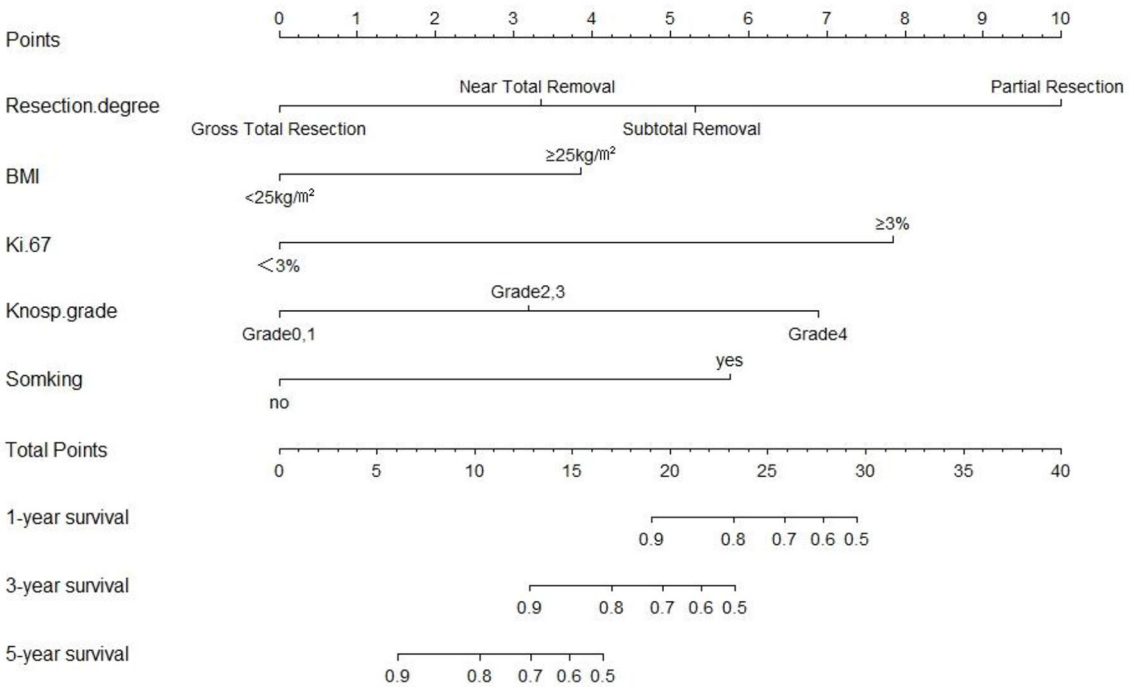

FIGURE 3 | The predictive nomogram based on resection degree, BMI, Ki-67, Knosp classification and smoking history.

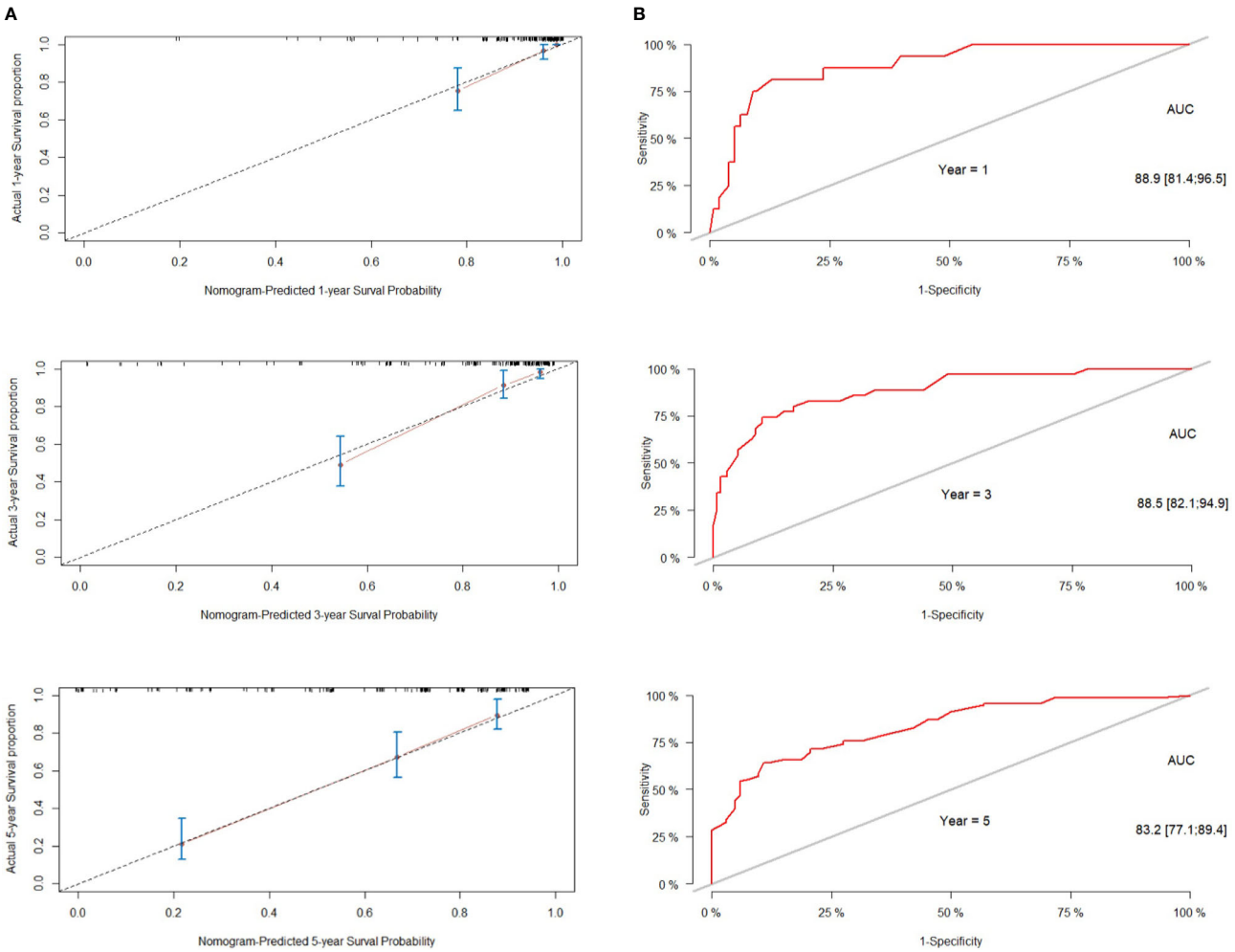

FIGURE 4 | Performance of the nomogram for predicting tumor recurrence or progression. **(A)** calibration curve of the nomogram. **(B)** The predictive performance of the nomogram was assessed by receiver operator characteristics (ROC) analysis and area under the curve (AUC).

< 3% Ki-67 positivity. Furthermore, Ki-67 ≥ 3% was identified an independent risk factor of postoperative recurrence or progression. However, P53 expression did not have any impact on the mean PFS. According to WHO 2017 classification, the pathological subtypes of PA include sparsely granulated somatotroph adenoma, lactotroph adenoma (in men), pluri-hormonal PIT-1 positive adenoma, silent corticotroph adenoma and crooke cell adenoma, all of which are considered high-risk (38). Due to limitations of specific markers and staining techniques, we were unable to include this pathological classification in our study. Therefore, predicting the proliferative potential of large and giant PAs classified on the basis of more rigorous pathological criteria remains to be elucidated.

The prognosis of PA is evaluated according to imaging features (tumor site, Knosp classification etc.) and pathological results (pathological classification, Ki-67, P53 etc.) (39), which do not take into account other clinical factors. In this study, we found that BMI ≧ 25 kg/m^2 and a history of smoking were independent risk factors of postoperative recurrence or progression. Obesity is an established risk factor for intracranial tumors (40, 41), and promotes tumor development through chronic insulin resistance, hyperinsulinemia and enhanced IGF-1 activity. In fact, more than half of meningiomas overexpress IGF-1 receptors, and IGF-1 can promote the growth of meningioma cells *in vitro* (42). Furthermore, overexpression of IGF-1 receptors in glioma cells promotes their proliferation and inhibits apoptosis (43, 44). In this study, the mean PFS of overweight patients (BMI≥25 kg/m^2) was significantly shorter than that of patients with a healthy weight (BMI < 25 kg/m^2). All these evidences provide new insights into the molecular mechanisms underlying recurrence or progression of large and giant PAs after surgery. Several studies have shown that smoking is a high-risk factor for lung

cancer, bladder cancer, head and neck cancer and other cancers (45–47). Taken together, the correlation of general health and smoking with PA progression warrants further study.

Although the association between PA recurrence or progression and clinical variables has been reported previously (48–50), multiple variables are rarely incorporated to assess prognosis. Nomograms are now widely used to predict the prognosis of other tumors, since they can simplify the statistical model, and estimate the probability of an event (such as death or recurrence) with a single value (51). In addition, a nomogram can integrate multiple prognostic variables and determinants that simulate complex biological and clinical scenarios for personalized medicine (52). On the basis of the univariate and multivariate models, we developed a nomogram to predict the recurrence or progression of PA after transnasal sphenoidal surgery by integrating the independent risk factors, and found that the model can predict tumor recurrence 1-, 3- and 5 years after surgery with satisfactory accuracy. This nomogram provided probability estimates that may be useful for individual patients, and help predict tumor recurrence or progression after surgery. We can use this scoring system after surgery by adding up the scores for all factors, objectively evaluate the possibility of tumor recurrence or progression, and provide a reference for clinical treatment to develop an individual follow-up plan.

However, this study has certain limitations that should be considered. First, this was a single-center retrospective study, which warrants further validation of the predictive model on a larger, multicenter cohort. Second, the association of the pathological subtypes of PA with tumor recurrence or progression should be further explored with a uniform and strict standard. In conclusion, partial resection, BMI ≧25 kg/m^2, Ki-67 ≥3%, Knosp classification grade 4 and smoking increase the risk of the recurrence or progression of large and giant PAs. The nomogram model incorporating these risk factors can facilitate prediction of tumor recurrence or progression after transnasal sphenoidal surgery in individual patients.

DATA AVAILABILITY STATEMENT

The original contributions presented in the study are included in the article/supplementary material. Further inquiries can be directed to the corresponding authors.

ETHICS STATEMENT

The study was reviewed and approved by Ethics Committee of Second Affiliated Hospital, School of Medicine, Zhejiang University.

AUTHOR CONTRIBUTIONS

YC and FC performed the analysis and co-wrote the manuscript. AZ, XH, YT, FG, YL, and JC collected the patient information. WY, YW, SC, and XD revised paper. QW and JZ supervised the project, conceived the study, and guided the editing of the manuscript. YC and FC contributed equally to the manuscript. QW and JZ are corresponding authors. All authors contributed to the article and approved the submitted version.

REFERENCES

1. Ostrom QT, Gittleman H, Truitt G, Boscia A, Kruchko C, Barnholtz-Sloan JS. CBTRUS Statistical Report: Primary Brain and Other Central Nervous System Tumors Diagnosed in the United States in 2011-2015. *Neuro Oncol* (2018) 20 (suppl_4):iv1–iv86. doi: 10.1093/neuonc/noy131
2. Chen Y, Wang CD, Su ZP, Chen YX, Cai L, Zhuge QC, et al. Natural History of Postoperative Nonfunctioning Pituitary Adenomas: A Systematic Review and Meta-Analysis. *Neuroendocrinology* (2012) 96(4):333–42. doi: 10.1159/000339823
3. Raappana A, Koivukangas J, Ebeling T, Pirilä T. Incidence of Pituitary Adenomas in Northern Finland in 1992-2007. *J Clin Endocrinol Metab* (2010) 95(9):4268–75. doi: 10.1210/jc.2010-0537
4. Raverot G, Jouanneau E, Trouillas J. Management of Endocrine Disease: Clinicopathological Classification and Molecular Markers of Pituitary Tumours for Personalized Therapeutic Strategies. *Eur J Endocrinol* (2014) 170(4):R121–32. doi: 10.1530/EJE-13-1031
5. Müslüman AM, Cansever T, Yılmaz A, Kanat A, Oba E, Çavuşoğlu H, et al. Surgical Results of Large and Giant Pituitary Adenomas With Special Consideration of Ophthalmologic Outcomes. *World Neurosurg* (2011) 76 (1-2):141–8; discussion 63-6. doi: 10.1016/j.wneu.2011.02.009
6. de Paiva Neto MA, Vandergrift A, Fatemi N, Gorgulho AA, Desalles AA, Cohan P, et al. Endonasal Transsphenoidal Surgery and Multimodality Treatment for Giant Pituitary Adenomas. *Clin Endocrinol (Oxf)* (2010) 72 (4):512–9. doi: 10.1111/j.1365-2265.2009.03665.x
7. Hofstetter CP, Nanaszko MJ, Mubita LL, Tsiouris J, Anand VK, Schwartz TH. Volumetric Classification of Pituitary Macroadenomas Predicts Outcome and Morbidity Following Endoscopic Endonasal Transsphenoidal Surgery. *Pituitary* (2012) 15(3):450–63. doi: 10.1007/s11102-011-0350-z
8. Juraschka K, Khan OH, Godoy BL, Monsalves E, Kilian A, Krischek B, et al. Endoscopic Endonasal Transsphenoidal Approach to Large and Giant Pituitary Adenomas: Institutional Experienceand Predictors of Extent of Resection. *J Neurosurg* (2014) 121(1):75–83. doi: 10.3171/2014.3.JNS131679
9. Shimon I, Jallad RS, Fleseriu M, Yedinak CG, Greenman Y, Bronstein MD. Giant GH-Secreting Pituitary Adenomas: Management of Rare and Aggressive Pituitary Tumors. *Eur J Endocrinol* (2015) 172(6):707–13. doi: 10.1530/EJE-14-1117
10. Gillam MP, Molitch ME, Lombardi G, Colao A. Advances in the Treatment of Prolactinomas. *Endocr Rev* (2006) 27(5):485–534. doi: 10.1210/er.2005-9998
11. Pratheesh R, Rajaratnam S, Prabhu K, Mani SE, Chacko G, Chacko AG. The Current Role Oftranscranial Surgery in the Management of Pituitary Adenomas. *Pituitary* (2013) 16(4):419–34. doi: 10.1007/s11102-012-0439-z
12. Jankowski R, Auque J, Simon C, Marchal JC, Hepner H, Wayoff MJL. Endoscopic Pituitarytumor Surgery. *Laryngoscope* (1992) 102(2):198–202. doi: 10.1288/00005537-199202000-00016
13. Dekkers OM, Pereira AM, Roelfsema F, Voormolen JHC, Neelis KJ, Schroijen MA, et al. Observation Alone After Transsphenoidal Surgery for Nonfunctioning Pituitary Macroadenoma. *J Clin Endocrinol Metab* (2006) 91(5):1796–801. doi: 10.1210/jc.2005-2552
14. Brochier S, Galland F, Kujas M, Parker F, Gaillard S, Raftopoulos C, et al. Factors Predicting Relapse of Nonfunctioning Pituitary Macroadenomas After Neurosurgery: A Study of 142 Patients. *Eur J Endocrinol* (2010) 163(2):193–200. doi: 10.1530/EJE-10-0255

15. Ferrante E, Ferraroni M, Castrignano T, Menicatti L, Anagni M, Reimondo G, et al. Non-Functioning Pituitary Adenoma Database: A Useful Resource to Improve the Clinical Management of Pituitary Tumors. *Eur J Endocrinol* (2006) 155(6):823–9. doi: 10.1530/eje.1.02298
16. Sassolas G, Trouillas J, Treluyer C, Perrin GJAE. Management of Nonfunctioning Pituitaryadenomas. *Acta Endocrinol (Copenh)* (1993) 129 (Suppl 1):21–6.
17. Sadik ZHA, Voormolen EHJ, Depauw PRAM, Burhani B, Nieuwlaat WA, Verheul J, et al. Treatment of Nonfunctional Pituitary Adenoma Postoperative Remnants: Adjuvant or Delayed Gamma Knife Radiosurgery? *World Neurosurg* (2017) 100:361–8. doi: 10.1016/j.wneu.2017.01.028
18. Losa M, Mortini P, Barzaghi R, Ribotto P, Terreni MR, Marzoli SB, et al. Early Results of Surgery in Patients With Nonfunctioning Pituitary Adenoma and Analysis of the Risk of Tumor Recurrence. *J Neurosurg* (2008) 108(3):525–32. doi: 10.3171/JNS/2008/108/3/0525
19. Micko AS, Wöhrer A, Wolfsberger S, Knosp E. Invasion of the Cavernous Sinus Space Inpituitary Adenomas: Endoscopic Verification and its Correlation With an MRI-Based Classification. *J Neurosurg* (2015) 122 (4):803–11. doi: 10.3171/2014.12.JNS141083
20. Witek P, Zieliński G, Szamotulska K, Maksymowicz M, Kamiński G. Clinicopathological Predictive Factors in the Early Remission of Corticotroph Pituitary Macroadenomas in a Tertiary Referral Centre. *Eur J Endocrinol* (2016) 174(4):539–49. doi: 10.1530/EJE-15-1226
21. Kato M, Inoshita N, Sugiyama T, Tani Y, Shichiri M, Sano T, et al. Differential Expression of Genes Related to Drug Responsiveness Between Sparsely and Densely Granulated Somatotroph Adenomas. *Endocr J* (2012) 59(3):221–8. doi: 10.1507/endocrj.ej11-0177
22. Delgrange E, Vasiljevic A, Wierinckx A, François P, Jouanneau E, Raverot G, et al. Expression of Estrogen Receptor Alpha Is Associated With Prolactin Pituitary Tumor Prognosis and Supports the Sex-Related Difference in Tumor Growth. *Eur J Endocrinol* (2015) 172(6):791–801. doi: 10.1530/EJE-14-0990
23. Williamson TJ, Kwon DM, Riley KE, Shen MJ, Hamann HA, Ostroff JS. Lung Cancer Stigma: Does Smoking History Matter? *Ann Behav Med Publ Soc Behav Med* (2020) 54(7):535–40. doi: 10.1093/abm/kaz063
24. Lelotte J, Mourin A, Fomekong E, Michotte A, Raftopoulos C, Maiter D. Both Invasivenessand Proliferation Criteria Predict Recurrence of Non-Functioning Pituitary Macroadenomas After Surgery: A Retrospective Analysis of a Monocentric Cohort of 120 Patients. *Eur J Endocrinol* (2018) 178(3):237–46. doi: 10.1530/EJE-17-0965
25. Lv L, Yin S, Zhou P, Hu Y, Chen C, Ma W, et al. Clinical Andpathologic Characteristics Predicted the Postoperative Recurrence and Progression of Pituitary Adenoma: A Retrospective Study With 10 Years Follow-Up. *World Neurosurg* (2018) 118:e428–35. doi: 10.1016/j.wneu.2018.06.210
26. Criscitiello C, Disalvatore D, De Laurentiis M, Gelao L, Fumagalli L, Locatelli M, et al. High Ki-67 Score Is Indicative of a Greater Benefit From Adjuvant Chemotherapy When Added to Endocrine Therapy in Luminal B HER2 Negative and Node-Positive Breast Cancer. *Breast* (2014) 23(1):69–75. doi: 10.1016/j.breast.2013.11.007
27. Fathalla H, Cusimano MD, Di Ieva A, Lee J, Alsharif O, Goguen J, et al. Endoscopic Versus Microscopic Approach for Surgical Treatment of Acromegaly. *Neurosurg Rev* (2015) 38(3):541–8; discussion 548-9. doi: 10.1007/s10143-015-0613-7
28. Harris FS, Rhoton AL. Anatomy of the Cavernous Sinus. A Microsurgical Study. *J Neurosurg* (1976) 45(2):169–80. doi: 10.3171/jns.1976.45.2.0169
29. Heaney A. Management of Aggressive Pituitary Adenomas and Pituitary Carcinomas. *JNeurooncol* (2014) 117(3):459–68. doi: 10.1007/s11060-014-1413-6
30. Yokoyama S, Hirano H, Moroki K, Goto M, Imamura S, Kuratsu JI. Are Nonfunctioningpituitary Adenomas Extending Into the Cavernous Sinus Aggressive and/or Invasive? *Neurosurgery* (2001) 49(4):857–62; discussion 862-3. doi: 10.1097/00006123-200110000-00014
31. Liu H, Wang G, Gu W, Mu Y, Cathepsin K. The Association Between Cathepsin K Expressionand Sphenoid Sinus Invasion of Pituitary Adenomas. *Med Hypotheses* (2016) 97:88–9. doi: 10.1016/j.mehy.2016.10.013
32. Araujo-Castro M, Pascual-Corrales E, Martínez-Vaello V, Baonza Saiz G, Quiñones de Silva J, Acitores Cancela A, et al. Predictive Model of Surgical Remission in Acromegaly: Age, Presurgical GH Levels and Knosp Grade as the Best Predictors of Surgical Remission. *J Endocrinol Invest* (2021) 44 (1):183–93. doi: 10.1007/s40618-020-01296-4
33. Buchy M, Lapras V, Rabilloud M, Vasiljevic A, Borson-Chazot F, Jouanneau E, et al. Predicting Early Post-Operative Remission in Pituitary Adenomas: Evaluation of the Modified Knosp Classification. *Pituitary* (2019) 22(5):467–75. doi: 10.1007/s11102-019-00976-6
34. Yuhan L, Zhiqun W, Jihui T, Renlong P. Ki-67 Labeling Index and Knosp Classification Ofpituitary Adenomas. *Br J Neurosurg* (2021) 27:1–5. doi: 10.1080/02688697.2021.1884186
35. Mete O, Lopes MB. Overview of the 2017 WHO Classification of Pituitary Tumors. *EndocrPathol* (2017) 28(3):228–43. doi: 10.1007/s12022-017-9498-z
36. Glebauskiene B, Liutkeviciene R, Vilkeviciute A, Gudinaviciene I, Rocyte A, Simonaviciute D, et al. Association of Ki-67 Labelling Index and IL-17A With Pituitary Adenoma. *BioMed Res Int* (2018) 2018:7490585. doi: 10.1155/2018/7490585
37. Petry C, Poli JHZ, de Azevedo Dossin I, Rech CGSL, Pereira Lima JFS, Ferreira NP, et al. Evaluation of the Potential of the Ki67 Index to Predict Tumor Evolution in Patients With Pituitary Adenoma. *Int J Clin Exp Pathol* (2019) 12 (1):320–6.
38. Lopes MBS. The 2017 World Health Organization Classification of Tumors of the Pituitarygland: A Summary. *Acta Neuropathol* (2017) 134(4):521–35. doi: 10.1007/s00401-017-1769-8
39. Trouillas J, Roy P, Sturm N, Dantony E, Cortet-Rudelli C, Viennet G, et al. Anew Prognostic Clinicopathological Classification of Pituitary Adenomas: A Multicentric Case-Control Study of 410 Patients With 8 Years Post-Operative Follow-Up. *Acta Neuropathol* (2013) 126(1):123–35. doi: 10.1007/s00401-013-1084-y
40. Lauby-Secretan B, Scoccianti C, Loomis D, Grosse Y, Bianchini F, Straif K, et al. Body Fatness and Cancer–Viewpoint of the IARC Working Group. *N Engl J Med* (2016) 375(8):794–8. doi: 10.1056/NEJMsr1606602
41. Wiedmann MKH, Brunborg C, Di Ieva A, Lindemann K, Johannesen TB, Vatten L, et al. Overweight, Obesity and Height as Risk Factors for Meningioma, Glioma, Pituitary Adenoma and Nerve Sheath Tumor: A Large Population-Based Prospective Cohort Study. *Acta Oncol* (2017) 56 (10):1302–9. doi: 10.1080/0284186X.2017.1330554
42. Kurihara M, Tokunaga Y, Tsutsumi K, Kawaguchi T, Shigematsu K, Niwa M, et al. Characterization of Insulin-Like Growth Factor I and Epidermal Growth Factor Receptors in Meningioma. *J Neurosurg* (1989) 71(4):538–44. doi: 10.3171/jns.1989.71.4.0538
43. Friend KE, Khandwala HM, Flyvbjerg A, Hill H, Li J, McCutcheon IE. Growth Hormone Andinsulin-Like Growth Factor-I: Effects on the Growth of Glioma Cell Lines. *Growth Horm IGF Res* (2001) 11(2):84–91. doi: 10.1054/ghir.2000.0183
44. Yin D, Tamaki N, Parent AD, Zhang JH. Insulin-Like Growth Factor-I Decreased Etoposide-Induced Apoptosis in Glioma Cells by Increasing Bcl-2 Expression and Decreasing CPP32 Activity. *Neurol Res* (2005) 27(1):27–35. doi: 10.1179/016164105X18151
45. Hecht SS. Tobacco Smoke Carcinogens and Lung Cancer. *J Natl Cancer Inst* (1999) 91(14):1194–210. doi: 10.1093/jnci/91.14.1194
46. van Imhoff LC, Kranenburg GG, Macco S, Nijman NL, van Overbeeke EJ, Wegner I, et al. Prognostic Value of Continued Smoking on Survival and Recurrence Rates in Patients With Head and Neck Cancer: A Systematic Review. *Head Neck* (2016) 38(Suppl 1):E2214–20. doi: 10.1002/hed.24082
47. Li HM, Azhati B, Rexiati M, Wang WG, Li XD, Liu Q, et al. Impact of Smoking Statusand Cumulative Smoking Exposure on Tumor Recurrence of non-Muscle-Invasive Bladder Cancer. *Int Urol Nephrol* (2017) 49(1):69–76. doi: 10.1007/s11255-016-1441-6
48. Batista RL, Trarbach EB, Marques MD, Cescato VA, da Silva GO, Herkenhoff CGB, et al. Nonfunctioning Pituitary Adenoma Recurrence and Its Relationship With Sex, Size, and Hormonal Immunohistochemical Profile. *World Neurosurg* (2018) 120:e241–6. doi: 10.1016/j.wneu.2018.08.043
49. Bodhinayake I, Ottenhausen M, Mooney MA, Kesayabhotla K, Christos P, Schwarz JT, et al. Results and Risk Factors for Recurrence Following Endoscopic Endonasal Transsphenoidal Surgery for Pituitary Adenoma. *Clin Neurol Neurosurg* (2014) 119:75–9. doi: 10.1016/j.clineuro.2014.01.020
50. Lyu W, Fei X, Chen C, Tang YQ. Nomogram Predictive Model of Post-Operative Recurrencein non-Functioning Pituitary Adenoma. *Gland Surg* (2021) 10(2):807–15. doi: 10.21037/gs-21-47
51. Iasonos A, Schrag D, Raj GV, Panageas KS. How to Build and Interpret a Nomogram Forcancer Prognosis. *J Clin Oncol* (2008) 26(8):1364–70. doi: 10.1200/JCO.2007.12.9791

52. Balachandran VP, Gonen M, Smith JJ, DeMatteo RP. Nomograms in Oncology: More Than meets the Eye. *Lancet Oncol* (2015) 16(4):e173–80. doi: 10.1016/S1470-2045(14)71116-7

Conflict of Interest: The authors declare that the research was conducted in the absence of any commercial or financial relationships that could be construed as a potential conflict of interest.

Publisher's Note: All claims expressed in this article are solely those of the authors and do not necessarily represent those of their affiliated organizations, or those of the publisher, the editors and the reviewers. Any product that may be evaluated in this article, or claim that may be made by its manufacturer, is not guaranteed or endorsed by the publisher.

frontiers in Endocrinology

ORIGINAL RESEARCH
published: 23 December 2021
doi: 10.3389/fendo.2021.771673

Clinical and Therapeutic Characteristics of Pituitary TSH-Secreting Adenoma in Adolescent-Onset Patients: Six Case Studies and Literature Review

Yamei Yang[1], Jie Liu[2], Kan Deng[2], Lin Lu[1], Huijuan Zhu[1], Xiaolan Lian[1], Xinjie Bao[2], Lian Duan[1] and Yong Yao[2]**

[1] Key Laboratory of Endocrinology of National Health Commission, Department of Endocrinology, Peking Union Medical College Hospital, Chinese Academy of Medical Science and Peking Union Medical College, Beijing, China, [2] Department of Neurosurgery, Peking Union Medical College Hospital, Chinese Academy of Medical Science and Peking Union Medical College, Beijing, China

OPEN ACCESS

Edited by:
Wang Haijun,
The First Affiliated Hospital of Sun Yat-sen University, China

Reviewed by:
Hiroshi Nishioka,
Toranomon Hospital, Japan
Akira Shimatsu,
Kusatsu General Hospital, Japan
Limei Zheng,
First Affiliated Hospital of Fujian Medical University, China
Jiwei Wang,
Tianjin Huanhu Hospital, China

***Correspondence:**
Lian Duan
duanlianpumc@163.com
Yong Yao
freetigeryao@163.com

Specialty section:
This article was submitted to Pituitary Endocrinology, a section of the journal Frontiers in Endocrinology

Received: 06 September 2021
Accepted: 29 November 2021
Published: 23 December 2021

Citation:
Yang Y, Liu J, Deng K, Lu L, Zhu H, Lian X, Bao X, Duan L and Yao Y (2021) Clinical and Therapeutic Characteristics of Pituitary TSH-Secreting Adenoma in Adolescent-Onset Patients: Six Case Studies and Literature Review. Front. Endocrinol. 12:771673. doi: 10.3389/fendo.2021.771673

Background: Thyrotropin-secreting adenoma (TSH-oma) is a very rare kind of functional pituitary adenoma, especially that which occurs in adolescents. However, its potential clinical and therapeutic characteristics are still unknown.

Objectives: The study was aimed to summarize the clinical and therapeutic characteristics of patients with adolescent-onset TSH-oma.

Methods: We retrospectively analyzed six (4.1%) adolescent-onset TSH-oma cases from 148 patients who were diagnosed with TSH-oma at our hospital between January 2012 and October 2020. A literature review was performed on the PubMed online database, and 14 adolescent-onset TSH-oma cases were retrieved. Then, the characteristics of clinical manifestations, treatment outcomes, and follow-ups were analyzed and compared to the adult TSH-oma patients.

Results: Altogether, 20 adolescent-onset cases were included in this study having mean onset age of 13.4 ± 3.3 years. Males were found to be slightly predominant (M: F = 1.5:1) in our study. The median baseline levels of TSH, FT3, and FT4 in adolescent-onset cases were found to be 6.30 [interquartile range (IQR) 9.82] μIU/ml, 9.18 (IQR 11.61) pg/ml, and 3.22 (IQR 1.90) ng/dl, respectively, which were all significantly higher than the adult patients of our hospital. Also, the adolescent-onset cases showed more large tumor ratio (36.8% vs. 9.3%, p = 0.007) compared to the adult patients. Compared to the patients of all ages in the literature, the biochemical remission rate of SSAs (57.1%) and remission rate of TSS (38.9%) were found to be considerably lower in adolescent-onset patients, while the recurrence rate (44.4%) was found to be considerably higher.

Conclusions: Adolescent-onset TSH-oma patients showed higher TSH and thyroid hormone levels, more large tumors, and worse treatment outcomes than adult cases. Hence, early diagnosis, multidisciplinary therapy, and close follow-up should be highlighted to improve the prognosis.

Keywords: thyrotropin-secreting adenoma, adolescent-onset, somatostatin analogs, transsphenoidal surgery, multidisciplinary therapy

1 INTRODUCTION

Thyrotropin (TSH)-secreting adenoma (TSH-oma) is a type of functional pituitary adenoma, which produces excessive amounts of TSH causing elevated levels of serum thyroid hormone. Also, it has a very rare occurrence and accounts for only 0.5 to 3% of all types of pituitary adenomas (1). The main manifestations of this disease are central hyperthyroidism and pituitary lesions. Most patients present with typical symptoms of hyperthyroidism, and inappropriate secretion of TSH which means elevated thyroid hormones with unsuppressed TSH levels. Further, pituitary macroadenomas usually result in visual field defects and vision loss. As Pit-1 lineage tumors, approximately 16% and 10% of the TSH-oma can co-secrete growth hormones (GH) and prolactin (PRL), respectively (2). Therefore, patients may also exhibit symptoms of gigantism, acromegaly, lactation, oligomenorrhea, etc. The first-line therapy for TSH-oma is transsphenoidal surgery (3). Further, somatostatin analogs can be used effectively to normalize the thyroid hormones, preoperatively (4). Adolescent-onset cases of TSH-oma are rare and have unknown potential differences between underage and adult TSH-oma patients. We presented the clinical features, treatments, and follow-ups of six adolescent-onset TSH-oma patients in our center along with reviewing 14 cases from the literature. Thus, we aimed to summarize the characteristics of adolescent-onset TSH-oma and gather some opinions about its management.

2 METHODS

2.1 Diagnostic and Remission Criteria for TSH-Oma

The diagnosis of TSH-oma was established based on endocrinological and radiological evidence and was as follows: (1) presented with clinical symptoms of hyperthyroidism, (2) high levels of circulating total or free thyroid hormones in the presence of non-suppressed TSH levels and these evidences were repeatable, and (3) Enhanced Magnetic Resonance Imaging (MRI) identified a tumor in the pituitary region (3, 5). According to the maximum diameter of the tumor, the pituitary TSH-oma was classified into microadenomas (<10 mm), macroadenomas (≥10 mm), and large adenomas (≥30 mm).

The remission criteria included cured hyperthyroidism symptoms along with normalized TSH and thyroid hormone levels and resolution of neuroradiological lesions.

2.2 Collection of the Patients

A total of 148 patients were diagnosed with TSH-oma at our hospital between January 2012 and October 2020. Out of these, we retrospectively analyzed six (4.1%) adolescent-onset TSH-oma patients. This study was approved by the Ethics Committee of our hospital. The inclusion criteria were: (1) meeting the diagnosis criteria of TSH-omas; (2) symptom onset before the patient turned 18 years old; and (3) being operated in our center with available medical records. The exclusion criteria were: (1) having undergone total or subtotal thyroidectomy previously; and (2) suffering from other thyroid diseases, such as Grave's disease.

We obtained the patients' data from the electronic medical records system of our hospital. The information included: (1) the demographic features and clinical symptoms; (2) serological tests involving the measurement of the concentrations of the TSH, free tetraiodothyronine (FT4), free triiodothyronine (FT3), thyroxine (T4), triiodothyronine (T3), growth hormone (GH), insulin-like growth factor 1 (IGF-1), prolactin (PRL), adrenocorticotropic hormone (ACTH), cortisol (F), follicle-stimulating hormone (FSH), luteinizing hormone (LH), estradiol (E2), testosterone (T), serum calcium (Ca), serum phosphorus (P), alkaline phosphatase (ALP), 25-hydroxyvitamin D [25(OH)D], parathyroid hormone (PTH), fasting blood glucose (FBG), fasting insulin, total cholesterol (TC), triglyceride (TG), high-density lipoprotein cholesterol (HDL-C), and low-density lipoprotein cholesterol (LDL-C), which were tested using the standard methods at the department of clinical laboratory of our hospital (6); (3) imaging examinations which were as follows: enhanced 3.0T pituitary MRI, somatostatin receptor scintigraphy (^{99}mTc labeled octreotide was administered as intravenous injection, then the whole-body scintigraphy was performed at 1 and 4 h after the administration), and thyroid ultrasound examination (Philips iU22, 8–15 MHz); (4) Octreotide suppression tests, which were performed using the 3-day method (Novartis octreotide was administered as subcutaneous injection with a dose of 0.1 mg q8h for 3 days. The TSH, FT3, and FT4 levels were measured at 0, 2, 4, 6, 8, 12, 24, 48, and 72 h. If the TSH levels decreased more than 50% during the tests, the patient was considered sensitive to octreotide); (5) pathological examinations included the following: H&E and immuno-histochemistry staining for pituitary hormones and transcription factors; and (6) treatments and outcomes. Finally, we enrolled six adolescent-onset and 107 adult-onset TSH-oma patients whose preoperative information was available at our center.

2.3 Literature Review

We conducted a literature search of the PubMed online database until January 1, 2021, and found 411 articles containing the

following keywords: [thyrotropinoma] OR [TSH-secreting adenoma] OR [thyrotropin-secreting adenoma] OR [thyroid-stimulating hormone-secreting adenoma]. The age filters were set as [child: birth-18 years] or [young adults: 19–24 years]. The exclusion criteria were as follows: (1) the age of the patient being older than 18 years at the symptom onset; (2) cases not being reported in English; and (3) no new cases being presented in the literature.

2.4 Statistical Analyses

Clinical data were analyzed using IBM SPSS v.23 (IBM Corporation, NY, USA). Categorical data were compared using a χ^2 or Fisher's exact test. The normality of continuous variables was analyzed by the Shapiro–Wilk test. Normally or non-normally distributed variables were compared using a student t-test or non-parametric Mann–Whitney U test. Data were presented as mean ± SD, or median (IQR). $P < 0.05$ was considered statistically significant.

3 RESULTS

3.1 The Presentation of Six Cases of TSH-Oma

3.1.1 Demographics and Baseline Characteristics

In our study, we enrolled six adolescent-onset patients from our hospital (**Table 1**). The corresponding ages of the patients ranged between 6.8 and 17.0 years at the symptom onset, while the female/male ratio was 2:1. The delay in diagnosis was 76.7 ± 67.3 months on an average (4–180 m). Except for case 3 who was diagnosed as TSH-GH-PRL mixed adenoma, all others were pure TSH-secreting adenomas with hyperthyroid symptoms such as polyphagia, sweating, hand tremor, and goiter. On pituitary MRI, four cases showed macroadenomas, out of which two were invasive (Knosp grade 4). The other two showed microadenomas, with one of them being ectopic and located on the left front of the pituitary stalk (**Figure 1**) (7). No patients were presented with headaches or visual impairments.

During their first visits, all patients were presented with elevated levels of serum FT3, FT4, and non-suppressed TSH levels (**Table 1**). The average value of the TSH, FT3, and FT4 were 6.11 ± 3.99 μIU/ml, 10.02 ± 5.38pg/ml, and 2.94 (1.90) ng/dl, respectively.

In terms of the development, two out of six (33.3%) patients were diagnosed before 10 years of age and had a height of +0.9 SD/+1.89 SD and weight of +0.34 SD/+2.31 SD, which was comparable to the same age and sex. The BMI of the other four cases at diagnosis was 24.5 ± 2.0 kg/m^2 on average. Especially, case 3 was overweight, showed hypogonadism, and had high fasting insulin which could be attributed to the patient's elevated levels of serum GH, IGF-1, and PRL. As for complications, pure TSH-oma cases showed normal glucose, lipids, and bone turnover indexes. Three out of the six (50.0%) cases suffered from arrhythmia, while two out of the six (33.3%) cases had mild valvular disease (**Table 1**).

Four out of the six (66.7%) cases were sensitive to octreotide sensitive suppression tests, with TSH suppression rates ranging between 70.0 and 90.5%. The TSH suppression rates in the two insensitive cases were 44.8 and 27.5%. However, in case 5, whose TSH level decreased 27.5%, the octreotide suppression test was discontinued at the eighth hour due to the high cost of Sandostatin. In the five cases that received somatostatin receptor scintigraphy, three (60.0%) cases showed radioactive concentration in the pituitary region while others showed no radioactive concentration in the pituitary region.

3.1.2 Medical Therapy

To normalize thyroid functions before the operation, all patients underwent medical therapies with somatostatin analogs (SSAs) before surgery. Due to the SSAs treatment, three cases (50.0%) became euthyroid. Another patient also turned euthyroid after using the combination treatment of SSA and bromocriptine. However, even after the SSAs therapy, the thyroid hormones in the two other cases (cases 1 and 6) showed only a decrease and were still abnormal. We used combined thyrozol treatment in the following month for case 1, while interrupted medical therapy in case 6 for a skin rash and endermic induration caused by SSA.

3.1.3 Surgery Therapy and Immunohistochemical (IHC) Staining

Endoscopic transsphenoidal pituitary tumor resection and sellar reconstruction (TSS) were performed at our hospital by an experienced neurosurgery team. The cerebrospinal linkage happened in two cases (case 2: postoperative, secondary to intracranial infection; case 3: intraoperative). Also, two out of six (33.3%) tumors were tough, while four out of six tumors (66.7%) had soft consistencies. The H&E staining was performed in all cases, while IHC staining was performed in five cases (cases 1–5). The H&E staining confirmed that the tumors were adenomas. TSH staining was positive in all the cases except in case 3, which might be due to the inappropriate sampling during the process of pathological sectioning. Only case 4 was stained by Pit-1, which showed a positive result. The Ki-67 index in case 1 was approximately 3%, while it was less than or equals to 1% in all other cases. P53 staining was negative in all cases.

3.1.4 Postoperative Therapy and Follow-Up

After performing the TSS, four cases were in remission during their 1 to 4 years of follow-up (**Table 1**). Case 1, whose macroadenoma was partly removed, relapsed two months after the TSS. Hence, γ-knife radiosurgery was performed, and antithyroid therapy was provided for two years, but the patient's residual tumor enlarged. Then, a second TSS was performed, resulting in temporary euthyroidism and relapse after two months. Next, regular sellar radiotherapy was performed. In case 3, the thyroid hormones were gradually reduced to normal levels after the TSS, but the GH, IGF-1, and PRL concentrations remained elevated. Thus, sellar radiotherapy was performed.

3.2 Literature Review

We found 14 adolescent-onset TSH-oma patients through elaborate retrieval from literature reported between 1964 and

TABLE 1 | Clinical features, examinations, treatments, and outcomes of six adolescent-onset TSH-oma cases at our center.

	Case 1	Case 2	Case 3	Case 4	Case 5	Case 6
Sex	F	F	M	F	M	F
Age at Onset (years)	6.8	8.3	15.0	15.0	17.0	17.0
Age at Diagnosis (years)	7.1	10.3	18.0	23.0	32.0	27.0
Ht (cm)	127.0	152.0	182.0	164.0	175.0	165.0
Wt (kg)	24.0	46.0	86.0	59.0	80.0	65.0
BMI (kg/m^2)	14.9	19.9	26.0	22.0	26.1	23.9
Diagnosis Delay (months)	4	24	36	96	180	120
Symptoms at Onset	Polyphagia, Heat intolerance	Polyphagia, Goiter	Abnormal growth of face, hands, and feet	Sweating, Palpitation	Sweating	Hand tremor, Heat intolerance
Hypopituitarism	No	No	Hypogonadism	No	No	No
Laboratory examination at the diagnosis of TSH-omas						
TSH (μIU/ml)	9.949	2.772	3.423	3.47	12.251	4.815
FT3 (pg/ml)	>20	6.43	9.47	5.28	11.57	7.37
FT4 (ng/dl)	6.249	2.12	3.263	2.04	3.18	2.7
T3 (ng/ml)	>8	2.15	3.429	1.64	3.26	ND
T4 (μg/dl)	>30	11.9	26.6	13.2	13.33	ND
GH (ng/ml)	1.7	0.2	59.1	0.7	<0.5	1.4
IGF-1 (ng/ml)	104	388	773	498	165	456
IGF-1 SDS	−1.58	0.75	3.73	2.92	−0.48	3.67
PRL (ng/ml)	5.27	ND	145.4	16.37	7.2	12.77
TSH suppression rates in OST	70.00%	73.00%	44.80%	88.90%	27.50%	90.50%
Imaging, IHC staining, and other examinations						
Pituitary Tumor Size (mm)	12 × 31 × 13	4.4	23 × 18 × 21	3.5 × 2	11 × 8.6	15 × 17 × 15
Knosp grade	4	0	4	1	2	2
SSTR scintigraphy	Positive	Negative	Positive	Negative	Positive	ND
Thyroid Ultrasound	Increased thyroid blood flow, consistent with hyperthyroidism	multiple cystic nodules with crystals, uneven echo	Thyroid enlargement, diffuse lesions, solid-cystic nodules in right lobe	Uneven echo, diffuse patchy hypoechoic areas	Diffuse lesions, multiple hypoechoic areas	Uneven echo, multiple cyclic nodules
Thyroid Palpation	II° enlargement	III° enlargement	0–I° enlargement	II° enlargement	I° enlargement	II° enlargement
IHC staining	TSH+/GH+/PRL−	TSH+/GH+/PRL−	TSH-/GH+/PRL−	TSH+/GH+ /PRL+	TSH+/GH+ /PRL−	ND
Ki-67 index	3%	<1%	1%	<1%	<1%	ND
Treatments and outcomes						
Preoperative medical therapy	Octreotide, Thyrozol	Octreotide	Octreotide, Bromocriptine	Octreotide	Octreotide	Octreotide
Surgery	Partly TSS	TSS	Partly TSS	TSS	TSS	TSS
Surgery Outcomes	Euthyroid, Relapsed 2 m later	Remission, Intracranial infection, CSF linkage.	No biochemical remission	Remission	Remission	Remission
Subsequent therapy	γknife + thyrozol→ second TSS→ sellar regional RT	Rhinosphenoid sinus repair surgery	RT	Propranolol	No	No
Outcomes	No biochemical remission	Remission	Euthyroid, Elevated GH and PRL levels	Remission	Remission	Remission
Follow-up time (year)	4	2	0.5	1	4	2

OST, Octreotide suppression tests; SSTR scintigraphy, somatostatin receptor scintigraphy; TSS, transsphenoidal surgery; CSF, cerebrospinal fluid; RT, radiotherapy; ND, not detected. Normal ranges: TSH: 0.38–4.34 μIU/ml, FT4: 0.81–1.89 ng/dl, FT3: 1.80–4.10 pg/ml, T3: 0.66–1.92 ng/ml, T4: 4.30–12.50 μg/dl, GH: <2.0 ng/ml, PRL<30 ng/ml.

2016 (**Table 2**). The average disease onset age was 13.5 ± 2.8 years, and the gender ratio was 2:5 (F/M). Of the 14 patients, 11 (18.6%) cases complained about hyperthyroid symptoms such as weight loss, hand tremors, and tachycardia, while six out of the 14 (42.9%) cases were presented with headaches, hemianopsia, or vision changes. Hypopituitarism was exhibited in one case. The mean diagnosis delay was 8.0 (28.0) months (0.75–72 m). Of the 14 patients, 12 (85.7%) cases had macroadenomas, of which six were large adenomas. Additionally, two cases were diagnosed as GH-TSH and GH-PRL-TSH secreting pituitary adenomas. During their first visits, the average concentrations of TSH, FT3, and FT4 were found to be 10.51 ± 7.45 μIU/ml, 9.18

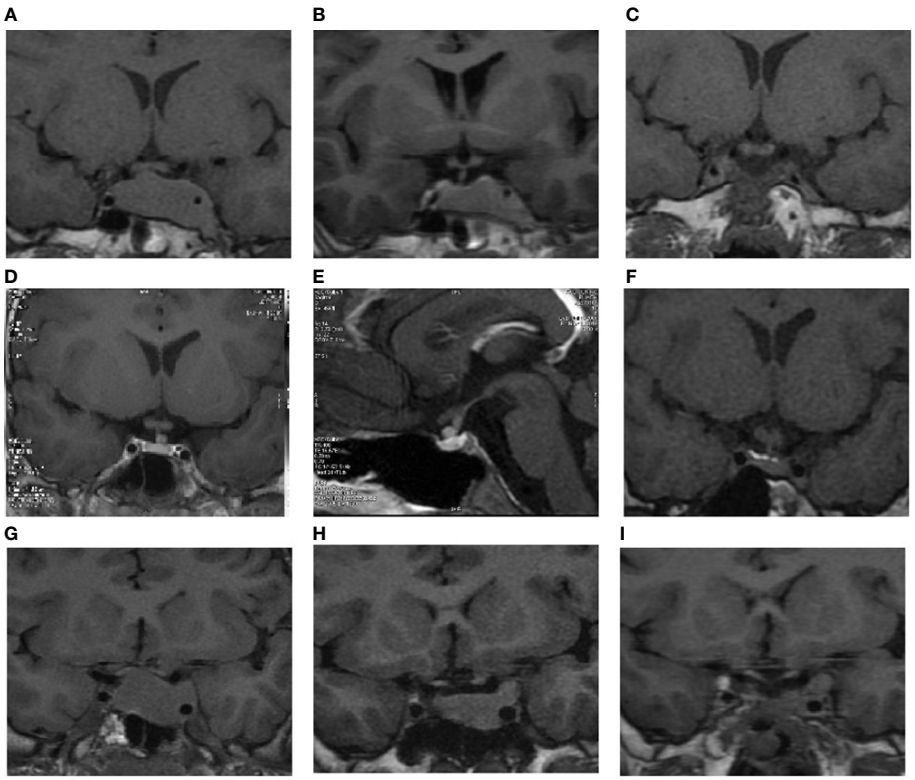

FIGURE 1 | The pituitary MRI imaging of cases 1, 2, and 3. **(A)** Coronal imaging of case 1 during the first visit. **(B)** Coronal imaging of case 1 after long-term SSA therapy. **(C)** Coronal imaging of case 1 during the last follow-up. **(D)** An ectopic pituitary stalk tumor in case 2 during the first visit. **(E)** Sagittal pituitary imaging of case 2 during the first visit. **(F)** Coronal pituitary imaging of case 2 during the last follow-up. **(G)** Coronal imaging of case 3 during the first visit. **(H)** Coronal imaging of case 3 after long-term SSA therapy. **(I)** Coronal imaging of case 3 at the last follow-up.

(81.91) pg/ml, and 3.40 (2.67) ng/dl, respectively. No significant differences were observed in the baseline hormone levels, and tumor sizes between adolescent-onset cases enrolled in our center and cases reviewed (**Table 3**).

In the treatment aspect, eight out of the 14 (57.1%) patients received preoperative medication therapies. However, except for one patient who was treated with lanreotide (40 mg, q2w), all other antithyroid preoperative preparations failed because of much higher TSH levels, emerging tumor compression symptoms, tumor enlargement or goiter progression. All patients received surgery therapy, but only three patients attained long-term remission. Of the 14 patients, two died postoperatively, while nine showed no remission or relapses. Then they received repeated surgeries, SSAs, RTs, and (or) antithyroid therapies. Four patients were still hyperthyroid during their last follow-up, including one who attained remission but relapsed after the SSA interruption.

3.3 Comparison Between Adolescent-Onset and Adult Cases

Compared to the 107 adult TSH-oma patients admitted to our hospital, the adolescent cases (n = 20) showed significantly higher baseline levels of TSH, FT3, FT4, T3, and T4 than that of the adult patients ($p = 0.012$, $p = 0.000$, $p = 0.007$, $p = 0.001$, and $p = 0.026$), whose values were 6.30 (9.82) μIU/ml, 9.18 (11.61) pg/ml, 3.22 (1.90) ng/dl, 3.34 (4.10) ng/ml, and 23.74 ± 13.21 μg/dl, respectively. Also, the large tumor ratio was higher compared to that of the adult cases (36.8% vs. 9.3%, $p = 0.007$) (**Table 3**). No significant differences were observed in the gender ratio, diagnosis delay, and heart complication incidences between adolescent-onset and adult patients in our hospital (gender: $p = 0.144$, diagnosis delay: $p = 0.570$, arrhythmia incidence: $p = 0.486$, valvular disease incidence: $p = 0.350$) (**Table 4**).

4 DISCUSSION

TSH-oma is extremely rare, especially in adolescent cases. Herein, we described six cases in our center and 14 cases retrieved from literature to summarize the characteristics of clinical manifestations and therapeutic outcomes in adolescent-onset TSH-oma patients. Of the 20 cases, 16 (80.0%) showed macroadenomas and four (20.0%) showed microadenomas, which was consistent with the overall 70–90% macroadenomas ratio summarized before (1). However, adolescent-onset patients may have more large pituitary tumors than adult patients (36.8% vs 9.3%) along with significantly higher baseline TSH, FT3, FT4,

TABLE 2 | Basic characteristics and treatment outcomes of 14 retrieved cases.

Cases	Onset Age/ Sex	Symptoms	Diagnosis delay (m)	TSH/FT3/ FT4/T3/T4	Tumor size (mm)	Hypopituitarism	Treatments	Pre-op MEDs	First Surgery Outcomes	Ki-67 index	Outcomes	Follow-up time (m)
7 (8)	8/M	Emaciation, Muscle weakness	2	13.17/113/ 3.8/NA/NA	Macro	No	TSS→LT4	No	Remission	NA	Remission	11
8 (9)	11/F	Headache, hemianopsia	24–36	NA	Large	NA	PTU→Craniotomy→death	III	NA	NA	Death	NA
9 (10)	11/F	Headache, Polyuria, Polydipsia, Diplopia, Hemianopia	8	NA	Large (48 × 62 × 58)	NA	craniotomy→RT→carbimazole	No	No remission	NA	No remission	20
10 (11)	11/M	Autoimmune polyglandular syndrome, Tachycardia	NA	16.8/18.12/ 3.52/NA/NA	Large (26 × 32)	No	TSS→RT→GH/LT4	No	Remission for 3 months	NA	Remission	72
11 (12)	12/F	Goiter, Sinus tachycardia, Tremors	18	21.11/9.25/ 2.21/NA/NA	Micro (6 × 5)	No	Thyrozol→TSS	III	Remission	NA	Remission	14
12 (13)	13/F	Poor weight gain, Pubertal delay	72	3.0/NA/NA/ 5.29/15.93	Micro (9)	NA	PTU→thyroidectomy→LT4→TSS→LT4	II	Remission	NA	Remission	24
13 (14)	13/M	School performance deterioration, Secondary enuresis	Several	9.8/NA/7.7/ 6/>24	Macro (20 × 15)	GH/ADH	PTU+SSA→TSS	III	NA	NA	Death	NA
14 (15)	13/M	Increased height velocity, Weight loss, Polyphagia, Visual impairment	6	3.54/6.75/ 1.94/2.48/ NA	Large (40 × 45)	NA	MMI→TSS*3→SSA→SSA+RT	NA	Remission for 2 months	11%	Hypothyroidism	7
15 (16)	15/M	Weight loss, Irritability, Difficulty sleeping, Headache	0.75	24.8/154.08/ 31/27.25/ 54.2	Large (30 × 30 × 30)	NA	PTU→TSS→RT	III	Remission for 1.5 months	NA	No remission	1.5
16 (17)	15/M	Headache, Weight loss	36	6.49/NA/NA/ 3.16/24.6	NA	No	craniotomy→PTU→SSA (in the plan)	No	No remission	NA	No remission	3
17 (18)	16/M	Mild thyrotoxicosis, Intermittent dizziness	8	1.8/8.31/ 3.28/NA/NA	Macro	No	TSS→BCT + Pergolide→SSA	No	Remission for 1 months	NA	No remission	5
18 (19)	16/M	Goiter, Hypertension	NA	13.6/NA/ 4.35/NA/NA	Macro (17 × 15)	No	MMI→TSS→MMI→SSA	III	Remission for 1 months	5–10%	Remission	48
19 (20)	17/M	Paroxysmal headache, Blurred vision, Palpitation, Hand tremor, Sweating	4	5.934/7.06/ 2.97/NA/NA	Large (44 × 39)	NA	SSA→TSS→γ knife RT	I	Remission for 4 months	<1%	Remission	24
20 (21)	18/M	NA	NA	6.1/9.11/ 2.62/NA/NA	Macro (22)	NA	TSS→SSA→TSS	NA	Remission for 5 years	NA	Remission	84

TSH, μIU/ml; FT3, pg/ml; FT4, ng/dl; T3, ng/ml, T4, μg/dl.

The outcomes of preoperatively medical therapy (pre-op MEDs) were classified into 3 grades: I: TSH and thyroid hormones normalized, no symptom or tumor size worsened; II: TSH and thyroid hormones decreased but still abnormal, no symptom or tumor size worsened; III: TSH or thyroid hormones levels rose, symptoms worsen, or tumor enlarged.

Na, not available; TSS, transsphenoidal surgery; LT4, levothyroxine; SSA, somatostatin analogs; PTU, propylthiouracil; MMI, methimazole; RT, radiotherapy; BCT, bromocriptine; ADH, antidiuretic hormone.

TABLE 3 | The comparison between adolescent-onset cases at our center and reviewed cases from literature along with the comparison between adolescent-onset cases and adult cases.

	Adolescent cases in our center (n = 6)	Adolescent cases reviewed (n = 14)	P-values	Adolescent-onset cases (n = 20)	Adult cases (n = 107)	P-values
Age	13.2 ± 4.5	13.5 ± 2.8	0.848	13.4 ± 3.3	38.8 ± 11.7	0.000**
Diagnosis delay	76.7 ± 67.3	8.0 (28.0)	0.050	21.0 (58.5)	24.0 (66.0)	0.570
TSH	6.11 ± 3.99	10.51 ± 7.45	0.199	6.30 (9.82)	4.39 (3.19)	0.012*
FT3	10.02 ± 5.38	9.18 (81.91)	0.439	9.18 (11.61)	5.84 (3.51)	0.000**
FT4	2.94 (1.90)	3.40 (2.67)	0.329	3.22 (1.90)	2.25 (1.13)	0.007**
T3	3.70 ± 2.52	5.29 (13.81)	0.347	3.34 (4.10)	2.01 (1.08)	0.001**
T4	19.01 ± 8.59	29.68 ± 16.82	0.253	23.74 ± 13.21	13.91 (5.27)	0.026*
Tumor max diameters (mm)	14.98 ± 10.81	28.70 ± 17.58	0.109	23.56 ± 16.48	18.07 ± 10.40	0.216

TSH, μlU/ml; FT3, pg/ml; FT4, ng/dl; T3, ng/ml; T4, μg/dl.
*$p < 0.05$, **$p < 0.01$.*

T3, and T4 levels (**Table 3**). Both of these observations contribute to the therapeutic challenges seen in adolescent-onset patients. In the case of complications, five pure TSH-oma cases in our center showed normal height growth and puberty development and also the lipid level and bone turnover indexes. Arrhythmia and valvular diseases were seen in more than 30% of the TSH-oma cases at our center. Recently, a meta-analysis revealed that atrial fibrillation or heart failure happened in 11.1% of 535 adult TSH-oma cases (22). Another research found that TSH-oma can significantly induce left atrial enlargement and subclinical atrial fibrillation since excess thyroid hormones can increase the arrhythmogenic activity of the pulmonary veins, and increase the hemodynamic load (23). Thus, the potential cardiovascular complications caused by the TSH-oma may be more common than reported and should be taken seriously.

SSAs can normalize thyroid functions without increasing the TSH levels, and reduce the operative difficulties. Thus, it is generally applied when the tumor is large or invasive. Compared to the 90% (24) or 73–100% (1) remission rates reported in all age patients, the effectiveness of SSAs can be considered worse in adolescent patients considering that only four out of seven (57.1%) patients achieved biochemical remission. For intractable cases, combination medical therapy such as SSAs combined with dopamine analogs and (or) antithyroid drugs may work well. There is a need to be cautious while using antithyroid drugs alone preoperatively because it may increase TSH levels through feedback regulation (19).

SSAs bind with high affinity to SSTR2 and lower affinity to SSTR3 and SSTR5, making *in vivo* effects by activating these specific SSTR subtypes (25). It is suggested that SSAs may inhibit TSH secretion in all TSH-omas that express SSTR2 while the coexistence of SSTR5 can enhance the effectiveness of SSAs (26, 27). Thus, the difference in the expression levels of SSTR5 and SSTR2 in TSH-omas may explain or even predict the different outcomes of treatment with SSAs. However, since SSTR staining has not yet been deployed in our center, the data on its expression remain unavailable in our cases.

TSS is the first-line therapy for TSH-omas. In the 20 cases, seven out of 18 (38.9%) were in remission, three out of 18 (16.7%) didn't relieve, while eight out of 18 (44.4%) relapsed. Two cases died from postoperative infection, probably due to failed primary therapies and limited surgical techniques used. The recurrences in adolescent-onset patients are more frequent than the overall 0–21.4% recurrence rates observed (28–31). Similarly, the cavernous sinus invasion and larger tumor size are related to the tendency of recurrence (28). Only three out of 14 (21.4%) macroadenoma patients attained remission after one TSS, while the remission rate in microadenoma patients was 100%. For relapsed cases, repeat surgeries, radiotherapies, and (or) SSAs were applied. Overall, relatively high occurrence rates highlight the importance of having multidisciplinary therapy and close follow-up in adolescent patients.

TABLE 4 | The comparison of gender ratio, baseline tumor types, and complications between adolescent-onset and adult cases.

		Adolescent-onset cases		Adult cases in our center		χ2	P
		number	%	Number	%		
Sex	M	12	60.0%	44	41.1%	2.436	0.144
	F	8	40.0%	63	58.9%		
Tumor type	Large	7	36.8%	10	9.3%	9.086	0.007**
	Macro	8	42.1%	74	69.2%		
	Micro	4	21.1%	23	21.5%		
Arrhythmia	Yes	3	50.0%	26	40.6%	/	0.486
	No	3	50.0%	38	59.4%		
Value diseases	Yes	2	33.3%	35	50.7%	/	0.350
	No	4	66.7%	34	49.3%		

**$p < 0.01$.*

The results of IHC showed that a special case diagnosed as TSH-GH-PRL mixed adenoma was found to be negative for TSH staining. However, the normalization of his thyroid functions after TSS suggested correct clinical diagnosis, so the negative pathological result may be due to inappropriate tissue sampling. Also, the positive staining of GH and (or) PRL in pure TSH-oma patients was actually understandable because positive IHC staining did not necessarily mean the hypersecretion of hormones, such as silent pituitary adenoma (4). Ki-67 index of case 1 was approximately 3% with the tumor invading into the cavernous sinus and surrounding the left internal carotid. According to recent studies, Ki-67 is a cell proliferation-associated antigen. A higher Ki-67 index usually means more aggressive tumor behavior and more recurrence risk with 2.5–3% cut-off points for pituitary adenomas (32–35). The treatment for TSH-oma in the case of higher Ki-67 index was also more challenging, for example, in one case where the Ki-67 index was 11%, three TSSs had to be performed along with providing SSAs and RTs. However, whether the Ki-67 index is generally higher in adolescent patients or not is still unknown. Meanwhile, it is necessary to understand the genetic background of TSH-oma tumorigenesis in early-onset patients. Current research has found a very uncommon germ-line MEN1 and AIP mutation in familial cases (4) and some somatic mutations and copy number changes in sporadic cases (36). But no oncogenes or proto-oncogene mutations have been identified (4). However, these findings are very limited in clarifying the molecular mechanisms of TSH-oma and need further studies. Additionally, our study has some limitations. As a retrospective study, some data are missing causing a loss of information about the follow-up. The postoperative heart functions, thyroid ultrasonographic manifestations, and glucolipid metabolisms have not been followed up adequately. Also, some studies were published long ago; hence, the diagnosis and treatments may be non-standard. Moreover, the indiscoverable pituitary microadenomas may cause misdiagnosis of TSH-oma along with a statistical bias.

Conclusion

In conclusion, adolescent-onset TSH-oma patients have higher baseline TSH and thyroid hormone levels, more large tumors, lower biochemical remission rates of SSAs, lower surgery remission rates, and higher postoperative recurrence rates than seen in the adult cases. Whether in primary therapies or postoperative management, more difficulties are faced in treating adolescent-onset patients, especially those with macroadenomas. Hence, early identification, preoperative SSA application, multidisciplinary therapy, and close follow-up can improve patients' prognoses and should be highlighted.

DATA AVAILABILITY STATEMENT

The raw data supporting the conclusions of this article will be made available by the authors, without undue reservation.

ETHICS STATEMENT

The studies involving human participants were reviewed and approved by the Ethics Committee of Peking Union Medical College Hospital. Written informed consent from the participants' legal guardian/next of kin was not required to participate in this study in accordance with the national legislation and the institutional requirements.

AUTHOR CONTRIBUTIONS

YMY wrote the manuscript and prepared figures and tables. YMY and JL collected the data. KD, LL, HJZ, XLL, XJB, LD, and YY diagnosed and provided treatments for the cases involved in this study. HJZ, LD, and YY designed the study and provided suggestions for the manuscript writing. All authors contributed to the article and approved the submitted version.

FUNDING

This work was supported by the Chinese Academy of Medical Sciences Innovation Fund for Medical Science (CAMS-2016-I2M-1-002).

REFERENCES

1. Amlashi FG, Tritos NA. Thyrotropin-Secreting Pituitary Adenomas: Epidemiology, Diagnosis, and Management. *Endocrine* (2016) 52(3):427–40. doi: 10.1007/s12020-016-0863-3
2. Beck-Peccoz P, Persani L, Mannavola D, Campi I. Pituitary Tumours: TSH-Secreting Adenomas. *Best Pract Res Clin Endocrinol Metab* (2009) 23(5):597–606. doi: 10.1016/j.beem.2009.05.006
3. Beck-Peccoz P, Lania A, Beckers A, Chatterjee K, Wemeau JL. 2013 European Thyroid Association Guidelines for the Diagnosis and Treatment of Thyrotropin-Secreting Pituitary Tumors. *Eur Thyroid J* (2013) 2(2):76–82. doi: 10.1159/000351007
4. Beck-Peccoz P, Giavoli C, Lania A. A 2019 Update on TSH-Secreting Pituitary Adenomas. *J Endocrinol Invest* (2019) 42(12):1401–6. doi: 10.1007/s40618-019-01066-x
5. Luo P, Zhang L, Yang L, An Z, Tan H. Progress in the Pathogenesis, Diagnosis, and Treatment of TSH-Secreting Pituitary Neuroendocrine Tumor. *Front Endocrinol (Lausanne)* (2020) 11:580264. doi: 10.3389/fendo.2020.580264
6. Wang L, Liu M, Ning D, Zhu H, Shan G, Wang D, et al. Low Serum ZAG Levels Correlate With Determinants of the Metabolic Syndrome in Chinese Subjects. *Front Endocrinol (Lausanne)* (2020) 11:154. doi: 10.3389/fendo.2020.00154
7. Li X, Zhao B, Hou B, Zhu J, Yao Y, Lian X. Case Report and Literature Review: Ectopic Thyrotropin-Secreting Pituitary Adenoma in the Suprasellar Region. *Front Endocrinol (Lausanne)* (2021) 12:619161. doi: 10.3389/fendo.2021.619161
8. Nakayama Y, Jinguji S, Kumakura S, Nagasaki K, Natsumeda M, Yoneoka Y, et al. Thyroid-Stimulating Hormone (Thyrotropin)-Secretion Pituitary

Adenoma in an 8-Year-Old Boy: Case Report. *Pituitary* (2012) 15(1):110–5. doi: 10.1007/s11102-010-0275-y
9. Nyhan WL, Green M. Hyperthyroidism in a Patient With a Pituitary Adenoma. *J Pediatr* (1964) 65:583–9. doi: 10.1016/s0022-3476(64)80292-4
10. Avramides A, Karapiperis A, Triantafyllidou E, Vayas S, Moshidou A, Vyzantiadis A. TSH-Secreting Pituitary Macroadenoma in an 11 -Year-Old Girl. *Acta Paediatr* (1992) 81(12):1058–60. doi: 10.1111/j.1651-2227.1992.tb12177.x
11. Mazerkina N, Trunin Y, Gorelyshev S, Golanov A, Kadashev B, Shishkina L, et al. Thyrotropin-Secreting Pituitary Adenoma in an 11-Year-Old Boy With Type 1 Autoimmune Polyglandular Syndrome. *J Pediatr Endocrinol Metab* (2016) 29(2):237–40. doi: 10.1515/jpem-2015-0018
12. Teng X, Jin T, Brent GA, Wu A, Teng W, Shan Z. A Patient With a Thyrotropin-Secreting Microadenoma and Resistance to Thyroid Hormone (P453T). *J Clin Endocrinol Metab* (2015) 100(7):2511–4. doi: 10.1210/jc.2014-3994
13. Korn EA, Gaich G, Brines M, Carpenter TO. Thyrotropin-Secreting Adenoma in an Adolescent Girl Without Increased Serum Thyrotropin-Alpha. *Horm Res* (1994) 42(3):120–3. doi: 10.1159/000184177
14. Phillip M, Hershkovitz E, Kornmehl P, Cohen A, Leiberman E. Thyrotropin Secreting Pituitary Adenoma Associated With Hypopituitarism and Diabetes Insipidus in an Adolescent Boy. *J Pediatr Endocrinol Metab* (1995) 8(1):47–50. doi: 10.1515/jpem.1995.8.1.47
15. Pereira BD, Raimundo L, Mete O, Oliveira A, Portugal J, Asa SL. Monomorphous Plurihormonal Pituitary Adenoma of Pit-1 Lineage in a Giant Adolescent With Central Hyperthyroidism. *Endocr Pathol* (2016) 27 (1):25–33. doi: 10.1007/s12022-015-9395-2
16. Stanley JM, Najjar SS. Hyperthyroidism Secondary to a TSH-Secreting Pituitary Adenoma in a 15-Year-Old Male. *Clin Pediatr (Phila)* (1991) 30 (2):109–11. doi: 10.1177/000992289103000212
17. Page KA, Roehmholdt BF, Jablonski M, Mayerson AB. Development of Thyroid Storm After Surgical Resection of a Thyrotropin-Secreting Pituitary Adenoma. *Endocr Pract* (2008) 14(6):732–7. doi: 10.4158/ep.14.6.732
18. Polak M, Bertherat J, Li JY, Kujas M, Le Dafniet M, Weizani H, et al. A Human TSH-Secreting Adenoma: Endocrine, Biochemical and Morphological Studies. Evidence of Somatostatin Receptors by Using Quantitative Autoradiography. Clinical and Biological Improvement by SMS 201-995 Treatment. *Acta Endocrinol (Copenh)* (1991) 124(4):479–86. doi: 10.1530/acta.0.1240479
19. Kessler M, David R, Pawelczak M, Hanono A, Shah B. Thyrotropin-Secreting Pituitary Adenoma in an Adolescent Boy: Challenges in Management. *Pediatrics* (2010) 126(2):e474–8. doi: 10.1542/peds.2009-2354
20. Zhao W, Ye H, Li Y, Zhou L, Lu B, Zhang S, et al. Thyrotropin-Secreting Pituitary Adenomas: Diagnosis and Management of Patients From One Chinese Center. *Wiener klinische Wochenschrift* (2012) 124(19-20):678–84. doi: 10.1007/s00508-012-0216-z
21. Beckers A, Abs R, Mahler C, Vandalem JL, Pirens G, Hennen G, et al. Thyrotropin-Secreting Pituitary Adenomas: Report of Seven Cases. *J Clin Endocrinol Metab* (1991) 72(2):477–83. doi: 10.1210/jcem-72-2-477
22. De Herdt C, Philipse E, De Block C. Endocrine Tumours: Thyrotropin-Secreting Pituitary Adenoma: A Structured Review of 535 Adult Cases. *Eur J Endocrinol* (2021) 185(2):R65–74. doi: 10.1530/EJE-21-0162
23. Yoshiki K, Sasagawa Y, Shimojima M, Takeshita Y, Takata S, Hayashi Y, et al. Thyrotropin-Secreting Pituitary Adenomas Induce Left Atrial Enlargement With Subclinical Atrial Fibrillation: An Echocardiographic Study. *Pituitary* (2021) 24(5):778–86. doi: 10.1007/s11102-021-01154-3
24. Molitch ME. Diagnosis and Treatment of Pituitary Adenomas: A Review. *JAMA* (2017) 317(5):516–24. doi: 10.1001/jama.2016.19699
25. Gatto F, Barbieri F, Castelletti L, Arvigo M, Pattarozzi A, Annunziata F, et al. *In Vivo* and *In Vitro* Response to Octreotide LAR in a TSH-Secreting Adenoma: Characterization of Somatostatin Receptor Expression and Role of Subtype 5. *Pituitary* (2011) 14(2):141–7. doi: 10.1007/s11102-010-0271-2
26. Yoshihara A, Isozaki O, Hizuka N, Nozoe Y, Harada C, Ono M, et al. Expression of Type 5 Somatostatin Receptor in TSH-Secreting Pituitary Adenomas: A Possible Marker for Predicting Long-Term Response to Octreotide Therapy. *Endocr J* (2007) 54(1):133–8. doi: 10.1507/endocrj.k06-133
27. Sharif N, Gendron L, Wowchuk J, Sarret P, Mazella J, Beaudet A, et al. Coexpression of Somatostatin Receptor Subtype 5 Affects Internalization and Trafficking of Somatostatin Receptor Subtype 2. *Endocrinology* (2007) 148 (5):2095–105. doi: 10.1210/en.2006-1266
28. Yamada S, Fukuhara N, Horiguchi K, Yamaguchi-Okada M, Nishioka H, Takeshita A, et al. Clinicopathological Characteristics and Therapeutic Outcomes in Thyrotropin-Secreting Pituitary Adenomas: A Single-Center Study of 90 Cases. *J Neurosurg* (2014) 121(6):1462–73. doi: 10.3171/2014.7.Jns1471
29. Mortini P, Barzaghi LR, Albano L, Panni P, Losa M. Microsurgical Therapy of Pituitary Adenomas. *Endocrine* (2018) 59(1):72–81. doi: 10.1007/s12020-017-1458-3
30. Malchiodi E, Profka E, Ferrante E, Sala E, Verrua E, Campi I, et al. Thyrotropin-Secreting Pituitary Adenomas: Outcome of Pituitary Surgery and Irradiation. *J Clin Endocrinol Metab* (2014) 99(6):2069–76. doi: 10.1210/jc.2013-4376
31. Van Varsseveld NC, Bisschop PH, Biermasz NR, Pereira AM, Fliers E, Drent ML. A Long-Term Follow-Up Study of Eighteen Patients With Thyrotrophin-Secreting Pituitary Adenomas. *Clin Endocrinol (Oxf)* (2014) 80(3):395–402. doi: 10.1111/cen.12290
32. Ng HY, Namboodiri D, Learoyd D, Davidson A, Champion B, Preda V. Clinical Challenges of a Co-Secreting TSH/GH Pituitary Adenoma. *Endocrinol Diabetes Metab Case Rep* (2019) 1–6. doi: 10.1530/edm-19-0068
33. Nishioka H, Inoshita N. New WHO Classification of Pituitary Adenomas (4th Edition): Assessment of Pituitary Transcription Factors and the Prognostic Histological Factors. *Brain Tumor Pathol* (2018) 35(2):57–61. doi: 10.1007/s10014-017-0307-7
34. Hasanov R, Aydogan BI, Kiremitci S, Erden E, Gullu S. The Prognostic Roles of the Ki-67 Proliferation Index, P53 Expression, Mitotic Index, and Radiological Tumor Invasion in Pituitary Adenomas. *Endocr Pathol* (2019) 30(1):49–55. doi: 10.1007/s12022-018-9563-2
35. Di Ieva A, Rotondo F, Syro LV, Cusimano MD, Kovacs K. Aggressive Pituitary Adenomas–Diagnosis and Emerging Treatments. *Nat Rev Endocrinol* (2014) 10(7):423–35. doi: 10.1038/nrendo.2014.64
36. Sapkota S, Horiguchi K, Tosaka M, Yamada S, Yamada M. Whole-Exome Sequencing Study of Thyrotropin-Secreting Pituitary Adenomas. *J Clin Endocrinol Metab* (2017) 102(2):566–75. doi: 10.1210/jc.2016-2261

Conflict of Interest: The authors declare that the research was conducted in the absence of any commercial or financial relationships that could be construed as a potential conflict of interest.

frontiers in Endocrinology

ORIGINAL RESEARCH
published: 28 February 2022
doi: 10.3389/fendo.2022.800135

Analysis of the Clinical Characteristics and Pituitary Function of Patients in Central China With Rathke's Cleft Cysts

*Lixia Zhang, Xueyuan Li, Chong Li, Zhifang Wang, Lili Zheng, Guijun Qin, Shoujun Wang and Lijun Xu**

Department of Endocrinology, The First Affiliated Hospital of Zhengzhou University, Zhengzhou, China

Objective: A Rathke's cleft cyst (RCC) is a common, benign, cystic disease that often leads to hypophyseal dysfunction or head symptoms. The relationship between RCCs and pituitary gland function is not clear. We therefore carried out a study to examine this relationship in greater detail.

Methods: The study was a retrospective, cohort design in patients diagnosed with a RCC between January 2019 to July 2021 at the First Affiliated Hospital of Zhengzhou University, China.

Results: A total of 221 patients were enrolled and then divided into study cohorts according to the diameter of the RCC, clinical manifestations, and surgical treatment received. The majority of patients were symptomatic (143/221), including 83 cases of dizziness and headache, 9 of vision loss and visual field defect, and 2 of diabetes insipidus. 52 cases had abnormal pituitary function, with 8 cases interestingly showing high adrenocorticotropic-hormone (ACTH) and cortisone levels, while 8 juvenile cases had developed central precocious puberty. Patients with larger RCCs were more likely to present with headaches and dizziness, with subjects who suffered from these symptoms having high ACTH and cortisone levels.

Conclusion: Although the size of a RCC is not an important factor influencing hypopituitary function, we consider that endocrine evaluation should be carried out in all patients with a RCC.

Keywords: Rathke's cleft cyst, hypopituitarism, pituitary tumor, central precocious puberty (CPP), central of China

OPEN ACCESS

Edited by:
Congxin Dai,
Capital Medical University, China

Reviewed by:
Changxiang Yan,
Capital Medical University, China
Nidan Qiao,
Fudan University, China

****Correspondence:***
Lijun Xu
107797673@qq.com

Specialty section:
This article was submitted to Pituitary Endocrinology, a section of the journal Frontiers in Endocrinology

Received: *22 October 2021*
Accepted: *18 January 2022*
Published: *28 February 2022*

Citation:
Zhang L, Li X, Li C, Wang Z, Zheng L, Qin G, Wang S and Xu L (2022) Analysis of the Clinical Characteristics and Pituitary Function of Patients in Central China With Rathke's Cleft Cysts. Front. Endocrinol. 13:800135. doi: 10.3389/fendo.2022.800135

INTRODUCTION

A Rathke's cleft cyst (RCC) is a common, benign, cystic lesion that originates from the remnant tissue of a Rathke's cyst (1). Different autopsy studies have shown the prevalence of RCCs ranges from 13% to 22%. The cysts are often located in the saddle or upon the saddle. Most patients have no clinical manifestations, with symptomatic Rathke's cysts being relatively uncommon (2). Medical management of RCCs has not yet been standardized (3), although it is generally accepted that

clinical and radiological monitoring is sufficient for cases of incidental asymptomatic RCCs. However, it is possible that RCC-related pituitary dysfunction and other manifestations, such as headaches and visual disturbances may be underestimated by this approach (4). Because of the benign features of RCC, there have only been a small number of clinical studies on pituitary function in patients with RCC in China, with pituitary dysfunction often ignored in diagnosis and treatment. To further assess pituitary function in patients with RCC, we performed a cross-sectional, retrospective study of patients with RCCs, diagnosed by magnetic resonance imaging (MRI) or histology following surgery.

PATIENTS AND METHODS

Patients

According to the guidelines of the ZhengZhou University Medical Ethical Committee, the data of patients diagnosed with a RCC who were admitted to the First Affiliated Hospital of Zhengzhou University from January 2019 to July 2021 were collected to establish a retrospective observational cohort study. Study eligibility criteria included a radiologically defined RCC and assessment of pituitary function. A total of 221 patients were enrolled in the study including 22 patients who underwent surgery and had a pathological diagnosis and 199 patients with a presumed diagnosis following an MRI. Basic information of the patient's gender, age, chief complaint, symptoms and signs were collected. Data on the function of endocrine glands were collected, including thyroid function free serum thyroxine (FT4), free triiodothyronine (FT3), thyroid stimulating hormone (TSH), serum ACTH and cortisone (at 8am and 0am), serum gonadotropin [luteinizing hormone (LH) and follicle-stimulating hormone (FSH)], prolactin (PRL), growth hormone (GH) and insulin-like growth factor-1 (IGF-1). Information on MRI imaging suprasellar area and pathological diagnosis was also recorded.

Data Analysis

RCC-related clinical manifestations were determined according to the patient's medical history and included headache, dizziness, decreased vision, visual field defects, sexual dysfunction, and diabetes insipidus. Pituitary dysfunction was diagnosed based on laboratory results and clinical signs and symptoms (The diagnostic criteria are detailed in **Appendix 1**) and defined as either hypoadrenalism(secondary), hypothyroidism(secondary), growth hormone deficiency, hypogonadotropic hypogonadism, precocious puberty, delayed puberty, or asymptomatic. For analysis, the data was grouped according to clinical manifestations, pituitary function, treatment methods, and the diameter of the RCC.

Statistical Analysis

SPSS16 software was used for the statistical analyses. Numeric variables were expressed as mean ± standard deviation (SD) and qualitative variables as numbers and percentages (%). The non-parametric Kruskal Wallis test or the Pearson 2 test were used to compare categorical variables. P values < 0.05 were considered statistically significant.

RESULTS

General Characteristics

A total of 221 patients with a mean age of 40.31 ± 18.58 years (range, 5 - 82 years), were enrolled in the study. Of the 221 patients, 117 (52.94%) were aged 30-50 years and 32 were younger than 18 years old. There were 107 males (aged 41.01 ± 19.79 years) and 114 females (aged 39.63 ± 17.42 years) in the study cohort. There was no significant difference in age between the male and female patients (t=0.561, p=0.575). 22 cases underwent surgery and were diagnosed pathologically, while the remaining 199 cases who received conservative treatment were diagnosed by a MRI of the sellar area. The ages of patients who accepted surgery or conservative treatment were 37.59 ± 19.29 years and 40.61 ± 18.52 years, respectively. The difference in age between the two groups was not statistically significant. A similar number of males and females underwent surgery (n=11 for each gender).

Clinical Manifestations

143 patients were symptomatic, including 83 cases who suffered from dizziness and headache, 9 cases who suffered vision loss or visual field defection, and 2 patients with diabetes insipidus. 52 patients showed symptoms due to abnormal pituitary function including afraid of the cold, poor appetite, loss of libido or gonadal growth retardation, early puberty development, and slow height growth. The remaining 78 cases were asymptomatic. When grouped according to clinical symptoms, the patients with headache and dizziness had larger cysts, with a mean diameter of 15.05 ± 5.92 mm, whereas patients without headache or dizziness had significant smaller cysts with a mean diameter of 0.30 ± 6.98 mm (p = 0.001).

Evaluation and Analysis of Endocrine Function

A total of 52 patients had hypopituitarism, including 23 cases of central hypothyroidism, 10 of hypogonadotropic hypogonadism, 5 of hypoadrenalism, 21 of growth hormone deficiency (14 partial deficiency and 7 complete deficiency), and 8 of increased ACTH level. As shown in **Table 1**, serum cortisone levels at 8am were highest in patients without hypopituitarism, while there was no significant difference in either the size of the cyst or age of the patient between cases with or without hypopituitarism.

Imaging Examination

All patients underwent a pituitary MRI examination, with the presumptive diagnosis of RCC made by at least two doctors (**Figure 1**). In 154 cases, the largest diameter of the cysts was <10 mm (mean 5.50 ± 2.42 mm), and in 67 cases the diameter of the cysts was ≥10 mm (mean 16.35 ± 5.20 mm). The patients were divided into two groups according to the diameter of the

TABLE 1 | Comparison of endocrine function indices between patients with or without hypopituitarism.

	Hypopituitarism n=52	Without Hypopituitarism n=169	*P*
Age (yr)	39.48 ± 20.1	40.57 ± 18.14	0.713
Diameter of RCC (mm)	12.41 ± 8.18	13.19 ± 6.25	0.620
FT3 (pmol/L)	4.96 ± 2.66	4.91 ± 1.33	0.843
FT4 (pmol/L)	11.32 ± 8.63	12.14 ± 4.33	0.363
TSH (μiu/mL)	2.2 ± 1.64	3.33 ± 11.88	0.496
IGF-1 (ng/mL)	181.54 ± 95.66	194.74 ± 96.14	0.514
GH (ng/mL)	0.68 ± 1.74	1.26 ± 4.57	0.497
FSH (mIU/mL)	9.47 ± 15.75	12.16 ± 17.09	0.254
LH (mIU/mL)	5.64 ± 7.85	9.11 ± 10.74	0.045*
PRL (ng/mL)	25.58 ± 24.52	25.09 ± 30.52	0.922
ACTH 0am (pg/mL)	9.36 ± 9.07	11.96 ± 12.79	0.270
ACTH 8am (pg/mL)	20.45 ± 17.39	42.87 ± 83.92	0.075
Cortisone 0am (μg/dL)	3.97 ± 5.43	3.59 ± 7.37	0.778
Cortisone 8am (μg/dL)	7.33 ± 5.96	12.12 ± 7.93	0.000*
24h UFC (nmol/d)	231.79 ± 230.22	290.78 ± 111.05	0.116

*24h UFC, 24-hour urine free cortisol, *P < 0.05.*

Function of hypothalamic-pituitary target gland axes, as shown above, only serum cortisone level at 8am was higher in patients without hypopituitarism, there was no significant difference in either the size of the cyst or age of the patient between cases with or without hypopituitarism. Levels of FT3, FT4, TSH, IGF-1, GH, FSH, LH, ACTH, cortisone at 0am, and 24hUFC in patients with hypopituitarism were slightly lower than that of patients without hypopituitarism, but not statistically significant.

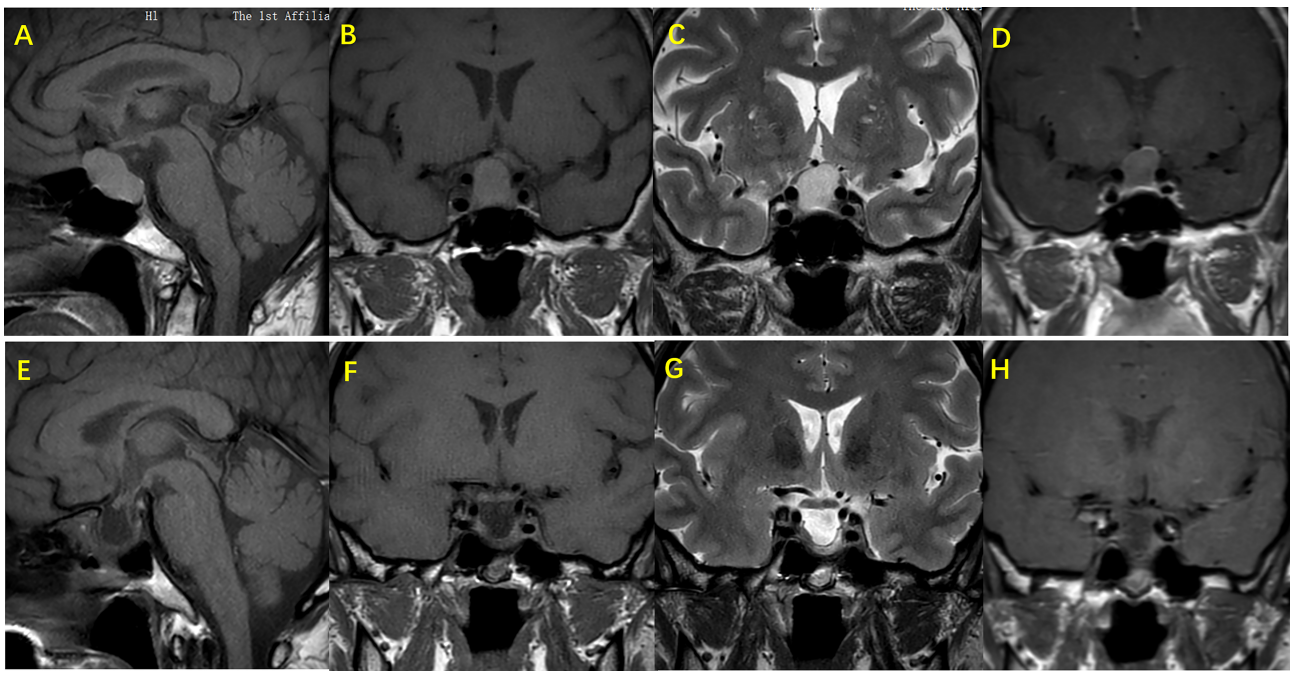

FIGURE 1 | Images of MRI and gadolinium-enhanced MRI sequencing for sella region in RCC patient. Female patient, age 47, suffers headache as the main symptoms, MRI shows a snowman appearance of the RCC, the cyst present isointense on T1W imaging. **(A, B)** and hypertense on T2W imaging. **(C)** and the wall has been partialy enhanced with gadolinium administration **(D)** In the preoperative picture of the patient, the RCC is compressing the sella - supraselar region causing compression of optic chiasm, while pituitary stalk is not visible as the result of compression. Pictures **(E–H)** show the 6 months post - operation evaluation of the pituitary gland. Hypertense on T1W **(E, F)** and heterogeneous intensity on T2W imaging **(G)** present in the sela - suprasellar region, with irregular enhancement after gadolinium administration. Also, pituitary stalk appears although it has been shifted, and the compression of optic chiasm is seen relieved.

cysts. Those with a largest diameter <10 mm were defined as group A, and patients with a largest diameter of ≥10 mm as group B. Comparison of these two groups showed that the difference in cyst diameter was statistically significantly, whereas the gender proportion and age at onset was similar. As shown in **Table 2**, the incidence of headache and dizziness was higher in group B. Among the pituitary function indexes, only the ACTH level at 8 am was significantly different in the two groups, but interesting, the level of ACTH in group B was higher than that in group A (**Table 3**).

TABLE 2 | Comparison of general information between groups A and B.

Name	Diameter of RCC		Total	*P* value
	<10mm (Group A)	≥10mm (Group B)		
With dizziness or headache	36	47	83	
Without dizziness or headache	118	20	138	0*
Male	81	26	107	
Female	73	41	114	0.059
<18years	24	8	32	
Adult	130	59	189	0.479

**P < 0.05.*

The incidence of headache and dizziness was higher in patients with large RCC. There is no difference in gender and age distribution between the two groups.

TABLE 3 | Comparison of endocrine function between groups A and B.

	Diameter <10mm	Diameter ≥10mm	*P*
Diameter of RCC (mm)	5.50 ± 2.42	16.35 ± 5.20	0.000*
Age (yr)	40.13 ± 19.11	40.169 ± 17.13	0.988
FT3 (pmol/L)	5.05 ± 1.51	5.12 ± 2.73	0.891
FT4 (pmol/L)	12.68 ± 5.98	12.18 ± 8.75	0.775
TSH (μiu/mL)	4.85 ± 15.18	3.65 ± 15.91	0.724
IGF1 (ng/mL)	223.69 ± 131.20	174.33 ± 75.05	0.115
GH (ng/mL)	0.94 ± 2.28	0.62 ± 0.86	0.451
FSH (mIU/mL)	11.76 ± 17.95	10.44 ± 15.37	0.142
LH (mIU/mL)	7.73 ± 8.82	8.61 ± 10.04	0.694
PRL (ng/mL)	21.22 ± 1346	23.64 ± 26.26	0.669
ACTH 0 am (pg/mL)	10.72 ± 10.37	14.85 ± 17.7	0.319
ACTH 8 am (pg/mL)	24.77 ± 15.48	37.33 ± 33.95	0.022*
Cortisone 0 am (μg/dL)	4.12 ± 5.57	3.62 ± 4.52	0.721
Cortisone 8 am (μg/dL)	10.18 ± 5.64	10.48 ± 6.26	0.841

**P < 0.05.*

Among the pituitary function indexes, only the ACTH level at 8 am was significantly different in the two groups, but interesting, the level of ACTH in group B was higher than that in group A.

The Relationship Between Endocrine Function and Clinical Manifestations

Headache and dizziness were the most common symptoms observed in our study cohort. We analyzed the difference between patients with head symptoms (named as group C)and those without head symptoms(named as group D). There was no significant difference in gender distribution between groups C and D, although the size of the cysts was significantly different (15.05 ± 5.92 mm vs. 10.30 ± 6.98 mm, respectively, $P<0.05$). The levels of serum ACTH at 0 am was significantly higher in patients with headache and dizziness than in patients without these symptoms (15.24 ± 17.29 vs. 9.16 ± 7.17 pg/mL, respectively, $P<0.05$). Eight patients had increased serum ACTH and cortisone levels, with all these patients suffering from headache or dizziness. The incidence of these symptoms was significantly different compared with those in patients with normal ACHT and cortisone levels (8/8 vs. 75/213, P <0.001). Patients with increased or normal serum ACTH and cortisone levels also had larger RCCs than patients without headache and dizziness (as described above). Compared with age-matched children with normal stature, eight juveniles with RCC were short in stature, all of whom received growth hormone excitation tests. The basic level of serum GH showed no difference between these two groups (0.41 ± 0.44 vs. 2.76 ± 3.80 ng/mL, $P>0.05$), whereas the peak level of GH was lower in short children compared to children with a normal stature (5.38 ± 2.28 vs. 10.04 ± 1.59 ng/mL, $P<0.05$). The serum levels of IGF-1 (228.80 ± 63.22 vs.358.72 ± 187.92 ng/mL) and LH (1.70 ± 1.35 vs. 4.97± 3.49) were also lower in short juveniles compared to that in juveniles with normal height (both $P<0.05$). However, there was no difference in cyst diameter between these two groups (7.00 ± 7.71 vs. 12.83 ± 5.076 mm, respectively, $P>0.05$).

Eight juveniles in the study (2 males, 6 females, mean age 7.88 ± 2.17 years) were diagnosed with precocious puberty, with a mean diameter of RCC of 9.80 ± 1.69 mm. With the exception of a pituitary-gonadal axis disorder, no other pituitary-target organ axis was affected. Unfortunately, no age-matched children were enrolled in the study as a control group.

Treatment Methods

A total of 22 patients received surgery for RCC, most of who were symptomatic patients, including those with headaches, dizziness, decreased vision, and visual field defects. All the patients underwent endoscopic endonasal transsphenoidal dissection of RCC surgery. A round fistula of no less than 5mm in diameter was produced in the wall of each RCC (**Figure 2**). The contents of the RCC were described as a jelly-like substance of different colors. After clear-up of the RCC-contents, the cystic parietal cells were destroyed to the great extent with a scraping circle to reduce the recurrence rate of RCC. A small amount of hemostatic material was filled in the operation cavity. Clinical pathological reports described a powder-

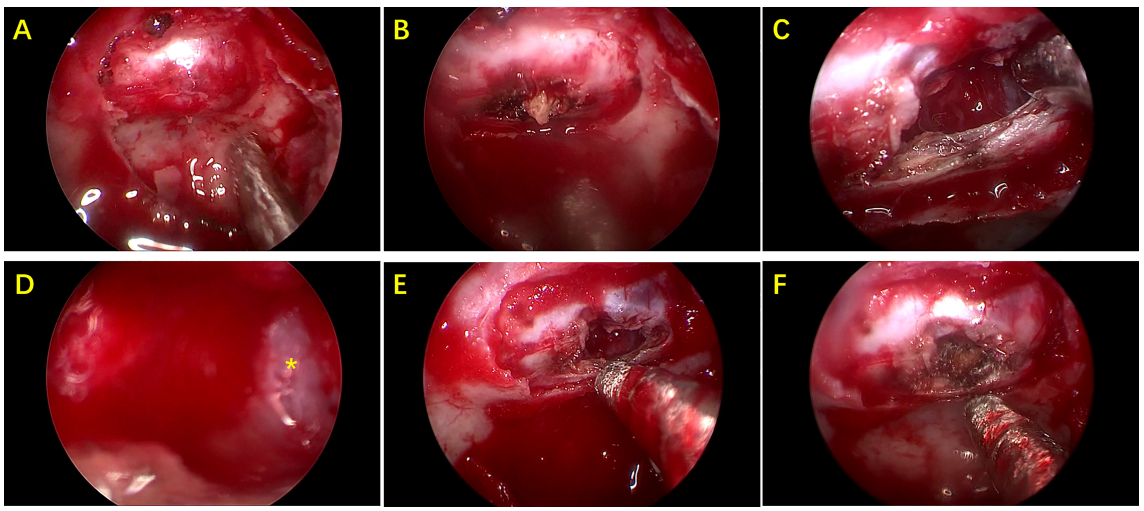

FIGURE 2 | Pictures during endoscopic endonasal transsphenoidal surgery. **(A)** Exposure of sellar dura mater. **(B)** After the dura mater is cut open, there is some cheese-like substance. **(C)** Capsule contents are cleared up. **(D)** Local enlarged view of capsule wall(*). **(E)** Final status of cyst wall fistula. **(F)** A small amount of hemostatic material are filled in the capsule.

stained amorphous substance, with the wall of the capsule composed of a single layer of cubic epithelial ciliated columnar epithelial cells or cubic epithelial cells (**Figure 3**). The maximum diameter of the cysts in the patients who received surgery was significantly greater than that of patients who received conservative treatment (17.70 ± 5.57 mm vs. 11.92 ± 6.58 mm, respectively, $p<0.05$). The level of ACTH at 0 am was higher in patients who underwent surgery than that measured in patients who received conservative treatment (30.76 ± 28.57 vs. 9.74 ± 8.046 pg/mL, respectively, $p<0.05$). The other indicators of endocrine function were similar in the two treatment groups.

DISCUSSION

We conducted a retrospective observational study to analyze the clinical manifestations of RCCs and the effect of a RCC on pituitary function. The study carried out in central China showed that RCC occurs at different ages and predominantly in females. Most patients with RCC are symptomatic and have head symptoms and abnormal pituitary function, not only hypopituitary, but also hyperfunction, such as high ACTH levels and precocious puberty. In the current study, the size of the RCC was not related closely to hypopituitary. The study also provided suggestions regarding evaluation of endocrine function in patients with RCC. A study conducted by Mizue Fujii on the Japanese also came up with similar results, RCC, even small ones, can cause pituitary dysfunction (5).

The findings of the study on the general characteristics of the patients were consistent with those of previous reports. The age distribution ranged from children to elderly people, with the highest incidence of RCCs in people aged 30-50 years. The majority of patients were symptomatic, with headache being

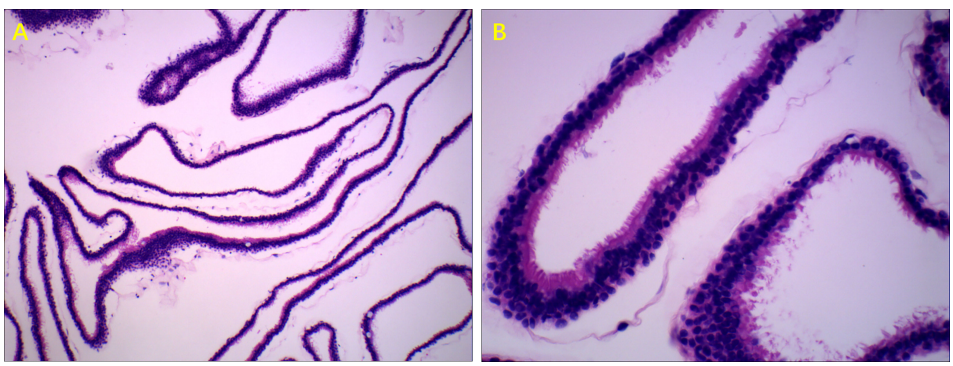

FIGURE 3 | Typical pathologic manifestations of RCC. Ciliated columnar epithelium of RCC, H&E stain. **(A)** (100× magnification). **(B)** (400× magnification).

the most common symptom (6), with an incidence of 64.7% in this study, similar to that reported in other studies (7, 8). We observed that about one third (67/221) of patients had a large RCC, and as expected the size of the RCC was related to the presence of headache and dizziness. Our data also showed that the incidence of headache and dizziness was higher in patients with a RCC diameter >10mm, a finding consistent with those reported in previous literature (9, 10).

Among the pituitary function indices, the level of ACTH at 8 am was significantly different between patients with different sized RCCs, and it is interesting that the level of ACTH was highest in patients with a larger RCC. We consider that headache and dizziness caused by a large RCC may be the reason for this increase in ACTH level (11), pain is a stressful stimulus that is likely to elicit ACTH and cortisol secretion and is commonly associated with hypercortisolism, ACTH-cortisone is a key player in the stress response (12). This is consistent with result in this study, the incidence of headache and dizziness was higher in patients with large RCC, and all the patients with a high ACTH level suffered from headache or dizziness. Other reasons for these results should be considered, because patients who underwent surgery received a pathological diagnosis, while in other symptomatic patients who received conservative treatment, the presence of a RCC and ACTH secreting pituitary microadenoma (13) or even a pituitary adenoma and concomitant RCC (14–16) could not be definitely excluded. Although both these states have been reported in the literature, we showed that none of our patients had been diagnosed with Cushing syndrome, while no symptoms and signs related to this syndrome were identified in the medical records.

Compared to other research, our study showed a low prevalence of hypopituitarism (17, 18), especially hypogonadotropic hypogonadism, with only 10 patients complaining about this symptom. However, we observed lower LH levels in patients with hypopituitarism. Consistent with the culture of central China, people are ashamed to talk about sexual function and this hesitation may be responsible for the low incidence of hypopituitarism we observed. Of note, no correlation between hypopituitarism and RCC size was observed in our study, a finding similar to that reported by other literature (6). However, a significant positive relationship between RCC size and the number of impaired hormones has been reported previously, although there is no consensus regarding this association.

RCC may be one of the causes of central precocious puberty, although this relationship is also controversial (7, 19, 20). In our study, eight cases showed precocious puberty, mainly girls, a finding different from data reported in some other papers (7). Han Hyuk Lim et al. reported smaller RCCs in cases of precocious puberty, although in our study the diameter of RCCs in patients with or without precocious puberty was similar. The mechanism of how RCCs leads to precocious puberty is unclear. Possible mechanisms reported as following, larger cysts may cause extreme pressure on the pituitary, lead to precocious puberty by interrupting a neuronal inhibitory mechanism for pituitary gonadotropin release. While smaller cysts may elicit endocrine dysfunction through inflammation of the pituitary or by interruption of normal inhibitory pathway. In our study there were also eight cases of RCC in people with a short stature who had low levels of GH, IGF-1, and LH and were diagnosed with delayed puberty or growth hormone deficiency, both of which may result from a RCC (21–23). The gene mutation is consider to be responsible role, such as the transcription factor ISL1, It's expressed in pituitary gland stem cells and thyrotrope and gonadotropin lineages, with the conditional Isl1 deletion causing development of multiple Rathke's cleft-like cysts, with 100% penetrance (24, 25).

Surgery and conservative treatment were both used for treatment of RCC in the patients in our study. Symptoms and signs were the basis for these treatment plans, and although our results showed that most patients were symptomatic, fewer patients underwent surgery compared with that reported in other literature (26). Chinese conservative thinking considers that surgery will destroy vitality, especially surgery on the head.

The pathogenesis of RCC remains controversial, classic RCCs are lined by a single layer of cuboidal or ciliated columnar epithelium, while stratified squamous epithelial cells lining a portion of RCCs are reported. This finding favors the hypothesis that RCCs and craniopharyngiomas, which are lined with multi-stratified squamous epithelium, may represent two extremes of a continuum of cystic sellar lesions. Due to the high rate of relapse and progressions (17, 24, 27, 28) and the homologous etiology of RCCs and craniopharyngioma (24, 29), patients with a RCC should receive regular clinical follow-up, especially juvenile patients.

LIMITATIONS

Our study had some limitations, the first of which was its retrospective cross-sectional design. Second, patients enrolled in the study were treated at a single medical center. Third, follow-up studies are needed to better understand the long-term effects of management of RCCs.

CONCLUSION

This study analyzed the impact of RCC on pituitary function and its relationship with RCC-related clinical manifestations. The majority of patients with RCC were symptomatic, mainly suffering from headaches and dizziness. RCC should therefore be considered as a possible reason for these symptoms. We observed that hypopituitary function was not closely related to cyst size, suggesting that clinicians need to evaluate endocrine function in patients with an identified RCC.

DATA AVAILABILITY STATEMENT

The original contributions presented in the study are included in the article/supplementary material. Further inquiries can be directed to the corresponding author.

ETHICS STATEMENT

The studies involving human participants were reviewed and approved by Ethics Committee of Zhengzhou University, Zhengzhou University. Written informed consent to participate in this study was provided by the participants' legal guardian/next of kin.

AUTHOR CONTRIBUTIONS

LXZ and XL performed the data analyses and wrote the manuscript. XL contributed to the conception of the study. CL and ZW performed the collection of data collection and recording. LLZ, GQ, and SW helped perform the analysis with constructive discussions. LX contributed significantly to analysis and manuscript preparation. All authors contributed to the article and approved the submitted version.

ACKNOWLEDGMENTS

The authors would like to express their gratitude to EditSprings (https://www.editsprings.cn/) for the expert linguistic services provided.

REFERENCES

1. Freda PU, Wardlaw SL, Post KD. Unusual Causes of Sellar/Parasellar Masses in a Large Transsphenoidal Surgical Series. *J Clin Endocrinol Metab* (1996) 81 (10):3455–9. doi: 10.1210/jcem.81.10.8855784
2. Jung JE, Jin J, Jung MK, Kwon A, Chae HW, Kim DH, et al. Clinical Manifestations of Rathke's Cleft Cysts and Their Natural Progression During 2 Years in Children and Adolescents. *Ann Pediatr Endocrinol Metab* (2017) 22(3):164–9. doi: 10.6065/apem.2017.22.3.164
3. Post KD. Rathke's Cleft Cysts: Unanswered Questions. *World Neurosurg* (2012) 78(5):428–9. doi: 10.1016/j.wneu.2012.01.043
4. Jeon H, Suh HB, Chung W, Choi HY. Ophthalmic Manifestations of Rathke's Cleft Cyst and Its Association to Radiological Characteristics. *Curr Eye Res* (2021) 46(8):1227–31. doi: 10.1080/02713683.2020.1863430
5. Fujii M, Nakagawa A, Tachibana O, Iizuka H, Koya D. Anterior Pituitary Function in Rathke's Cleft Cysts Versus Nonfunctioning Pituitary Adenomas. *Endocr J* (2021) 68(8):943–52. doi: 10.1507/endocrj.EJ21-0050
6. Raper DM, Besser M. Clinical Features, Management and Recurrence of Symptomatic Rathke's Cleft Cyst. *J Clin Neurosci* (2009) 16(3):385–9. doi: 10.1016/j.jocn.2008.04.023
7. Lim HH, Yang SW. Risk Factor for Pituitary Dysfunction in Children and Adolescents With Rathke's Cleft Cysts. *Korean J Pediatr* (2010) 53(7):759–65. doi: 10.3345/kjp.2010.53.7.759
8. Truong L, Bazin C, Gomis P, Decoudier B, Delemer B, Litre CF. Surgery Versus Conservative Care for Rathke's Cleft Cyst. *Neurochirurgie* (2021) 67 (2):104–11. doi: 10.1016/j.neuchi.2020.12.010
9. Ozoner B, Aydin S, Akgun MY, Durmaz ES, Sahin S, Gazioglu N, et al. Predictive Factors for Rathke's Cleft Cyst Consistency. *World Neurosurg* (2019) 128:e522–30. doi: 10.1016/j.wneu.2019.04.188
10. Cabuk B, Selek A, Emengen A, Anik I, Canturk Z, Ceylan S. Clinicopathologic Characteristics and Endoscopic Surgical Outcomes of Symptomatic Rathke's Cleft Cysts. *World Neurosurg* (2019) 132:e208–16. doi: 10.1016/j.wneu.2019.08.196
11. McBeth J, Chiu YH, Silman AJ, Ray D, Morriss R, Dickens C, et al. Hypothalamic-Pituitary-Adrenal Stress Axis Function and the Relationship With Chronic Widespread Pain and Its Antecedents. *Arthritis Res Ther* (2005) 7(5):R992–1000. doi: 10.1186/ar1772
12. Tsigos C, Chrousos GP. Hypothalamic-Pituitary-Adrenal Axis, Neuroendocrine Factors and Stress. *J Psychosom Res* (2002) 53(4):865–71. doi: 10.1016/s0022-3999(02)00429-4
13. Sagan KP, Andrysiak-Mamos E, Sagan L, Nowacki P, Małkowski B, Syrenicz A. Cushing's Syndrome in a Patient With Rathke's Cleft Cyst and ACTH Cell Hyperplasia Detected by (11)C-Methionine PET Imaging-A Case Presentation. *Front Endocrinol (Lausanne)* (2020) 11:460. doi: 10.3389/fendo.2020.00460
14. Wu W, Jia G, Jia W, Li G, Zhang J, Zhang L. Pituitary Adenoma Associated With Rathke's Cleft Cyst: Report of 15 Cases. *Can J Neurol Sci* (2018) 45 (1):68–75. doi: 10.1017/cjn.2017.252
15. Wang K, Ma L, You C. Pituitary Adenoma and Concomitant Rathke's Cleft Cyst: A Case Report and Review of the Literature. *Neurol India* (2012) 60 (3):309–10. doi: 10.4103/0028-3886.98520
16. Noh SJ, Ahn JY, Lee KS, Kim SH. Pituitary Adenoma and Concomitant Rathke's Cleft Cyst. *Acta Neurochir (Wien)* (2007) 149(12):1223–8. doi: 10.1007/s00701-007-1295-x
17. Sala E, Moore JM, Amorin A, Carosi G, Martinez HJ, Harsh GR, et al. Natural History of Rathke's Cleft Cysts: A Retrospective Analysis of a Two Centres Experience. *Clin Endocrinol (Oxf)* (2018) 89(2):178–86. doi: 10.1111/cen.13744
18. Fujii M, Nakagawa A, Tachibana O, Iizuka H, Koya D. Anterior Pituitary Function in Rathke's Cleft Cysts Versus Nonfunctioning Pituitary Adenomas. *Endocr J* (2021) 68(8):943–52. doi: 10.1507/endocrj.EJ21-0050
19. Chiu CF, Wang CJ, Chen YP, Lo FS. Pathological and Incidental Findings in 403 Taiwanese Girls With Central Precocious Puberty at Initial Diagnosis. *Front Endocrinol (Lausanne)* (2020) 11:256. doi: 10.3389/fendo.2020.00256
20. Oh YJ, Park HK, Yang S, Song JH, Hwang IT. Clinical and Radiological Findings of Incidental Rathke's Cleft Cysts in Children and Adolescents. *Ann Pediatr Endocrinol Metab* (2014) 19(1):20–6. doi: 10.6065/apem.2014.19.1.20
21. Briceno LG, Gunczler P, Solis O. Rathke Cleft Cyst as Cause of Growth Hormone Deficiency in a 9-Year-Old Girl. *J Pediatr* (2012) 160(4):708–708.e1. doi: 10.1016/j.jpeds.2011.10.006
22. Kim E. Symptomatic Rathke Cleft Cyst: Clinical Features and Surgical Outcomes. *World Neurosurg* (2012) 78(5):527–34. doi: 10.1016/j.wneu.2011.12.091
23. Kim CW, Hwang K, Joo JD, Kim YH, Han JH, Kim CY. Spontaneous Involution of Rathke's Cleft Cysts Without Visual Symptoms. *Brain Tumor Res Treat* (2016) 4(2):58–62. doi: 10.14791/btrt.2016.4.2.58
24. Brinkmeier ML, Bando H, Camarano AC, Fujio S, Yoshimoto K, de Souza FS, et al. Rathke's Cleft-Like Cysts Arise From Isl1 Deletion in Murine Pituitary Progenitors. *J Clin Invest* (2020) 130(8):4501–15. doi: 10.1172/JCI136745
25. Castinetti F, Brinkmeier ML, Mortensen AH, Vella KR, Gergics P, Brue T, et al. ISL1 Is Necessary for Maximal Thyrotrope Response to Hypothyroidism. *Mol Endocrinol* (2015) 29(10):1510–21. doi: 10.1210/me.2015-1192
26. Sade B, Albrecht S, Assimakopoulos P, Vezina JL, Mohr G. Management of Rathke's Cleft Cysts. *Surg Neurol* (2005) 63(5):459–66; discussion 466. doi: 10.1016/j.surneu.2004.06.014
27. Wedemeyer MA, Lin M, Fredrickson VL, Arakelyan A, Bradley D, Donoho DA, et al. Recurrent Rathke's Cleft Cysts: Incidence and Surgical Management in a Tertiary Pituitary Center Over 2 Decades. *Oper Neurosurg (Hagerstown)* (2019) 16(6):675–84. doi: 10.1093/ons/opy258
28. Wang M, Fu Q, Song M, Zhao Z, Wang R, Zhang J, et al. A Potential Concomitant Sellar Embryonic Remnant-Associated Collision Tumor: Systematic Review. *Front Oncol* (2021) 11:649958. doi: 10.3389/fonc.2021.649958
29. Gunes A, Ozbal GS. The Neuroimaging Features of Rathke's Cleft Cysts in Children With Endocrine-Related Diseases. *Diagn Interv Radiol* (2020) 26 (1):61–7. doi: 10.5152/dir.2019.19352

Conflict of Interest: The authors declare that the research was conducted in the absence of any commercial or financial relationships that could be construed as a potential conflict of interest.

this article, or claim that may be made by its manufacturer, is not guaranteed or endorsed by the publisher.

APPENDIX 1

Diagnostic Criteria

1. Secondary Hypoadrenalism, defined as patients with low level of cortisone in serum or urine (serum cortisone < 5μg/dl, 24hUFC < 73nmol/d Chemiluminescence immunoassay), and low serum ACTH at 8am (serum ACTH < 7pg/ml, Chemiluminescence analysis)
2. Secondary Hypothyroidism, defined as patients with low level of serum FT4 or FT3 (FT4 <7.9 pmol/ml, or FT4 <3.28 pmol/ml, Chemiluminescence immunoassay), and low TSH in serum (TSH < 5.91U μ iu/ml, Chemiluminescence immunoassay)
3. Growth hormone deficiency (GHD), GHD is defined by a peak GH response to insulin-induced hypoglycemia (insulin tolerance test, ITT), less than 5 ng/ml or 10 ng/ml, named complete growth hormone deficiency and partial growth hormone deficiency respectively.
4. Hypogonadotropic hypogonadism (HH). In teenagers (<18 years), HH diagnosed by low blood testosterone/ estrogen levels and low pituitary hormone level (LH), confirmed by GnRHa provocation test, peak LH response to gonadotropin stimulation test (0.1mg im) less than 12 mIU/ml (Chemiluminescence immunoassay). In adults with RCC, HH diagnosed by low blood testosterone/ estrogen levels and low pituitary hormone levels.
5. Abnormal puberty, include precious puberty and delayed puberty. precious puberty refers to puberty begins before age 8 in girls and before age 9 in boys, delayed puberty is defined by the absence of testicular development in boys beyond 14 years (or a testicular volume lower than 4 ml) and by the absence of breast development in girls beyond 13 years.

frontiers in Endocrinology

ORIGINAL RESEARCH
published: 15 March 2022
doi: 10.3389/fendo.2022.848762

Observation of Clinicopathologic Features of Pituitary Adenoma With Neuronal Differentiation

Limei Zheng[1†], Xiaorong Yan[2†], Chengcong Hu[1], Peng Zhang[3], Yupeng Chen[1], Qiaoyan Zheng[1], Liwen Hu[1], Mi Wang[1], Guoping Li[1], Ping Wu[1], Changzhen Jiang[2], Jing Tian[4], Sheng Zhang[1] and Xingfu Wang[1]*

[1] Department of Pathology, The First Affiliated Hospital of Fujian Medical University, Fuzhou, China, [2] Department of Neurosurgery, The First Affiliated Hospital of Fujian Medical University, Fuzhou, China, [3] Department of Cardiovascular Surgery, Renji Hospital, Shanghai Jiaotong University School of Medicine, Shanghai, China, [4] Department of Immunology and Microbiology, Shanghai Institute of Immunology, Shanghai Jiao Tong University School of Medicine, Shanghai, China

Objective: To investigate the clinicopathologic features of pituitary adenoma with neuronal differentiation.

Methods: Four patients with mixed gangliocytoma-pituitary adenomas between January 2011 and January 2021 and 111 new-onset patients with adenomas between January 2019 and June 2021 who attended the First Affiliated Hospital of Fujian Medical University were included in the study. The histological and immunohistochemical findings were analyzed. Neuronal differentiation marker staining was performed on new-onset adenomas, and the related literature was reviewed.

Results: Altogether, more than 100 mixed gangliocytoma-pituitary adenoma cases have been reported in the literature until now, of which pituitary-specific POU-class homeodomain transcription 1 (PIT1) positive adenomas are more frequently observed. In the present study, all 4 patients we described were female, aged 29 to 53 years (mean 39 years). Clinically, 3/4 patients presented with acromegaly, and 1/2 patients presented with headache. Histologically, the tumor was composed of two distinct mixed components. The one was a population of neoplastic ganglionic cells with large nuclei, prominent nucleoli, and abundant basophilic cytoplasm embedded in a fibrillary background. Stains of chromograninA (CgA), synaptophysin (Syn), Calretinin (CR) were positive. Axotomy-like expression was observed in neurofilament (NF) staining. PIT1 was expressed in partial ganglionic cells in all cases. The other component was a population of small uniform cells with round nuclei and acidophilic cytoplasm. Prolactin (PRL) and growth hormone (GH) were positive in all 4 cases. PIT1 was positive in the nuclei of adenomas. Although adenomas and ganglionic regions varied in histology, there was a population of cells with neuronal differentiation expressing PIT1. Additionally, axotomy-like expression of NF staining could be seen in a distant area of adenoma regions. A total of 111 cases of adenomas without ganglionic cells were included in this study, including 7 cases with neuronal differentiation. Among them, 4 cases were prolactinomas, 2 cases were somatotroph adenomas, and 1 case was corticotroph adenoma. 6/7 cases were PIT1-positive adenomas. And the remaining one case is T-PIT-positive adenoma.

OPEN ACCESS

Edited by:
Congxin Dai,
Capital Medical University, China

Reviewed by:
Xiaobiao Zhang,
Fudan University, China
Murat Aydin Sav,
Yeditepe University, Turkey

****Correspondence:***
Xingfu Wang
wang_xfu@126.com

†These authors have contributed equally to this work

Specialty section:
This article was submitted to Pituitary Endocrinology, a section of the journal Frontiers in Endocrinology

Received: *05 January 2022*
Accepted: *10 February 2022*
Published: *15 March 2022*

Citation:
Zheng L, Yan X, Hu C, Zhang P, Chen Y, Zheng Q, Hu L, Wang M, Li G, Wu P, Jiang C, Tian J, Zhang S and Wang X (2022) Observation of Clinicopathologic Features of Pituitary Adenoma With Neuronal Differentiation. Front. Endocrinol. 13:848762. doi: 10.3389/fendo.2022.848762

Conclusions: Mixed gangliocytoma-pituitary adenomas are rare tumors with neuronal differentiation. The majority of MGAs are associated with endocrinopathies, mainly acromegaly. Our results suggest that PIT1-positive pituitary adenomas may have neural differentiation potential, which may not be unusual. This indication supports the possibility that the neuronal transdifferentiation of adenomatous cells is a possible mechanism, and the underlying mechanism requires further elucidation.

Keywords: mixed-gangliocytoma pituitary adenoma, pituitary tumor, neural differentiation, acromegaly, PIT1

INTRODUCTION

Gangliocytomas/mixed gangliocytoma-adenomas (GCs/MGAs) are rare entities in the sellar region and are categorized as neuronal and paraneuronal tumors according to the 2017 World Health Organization Neuroendocrine Tumor Classification Guideline (1). Most cases reported are composed of ganglion cells with pituitary adenomas (2), forming so-called mixed gangliocytoma adenomas. Isolated gangliocytomas are extremely rare. In the present study, 4 cases of mixed gangliocytoma adenoma and 111 new-onset cases of pituitary adenoma were analyzed. The purpose of this study was to investigate the clinicopathologic features of pituitary adenoma with neuronal differentiation.

MATERIALS AND METHODS

We retrospectively studied the histological examinations of 4 patients with mixed gangliocytoma-pituitary adenomas between January 2011 and January 2021 and 111 new-onset patients with adenomas between January 2019 and June 2021 who attended the First Affiliated Hospital of Fujian Medical University. For histology and immunohistochemistry, the tissue was fixed in 10% formalin and subsequently paraffin embedded. Paraffin-embedded sections (4–6μm thick) were processed, and then selected blocks were stained with antibodies to transcription factors and pituitary hormones, including PIT1 (1:500, G-2; Zsbio), steroidogenic factor 1 (SF-1) (1:500, OTI1H2; Zsbio), T-box family member TBX19 (T-PIT) (1:500, OTI2G1; Zsbio), adrenocorticotropic hormone (ACTH) (RAB-0010; Maxim), PRL (MAB-0886; Maxim), follicle-stimulating hormone (FSH) (MAB-0782; Maxim), GH (MAB-0883; Maxim), luteal hormone (LH) (MAB-0788; Maxim) and thyroid stimulating hormone (TSH) (MAB-0796; Maxim). Immunohistochemistry (IHC) stains that have been utilized for the detection of neuronal structures include neuronal nuclei (NeuN) (1:200; MAB-0578; Maxim), CR (1:200; ZA-0026; Zsbio), NF (1:300; TA309765; Zsbio), Syn (1:600; ZA-0263; Zsbio) and MAP2 (1:200; ZA-0380; Zsbio). Other antibodies for diagnosis and differential diagnosis includes CK8 (MAB-1002; Maxim), thyroid transcription factor 1 (TTF-1) (HPA054837; Roche), BRAF (HPA001328; Roche), CD34 (Kit-0004; Maxim), GFAP (1:300; ZM-0118; Zsbio), P53 (MAB-0674; Maxim) and Ki-67 (1:400; ZM-0378; Zsbio). Double-labeling IHC assay PIT-1/MAP2 was performed using dual detection kit (Roche) in BenchMark ULTRA system.

Medical files were retrospectively reviewed, and magnetic resonance imaging (MRI) studies of the patients were also analyzed. The follow-up information came from outpatient follow-up review or telephone follow-up.

RESULTS

Case 1

A 53-year-old female presented with a 12-month history of acromegaly. She had a history of surgical thyroidectomy. MRI showed an intrasellar mass measuring 2.1 cm×1.6 cm×1.5 cm. The tumor passed the intercarotid line, but not beyond the tangent on the lateral aspects of the intracavernous. Random GH serum level was elevated at 19.48 μg/L on admission. Insulin-like growth factor-1 (IGF-1) level was 408 ng/mL (normal value 87-238 ng/mL). A 75g oral glucose tolerance test (OGTT) achieved inadequate suppression of nadir GH level (17.97ng/mL; normal value 0.06-5μg/L). Other hormones were within normal range. She underwent a transsphenoidal endoscopic approach resection of the tumor. At the 50th month follow-up after the surgery, the clinical symptoms of the patient markedly improved.

Case 2

A 29-year-old female with acromegaly complained of a 1-year history of headache with aggravation for 1 week. MRI showed a mass measuring 2.4 cm×2.3 cm×1.8 cm in the sella turcica. On coronal contrast imaging, the intracavernous artery was totally encased by the tumor. The boundaries were relatively clear. Preoperative growth hormone level was 4.28μg/L and IGF-1 level was 516.6 ng/mL (normal value 63-373ng/mL). 75g OGTT found nadir GH level of 4.79ng/mL, resulting in no suppression of less than 1μg/L. PRL serum level was elevated at 565.4mIU/L. Other pituitary hormones were within normal range. The patient was followed up for 12 months after transsphenoidal resection, and her general condition was good.

Case 3

A 35-year-old female had a 5-year history of secondary amenorrhea and a 1-year history of acromegaly. MRI revealed an intra- and suprasellar lesion with a prominent waist sign (**Figure 1**) measuring 3.0 cm×2.7 cm×2.0 cm. The tumor passed the medial tangent, but did not extend beyond the intercarotid line. In addition, it was heterogeneous enhanced after contrast. Laboratory tests revealed high levels of GH (70.10μg/L), PRL (1160.0mIU/L) and IGF-1

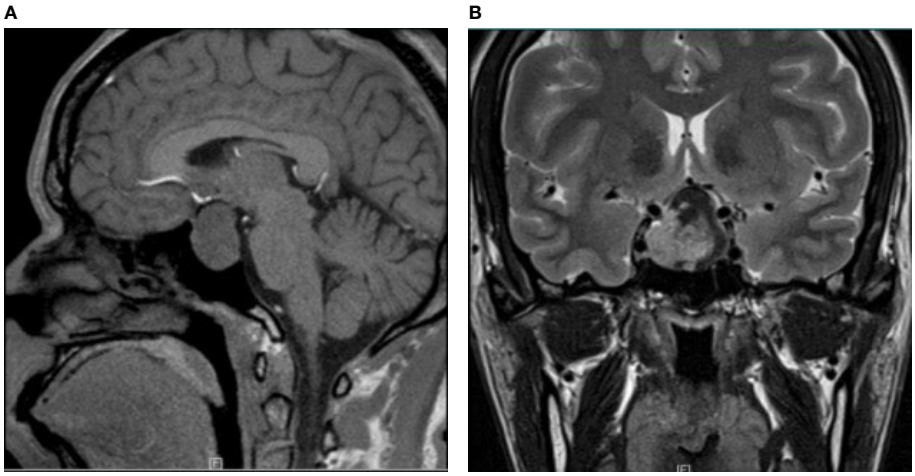

FIGURE 1 | Radiological image of mixed gangliocytoma-pituitary adenoma. **(A)** Preoperative MRI shows a lesion with sagittal hypointensity on T1-weighted imaging. **(B)** T2-weighted coronal contrast imaging shows a hyperintensity signal with a prominent waist sign. The tumor passed the tangent of the medial aspects of the intracavernous and supracavernous internal carotid arteries, but did not extend beyond the intercarotid line.

(545.2ng/mL, normal value 63-373ng/mL). Other hormones were within normal range. Transsphenoidal endoscopic gross total tumor resection was performed. At a follow-up visit 7 months after surgery, all clinical symptoms had disappeared. Menstruation was restored following surgery but irregular.

Case 4

A 39-year-old female was admitted to the hospital with severe headache for ten days. MRI showed an intrasellar equal T1 and slightly long T2 signal, within the intercarotid line. The size of the lesion was 1.8 cm×1.5 cm×1.4 cm. GH serum level was elevated at 16.55μg/L and IGF-1 level was elevated at 640 ng/mL (normal value 63-373ng/mL). Serum PRL level was elevated at 437.9mIU/L. Other hormones were within normal range. The mass was excised *via* an endoscopic transsphenoidal procedure. The postoperative record was taken at 4 months after surgery, and the clinical symptoms improved significantly.

The patients' clinical characteristics are summarized in **Table 1**.

Macroscopically, the resected surgical specimens were grayish brown tissue with soft texture, and the size ranged from 1.8 cm×1.5 cm×1.4 cm to 3.0 cm×2.7 cm×2.0 cm. Histologically, four cases were composed of pituitary adenomas admixed with ganglionic cells (**Figure 2A**). The adenomatous component consisted of small uniform cells with acidophilic cytoplasm (**Figure 2B**). The ganglionic component showed polyhedral, occasionally binucleated neurons, with prominent fibrillary neuropils in the stroma (**Figures 2C, D**).

The expressions of the transcriptional factors were as follows. PIT1 were found to be expressed in all four cases. T-PIT and SF-1 were all negative. In all four cases, the expression of GH, PRL (**Figure 3A**) and PIT1 (**Figure 3B**) was observed in both the adenomatous component and a fraction of the ganglionic component. Large ganglionic cells were positive for microtubule-associated protein 2 (MAP2) (**Figure 3C**). Furthermore, PIT1/

TABLE 1 | List of clinical characteristics of the patients.

	Case1	Case2	Case3	Case4
Gender	F	F	F	F
Age (year)	53	29	35	39
Location	intrasellar	Intrasellar, suprasellar, cavernous sinus	Intrasellar, suprasellar	intrasellar
Clinical presentation	Acromegaly progressing	Headache, acromegaly	Acromegaly, amenorrhea	Headache
Tumor size (cm)	2.07×1.58×1.52	2.4×2.3×1.8	3.0×2.7×2.0	1.8×1.5×1.4
Knosp grade	II	IV	I	I
GH level (μg/L)	19.48	4.28	70.10	16.55
nadir GH level after OGTT	17.97	4.79	/	/
IGF-1 level(ng/mL)	408	516.6	545.2	640
PRL level(mIU/L)	53.2	565.4	1160.0	437.9
Surgery	ETS	ETS	ETS	ETS
Follow-up (month)	50, NED	12, NED	7, NED	4, NED

F, Female; ETS, endoscopic transsphenoidal surgery; NED, No evidence of disease.
Normal ranges: GH: 0.06-5μg/L, IGF-1:63-373ng/mL (Case1: 87-238 ng/mL), PRL: 86-324 mIU/L.

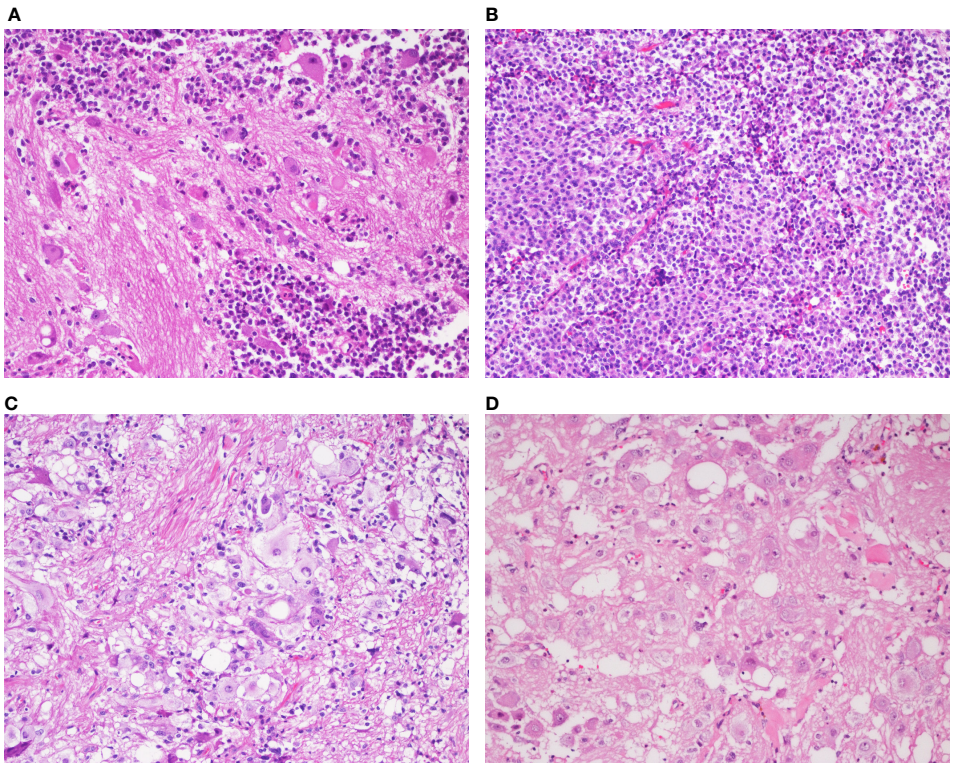

FIGURE 2 | Histopathological analysis of the mixed gangliocytoma-pituitary adenoma in a representative case (Case 3) **(A)** Two distinct mixed neoplastic cell populations are observed. **(B)** The adenomatous component consists of small monomorphic cells with oval nuclei and eosinophilic cytoplasm. **(C)** Binucleated cells and masses of neuropils are detected in the neural component. **(D)** The ganglionic cells are large, immature with abundant cytoplasm and decentralized nuclei containing prominent nucleoli. [**(A–D)**, magnification×200].

MAP2 double-IHC staining was performed. MAP2 and PIT1 were coexpressed in some ganglionic cells (**Figure 3D**). Although adenomatous and ganglionic regions varied in histology, there were different numbers of cells with neuronal differentiation expressing PIT1. Axotomy-like expression was observed in ganglionic cells by NF staining (**Figure 4A**), while typical adenomatous cells did not express NF. Additionally, the axotomy-like appearance of NF staining can be seen in a distant area of adenoma regions. A typical dot-like paranuclear CK8 immunoreactivity pattern was observed in ganglion cells (**Figure 4B**), in addition to expression in the fibrous bodies of the adenomatous cytoplasm. TTF-1, GFAP and CD34 were negative in all four cases. Immunostain for a mutation-specific antibody and mutation testing has shown no BRAF V600E mutation (4 case tested). Ki-67 proliferation index was from 1% to 7%. The immunohistochemical results of pituitary transcription factors, pituitary hormones, neuronal markers and Ki-67 proliferation indexs are summarized in **Table 2**. According to the 2017 World Health Organization Neuroendocrine Tumor Classification Guideline, final pathological diagnoses of four cases were mixed gangliocytoma-adenomas. The adenomatous components were all sparsely granulated mammosomatotroph adenomas.

A total of 111 cases of adenomas without ganglionic cells were included in this study. The expression of NF was investigated in this series. Accordingly, NF positivity was noted in 7 cases. The incidence of neuronal differentiation in this series was 6%. Among them, 4 cases were prolactinomas, 2 cases were somatotroph adenomas, and 1 case was corticotroph adenoma. 6/7 cases were PIT1-positive adenomas. And the remaining one case is T-PIT-positive adenoma. NF immunostaining showed diverse expression patterns, such as paranuclear, cytoplasmic (**Figure 4C**) and axotomy-like coloring (**Figure 4D**). From these findings, we deduce that neuronal differentiation in adenomas without ganglionic cells may not be a rare phenomenon.

DISCUSSION

Mixed gangliocytoma adenoma is composed of neoplastic mature ganglion cells in combination with pituitary adenomas accompanied by clinical symptoms caused by hypersecretion. GC/MGA was first reported in 1919 by Greenfield et al. and was named choristoma (3). With a deeper understanding of the disease, more varying terminologies have been used to describe it, including neuronal choristoma, choristoma, adenohypophysial choristoma, ganglioneuroma, and pituitary adenoma with neuronal choristoma [PANCH] (4).

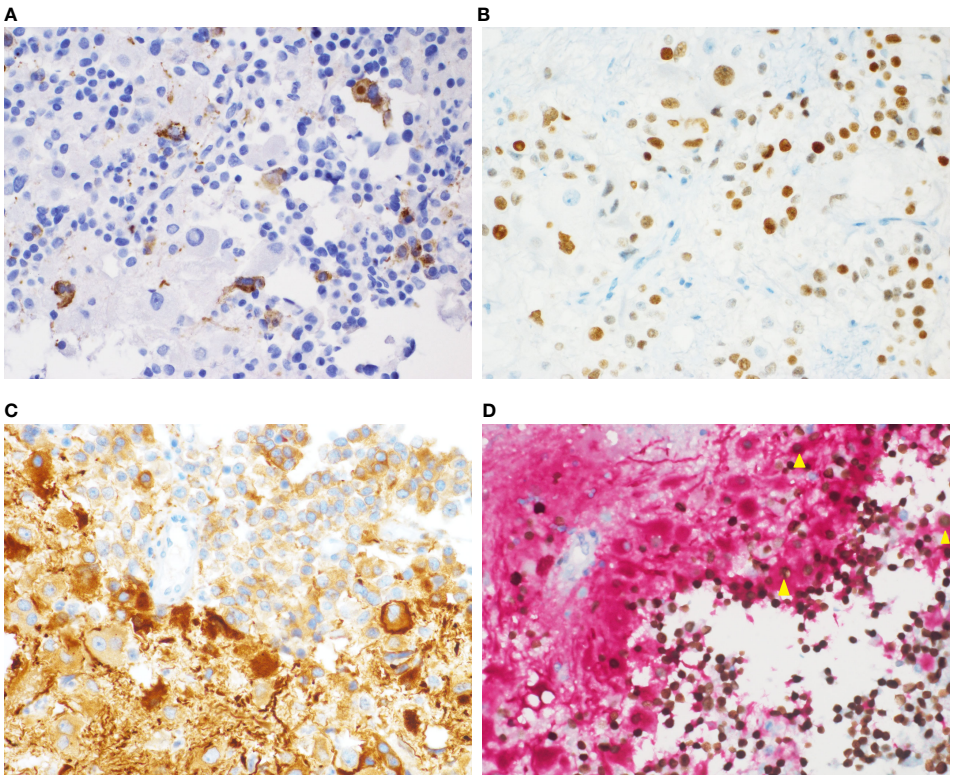

FIGURE 3 | Immunochemical staining of the mixed gangliocytoma-pituitary adenoma. **(A)** Some ganglion-like cells express PRL in the cytoplasm. **(B)** Nuclear PIT1 immunoreactivity is observed in both adenomatous cells and ganglionic cells. **(C)** Fibrillar matrix and large ganglion cells with prominent nucleoli show strong cytoplasmic reactivity for MAP2. **(D)** Double-IHC staining for PIT1 (nuclear; brown) and MAP2 (cytoplasmic; red) shows the coexpression of PIT1 (nuclear) and MAP2 (cytoplasmic) in individual cells (yellow triangle). [**(A–D)**, magnification×400].

To date, 148 cases of GC/MGA have been reported in the literature (5–35). Most of the cases involved female patients with an average age of 44.5 years. The main clinical manifestations of GC/MGA are acromegaly and lactational amenorrhea syndrome, while a few cases present as Cushing´s syndrome or hyperprolactinemia. Patients with acromegaly presented with coarse facial features and acral enlargement. A diagnosis of acromegaly is confirmed biochemically by detection of increased serum IGF-1 concentrations and high serum levels of GH that are not suppressed in an OGTT. Random GH level <1.0μg/L associated with a normal IGF-1 level represents the therapeutic goal and correlates with optimal disease control. A nadir GH level <1 μg/L after OGTT is associated with improved long-term outcomes and lower mortality risk in patients after surgery. Of the 4 MGA patients in this study, 3/4 patients suffered acromegaly, 1/2 patients exhibited headaches, and 1/4 patient experienced amenorrhea, in accordance with the literature. GH serum level was elevated in all cases but Case 2. Nadir GH level after OGTT was >1.0μg/L in Case 2. After 3 months of follow-up, the serum GH levels returned to the normal range in all patients.

Concomitant pituitary adenomas demonstrated by immunohistochemistry in MGAs include somatotroph adenoma, corticotroph adenoma, lactotroph adenoma, mammosomatotroph adenoma and thyrotroph adenoma. Furthermore, GH, PRL, and corticotropin-releasing hormone (CRH) are usually positive in the majority of cases. Radiographically, there was no significant difference in imaging examination between MGA and pituitary adenomas. The lesion was hypointense on the T1-weighted image without enhancement of the mass and hyperintense on the T2-weighted image (15).

Histologically, MGA is composed of two distinct neoplastic cell populations with no clear boundaries. One is a cluster of ganglion cells, and the other is pituitary adenoma. The gangliocytic component consists of irregularly oriented cells with eccentric nuclei containing prominent nucleoli and basophilic cytoplasm. The adenoma component consists of small monomorphic cells with round to ovoid nuclei, delicately stippled chromatin and moderately abundant cytoplasm. A preponderance of pituitary adenoma is sparsely granulated somatotroph adenoma.

Differential diagnosis may mainly concern ganglioglioma. Ganglioglioma is composed of neoplastic mature ganglion cells in combination with neoplastic glial cells. GC/MGA is devoid of neoplastic glial cells. GFAP may aid the differential diagnosis. Meanwhile, CD34 is consistently expressed in 70-80% and BRAF V600E mutation occur in 20-60% of investigated cases of

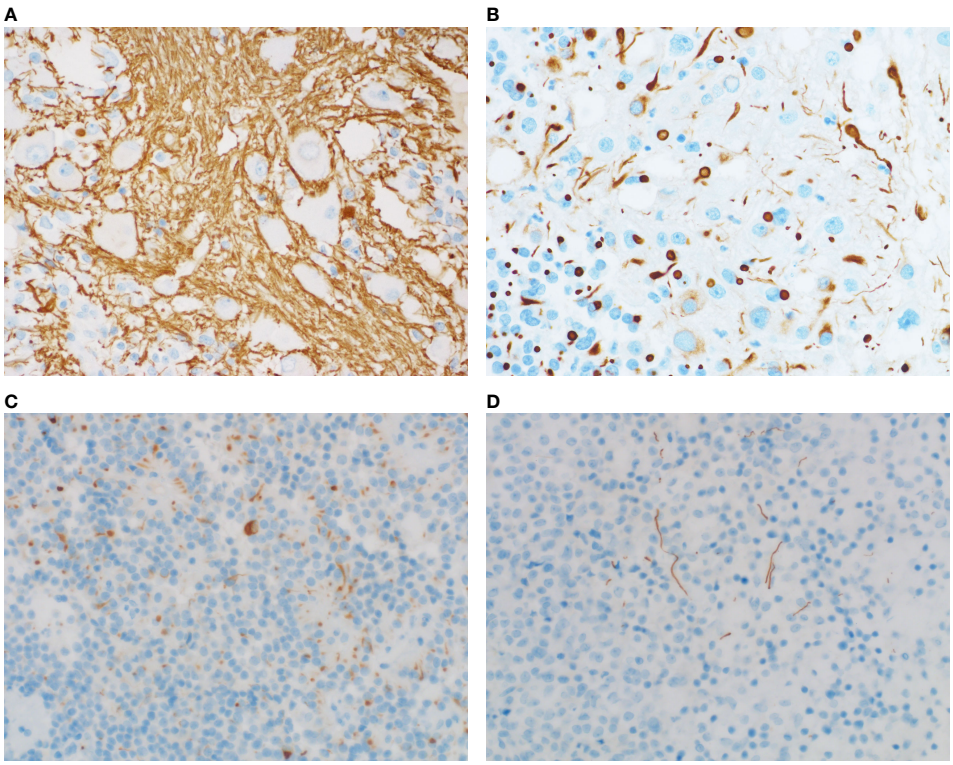

FIGURE 4 | NF staining and CK staining of adenomas with or without neuronal differentiation. **(A)** NF immunostaining shows axotomy-like expression. **(B)** Prominent CK8 staining is noted within fibrous bodies of the ganglion cells. **(C)** NF staining shows a dot-like/cytoplasmic staining pattern. **(D)** Axotomy-like NF coloring can also be seen in adenomas without ganglionic cells. [**(A–D)**, magnification×400].

TABLE 2 | List of immunohistochemical results.

	Case1		Case2		Case3		Case4	
	Ad	**GC**	**Ad**	**GC**	**Ad**	**GC**	**Ad**	**GC**
SF-1	–	–	–	–	–	–	–	–
T-PIT	–	–	–	–	–	–	–	–
PIT1	+	+	+	+	+	+	+	+
PRL	+	+	+	+	+	+	+	+
GH	w+	w+	+	+	+	+	+	+
ACTH	–	–	–	–	–	–	–	–
LH	–	–	–	–	–	–	–	–
TSH	–	–	–	–	–	–	–	–
FSH	–	–	–	–	–	–	–	–
CK8	+	+	+	+	+	–	+	–
Syn	+	+	+	+	+	+	+	+
NeuN	–	–	–	–	–	–	–	–
MAP2	–	+	–	+	–	+	–	+
CR	–	+	–	+	–	+	–	+
NF	–	+	–	+	–	+	–	+
P53	/	/	+	+	+	+	+	+
Ki-67	2%	<1%	7%	<1%	3%	<1%	1%	<1%
TTF-1	–	–	–	–	–	–	–	–
GFAP	–	–	–	–	–	–	–	–
CD34	–	–	–	–	–	–	–	–
BRAF	–	–	–	–	–	–	–	–

A, Adenomatous component; GC, ganglionic cells; w+, weak positive.

gangliogliomas. The detection of CD34 and BRAF V600E may also be useful for the differential diagnosis.

The histogenesis of pituitary GC/MGA is currently not clear. There are three main hypotheses about the pathogenesis of these tumors: (1) Excess GHRH produced by primary gangliocytoma stimulates the adenomatous formation (36); (2) Both ganglion cells and adenoma cells might arise from a common stem/progenitor cell (37); (3) The neuronal component originates from neuronal differentiation of a preexisting pituitary adenoma (38).

The theory of neuronal differentiation has received increasing recognition. Neuronal transformation is observed in many neuroendocrine cells *in vitro*, including carcinoid tumors, small cell carcinoma of the lung, pheochromocytoma and insulin-producing pancreatic islet cell tumors (39–41). Ultrastructural analysis has found evidence of intermediate cells between adenomatous and ganglionic cells, characterized by neuronal type RER and immunoreactivity for pituitary hormones and low-molecular weight keratin in the perikarya (38). In the present cases, both adenomatous and ganglionic components expressed PIT1. Immunostaining for PRL showed cytoplasmic positivity, and CK8 immunostaining showed strong dot-like perinuclear positivity in ganglionic cells. Meanwhile, a few pituitary adenomatous cells had a neuronal phenotype confirmed by the neuron-related marker NF without morphological characterization of neurons. This result supports the possibility that transdifferentiation could be a potential underlying mechanism of mixed pituitary adenoma–gangliocytomas. Due to the limited number of cases, the effect of neuronal components on the prognosis of MGAs is not yet clear.

Surgery constitutes the primary form of treatment for most patients with MGA/GC. Transsphenoidal tumor resection is the procedure of choice. The rate of surgical success is closely associated with the size and degree of invasiveness of the tumor. Results with large tumors are worse and tumors with evidence of invasion have poor long-term results. Medical therapy has an important role in the management of acromegaly, including dopamine agonists (DAs), the GH receptor antagonist pegvisomant (PEG) and the second-generation SRL pasireotide (PAS) (42). The existence of neural components, however, has no influence on aggressiveness and the risk of recurrence after surgical resection (2).

DATA AVAILABILITY STATEMENT

The raw data supporting the conclusions of this article will be made available by the authors, without undue reservation.

ETHICS STATEMENT

Written informed consent was obtained from the individual(s) for the publication of any potentially identifiable images or data included in this article.

AUTHOR CONTRIBUTIONS

LZ and XY: Conceptualization, Methodology, Formal Analysis, Writing - Original Draft. HC, PZ, YC, QZ, LH, MW, GL, and PW: Immunohistochemistry. CJ, JT, and SZ: Supervision, Writing -Review & Editing. XW: Conceptualization, Funding Acquisition, Resources, Supervision, Writing - Review and Editing. All authors contributed to the article and approved the submitted version.

FUNDING

This work was supported in part by Fujian Medical University Startup Fund for scientific research (2020QH1053), in part by National Natural Science Foundation of China (81900767), Natural Science Foundation of Fujian Province (2018J01155).

REFERENCES

1. Lopes MBS. The 2017 World Health Organization Classification of Tumors of the Pituitary Gland: A Summary. *Acta Neuropathologica* (2017) 134(4):521–35. doi: 10.1007/s00401-017-1769-8
2. Cossu G, Daniel RT, Messerer M. Gangliocytomas of the Sellar Region: A Challenging Diagnosis. *Clin Neurol neurosurg* (2016) 149:122–35. doi: 10.1016/j.clineuro.2016.08.002
3. Greenfield JG. The Pathological Examination of Forty Intracranial Neoplasms. *Brain* (1919) 42(1):29–85. doi: 10.1093/brain/42.1.29
4. Lloyd RV OR, Kloppel G, Rosai J. *WHO Classification of Tumours of the Endocrine Organs. 4th edn*. Lyon: International Agency for Research on Cancer (2017) p. 48–9.
5. Balci S, Saglam A, Oruckaptan H, Erbas T, Soylemezoglu F. Pituitary Adenoma With Gangliocytic Component: Report of 5 Cases With Focus on Immunoprofile of Gangliocytic Component. *Pituitary* (2015) 18(1):23–30. doi: 10.1007/s11102-013-0551-8
6. Domingue ME, Marbaix E, Do Rego JL, Col V, Raftopoulos C, Duprez T, et al. Infrasellar Pituitary Gangliocytoma Causing Cushing's Syndrome. *Pituitary* (2015) 18(5):738–44. doi: 10.1007/s11102-014-0595-4
7. Petrakakis I, Pirayesh A, Krauss JK, Raab P, Hartmann C, Nakamura M, et al. The Sellar and Suprasellar Region: A "Hideaway" of Rare Lesions. Clinical Aspects, Imaging Findings, Surgical Outcome and Comparative Analysis. *Clin Neurol Neurosurg* (2016) 149:154–65. doi: 10.1016/j.clineuro.2016.08.011
8. Donadille B, Villa C, Gaillard S, Christin-Maitre S. Gangliocytoma: Outcome of a Rare Silent Pituitary Tumour. *BMJ Case Rep* (2017) 2017. doi: 10.1136/bcr-2016-218859
9. Teramoto S, Tange Y, Ishii H, Goto H, Ogino I, Arai H, et al. Mixed Gangliocytoma-Pituitary Adenoma Containing GH and GHRH Co-Secreting Adenoma Cells. *Endocrinol Diabetes Metab Case Rep* (2019) 2019. doi: 10.1530/EDM-19-0099
10. Robertson DM, Hetherington RF. A Case Of Ganglioneuroma Arising In The Pituitary Fossa. *J Neurol Neurosurg Psychiatry* (1964) 27(3):268–72. doi: 10.1136/jnnp.27.3.268
11. Asa SL, Kovacs K, Tindall GT, Barrow DL, Horvath E, Vecsei P, et al. Cushing's Disease Associated With an Intrasellar Gangliocytoma Producing Corticotrophin-Releasing Factor. *Ann Internal Med* (1984) 101(6):789–93. doi: 10.7326/0003-4819-101-6-789
12. McCowen KC, Glickman JN, Black PM, Zervas NT, Lidov HG, Garber JR, et al. Gangliocytoma Masquerading as a Prolactinoma. Case Report. *J neurosurg* (1999) 91(3):490–5. doi: 10.3171/jns.1999.91.3.0490
13. Geddes JF, Jansen GH, Robinson SF, Gömöri E, Holton JL, Monson JP, et al. 'Gangliocytomas' of the Pituitary: A Heterogeneous Group of Lesions With Differing Histogenesis. *Am J Surg Pathol* (2000) 24(4):607–13. doi: 10.1097/00000478-200004000-00017

14. Isidro ML, Iglesias Díaz P, Matías-Guiu X, Cordido F. Acromegaly Due to a Growth Hormone-Releasing Hormone-Secreting Intracranial Gangliocytoma. *J Endocrinol Invest* (2005) 28(2):162–5. doi: 10.1007/BF03345360
15. Qiao N, Ye Z, Wang Y, Li S, Mao Y, Bao W, et al. Gangliocytomas in the Sellar Region. *Clin Neurol neurosurg* (2014) 126:156–61. doi: 10.1016/j.clineuro.2014.08.034
16. Levitus CF, Charitou MM. AN INCIDENTAL COLLISION TUMOR OF THE SELLA TURCICA. *AACE Clin Case Rep* (2019) 5(4):e247–9. doi: 10.4158/ACCR-2019-0013
17. He M, Zheng N, Zhang J, Hu Z, You G, Ren Q, et al. Growth Hormone-Secreting Adenoma Coexisted With Gangliocytoma: A Rare Case. *Int J Clin Exp Pathol* (2018) 11(7):3785–8.
18. Novello M, Gessi M, Doglietto F, Anile C, Lauriola L, Coli A, et al. Characteristics of Ganglion Cells in Pituitary Gangliocytomas. *Neuropathol Off J Japanese Soc Neuropathol* (2017) 37(1):64–8. doi: 10.1111/neup.12322
19. Lopes MB, Sloan E, Polder J. Mixed Gangliocytoma-Pituitary Adenoma: Insights on the Pathogenesis of a Rare Sellar Tumor. *Am J Surg Pathol* (2017) 41(5):586–95. doi: 10.1097/PAS.0000000000000806
20. Yano S, Hide T, Uekawa K, Honda Y, Mikami Y, Kuratsu JI, et al. Mixed Pituitary Gangliocytoma and Prolactinoma Resistant to the Cabergoline Treatment. *World neurosurg* (2016) 95:620.e617–620.e622. doi: 10.1016/j.wneu.2016.08.011
21. Jukes A, Allan R, Rawson R, Buckland ME. Growth Hormone Secreting Pituitary Adenoma With Admixed Gangliocytoma and Ganglioglioma. *J Clin Neurosci Off J Neurosurg Soc Australasia* (2016) 31:202–4. doi: 10.1016/j.jocn.2016.02.024
22. Angelstein I. Pathogenesis of Acromegaly. *Deutsche Z fur Nervenheilkunde* (1953) 170(4):337–48. doi: 10.1007/BF00242976
23. Muller W, Marcos F. [The Occurrence of Ganglion Cells in a Pituitary Tumor]. *Virchows Archiv fur pathologische Anatomie und Physiologie und fur klinische Med* (1954) 325(6):733–6. doi: 10.1007/BF00955104
24. Jakumeit HD, Zimmermann V, Guiot G. Intrasellar Gangliocytomas. Report of Four Cases. *J neurosurg* (1974) 40(5):626–30. doi: 10.3171/jns.1974.40.5.0626
25. Asa SL, Bilbao JM, Kovacs K, Linfoot JA. Hypothalamic Neuronal Hamartoma Associated With Pituitary Growth Hormone Cell Adenoma and Acromegaly. *Acta Neuropathologica* (1980) 52(3):231–4. doi: 10.1007/BF00705811
26. Rhodes RH, Dusseau JJ, Boyd AS Jr., Knigge KM. Intrasellar Neural-Adenohypophyseal Choristoma. A Morphological and Immunocytochemical Study. *J neuropathol Exp Neurol* (1982) 41(3):267–80. doi: 10.1097/00005072-198205000-00003
27. Burchiel KJ, Shaw CM, Kelly WA. A Mixed Functional Microadenoma and Ganglioneuroma of the Pituitary Fossa. Case Report. *J Neurosurg* (1983) 58 (3):416–20. doi: 10.3171/jns.1983.58.3.0416
28. Fischer EG, Morris JH, Kettyle WM. Intrasellar Gangliocytoma and Syndromes of Pituitary Hypersecretion. Case Report. *J Neurosurg* (1983) 59 (6):1071–5. doi: 10.3171/jns.1983.59.6.1071
29. Asa SL, Scheithauer BW, Bilbao JM, Horvath E, Ryan N, Kovacs K, et al. A Case for Hypothalamic Acromegaly: A Clinicopathological Study of Six Patients With Hypothalamic Gangliocytomas Producing Growth Hormone-Releasing Factor. *J Clin Endocrinol Metab* (1984) 58(5):796–803. doi: 10.1210/jcem-58-5-796
30. Bevan JS, Asa SL, Rossi ML, Esiri MM, Adams CB, Burke CW, et al. Intrasellar Gangliocytoma Containing Gastrin and Growth Hormone-Releasing Hormone Associated With a Growth Hormone-Secreting Pituitary Adenoma. *Clin Endocrinol* (1989) 30(3):213–24. doi: 10.1111/j.1365-2265.1989.tb02229.x
31. Kamel OW, Horoupian DS, Silverberg GD. Mixed Gangliocytoma-Adenoma: A Distinct Neuroendocrine Tumor of the Pituitary Fossa. *Hum Pathol* (1989) 20(12):1198–203. doi: 10.1016/S0046-8177(89)80012-7
32. Li JY, Racadot O, Kujas M, Kouadri M, Peillon F, Racadot J. Immunocytochemistry of Four Mixed Pituitary Adenomas and Intrasellar Gangliocytomas Associated With Different Clinical Syndromes: Acromegaly, Amenorrhea-Galactorrhea, Cushing's Disease and Isolated Tumoral Syndrome. *Acta Neuropathologica* (1989) 77(3):320–8. doi: 10.1007/BF00687585
33. Asada H, Otani M, Furuhata S, Inoue H, Toya S, Ogawa Y, et al. Mixed Pituitary Adenoma and Gangliocytoma Associated With Acromegaly–Case Report. *Neurologia Medico-Chirurgica* (1990) 30(8):628–32. doi: 10.2176/nmc.30.628
34. Slowik F, Fazekas I, Bálint K, Gazsó L, Pásztor E, Czirják S, et al. Intrasellar Hamartoma Associated With Pituitary Adenoma. *Acta neuropathologica* (1990) 80(3):328–33. doi: 10.1007/BF00294652
35. Saeger W, Puchner MJ, Lüdecke DK. Combined Sellar Gangliocytoma and Pituitary Adenoma in Acromegaly or Cushing's Disease. A Report of 3 Cases. *Virchows Archiv an Int J Pathol* (1994) 425(1):93–9. doi: 10.1007/BF00193956
36. Kurosaki M, Saeger W, Lüdecke DK. Intrasellar Gangliocytomas Associated With Acromegaly. *Brain Tumor Pathol* (2002) 19(2):63–7. doi: 10.1007/BF02478929
37. Kontogeorgos G, Mourouti G, Kyrodimou E, Liapi-Avgeri G, Parasi E. Ganglion Cell Containing Pituitary Adenomas: Signs of Neuronal Differentiation in Adenoma Cells. *Acta Neuropathologica* (2006) 112(1):21–8. doi: 10.1007/s00401-006-0055-y
38. Horvath E, Kovacs K, Scheithauer BW, Lloyd RV, Smyth HS. Pituitary Adenoma With Neuronal Choristoma (PANCH): Composite Lesion or Lineage Infidelity? *Ultrastructural Pathol* (1994) 18(6):565–74. doi: 10.3109/01913129409021900
39. Lach B, Rippstein P, Benott BG, Staines W. Differentiating Neuroblastoma of Pituitary Gland: Neuroblastic Transformation of Epithelial Adenoma Cells. Case Report. *J Neurosurg* (1996) 85(5):953–60. doi: 10.3171/jns.1996.85.5.0953
40. Chen J, Hersmus N, Van Duppen V, Caesens P, Denef C, Vankelecom H, et al. The Adult Pituitary Contains a Cell Population Displaying Stem/Progenitor Cell and Early Embryonic Characteristics. *Endocrinology* (2005) 146(9):3985–98. doi: 10.1210/en.2005-0185
41. Taniguchi Y, Yasutaka S, Kominami R, Shinohara H. Proliferation and Differentiation of Rat Anterior Pituitary Cells. *Anat Embryol* (2002) 206(1-2):1–11. doi: 10.1007/s00429-002-0271-8
42. Colao A, Grasso LFS, Giustina A, Melmed S, Chanson P, Pereira AM, et al. Acromegaly. *Nat Rev Dis Primers* (2019) 5(1):20. doi: 10.1038/s41572-019-0071-6

Conflict of Interest: The authors declare that the research was conducted in the absence of any commercial or financial relationships that could be construed as a potential conflict of interest.

frontiers | Frontiers in Endocrinology

ORIGINAL RESEARCH
published: 06 April 2022
doi: 10.3389/fendo.2022.800923

Surgical Outcomes of Clival Chordoma Through Endoscopic Endonasal Approach: A Single-Center Experience

Ge Chen[1,2], *Mingchu Li*[1,2], *Wenlong Xu*[1,2], *Xu Wang*[1,2], *Ming Feng*[2,3], *Renzhi Wang*[2,3] *and Xiaohai Liu*[1,2*]

[1] Department of Neurosurgery, Xuanwu Hospital Capital Medical University, Beijing, China, [2] Chinese Pituitary Specialists Congress, Beijing, China, [3] Department of Neurosurgery, Peking Union Medical College Hospital, Chinese Academy of Medical Sciences and Peking Union Medical College, Beijing, China

OPEN ACCESS

Edited by:
Run Yu,
University of California, Los Angeles, United States

Reviewed by:
Xiaorong Yan,
First Affiliated Hospital of Fujian Medical University, China
Xingfu Wang,
First Affiliated Hospital of Fujian Medical University, China
Qi Cao,
LAC+USC Medical Center, United States

***Correspondence:**
Xiaohai Liu
liuxiaohai09@126.com

Specialty section:
This article was submitted to Pituitary Endocrinology, a section of the journal Frontiers in Endocrinology

Received: 24 October 2021
Accepted: 14 March 2022
Published: 06 April 2022

Citation:
Chen G, Li M, Xu W, Wang X, Feng M, Wang R and Liu X (2022) Surgical Outcomes of Clival Chordoma Through Endoscopic Endonasal Approach: A Single-Center Experience. Front. Endocrinol. 13:800923. doi: 10.3389/fendo.2022.800923

Objective: Clival chordoma is a locally aggressive tumor with low metastatic potential. In the past decade, endoscopic endonasal approach (EEA) for clival chordoma has had a higher resection rate and a lower morbidity rate than transcranial approaches. Here, we present our initial single-center experience after EEA of clival chordomas.

Patients and methods: This study retrospectively analyzed 17 consecutive patients with clival chordoma who received EEA in our department between March 2015 and September 2021. The operation was performed by a single surgeon with EEA. The clinical and pathological characteristics were analyzed along with the surgical outcomes and complications.

Results: A total of 17 consecutive patients with clival chordoma received EEA with a median follow-up of 29.2 months (range 1-79). Gross total resection (GTR) was performed in 7 cases (41%), subtotal resection (STR) in 7 case (41%) and partially resection (PR) in 3 cases (18%). Cerebrospinal fluid leakage occurred in 2 cases (12%) and meningitis developed in 3 patients (18%) which were all successfully treated with intravenous antibiotics without any complications. There were no perioperative deaths or new focal neurological deficits postoperatively. Four in 7 patients with STR have had radiotherapy while the other three chose to be monitored. Till the last follow-up, three patients in STR group who received radiotherapy (3 in 4) had no tumor regrowth, while one in STR group with radiotherapy (1 in 4) showed tumor progression. Two patients in STR group without radiotherapy (2 in 3) showed stable tumor while the left one (1 in 3) showed tumor progression. One patient in the PR group died of tumor progression 2 years postoperation and the other one showed tumor progression and died of lung cancer 1 year postoperation. In addition, 1 in 7 patients with GTR had tumor recurrence *in situ* after

10 months and developed surgical pathway seeding in the spinal canal in C1 after 16 months. No recurrence occurred in the other 6 cases with GTR during the follow-up.

Conclusion: Although more cases are needed, our case series showed EEA is a safe and reliable method for clival chordoma with high resection rates and low morbidity rates. GTR without tumor residuum would improve the outcome.

Keywords: clival chordoma, endoscopic transnasal approach, surgical outcome, surgical complications, single center experience

INTRODUCTION

Chordomas are rare and locally invasive bone tumors originating from remnants of the embryologic notochord with an incidence of approximately 0.1/100,000/year (1). The most common site of chordoma is the sacrococcygeal region (50%), followed by the skull base (35%), especially the clival region and vertebra (15%) (2). Although clival chordomas account for only 0.2% of all central nervous system tumors, they are characterized by local destruction, dural invasion, bone erosion, and cranial nerve palsy, and even metastasis, resulting in challenges for the surgical removal of this lesion. Moreover, local recurrence rates of clival chordoma are very high even after radical resection and adjuvant radiotherapy (3, 4), while chemotherapeutic agents are rare and are largely ineffective (5).

Most recently, endoscopic endonasal approach (EEA) was recommended as a first-line option with a higher resection rate and a lower surgical complication rate compared to the transcranial surgery for the treatment of clival chordomas, which is not yet widely accepted yet (6, 7). In this study, we aimed to report our single-center experience and surgical outcomes after EEA for the resection of clival chordomas, and showed that EEA provided a safe and reliable method for the resection of clival chordoma.

PATIENTS AND METHODS

Patients

A total of 17 consecutive patients with clival chordoma who underwent EEA in Beijing Xuanwu Hospital between January 2015 and December 2021 were retrospectively analyzed. All the patients included had complete clinical, radiological, and biochemical data, over 18 years old, were treated with EEA and had at least half a year of follow-up. Histopathological and immunohistochemical examinations confirmed clival chordoma in all patients. The surgical procedures were performed by a single neurosurgeon (Ge Chen) with the surgical goal of total tumor resection. MRI was performed in all patients pre- and 1 week, 3 months, 6 months and every year post-operatively. The tumor size was measured as the maximum tumor diameter on MRI. The study was approved by the Research Ethics Committee of our hospital and written informed consent was obtained from all patients.

Abbreviations: EEA, endoscopic endonasal approach; GTR, Gross total resection; PR, partially resection; STR, subtotal resection.

Surgical Procedures

All EEAs were performed endoscopically using a Karl Storz endoscope through bi-nostrils, following the protocols described by the Pittsburg group (8). Hadad-Bassagasteguy (H-B) vascularized septal flaps with blood supply were performed in all cases (9). Septostomy and large sphenoidotomy were performed to provide access to the sellar area and clivus. Further surgical approaches depend on the location of the tumor and its upper and lateral extent. During the operation, we tried to detect the pseudocapsule of the tumor before the tumor resection. The adjacent dura mater was resected in all cases to achieve maximum surgical resection. All patients underwent multilayer closure with dura implantation, fat transplantation (when necessary), and a vascularized H-B flap. The internal carotid artery and basal artery were confirmed using Doppler in the patients with vascular invasion. Cerebrospinal fluid lumbar drainage was given postoperatively in all cases and was removed within 7 days after surgery. The MRI scans were evaluated by a neuroradiologist and another endoscopic surgeon to determine the extent of the tumor removal.

Statistical Analysis

Statistical analysis was performed with SPSS 18.0 software (SPSS, Inc., Chicago, IL, USA). Descriptive statistics were performed to report data related to patients' demographics and clinicopathological characteristics.

RESULTS

Patient Characteristics

A total of 17 EEAs were performed in 17 patients. Three patients received one or two craniotomies while no one received radiotherapy before EEA and 2 cases with preoperative occipitocervical fusion surgery. The median age at diagnosis was 45 years and ranged from 10 to 67 years. The male to female ratio is 7:10. Nine patients out of 17 (53%) had headache, and eight patients were diagnosed with visual impairment or field defect (47%). Diplopia was the third most common symptom, which occurred in 6 patients (35%). Two patients exhibited dysphagia and dysphonia (12%) and hypophysis were seen in five patients at the time of diagnosis (29%). The average time from symptoms onset to diagnosis were 10.6 months (range 0.5–24 months). The maximum diameter and location of tumors are shown in **Table 1**. The maximum diameter of the 17 tumors arranged from 24.4 to 83.4 mm, with the mean diameter 45.9

mm. The mean tumor volume was 49.7 cm3 (range 3.1–220.5 cm3). Fourteen tumors (82%) were solid while only three were cystic. The tumor involved the clivus in 15 cases (88%), the sphenoid sinus in 6 cases (35%), the sella in 11 cases (65%), suprasella in 3 cases (18%) and in cavernous sinus 6 cases (35%). In one case, the tumor was located extended to the craniocervical junction. The pre- and post- MRIs of all the patients were shown in **Figure 1**.

Surgical Outcome

Gross total resection was performed in 7 cases (41%), STR in 7 case (41%) and PR in 3 case (18%) (**Figure 1**). The mean maximum diameters of the GTR, STR, and PR groups were 38.1, 51.1, and 64.3 mm, respectively. The value in the GTR group was significantly smaller than in the other 2 groups by multiple comparisons ($P < 0.001$, $P < 0.001$, respectively). The residual tumor was either in the cavernous sinus or in the subdural space, which could be adhered tightly to the dura and to the important vessels, such as the basal artery. Another reason for the tumor residual was due to the texture of the tumor. Headache and visual impairment or field defect were improved in most of the patients while five patients with the symptom of diplopia (5 in 6) resolved within 6 months after surgery. All the two patients with dysphagia and dysphonia were recovered within one year postoperation. The Ki-67 index ranged from 3-20%, with a mean value of 7.6%, showing its active proliferation capacity. Interestingly, the residual tumor in one of the three patients in the PR group showed rapid tumor growth in the follow up and died 12 months after surgery with a Ki-67 index of 20%.

Surgical Complications and Follow-Up

As the tumor invaded the dura in 13 patients, the repair using the fascia of thigh muscle and H-B flap were performed in these patients. A second lumbar drainage after operation was used to manage the cerebrospinal fluid leakage. One patient developed cerebrospinal fluid leakage 2 weeks after the operation and required a secondary endoscopic repair. Postoperative bacterial meningitis was found in 3 patients who had no significant cerebrospinal fluid leakage. All three patients were successfully treated with intravenous antibiotics without any complications. One patient who received GTR developed deterioration of pituitary function after the EEA and received adrenocorticoid and thyroid hormone replacement therapy, while one in four patient who had pituitary function failure had normal function in the last follow-up. Two patients with GTR developed temporary diabetes after the EEA and were successfully treated with desmopressin. None of these patients developed persistent diabetes or new-onset neurological dysfunction. All the 7 patients with STR were considered for adjuvant radiotherapy, while only 4 of them have had radiotherapy and the other three chose to be monitored, including one female patient aged 10 years who were not suitable for radiotherapy. Till the last follow-up, three patients in STR group who received radiotherapy (3 in 4) had no tumor regrowth, while one in STR group with radiotherapy (1 in 4) showed tumor progression. Two patients in STR group without radiotherapy (2 in 3) showed stable tumor while the left one (1 in 3) showed tumor progression. One patient in the PR group died of tumor progression 2 years postoperation and the other one showed tumor progression and died of lung cancer 1 year postoperation. In addition, 1 in 7 patients with GTR had tumor recurrence *in situ* after 10 months and developed surgical pathway seeding in the spinal canal in C1 after 16 months. No recurrence occurred in the other 6 cases with GTR during the follow-up.

DISCUSSION

Chordomas were first described by Virchow in 1857 (10), while the term chordoma was first proposed by Ribbert in the 1890s, representing the microscopic characteristics of the tumor derived from undifferentiated notochordal remnants (11). According to the Surveillance, Epidemiology and End Results (SEER) database, the incidence of chordomas is 0.08 per 100,000, which occurs mainly in males, and occurs between 50 and 60 years of age, with a median survival of 6.29 years (12). Although chordomas represent only 0.2% of all central nervous system tumors, the most common site of origin is the clivus for intracranial chordomas. Because they are characterized by local destruction, dural invasion, bone erosion, and cranial nerve palsy, and even metastasis, clival chordomas are difficult to manage and easily recur, resulting in poor prognosis (13).

Chordomas may be located on the upper clivus, along the caudal edge of the clivus, the sellar area, sphenoid sinus, nasopharynx, maxilla, or even the intradural area (14). The clinical manifestations are varied and are associated with the location and involvement of adjacent structures of the clival chordoma. Patients usually present with headache, diplopia and vision loss. In rare oropharyngeal manifestations, dysphagia and speaking difficulties are present, which is common in clival chordoma with parapharyngeal and retropharyngeal extension (15). Although a definitive diagnosis of clival chordoma requires histopathological results with the characteristic material-like appearance of cells, typical clinical signs should be evaluated for the early diagnosis and treatment (16).

Although the lateral transcranial approach provides better vascular control and a better view of the brainstem-tumor interface (17), some have argued that EEA may not only provide direct surgical access but also provide a better visualization of surrounding structures, which is safer and minimally invasive (18). In the past decade, the use of EEA has been recommended more with increasing indications and better results (12). Here, we present our initial single-center experience and short-term outcomes after endoscopic endonasal approach resection of clival chordomas.

As surgery is the first-line treatment for clival chordoma, there are many surgical approaches for chordoma resection. Traditional transcranial approaches often lead to more brain tissue retraction with increased cerebral edema, hematoma and more damage to surrounding structures such as the basilar artery and optic nerve (19). As clival chordoma is located in the middle line of the skull base, EEA for clival chordoma resection can easily provide the surgical pathway and excellent exposure of the tumor and adjacent structures (especially the anterior dura and basilar arteries) (20, 21).

TABLE 1 | Clinical characteristics and surgical outcomes of the 17 patients with clival chordoma.

Case No.	Sex/Age	Symptoms	Tumor Location	Pituitary function	Tumor size (cm)	Tumor volume (cm^3)	Surgical Outcome	Tumor residuum	Ki-67	Complications	Management of complication	Adjuvant radiotherapy	Follow up (Months)	Last imaging result
1	M/42	Headaches, vision loss of right eye, dysphagia and dysphonia	Sphenoid sinus, upper and middle clivus, right cavernous sinus, subdural	Normal	6.2	71.4	STR	right cavernous sinus, tumor attached to the basal artery	10	Intracranial Infection	Antibiotics	Gamma Knife	79	Recurrence
2	F/54	Vision loss and visual field defect	Sphenoid sinus, sella, upper clivus	Normal	3.9	23.8	GTR	—	5	—	—	—	69	No Recurrence
3	F/35	Headaches and, diplopia, CN 6^{th} nerve palsy	right cavernous sinus, upper and middle clivus, subdural	Normal	3.7	21.0	STR	right cavernous sinus	5	—	—	Proton knife	64	Stable
4	F/60	Headaches, vision loss of right eye and two craniotomies	Anterior cranial fossa, right orbital cavity	ND	5.2	59.8	PR	Anterior cranial fossa, right orbital cavity	15	—	—	—	12	Tumor progression and died of lung cancer
5	F/48	Headaches and vision loss of both eyes	Sella and suprasella, subdural	Normal	2.4	3.8	GTR	—	3	—	—	—	50	No Recurrence
6	M/49	Headaches	Sella, right cavernous sinus and upper clivus, subdural	ND	3.4	12.4	GTR	—	2	Intracranial Infection	—	—	44	No Recurrence
7	M/67	Headaches, vision loss of right eye and one craniotomy	Sphenoid sinus, sella, upper and middle clivus	Low	3.0	11.1	GTR	—	3	Intracranial Infection	—	—	25	No Recurrence
8	M/62	Vision loss of both eyes	Sphenoid sinus, sella, upper and middle clivus	Low	8.3	220.5	STR	—	3	—	—	—	25	Stable
9	M/49	Diplopia, CN 3^{rd} and 6^{th} nerves palsy	Sella, left cavernous sinus and upper, middle and lower clivus, subdural	Low	6.6	79.0	PR	left cavernous sinus	20	—	—	—	24	Died of recurrence
10	F/49	gait instability	Sella, upper and middle clivus, subdural	Low	6.7	115.4	GTR	—	5	—	—	Gamma Knife	22	Tumor recurrence and Intradural spinal seeding
11	M/38	Headaches, stiff neck, dysphagia and dysphonia	upper, middle and lower clivus, craniocervical junction, subdural	ND	5.2	59.9	STR	—	20	—	—	Gamma Knife	17	Stable
12	F/55	Diplopia	Sella, right cavernous sinus and upper and middle clivus, subdural	ND	3.2	12.5	STR	right cavernous sinus	10	—	—	Proton knife	16	Stable
13	F/63	Headaches and vision loss of both eyes	Sphenoid sinus, sella and suprasella, upper and middle clivus, intradural	Normal	4.4	24.4	STR	suprasella	5	—	—	—	28	Recurrence
14	F/39	Diplopia, left CN 6^{th} nerve palsy	upper and middle clivus, intradural	Normal	4.1	20.7	GTR	—	5	—	—	—	12	No Recurrence
15	F/11	Diplopia, left CN 6^{th} nerve palsy	upper and middle clivus, intradural	Low	3.2	11.2	GTR	—	3	—	—	—	6	No Recurrence
16	M/33	Headaches and vision loss	Sphenoid sinus, sella and suprasella, upper and middle clivus, subdural	Normal	7.5	71.4	PR	subdural	5	—	—	—	1	Stable
17	F/10	Diplopia, CN 6^{th} nerve palsy and two craniotomies	Sella, left cavernous sinus, upper and middle clivus, subdural	Normal	4.8	26.9	STR	subdural	5	—	—	—	3	Stable

ND, Not done.

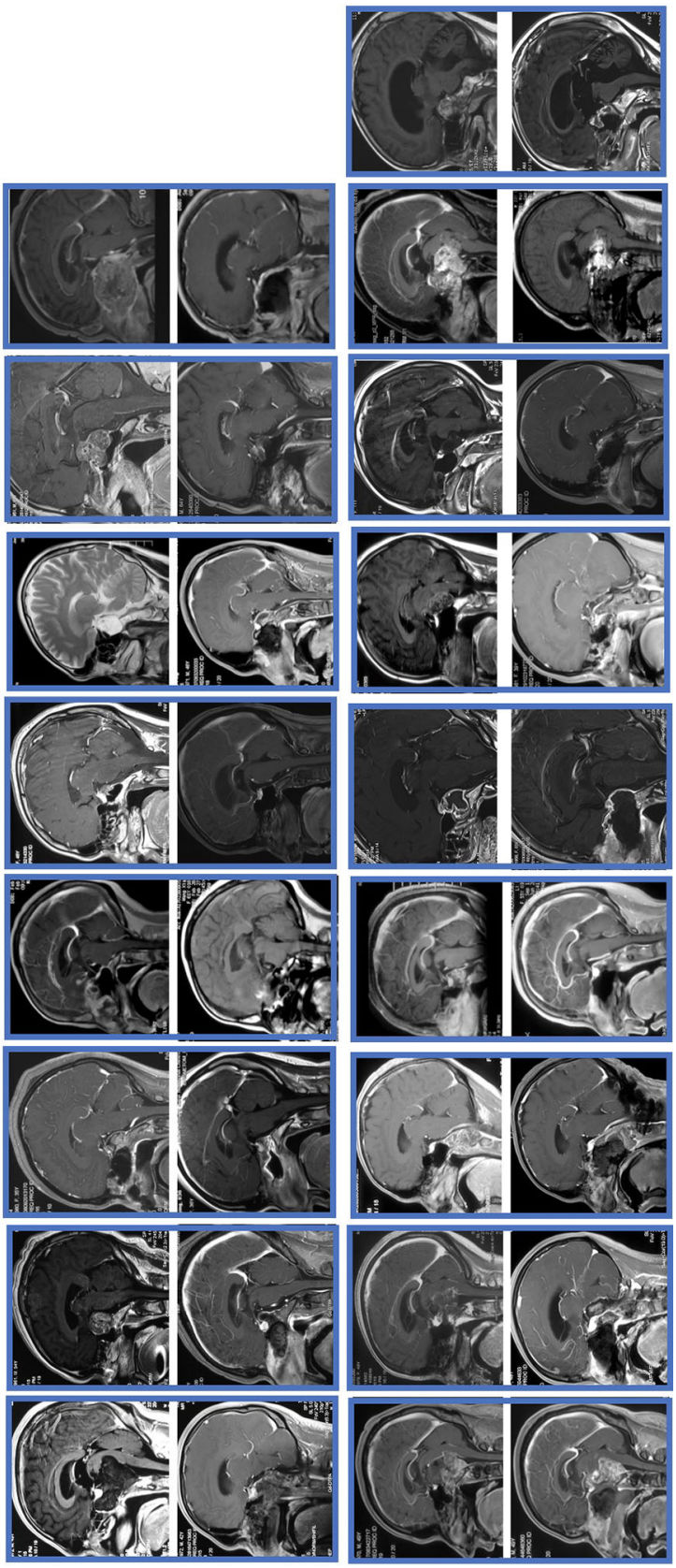

FIGURE 1 | The pre- and post- MRIs of all the patients.

The use of angled endoscopy has an advantage in showing hidden areas that cannot be seen with the transcranial approach. Zhang et al. proposed a surgical strategy for EEA according to the tumor growth directions, contributing to increasing the GTR rate (22). Therefore, EEA for clival chordoma resection has less morbidity compared to the transcranial approach (23). In our study, EEA resulted in a high GTR rate and a low surgical complication rate. Although intraoperative cerebrospinal fluid is very common, it is still inevitable during endoscopic surgery as cerebrospinal fluid repair could be performed after tumor resection with improved reconstructive techniques.

When the neurovascular structures of the surrounding area are locally invaded by the clival chordoma, the surgical principle is to minimize neurological dysfunction, even at the expense of having a postoperative residual tumor (12). After aggressive resection, radiotherapy could be used, with which residual tumors, especially small ones, can be effectively treated by radiotherapy. In 19 patients who underwent surgery and postoperative stereotactic radiotherapy, high-dose radiotherapy effectively controlled the small residual tumor volume (24). In a previous report, eleven patients underwent chordoma resection, of which 7 had subtotal or partial resections (24). Transient neurological deterioration (cranial nerve defects) occurred in seven patients, all of whom returned to neurological baseline. Following these considerations, 2 patients developed diplopia postoperatively but both returned to normal within 6 months in our case series, providing the evidence that the surgical strategies should not be overly aggressive, but should consider the option of radiotherapy and residual tumor observation.

Local recurrence is the main form of treatment failure (25). Radiotherapy can be used to treat recurrent clival chordoma patients who are not suitable for surgery (26). En bloc excision plus high dose radiation (27) or en bloc resection with proton beam radiation (28) were both the best evidences for improving survival in these patients. In our case series, one patient showed a recurrence *in situ* after EEA and gamma knife treatment was performed. After a follow-up of 16 months, a new lesion was seen in the spinal canal at C1 to C2, where an intradural spinal seeding chordoma was highly suspected. After a craniotomy, the lesion in the spinal canal was totally removed and the pathology confirmed a chordoma with increasing proliferative potential. And the patient was still in intensive follow-up.

Although the pathogenesis of chordoma is still unclear, loss of heterozygosity (LOH) of 1p36 is very common among sporadic chordomas and is related to tumorigenesis (29). As the molecular pathogenesis of clival chordoma is still unknown, no chemotherapy or targeted therapy has been developed until now. There is no specific genetic biomarker involved in predicting the recurrence and metastatic potential of chordomas. Although long-term prospective studies should be carried out to evaluate the role of endoscopic endonasal surgery in clival chordoma, endoscopic endonasal resection of clival chordoma is minimally invasive and reliable, which is correlated with a high GRT rate and a low morbidity.

CONCLUSION

Although more cases are needed, our case series showed EEA is a safe and reliable method for clival chordoma with high resection rates and low morbidity rates. GTR without tumor residuum would improve the outcome.

DATA AVAILABILITY STATEMENT

The raw data supporting the conclusions of this article will be made available by the authors, without undue reservation.

ETHICS STATEMENT

The studies involving human participants were reviewed and approved by Ethics Committee of Xuanwu Hospital Capital Medical University, Written informed consent to participate in this study was provided by the participants' legal guardian/next of kin.

Written informed consent was obtained from the individual(s), and minor(s)' legal guardian/next of kin, for the publication of any potentially identifiable images or data included in this article

AUTHOR CONTRIBUTIONS

Design, provision of patients, collection and assembly of data, data analysis and interpretation, manuscript writing. All authors contributed to the article and approved the submitted version.

FUNDING

The financial support for this study was provided by Beijing Hospitals Authority Youth Program (Code: QMS20210802 to XL).

REFERENCES

1. Castellanos LE, Gutierrez C, Smith T, Laws ER, Iorgulescu JB. Epidemiology of Common and Uncommon Adult Pituitary Tumors in the U.S. According to the 2017 World Health Organization Classification. *Pituitary* (2021) 27 (1):201–9. doi: 10.1007/s11102-021-01189-6
2. Erdem E, Angtuaco EC, Van Hemert R, Park JS, Al-Mefty O. Comprehensive Review of Intracranial Chordoma. *Radiographics* (2003) 23(4):995–1009. doi: 10.1148/rg.234025176
3. Hug EB, Slater JD. Proton Radiation Therapy for Chordomas and Chondrosarcomas of the Skull Base. *Neurosurg Clin N Am* (2000) 11 (4):627–38. doi: 10.1016/S1042-3680(18)30088-3
4. Noël G, Habrand JL, Jauffret E, de Crevoisier R, Dederke S, Mammar H, et al. Radiation Therapy for Chordoma and Chondrosarcoma of the Skull Base and the Cervical Spine. Prognostic Factors and Patterns of Failure. *Strahlenther Onkol* (2003) 179(4):241–8. doi: 10.1007/s00066-003-1065-5
5. Chugh R, Dunn R, Zalupski MM, Biermann JS, Sondak VK, Mace JR, et al. Phase II Study of 9-Nitro-Camptothecin in Patients With Advanced

Chordoma or Soft Tissue Sarcoma. *J Clin Oncol* (2005) 23(15):3597–604. doi: 10.1200/JCO.2005.02.170
6. Zoli M, Milanese L, Bonfatti R, Faustini-Fustini M, Marucci G, Tallini G, et al. Clival Chordomas: Considerations After 16 Years of Endoscopic Endonasal Surgery. *J Neurosurg* (2018) 128(2):329–38. doi: 10.3171/2016.11.JNS162082
7. Yousaf J, Afshari FT, Ahmed SK, Chavda SV, Sanghera P, Paluzzi A. Endoscopic Endonasal Surgery for Clival Chordomas - A Single Institution Experience and Short Term Outcomes. *Br J Neurosurg* (2019) 33(4):388–93. doi: 10.1080/02688697.2019.1567683
8. Stippler M, Gardner PA, Snyderman CH, Carrau RL, Prevedello DM, Kassam AB. Endoscopic Endonasal Approach for Clival Chordomas. *Neurosurgery* (2009) 64(2):268–77. discussion 277-8. doi: 10.1227/01.NEU.0000338071.01241.E2
9. Hadad G, Bassagasteguy L, Carrau RL, Mataza JC, Kassam A, Snyderman CH, et al. A Novel Reconstructive Technique After Endoscopic Expanded Endonasal Approaches: Vascular Pedicle Nasoseptal Flap. *Laryngoscope* (2006) 116(10):1882–6. doi: 10.1097/01.mlg.0000234933.37779.e4
10. Virchow RL. Untersuchungen Ueber Die Entwicklung Des Schaedelgrundes. *Berlin: G Rimer* 1857.
11. Horten BC, Montague SR. *In Vitro* Characteristics of a Sacrococcygeal Chordoma Maintained in Tissue and Organ Culture Systems. *Acta Neuropathol* (1976) 35(1):13–25. doi: 10.1007/BF00688940
12. McMaster ML, Goldstein AM, Bromley CM, Ishibe N, Parry DM. Chordoma: Incidence and Survival Patterns in the United States, 1973–1995. *Cancer Causes Control* (2001) 12:1–11. doi: 10.1023/A:1008947301735
13. Walcott BP, Nahed BV, Mohyeldin A, Coumans JV, Kahle KT, Ferreira MJ. Chordoma: Current Concepts, Management, and Future Directions. *Lancet Oncol* (2012) 13(2):e69–76. doi: 10.1016/S1470-2045(11)70337-0
14. Burge AJ. A Case of Oropharyngeal Chordoma. *J Laryngol Otol* (1975) 89 (1):115–9. doi: 10.1017/S0022215100080142
15. Mindell ER. Chordoma. *J Bone Joint Surg Am* (1981) 63(3):501–5. doi: 10.2106/00004623-198163030-00035
16. Castro JR, Linstadt DE, Bahary JP, Petti PL, Daftari I, Collier JM, et al. Experience in Charged Particle Irradiation of Tumors of the Skull Base: 1977-1992. *Int J Radiat Oncol Biol Phys* (1994) 29(4):647–55. doi: 10.1016/0360-3016(94)90550-9
17. Tzortzidis F, Elahi F, Wright D, Natarajan SK, Sekhar LN. Patient Outcome at Long-Term Follow-Up After Aggressive Microsurgical Resection of Cranial Base Chordomas. *Neurosurgery* (2006) 59(2):230–37. doi: 10.1227/01.NEU.0000223441.51012.9D
18. Dehdashti AR, Karabatsou K, Ganna A, Witterick I, Gentili F. Expanded Endoscopic Endonasal Approach for Treatment of Clival Chordomas: Early Results in 12 Patients. *Neurosurgery* (2008) 63(2):299–307. doi: 10.1227/01.NEU.0000316414.20247.32
19. Hong Jiang W, Ping Zhao S, Hai Xie Z, Zhang H, Zhang J, Yun Xiao J. Endoscopic Resection of Chordomas in Different Clival Regions. *Acta Otolaryngol* (2009) 129(1):71–83. doi: 10.1080/00016480801995404
20. Koutourousiou M, Gardner PA, Tormenti MJ, Henry SL, Stefko ST, Kassam AB, et al. Endoscopic Endonasal Approach for Resection of Cranial Base Chordomas: Outcomes and Learning Curve. *Neurosurgery* (2012) 71(3):614–25. doi: 10.1227/NEU.0b013e31825ea3e0
21. Kassam AB, Prevedello DM, Carrau RL, Snyderman CH, Thomas A, Gardner P, et al. Endoscopic Endonasal Skull Base Surgery: Analysis of Complications in the Authors' Initial 800 Patients. *J Neurosurg* (2011) 114(6):1544–68. doi: 10.3171/2010.10.JNS09406
22. Bai J, Li M, Xiong Y, Shen Y, Liu C, Zhao P, et al. Endoscopic Endonasal Surgical Strategy for Skull Base Chordomas Based on Tumor Growth Directions: Surgical Outcomes of 167 Patients During 3 Years. *Front Oncol* (2021) 22(11):724972. doi: 10.3389/fonc.2021.724972
23. Bongers MER, Dea N, Ames CP, Schwab JH. Surgical Strategies for Chordoma. *Neurosurg Clin N Am* (2020) 31(2):251–61. doi: 10.1016/j.nec.2019.11.007
24. Potluri S, Jefferies SJ, Jena R, Harris F, Burton KE, Prevost AT, et al. Residual Postoperative Tumor Volume Predicts Outcome After High-Dose Radiotherapy for Chordoma and Chondrosarcoma of the Skull Base and Spine. *Clin Oncol (R Coll Radiol)* (2011) 23(3):199–208. doi: 10.1016/j.clon.2010.09.011
25. Gheorghiu ML, Gheorghisan-Galateanu AA. Clivus Chordoma. *Acta Endocrinol (Buchar)* (2019) 15(3):406. doi: 10.4183/aeb.2019.406
26. Hafez RFA, Fahmy OM, Hassan HT. Gamma Knife Surgery Efficacy in Controlling Postoperative Residual Clival Chordoma Growth. *Clin Neurol Neurosurg* (2019) 178:51–5. doi: 10.1016/j.clineuro.2019.01.017
27. Boriani S, Chevalley F, Weinstein JN, Biagini R, Campanacci L, De Iure F, et al. Chordoma of the Spine Above the Sacrum. Treatment and Outcome in 21 Cases. *Spine (Phila Pa 1976)* (1996) 21(13):1569–77. doi: 10.1097/00007632-199607010-00017
28. Hug EB, Loredo LN, Slater JD, DeVries A, Grove RI, Schaefer RA, et al. Proton Radiation Therapy for Chordomas and Chondrosarcomas of the Skull Base. *J Neurosurg* (1999) 91(3):432–9. doi: 10.3171/jns.1999.91.3.0432
29. Riva P, Crosti F, Orzan F, Dalprà L, Mortini P, Parafioriti A, et al. Mapping of Candidate Region for Chordoma Development to 1p36.13 by LOH Analysis. *Int J Cancer* (2003) 107(3):493–7. doi: 10.1002/ijc.11421

Conflict of Interest: The authors declare that the research was conducted in the absence of any commercial or financial relationships that could be construed as a potential conflict of interest.

Publisher's Note: All claims expressed in this article are solely those of the authors and do not necessarily represent those of their affiliated organizations, or those of the publisher, the editors and the reviewers. Any product that may be evaluated in this article, or claim that may be made by its manufacturer, is not guaranteed or endorsed by the publisher.

frontiers | Frontiers in Endocrinology

ORIGINAL RESEARCH
published: 25 April 2022
doi: 10.3389/fendo.2022.837025

Outcome of Endoscopic Transsphenoidal Surgery for Recurrent or Residual Pituitary Adenomas and Comparison to Non-Recurrent or Residual Cohort by Propensity Score Analysis

Xuan Gong[1], Yang Zhuo[1], Huichun Yuan[2], Kui Yang[1], Chuntao Li[1], Songshan Feng[1], Mingyu Zhang[1], Zhenyan Li[1], Hongshu Zhou[1] and Zhixiong Liu[1]**

[1] Department of Neurosurgery, Xiangya Hospital, Central South University, Changsha, China, [2] Department of Neurosurgery, The First People's Hospital of Changde, Changde, China

OPEN ACCESS

Edited by:
Run Yu, University of California, Los Angeles, CA, United States

Reviewed by:
Mehdi Zeinalizadeh, Tehran University of Medical Sciences, Iran
Sauradeep Sarkar, Christian Medical College & Hospital, India

***Correspondence:**
Zhixiong Liu
zhixiongliu@csu.edu.cn
Hongshu Zhou
zhou_hs@csu.edu.cn

Specialty section:
This article was submitted to Pituitary Endocrinology, a section of the journal Frontiers in Endocrinology

Received: *16 December 2021*
Accepted: *21 March 2022*
Published: *25 April 2022*

Citation:
Gong X, Zhuo Y, Yuan H, Yang K, Li C, Feng S, Zhang M, Li Z, Zhou H and Liu Z (2022) Outcome of Endoscopic Transsphenoidal Surgery for Recurrent or Residual Pituitary Adenomas and Comparison to Non-Recurrent or Residual Cohort by Propensity Score Analysis. Front. Endocrinol. 13:837025. doi: 10.3389/fendo.2022.837025

Objective: To evaluate the long-term outcomes and safety of endoscopic transsphenoidal surgery (ETS) in recurrent and residual pituitary adenomas (rrPAs), as well as the predictors of gross total resection (GTR) and intraoperative CSF leakage. Furthermore, to compare outcomes and complications with non-rrPAs cohort.

Methods: Clinical and radiological characteristics of patients with rrPAs who underwent ETS were collected between 2017 and 2020. Data of patients with non-rrPAs were collected from 2019 to 2020. Logistic regression analyses were performed to investigate the factors influencing gross total resection (GTR) and intraoperative CSF leakage. Between-group comparisons of outcomes and complications were performed through propensity score analysis.

Results: We enrolled 73 patients with rrPAs. GTR was achieved in 41 (56.1%) cases; further, GTR or near-total resection was achieved in 93.2% of patients. The mean tumor volumes for GTR and non-GTR cases were 6.2 ±7.2 cm^3 and 11.1 ±9.1 cm^3, respectively. Multivariate regression analysis of the GTR rate in patients with rrPAs revealed that Knosp grade was an independent factor (odds ratio [OR] = 0.324; p=0.005). Moreover, previous transcranial surgery and non-functional pituitary adenomas were risk factors for intraoperative CSF leakage in patients with rrPAs (OR=6.450, p=0.019 and OR=7.472, p=0.012, respectively). After propensity score matching, There was no significant difference in the GTR rate between patients with rrPAs and patients with non-rrPAs. Contrastingly, patients with rrPAs had a higher rate of intraoperative CSF leakage and longer postoperative hospital stay than patients with non-rrPAs. During the follow-up, vision improved in 9 (22.0%) and 24 (62.5%) patients with rrPAs and non-rrPAs, respectively. Although there was a trend that reoperation of rrPAs involved a lower

hypopituitarism recovery rate and biochemical remission rate, as well as a higher hypopituitarism rate, there was no statistically significant between-group difference.

Conclusions: Knosp grade was an independent factor for GTR in endoscopic transsphenoidal surgery in patients with rrPAs. Previous transcranial surgery and non-functional PAs were risk factors for intraoperative CSF leakage. Although associated with longer hospital stay, rrPAs did not associate with lower GTR rate or more frequent postoperative complications than non-rrPAs cohort.

Keywords: pituitary adenoma, endonasal endoscopic surgery, recurrence, gross total resection, repeat transsphenoidal surgery

INTRODUCTION

Transsphenoidal surgery is the initial treatment of choice for most non-prolactin-secreting pituitary adenomas (PAs) (1, 2). Since the introduction of endoscopy into transsphenoidal surgery, it has gained acceptance due to allowing better visualization of the supra- and parasellar regions, as well as minimal structures. There have been promising results regarding the tumor resection rates and postoperative complications after endoscopic transsphenoidal surgery (ETS) (3–7). However, PAs are likely to recur even after complete resection, especially in the long term. The reported overall recurrence rate after gross total resection (GTR) is 7%–33%, with cases of incomplete resection showing higher recurrence rates (8–12). Risk factors for recurrence include labeling index, cavernous sinus invasiveness, and young age at diagnosis (9, 13, 14).

Radiation therapy and medication are relatively safe treatment options for recurrent PAs (15, 16). However, repeat surgery is often preferred when the tumor is very large, close to optic chiasm or hormone secreting (17–19). Repeat surgery for recurrent or residual PAs (rrPAs) is technically challenging due to the absence of anatomical landmarks and presence of scar tissue. Compared with initial surgeries, re-operative pituitary surgeries have more frequent complications and a lower GTR rate (20–23). However, few studies explored factors affecting GTR or risk factors for complications of re-operative pituitary surgery. Perhaps even less studies compared the outcomes of ETS for rrPAs with those for non-recurrent or residual pituitary adenomas (non-rrPAs). This study aimed to describe a series of cases of rrPAs resected through ETS and to explore factors related to GTR and intraoperative CSF leakage. Furthermore, we aimed to compare the outcomes and complications of ETS for rrPAs and non-rrPAs.

METHODS

Data Collection

After obtaining institutional review board approval and full patient consent, we collected data from consecutive patients diagnosed with rrPAs who underwent planned ETS in the Department of Neurosurgery of Xiangya Hospital, Central South University from January 2017 to June 2020. Besides, we included patients with non-rrPAs who underwent ETS in the same hospital from January 2019 to June 2020. All surgical procedures were performed by the senior authors ZY Li, and ZX Liu. Further, we retrospectively analyzed demographic, clinical, radiological, and surgical outcomes.

Perioperative Evaluation

Pre- and post-operative hormone levels, including cortisol (8 am), adrenocorticotropic hormone (ACTH) (8 am), T3, T4, thyroid-stimulating hormone, prolactin, growth hormone, testosterone, estradiol, luteinizing hormone, and follicle-stimulating hormone, were examined in each patient. Prolactinoma, acromegaly, and Cushing disease were diagnosed as previously described (2, 24, 25). For patients with prolactinomas, remission was indicated by prolactin levels < 20 ng/mL and <15 ng/mL in women and men, respectively, on the day after surgery. For patients with growth hormone (GH)-secreting adenomas, biochemical remission was defined by a GH value < 0.4 ng/mL after a 75-g oral glucose load or a random GH value < 1.0 ng/ml and normal levels of insulin-like growth factor with adjustment for sex and age (19, 26). Remission of Cushing's disease was indicated by early-morning cortisol levels of 1.8 mg/ml in the first 48 postoperative hours and normalization of the 24-h levels of urinary free cortisol (27). Ophthalmologists blinded to the surgery outcomes evaluated the vision and visual fields pre- and post-operatively. High-resolution and regular CT scans were used to evaluate the bony anatomy of the skull base before surgery and hematoma after surgery. All patients underwent contrast-enhanced magnetic resonance (MR) imaging preoperatively and 1–2 days postoperatively.

Surgical Techniques

All surgical procedures were performed using an endoscopic transsphenoidal approach with a 0° and 30° rigid endoscope. For cases with a large portion of suprasellar extension or cavernous sinus invasion, an extended transsphenoidal or trans-cavernous sinus approach was applied as previously described (5, 28–32). Surgical navigation and mini-Doppler were routinely performed, especially in cases with tumor invasion in the cavernous sinus. A pedicled nasal mucosal flap was routinely formed, as appropriate. In case of an intraoperative high-flow CSF leakage, a fascia lata graft was harvested and placed in the sellar turcica, followed by covering with a pedicled mucosal flap, application of absorbable

fibrin glue, and nasal packing. Postoperative low flow or high flow CSF leaks were evaluated not only based on the symptoms but also on the radiologic findings. In patients with no intraoperative CSF leak, if pneumocephalus presented on the CT after surgery, high-flow postoperative CSF leak was considered. While in patients with high-flow intraoperative CSF leak, If pneumocephalus on the CT scan increased or reoccurred several days after surgery, even a little amount of CSF discharge from the nose, high-flow postoperative CSF leak was also considered. In case of postoperative low-flow CSF leakage, conservative measures were applied, including 7-day bed rest with a head elevated 30 to 45 degrees and avoidance of nose blowing or coughing during lumbar drainage. Repair surgery was performed in case of postoperative high-flow CSF leakage that continued after lumbar drainage.

Follow-up

Patients were followed up at 1, 3 and 6 postoperative months and subsequently annually. Neurological, endocrinological and MR images evaluations were performed for each patient. The extent of resection was evaluated on MRI at 3 postoperative months. A picture archiving and communication system was used to review all MR images. Two senior radiologists calculated the tumor volume using the ellipsoid model "(ABC)/2" equation. GTR, near-total resection, subtotal resection, and partial removal were indicated by removal of 100%, 90%–99%, 50%–90%, and < 50% of the tumor volume, respectively. For the functional pituitary adenomas, GTR was also required to meet the criteria of biochemical remission.

Statistical Analysis and Propensity Score Matching

Continuous variables are presented as mean ± standard deviation and range. Categorical and continuous variables were analyzed using Pearson's chi-square test and Mann-Whitney U-test, respectively. Logistic regression analysis was performed to determine independent predictive factors for postoperative CSF leakage. Statistical significance was set at $p < 0.05$. Statistical analyses were performed using SPSS 22.0 (IBM Corporation).

Postoperative outcomes were compared between patients with rrPAs and non- rrPAs using propensity score analysis. This methodology was applied to reduce between-group imbalance in the baseline patient characteristics. Based on covariates from the logistic model, we generated a propensity score for each patient in terms of age, sex, functional adenomas, tumor volume, and Knosp grade. Based on the inclusion criteria, 212 patients with non-rrPAs were consecutively recruited. We used a nearest-matching algorithm with a 1:1 ratio. Statistical analysis was performed using the R statistical program (version 4.4.0; R Core Team).

RESULTS

Clinical Characteristics

According to the inclusion criteria, we enrolled 73 patients with rrPAs (mean age: 48.0±12.5 years). Among them, 41 (56.2%) and 14 (19.2%) presented with vision impairment and headaches. Moreover, 17 patients presented with endocrinological hyperfunction, including 3, 11, and 3 with prolactinomas, acromegaly, and Cushing's disease, respectively. Additionally, 12 (16.4%) patients were asymptomatic upon admission (**Table 1**). With respect to initial surgery, 58 (79.5%) and 15 (20.5%) patients underwent initial endoscopic transsphenoidal surgery and microscopic transcranial surgery, respectively. The mean interval between initial and repeat surgery was 65.9 ±59.2 months. Six patients (8.8%) in the rrPA group received prior stereotactic radiotherapy and three patients (4.4%) had bromocriptine before repeat surgery. Upon reoperation, the mean tumor volume was 8.4 ±8.4 cm^3. In our series, 57 (78.1%) and 16 (21.9%) patients had tumors of Knosp-Steiner grades 3–4 and 1–2 for invasion, respectively.

Extent of Tumor Resection

Among the 73 rrPA patients, 41 (56.2%) achieved GTR (**Figure 1**), 27 (37.0%) underwent near-total resection (**Figure 2**), 4 (5.5%) underwent subtotal resection, and 1 (1.4%) underwent partial resection (**Table 1**). **Table 2** presents a comparison of the patients' baseline characteristics between the GTR and non-GTR groups. Overall, there was no significant between-group difference in age and sex distributions. Among patients who achieved GTR in repeat surgery, 35 and 6 patients underwent prior transsphenoidal and transcranial surgeries, respectively. In the non-GTR group, 23 and 9 patients underwent prior transsphenoidal and transcranial surgeries, respectively. GTR showed a non-significant tendency to be achieved in patients with prior transsphenoidal surgery. The mean interval between the initial surgery and reoperation in the GTR and non-GTR groups were 59.3 ±38.1 and 74.3 ±78.4 months, respectively. Among functional PAs, GTR and non-GTR were achieved in nine and eight patients, respectively. The GTR group had a significantly lower mean tumor volume than the non-GTR group (6.2 ±7.2 cm^3 vs. 11.1 ±9.1 cm^3, $p = 0.012$). Proportion of high Knosp grade cases was found to be significantly higher in non-GTR group than in GTR group (93.8% vs 65.9%, p=0.002).

TABLE 1 | Clinical characteristics of rrPAs.

Characteristics	No. of Patients (%)
Onset symptoms	
Visual loss/Visual field cuts	41 (56.2)
Headaches	14 (19.2)
Asymptomatic	12 (16.4)
Hormonal hyperfunction	17 (23.3)
Acromegaly	11 (15.1)
Prolactinomas	3 (4.1)
Cushing diseases	3 (4.1)
Preoperative hormonal deficiency	35 (47.9)
Single axis	23 (31.5)
Multiple axis	12 (16.4)
None	38 (52.1)
Extent of resection	
Gross total resection	41 (56.2)
Near-total resection	27 (37.0)
Subtotal resection	4 (5.5)
Partial resection	1 (1.4)

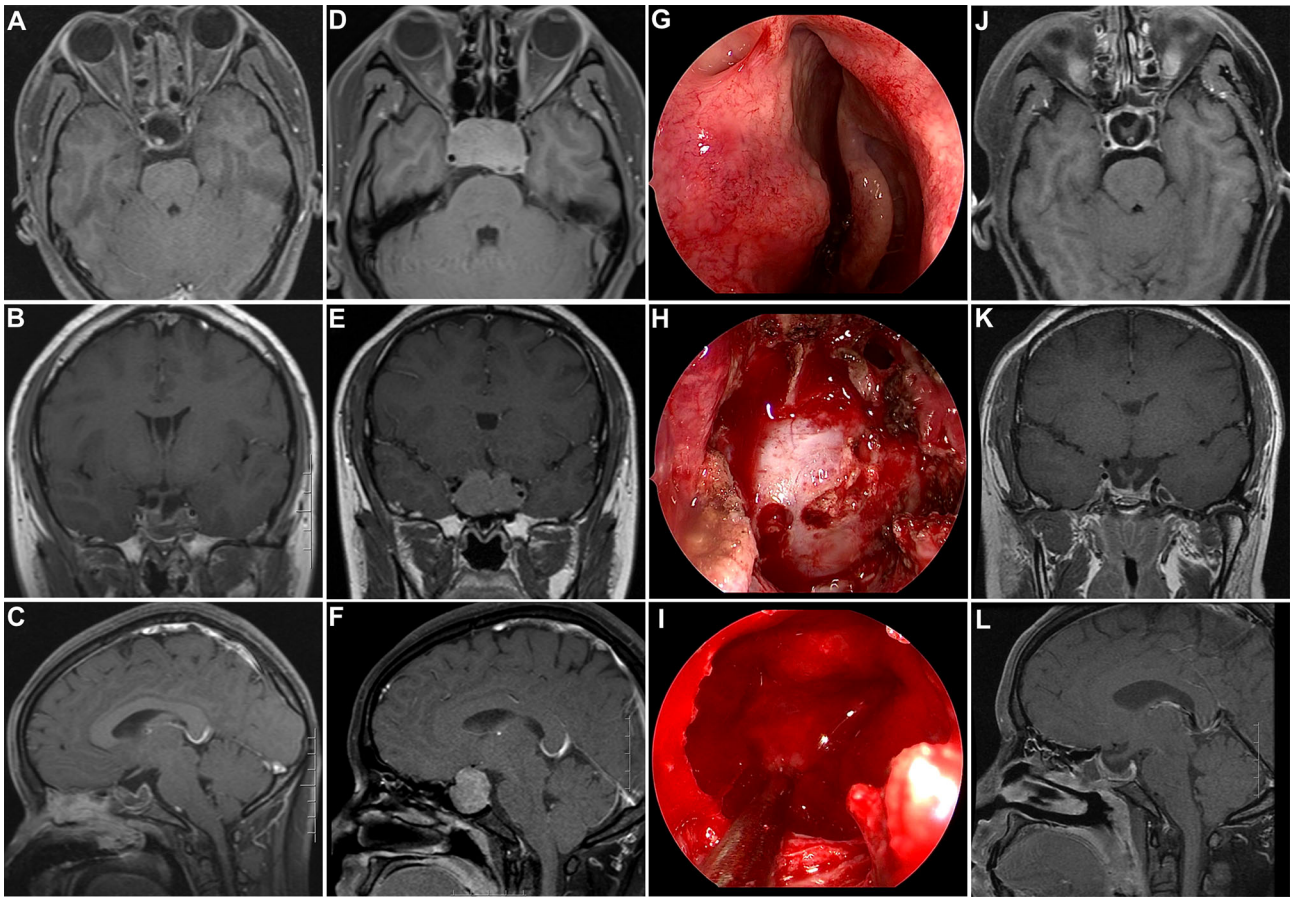

FIGURE 1 | Illustrative case of a recurrent non-functional PA after prior transsphenoidal surgery. **(A–C)** Postoperative post-contrast T1-weighted MR images showing GTR after initial transsphenoidal surgery. **(D–F)** Post-contrast T1-weighted MR images showing tumor recurrence after 6 years. **(G–I)** Intraoperative photographs during repeat transsphenoidal surgery. **(H)** Wide sphenoidotomy was performed and a dural defect caused by the initial surgery was observed. **(I)** After tumor removal, the compressed pituitary and intact diaphragm sellae were displayed. **(J–L)** Post-contrast T1-weighted MR images acquired 3 months after repeated surgery showed complete tumor removal; additionally, both the pituitary and stalk were discernable.

Preoperative Predictors for GTR of rrPAs

To investigate factors related to the GTR rate in rrPAs, we performed logistic regression analysis with clinical characteristics, tumor volume, and Knosp grade. Univariate regression analysis revealed that patients with a larger tumor volume or higher Knosp grade had a higher risk of undergoing non-GTR. After adjustment for confounding factors in multivariate analysis, only Knosp grade was a significant adverse predictor (OR 0.324, 95% CI 0.147–0.715, p = 0.005), which indicated that tumors with higher Knosp grade are more difficult to achieve GTR (**Figure 3**).

Clinical Outcomes

Among the 41 patients with preoperative vision impairment, vision status improved and remained stable in 9 (22.0%) and 30 (73.2%) patients, respectively. Two patients (4.9%) complained of postoperative vision deterioration, with both showing partial improvement after hyperbaric oxygen therapy during follow-up. At the final follow-up, 18 patients recovered from preoperative hypopituitarism and 5 patients developed hormonal deficiency requiring hormonal replacement therapy. Endocrinological remission was achieved in 8 cases, including 1, 5, and 2 with prolactinoma, GH-secreting adenomas, and ACTH-secreting adenomas, respectively. The other patient with ACTH-secreting adenoma showed temporary biochemical relief without residue on postoperative MRI. However, the patient developed Cushing syndrome at one postoperative year, with no mass being observed on dynamic contrast-enhanced MRI.

Postoperative Complications

Postoperative CSF leakage occurred in five (9.6%) cases and ceased in five patients after lumbar drainage, with the remaining two patients undergoing repair surgery. Meningitis occurred in four cases and was successfully treated using antibiotics. Epistaxis occurred in four patients. Two patients were cured by nasal packing; the other 2 patients relieved after surgical treatment. Diabetes insipidus temporarily existed in 29 (39.7%) patients, with all patients showing relief during follow-up.

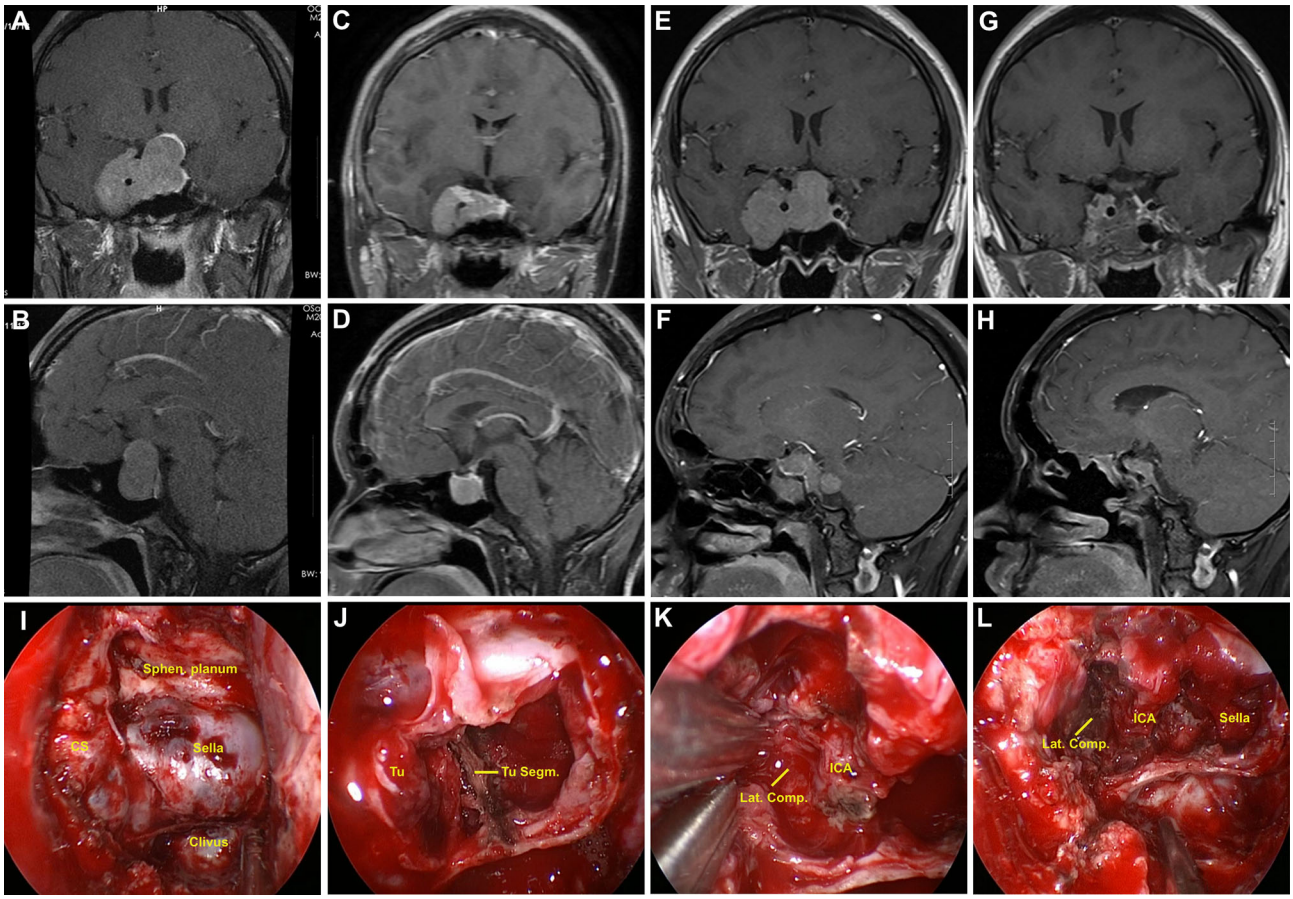

FIGURE 2 | Illustrative case of a residual GH-secreting PA after prior transcranial surgery. **(A, B)** Preoperative coronal and sagittal post-contrast MR images showing a giant PA (Knosp grade 4), with the mass extending to the suprasellar area and cavernous sinus; moreover, cavernous segment of internal carotid artery (ICA) was totally encased by the tumor. **(C, D)** The patient had undergone transcranial surgery at another hospital. Early postoperative follow-up MR images revealed partial tumor removal. **(E, F)** Post-contrast T1-weighted MR images acquired one year after initial surgery showed residual tumor regrowth. **(G–H)** Postoperative MR images revealed near-total tumor removal. A small tumor piece was present at superior lateral compartment (Lat. Comp.)of cavernous sinus owing to adhesion. **(I–L)** Intraoperative photographs during repeat transsphenoidal surgery. **(I)** Sella and right cavernous sinus were widely exposed. **(J)** After debulking, tumor segmentation (Tu. Segm.) was observed. **(K)** Tumor in the right cavernous sinus presented fibrous and rubbery texture, and was sharply dissected from ICA. **(L)** Cavernous segment of ICA was observed after tumor removal. Sphen, sphenoidal.

Risk Factors for Intraoperative CSF Leakage of rrPAs

Almost all patients with postoperative CSF leakage experienced intraoperative CSF leakage. During reoperation, intraoperative CSF leakage occurred in 35 patients. We divided all the 73 patients into those with or without intraoperative CSF leakage. Patients with intraoperative CSF leakage had a longer postoperative hospital stay (12.5 ±10.9 days) than those without (8.1 ±5.8 days, $p = 0.041$). Logistic regression analyses were performed to determine the risk factors for intraoperative CSF leakage. Prior transcranial approach (OR 6.450, 95% CI 1.35511–30.696, $p = 0.019$) and non-functional adenomas (OR 7.472, 95% CI 1.562–35.737, $p = 0.012$) were significantly associated with intraoperative CSF leakage during reoperation (**Figure 4**).

Outcomes and Complications Comparison Between rrPAs and Non-rrPAs

We then matched 73 cases of non-rrPAs from 212 patients with each case of the rrPAs group using propensity-score matching. After matching, there was no significant between-group difference in preoperative clinical characteristics. The rrPA group had a non-significantly higher GTR rate than the non-rrPA group (61.6% vs. 58.9%). There were no significant between-group differences in postoperative complications, including postoperative CSF leakage and meningitis. However, the rrPA group had a significantly higher incidence of intraoperative CSF leakage and a longer postoperative hospital stay than the non-rrPA group ($p < 0.0001$ and $p = 0.017$, respectively). Epistaxis was observed in four and no patients in

TABLE 2 | Preoperative characteristics of rrPAs classified by GTR.

Characteristics	No. of Patients (%)			p Value
	Total	GTR	Non-GTR	
	73	41 (56.2)	32 (43.8)	
Gender				0.501
Male	31 (42.5)	16 (39.5)	15 (48.0)	
Female	42 (57.5)	25 (60.5)	17 (52.0)	
Mean age at op (yrs)	48.0 ± 12.5	47.9 ± 11.4	48.2 ± 14.0	0.903
Prior Approach				0.157
TSS	58 (79.5)	35 (85.4)	23 (71.9)	
TC	15 (20.5)	6 (14.6)	9 (28.1)	
Interval btwn initial & reop (mos)	65.9 ± 59.2	59.3 ± 38.1	74.3 ± 78.4	0.325
Function				
Functional	17 (23.3)	9 (22.0)	8 (25.0)	0.760
Non-functional	56 (76.7)	32 (78.0)	24 (75.0)	
Tumor volume (cm^3)	8.4 ± 8.4	6.2 ± 7.2	11.1 ± 9.1	0.012
Knosp grade				0.002
0	5 (6.8)	5 (12.2)	0 (0.0)	
1	5 (6.8)	5 (12.2)	0 (0.0)	
2	6 (8.2)	4 (9.8)	2 (6.3)	
3 (3a,3b)	32 (43.8)	20 (48.8)	12 (37.5)	
4	25 (34.2)	7 (17.1)	18 (56.3)	

Op, operation; TSS, transsphenoidal surgery; TC, transcranial surgery; reop, reoperation.

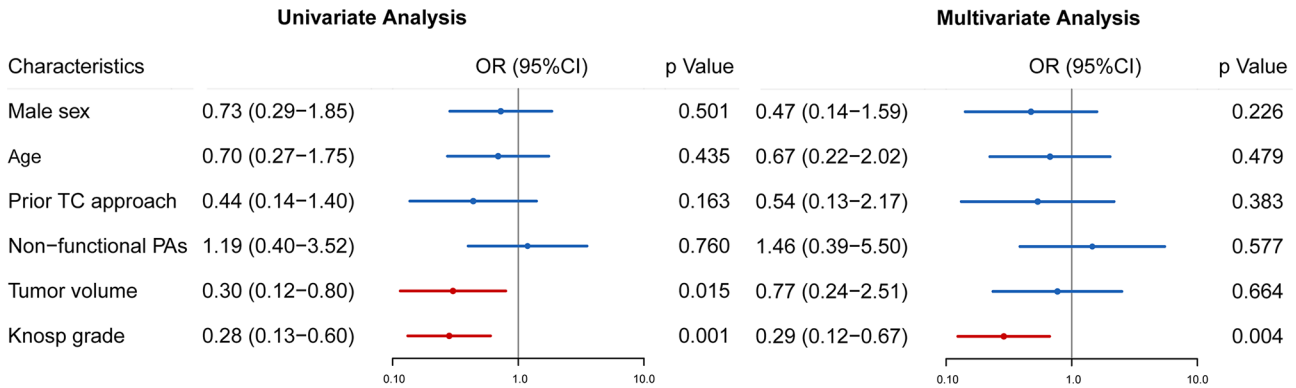

FIGURE 3 | Univariate and multivariate analyses were performed to identify preoperative factors influencing GTR in patients with rrPAs. Odds ratio (OR), 95% confidence intervals (CI) and p value are exhibited for comparison.

the rrPA and non-rrPA groups, respectively. Among the patients who presented preoperative vision impairment, 24 (57.1%) and 9 (22%) patients in the non-rrPA and rrPA groups, respectively, showed postoperative vision improvement (p = 0.002). There was no significant between-group difference in the rate of hypopituitarism recovery or biochemical remission (**Table 3**).

DISCUSSION

Surgical Outcomes

In our series, most symptomatic patients showed improvement after endoscopic transsphenoidal surgery. Specifically, 97.3% (71/73) of the patients showed improved/stable visual acuity while 51.4% of the patients recovered from preoperative hypopituitarism. Endocrinological remission was achieved in 47.1% of the patients. Do et al. reported biochemical remission in 9 out of 12 (75%) functional PAs and improved/stable visual acuity in 38 out of 40 (95%) non-functional PAs (33). Hwang et al. reported vision improvement in 19 (79%) patients (34). Our findings are generally comparable with these previous reports.

The average postoperative follow-up duration for patients with rrPAs was 29 months (range, 8–55 months). GTR was achieved in 42 (56.1%) patients, which is higher than previously reported values (14, 22, 33, 35, 36). Most tumors in re-operative patients were residual from the initial surgery rather than recurrence. For maximal resection of rrPAs, it is important to evaluate the location and reason of the residual tumor. In our series, residual tumors were more common in the parasellar and suprasellar regions after prior transsphenoidal surgery. Contrastingly, residual tumors were more common in the sphenoidal sinus and parasellar region after initial transcranial

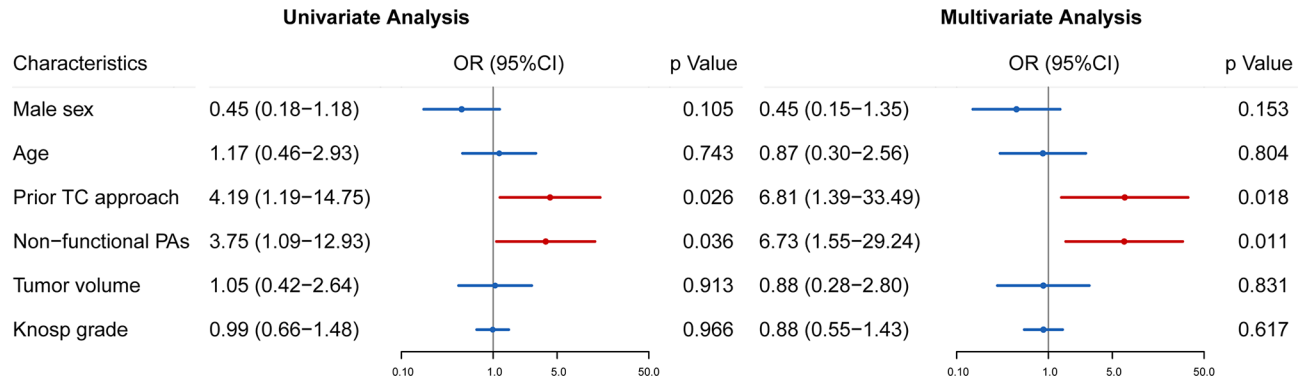

FIGURE 4 | Univariate and multivariate analyses were used to identify risk factors for intraoperative CSF leakage in reoperation of rrPAs. Odds ratio (OR), 95% confidence intervals (CI) and p value are exhibited for comparison.

TABLE 3 | Preoperative Characteristics of non-rrPAs and rrPAs after propensity score matching.

	No. of Patients(%)			
Characteristics	**Total**	**Non-rrPAs**	**rrPAs**	**p value**
Gender	146	73	73	0.320
Male	68 (46.6)	37 (50.7)	31 (42.5)	
Female	78 (53.4)	36 (49.3)	42 (57.5)	
Mean age at op (yrs)	47.2 ± 13.7	46.5 ± 14.7	48.0 ± 12.5	0.499
Function				0.701
Functional PAs	36 (24.7)	19 (26.0)	17 (23.3)	
Non-functional PAs	110 (75.3)	54 (74.0)	56 (76.7)	
Tumor volume (cm^3)	9.1 ± 9.9	9.8 ± 11.2	8.4 ± 8.4	0.383
Knosp grade				0.825
0	11 (7.5)	6 (8.2)	5 (6.8)	
1	8 (5.5)	3 (4.1)	5 (6.8)	
2	10 (6.8)	4 (5.5)	6 (8.2)	
3 (3a,3b)	62 (42.5)	30 (41.1)	32 (43.8)	
4	55 (37.7)	30 (41.1)	25 (34.2)	
Extent of resection				0.501
GTR	86 (58.9)	45 (61.6)	41 (56.2)	
Non-GTR	60 (41.1)	28 (38.4)	32 (43.8)	
Intraoperative CSF leak	46 (31.5)	11 (15.1)	35 (47.9)	<0.0001
Postoperative CSF leak	9 (61.6)	2 (2.7)	7 (9.6)	0.275
Meningitis	6 (41.1)	2 (2.7)	4 (5.5)	0.681
Epistaxis	4 (2.7)	0 (0)	4 (5.5)	0.120
LOS (days)	8.8 ± 7.2	7.34 ± 4.9	10.2 ± 8.8	0.017
Vision improved	33/83 (39.8)	24/42 (57.1)	9/41 (22.0)	0.002
Hypopituitarism recovered	33/59 (55.9)	15/24 (62.5)	18/35 (51.4)	0.436
Biochemical remission	21/36 (58.3)	13/19 (68.4)	8/17 (47.1)	0.311
Newly hypopituitarism	9/87(10.3)	4/49 (2.0)	5/38 (13.2)	0.496

Op, operation; LOS, length of postoperative hospital stay.

surgery. Inadequate opening of the sphenoid and sella is frequently observed. Therefore, for re-operation, we prefer wide sphenoidotomy and wide exposure of the sellar floor. For tumors extensively invading the supra-diaphragmatic region, the tuberculum sellae and planum were also removed. The anterior wall of the cavernous sinus was opened when the mass invaded the lateral compartment of the cavernous sinus (30). Moreover, the scar and tumor segmentation can impede the achievement of GTR during repeat surgery. Specifically, several tumor parts can be hidden by a tough fibrous septum to misguide the surgeon. It is important to thoroughly examine the tumor segmentation on preoperative MRI and to distinguish it from the normal boundary during surgery for complete mass removal. Doppler devices and precise neuronavigation facilitate accurate mapping of the carotid artery, as well as distinguishing the tumor compartment and anatomical boundary.

Preoperative factors influencing GTR remain unclear. The extent of resection is reported to be correlated with cavernous sinus invasion, tumor size, and initial surgery (endoscopic or microscopic transsphenoidal approach) (21, 33). Another study

reported that Knosp-Steiner Grade 3–4 status was significantly associated with a non-GTR; however, GTR did not differ according to the prior approach (19). In our study, univariate analysis revealed a higher tumor volume and Knosp grade indicated a lower GTR rate. However, in the logistic regression model, only Knosp grade was an independent predictor of GTR. Tumors invading the lateral compartment of the cavernous sinus (Knosp grade 4) are challenging even with a trans-cavernous sinus approach, which could be attributed to the invasive tumor nature indicated by extension into the lateral compartment of the cavernous sinus and the resulting anatomical complexity (37, 38). Do et al. reported a GTR rate of 51.7% in patients who underwent reoperation for PA (70.3% and 21.7% for patients with Knosp grade 0–2 and 3–4, respectively) (33). In our cases, the GTR rate was 87.5% and 47.4% for patients with Knosp grade 0–2 and 3–4, respectively, which was higher than those in previous studies.

Complications

Although there was a frequent occurrence of postoperative temporary DI in our series, all the patients were relieved during follow-up. Other complications of ETS include CSF leakage, meningitis, and epistaxis. Without prompt care, postoperative CSF leakage can cause severe outcomes, including meningitis or pneumocephalus. Intraoperative CSF leakage is reported to be an independent risk factor for postoperative CSF leakage (39–41). We found that prior transcranial surgery was an independent risk factor for intraoperative CSF leakage in re-operative ETS. Among patients who were previously treated with transcranial and transsphenoidal surgery, intraoperative CSF leakage occurred in 12 (80%) and 23 (39.7%) patients, respectively. This could be attributed to destruction of the diaphragm sellae and opening of the optic chiasmatic cistern during the prior transcranial surgery. Further, initial transcranial approach is generally chosen when the tumor has a large suprasellar component, where the residual tumor may remain. This may increase the risk of intraoperative CSF leakage during repeat surgery.

Given the morbidity of repeat transsphenoidal surgery, Radiation therapy including fractionated RT or stereotactic radiosurgery and medication (such as temozolomide) are also relatively safe treatment options for recurrent PAs.

RrPAs Versus Non-rrPAs

Numerous reports have indicated that patients with rrPAs have a lower GTR and present with more complications than patients with non-rrPAs. However, most studies comparing GTR and complications between non-rrPAs and rrPAs were based on meta-analyses or previously published data (9, 11, 19, 32, 42). In this study, we used propensity score matching to mitigate between-group imbalance and found that the rrPA group had a significantly higher rate of intraoperative CSF leakage and longer postoperative hospital stay than the non-rrPA group. However, there was no between-group difference in the GTR rate and postoperative complications, which were inconsistent with previous findings. This could be attributed to the between-group differences in preoperative characteristic which may have resulted in outcome bias. Furthermore, the re-operations for rrPAs and surgery for non-rrPAs in previous studies were not performed by the same surgeons. Additionally, there are among-surgeon differences in techniques and experience, as well as among-institution differences in available armamentarium and materials. Yamada et al. also reported no difference in the complication rate between initial and repeat surgeries for rrPAs performed by experienced surgeons (11). Our study indicated that the extent of resection was affected by preoperative clinical features, including Knosp grade, but not by scarring and distorted anatomy caused by initial surgery. Although the rate of intraoperative CSF leak was higher for repeat surgery than for first-time surgery, a thorough multi-layer reconstruction technique could mitigate the rate of postoperative CSF leak after repeat surgery.

Limitations

This study had several limitations. First, this was a single-institution study, potential bias may exist in patient selection for the different surgical procedures Second, although we included numerous clinical factors, several other preoperative characteristics including tumor segmentation, tumor lobulation, tumor fibrosis and Hardy stage were not analyzed in this study.

CONCLUSION

The current study reported a series of re-operative endoscopic transsphenoidal surgeries performed on patients with rrPAs, which exhibited excellent outcomes and relatively low complication rates. Knosp grade was an independent predictor of GTR in repeat transsphenoidal surgeries. Previous transcranial surgery and non-functional PAs were significantly associated with intraoperative CSF leakage during reoperation. There is a need for careful decision-making for patients with previous transcranial surgery or non-functional PA regarding undergoing revision transsphenoidal surgery in case of CSF leakage. Compared with initial surgery, endonasal endoscopic reoperation allows comparable outcomes and complication rates.

DATA AVAILABILITY STATEMENT

The raw data supporting the conclusions of this article will be made available by the authors, without undue reservation.

ETHICS STATEMENT

Studies involving human participants were reviewed and approved by Medical Ethics Committee of the Xiangya Hospital, Central South University (No.201612816). Written informed consent was obtained from the individual(s) for publication of any potentially identifiable images included in this article.

AUTHOR CONTRIBUTIONS

Conception and design: XG and ZXL. Acquisition of data: HSZ, YZ, and HCY. Analysis and interpretation of data: HSZ

and XG. Drafting the article: HSZ and XG. Critically revising the article: XG, HSZ and ZXL. Statistical analysis: XG and HSZ. Administrative/technical/material support: CTL, KY, SSF, MYZ, and ZYL. Study supervision: ZXL. All authors contributed to the article and approved the submitted version.

FUNDING

This study was supported by the National Natural Science Foundation of China (grant No. 81701285, 81873635, 82172685) and the Natural Science Foundation of Hunan Province (grant No. 2018JJ3824).

REFERENCES

1. Ammirati M, Wei L, Ciric I. Short-Term Outcome of Endoscopic Versus Microscopic Pituitary Adenoma Surgery: A Systematic Review and Meta-Analysis. *J Neurol Neurosurg Psychiatry* (2013) 84(8):843–9. doi: 10.1136/jnnp-2012-303194
2. Molitch ME. Diagnosis and Treatment of Pituitary Adenomas: A Review. *JAMA* (2017) 317(5):516–24. doi: 10.1001/jama.2016.19699
3. Chowdhury T, Prabhakar H, Bithal PK, Schaller B, Dash HH. Immediate Postoperative Complications in Transsphenoidal Pituitary Surgery: A Prospective Study. *Saudi J Anaesth* (2014) 8(3):335–41. doi: 10.4103/1658-354X.136424
4. Cappabianca P, Cavallo LM, Solari D, Stagno V, Esposito F, de Angelis M. Endoscopic Endonasal Surgery for Pituitary Adenomas. *World Neurosurg* (2014) 82(6 Suppl):S3–11. doi: 10.1016/j.wneu.2014.07.019
5. Hofstetter CP, Shin BJ, Mubita L, Huang C, Anand VK, Boockvar JA, et al. Endoscopic Endonasal Transsphenoidal Surgery for Functional Pituitary Adenomas. *Neurosurg Focus* (2011) 30(4):E10. doi: 10.3171/2011.1.FOCUS10317
6. Ciric I, Ragin A, Baumgartner C, Pierce D. Complications of Transsphenoidal Surgery: Results of a National Survey, Review of the Literature, and Personal Experience. *Neurosurgery* (1997) 40(2):225–236; discussion 236-227. doi: 10.1097/00006123-199702000-00001
7. Penn DL, Burke WT, Laws ER. Management of Non-Functioning Pituitary Adenomas: Surgery. *Pituitary* (2018) 21(2):145–53. doi: 10.1007/s11102-017-0854-2
8. Roelfsema F, Biermasz NR, Pereira AM. Clinical Factors Involved in the Recurrence of Pituitary Adenomas After Surgical Remission: A Structured Review and Meta-Analysis. *Pituitary* (2012) 15(1):71–83. doi: 10.1007/s11102-011-0347-7
9. Cavallo LM, Solari D, Tasiou A, Esposito F, de Angelis M, D'Enza AI, et al. Endoscopic Endonasal Transsphenoidal Removal of Recurrent and Regrowing Pituitary Adenomas: Experience on a 59-Patient Series. *World Neurosurg* (2013) 80(3-4):342–50. doi: 10.1016/j.wneu.2012.10.008
10. Cappabianca P, Solari D. The Endoscopic Endonasal Approach for the Treatment of Recurrent or Residual Pituitary Adenomas: Widening What to See Expands What to do? *World Neurosurg* (2012) 77(3-4):455–6. doi: 10.1016/j.wneu.2011.08.047
11. Yamada S, Fukuhara N, Oyama K, Takeshita A, Takeuchi Y. Repeat Transsphenoidal Surgery for the Treatment of Remaining or Recurring Pituitary Tumors in Acromegaly. *Neurosurgery* (2010) 67(4):949–56. doi: 10.1227/NEU.0b013e3181ec4379
12. Benveniste RJ, King WA, Walsh J, Lee JS, Delman BN, Post KD. Repeated Transsphenoidal Surgery to Treat Recurrent or Residual Pituitary Adenoma. *J Neurosurg* (2005) 102(6):1004–12. doi: 10.3171/jns.2005.102.6.1004
13. Noh TW, Jeong HJ, Lee MK, Kim TS, Kim SH, Lee EJ. Predicting Recurrence of Nonfunctioning Pituitary Adenomas. *J Clin Endocrinol Metab* (2009) 94 (11):4406–13. doi: 10.1210/jc.2009-0471
14. Alahmadi H, Dehdashti AR, Gentili F. Endoscopic Endonasal Surgery in Recurrent and Residual Pituitary Adenomas After Microscopic Resection. *World Neurosurg* (2012) 77(3-4):540–7. doi: 10.1016/j.wneu.2011.07.012
15. Minniti G, Paolini S, Rea MLJ, Isidori A, Scaringi C, Russo I, et al. Stereotactic Reirradiation With Temozolomide in Patients With Recurrent Aggressive Pituitary Tumors and Pituitary Carcinomas. *J Neurooncol* (2020) 149(1):123–30. doi: 10.1007/s11060-020-03579-5
16. Iwata H, Sato K, Tatewaki K, Yokota N, Inoue M, Baba Y, et al. Hypofractionated Stereotactic Radiotherapy With CyberKnife for Nonfunctioning Pituitary Adenoma: High Local Control With Low Toxicity. *Neuro Oncol* (2011) 13(8):916–22. doi: 10.1093/neuonc/nor055
17. Moraes AB, Silva CM, Vieira Neto L, Gadelha MR. Giant Prolactinomas: The Therapeutic Approach. *Clin Endocrinol (Oxf)* (2013) 79(4):447–56. doi: 10.1111/cen.12242
18. Rahimli T, Hidayetov T, Yusifli Z, Memmedzade H, Rajabov T, Aghayev K. Endoscopic Endonasal Approach to Giant Pituitary Adenomas: Surgical Outcomes and Review of the Literature. *World Neurosurg* (2021) 149: e1043–55. doi: 10.1016/j.wneu.2021.01.019
19. Negm HM, Al-Mahfoudh R, Pai M, Singh H, Cohen S, Dhandapani S, et al. Reoperative Endoscopic Endonasal Surgery for Residual or Recurrent Pituitary Adenomas. *J Neurosurg* (2017) 127(2):397–408. doi: 10.3171/2016.8.JNS152709
20. Long H, Beauregard H, Somma M, Comtois R, Serri O, Hardy J. Surgical Outcome After Repeated Transsphenoidal Surgery in Acromegaly. *J Neurosurg* (1996) 85(2):239–47. doi: 10.3171/jns.1996.85.2.0239
21. Farrell CJ, Garzon-Muvdi T, Fastenberg JH, Nyquist GG, Rabinowitz MR, Rosen MR, et al. Management of Nonfunctioning Recurrent Pituitary Adenomas. *Neurosurg Clin N Am* (2019) 30(4):473–82. doi: 10.1016/j.nec.2019.05.006
22. Bernat AL, Troude P, Priola SM, Elsawy A, Farrash F, Mete O, et al. Endoscopic Endonasal Pituitary Surgery For Nonfunctioning Pituitary Adenomas: Long-Term Outcomes and Management of Recurrent Tumors. *World Neurosurg* (2021) 146:e341–50. doi: 10.1016/j.wneu.2020.10.083
23. Jahangiri A, Wagner J, Han SW, Zygourakis CC, Han SJ, Tran MT, et al. Morbidity of Repeat Transsphenoidal Surgery Assessed in More Than 1000 Operations. *J Neurosurg* (2014) 121(1):67–74. doi: 10.3171/2014.3.JNS131532
24. Lake MG, Krook LS, Cruz SV. Pituitary Adenomas: An Overview. *Am Fam Phys* (2013) 88(5):319–27.
25. Melmed S, Casanueva FF, Hoffman AR, Kleinberg DL, Montori VM, Schlechte JA, et al. Diagnosis and Treatment of Hyperprolactinemia: An Endocrine Society Clinical Practice Guideline. *J Clin Endocrinol Metab* (2011) 96(2):273–88. doi: 10.1210/jc.2010-1692
26. Giustina A, Chanson P, Bronstein MD, Klibanski A, Lamberts S, Casanueva FF, et al. A Consensus on Criteria for Cure of Acromegaly. *J Clin Endocrinol Metab* (2010) 95(7):3141–8. doi: 10.1210/jc.2009-2670
27. Chanson P, Salenave S. Diagnosis and Treatment of Pituitary Adenomas. *Minerva Endocrinol* (2004) 29(4):241–75.
28. Paluzzi A, Fernandez-Miranda JC, Tonya Stefko S, Challinor S, Snyderman CH, Gardner PA. Endoscopic Endonasal Approach for Pituitary Adenomas: A Series of 555 Patients. *Pituitary* (2014) 17(4):307–19. doi: 10.1007/s11102-013-0502-4
29. Koutourousiou M, Vaz Guimaraes Filho F, Fernandez-Miranda JC, Wang EW, Stefko ST, Snyderman CH, et al. Endoscopic Endonasal Surgery for Tumors of the Cavernous Sinus: A Series of 234 Patients. *World Neurosurg* (2017) 103:713–32. doi: 10.1016/j.wneu.2017.04.096
30. Fernandez-Miranda JC, Zwagerman NT, Abhinav K, Lieber S, Wang EW, Snyderman CH, et al. Cavernous Sinus Compartments From the Endoscopic Endonasal Approach: Anatomical Considerations and Surgical Relevance to Adenoma Surgery. *J Neurosurg* (2018) 129(2):430–41. doi: 10.3171/2017.2.JNS162214
31. Dhandapani S, Singh H, Negm HM, Cohen S, Anand VK, Schwartz TH. Cavernous Sinus Invasion in Pituitary Adenomas: Systematic Review and Pooled Data Meta-Analysis of Radiologic Criteria and Comparison of Endoscopic and Microscopic Surgery. *World Neurosurg* (2016) 96:36–46. doi: 10.1016/j.wneu.2016.08.088
32. Cappabianca P, Alfieri A, Colao A, Cavallo LM, Fusco M, Peca C, et al. Endoscopic Endonasal Transsphenoidal Surgery in Recurrent and Residual Pituitary Adenomas: Technical Note. *Minim Invasive Neurosurg* (2000) 43 (1):38–43. doi: 10.1055/s-2000-8814

33. Do H, Kshettry VR, Siu A, Belinsky I, Farrell CJ, Nyquist G, et al. Extent of Resection, Visual, and Endocrinologic Outcomes for Endoscopic Endonasal Surgery for Recurrent Pituitary Adenomas. *World Neurosurg* (2017) 102:35–41. doi: 10.1016/j.wneu.2017.02.131
34. Hwang JM, Kim YH, Kim JW, Kim DG, Jung HW, Chung YS. Feasibility of Endoscopic Endonasal Approach for Recurrent Pituitary Adenomas After Microscopic Trans-Sphenoidal Approach. *J Korean Neurosurg Soc* (2013) 54 (4):317–22. doi: 10.3340/jkns.2013.54.4.317
35. Esquenazi Y, Essayed WI, Singh H, Mauer E, Ahmed M, Christos PJ, et al. Endoscopic Endonasal Versus Microscopic Transsphenoidal Surgery for Recurrent and/or Residual Pituitary Adenomas. *World Neurosurg* (2017) 101:186–95. doi: 10.1016/j.wneu.2017.01.110
36. Tajudeen BA, Mundi J, Suh JD, Bergsneider M, Wang MB. Endoscopic Endonasal Surgery for Recurrent Pituitary Tumors: Technical Challenges to the Surgical Approach. *J Neurol Surg B Skull Base* (2015) 76(1):50–6. doi: 10.1055/s-0034-1383856
37. Micko AS, Wohrer A, Wolfsberger S, Knosp E. Invasion of the Cavernous Sinus Space in Pituitary Adenomas: Endoscopic Verification and its Correlation With an MRI-Based Classification. *J Neurosurg* (2015) 122 (4):803–11. doi: 10.3171/2014.12.JNS141083
38. Micko A, Oberndorfer J, Weninger WJ, Vila G, Hoftberger R, Wolfsberger S, et al. Challenging Knosp High-Grade Pituitary Adenomas. *J Neurosurg* (2019) 132(6):1739–46. doi: 10.3171/2019.3.JNS19367
39. Rolf W. Seiler LM. Sellar Reconstruction With Resorbable Vicryl Patches, Gelatin Foam, and Fibrin Glue in Transsphenoidal Surgery_ a 10-Year Experience With 376 Patients. *J Neurosurg* (2000) 93(5):762–5. doi: 10.3171/jns.2000.93.5.0762
40. Shiley SG, Limonadi F, Delashaw JB, Barnwell SL, Andersen PE, Hwang PH, et al. Incidence, Etiology, and Management of Cerebrospinal Fluid Leaks Following Trans-Sphenoidal Surgery. *Laryngoscope* (2003) 113(8):1283–8. doi: 10.1097/00005537-200308000-00003
41. Dlouhy BJ, Madhavan K, Clinger JD, Reddy A, Dawson JD, O'Brien EK, et al. Elevated Body Mass Index and Risk of Postoperative CSF Leak Following Transsphenoidal Surgery. *J Neurosurg* (2012) 116(6):1311–7. doi: 10.3171/2012.2.JNS111837
42. Tabaee A, Anand VK, Barron Y, Hiltzik DH, Brown SM, Kacker A, et al. Endoscopic Pituitary Surgery: A Systematic Review and Meta-Analysis. *J Neurosurg* (2009) 111(3):545–54. doi: 10.3171/2007.12.17635

Conflict of Interest: The authors declare that the research was conducted in the absence of any commercial or financial relationships that could be construed as a potential conflict of interest.

frontiers | Frontiers in Endocrinology

MINI REVIEW
published: 04 May 2022
doi: 10.3389/fendo.2022.895054

Sellar Glomus Tumor Misdiagnosed as Pituitary Adenoma: A Case Report and Review of the Literature

*Yijun Cheng, Hao Tang and Zhe Bao Wu**

Department of Neurosurgery, Center of Pituitary Tumor, Ruijin Hospital, Shanghai Jiao Tong University School of Medicine, Shanghai, China

Glomus tumor is a rare mesenchymal tumor with an organ-like structure. Sellar glomus tumors are extremely rare with only six reported cases in the literature. Because of the lack of special clinical manifestations and imaging features, the disorder may be easily misdiagnosed as other sellar tumors, especially pituitary adenomas. Here, the present study showed a case of a 69-year-old male with hypopituitarism who was preliminarily misdiagnosed as non-functional pituitary adenoma.

Keywords: sellar, glomus tumor, hypopituitarism, pituitary adenoma, endoscopic transsphenoidal approach

OPEN ACCESS

Edited by:
Run Yu,
University of California, Los Angeles, United States

Reviewed by:
Sergei I. Bannykh,
Cedars Sinai Medical Center, United States

***Correspondence:**
Zhe Bao Wu
zhebaowu@aliyun.com

Specialty section:
This article was submitted to Pituitary Endocrinology, a section of the journal Frontiers in Endocrinology

Received: *12 March 2022*
Accepted: *28 March 2022*
Published: *04 May 2022*

Citation:
Cheng Y, Tang H and Wu ZB (2022) Sellar Glomus Tumor Misdiagnosed as Pituitary Adenoma: A Case Report and Review of the Literature. Front. Endocrinol. 13:895054. doi: 10.3389/fendo.2022.895054

INTRODUCTION

Sellar tumors consist of a broad range of benign and malignant lesions due to the complex anatomy of the sellar region. Notably, many of the sellar tumors are newly described or have recently revised nomenclature in the 2017 Revision of the World Health Organization (WHO) classification system (1). Despite this wide range, approximately 80% of sellar tumors are due to the five most common lesions, including the pituitary adenomas, meningiomas, aneurysms, glioma, and craniopharyngiomas (2). In particular, pituitary adenomas are the most common sellar tumors that can account for as high as 10%–15% of all intracranial tumors. Compared to other intracranial lesions, imaging features for sellar tumors are relatively less specific, which always results in a misdiagnosis (3). Here, we report an extremely rare case of sellar glomus tumors in a 69-year-old male who was misdiagnosed as non-functional pituitary adenoma with hyperthyroidism for more than 5 years.

CLINICAL PRESENTATION

A 69-year-old man presented with sellar mass for more than 5 years and visual deficits for about 3 months. Five years ago, the patient was hospitalized in the department of endocrinology due to hypopituitarism. During hospitalization, the high-resolution contrast enhanced MRI was performed and suggested an incidental lesion (21.0 × 14.5 × 12 mm) in the sellar region. The lesion had cystic structures and was heterogeneously enhanced, suggesting a "macroadenoma" (**Figures 1A, B**). However, the patient refused further surgery treatment. After discharge, the patient was followed up regularly clinically and radiologically. The sellar mass did not grow significantly, and no other symptoms appeared during follow-up. Three months ago, the patient presented with acute onset of diminished visual acuity and fields. The high-resolution contrast enhanced MRI revealed a giant hetereogenous sellar mass with multiple apoplectic events, measuring 37 × 35 × 24 mm in size (**Figures 1C, D**). In addition, the pituitary

hormone test demonstrated low basal level of serum cortisol (8:00 AM, 0.54 μg/dl; normal, 6.7–22.6 μg/dl). On the basis of these findings, hypopituitarism secondary to a non-functional pituitary macroadenoma was suspected. Afterward, the patient underwent a neurosurgery *via* the endonasal endoscopic transsphenoidal approach (TSA) under general anesthesia. The visual acuity and field recovered soon after operation.

The paraffin sellar tumor specimen were cut (4 μm thickness), dewaxed, and then rehydrated. An antigen retrieval procedure was performed. Afterward, the sections were incubated in 3% H_2O_2 in phosphate-buffered saline (PBS) for about 10 min, blocked in PBS containing 5% normal goat serum at the room temperature for nearly 1 h, followed by incubation with the primary antibodies (**Supplementary Table 1**) at 4°C overnight. After washing three times, these sections were developed with the ABC kit and detected by Diaminobenzidine (DAB) staining (both from Vector Laboratories, Burlingame, CA, USA). Subsequently, the sections were stained with hematoxylin. Histopathological examination revealed mild cell morphology with rare nuclear division (**Figure 1E**) . Immunohistochemical (IHC) staining indicated tumor cells positive for Vimentin (**Figure 1F**), SMA (**Figure 1G**), SYN (**Figure 1H**), h-caldesmon (**Figure 1I**), Desmin (weak, **Figure 1J**), Collagen IV (**Figure 1K**), and CD34 (vascular, **Figure 1L**). Moreover, immunostains for AE1/AE3, Pit-1, ER, CgA, SF-1, T-pit, S-100, GFAP, EMA, STAT-6, and PAS were negative (data not shown).

DISCUSSION

Glomus tumor originates from the normal globular aberrant smooth muscle cells. It is a rare mesenchymal tumor with an organ-like structure (4). More than 96% of the tumor occurs in the fingertips, and mostly in the nail bed area. Glomus tumor was first reported by Wood in 1812. In 1924, Barre and Masson for the first time gave a relatively complete description of its histology, and put forward the term "glomus tumor". In 1951, Kay et al. first reported a case of non-phalangeal glomus tumor, gastric glomus tumor (5). Since then, breast (6), penis (7), nerve (8), bone (9), lung (10), and other tissues glomus tumors have also been reported successively. In 1984, Asa et al. (11) first described the features of glomus tumors in the sellar region. Since this first description, other five cases have been reported successively (12–15), which are summarized in **Table 1**.

Vascular spherules are composed of vascular cells, vascular structures, and smooth muscle tissues. According to the difference of composition proportions, glomus tumor is specifically subdivided into three subtypes: glomus tumor proper, glomangioma, and glomangiomyoma. According to the biological behavior, the tumor was classified as benign, uncertain malignant potential, and malignant. In the updated WHO classification, the criteria for malignant glomus tumor are as follows: (i) marked nuclear atypia and any level of mitotic activity; or (ii) atypical mitotic figures. Tumor should be categorized as uncertain malignant potential glomus tumor if it possesses any of the following characteristics: (i) tumor size >2 cm or deep location; (ii) atypical nuclear division (>5/50 HPF); (iii) atypical cells with round or fusiform appearance; and (iv) invading extra-capsular and surrounding tissues. In the current case, the tumor size was bigger than 2 cm, located in the sellar area, and had uncertain biological behavior, indicating that it was an uncertain malignant potential glomus tumor.

Because of the rare occurrence and non-specific clinical manifestations, the imaging may be still the most valuable

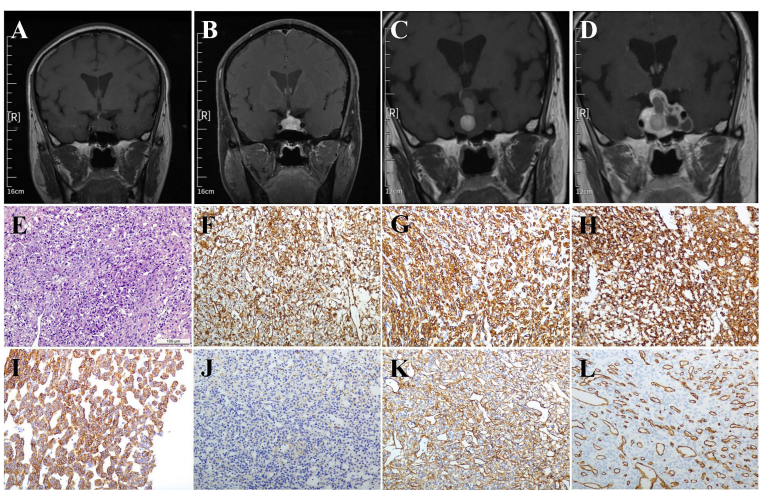

FIGURE 1 | MRI and pathological images. **(A, B)** Five years before the operation: Coronal MRI and enhanced MRI images indicated the sellar lesions with a size of approximately 21.0 × 14.5 × 12 mm had cystic structures and was inhomogenously enhanced. **(C, D)** Three months before the operation: Coronal MRI and enhanced MRI images indicated the sellar lesions with a size of about 37 × 35 × 24 mm had variable signal intensity and multiple apoplectic events. **(E)** Hematoxylin-eosin (H&E) staining indicated the mild cell morphology with rare nuclear division; immunohistochemical staining indicated that the tumor cells were positive for **(F)** Vimentin, **(G)** SMA, **(H)** SYN, **(I)** h-caldesmon, **(J)** Desmin, **(K)** Collagen IV, and **(L)** CD34. Magnification, ×200; Bar = 100 μm.

TABLE 1 | Summary of the patients' clinical data.

Year	Authors	Age	Sex	Symptom	Pituitary function	Treatment	Outcomes
1984	Asa et al. (11)	42	M	Decreased visual accuracy	Not Available	Surgery and radiotherapy	Recurrence
2005	Hanggi et al. (12)	47	F	Diplopia	Not Available	Surgery and radiotherapy	Recurrence
2011	Ebinu et al. (13)	72	M	Bitemporal hemianopia	Not Available	Surgery	
2020	Tsang et al. (14)	8	F	Decreased visual accuracy	Hypopituitarism	Surgery and Gamma Knife radiosurgery	Recurrence
2021	Quah et al. (15)	63	M	Blurred vision	Hypopituitarism	Surgery and radiotherapy	Not Available
		30	F	Intracranial hypertension	Hypopituitarism	Surgery	Death

method for the diagnosis of non-phalangeal glomus tumor. Considering that glomus tumor is filled with poorly circulated blood, MRI shows hypointensive signal on T1-weighted images, hyperintensive signal on T2-weighted images, and enhancement on T1-weighted images following gadolinium injection. As glomus tumor has a well-defined capsule, a more specific characteristic of a linear hyperintensive nidus surrounded by a rim of hypointensive signal could be showed on MRI. In a series of 42 glomus tumor patients study, MRI was reported to have a sensitivity of 90% and positive predictive value of 97% in diagnosis. However, the specificity was only 50%, and the negative predictive value was as low as 20% (16). In this case, the sellar mass showed clear tumor boundaries, obvious tumor capsule, mixed signals (mainly hypointensive signal) on T1-weighted images, mixed signals (mainly hyperintensive signal) on T2-weighted images, and heterogeneous enhancement with gadolinium on MRI scanning. Thus, the probable diagnosis of non-phalangeal glomus tumor should be considered, and further Digital subtraction angiography (DSA) examination is recommended.

The golden standard for treatment of glomus tumor is complete resection (17). According to the anatomical tumor position, we selected the transnasal TSA with endoscopic visualization. Unlike other solid sellar tumors, glomus tumor is a mesenchymal hemangioma essentially, which bleed easily during operation. Fortunately, the tumor was completely removed through concerted efforts of our multidisciplinary team (MDT), including experts from departments of anesthesiology, blood transfusion, and radiology. Imaging follow-up examination at 12 months after operation suggested that the tumor was resected totally without evidence of recurrence or metastasis.

CONCLUSION

In conclusion, the current case reminds us that the glomus tumor should be considered as a differential diagnosis for sellar mass. Preoperative DSA examination can be performed if necessary. Surgical resection is the first choice for sellar glomus tumor. Notably, sufficient preoperative planning, including the image test, MDT discussion, hormone replacement therapy, and preoperative blood preparation, should be well prepared. Moreover, the long-term follow-up is needed due to the high recurrence rate, as evidenced in **Table 1**.

AUTHOR CONTRIBUTIONS

YC took charge of original draft writing. HT performed follow-up and management of the patient. ZBW contributed to manuscript review and editing. All authors contributed to the article and approved the submitted version.

SUPPLEMENTARY MATERIAL

The Supplementary Material for this article can be found online at: https://www.frontiersin.org/articles/10.3389/fendo.2022.895054/full#supplementary-material

REFERENCES

1. Lopes MBS. The 2017 World Health Organization Classification of Tumors of the Pituitary Gland: A Summary. *Acta Neuropathol* (2017) 134(4):521–35. doi: 10.1007/s00401-017-1769-8
2. Jesser J, Schlamp K, Bendszus M. Pituitary Gland Tumors. *Radiologe* (2014) 54(10):981–8. doi: 10.1007/s00117-014-2688-5
3. Schwetye KE, Dahiya SM. Sellar Tumors. *Surg Pathol Clin* (2020) 13(2):305–29. doi: 10.1016/j.path.2020.02.006
4. Gombos Z, Zhang PJ. Glomus Tumor. *Arch Pathol Lab Med* (2008) 132:1448–1452. doi: 10.5858/2008-132-1448-GT
5. Kay S, Callahan WPJr, Murray MR, Randall HT, Stout AP. Glomus Tumors of the Stomach. *Cancer* (1951) 4(4):726–36. doi: 10.1002/1097-0142(195107)4:4<726::AID-CNCR2820040410>3.0.CO;2-Z
6. Barajas D. Glomus Tumor of the Male Breast. *Breast J* (2020) 26(2):297–8. doi: 10.1111/tbj.13549
7. Dagur G, Warren K, Miao Y, Singh N, Suh Y, Khan SA. Unusual Glomus Tumor of the Penis. *Curr Urol* (2016) 9(3):113–8. doi: 10.1159/000442864
8. Shamsi ZA, Shaikh FA, Wasif M, Chaudhry MB, Siddiqui NA, Sophie Z. Hypoglossal Nerve Paraganglioma Depicting as Glomus Tumor of Neck. *Iran J Otorhinolaryngol* (2021) 33(115):113–7. doi: 10.22038/ijorl.2020.43602.2448
9. Bouayyad S, Abdelaty M, Mishra A. A 15-Year Mystery Resolved: A Large Bone-Boring Glomus Tumor Mistaken as Dermatitis. *J Surg Case Rep* (2020) 2020(2):rjaa013. doi: 10.1093/jscr/rjaa013
10. Singh D, Dixit R, Goyal M, Bhandari C, Gupta N. Pulmonary Involvement in Malignant Glomus Tumor. *Lung India* (2021) 38(3):284–6. doi: 10.4103/lungindia.lungindia_266_20
11. Asa SL, Kovacs K, Horvath E, Ezrin C, Weiss MH. Sellar Glomangioma. *Ultrastruct Pathol* (1984) 7(1):49–54. doi: 10.3109/01913128409141853
12. Hanggi D, Adams H, Hans VH, Probst A, Tolnay M. Recurrent Glomus Tumor of the Sellar Region With Malignant Progression. *Acta Neuropathol* (2005) 110(1):93–6. doi: 10.1007/s00401-005-1006-8

13. Ebinu JO, Shahideh M, Ibrahim GM, Vescan A, Gentili F, Ridout R, et al. Sellar Glomangioma. *Endocr Pathol* (2011) 22(4):218–21. doi: 10.1007/s12022-011-9179-2
14. Tsang JCH, Ng CS, Fung CF, Chan JKC, Cheuk W. Glomus Tumor of Sella Turcica With Synaptophysin Expression Mimicking Pituitary Adenoma. *Int J Surg Pathol* (2020) 28(4):401–5. doi: 10.1177/1066896919900550
15. Quah BL, Donofrio CA, La Rosa S, Brouland JP, Cossu G, Djoukhadar I, et al. Primary Glomus Tumour of the Pituitary Gland: Diagnostic Challenges of a Rare and Potentially Aggressive Neoplasm. *Virchows Arch* (2021) 478(5):977–84. doi: 10.1007/s00428-020-02923-4
16. Al-Qattan MM, Al-Namla A, Al-Thunayan A, AI-Subhi F, EI-Shayeb AF. Magnetic Resonance Imaging in the Diagnosis of Glomus Tumours of the Hand. *J Handb Surg* (2005) 30:535–40. doi: 10.1016/j.jhsb.2005.06.009
17. Chou T, Pan SC, Shieh SJ, Lee JW, Chiu HY, Ho CL. Glomus Tumor: Twenty-Year Experience and Literature Review. *Ann Plast Surg* (2106) 76:S35–40. doi: 10.1097/SAP.0000000000000684

Conflict of Interest: The authors declare that the research was conducted in the absence of any commercial or financial relationships that could be construed as a potential conflict of interest.

frontiers | Frontiers in Endocrinology

ORIGINAL RESEARCH
published: 06 May 2022
doi: 10.3389/fendo.2022.879702

Transsphenoidal Surgery of Giant Pituitary Adenoma: Results and Experience of 239 Cases in A Single Center

Yike Chen[1†], Xiaohui Xu[2†], Jing Cao[3], Yuanqing Jie[4], Linkai Wang[1], Feng Cai[1], Sheng Chen[1], Wei Yan[1], Yuan Hong[1], Jianmin Zhang[1] and Qun Wu[1*]*

[1] Department of Neurosurgery, The Second Affiliated Hospital, School of Medicine, Zhejiang University, Hangzhou, China, [2] Department of Neurosurgery, The Fourth Affiliated Hospital, School of Medicine, Zhejiang University, Yiwu, China, [3] Department of Statistical Office, The Affiliated Changsha Central Hospital, Hengyang Medical School, University of South, Changsha, China, [4] Department of Neurosurgery, The Affiliated Quzhou People's Hospital of Wenzhou Medical University, Quzhou, China

OPEN ACCESS

Edited by:
Congxin Dai,
Capital Medical University, China

Reviewed by:
Andrea Glezer,
University of São Paulo, Brazil
Gao Dakuan,
The Fourth Military Medical University, China

***Correspondence:**
Qun Wu
2192010@zju.edu.cn
Jianmin Zhang
zjm135@zju.edu.cn

[†]These authors have contributed equally to this work and share first authorship

Specialty section:
This article was submitted to Pituitary Endocrinology, a section of the journal Frontiers in Endocrinology

Received: *20 February 2022*
Accepted: *08 April 2022*
Published: *06 May 2022*

Citation:
Chen Y, Xu X, Cao J, Jie Y, Wang L, Cai F, Chen S, Yan W, Hong Y, Zhang J and Wu Q (2022) Transsphenoidal Surgery of Giant Pituitary Adenoma: Results and Experience of 239 Cases in A Single Center. Front. Endocrinol. 13:879702. doi: 10.3389/fendo.2022.879702

Background: Transsphenoidal surgery (TSS) is first-line treatment for giant pituitary adenomas (PAs). Although PA is a benign neuroendocrine tumor that originates from adenohypophysial cells, the surgical outcomes and prognosis of giant PAs differ significantly due to multiple factors such as tumor morphology, invasion site, pathological characteristics and so on. The aim of this study was to evaluate surgical outcomes of giant PAs in a single-center cohort.

Methods: The clinical features and outcomes of 239 patients with giant PA who underwent sphenoidal surgery at the Second Affiliated Hospital of Zhejiang University School of Medicine from January 2015 to October 2021 were collected from medical records. The basic clinical information (age, gender, function etc.), surgical procedure, imaging features (maximum diameter, invasion characteristics, tumor shape etc.) and histopathological characteristics (pathological results, Ki-67, P53 etc.) were retrospectively reviewed. SPSS 25.0 and Stata 12.0 software were used for statistical analysis.

Results: A total of 239 patients with giant PAs underwent TSS, of which 168 surgeries (70.29%) were endoscopic endonasal transsphenoidal (EETS) and 71 (29.71%) were microscopic transsphenoidal (MTS). The mean preoperative maximum diameter in the cohort was 45.64 mm. Gross-total resection was achieved in 46 patients (19.25%), near-total in 56 (23.43%), subtotal in 68 (28.45%), and partial in 69 (28.87%) patients. The maximum tumor diameter and Knosp grade were the significant factors that limited the extent of the resection of giant PAs. A total of 193 patients (80.75%) experienced surgical complications, and the most common complications were postoperative diabetes insipidus (DI) (91, 38.08%), intracranial infection (36, 15.06%) and cerebrospinal fluid (CSF) leaks (37, 15.48%). In addition, there was a significant difference in the incidence of CSF leaks between the neuroendoscopy group and the microscopic group ($P < 0.05$).

Conclusion: The management of giant PAs remains a therapeutic challenge due to their large size and postoperative complications. The maximum diameter and Knosp grade of giant PAs significantly limited the extent of resection, which warrants a reasonable surgical plan.

Keywords: giant pituitary adenoma, transsphenoidal surgery, CSF leak, Knosp grade, extent of resection

INTRODUCTION

Pituitary adenoma (PA) is a benign neuroendocrine tumor that originates from adenohypophysial cells, and accounts for 10%-20% of all primary intracranial tumors (1, 2). Giant PAs are defined as tumors with largest diameter ≥4 cm (3–5), and are characterized by high invasiveness and irregular growth. In addition, giant PAs tend to compresses the optic chiasm and third ventricle, encase the internal carotid artery, and affect hormone secretion from the pituitary gland and hypothalamus (6, 7).

Surgical resection is the first-line treatment for most giant PAs except prolactinoma. Either transcranial or transsphenoidal approaches can be adopted for the surgical removal of giant PAs. Since craniotomy causes greater damage to normal brain tissues and results in more postoperative complications, it is now gradually being replaced with the transnasal sphenoidal approach (8). However, the efficacy of transsphenoidal surgery (TSS) for giant adenomas is poor and is associated with a higher complication rate compared to the smaller PAs (9–11), which can be attributed to the intricate anatomy and secretory functions of the pituitary gland. In this study, we have reviewed the outcomes following TSS of 239 giant PAs from a single-center and analyzed the factors that limit the extent of resection.

MATERIALS AND METHODS

Study Population

The clinical data of 239 patients with giant PAs who underwent TSS at The Second Affiliated Hospital Zhejiang University School of Medicine between January 2015 and October 2021 was retrospectively analyzed. The study was approved by the Research Ethics Committee of SAHZU. The inclusion criteria were as follows: 1) histologically confirmed PAs, 2) maximal diameter of PAs not less than 4 cm according to preoperative MRI, 3) tumor resection through TSS, and 4) regular follow-up for a minimum of 3 months. Patients were excluded if the medical records were not complete, or if the pathological report or follow-up data were missing.

Data Collection

The basic, surgical, radiological and pathological data was collected. Basic information included age, gender, functional status, clinical presentation. Radiological characteristics included maximum diameter (mm), tumor shape (rounded, dumbbell-shaped, multilobular), invasion characteristics and Knosp classification. Surgical procedures included the surgical method (microscopy or neuroendoscopy), unilateral/bilateral nostrils, the amount of blood loss, the duration of surgery, postoperative hospital stay, extent of resection (gross total resection, GTR (≥95%); near total resection, NTR (≥90%); subtotal resection, STR (≥70%); partial resection, PR [<70%) (12)], endocrine remission and surgical complications. The pathological classification, P53 and Ki-67 positive rates were also collected.

Tumor Volume Measurement

MRI was typically performed within 2 weeks before surgery and 3 months postoperatively at our institution. The imaging data were obtained through the imaging information-management system. The diameters of the tumors were measured in all direction using a measuring tool in the system, and the extent of resection was determined by comparing pre- and postoperative MRI data.

Surgical Approach

All patients underwent TSS, and the major surgical procedures were conducted by neurosurgeons with more than 15 years of experience. The objectives of the surgery were to: 1) achieve maximal resection and maximal remission of symptoms with least disturbance to neural and vascular structures, and 2) maintain or reinstate endocrine function.

Patients were positioned supine with the head raised and tilted back slightly. After the induction of general anesthesia, the nasal mucosa and skin of the surgical site was fully disinfected. The following operations are performed under an endoscope (with the aid of a 0° or 30° 4-mm endoscope) or microscope. To avoid nasal mucosal damage, a uninostril approach is used in most cases. Bilateral nostrils technique was performed if the operating space is too narrow. After covering the nasal mucosa with epinephrine cotton pad, the nasal turbinates are lateralized to expand the surgical space. The right pedicled nasoseptal flap was partially resected, then it was stored inferior the surgical channel and was fully harvested if an intraoperative CSF leak occurred. A high-speed drill or osteotome was used to open the sphenoid sinus and the sellar floor was removed. Once the tumor was fully exposed, the lesions localized in the intrasellar and suprasellar region was removed with suction and ring curettes first, then removed the residual lesions in cavernous sinus under direct vision. To protect the carotid arteries and other lateral structures, neuronavigation and Doppler ultrasound were used during resection. Finally, the skull base was reconstructed using the prepared autologous tissue and artificial materials after efficient hemostasis.

Data Analysis

SPSS 25.0 and STATA 12.0 software were used for statistical analysis. Continuous variables with normal distribution were expressed as mean ± SD and compared by one-way ANOVA. Mann-Whitney U test and Kruskal-Wallis H test were used for categorical variables. Enumeration data were compared using the chi-square and Fisher exact tests. Ordinal logistic regression model was used to identify factors affecting the extent of resection. Two-sided P values < 0.05 were considered statistically significant.

RESULTS

General Characteristics

A total of 239 patients (137 females and 102 males) with pathologically confirmed PA were included. The mean age was 51.12 ± 13.8 years (range, 19-84 years). Non-functional PAs was detected in 158 patients (66.11%) and 81 patients (33.89%) had functional PAs. In this series, patients mainly presented with visual impairment 175 (73.22%), including visual acuity (162, 67.78%) and/or visual field (122, 51.05%) deficits. In addition, 67 patients (28.03%) presented with headache, and 41 patients (17.15%) exhibited symptoms of endocrine dysfunction prior to surgery, including irregular menstruation (13, 5.44%), galactorrhea (2, 0.84%), sexual dysfunction (3, 1.26%), acromegaly (6, 2.51%), concentric obesity (2, 0.84%) and thyroid dysfunction (15, 6.28%). Furthermore, 10 patients (4.18%) experienced diabetes insipidus and 23 (9.62%) had apoplexy (confirmed by radiographic and intraoperative findings) prior to surgery (**Table 1**).

TABLE 1 | General characteristics.

Variables	Value*
Age (years)	
mean ± SD	51.12 ± 13.80
median	53
range	19-84
Gender	
male	102 (42.68)
female	137 (57.32)
Functional Status	
nonfunctioning	158 (66.11)
functioning	81 (33.89)
Clinical presentation	
headache	67 (28.03)
visual acuity deficits	162 (67.78)
visual field deficits	122 (51.05)
irregular menstruation	13 (5.44)
galactorrhea	2 (0.84)
sexual dysfunction	3 (1.26)
acromegaly	6 (2.51)
concentric obesity	2 (0.84)
thyroid dysfunction	15 (6.28)
diabetes insipidus	10 (4.18)
apoplexy	23 (9.62)

Values are number of patients (%) unless stated otherwise.

The average maximum diameter for the giant PAs was 45.64 ± 6.7 mm (range 40–75 mm). The tumors were round in 14 cases (5.86%), dumbbell shaped in 89 cases (37.24%), and multilobular in 136 cases (56.9%). Based on the preoperative MRI results and intraoperative observations, 220 cases (92.05%) had cavernous sinus invasion, 165 (69.04%) had sphenoid sinus invasion and 221 cases (92.47%) showed suprasellar invasion. The highest Knosp grade was 0-1 for 26 patients (10.88%), 2 for 46 patients (19.25%), 3A for 38 patients (15.90%), 3B for 21 patients (8.79%) and 4 for 108 patients (45.19%), which were indicative of the extent of cavernous sinus invasion and aggressiveness of the giant PAs (**Table 2**).

As expected, the predominant pathological type of the giant PAs was gonadotrophic adenomas (76, 31.8%), followed by lactotroph adenomas (27, 11.3%), corticotroph adenomas (27, 11.3%), plurihormonal and double adenomas (22, 9.21%), null cell adenomas (20, 8.4%), and somatotroph adenomas (3, 1.26%). 64 pathological results that were not based on latest WHO criteria and lack of transcription factors evaluation were excluded. Furthermore, Ki-67 labeling index was ≥ 5% in 19 patients (7.95%), < 3% in 178 patients (74.48%) and 3%-5% in 42 patients (17.57%). Positive staining for P53 was 14.64%, and 200 patients (83.68%) were negative and 4 patients (1.67%) had weak staining (**Table 3**).

Surgical Procedure

All patients underwent TSS, of which 168 patients (70.29%) were treated with neuroendoscopy and 71 (29.71%) with microscopy. The average operating duration was 143.18 ± 80.26 minutes (range, 46-475 minutes) and the mean intraoperative blood loss was 160.46 ± 285.71ml (range, 10-3500 ml). Four cases had more than 1000 ml of intraoperative blood loss. In addition, the two-nostril approach was taken in 39 cases and 200 patients were treated with the one-nostril approach. The mean length of stay after surgery was 9.59 ± 7.52 days and 7 patients were hospitalized for more than 1 month, mainly because of endocrine dysfunction and intracranial infection. According to

TABLE 2 | Radiological characteristics.

Variables	Value*
Maximum Diameter (mm)	
mean ± SD	45.64 ± 6.70
median	44
range	40-75
Tumor Shape	
rounded	14 (5.86)
dumbbell shaped	89 (37.24)
multilobular	136 (56.90)
Invasion Characteristics	
cavernous sinus invasion	220 (92.05)
sphenoid sinus invasion	165 (69.04)
suprasellar invasion	221 (92.47)
Knosp Grade	
0-1	26 (10.88)
2	46 (19.25)
3A	38 (15.90)
3B	21 (8.79)
4	108 (45.19)

Values are number of patients (%) unless stated otherwise.

TABLE 3 | Pathological characteristics.

Variables	Value*
Cell Type	
Somatotroph adenomas	3 (1.26)
lactotroph adenomas	27 (11.30)
TSH adenomas	0 (0.00)
corticotroph adenomas	27 (11.30)
gonadotrophic adenomas	76 (31.80)
null cell adenomas	20 (8.4)
Pluri-hormonal and double adenomas	22 (9.21)
unknown	64 (26.78)
Ki-67	
<3%	178 (74.48)
3%-5%	42 (17.57)
≥5%	19 (7.95)
P53	
negative	200 (83.68)
positive	35 (14.64)
weak	4 (1.67)

**Values are number of patients (%) unless stated otherwise.*

postoperative MRI, GTR was achieved in 46 cases (19.25%), NTR in 56 cases (23.43%), STR in 68 cases (28.45%) and PR in 69 cases (28.87%). Improvement of vision was achieved in 133 patients (76.00%). Endocrine tests were performed 3 days, 1 week, and 3 months postoperatively. Sixty-five patients with functional giant PAs achieved endocrine remission after TSS. All details are summarized in **Table 4**.

TABLE 4 | Surgical characteristics.

Variables	Value*
Surgical Method	
neuroendoscopy	168 (70.29)
Microscopy	71 (29.71)
Unilateral/Bilateral Nostrils	
unilateral nostrils	200 (83.68)
bilateral nostrils	39 (16.32)
Blood Loss	
mean ± SD	160.46 ± 285.712
median	100
range	10-3500
Operating Duration (min)	
mean ± SD	143.18 ± 80.26
median	125
range	46-475
Postoperative Length of stay (days)	
mean ± SD	9.59 ± 7.52
median	8
range	1-49
Extent of Resection	
PR	69 (28.87)
STR	68 (28.45)
NTR	56 (23.43)
GTR	46 (19.25)
Visual Improvement	133 (76.00)
Endocrine Dysfunction	
non-remission	10 (4.18)
remission	65 (27.20)

*GTR, gross total resection; NTR, near total resection; STR, subtotal resection; PR, partial resection. *Values are number of patients (%) unless stated otherwise.*

A total of 193 patients (80.75%) experienced surgical complications (**Table 5**), and the most common complication was postoperative diabetes insipidus (DI), which occurred in 91 patients (38.08%). The incidence of intracranial infection and cerebrospinal fluid (CSF) leaks was 15.48% (13) and 15.06% (14) respectively. Furthermore, 18 patients with CSF leaks developed secondary intracranial infections, and 8 patients experienced postoperative intracranial hemorrhage due to abundant tumor blood supply and inadequate hemostasis of residual tumor. Cranial nerve palsies were observed in 5 cases, all of whom experienced impaired visual field and limited eye movement. One patient experienced intraoperative internal carotid artery injury and was discharged after interventional therapy. Two patients died of intracranial infection and multiorgan failure. In addition, there was a significant difference in the incidence of CSF leaks between the neuroendoscopy and the microscopy groups ($P < 0.05$) (**Table 6**).

Risk Factors of Extent of Resection

The effect of various tumor characteristics on the extent of resection are outlined in **Table 7**, factors ($P > 0.05$) including age, gender, functional status, surgical method, unilateral/bilateral nostrils, tumor shape, invasion characteristics, Ki-67 labeling index, P53 were not significantly correlated with the extent of resection. Univariate analysis showed the maximum diameter of giant PAs maybe a significant factor limiting the extent of resection ($P < 0.05$). In the ordinal logistic regression model, the OR of maximum diameter was 0.95 ($P < 0.05$; 95%CI: 0.92-0.98) (**Table 8**). The Knosp grade was showed a significant effect on the extent of resection ($P < 0.001$). GTR was more likely achieved in giant PAs with lower Knosp grade, especially Knosp grade 0-1 ($P < 0.05$; OR: 2.96; 95%CI: 1.27, 6.90) (**Table 8**).

TABLE 5 | Surgical complications.

Variables	No. of Patients (%)
CSF leaks	36 (15.06)
DI	91 (38.08)
Intracranial infection	37 (15.48)
Epistaxis	0 (0.00)
Intracranial hemorrhage	8 (3.35)
Cranial nerve palsies	5 (2.09)
Internal carotid artery injury	1 (0.42)
Death	2 (0.84)

CSF leaks, cerebrospinal fluid leaks; DI, diabetes insipidus.

TABLE 6 | Complications comparison of ETTS and MTTS.

Surgical Complications	EETS (n = 168)	MTS (n = 71)	X^2	P
CSF leaks	32 (19.05)	4 (5.63)	7.019	0.008
DI	64 (38.1)	27 (38.03)	0.000	1.000
Intracranial infection	28 (16.67)	9 (12.68)	0.607	0.436
Epistaxis	0 (0.00)	0 (0.00)	0.000	1.000
Intracranial hemorrhage	3 (1.79)	5 (7.04)	–	0.053#
Cranial nerve palsies	4 (2.38)	1 (1.41)	–	1.000#
Internal carotid artery injury	1 (0.60)	0 (0.00)	–	1.000#

EETS, endoscopic endonasal transsphenoidal; MTS, microscopic transsphenoidal; CSF leaks, cerebrospinal fluid leaks; DI, diabetes insipidus. #means using Fisher's exact test.

TABLE 7 | The effect of various tumor characteristics on the extent of resection.

Variables	PR (n = 69)	STR (n = 68)	NTR (n = 56)	GTR (n = 46)	x^2/F	*P*
Gender					0.682	0.878
M	32 (46.38)	29 (42.65)	23 (41.07)	18 (39.13)		
F	37 (53.62)	39 (57.35)	33 (58.93)	28 (60.87)		
Age (years)	51.64 ± 14.95	51.59 ± 12.83	53.00 ± 11.42	47.35 ± 15.66	1.562	0.199
Functional Status					6.920	0.075
N	47 (68.11)	42 (61.76)	32 (57.14)	37 (80.43)		
Y	22 (31.89)	26 (38.24)	24 (42.86)	9 (19.57)		
Surgical Method					6.921	0.074
neuroendoscopy	42 (60.87)	52 (76.47)	37 (66.07)	37 (80.43)		
microscopy	27 (39.13)	16 (23.53)	19 (33.93)	9 (19.57)		
Unilateral/Bilateral Nostrils						
unilateral nostrils	60 (86.96)	57 (83.82)	44 (78.57)	39 (84.78)	1.655	0.647
bilateral nostrils	9 (13.04)	11 (16.18)	12 (21.43)	7 (15.22)		
Maximum Diameter (mm)	48.26 ± 8.14	44.72 ± 6.37	44.8 ± 5.46	44.09 ± 5.05	5.333	0.001
Tumor Shape					–	0.095#
rounded	3 (4.35)	2 (2.94)	2 (3.57)	7 (15.22)		
dumbbell shaped	21 (30.43)	29 (42.65)	25 (44.64)	14 (30.43)		
multilobular	45 (65.22)	37 (54.41)	29 (51.79)	25 (54.35)		
Cavernous Sinus Invasion					–	0.065#
N	3 (4.35)	10 (14.71)	5 (8.93)	1 (2.17)		
Y	66 (95.65)	58 (85.29)	51 (91.07)	45 (97.83)		
Sphenoid Sinus Invasion					1.577	0.665#
N	24 (34.78)	21 (30.88)	18 (32.14)	11 (23.91)		
Y	45 (65.22)	47 (69.12)	38 (67.86)	35 (76.09)		
Suprasellar Invasion					–	0.259#
N	2 (2.9)	7 (10.29)	6 (10.71)	3 (6.52)		
Y	67 (97.1)	61 (89.71)	50 (89.29)	43 (93.48)		
Knosp Grade					18.417	<0.001
0-1	8	4	3	11		
2	12	11	8	15		
3	13	16	21	9		
4	36	37	24	11		
Ki-67					0.781	0.854
<3%	49	51	42	36		
3%-5%	15	10	9	8		
≥5%	5	7	5	2		
P53					1.819	0.611
negative	60	54	46	40		
positive	7	13	9	6		
weak	2	1	1	0		

GTR, gross total resection; NTR, near total resection; STR, subtotal resection; PR, partial resection. #means using Fisher's exact test.

TABLE 8 | Ordinal logistic regression for factors of GTR.

Variables	P	OR	95%CI
Knosp Grade			
0-1	0.012	2.96	1.27, 6.90
2	0.009	2.52	1.26, 5.07
3	0.031	2.03	1.07, 3.88
4	–	1.00	–
Maximum Diameter	0.004	0.95	0.92, 0.98

DISCUSSION

Although relatively rare, giant PAs present significant challenges in terms of surgical resection and postoperative management on account of their size and frequent invasion into the surrounding normal tissues. In this study, we retrospectively analyzed the clinical data and surgical outcomes of 239 patients with giant PAs, and identified risk factors for the extent of resection.

Around 6-10% of PAs are defined as giant PAs based on their largest diameter (15, 16). A total of 2829 patients with PAs were treated at our center from January 2015 to October 2021, of which 8.4% had giant PAs. The frequency of the clinically non-functioning giant PAs (158; 66.11%) was twice as high as that of the functioning adenomas (81; 33.89%). This finding is consistent with that reported by Pedro et al. (6). This could be due to the difficulty in detecting silent PAs till they grow to a certain size and become symptomatic. Furthermore, 16 cases of clinically non-functioning giant PAs were confirmed as corticotroph adenomas, which are commonly found in large size of PAs and have been recognized as a more aggressive subtype of pituitary adenomas (17).

TSS is the first-line treatment for giant PAs (18) except the prolactinomas that can be effectively treated with dopamine agonists. The main goals of surgical resection of PAs are the restoration of normal pituitary function, nerve and vascular decompression, and minimal damage to the surrounding tissues. Since the 1990s, the endoscopic endonasal transsphenoidal

(EETS) approach has been widely practiced for its improved surgical visualization (19–22), since endoscopes with angled lenses can be used to access areas that are not visible under a microscope. Komotar et al. conducted a systematic review (1995–2010) to compare the outcomes of EETS and microscopic transsphenoidal approach (MTS), and found the EETS group had higher rates of GTR (47.2%) compared to the MTS group (30.9%) (23). Michael et al. further reported significantly higher mean reduction of tumor volume with EETS (91%) compared to MTS (63%) in a cohort of 72 patients with giant PAs (21). In this study, the extent of resection in the EETS group was higher than that in the MTS group, albeit without statistical significance.

Giant PAs are associated with a higher surgical complication rate compared to normal PAs, and the most common complications are DI, CSF leaks, postoperative intracranial hemorrhage, intracranial infections, cranial nerve palsies, hypopituitarism and epistaxis (12, 24, 25). Consistent with previous reports (25–28), the three most frequent complications in our cohort were DI (91, 38.08%) and 6 patients developed permanent DI, CSF leaks (36, 15.06%), and intracranial infection (37, 15.48%). DI is caused by posterior pituitary disfunction, and its incidence rate typically ranges from 9% to 22%, and may increase up to 53% at some centers (29–34). Nevertheless, only 2-7% of the patients develop permanent DI (35,36). PA patients with visual abnormalities, suprasellar extension or large tumors are at a higher risk of developing DI postoperatively (36), which could be the reason for the high incidence of DI in our cohort.

CSF leaks are generally the result of surgical injury and tumor invasion, especially in case of giant PAs with anterior cranial fossa extension (37) and suprasellar expansion (14). In our cohort, most cases of CSF leaks occurred during tumor removal. After reconstructing the skull base with the vascularized nasoseptal flap or the fascia and subcutaneous fat of the thigh, the CSF leaks in most patients receded within 3-6 days. In addition, we found that the rate of CSF leaks was higher in the EETS group than in the MTS group, which was consistent with the results of Yoshua et al. (13). This may be related to the imaging features of neuroendoscopy, which only provides 2D images without the important depth and three-dimensional sense. A previous study reported a significant association between CSF leak and postoperative intracranial infection (38), indicating that despite advanced skull base reconstruction and antibiotic treatment, some patients with CSF leaks may still develop intracranial infection. In this study, 37 patients experienced intracranial infection and 2 patients died as a result. Therefore, intracranial infection still represents a common and feared complication of this approach.

In our cohort, postoperative intracranial hemorrhage was reported in 8 (3.35%) cases. This is a terrible postoperative complication, which can cause great risk to the patient's life and economic pressure. Residual tumor and inadequate hemostasis were main reasons for this complication, so extreme caution should be exercised after giant PAs surgery. Once a hematoma in the operative cavity is found, an early evacuation of the hematoma and decompression of cranial nerve are urgent needed.

Internal carotid artery rupture is a rare complication but carries the greatest risk of short-term mortality, and there are reports describing fatal bleeds from damaged carotid arteries (39–41). In this study, one patient experienced internal carotid artery damage and formed a false aneurysm, which was managed by interventional endovascular treatment. In addition, cranial nerves are easily damaged during resection of tumors invading the cavernous sinus. Therefore, maintaining a strictly midline approach, familiarity with MRI results and the use of Doppler ultrasound is essential for neurovascular protection.

Since gross total resection is the optimal surgical outcome of giant PAs, we identified independent risk factors of the extent of resection in order to plan a suitable surgical strategy. Tumor size and the invasiveness of giant PAs into surrounding structures are key factors that limit the extent of resection. In our study, we found that each 1 mm increase in tumor diameter corresponded to a 5% decrease in the chance of achieving a GTR. Likewise, giant PAs with Knosp grades 0-1, 2 and 3 were more than twice as likely to achieve GTR compared to those with grade 4 (**Table 8**). Therefore, both the maximum diameter and the Knosp grade are independent factors of the extent of resection. Sanmillan et al. (42) also identified tumor volume and the Knosp grade as independent risk factors of the extent of resection in a study conducted on 294 patients with PAs, and found that the Knosp grade had a greater impact. Consistent with this, we found that some giant PAs with low Knosp grade could be satisfactorily removed despite their large size. Thus, cavernous sinus invasion of the PAs is crucial for planning surgical procedures, and tumor size can provide complementary information.

The primary aim of identifying risk factors limiting the extent of resection is to guide the neurosurgeons to distinguish the operation terminal and avoid complex complications rather than achieve complete removal of giant PAs. Therefore, the ultimate goals of the surgical resection of giant PAs are decompression of neurovascular structures, especially the optic nerve and internal carotid artery, relieving endocrine dysfunction and controlling the tumor progression, instead of gross total resection of the giant PAs. However, this study has certain limitations that are largely related to its single-center retrospective nature, and a longer follow-up and multicenter cohort are needed to validate our results.

DATA AVAILABILITY STATEMENT

The raw data supporting the conclusions of this article will be made available by the authors, without undue reservation.

ETHICS STATEMENT

The studies involving human participants were reviewed and approved by Ethics Committee of Second Affiliated Hospital, School of Medicine, Zhejiang University. Written informed consent for participation was not required for this study in accordance with the national legislation and the institutional requirements.

AUTHOR CONTRIBUTIONS

YC and XX performed the analysis and co-wrote the manuscript. LW, XX, YJ, FC, SC, and JC collected the patient information. WY and YH revised paper. QW and JZ supervised the project, conceived the study, and guided the editing of the manuscript. YC and XX contributed equally to the manuscript. QW and JZ are corresponding authors. All authors contributed to the article and approved the submitted version.

REFERENCES

1. Ostrom QT, Gittleman H, Truitt G, Boscia A, Kruchko C, Barnholtz-Sloan JS. CBTRUS Statistical Report: Primary Brain and Other Central Nervous System Tumors Diagnosed in the United States in 2011-2015. *Neuro Oncol* (2018) 20 (suppl_4):iv1–iv86. doi: 10.1093/neuonc/noy131
2. Chen Y, Wang CD, Su ZP, Chen YX, Cai L, Zhuge QC, et al. Natural History of Postoperative Nonfunctioning Pituitary Adenomas: A Systematic Review and Meta-Analysis. *Neuroendocrinology* (2012) 96(4):333–42. doi: 10.1159/000339823
3. Raverot G, Jouanneau E, Trouillas J. Management of Endocrine Disease: Clinicopathological Classification and Molecular Markers of Pituitary Tumours for Personalized Therapeutic Strategies. *Eur J Endocrinol* (2014) 170(4):R121–32. doi: 10.1530/EJE-13-1031
4. Müslüman AM, Cansever T, Yılmaz A, Kanat A, Oba E, Çavuşoğlu H, et al. Surgical Results of Large and Giant Pituitary Adenomas With Special Consideration of Ophthalmologic Outcomes. *World Neurosurg* (2011) 76 (1-2):141–8; discussion 63-6. doi: 10.1016/j.wneu.2011.02.009
5. Chen Y, Cai F, Cao J, Gao F, Lv Y, Tang Y, et al. Analysis of Related Factors of Tumor Recurrence or Progression After Transnasal Sphenoidal Surgical Treatment of Large and Giant Pituitary Adenomas and Establish a Nomogram to Predict Tumor Prognosis. *Front Endocrinol* (2021) 12:793337. doi: 10.3389/fendo.2021.793337
6. Iglesias P, Rodríguez Berrocal V, Díez JJ. Giant Pituitary Adenoma: Histological Types, Clinical Features and Therapeutic Approaches. *Endocrine* (2018) 61(3):407–21. doi: 10.1007/s12020-018-1645-x
7. Fallah N, Taghvaei M, Sadaghiani S, Sadrhosseini SM, Esfahanian F, Zeinalizadeh M. Surgical Outcome of Endoscopic Endonasal Surgery of Large and Giant Pituitary Adenomas: An Institutional Experience From the Middle East. *World Neurosurg* (2019) 132:e802–e11. doi: 10.1016/j.wneu.2019.08.004
8. Pratheesh R, Rajaratnam S, Prabhu K, Mani SE, Chacko G, Chacko AG. The Current Role of Transcranial Surgery in the Management of Pituitary Adenomas. *Pituitary* (2013) 16(4):419–34. doi: 10.1007/s11102-012-0439-z
9. de Paiva Neto MA, Vandergrift A, Fatemi N, Gorgulho AA, Desalles AA, Cohan P, et al. Endonasal Transsphenoidal Surgery and Multimodality Treatment for Giant Pituitary Adenomas. *Clin Endocrinol* (2010) 72 (4):512–9. doi: 10.1111/j.1365-2265.2009.03665.x
10. Goel A, Nadkarni T, Muzumdar D, Desai K, Phalke U, Sharma P. Giant Pituitary Tumors: A Study Based on Surgical Treatment of 118 Cases. *Surg Neurol* (2004) 61(5):436–45; discussion 45-6. doi: 10.1016/j.surneu.2003.08.036
11. Mortini P, Barzaghi R, Losa M, Boari N, Giovanelli M. Surgical Treatment of Giant Pituitary Adenomas: Strategies and Results in a Series of 95 Consecutive Patients. *Neurosurgery* (2007) 60(6):993–1002; discussion 3-4. doi: 10.1227/01.NEU.0000255459.14764.BA
12. Juraschka K, Khan OH, Godoy BL, Monsalves E, Kilian A, Krischek B, et al. Endoscopic Endonasal Transsphenoidal Approach to Large and Giant Pituitary Adenomas: Institutional Experience and Predictors of Extent of Resection. *J Neurosurg* (2014) 121(1):75–83. doi: 10.3171/2014.3.JNS131679
13. Esquenazi Y, Essayed WI, Singh H, Mauer E, Ahmed M, Christos PJ, et al. Endoscopic Endonasal Versus Microscopic Transsphenoidal Surgery for Recurrent and/or Residual Pituitary Adenomas. *World Neurosurg* (2017) 101:186–95. doi: 10.1016/j.wneu.2017.01.110
14. do Amaral LC, Reis BL, Ribeiro-Oliveira AJr., da Silva Santos TM, Giannetti AV. Comparative Study of Complications After Primary and Revision Transsphenoidal Endoscopic Surgeries. *Neurosurg Rev* (2021) 44(3):1687–702. doi: 10.1007/s10143-020-01360-w
15. Mohr G, Hardy J, Comtois R, Beauregard H. Surgical Management of Giant Pituitary Adenomas. *Can J Neurol Sci Le J Canadien Des Sci Neurol* (1990) 17 (1):62–6. doi: 10.1017/s0317167100030055
16. Trouillas J, Roy P, Sturm N, Dantony E, Cortet-Rudelli C, Viennet G, et al. A New Prognostic Clinicopathological Classification of Pituitary Adenomas: A Multicentric Case-Control Study of 410 Patients With 8 Years Post-Operative Follow-Up. *Acta Neuropathol* (2013) 126(1):123–35. doi: 10.1007/s00401-013-1084-y
17. Cho HY, Cho SW, Kim SW, Shin CS, Park KS, Kim SY. Silent Corticotroph Adenomas Have Unique Recurrence Characteristics Compared With Other Nonfunctioning Pituitary Adenomas. *Clin Endocrinol (Oxf)* (2010) 72(5):648–53. doi: 10.1111/j.1365-2265.2009.03673.x
18. Wang WF, Yang LH, Han L, Li MJ, Xiao JQ. Efficacy of Transsphenoidal Surgery for Pituitary Tumor: A Protocol for Systematic Review. *Medicine* (2019) 98(6):e14434. doi: 10.1097/MD.0000000000014434
19. Jho HD, Carrau RL. Endoscopic Endonasal Transsphenoidal Surgery: Experience With 50 Patients. *J Neurosurg* (1997) 87(1):44–51. doi: 10.3171/jns.1997.87.1.0044
20. Cappabianca P, Alfieri A, de Divitiis E. Endoscopic Endonasal Transsphenoidal Approach to the Sella: Towards Functional Endoscopic Pituitary Surgery (FEPS). *Minim Invasive Neurosurg: MIN* (1998) 41(2):66–73. doi: 10.1055/s-2008-1052019
21. Cusimano MD, Kan P, Nassiri F, Anderson J, Goguen J, Vanek I, et al. Outcomes of Surgically Treated Giant Pituitary Tumours. *Can J Neurol Sci Le J Canadien Des Sci Neurol* (2012) 39(4):446–57. doi: 10.1017/s0317167100013950
22. Sanchez MM, Karekezi C, Almeida JP, Kalyvas A, Castro V, Velasquez C, et al. Management of Giant Pituitary Adenomas: Role and Outcome of the Endoscopic Endonasal Surgical Approach. *Neurosurg Clin N Am* (2019) 30 (4):433–44. doi: 10.1016/j.nec.2019.05.004
23. Komotar RJ, Starke RM, Raper DM, Anand VK, Schwartz TH. Endoscopic Endonasal Compared With Microscopic Transsphenoidal and Open Transcranial Resection of Giant Pituitary Adenomas. *Pituitary* (2012) 15 (2):150–9. doi: 10.1007/s11102-011-0359-3
24. Koutourousiou M, Gardner PA, Fernandez-Miranda JC, Paluzzi A, Wang EW, Snyderman CH. Endoscopic Endonasal Surgery for Giant Pituitary Adenomas: Advantages and Limitations. *J Neurosurg* (2013) 118(3):621–31. doi: 10.3171/2012.11.JNS121190
25. Gondim JA, Almeida JP, Albuquerque LA, Gomes EF, Schops M. Giant Pituitary Adenomas: Surgical Outcomes of 50 Cases Operated on by the Endonasal Endoscopic Approach. *World Neurosurg* (2014) 82(1-2):e281–90. doi: 10.1016/j.wneu.2013.08.028
26. Xue-Fei S, Yong-Fei W, Shi-Qi L, Jing-Song W, Yao Z, Ying M, et al. Microsurgical Treatment for Giant and Irregular Pituitary Adenomas in a Series of 54 Consecutive Patients. *Br J Neurosurg* (2008) 22(5):636–48. doi: 10.1080/02688690802346083
27. Sinha S, Sharma BS. Giant Pituitary Adenomas–an Enigma Revisited. Microsurgical Treatment Strategies and Outcome in a Series of 250 Patients. *Br J Neurosurg* (2010) 24(1):31–9. doi: 10.3109/02688690903370305
28. Rahimli T, Hidayetov T, Yusifli Z, Memmedzade H, Rajabov T, Aghayev K. Endoscopic Endonasal Approach to Giant Pituitary Adenomas: Surgical Outcomes and Review of the Literature. *World Neurosurg* (2021) 149: e1043–e55. doi: 10.1016/j.wneu.2021.01.019
29. Devin JK. Hypopituitarism and Central Diabetes Insipidus: Perioperative Diagnosis and Management. *Neurosurg Clinics North Am* (2012) 23(4):679–89. doi: 10.1016/j.nec.2012.06.001
30. Kadir ML, Islam MT, Hossain MM, Sultana S, Nasrin R, Hossain MM. Incidence of Diabetes Insipidus in Postoperative Period Among the Patients

Undergoing Pituitary Tumour Surgery. *Mymensingh Med J: MMJ* (2017) 26 (3):642–9.
31. Nemergut EC, Zuo Z, Jane JAJr., Laws ERJr. Predictors of Diabetes Insipidus After Transsphenoidal Surgery: A Review of 881 Patients. *J Neurosurg* (2005) 103(3):448–54. doi: 10.3171/jns.2005.103.3.0448
32. Qari FA, AbuDaood EA, Nasser TA. Diabetes Insipidus Following Neurosurgery at a University Hospital in Western Saudi Arabia. *Saudi Med J* (2016) 37(2):156–60. doi: 10.15537/smj.2016.2.12848
33. Zhan R, Ma Z, Wang D, Li X. Pure Endoscopic Endonasal Transsphenoidal Approach for Nonfunctioning Pituitary Adenomas in the Elderly: Surgical Outcomes and Complications in 158 Patients. *World Neurosurg* (2015) 84 (6):1572–8. doi: 10.1016/j.wneu.2015.08.035
34. Constantino ER, Leal R, Ferreira CC, Acioly MA, Landeiro JA. Surgical Outcomes of the Endoscopic Endonasal Transsphenoidal Approach for Large and Giant Pituitary Adenomas: Institutional Experience With Special Attention to Approach-Related Complications. *Arq Neuropsiquiatr* (2016) 74(5):388–95. doi: 10.1590/0004-282X20160042
35. Vance ML. Perioperative Management of Patients Undergoing Pituitary Surgery. *Endocrinol Metab Clinics North Am* (2003) 32(2):355–65. doi: 10.1016/s0889-8529(03)00003-3
36. Nayak P, Montaser AS, Hu J, Prevedello DM, Kirschner LS, Ghalib L. Predictors of Postoperative Diabetes Insipidus Following Endoscopic Resection of Pituitary Adenomas. *J Endocr Soc* (2018) 2(9):1010–9. doi: 10.1210/js.2018-00121
37. Karnezis TT, Baker AB, Soler ZM, Wise SK, Rereddy SK, Patel ZM, et al. Factors Impacting Cerebrospinal Fluid Leak Rates in Endoscopic Sellar Surgery. *Int Forum Allergy Rhinol* (2016) 6(11):1117–25. doi: 10.1002/alr.21783
38. Parikh A, Adapa A, Sullivan SE, McKean EL. Predictive Factors, 30-Day Clinical Outcomes, and Costs Associated With Cerebrospinal Fluid Leak in Pituitary Adenoma Resection. *J Neurol Surg Part B Skull Base* (2020) 81 (1):43–55. doi: 10.1055/s-0039-1679896
39. Ahuja A, Guterman LR, Hopkins LN. Carotid Cavernous Fistula and False Aneurysm of the Cavernous Carotid Artery: Complications of Transsphenoidal Surgery. *Neurosurgery* (1992) 31(4):774–8; discussion 8-9. doi: 10.1227/00006123-199210000-00025
40. Kachhara R, Menon G, Bhattacharya RN, Nair S, Gupta AK, Gadhinglajkar S, et al. False Aneurysm of Cavernous Carotid Artery and Carotid Cavernous Fistula: Complications Following Transsphenoidal Surgery. *Neurol India* (2003) 51(1):81–3. doi: 10.1179/016164103101201247
41. Reddy K, Lesiuk H, West M, Fewer D. False Aneurysm of the Cavernous Carotid Artery: A Complication of Transsphenoidal Surgery. *Surg Neurol* (1990) 33(2):142–5. doi: 10.1016/0090-3019(90)90024-j
42. Sanmillán JL, Torres-Diaz A, Sanchez-Fernández JJ, Lau R, Ciller C, Puyalto P, et al. Radiologic Predictors for Extent of Resection in Pituitary Adenoma Surgery. A Single-Center Study. *World Neurosurg* (2017) 108:436–46. doi: 10.1016/j.wneu.2017.09.017

Conflict of Interest: The authors declare that the research was conducted in the absence of any commercial or financial relationships that could be construed as a potential conflict of interest.

frontiers | Frontiers in Endocrinology

ORIGINAL RESEARCH
published: 12 May 2022
doi: 10.3389/fendo.2022.857314

Surgical Experience of Transcranial Approaches to Large-to-Giant Pituitary Adenomas in Knosp Grade 4

Xiudong Guan[1†], *Yangyang Wang*[1†], *Chengkai Zhang*[1†], *Shunchang Ma*[2], *Wenjianlong Zhou*[1], *Guijun Jia*[1] *and Wang Jia*[1,2*]

[1] Department of Neurosurgery, Beijing Tiantan Hospital, Capital Medical University, Beijing, China, [2] Beijing Neurosurgical Institute, Beijing, China

Pituitary adenomas in Knosp grade 4 are difficult to resect completely and are generally involved in poor prognosis, because of the close relationship between the tumor and internal carotid. In this study, the authors retrospectively reviewed the outcome of different transcranial approaches in the management of large-to-giant pituitary adenomas in Knosp grade 4. A total of 42 patients with large-to-giant pituitary adenomas in Knosp grade 4, who underwent craniotomy in the Pituitary Disease Subdivision, Department of Neurosurgery, Beijing Tiantan Hospital, between March 2012 and March 2015 were included in this study. Clinical characteristics, surgical methods, complications, and outcomes were evaluated. The median age was 45 years (range, 19–73 years old), and 42.9% of the enrolled cases were men. The mean tumor diameter was 43.6 mm, and the mean volume was 30.9 cm^3. 26 patients underwent the frontolateral approach, while 16 cases accepted the frontotemporal approach. Gross total resection was achieved in 11 patients (26.2%), near total in 26 (61.9%), and subtotal in 5 (11.9%). The adenomas were larger, and the distance of the tumor extending to the lateral skull base was also further in the frontotemporal approach cases. The surgical time was shorter, and the bleeding volume was less in the frontolateral approach cases. Subsellar extension was associated with incomplete resection in pituitary macroadenomas of Knosp grade 4. The craniotomy is still an effective treatment for pituitary macroadenomas in Knosp grade 4.

Keywords: pituitary macroadenoma, Knosp grade 4, transcranial approach, outcome, frontolateral approach, frontotemporal approach

OPEN ACCESS

Edited by:
Congxin Dai,
Capital Medical University, China

Reviewed by:
Bing Xing,
Peking Union Medical College Hospital (CAMS), China
Yong Yao,
Peking Union Medical College Hospital (CAMS), China

***Correspondence:**
Wang Jia
jwttyy@126.com

[†]*These authors have contributed equally to this work and share first authorship*

Specialty section:
This article was submitted to Pituitary Endocrinology, a section of the journal Frontiers in Endocrinology

Received: *18 January 2022*
Accepted: *04 April 2022*
Published: *12 May 2022*

Citation:
Guan X, Wang Y, Zhang C, Ma S, Zhou W, Jia G and Jia W (2022) Surgical Experience of Transcranial Approaches to Large-to-Giant Pituitary Adenomas in Knosp Grade 4. Front. Endocrinol. 13:857314. doi: 10.3389/fendo.2022.857314

INTRODUCTION

As one of the most common benign tumors in the brain, pituitary adenoma accounts for 10%–15% of all intracranial tumors (1, 2). However, approximately 20%–55% of pituitary adenomas present an aggressive behavior and invade surrounding structures, such as the third ventricle, cavernous sinus, and sphenoid sinus. According to the Knosp classification, Knosp 3–4 was considered as a cavernous sinus invasion (3). The surgical strategy for pituitary adenomas with the cavernous sinus invasion and large tumor volume is particularly challenging, due to the deep intracranial location and being close to critical neurovascular structures.

The transsphenoidal approach is the preferred treatment in the surgical therapy of pituitary adenoma, which involves fewer complications (4). The improvements in visualization and additional lighting and the application of neuroendoscopy allow neurosurgeons to better distinguish tumor from normal tissue (5). The transsphenoidal approach is the preferred choice for pituitary adenomas with mild cavernous sinus invasion (Knosp grades 1–2), even part of adenomas in Knosp grade 3. However, endoscopic surgery still works less well in large-to-giant adenomas with multilobular configuration and extension beyond the lateral wall of the cavernous sinus, due to a narrow surgical working channel (6). Because of the adjacency of neurovascular structures in the cavernous sinus and the complicated anatomy of the skull base, it is difficult to completely remove the pituitary adenomas in Knosp grade 4 (7, 8). The incomplete resection rate is still up to 50%–65% of pituitary adenomas with the cavernous sinus invasion, even though the extended endoscopy technique has been gradually employed (9–11).

The transcranial approach is still essential for 1%–10% of large-to-giant adenomas with irregular shape and extension into the subfrontal region, retrochiasmatic area, or temporal region (6, 12). Recently, limited articles have addressed the transcranial approach to large-to-giant adenomas in Knosp grade 4.

The present study provides the outcome and complications of 42 patients with large-to-giant pituitary adenomas in Knosp grade 4 treated by the transcranial approach.

MATERIALS AND METHODS

Data Collection

The ethical review committee at the Capital Medical University approved this study. A prospectively acquired database on all patients with pituitary adenoma who underwent surgery in the Pituitary Disease Subdivision, Department of Neurosurgery, Beijing Tiantan Hospital, Capital Medical University, between March 2012 and March 2015 was retrospectively reviewed. All surgeries were performed by the senior authors (WJ and GJ). A total of 625 patients were pathologically confirmed to be pituitary adenoma during this time period. After excluding patients who are <18 years old or underwent transsphenoidal approach surgery, we finally confirmed 42 cases of craniotomy with pituitary adenomas in Knosp grade 4. The surgical approaches were discussed by neurosurgeons in our department and finally determined by two senior neurosurgeons (WJ and GJ). Tumors with mainly suprasellar invasion or a dumbbell shape tended to be treated with the frontolateral approach (**Figures 1A–C**). Pituitary adenoma in Knosp grade 4 with a large eccentric extension into the middle or posterior cranial fossa or temporal lobe tended to be dealt with using the frontotemporal approach (**Figures 2A–C**).

Radiological Findings

Magnetic resonance images (MRI) were acquired in each patient using a standard 3.0-T scanner preoperatively and postoperatively. The neurosurgeons interpreted the pre- and postsurgical MRI findings based on the T1-weighted coronal slices with and without contrast enhancement. Parasellar extension was evaluated by the Knosp grading scale (3) (grade 3 and grade 4). Suprasellar extension was identified according to the Wilson–Hardy grade (2) (grade C and grade D). Subsellar extension was estimated by the results of computed tomography (CT) combined with the MRI findings and intraoperative observation. The invasion and resection status of pituitary adenomas was respectively assessed by WJ, XG, and WZ, who provided independent evaluations in an attempt to decrease the reporting bias. To quantitatively define the tumor size, the maximum diameter of the tumor was measured based on the T1-weighted coronal slices with and without contrast enhancement from the axial, sagittal, and coronal images. The tumor volume was calculated according to the formula: $V = abc\pi/6$ (a: length; b: width; c height).

Endocrinological and Ophthalmological Evaluations

Pituitary hormone measurements, visual field tests, and visual acuity tests were performed in all patients preoperatively and 3 months postoperatively. The hormone panels included prolactin, GH, IGF-1, cortisol, ACTH, LH/FSH, progesterone, estradiol, testosterone, FT3, TT3, FT4, TT4, and TSH levels. Hormone remission was defined according to the following criteria: for patients with prolactinoma, serum PRL <20 ng/ml in women or <15 ng/ml in men (13); for patients with acromegaly, normalized age-adjusted insulin-like growth factor-1 level (IGF-1) and GH random level <1 ng/ml, or an oral glucose tolerance test <0.4 ng/ml (14, 15); and for patients with Cushing's syndrome, morning serum cortisol values <5 μg/dl or urine free cortisol <10–20 g/day (16). Male patients with reduced testosterone or female patients with low FSH levels were considered as hypogonadism. Patients with reduced fT4 and/or elevated TSH were identified as hypothyroidism. Patients with low cortisol levels were defined as hypocortisolism. Patients with low levels of all pituitary hormones were considered as panhypopituitarism.

Tumor Subtypes

Tumors were classified according to the hormone level and pathological diagnosis (17, 18). According to hormone level, tumors were classified into functioning adenomas and non-functioning adenomas. According to the histopathologic findings, non-functioning adenomas were further divided into null cell adenomas and silent pituitary adenomas (including PRL positive, GH positive, ACTH positive, FSH/LH positive, TSH positive, or plurihormonal positive).

Follow-Up

The MRI, neurological, and endocrinological evaluations were repeated at 3, 6, and 12 months followed by per year after surgery.

Statistics Analysis

Statistics analysis was performed using IBM SPSS Statistics software (version 24.0, Armonk, NY: IBM Corp). Figures were made by GraphPad Prism 7.0 for Mac OS (GraphPad Software, La Jolla CA, USA). The chi-square test was used to compare

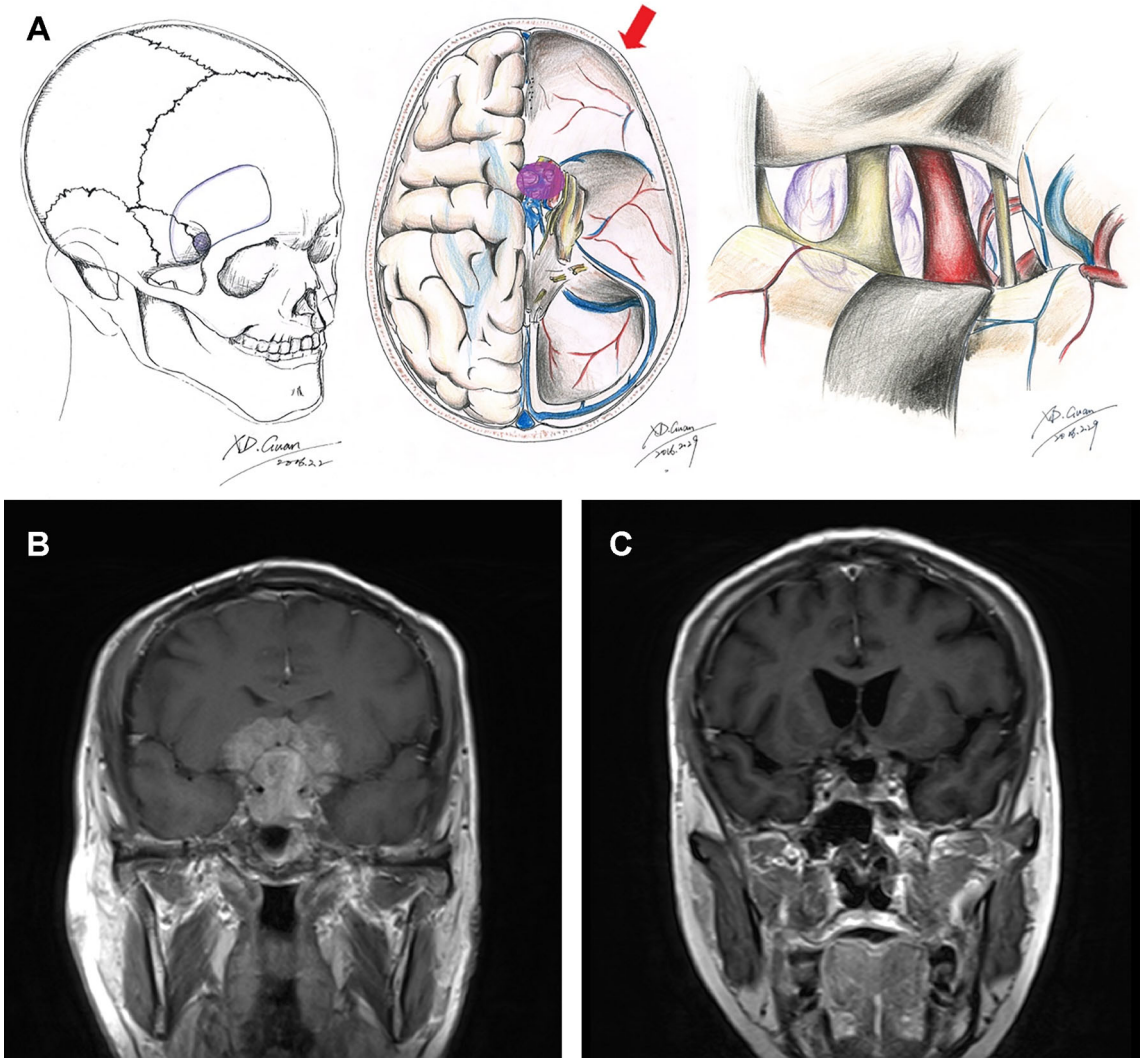

FIGURE 1 | Schematic diagrams and MRI images of frontolateral approach. Schematic diagrams of incision, surgical field, and microanatomy of frontolateral approach **(A)**. Preoperative **(B)** and 3-month postoperative **(C)** coronal enhanced MRI images of a giant pituitary adenoma in Knosp grade 4 that underwent the frontolateral approach.

categorical data, whereas an unpaired t-test was used to compare subgroup means. The Mann–Whitney U test was performed to compare the postoperative visual acuity, visual field, and resection rate between two surgical approaches. Univariable logistic regressions were performed to analyze predictors of gross total resection. A two-tailed P-value < 0.05 was considered statistically significant.

RESULTS

Clinical Features

A total of 42 patients (18 men; 42.9%) fulfilled the criteria for this study. The median age was 44 years (range, 19–73 years old). As shown in **Table 1**, the primary presenting symptom was progressive visual loss (83.3%), followed by headache (35.7%) and endocrinopathy (23.8%). The majority of patients were diagnosed with non-functioning pituitary adenomas (36/42, 85.7%). 6 patients were diagnosed with functioning pituitary adenomas, including 2 PRL-secreting adenomas, 3 GH-secreting adenomas, and 1 ACTH-secreting adenoma. 6 patients had recurrent tumors after prior microscopic transsphenoidal or transcranial surgery. Hemianopsia was observed in 31 patients (73.8%) *via* visual field testing. 3 patients (7.1%) had other cranial nerve palsies. 44.4% (8/18) of men had hypogonadism, while 37.5% (9/24) of women presented with hypogonadism. 5 patients had hypothyroidism, 5 patients had hypocortisolism, and 3 patients presented panhypopituitarism (**Table 1**).

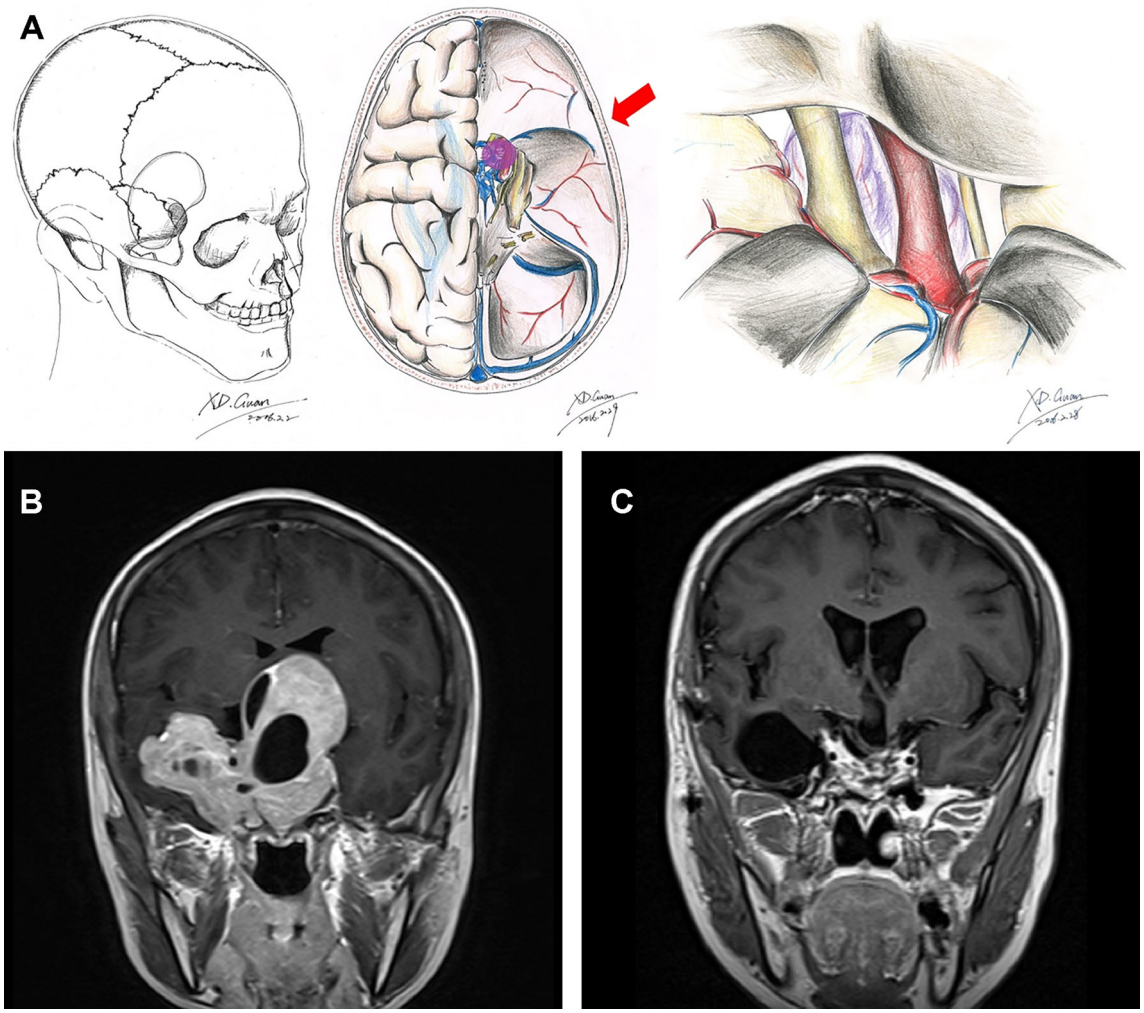

FIGURE 2 | Schematic diagram and MRI images of the frontotemporal approach. Schematic diagrams of incision, surgical field, and microanatomy of frontolateral approach **(A)**. Preoperative **(B)** and 3-month postoperative **(C)** coronal enhanced MRI images of a giant pituitary adenoma in Knosp grade 4 that underwent the frontotemporal approach.

Preoperative MRI findings demonstrated macroadenomas (>10 mm) in all patients. The maximum diameter of the tumor ranged from 25 to 76 mm (mean, 43.6 mm; SD, 11.9 mm). The maximal diameters in most adenomas (61.9%) were more than 40 mm, followed by 30 to 40 mm (26.2%) and 20 to 30 mm (11.9%). The mean approximated volume was 30.9 ± 27.8 cm^3. Besides, 76.2% of adenomas were more than 10 cm^3. Moreover, 21.4% of adenomas were the bilateral parasellar invasion. All adenomas were accompanied by suprasellar extension and compression of the optic chiasm. 40.5% of adenomas were exhibited with subsellar extension. 14.3% of tumors had a cystic formation (**Table 2**).

Surgical Approach

In this study, all patients underwent craniotomy. Surgical data were summarized as shown in **Table 3**. Among these, 61.9% of tumors were removed by the frontolateral approach (FL), and the others were *via* the frontotemporal approach (FT). The mean surgical time was 286 ± 83 min, while the mean amount of bleeding volume was 745 ± 696 ml. Near-total resection (61.9%) was the most, followed by gross total resection (26.2%) and subtotal resection (11.9%).

In our study, we found that the maximum diameter of tumors removed by the frontolateral approach (mean ± SD, 39.9 ± 11.8 mm) was significantly smaller than that of tumors resected by the frontotemporal approach (mean ± SD, 49.6 ± 10.2 mm) (P = 0.009) (**Figure 3A**). Besides, the tumor volumes in the FL group were smaller compared with the FT group (mean ± SD, 21.9 ± 19.1 cm^3 vs. 45.4 ± 33.6 cm^3, P = 0.006), (**Figure 3B**). According to the classification of tumor size, the number of giant adenomas in the FT group was also higher than that in the FL group (P = 0.003, χ^2 = 9.040) (**Table 4**). Furthermore, we measured the

TABLE 1 | Clinical characteristics of 42 patients with large to giant pituitary adenomas in Knosp grade 4.

Clinical characteristics	Value
Sex, male/female	18/24
Age (median ± SD [range]) (years)	44 ± 13 (19–73)
Presenting symptoms, n (%)	
Impaired visual acuity	35 (83.3)
Headache	15 (35.7)
Endocrinopathy	10 (23.8)
Incidental	1 (2.4)
Recurrence	6 (14.3)
Vision, n (%)	
Hemianopsia	31 (73.8)
Cranial nerve deficit	3 (7.1)
Other	5 (11.9)
Normal	4 (9.5)
Endocrinological types, n (%)	
Non-functioning adenomas	36 (85.7)
Functioning adenomas	6 (14.3)
PRL	2 (4.8)
GH	3 (7.1)
ACTH	1 (2.4)
Endocrine function, n (%)	
Hypogonadism, male	8 (44.4[a])
Hypogonadism, female	9 (37.5[b])
Hypothyroidism	5 (11.9)
Hypocortisolism	5 (11.9)
Panhypopituitarism	3 (7.1)

[a]*Number of hypogonadism in male/total number of male patients.*
[b]*Number of hypogonadism in female/total number of female patients.*

TABLE 2 | Imaging characteristics of large to giant pituitary adenomas in Knosp grade 4.

Tumor characteristic	Value
Tumor diameter, mean ± SD, mm	43.6 ± 11.9
≤30 mm, >20 mm, n (%)	5 (11.9)
≤40 mm, >30 mm, n (%)	11 (26.2)
>40 **mm**, n (%)	26 (61.9)
Tumor volume, mean ± SD, cm^3	30.9 ± 27.8
≤10 cm^3, n (%)	10 (23.8)
>10 cm^3, n (%)	32 (76.2)
Chiasm compression, n (%)	42 (100)
Parasellar invasion, n (%)	
Unilateral	33 (78.6)
Bilateral	9 (21.4)
Invasive localization, n (%)	
With suprasellar extension	42 (100)
With subsellar extension	17 (40.5)
Cystic formation, n (%)	6 (14.3)

TABLE 3 | Surgery and extent of resection.

Characteristic	Value
Surgical procedures, n (%)	
Frontolateral approach	26 (61.9)
Frontotemporal approach	16 (38.1)
Surgical time, mean ± SD, min	286 ± 83
Bleeding volume, mean ± SD, ml	745 ± 696
Extent of resection, n (%)	
Gross total	11 (26.2)
Near total	26 (61.9)
Subtotal	5 (11.9)

distance from the tumor border in the lateral skull base to the tumor center. The expanding distance in the FL (mean ± SD, 26.9 ± 1.6 mm) was also shorter compared with the FT group (mean ± SD, 33.9 ± 2.3 mm) ($P = 0.014$) (**Figure 3C**). Due to the invasion of tumors, the number of patients with subsellar extension in the FL group was more than in the FT group ($P = 0.023$, $\chi^2 = 5.203$) (**Table 4**). However, there was no significance between the two groups in the unilateral or bilateral parasellar invasion. Two groups also had no difference in the status of cystic formation and endocrinological types (**Table 4**).

Clinical Outcome and Complications

According to the postoperative histopathological testing, there were 22 null cell adenomas, 12 silent adenomas (including 1 PRL-positive, 1 GH-positive, 1 ATCH-positive, 5 FSH/LH-positive, 2 TSH-positive, and 4 plurihormonal-positive) among non-functioning adenomas. Among functioning adenomas, there were 2 PRL-positive adenomas, 1 GH-positive adenoma, 1 ACTH-positive adenoma, and 2 plurihormonal positive adenomas (**Table 5**). In functioning adenomas, the remission ratio was 1/2 in PRL adenomas, 0/3 in GH adenomas, and 1/1 in ACTH adenomas (**Table 5**).

No serious complications such as perioperative death or internal carotid artery injury occurred in the cohort. According to postoperative visual acuity testing, 11 of 35 patients with impaired visual acuity exhibited visual development after surgery, while the visual acuity of 8 patients decreased (**Table 5**). Meanwhile, 7 of 31 patients with hemianopsia revealed improvement in the visual field (**Table 5**). However, the defect of the visual field was worsened in 4 patients. Meanwhile, hemorrhage happened in two cases after surgery. 21.4% of patients suffered from postoperative infection. 16 patients presented nerve palsies, and electrolyte disturbance was shown in 20 cases (**Table 5**).

There was no difference in the extent of resection, change of visual acuity, and visual field between the two approaches. The hormone remission ratios of the FL and FT groups were 1/4 and 1/2, respectively. It was a trend that hemorrhage, infection, nerve palsies, or electrolyte disorder were more prevalent in the FT group than in the FL group, although there was no significant difference in the outcome between the two groups (**Table 6**).

Preoperative patients' clinical and radiological characteristics were analyzed to investigate the ability to predict gross total resection (**Table 7**). The subsellar extension was a potential unfavorable factor for gross total resection of pituitary macroadenomas in Knosp grade 4 (P = 0.033, OR 10.667, 95% CI 1.214–93.699). However, tumor volume and expanding distance showed no significance, although it was a trend that large volume or expanding distance contributed to the incomplete resection. Sex, age, cystic formation, and surgical approach were not significant predictors for gross total resection.

Follow-Up

36 patients (85.7%) were followed up by 15–46 months after surgery (median 30 months). Among them, 13 patients accepted adjuvant gamma knife treatment. Moreover, 3 of 36 patients presented recurrence. 18 patients presented the progression of

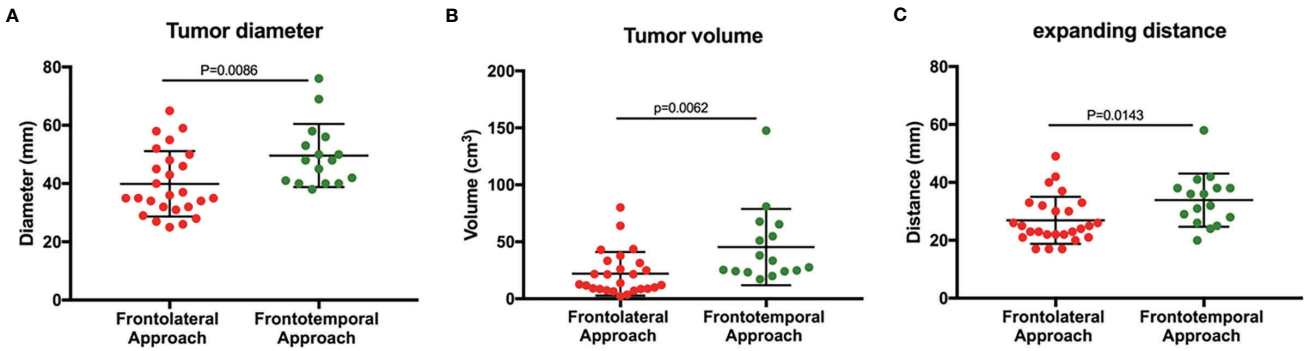

FIGURE 3 | Tumor size in the patients who underwent different surgical approaches. **(A)** The maximum diameter of tumors in two groups. **(B)** The tumor volume in two groups. **(C)** The distance of tumors expanding to the lateral skull base (Student t-test, $P < 0.05$).

TABLE 4 | Surgical approach based on preoperative imaging characteristic.

	Frontolateral approach (N = 26) n (%)	Frontotemporal approach (N = 16) n (%)	*P* value
Tumor diameter			
Macroadenoma (≤40 mm, >10 mm)	15 (57.7)	1 (6.3)	0.003[a]
Giant adenoma (>40 mm)	11 (42.3)	15 (93.8)	
Tumor volume			
Macroadenoma (≤10 cm^3)	10 (38.5)	0 (0.0)	0.007[b]
Giant adenoma (>10 cm^3)	16 (61.5)	16 (100)	
Endocrinological types			
Non-function adenomas	24 (92.3)	12 (75)	0.27[a]
Functioning adenomas	2 (7.7)	4 (25)	
Parasellar invasion			
Unilateral	23 (88.5)	10 (62.5)	0.109[a]
Bilateral	3 (11.5)	6 (37.5)	
With subsellar extension	7 (26.9)	10 (62.5)	0.023[c]
Cystic formation	3 (11.5)	3 (18.8)	0.846[c]

[a]*Continuity correction.*
[b]*Fisher's exact test.*
[c]*Pearson chi-square test.*

residual tumors. Meanwhile, the residual adenomas were stable in 13 cases. The visual acuity of 4 patients was improved during the follow-up period. However, one patient's visual acuity deteriorated. 4 patients still exhibited endocrine disorder.

DISCUSSION

As the most common lesion in the saddle area, some pituitary adenomas exhibit infiltration into the cavernous sinus structure and a close relationship with the internal carotid. Besides, neurosurgeons are in deep trouble with invasive pituitary macroadenomas as the result of low total removal rate, serious complaints, and high recurrent rate. In this study, we retrospectively reviewed 42 cases with pituitary macroadenomas in Knosp grade 4 who underwent craniotomies. A total of 26 patients underwent frontolateral approaches to remove the tumor, and 16 macroadenomas were excised by frontotemporal approaches. The gross total resection rate, near-total resection rate, and subtotal resection rate were 26.2%,11.9%, and 61.9%, respectively. In the surgical findings, the surgical time was shorter, and the bleeding volume was less through the frontolateral approach than through the frontotemporal approach. However, there was no statistical significance in postoperative complaints. The subsellar invasion was a predictor for incomplete resection.

Patients with pituitary macroadenomas generally have a poor prognosis, such as low gross total resection (GTR) rate, high rate

TABLE 5 | Clinical outcome and complications.

Characteristic	Value
Histopathology, n (%)	
Non-functioning adenomas	36 (85.7)
Null cell	22 (52.4)
PRL positive	1 (2.4)
GH positive	1 (2.4)
ACTH positive	1 (2.4)
FSH/LH positive	5 (11.9)
TSH positive	2 (4.8)
Plurihormonal positive	4 (9.5)
Functioning adenomas	6 (14.3)
PRL positive	2 (4.8)
GH positive	1 (2.3)
ACTH positive	1 (2.3)
Plurihormonal positive	2 (4.8)
Hormone remission, remission/total	
PRL	1/2
GH	0/3
ACTH	1/1
Visual acuity	
Improve	11 (26.2)
No change	23 (54.8)
Worsen	8 (19.0)
Visual field	
Improve	7 (16.7)
No change	31 (73.8)
Worsen	4 (9.5)
Complications	
Hemorrhage	2 (4.8)
Infection	9 (21.4)
Nerve palsies	16 (38.1)
Electrolyte disorder	20 (47.6)

TABLE 6 | Outcome and complications between different surgical approach.

	Frontolateral approach (N = 26)	Frontotemporal approach (N = 16)	*P* value
Extent of resection, n (%)			
Gross total	8 (30.8)	3 (18.8)	0.102[a]
Near total (>90%)	17 (65.4)	9 (56.3)	
Subtotal	1 (3.8)	4 (25.0)	
Outcome, n (%)			
Visual acuity			
Improve	7 (26.9)	4 (25.0)	0.943[a]
No change	14 (53.8)	9 (56.3)	
Worsen	5 (19.2)	3 (18.8)	
Visual field, n (%)			
Improve	5 (19.2)	2 (12.5)	0.480[a]
No change	19 (73.1)	12 (75.0)	
Worsen	2 (7.7)	2 (12.5)	
Hormone remission, remission/total	1/4	1/2	
Complications, n (%)			
Hemorrhage	1 (3.8)	1 (6.3)	
Infection	5 (19.2)	4 (25.0)	0.956[b]
Nerve palsies	9 (34.6)	7 (43.8)	0.554[c]
Electrolyte disorder	10 (38.5)	10 (62.5)	0.130[c]

[a]*Mann–Whitney U test.*
[b]*Continuity correction.*
[c]*Pearson chi-square test.*

TABLE 7 | Univariable logistic regression analyses of predictors for gross total resection.

Characteristics	OR	95% CI	*P* value
Sex (male)	2.500	0.557–11.230	0.232
Age (≥45 years)	0.889	0.224–3.534	0.867
Max diameter (>40 mm)	2.520	0.618–10.276	0.197
Tumor volume (>10 cm^3)	4.333	0.843–19.905	0.059
Expanding (≥27 mm)	3.692	0.819–16.656	0.089
Subsellar extension (with)	10.667	1.214–93.699	0.033
Cystic formation (with)	0.667	0.104–4.272	0.669
Surgical approach (frontotemporal)	1.926	0.427–8.688	0.394

of complications, and recurrence (19–24). Besides, the surgery for parasellar invasive adenomas, especially in Knosp grade 4, is a hot topic in neurosurgeons. As a result, our study focused on the outcome of patients with pituitary macroadenomas in Knosp grade 4. It is a common view that transsphenoidal surgery is the first-line treatment for patients with pituitary adenomas. With advances in technique and experience, mounting evidence suggests that endoscopic transsphenoidal surgery is a substitute for microscopic surgery for properly selected patients with pituitary macroadenomas (6, 25–27). With the development of endoscopic techniques, the endoscopic transsphenoidal approach has become the first-line treatment for the majority of pituitary adenomas. The proportion of patients undergoing the endoscopic transsphenoidal approach gradually increased (28). However, the endoscopic transsphenoidal approach also has some limitations for pituitary adenomas with parasellar invasion or Knosp grade 4. Previous retrospective studies has shown that the GTR rates for tumor extended into the anterior fossa, middle fossa, and posterior fossa were only 7.7%, 19.6%, and 14.3%, respectively (6). For giant pituitary adenomas that dealt with the transsphenoidal endoscopic approach, the GTR rate for rounded, dumbbell, and multilobular tumors was 46.7%–64%, 33.3%–46%, and only 6.1%–8%, respectively (6, 29). For patients with partial resection and intracranial remnant, transcranial reoperation was usually considered (29). In recent years, the indications of the endoscopic transsphenoidal approach gradually became broader. The extended endoscopic transsphenoidal approach can also be applied in selected pituitary adenomas in Knosp grade 4. Although a cohort of pituitary adenomas in Knosp grade 4 reached 70.6% (72/102) after aggressive endoscopic transsphenoidal surgery, life-threating internal carotid artery (ICA) injury occurred in 2 cases (30).

Providing a more panoramic visualization and wider corridor compared with microscopic surgery, extended endoscopic endonasal transsphenoidal surgery does not take the invasion of the medial wall of the cavernous sinus as a contraindication of tumor resection (6, 27, 31). However, the invasion of the lateral wall of the cavernous sinus, even the extension to the temporal lobe, is labeled as a limitation of gross total resection (6). The rate of GTR was 0% to 8% in the cases of macro or giant adenomas with Knosp grade 4 invasion (6, 27, 32, 33). Also, another reason that extensive macro or giant adenomas can be resected through craniotomy is that continuous stable displacement of the neurovascular structures, due to the slow progression of the tumor over decades, provides a potentially large preformed space for resection corridors. The exposure in the frontolateral craniotomy from the contralateral optic nerve to the ipsilateral oculomotor nerve supplies neurosurgeons variety of corridors to resect tumor through the classic subchiasmina, opticocarotid, carotid-oculomotor, and translamina terminalis pathways, allowing resection of deeply located parts of the tumor (**Figure 1A**). These kinds of multiple corridors avoid the collapse of the tumor bed after the previous steps of resection and maintains the exposure of tumor mass, allowing access to the deeper parts of the tumor (34). As a result of the exposure in this approach including the corridors in the subfrontal approach and frontotemporal approach, we do not require a larger opening at the skull surface to remove a deep lesion. Besides, the frontolateral approach could reduce the incidence of damage to the branch of the facial nerve, supraorbital nerve, and temporal muscle and protect the frontal lobe. However, using this approach is difficult to overcome parts of the lesion extending to the third ventricle, which is not available to get a good surgery field, and is difficult to protect the frontal lobe.

Provided drilling the sphenoid ridge as far down as the superior orbital fissure, the frontotemporal (pterional) approach allows neurosurgeons to reach the tumor *via* the lateral fissure (**Figure 2A**), which is the natural space between two lobes. The exposure in the frontotemporal approach from the ipsilateral optic nerve to the oculomotor supplies opticocarotid and carotid-oculomotor pathways to remove the deeply located parts of the tumor (**Figure 2A**). Besides, this approach also provides a chance

to remove the parts of the tumor invading into the cavernous sinus structure *via* opening the lateral wall of the cavernous sinus. Nevertheless, this surgical approach requires consideration of protecting the temporal branches of the facial nerve (35). Damaging them in the surgery may lead to the paralysis of the frontalis, orbicularis oculi, and corrugator supercilii muscles.

In our study, GTR, evaluated by no residual lesion on the postoperative MRI, was achieved in 26.2% of patients. In addition, the rate of near-total resection was 61.9%. These rates of resection correlate well with some other reports, whose rates are less than 10% (7, 8, 24, 36). The GTR of patients, who underwent the frontolateral approach, was not significantly different from the frontotemporal approach, although a trend toward the GTR in the frontolateral approach was better. Compared with the FL group, the tumor size in the FT group was larger. More importantly, the tumor treated by the FT approach extended further to the lateral skull base than those treated by the TL approach. We chose the frontotemporal approach to protect the frontal lobe. However, the frontotemporal approach was more complex than in the frontolateral craniotomy, leading to a long surgical time and more bleeding volume. Furthermore, the extent of resection and complications did not reach statistical significance between the two surgical approaches.

The complete resection contributes to a decrease in the risk of recurrence and an increase in the chance of endocrinological remission. Although the endoscopic transsphenoidal approach is viewed as the first-line treatment, transcranial surgery still has the advantage of removing the pituitary adenomas with parasellar invasion, especially Knosp grade 4. In this study, we analyzed the preoperative characters of the tumors to predict the extent of resection. Our experience showed that subsellar extension increased the risk of the residual lesion for macroadenomas in Knosp grade 4 when treated by the transcranial approach. In such cases, staging surgery would be a better choice to increase the chance of cure.

There were also some limitations in this study. This study was a retrospective research, and risks of selection bias existed. The operations performed in this series were designed by neurosurgeons in a single center, after a conference discussion according to the preoperative examination. Therefore, the choice of the surgical approach was subjective to some extent. We focused on the transcranial approaches for Knosp grade 4 adenoma. However, we did not discuss combined transsphenoidal and transcranial approaches.

CONCLUSION

Although the endoscopic transsphenoidal approach is the first-line treatment for pituitary adenoma, the transcranial approach acts as an alternative and still has its value for pituitary adenoma in Knosp grade 4. In the present study, 26.2% (11/42) pituitary adenoma in Knosp grade 4 achieved gross total resection after the transcranial approach. Compared with the frontolateral approach, the frontotemporal approach was more appropriate for tumors in large volume and further extended into the lateral skull base. At the same time, the frontotemporal approach was associated with longer surgical time and more bleeding volume. Subsellar extension was associated with incomplete resection in pituitary macroadenomas of Knosp grade 4. Our analysis summarized the risks and benefits of common transcranial approaches and provided evidence for the design of surgical procedures for large to giant pituitary adenomas in Knosp grade 4.

DATA AVAILABILITY STATEMENT

The raw data supporting the conclusions of this article will be made available by the authors, without undue reservation.

ETHICS STATEMENT

The studies involving human participants were reviewed and approved by the ethical review committee at the Capital Medical University. Written informed consent for participation was not required for this study in accordance with the national legislation and the institutional requirements.

AUTHOR CONTRIBUTIONS

WJ and XG designed the study. XG, YW, CZ, and WZ acquired the data. XG, CZ, and SM analyzed and interpreted the data. WJ and GJ performed surgery on patients. XG and YW wrote the first draft. WJ was responsible for the integrity and accuracy of the data and was the supervisor. All authors contributed to the article and approved the submitted version.

FUNDING

This work was supported by the Capital Health Research and Development of Special (2014–2–1072) and the Beijing Municipal Natural Science Foundation (7142054).

ACKNOWLEDGMENTS

The authors are particularly grateful to WJ for consecutive help and guidance during the study.

REFERENCES

1. Kovacs K, Horvath E. Pathology of Pituitary Tumors. *Endocrinol Metab Clin North Am* (1987) 16(3):529–51. doi: 10.1016/S0889-8529(18)30463-8
2. Wilson CB. A Decade of Pituitary Microsurgery. The Herbert Olivecrona Lecture. *J Neurosurg* (1984) 61(5):814–33. doi: 10.3171/jns.1984.61.5.0814
3. Knosp E, Steiner E, Kitz K, Matula C. Pituitary Adenomas With Invasion of the Cavernous Sinus Space: A Magnetic Resonance Imaging Classification Compared With Surgical Findings. *Neurosurgery* (1993) 33(4):610–7; discussion 7-8. doi: 10.1227/00006123-199310000-00008
4. Fahlbusch R, Buchfelder M. Transsphenoidal Surgery of Parasellar Pituitary Adenomas. *Acta Neurochirurgica* (1988) 92(1-4):93–9. doi: 10.1007/BF01401978
5. Eseonu CI, ReFaey K, Rincon-Torroella J, Garcia O, Wand GS, Salvatori R, et al. Endoscopic Versus Microscopic Transsphenoidal Approach for Pituitary Adenomas: Comparison of Outcomes During the Transition of Methods of a Single-Surgeon. *World Neurosurg* (2016) 97:317–25. doi: 10.1016/j.wneu.2016.09.120
6. Koutourousiou M, Gardner PA, Fernandez-Miranda JC, Paluzzi A, Wang EW, Snyderman CH. Endoscopic Endonasal Surgery for Giant Pituitary Adenomas: Advantages and Limitations. *J Neurosurg* (2013) 118(3):621–31. doi: 10.3171/2012.11.JNS121190
7. Nishioka H, Fukuhara N, Horiguchi K, Yamada S. Aggressive Transsphenoidal Resection of Tumors Invading the Cavernous Sinus in Patients With Acromegaly: Predictive Factors, Strategies, and Outcomes. *J Neurosurg* (2014) 121(3):505–10. doi: 10.3171/2014.3.JNS132214
8. Micko AS, Wohrer A, Wolfsberger S, Knosp E. Invasion of the Cavernous Sinus Space in Pituitary Adenomas: Endoscopic Verification and its Correlation With an MRI-Based Classification. *J Neurosurg* (2015) 122(4):803–11. doi: 10.3171/2014.12.jns141083
9. Dhandapani S, Singh H, Negm HM, Cohen S, Anand VK, Schwartz TH. Cavernous Sinus Invasion in Pituitary Adenomas: Systematic Review and Pooled Data Meta-Analysis of Radiologic Criteria and Comparison of Endoscopic and Microscopic Surgery. *World Neurosurg* (2016) 96:36–46. doi: 10.1016/j.wneu.2016.08.088
10. Paluzzi A, Fernandez-Miranda JC, Tonya Stefko S, Challinor S, Snyderman CH, Gardner PA. Endoscopic Endonasal Approach for Pituitary Adenomas: A Series of 555 Patients. *Pituitary* (2014) 17(4):307–19. doi: 10.1007/s11102-013-0502-4
11. Dehdashti AR, Ganna A, Karabatsou K, Gentili F. Pure Endoscopic Endonasal Approach for Pituitary Adenomas: Early Surgical Results in 200 Patients and Comparison With Previous Microsurgical Series. *Neurosurgery* (2008) 62(5):1006–15; discussion 15-7. doi: 10.1227/01.neu.0000325862.83961.12
12. Pratheesh R, Rajaratnam S, Prabhu K, Mani SE, Chacko G, Chacko AG. The Current Role of Transcranial Surgery in the Management of Pituitary Adenomas. *Pituitary* (2013) 16(4):419–34. doi: 10.1007/s11102-012-0439-z
13. Casanueva F, Molitch M, Schlechte J, Abs R, Bonert V, Bronstein M, et al. Guidelines of the Pituitary Society for the Diagnosis and Management of Prolactinomas. *Clin Endocrinol* (2006) 65(2):265–73. doi: 10.1111/j.1365-2265.2006.02562.x
14. Katznelson L, Laws E, Melmed S, Molitch M, Murad M, Utz A, et al. Acromegaly: An Endocrine Society Clinical Practice Guideline. *J Clin Endocrinol Metab* (2014) 99(11):3933–51. doi: 10.1210/jc.2014-2700
15. Giustina A, Chanson P, Bronstein M, Klibanski A, Lamberts S, Casanueva F, et al. A Consensus on Criteria for Cure of Acromegaly. *J Clin Endocrinol Metab* (2010) 95(7):3141–8. doi: 10.1210/jc.2009-2670
16. Nieman L, Biller B, Findling J, Murad M, Newell-Price J, Savage M, et al. Treatment of Cushing's Syndrome: An Endocrine Society Clinical Practice Guideline. *J Clin Endocrinol Metab* (2015) 100(8):2807–31. doi: 10.1210/jc.2015-1818
17. Lim C, Korbonits M. Update on the Clinicopathology of Pituitary Adenomas. *Endocrine Pract* (2018) 24(5):473–88. doi: 10.4158/ep-2018-0034
18. Drummond J, Roncaroli F, Grossman A, Korbonits M. Clinical and Pathological Aspects of Silent Pituitary Adenomas. *J Clin Endocrinol Metab* (2019) 104(7):2473–89. doi: 10.1210/jc.2018-00688
19. Przybylowski CJ, Dallapiazza RF, Williams BJ, Pomeraniec IJ, Xu Z, Payne SC, et al. Primary Versus Revision Transsphenoidal Resection for Nonfunctioning Pituitary Macroadenomas: Matched Cohort Study. *J Neurosurg* (2017) 126(3):889–96. doi: 10.3171/2016.3.jns152735
20. Mehta GU, Oldfield EH. Prevention of Intraoperative Cerebrospinal Fluid Leaks by Lumbar Cerebrospinal Fluid Drainage During Surgery for Pituitary Macroadenomas. *J Neurosurg* (2012) 116(6):1299–303. doi: 10.3171/2012.3.jns112160
21. Magro E, Graillon T, Lassave J, Castinetti F, Boissonneau S, Tabouret E, et al. Complications Related to the Endoscopic Endonasal Transsphenoidal Approach for Nonfunctioning Pituitary Macroadenomas in 300 Consecutive Patients. *World Neurosurg* (2016) 89:442–53. doi: 10.1016/j.wneu.2016.02.059
22. Hoang N, Tran DK, Herde R, Couldwell GC, Osborn AG, Couldwell WT. Pituitary Macroadenomas With Oculomotor Cistern Extension and Tracking: Implications for Surgical Management. *J Neurosurg* (2016) 125(2):315–22. doi: 10.3171/2015.5.jns15107
23. Dallapiazza R, Bond AE, Grober Y, Louis RG, Payne SC, Oldfield EH, et al. Retrospective Analysis of a Concurrent Series of Microscopic Versus Endoscopic Transsphenoidal Surgeries for Knosp Grades 0-2 Nonfunctioning Pituitary Macroadenomas at a Single Institution. *J Neurosurg* (2014) 121(3):511–7. doi: 10.3171/2014.6.jns131321
24. Chabot JD, Chakraborty S, Imbarrato G, Dehdashti AR. Evaluation of Outcomes After Endoscopic Endonasal Surgery for Large and Giant Pituitary Macroadenoma: A Retrospective Review of 39 Consecutive Patients. *World Neurosurg* (2015) 84(4):978–88. doi: 10.1016/j.wneu.2015.06.007
25. Nakao N, Itakura T. Surgical Outcome of the Endoscopic Endonasal Approach for non-Functioning Giant Pituitary Adenoma. *J Clin Neurosci* (2011) 18(1):71–5. doi: 10.1016/j.jocn.2010.04.049
26. Cusimano MD, Kan P, Nassiri F, Anderson J, Goguen J, Vanek I, et al. Outcomes of Surgically Treated Giant Pituitary Tumours. *Can J Neurol Sci Le J Canadien Des Sci Neurol* (2012) 39(4):446–57. doi: 10.1017/S0317167100013950
27. Juraschka K, Khan OH, Godoy BL, Monsalves E, Kilian A, Krischek B, et al. Endoscopic Endonasal Transsphenoidal Approach to Large and Giant Pituitary Adenomas: Institutional Experience and Predictors of Extent of Resection. *J Neurosurg* (2014) 121(1):75–83. doi: 10.3171/2014.3.JNS131679
28. Crowther S, Rushworth R, Rankin W, Falhammar H, Phillips L, Torpy D. Trends in Surgery, Hospital Admissions and Imaging for Pituitary Adenomas in Australia. *Endocrine* (2018) 59(2):373–82. doi: 10.1007/s12020-017-1457-4
29. Micko A, Agam M, Brunswick A, Strickland B, Rutkowski M, Carmichael J, et al. Treatment Strategies for Giant Pituitary Adenomas in the Era of Endoscopic Transsphenoidal Surgery: A Multicenter Series. *J Neurosurg* (2022) 136(3):776–85. doi: 10.3171/2021.1.Jns203982
30. Ouyang T, Zhang N, Xie S, Tang B, Li J, Xiao L, et al. Outcomes and Complications of Aggressive Resection Strategy for Pituitary Adenomas in Knosp Grade 4 With Transsphenoidal Endoscopy. *Front Oncol* (2021) 11:693063. doi: 10.3389/fonc.2021.693063
31. Di Maio S, Cavallo LM, Esposito F, Stagno V, Corriero OV, Cappabianca P. Extended Endoscopic Endonasal Approach for Selected Pituitary Adenomas: Early Experience. *J Neurosurg* (2011) 114(2):345–53. doi: 10.3171/2010.9.jns10262
32. Woodworth GF, Patel KS, Shin B, Burkhardt JK, Tsiouris AJ, McCoul ED, et al. Surgical Outcomes Using a Medial-To-Lateral Endonasal Endoscopic Approach to Pituitary Adenomas Invading the Cavernous Sinus. *J Neurosurg* (2014) 120(5):1086–94. doi: 10.3171/2014.1.jns131228
33. de Paiva Neto MA, Vandergrift A, Fatemi N, Gorgulho AA, Desalles AA, Cohan P, et al. Endonasal Transsphenoidal Surgery and Multimodality Treatment for Giant Pituitary Adenomas. *Clin Endocrinol* (2010) 72(4):512–9. doi: 10.1111/j.1365-2265.2009.03665.x
34. Gerganov V, Metwali H, Samii A, Fahlbusch R, Samii M. Microsurgical Resection of Extensive Craniopharyngiomas Using a Frontolateral Approach: Operative Technique and Outcome. *J Neurosurg* (2014) 120(2):559–70. doi: 10.3171/2013.9.JNS122133
35. Poblete T, Jiang X, Komune N, Matsushima K, Rhoton ALJr. Preservation of the Nerves to the Frontalis Muscle During Pterional Craniotomy. *J Neurosurg* (2015) 122(6):1274–82. doi: 10.3171/2014.10.JNS142061
36. Yamada S, Fukuhara N, Horiguchi K, Yamaguchi-Okada M, Nishioka H, Takeshita A, et al. Clinicopathological Characteristics and Therapeutic Outcomes in Thyrotropin-Secreting Pituitary Adenomas: A Single-Center

Study of 90 Cases. *J Neurosurg* (2014) 121(6):1462–73. doi: 10.3171/2014.7.jns1471

Conflict of Interest: The authors declare that the research was conducted in the absence of any commercial or financial relationships that could be construed as a potential conflict of interest.

Publisher's Note: All claims expressed in this article are solely those of the authors and do not necessarily represent those of their affiliated organizations, or those of the publisher, the editors and the reviewers. Any product that may be evaluated in this article, or claim that may be made by its manufacturer, is not guaranteed or endorsed by the publisher.

frontiers | Frontiers in Endocrinology

ORIGINAL RESEARCH
published: 18 May 2022
doi: 10.3389/fendo.2022.861540

A Clinicopathological and Molecular Analysis of Sellar/Suprasellar Neurocytoma Mimicking Pituitary Adenoma

Lifeng Zhang[1†], Weiwei Fu[2†], Limei Zheng[3], Fangling Song[3], Yupeng Chen[3], Changzhen Jiang[4], Zhen Xing[5], Chengcong Hu[3], Yuhong Ye[3], Sheng Zhang[3], Xiaorong Yan[4] and Xingfu Wang[3*]*

[1] Department of Endocrinology, Fujian Provincial Governmental Hospital, Fuzhou, China, [2] Department of Pathology, The Affiliated Hospital of Qingdao University, Qingdao, China, [3] Department of Pathology, The First Affiliated Hospital of Fujian Medical University, Fuzhou, China, [4] Department of Neurosurgery, The First Affiliated Hospital of Fujian Medical University, Fuzhou, China, [5] Department of Radiology, The First Affiliated Hospital of Fujian Medical University, Fuzhou, China

OPEN ACCESS

Edited by:
Congxin Dai,
Capital Medical University, China

Reviewed by:
Shun Yao,
Sun Yat-sen University, China
Ting Lei,
Tongji Hospital, China

***Correspondence:**
Xingfu Wang
wang_xfu@126.com
Xiaorong Yan
178603351@qq.com

[†]These authors have contributed equally to this work

Specialty section:
This article was submitted to Pituitary Endocrinology, a section of the journal Frontiers in Endocrinology

Received: 24 January 2022
Accepted: 08 April 2022
Published: 18 May 2022

Citation:
Zhang L, Fu W, Zheng L, Song F, Chen Y, Jiang C, Xing Z, Hu C, Zhang S, Ye Y, Yan X and Wang X (2022) A Clinicopathological and Molecular Analysis of Sellar/Suprasellar Neurocytoma Mimicking Pituitary Adenoma. Front. Endocrinol. 13:861540. doi: 10.3389/fendo.2022.861540

Objective: To investigate the clinicopathological characteristics, molecular genetic characteristics and prognosis of extraventricular neurocytoma located in the sellar/suprasellar region.

Methods: Seven archived tumor samples derived from 4 patients with neurocytoma in the sellar/suprasellar region were collected from the First Affiliated Hospital of Fujian Medical University and the Affiliated Hospital of Qingdao University and retrospectively analyzed for clinical manifestations, imaging features, and histopathological features. Neuronal and pituitary biomarkers and molecular features were detected in these tumor tissues by immunohistochemistry and FISH or Sanger sequencing. The related literature was reviewed.

Results: Three patients were female, while 1 was male, with an average age of 35.5 years (range: 27 to 45 years). The initial manifestations were mainly headache and blurred vision in both eyes. The first MRI examination showed marginally enhancing masses in the intrasellar or intra- to suprasellar region. The diagnosis of pituitary adenomas was based on imaging features. The levels of pituitary hormones were normal. Histologically, the tumor cells were arranged in a sheet-like, monotonous architecture and were uniform in size and shape with round to oval, exquisite and hyperchromatic nuclei, which densely packed close to one another and were separated only by a delicate neuropil background. There was no evident mitosis, necrosis or microvascular proliferation. The three cases of recurrent tumors were highly cellular and showed increased mitotic activity. Immunohistochemically, the tumor cells were positive for syn, CR, CgA, and vasopressin and were focally positive for NeuN, TTF-1, NF, CK8, vimentin, and S100 proteins. Other markers, including IDH1, BRAF VE1, Olig-2, and EMA, were negative. Pituitary transcription factors and anterior pituitary hormones were negative. Molecular genetic testing showed that the tumor cells lacked IDH gene mutations, LOH of 1p/19q,

MYCN amplification, and EGFR alteration. With a median follow-up of 74.5 months (range 23 to 137 months), 3 patients relapsed at 11, 50, and 118 months after the initial surgery.

Conclusion: The morphological features and immunophenotypes of neurocytoma in the sellar/suprasellar region are similar to those of classic central neurocytoma. The prognosis is relatively good. Gross-subtotal resection and atypical subtype may be related to tumor recurrence.

Keywords: neurocytoma, extraventricular neurocytoma, sellar and suprasellar region, pituitary tumor, clincopathology

INTRODUCTION

The first case of neurocytoma was reported by Hassoun et al. in 1982, who described two cases of third ventricle tumors with neuronal differentiation and proposed the term "central neurocytoma" (CN) (1). Thereafter, tumors with clinicopathological features similar to central neurocytoma were found outside the ventricles, including the hemispheric parenchyma, cerebellum, pons, spinal cord, cauda equina, and retina, which have been termed "extraventricular neurocytoma" (EVN) (2). In 2007, EVN was officially recognized by the World Health Organization (WHO) classification of central nervous system tumors as a distinct entity among glioneuronal tumors, making up 10% of all neurocytomas.

The radiological, histopathological, and immunophenotypic features of EVNs resemble those of CNs. Contrary to CNs, EVNs have a marked tendency for ganglionic differentiation. In addition, EVNs have molecular characteristics distinct from those of CNs (3). The prognosis is generally good for patients with CNs or EVNs who can undergo complete removal. EVN arising in the sellar or suprasellar region is an extremely rare tumor proposed to be within the family of CNS neurocytomas. To the best of our knowledge, there are only 21 cases of sellar/suprasellar neurocytoma reported in the English literature. The neuroimaging features of EVNs arising from the sellar/suprasellar region are indistinguishable from those seen in tumors of the pituitary gland. Histopathologically, the differential diagnosis of sellar/suprasellar EVNs includes pituitary adenoma/pituitary neuroendocrine tumors that can also invade the sinuses, paraganglioma, and olfactory neuroblastoma (4). The biological behavior of sellar/suprasellar EVNs is unclear because few cases have been reported. Here, we retrospectively analyzed the clinicopathological and molecular features of 4 cases of extraventricular neurocytoma arising in the sellar or suprasellar region and reviewed the related literature.

MATERIALS AND METHODS

Seven tumor samples from 4 patients with sellar/suprasellar EVN were retrieved from the archives of the Department of Pathology of the First Affiliated Hospital of Fujian Medical University and the Affiliated Hospital of Qingdao University between 2000 and 2020 with the approval of the research ethics board. Written informed consent was obtained from the individual(s) AND/OR minor(s)' legal guardian/next of kin for the publication of any potentially identifiable images or data included in this article. Clinical data of the patients were obtained from their medical records.

All available immunohistochemical stains were reviewed and documented. If not performed at the time of pathological diagnosis, immunostaining including pituitary transcription factors and so on was performed for each tissue sample with the available formalin-fixed paraffin-embedded tissue blocks. Primary antibodies used for immunostaining are against the following proteins: pituitary-specific positive transcription factor 1 (Pit1), T-box transcription factor 19 (T-Pit), splicing factor 1(SF1), estrogen receptor alpha (ERα), GATA binding protein 2 (GATA2), thyroid transcription factor 1 (TTF1, SPT24), synaptophysin(syn), chromogranin A(CgA), cytokeratin 8 (CK8), prolactin, growth hormone (GH), thyroid-stimulating hormone (TSH), adrenocorticotropic hormone (ACTH), follicle-stimulating hormone (FSH), luteinizing hormone(LH), S100, neuron-specific enolase (NSE), neuronal nuclei (NeuN), calretinin, glial fibrillary acidic protein (GFAP), oligodendrocyte transcription factor 2(Olig2), neurofilament protein (NF), Ki-67, GATA3, p53, E-cadherin, and vasopressin. Staining was performed on a BenchMark ULTRA system (Ventana Medical Systems, Tucson, AZ). A reticulin stain was also performed.

All 7 samples were tested by fluorescence *in situ* hybridization for bHLH transcription factor (MYCN), fibroblast growth factor receptor 1 (FGFR1), epidermal growth factor receptor (EGFR), 1p/19q and cyclin dependent kinase inhibitor 2A (CDKN2A) gene alterations and sequencing by Sanger sequencing for isocitrate dehydrogenase 1 (IDH1), IDH2, and BRAF V600E mutations. All probes were obtained from Gene Company Limited (Hong Kong).

RESULTS

Clinical and Radiologic Findings

The study group included 3 women and 1 man whose age at the onset of symptoms ranged from 27 to 46 years with a median age of 34 years. Patients presented mainly with worsening visual disturbances and headaches for 5 months to 2 years. All patients had no abnormalities of adenohypophyseal hormones on the preoperative examination. CT scan demonstrated a well-circumscribed lesion isodense with the brain parenchyma. Focal calcification in the tumor was present in case 4. Brain

magnetic resonance imaging (MRI) revealed a sellar solid mass, with focal cysts in cases 3 and 4 extending to the suprasellar region, causing enlargement of the sellar, infiltrating the cavernous sinus, and encasing the internal carotid artery. The masses were isointense or hypointense on T1-weighted imaging and heterogeneously hyperintense on T2-weighted imaging. Post-contrast T1 images showed moderate enhancement (**Figure 1**) (**Table 1**).

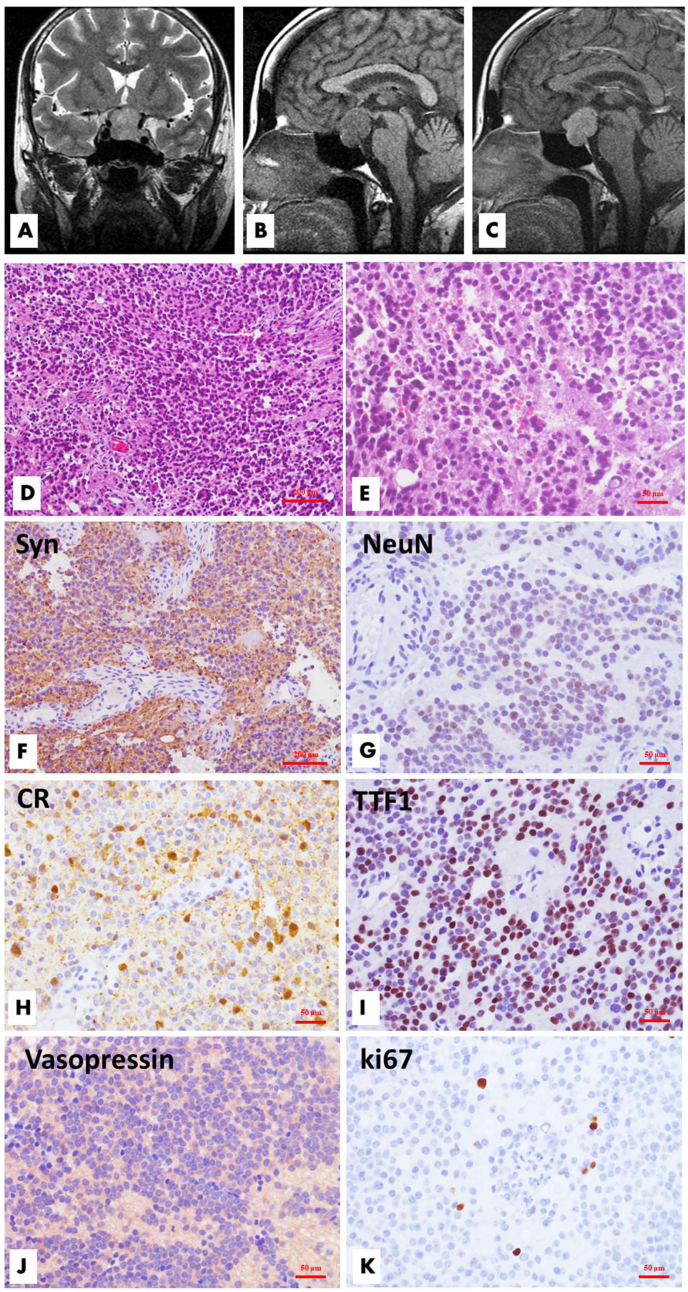

FIGURE 1 | Radiological, histological and immunohistochemical features of sellar/suprasellar neurocytoma (Case 1). MR imaging demonstrated a well-circumscribed mass located in the sellar and suprasellar regions. The tumor was inhomogeneously hyperintense on coronal T2WI, and the left suprasellar sinus space was involved **(A)**, while the lesion was hypointense on sagittal T1WI, and the optic chiasma was displaced upwardly **(B)**. The lesion showed significant homogeneous enhancement on enhanced T1WI **(C)**. Microscopically, the tumor is comprised of solid nests or sheets of noncohesive monotonous small round cells with round to oval nuclei and fine chromatin. The poorly defined cytoplasm merges with the neuropil. Necrosis and mitotic figures are absent. **(D**, H&E, ×100; **E**, H&E, ×200**)** Immunohistochemical analysis revealed that the tumor cells had neuronal differentiation and were positive for synaptophysin **(F**, ×100**)**, NeuN **(G**, ×200**)**, and calretinin **(H**, ×200**)**. TTF1 **(I**, ×200**)** and vasopressin **(J**, ×200**)** had variable reactivities. The Ki-67 labeling index is approximately 1.5% **(K**, ×200**)**.

TABLE 1 | Clinicopathological details of the present 4 cases of sellar/suprasellar neurocytoma.

case	Sex	Age	Initial symptoms	Serum vasopressin	Pituitary hormone	Location	Focal infiltrations	Preoperative impression	Type	Initial operation	Adjuvant radiotherapy	Recurrence (months)	second operation	Type	follow-up (months)
1	F	28	Visual disturbances; 2-year	normal	normal	S/S	yes	Pituitary adenoma	typical	STR	No	Yes (50)	STR	atypical	(live) 63
2	M	46	Visual impairment; 2-year	NA	NA	S/S	yes	Pituitary adenoma	typical	STR	No	Yes (118)	STR	typical	(live) 137
3	F	27	Blurred vision; 5-month	NA	normal	S/S	yes	Pituitary benign tumor	typical	GTR	No	No	No	No	(live) 65
4	F	40	Bitemporal hemianopsia; 10-month	NA	normal	S/S	yes	Pituitary adenoma	atypical	STR	No	Yes (11)	STR	atypical	(live) 23

NA, Not available; S/S, Sellar/Suprasellar; S, Sellar; PA, Pituitary adenoma; STR, Subtotal resection; GTR, Gross total resection.

Histopathological Features

Histopathological examination revealed a moderately hypercellular neoplasm comprised of sheets of small- to medium-sized cells with round-to-oval, monomorphic nuclei with dispersed chromatin and inconspicuous nucleoli (**Figure 1**). The nuclei were surrounded by scant finely granular eosinophilic cytoplasm or perinuclear halos. Focal areas of the tumor were less cellular and had anuclear areas with fine fibrillary neuropil. Rare mitotic figures were present. Necrosis and vascular proliferation were absent. There was focal fibrosis and calcification. The recurrent tumor tissues of case 1 (**Figure 2**) and case 4 showed atypical histologic features, including focal necrosis, microvascular proliferation, and active mitoses. In addition, the recurrence of case 1 was comprised of smaller-sized and partly markedly hypercellular tumor cells. Classical large gangliocytes were lacking in the tumor tissues of all 7 samples.

Immunophenotypic Features and Molecular Genetics Results

Immunohistochemically, the tumor cells were positive for synaptophysin, chromogranin A, and calretinin and were focally positive for NeuN, TTF1, NF, CK8, vimentin, and S100 proteins. A few entrapped or reactive astrocytes expressed GFAP, but the tumor cells were negative. Other markers, including IDH1, BRAF VE1, Olig-2, EMA, E-cadherin and GATA3, were negative. All pituitary transcription factors, including Pit-1, T-pit, SF1, ER_{α}, and GATA2, and anterior pituitary hormones, such as GH, PRL, TSH, FSH, LH and ACTH, were negative. However, vasopressin expression was identified in all 7 samples. The Ki-67 labeling index of cases 1-3 was 1% to 2%, and it was 6% in case 4, while those of the recurrent cases 1, 2 and 4 were 5%, 2%, and 10%, respectively.

Sanger sequencing did not detect IDH1, IDH2 or *H3F3A* mutations in 5 of 7 FFPE samples (case 1 and its recurrence, recurrence of case 2 and case 4, and case 3), while loss of ATRX expression was absent by immunostaining. Fluorescence *in situ* hybridization (FISH) detection showed that tumor cells were intact on chromosomes 1p and 19q, CDKN2A nondeletion, and EGFR nonamplification. Rearrangement of fibroblast growth factor receptor 1 (*FGFR1*) was not found by *FGFR1 break*-apart *probe FISH*. The BRAF V600E mutation and TERT promoter mutations were negative by tetraprimer amplification refractory mutation system-polymerase chain reaction (ARMS-PCR), and the absence of O6-methylguanine-*DNA* methyltransferase (*MGMT*) gene promoter methylation was identified by pyrosequencing in the 3 cases of recurrence (**Table 2**).

Treatments and Prognosis

All 4 patients underwent surgical treatment. Case 2 was excised *via* a transsphenoidal procedure tumor resection, and transsphenoidal endoscopic approach resection of the mass was performed in the other three cases. The tumors in case 1, case 2 and case 4 were resected subtotally through the nasal sella. In case 4, only approximately 2/3 of the mass could be removed.

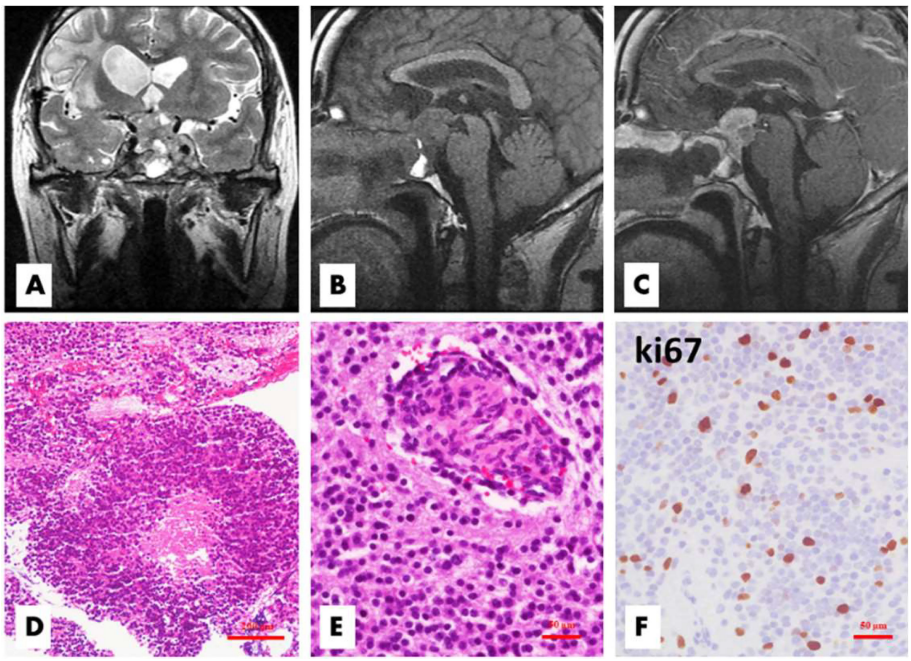

FIGURE 2 | Patient 1 relapsed 50 months after the first surgery. The tumor located in the sellar and suprasellar regions demonstrated inhomogeneous hyperintensity on coronal T2WI, and the bilateral cavernous sinuses were involved **(A)**. On sagittal T1WI images, the lesion exhibited inhomogeneous hypointensity and irregular margins **(B)**, with significant inhomogeneous enhancement on enhanced T1WI **(C)**. Histologically, there were some atypical or anaplastic features, including focal necrosis **(D**, H&E, ×100**)** and microvascular proliferation **(E**, H&E,×200**)**, with a high Ki-67 index **(F**, ×200**)**.

With a median follow-up of 74.5 months (range 23 to 137 months), all 4 patients survived. Case 1, case 2 and case 4 relapsed at 50, 118 and 11 months after initial surgery, and they underwent a transsphenoidal endoscopic approach resection for subtotal removal of the tumor again. Radiation therapy was performed after the second surgery (**Table 1**).

DISCUSSION

Sellar/suprasellar neurocytoma is an extraventricular neurocytoma arising from the hypothalamic-pituitary region. Only 21 cases of EVNs arising in the sellar/suprasellar region have ever been reported in the English literature. The clinical, radiological, and pathological features of the patients are shown in **Table 3**. The ages of the patients at first diagnosis ranged from 14 to 70 years, with an average of 44 years, and the female-to-male ratio was 1:1. The original complaints were reduced visual acuity with bitemporal or asymmetrical hemianopsia related to focal compression. Headache and dizziness would also occur. Radiological examination revealed that the sellar/suprasellar neurocytomas were generally well-defined, solid, homogeneous, and with limited or no peritumoral swelling. Small–scattered calcifications and cystic components occurred in a few cases. The vast majority of tumors, including the present 4 cases we reported, presented with invasion of the cavernous sinus. The CT scans revealed discreetly iso/hyperdense and heterogeneous enhancing appearances. In general, magnetic resonance imaging (MRI) showed that the EVNs were iso-signal to gray matter on T1- and T2-weighted images, with a variable heterogeneous enhancement pattern (6, 9, 23).

Histopathologically, EVNs arising in the sellar/suprasellar region have similar features of central neurocytoma and EVNs arising from other loci (4, 18, 19). These tumors are comprised of sheets of uniform round cells with "salt and pepper" chromatin and inconspicuous nucleoli. The tumor cells are usually embedded in a neuropil-like fibrillary background. Calcifications and 'chicken wire'-like capillaries are also common. Ganglion cell differentiation is uncommon in central neurocytomas but is relatively frequent, up to approximately 50%, in extraventricular neurocytomas (24–26). EVN with ganglioid differentiation mainly arises from the frontal, temporal, and parietal lobes. There are only 2 cases of EVN with ganglioid differentiation occurring in the sellar/suprasellar region reported in the literature (20). No evidence of ganglioid differentiation was shown in any of the 7 sample tissues in this study. Necrosis and microvascular proliferation occur in a few cases with aggressive growth. In our cases, 2 recurrences showed anaplastic characteristics and progressed into atypical EVNs.

Immunohistochemistry confirmed that neurocytomas are positive for neuronal differentiation markers such as synaptophysin and chromogranin A and variable neurofilaments, NeuN and calretinin. Hypothalamic hormone vasopressin and focal TTF-1 expression are seen, and some

TABLE 2 | Immunohistochemical and molecular features of all 7 samples of 4 cases of sellar/suprasellar neurocytoma.

Case	Syn	NeuN	NF	TTF1	vasopressin	calretinin	MAP2	TFs	hormones	Ki67 (+,%)	IDH1/2 (Sanger Sequencing)	1p/19q (FISH)	EGFR (FISH)	TERT (Sanger sequencing)	CDKN2A (FISH)	FGFR1 (FISH)	MGMT (Pyro-sequencing)
1	++	f+	f+	S+	+	+	+	–	–	1.5	wildtype	intact	nonamp	wildtype	intact	nonrearrangement	NA
R1	++	f+	–	–	+	+	+	–	–	5	wildtype	intact	nonamp	wildtype	intact	nonrearrangement	unmethylated
2	++	+	f+	S+	+	+	+	–	–	1	NA	NA	NA	NA	NA	nonrearrangement	NA
R2	++	S+	f+	–	+	+	+	–	–	2	wildtype	intact	nonamp	wildtype	intact	nonrearrangement	unmethylated
3	++	+	f+	+	+	++	+	–	–	1.5	wildtype	intact	nonamp	wildtype	intact	nonrearrangement	NA
4	++	f+	f+	+	+	+	+	–	–	6	NA	NA	nonamp	NA	intact	nonrearrangement	NA
R4	++	f+	f+	S+	+	W+	+	–	–	10	wildtype	intact	nonamp	wildtype	intact	nonrearrangement	unmethylated

+, positive; ++, strongly positive; f, focally; s, scattered; w, weakly; -, negative; TFs, transcr factors of adenohypophysis; NA, not available; FISH, fluorescence in situ hybridization.

researchers have suggested that these tumors may be derived from the basal hypothalamus, which could provide a useful diagnostic tool for differential diagnosis. They were all negative for pituitary transcription factors and hormones, GFAP, keratins, EMA, IDH1, BRAF VE1, Olig-2 and so on. Most CNs usually show a Ki-67 labeling index of less than 2%; however, a small portion of tumors that are termed atypical CNs are characterized by an increased Ki-67 labeling index of more than 2% or 3%. Atypical CN was recognized by the WHO in 2016, accounting for approximately 25% of all CNs (27). A strict definition of "atypical EVN" has not been clarified by the WHO, and the Ki-67 labeling index for the definition of atypia ranges from 2% to 5% among different studies (28, 29). Generally, atypical EVNs are characterized by increased mitotic activity or a higher Ki-67 labeling index and other atypical features, such as necrosis or microvascular proliferation (29, 30). Compared with atypical CNs, the proportion of atypical EVNs is approximately 30% higher than that of all EVNs. The atypical cases of sellar/suprasellar EVNs in the literature and this study had a similar rate, accounting for 32% (8/25).

To date, little is known about the molecular genetic features of extraventricular neurocytoma. A study from Slevers et al. revealed that the presence of FGFR1-TACC1 or FGFR3-TACC3 gene fusions in extraventricular neurocytoma located in the supratentorial brain is a frequent molecular event, especially the former, accounting for approximately 60% (3). However, these gene fusions have not been reported in EVN in the sellar or parasellar regions. In the present 4 patients, no FGFR1 gene breakage or rearrangement was found by FISH detection, suggesting that sellar/suprasellar neurocytomas may not have the same molecular biological characteristics as those originating from other parts. A microarray-based comparative genomic hybridization investigation revealed distinct profiles, with loss and gain of multiple chromosomal loci, which concluded that MYCN gene amplification, together with loss of BIN1 expression, were typical of central neurocytoma (31). EGFR amplification mutations have been reported in two cases of atypical EVNs (32, 33). In our cases, there was no amplification of MYCN or EGFR, and no alterations in IDH1, IDH2, BRAF V600E, 1p/19q, H3F3A or CDKN2A were found.

Several cases of sellar/suprasellar EVN reported in the literature have confirmed that the tumor cells are immunoreactive for vasopressin (5, 21). Through electron microscopic observation, Maguire et al. found that the perinuclear cytoplasm of the tumor cells contains neurosecretory granules, which are also packed in swollen neuritic processes that resemble Herring bodies (5). They interpreted the immunohistochemical and ultrastructural features of this tumor as suggestive of primary hypothalamic derivation. All samples in this study were positive for vasopressin, supporting the above view. Asa et al. reported that 3 patients with sellar/suprasellar EVN had a syndrome of inappropriate antidiuresis, which is associated with excess vasopressin production by tumors (21). However, serum vasopressin levels were not investigated preoperatively or postoperatively in our cases, which is a limitation of this study.

TABLE 3 | Clinicopathological details of the 21 reported cases of sellar/suprasellar neurocytoma.

Case	Reference	Sex	Age	Initial symptoms	Serum vaso-pressin	Pituitary hormone	Location	Focal infil-trations	Preoperative impression	Type	Resection	Adjuvant radiotherapy	Recurrence
1	Maguire et al. (5)	F	55	Visual disturbances; 6 months	NA	normal	S/S	no	PA	typical	STR	NA	NA
2	Yang GF et al. (6)	F	46	Visual impairment; 1 year	NA	normal	S/S	yes	Meningioma	typical	STR	NA	NA
3	Chen H et al. (7)	M	52	Blurred vision; 6-month	NA	normal	S	no	NA	typical	GTR	no	NA
4	Wang Y et al. (8)	F	50	Decreasing vision; 2-month	NA	normal	S/S	yes	PA or craniopharyngioma	typical	STR	yes	no
5	Liu K et al. (9)	M	40	Visual impairment; NA	NA	normal	S/S	yes	PA	typical	NA	no	no
6	Wang Y et al. (10)	F	23	Bitemporal visual deficit and headache;4-month	NA	NA	S/S	yes	NA	typical	STR	yes	NA
7	Kawaji H et al. (11)	M	48	Visual impairment	NA	PRL↑	S/S	yes	PA	atypical	STR	yes	6 years
8	Xiong Z et al. (12)	NA	56	NA	NA	NA	S	NA	NA	typical	NA	NA	NA
9	Makis W et al. (13)	F	64	Bitemporal hemianopsia;30-year history of recurrent sellar masses	NA	NA	S/S	NA	Recurrent PA	atypical	NA	yes	30yrs ago (typical) 4yrs ago (atypical)
10	Peng P et al. (14)	M	56	Bitemporal hemianopsia	NA	ACTH↓	S/S	yes	PA	typical	GTR	no	no
11	Chen S et al. (15)	F	50	Decreasing vision in left eye and diplopia; 2-month	NA	normal	S/S	yes	NA	typical	STR	yes	no
12	Chen S et al. (15)	M	62	Homonymous hemianopsia, temporal both eyes; 1 year	NA	PRL↓	S/S	no	NA	typical, ganglion	STR	yes	no
13	Cho et al. (16)	M	14	Bitemporal hemianopsia, decreased visual acuity; 0	NA	NA	S/S	yes	Hypothalamic glioma	typical	STR	yes	1 year
14	Wang et al. (16)	M	25	Worsening vision; 7-month	NA	normal	S/S	yes	PA or meningioma	typical	STR	yes	no
15	Tan CL et al. (17)	F	59	Visual disturbances; 2-year; with a history of osteoporosis and SIADH	NA	NA	S/S	yes	PA	typical	STR	yes	no
16	Nery B et al. (18)	M	27	Progressive bilateral vision loss; 4-year	NA	normal	S/S	yes	PA	typical	GTR	no	no
17	Tish S et al. (19)	M	70	Imbalance and dizziness	NA	normal	S/S	yes	NA	atypical, ganglion	biopsy	yes	no
18	Asa et al. (21)	F	39	5-month history of worsening visual field loss; idiopathic SIADH; 6-year	vasopressin excess with SIAD	normal	S/S	yes	PA	atypical	STR	no	NA
19	Asa et al. (21)	F	34	Galactorrhea, amenorrhea, hyponatremia; 18-month	vasopressin excess with SIAD	PRL↑	S/S	NA	PA	atypical	STR	yes	30yrs, death
20	Asa et al. (21); Zhang D et al. (22)	M	17	Progressive abdominal pain, nausea and emesis; 3-year	vasopressin excess with SIAD	low total testosterone	S	yes	NA	atypical	STR	no	no
21	Asa et al. (21)	F	40	Visual disturbance and headache	no	normal	S/S	yes	PA	atypical	STR	no	<1 year

NA, Not available; SIADH, Syndrome of inappropriate antidiuretic hormone secretion; S/S, Sellar/Suprasellar; S, Sellar; PA, Pituitary adenoma; STR, Subtotal resection; GTR, Gross total resection.

Therefore, whether the serum level of vasopressin can hint at the diagnosis of this tumor is unclear, and more case studies are needed.

Most of the reported cases and the present cases were diagnosed as giant pituitary adenomas before surgery, and none of them were suspected to be EVNs based on preoperative imaging. A large pituitary adenoma suspected to involve the sellar/suprasellar region with invasion of the venous sinuses and nonfunctional clinical changes always has the possibility of being a neurocytoma. Histopathologically, pituitary endocrine tumors are the first differential diagnosis. In most cases, the histological characteristics of pituitary endocrine tumors as well as the pattern of expression of transcription factors and pituitary hormone markers can easily distinguish them. However, it is difficult to make a differential diagnosis from null cell adenoma, a very rare group of pituitary neuroendocrine tumors (PitNETs) that are negative for all adenohypophyseal hormones and transcription factors. The main points of differential diagnosis include the identification of neuropils and the expression of NeuN and TTF1 in sellar/suprasellar EVNs. In addition, we found that E-cadherin and P120 are also useful markers for differential diagnosis (unpublished), which are immune-positive in pituitary adenomas but immune-negative in neurocytomas. Other differential diagnoses include paraganglioma and olfactory neuroblastoma. Immunohistochemical markers are helpful. For example, paraganglioma generally expresses GATA3 and tyrosine hydroxylase, while neurocytoma does not (34).

Gross total resection is the preferred treatment for EVN (35, 36). EVN that occurs in the sellar/suprasellar region often invades the sphenoid sinus and cavernous sinus and usually compresses the optic nerve and envelops the internal carotid artery, so gross total resection is quite difficult, and thus subtotal resection is often performed. Adjuvant radiotherapy, either conventional or radiosurgery with gamma knife, can improve both local control and survival in patients who undergo subtotal resection (37, 38). The effect of chemotherapy on EVNs as an adjuvant management tool remains unclear. The overall prognosis of EVNs is good, although the recurrence rate is higher than that of CNs. In addition to incomplete resection affecting the prognosis, atypical or anaplastic features are associated with a higher recurrence rate and generally worse outcomes. In our cases, all 4 patients underwent surgical treatment radiotherapy or chemotherapy was not performed postoperatively, and 3 cases underwent subtotal resection have relapsed after initial surgery.

In summary, neurocytoma of the sellar/suprasellar region is an extremely rare tumor. The morphological features and immunophenotypes of a neurocytoma in the sellar/suprasellar region are similar to classic central neurocytoma. The tumor is often not completely resected, and adjuvant radiotherapy is feasible after surgery. Attention should be given to the differential diagnosis of pituitary endocrine tumors. The overall prognosis is good. Atypical histological features and subtotal resection may be related to tumor recurrence. Its biological behaviors and molecular genetics/epigenetics characteristics need to be studied further with a larger sample.

DATA AVAILABILITY STATEMENT

The original contributions presented in the study are included in the article/supplementary material. Further inquiries can be directed to the corresponding authors.

AUTHOR CONTRIBUTIONS

LFZ: Investigation, Data curation, Writing- Original draft preparation. WF: Investigation, Data curation, Writing-Original draft preparation. LMZ and YHY: Data curation, Visualization. FS: Methodology. YC: Methodology. CJ: Data curation. ZX: Data curation. CH: Data curation. SZ: Project administration. XY: Data curation, Supervision, Writing-Reviewing and Editing. XW: Funding acquisition, Supervision, Writing- Reviewing and Editing. All authors contributed to the article and approved the submitted version.

FUNDING

This study was supported by Natural Science Foundation of Fujian Province (2018J01155), Fujian Medical University Startup Fund for scientific research (2020QH1053) and Fujian Provincial Health and Family Planning Training Project for Young and Middle-aged Key Talents (2019-ZQN-61).

REFERENCES

1. Hassoun J, Gambarelli D, Grisoli F, Pellet W, Salamon G, Pellissier JF, et al. Central Neurocytoma. An Electron-Microscopic Study of Two Cases. *Acta Neuropathol* (1982) 56(2):151–6. doi: 10.1007/BF00690587
2. Giangaspero F, Cenacchi G, Losi L, Cerasoli S, Bisceglia M, Burger PC. Extraventricular Neoplasms With Neurocytoma Features. A Clinicopathological Study of 11 Cases. *Am J Surg Pathol* (1997) 21(2):206–12. doi: 10.1097/00000478-199702000-00011
3. Sievers P, Stichel D, Schrimpf D, Sahm F, Koelsche C, Reuss DE, et al. FGFR1: TACC1 Fusion is a Frequent Event in Molecularly Defined Extraventricular Neurocytoma. *Acta Neuropathol* (2018) 136(2):293–302. doi: 10.1007/s00401-018-1882-3
4. Xu L, Ouyang Z, Wang J, Liu Z, Fang J, Du J, et al. A Clinicopathologic Study of Extraventricular Neurocytoma. *J Neurooncol* (2017) 132(1):75–82. doi: 10.1007/s11060-016-2336-1
5. Maguire JA, Bilbao JM, Kovacs K, Resch L. Hypothalamic Neurocytoma With Vasopressin Immunoreactivity: Immunohistochemical and Ultrastructural Observations. *Endocr Pathol* (1992) 3(2):99–104. doi: 10.1007/BF02921349
6. Yang GF, Wu SY, Zhang LJ, Lu GM, Tian W, Shah K. Imaging Findings of Extraventricular Neurocytoma: Report of 3 Cases and Review of the Literature. *AJNR Am J Neuroradiol* (2009) 30(3):581–5. doi: 10.3174/ajnr.A1279
7. Chen H, Zhou R, Liu J, Tang J. Central Neurocytoma. *J Clin Neurosci* (2012) 19(6):849–53. doi: 10.1016/j.jocn.2011.06.038
8. Wang YY, Kearney T, du Plessis D, Gnanalingham KK. Extraventricular Neurocytoma of the Sellar Region. *Br J Neurosurg* (2012) 26(3):420–2. doi: 10.3109/02688697.2011.633635

9. Liu K, Wen G, Lv XF, Deng YJ, Deng YJ, Hou GQ, et al. MR Imaging of Cerebral Extraventricular Neurocytoma: A Report of 9 Cases. *AJNR Am J Neuroradiol* (2013) 34(3):541–6. doi: 10.3174/ajnr.A3264
10. Wang Y, Tao R, Liu B. Response to: Extraventricular Neurocytoma of the Sellar Region. *Br J Neurosurg* (2013) 27(4):551–2. doi: 10.3109/02688697.2013.798861
11. Kawaji H, Saito O, Amano S, Kasahara M, Baba S, Namba H. Extraventricular Neurocytoma of the Sellar Region With Spinal Dissemination. *Brain Tumor Pathol* (2014) 31(1):51–6. doi: 10.1007/s10014-012-0128-7
12. Xiong Z, Zhang J, Li Z, Jiang J, Han Q, Sun S, et al. A Comparative Study of Intraventricular Central Neurocytomas and Extraventricular Neurocytomas. *J Neurooncol* (2015) 121(3):521–9. doi: 10.1007/s11060-014-1659-z
13. Makis W, McCann K, McEwan AJ. Extraventricular Neurocytoma Treated With 177Lu DOTATATE PRRT Induction and Maintenance Therapies. *Clin Nucl Med* (2015) 40(3):234–6. doi: 10.1097/RLU.0000000000000668
14. Peng P, Chen F, Zhou D, Liu H, Li J. Neurocytoma of the Pituitary Gland: A Case Report and Literature Review. *BioMed Rep* (2015) 3(3):301–3. doi: 10.3892/br.2015.430
15. Chen S, Ji N, Wang B, Wang J, Yu S, Wang J. Extraventricular Neurocytoma of the Sellar Region: Report of Two Cases and Literature Review. *Int J Clin Exp Pathol* (2016) 9(1):165–70.
16. Cho M, Joo JD, Kim BH, Choe G, Kim CY. Hypothalamic Extraventricular Neurocytoma (EVN) in a Pediatric Patient: A Case of EVN Treated With Subtotal Removal Followed by Adjuvant Radiotherapy. *Brain Tumor Res Treat* (2016) 4(1):35–9. doi: 10.14791/btrt.2016.4.1.35
17. Wang J, Song DL, Deng L, Sun SY, Liu C, Gong DS, et al. Extraventricular Neurocytoma of the Sellar Region: Case Report and Literature Review. *Springerplus* (2016) 5(1):987. doi: 10.1186/s40064-016-2650-2
18. Tan CL, Pang YH, Lim KHC, Sein L, Codd PJ, McLendon RE. Two Extraordinary Sellar Neuronal Tumors: Literature Review and Comparison of Clinicopathologic Features. *Am J Clin Pathol* (2019) 151(3):241–54. doi: 10.1093/ajcp/aqy155
19. Nery B, Bernardes Filho F, Costa RAF, Pereira LCT, Quaggio E, Queiroz RM, et al. Neurocytoma Mimicking Macroadenoma. *Surg Neurol Int* (2019) 10:8. doi: 10.4103/sni.sni_387_18
20. Tish S, Habboub G, Prayson RA, Woodard TD, Kshettry VR, Recinos PF. Extraventricular Neurocytoma With Ganglioid Differentiation of the Sellar and Parasellar Regions in an Elderly Patient: A Case Report. *Surg Neurol Int* (2019) 10:82. doi: 10.25259/SNI-30-2019
21. Asa SL, Ezzat S, Kelly DF, Cohan P, Takasumi Y, Barkhoudarian G, et al. Hypothalamic Vasopressin-Producing Tumors: Often Inappropriate Diuresis But Occasionally Cushing Disease. *Am J Surg Pathol* (2019) 43(2):251–60. doi: 10.1097/PAS.0000000000001185
22. Zhang D, Kim SSR, Kelly DF, Asa SL, Movassaghi M, Mareninov S, et al. Somatostatin Receptor Ligand Therapy-A Potential Therapy for Neurocytoma. *J Clin Endocrinol Metab* (2019) 104(6):2395–402. doi: 10.1210/jc.2018-02419
23. Romano N, Federici M, Castaldi A. Imaging of Extraventricular Neurocytoma: A Systematic Literature Review. *Radiol Med* (2020) 125 (10):961–70. doi: 10.1007/s11547-020-01198-8
24. Chou S, Varikatt W, Dexter M, Ng T. Extraventricular Neurocytoma With Atypical Features and Ganglionic Differentiation. *J Clin Neurosci* (2010) 17 (7):920–2. doi: 10.1016/j.jocn.2009.10.022
25. Zhu P, Yan F, Ma Y, Ao Q. Clinicopathological Analysis of Central and Extraventricular Neurocytoma: A Report of 17 Cases. *J Huazhong Univ Sci Technolog Med Sci* (2010) 30(6):746–50. doi: 10.1007/s11596-010-0651-x
26. Nabavizadeh SA, Chawla S, Baccon J, Zhang PJ, Poptani H, Melhem ER, et al. Extraventricular Neurocytoma and Ganglioneurocytoma: Advanced MR Imaging, Histopathological, and Chromosomal Findings. *J Neuroimaging* (2014) 24(6):613–6. doi: 10.1111/jon.12081
27. AbdelBari Mattar M, Shebl AM, Toson EA. Atypical Central Neurocytoma: An Investigation of Prognostic Factors. *World Neurosurg* (2021) 146:e184–93. doi: 10.1016/j.wneu.2020.10.068
28. Lampros MG, Vlachos N, Voulgaris S, Alexiou GA. Extraventricular Neurocytomas: A Systematic Review of the Literature in the Pediatric Population. *Childs Nerv Syst* (2021) 37(8):2465–74. doi: 10.1007/s00381-021-05257-x
29. Brat DJ, Scheithauer BW, Eberhart CG, Burger PC. Extraventricular Neurocytomas: Pathologic Features and Clinical Outcome. *Am J Surg Pathol* (2001) 25(10):1252–60. doi: 10.1097/00000478-200110000-00005
30. Moriguchi S, Yamashita A, Marutsuka K, Yoneyama T, Nakano S, Wakisaka S, et al. Atypical Extraventricular Neurocytoma. *Pathol Int* (2006) 56(1):25–9. doi: 10.1111/j.1440-1827.2006.01914.x
31. Jay V, Edwards V, Hoving E, Rutka J, Becker L, Zielenska M, et al. Central Neurocytoma: Morphological, Flow Cytometric, Polymerase Chain Reaction, Fluorescence *in Situ* Hybridization, and Karyotypic Analyses. *Case Rep J Neurosurg* (1999) 90(2):348–54. doi: 10.3171/jns.1999.90.2.0348
32. Yu B, Li J, Jing L, Man W, Wang G. A Rare Case of Atypical Spinal Neurocytoma With EGFR Mutation in a 12-Year-Old Boy. *Childs Nerv Syst* (2021) 37(7):2399–403. doi: 10.1007/s00381-020-04912-z
33. Myung JK, Cho HJ, Park CK, Chung CK, Choi SH, Kim SK, et al. Clinicopathological and Genetic Characteristics of Extraventricular Neurocytomas. *Neuropathology* (2013) 33(2):111–21. doi: 10.1111/j.1440-1789.2012.01330.x
34. Tischler AS, deKrijger RR. 15 YEARS OF PARAGANGLIOMA: Pathology of Pheochromocytoma and Paraganglioma. *Endocr Relat Cancer* (2015) 22(4): T123–133. doi: 10.1530/ERC-15-0261
35. Patil AS, Menon G, Easwer HV, Nair S. Extraventricular Neurocytoma, a Comprehensive Review. *Acta Neurochir (Wien)* (2014) 156(2):349–54. doi: 10.1007/s00701-013-1971-y
36. Mallick S, Benson R, Rath GK. Patterns of Care and Survival Outcomes in Patients With an Extraventricular Neurocytoma: An Individual Patient Data Analysis of 201 Cases. *Neurol India* (2018) 66(2):362–7. doi: 10.4103/0028-3886.227262
37. Samhouri L, Meheissen MAM, Ibrahimi AKH, Al-Mousa A, Zeineddin M, Elkerm Y, et al. Impact of Adjuvant Radiotherapy in Patients With Central Neurocytoma: A Multicentric International Analysis. *Cancers (Basel)* (2021) 13(17):4308. doi: 10.3390/cancers13174308
38. Chen S, Duan H, Liu R, Luo J, Wang H, Zhang S, et al. Cerebellar Neurocytoma With Excellent Response to Radiotherapy. *World Neurosurg* (2020) 141:327–30. doi: 10.1016/j.wneu.2020.06.133

Conflict of Interest: The authors declare that the research was conducted in the absence of any commercial or financial relationships that could be construed as a potential conflict of interest.

frontiers | Frontiers in Endocrinology

ORIGINAL RESEARCH
published: 09 June 2022
doi: 10.3389/fendo.2022.882381

Neoadjuvant B-RAF and MEK Inhibitor Targeted Therapy for Adult Papillary Craniopharyngiomas: A New Treatment Paradigm

Francesco Calvanese[1,2*], *Timothée Jacquesson*[1,3,4], *Romain Manet*[1], *Alexandre Vasiljevic*[3,5,6,7], *Hélène Lasolle*[3,6,8], *Francois Ducray*[3,9,10], *Gerald Raverot*[3,6,8] *and Emmanuel Jouanneau*[1,3,4,6]

[1] Pituitary and Skull Base Neurosurgical Department, Reference Center for Rare Pituitary Diseases HYPO, "Groupement Hospitalier Est" Hospices Civils de Lyon, "Claude Bernard" Lyon 1 University, Hôpital Pierre Wertheimer, Lyon, France, [2] Department of Neurosurgery, I.R.C.C.S. San Raffaele Scientific Institute, Vita-Salute University, Milan, Italy, [3] Lyon University, Université Claude Bernard Lyon 1, Lyon, France, [4] CREATIS Laboratory CNRS UMR5220, Inserm U1206, INSA-Lyon, University of Lyon 1, Lyon, France, [5] Department of Pathology, Groupement Hospitalier, Lyon, France, [6] INSERM U1052, CNRS UMR5286, Cancer Research Center of Lyon, Lyon, France, [7] INSERM U1028, CNRS UMR5292, Lyon Neuroscience Research Center, Neuro-Oncology & Neuro–Inflammation Team, Lyon, France, [8] Endocrinology Department, Reference Center for Rare Pituitary Diseases HYPO, "Groupement Hospitalier Est" Hospices Civils de Lyon, "Claude Bernard" Lyon 1 University, Hôpital Louis Pradel, Lyon, France, [9] Cancerology Research Center of Lyon, INSERM U1052, CNRS UMR 5286, Cancer Cell Plasticity Department, Transcriptome Diversity in Stem Cells Laboratory, Lyon, France, [10] Service of Neuro-Oncology, Hospices Civils de Lyon, Groupement Hospitalier Est, Neurology Hospital, Lyon, France

OPEN ACCESS

Edited by:
Congxin Dai,
Capital Medical University, China

Reviewed by:
Hiroshi Nishioka,
Toranomon Hospital, Japan
Ann McCormack,
St Vincent's Hospital Sydney, Australia

***Correspondence:**
Francesco Calvanese
dr.fcalvanese@gmail.com
orcid.org/0000-0002-0966-2487

Specialty section:
This article was submitted to Pituitary Endocrinology, a section of the journal Frontiers in Endocrinology

Received: *23 February 2022*
Accepted: *04 April 2022*
Published: *09 June 2022*

Citation:
Calvanese F, Jacquesson T, Manet R, Vasiljevic A, Lasolle H, Ducray F, Raverot G and Jouanneau E (2022) Neoadjuvant B-RAF and MEK Inhibitor Targeted Therapy for Adult Papillary Craniopharyngiomas: A New Treatment Paradigm. Front. Endocrinol. 13:882381. doi: 10.3389/fendo.2022.882381

Background: Surgical and clinical management of craniopharyngiomas is associated with high long-term morbidity especially in the case of hypothalamic involvement. Improvements in knowledge of craniopharyngioma molecular biology may offer the possibility of safe and effective medical neoadjuvant treatments in a subset of patients harboring papillary subtype tumors with a BRAFV600E mutation.

Method: We report herein two cases of tubero-infundibular and ventricular Papillary Craniopharyngiomas in which BRAF/MEK inhibitor combined therapy was used as adjuvant (Case 1) or neoadjuvant (Case 2) treatment, with a 90% reduction in tumor volume observed after only 5 months. In Case 2 the only surgical procedure used was a minimal invasive biopsy by the trans-ventricular neuroendoscopic approach. As a consequence, targeted therapy was administered in purely neoadjuvant fashion. After shrinkage of the tumor, both patients underwent fractionated radiotherapy on the small tumor remnant to achieve long-term tumor control. A review of a previously reported case has also been performed.

Result: This approach led to tumor control with minimal long-term morbidity in both cases. No side effects or complications were reported after medical treatment and adjuvant radiotherapy.

Conclusion: Our experience and a review of the literature argue for a change in the current treatment paradigm for Craniopharyngiomas (CPs). In giant and invasive tumors, confirmation of BRAFV600E mutated PCPs by biopsy and BRAF/MEK inhibitor therapy before proposing other treatments may be useful to improve long term outcomes for patients.

Keywords: papillary craniopharyngiomas, tumor biopsy, V600E BRAF mutation, B-RAF and MEK inhibitor targeted therapy, neoadjuvant treatment

INTRODUCTION

Craniopharyngiomas (CPs) are rare suprasellar tumors arising from the epithelium of craniopharyngeal duct remnants with a global incidence of 0.5-2.5 new cases per 1 million population (1, 2). They develop along the hypothalamic-pituitary axis and exhibit two distinct histological subtypes: Adamantinomatous (ACPs) and Papillary (PCPs) craniopharyngiomas. ACPs account for 90% of all and present a bimodal peak of incidence in childhood and in adulthood whereas, PCP represents 10% of all craniopharyngiomas and usually affect adult patient in 4^{th}-5^{th} decade of life (1–3).

Despite CPs being classified as low-grade neoplasms (Grade I, WHO), they show an aggressive local behavior and a high rate of recurrence (i.e., from 9 to 62%), requiring multimodal invasive treatments to achieve tumor control (1, 2, 4–6). The involvement of the third ventricle is a critical factor increasing long-term morbidity and limiting the effectiveness of surgery and/or radiotherapy (5, 7–11). Pascal and Prieto (8, 12, 13) classified CPs topographically into four categories based on their relationship with third ventricular floor: Suprasellar (SS) or pseudo-intraventricular, SS secondary intraventricular, infundibular-tuberal or not strictly intraventricular and "purely" intra-ventricular tumors. The surgical resection of intraventricular and/or giant CPs is particularly challenging due to the frequent third ventricular floor invasion and narrow surgical corridors (4, 9, 12–14). Although in some cases the third ventricle portion can be safely resected, ventricular remnants are frequent after surgery, require adjuvant radiotherapy, and increase the risk of long-term recurrence and morbidity (10).

Improving our knowledge of the genetic landscape of craniopharyngiomas has led to characterization of two different clonal driver mutations that control oncogenesis of the two histological subtypes (3). ACPs are characterized by alterations in the Wnt/β-catenin pathway, mainly involving the central regulatory gene CTNNB1, whereas most PCPs are driven by the V600E mutation in the BRAF gene, which activates the mitogen-activated protein kinase (MAPK) signaling pathway (3, 5, 15, 16). These molecular changes have revealed potential targets for new therapeutics that could improve long term control of tumor volume with less morbidity (6, 16).

To date, no target agents have been found to have efficacy in blocking Wnt/B-catenin pathway in ACPs (1, 3, 16). Nonetheless, target therapy with B-RAF and MEK inhibitor agents has shown good results in the treatment of a number of human cancers (6, 16–18) and glial tumors (16, 18, 19) harboring the V600E BRAF mutation. These results have led to successful use of these agents for aggressive PCPs that present with a high frequency of BRAF V600E mutation (3, 16–21).

We present herein two cases that showed efficacy of combined anti-BRAF/MEK therapy as adjuvant and neoadjuvant treatment of a PCP. In view of our results and a review of the literature we then discuss a new concept for the management of invasive CPs.

MATERIALS AND METHODS

Two patients were treated for ventriculo-tuberal complex PCP with adjuvant (Case 1) and neoadjuvant (Case 2) anti-BRAF/MEK therapy at the Pierre Wertheimer Neurological Institute between 2019 and 2021. Preoperative, postoperative and follow-up radiological, biochemical, and clinical findings for both patients were collected and are reported in the results section and in **Figures 1**, **2**. In accordance with our institutional policy, both patients gave their informed consent for surgical operations, medical treatment and radiotherapy and for the use of their clinical data for research and publication purposes.

A systematic review of the pertinent medical literature was performed within PUBMED and Google scholar databases. All research which included the following keywords: "Papillary craniopharyngioma", "Papillary craniopharyngioma AND medical treatment", "Papillary craniopharyngioma AND BRAF inhibitors" and "Papillary craniopharyngioma AND BRAF/MEK inhibitors" was reviewed. Using the bibliographies of articles identified in our primary search we then performed a secondary search. Articles were reviewed by title and abstract for potential relevance as well as being reviewed completely if the title or/and abstract did not clearly indicate the degree of relevance. The search was limited to human subjects and English language publications. Only full papers and relevant publications as well as original communications were selected.

RESULTS

Case Reports

CASE 1

A 40-year-old man was admitted to our institution with a 2-month history of bitemporal inferior quadraniopsia and a decrease in right visual acuity confirmed by ophthalmological evaluation. Cerebral MRI showed a tuberoinfundibular solid-cystic mass, infiltrating the third ventricular floor and measuring

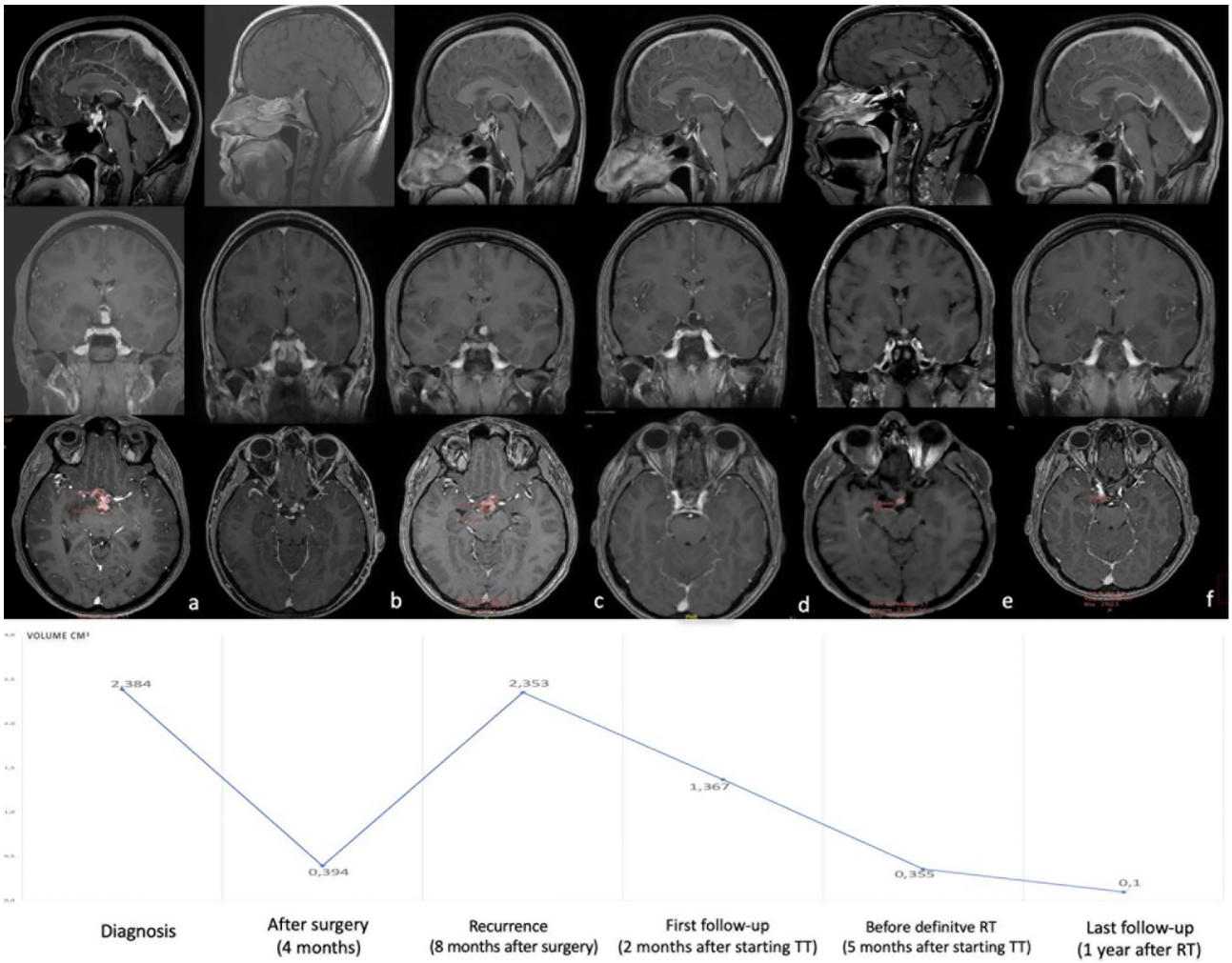

FIGURE 1 | Post-gadolinium axial, coronal and sagittal T1WI MRI images, representing the clinical course in case 1. **(A, B)** Shows the tumor volume and presentation at time of diagnosis (25.4 x 15.0 mm maximal axis and 2.384 cm3 volume) and after surgery (maximal axis: 7.5 x 11.5 mm, volume: 0.394 cm3). **(C)** Shows tumor recurrence/regrowth at 12 months postoperatively (13 x 24 mm and a volume of 2.353 cm3). **(D, E)** Show dramatic and rapid reduction in tumor volume at 2 months (80 %) and 4 months (90%) after starting combined anti-BRAF/MEK therapy. **(F)** Shows results at 1 year after final radiotherapy (near complete response). Volume curve has been reported in the inferior part of figure. TT: B-RAF and MEK inhibitor targeted therapy; RT: radiotherapy.

25.4 x 15.0 mm maximal axis and 2.384 cm^3 in volume (**Figure 1A**). The lesion showed heterogenous contrast enhancement after gadolinium on T1WI and hyperintensity on T2WI without intra-tumoral calcification on CT scan. Endocrinological pituitary screening showed a central hypogonadism without other deficits nor diabetes insipidus.

The patient underwent a near-total resection through an extended trans tubercular transsphenoidal endoscopic approach. Post-operative cerebral MRI showed tumor volume reduction of 90% (maximal axis: 7.5 x 11.5 mm, volume: 0.394 cm^3) without posterior III floor hypothalamic damage (**Figure 1B**). The post-operative course showed a complete regression of visual symptoms but the patient developed diabetes insipidus and central hypothyroidism requiring substitutive treatment. The patient was discharged from hospital after seven days. Histopathological analysis demonstrated a papillary Craniopharyngioma harboring the BRAF V600E mutation. The first MRI at 4 months showed stable disease but the second MRI, 8 months post-surgery, demonstrated tumor growth and there was new visual impairment. The lesion showed a maximal axis of 13 x 24 mm and a volume of 2.353 cm^3 (94% increase in tumor volume, **Figure 1C**). After discussion within our Multidisciplinary Pituitary Tumor Board, the patient commenced target therapy with Dobrafenib (150 mg Twice daily) and Trametinb (2 mg once daily) for 5 months. Indeed, in view of both hypothalamus and chiasma infiltration and the rapidity of recurrence, a second surgery was excluded, and radiotherapy was delayed in the hope

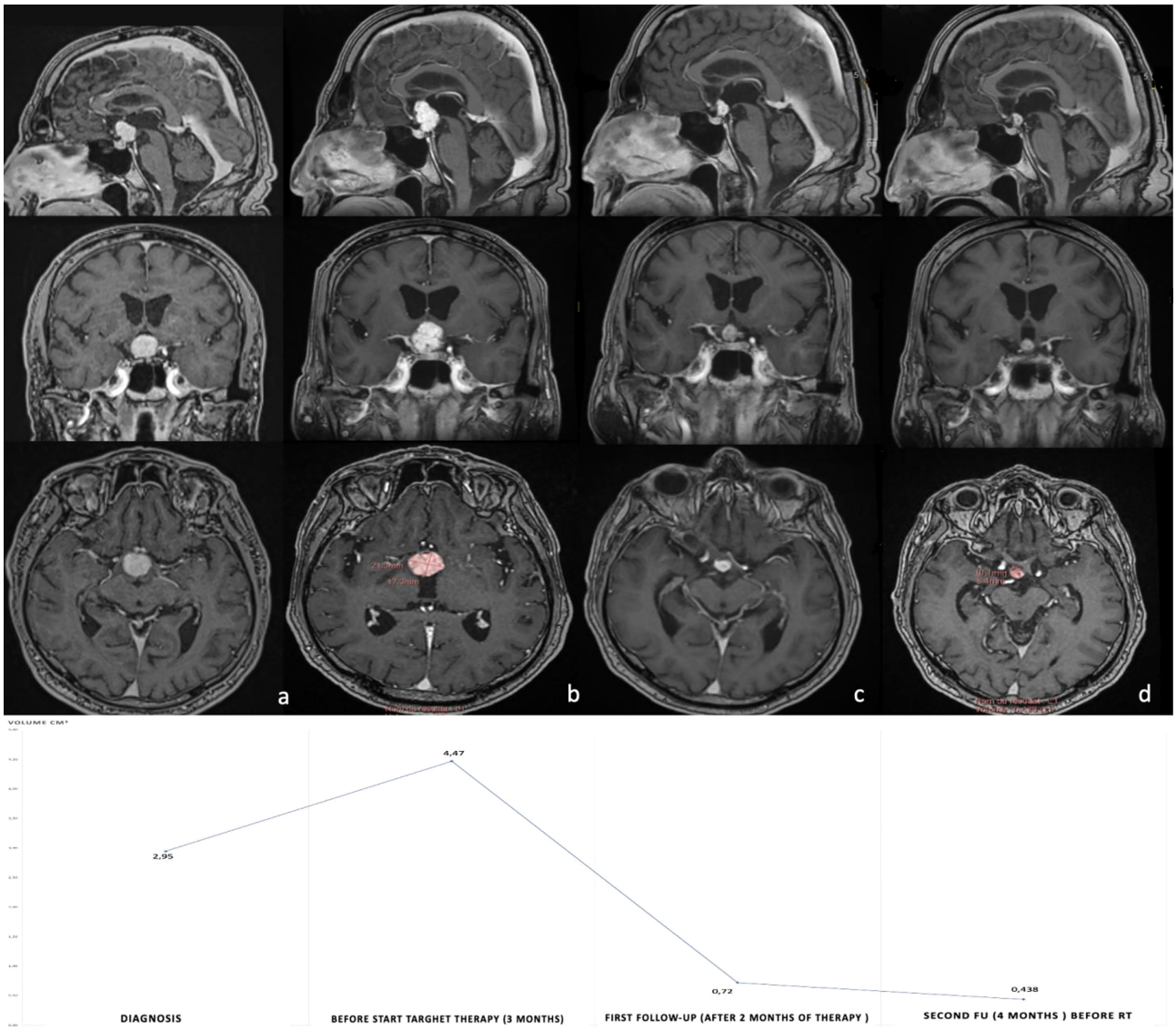

FIGURE 2 | Post-gadolinium axial, coronal and sagittal T1WI MRI images of case 2. **(A)** Postcontrast T1-weighted image shows large homogeneously enhanced intraventricular mass measuring 19 x 18.5 mm maximal axis and 2.945 cm^3 volume. **(B)** Shows progression of the intraventricular tumor portion after trans-ventricular endoscopic biopsy (18% of tumor volume). Panels c and d show a dramatic reduction in volume at 2 months **(C)** and 4 months **(D)** after commencing combined BRAF/MEK inhibitor treatment. Note complete resolution of the mass effect on suprasellar neurovascular structures and on Monro's foramen. Volume curve has been reported in the inferior part of figure. RT, radiotherapy.

of having a smaller target. The first follow-up cerebral MRI, performed 2 months after start of treatment, showed a 40% reduction in tumor volume. (1.367 cm^3) (**Figure 1D**). Ophthalmologic examination showed a normal result. Combined treatment was continued and well-tolerated without side effects. Cerebral MRI performed at 5 months post-treatment showed a 90% reduction in tumor volume (0.355 cm^3). (**Figure 1E**). Subsequently, fractionated VMAT (Volumetric Modulated Arc Therapy) radiotherapy with a total dose of 52.2 Gy in 29 fractions was applied, while combined treatment was interrupted one month before radiotherapy to prevent radiosensitization. At last follow up, one year after radiotherapy, the tumor showed a "near complete" radiological response, the patient was symptom-free and had resumed normal life (**Figure 1F**).

CASE 2

A 69-year-old HIV-seropositive man was referred to our center after a one year history of frontal headaches, a right visual impairment and psychiatric changes (aggressivity and behavior

changes). Cerebral MRI revealed a large solid third ventricular lesion measuring 19 x18.5 mm in maximal axis and 2.945 cm^3 in volume (**Figure 2A**). The lesion was implanted on the infundibular recess and bilaterally reached Monro's foramen. The lesion showed non-homogeneous contrast enhancement and was hypointense on T1WI and hyperintense on T2WI MRI. Hormonal screening showed normal pituitary function except for a slight disconnection hyperprolactinemia and no evidence of diabetes insipidus. Ophthalmologic evaluation revealed a left optic atrophy but visual field and acuity were normal. A biopsy by a trans-ventricular neuroendoscopic approach was performed in order to confirm the diagnosis and exclude differential diagnoses such as primary cerebral lymphoma. Histopathological analysis showed a papillary craniopharyngioma harboring classical BRAF V600E mutation.

After discussion within our Multidisciplinary Pituitary board, considering the invasion of the hypothalamus, neoadjuvant targeted therapy treatment was decided. A combination of dobrafenib (150 mg Twice daily) and Trametinb (2 mg once daily), after optimization of antiviral drug to avoid pharmacokinetic interactions, was started. MRI performed 3 months after the diagnosis and before starting targeted therapy showed tumor progression with a volume of 4.469 cm^3 and maximal axis of 21.3 x17.3 mm (an increase of 18% in tumor volume) (**Figure 2B**). After two months of therapy, the patient showed a complete regression of visual dysfunction and an improvement in psychiatric symptoms. Treatment was well-tolerated without side effects. At that date, MRI showed a near total response with an 80% reduction in tumor volume (0.72 cm^3) (**Figure 2C**) associated with complete resolution of the Monro's foramen obstruction. The tumor volume continued to diminish with 4 month follow-up imaging showing a total volume reduction of 90% (0.438 cm^3) (**Figure 2D**), allowing us to perform fractionated radiation treatment as initially planned. Fractionated Radiation therapy (52 Gy/30 Fraction) was scheduled 6 months after treatment initiation and targeted therapy was stopped 2 weeks before the start of radiation.

Literature Review

Our primary search identified 170 papers. Twenty-two articles were selected for clinical and subject relevance. Only 11 previously reported cases of PCP treated by targeted therapy were found in the English language publications (16, 17, 19, 22–29) and a summary of these findings is shown in **Table 1**. The preliminary data of one randomized study, which analyzed adjuvant anti-BRAF/MEK inhibitor therapy for PCP, have been published and are discussed in the following section (30).

Two specific surgical series were identified (31, 32). The other studies were earlier literature reviews on related topics (1–3, 5–7, 15, 18, 33).

DISCUSSION

Harvey Cushing referred to craniopharyngiomas as "the most forbidding of the intracranial tumors" (5). Despite improvements in microsurgical and endoscopic techniques, as well as in radiation therapy and radiosurgery, the long-term morbidity of CPs remains high, conferring a sometimes poor quality of life on these patients (1, 2, 10, 11, 14). The long-term morbidity of such tumors is mainly related to hypothalamic damage resulting either from the tumor invading neural structures or by treatment-related injury (10, 14). Consequently, craniopharyngiomas that involve the third ventricle and tuberoinfundibular areas represent the lesions which are extremely difficult to excise surgically and their subsequent management is equally difficult due to their intimate anatomical and functional relationships with the hypothalamus (9, 13, 14). According to the MRI classification proposed by Prieto et al. (8, 12), the surgical approach should be selected based on the relation of the tumor with the third ventricle floor and the value of the brainstem-mammillary body angle. In a preoperative setting, these findings must be carefully assessed to choose the best surgical approach (endonasal versus cranial) in order to reduce the aggressiveness of the surgery by avoiding, when possible, crossing the third ventricle floor or removing the hypothalamic walls (8, 10). Purely intraventricular CPs are tumors where not only the hypothalamic but also the pituitary functions can be preserved with adequate approach. However, in the case of large infundibulo-tuberal or ventricular tumors which frequently show invasion of hypothalamic structures, resection must be incomplete to avoid very serious adverse outcomes (13).

Even though PCPs account for 10% of all craniopharyngiomas in adults, they show a tendency to arise at the level of third ventricle floor and in the tuberoinfundibular area (75-90% of cases) with frequent hypothalamic involvement (1, 2, 5). This justifies their frequent presentation with hypothalamic symptoms including neuropsychiatric disorders, neurocognitive impairment and also neuroendocrine dysfunction (14, 16). Thus, complex PCPs represent a perfect example in which an effective neoadjuvant medical therapy, producing tumor shrinkage, could provide a reduction in long-term morbidity and facilitate both surgery and radiotherapy (5, 7, 21).

Brastianos et al. (20) reported in their original genetic study that PCPs harbor BRAF V600E mutation in 94.4% of cases and no other recurrent mutation or genomic alterations have been since identified (3, 20). B-RAF is an upstream regulator of the MAPK pathway which controls the cell cycle and cell proliferation (1, 16, 19, 23). BRAF V600E mutation encodes a constitutively activated B-RAF serine/threonine kinase that leads to a chronic hyperactivation of the RAS/RAF/MEK/ERK signaling pathway, driving oncogenesis in about 7% of human cancers (3, 15–18). In PCPs the mechanism by which BRAFV600E mutation is oncogenic has not yet been fully understood but it may give both a proliferative advantage to tumor SOX2+ stem cells and impair their differentiation potential (1, 15, 16).

Since the pioneering cases reported by Alwys at al. (17). and Brastianos et al. (24) in 2015, other authors have reported significant reductions in tumor volume and clinical improvement after administration of a single-agent BRAF

TABLE 1 | Literary review of all PCPs reported case treated with BRAF/MEK inhibitor agents.

Author, Year	Sex, age (year)	Previous treatments	Symptoms before target therapy	B-RAFi-Meki treatments	Duration of treatments (month)	Response (% volume reduction)	Symptoms relive	Recurrence (solid/ cystic), time of recurrence	Definitive treatments for residual or recurrence	Adverse effect	Follow-up (months)
Aylwin et al, 2015 (17)	F, 27	Surgery: STRc (EEA) x2 - RT- Surgery: STRc (EEA)	VS (temporal hemianopia, LE 6/ 60)	Vemurafenib 960 mg BID	3	NCR (95%)	Yes (LE 6/ 24)	Yes (solid), 6-week	re-started vemurafenib	CSF-leak/meningitis	7
Bastianos PK. et al, 2015 (24)	M,39	Multiple Surgery: STRc (TCA x3/EEA x1)	ICHTsymptoms	Dabrafenib 150 mg BID-trametinib 2 mg BID	1.25 (38 days)	PR (81% solid part; 85% Cystic part)	Yes	No	Surgery (EEA)-RT	Low grade Fever (1 day)	18
Roque & Odia, 2016 (29)	F,47	Surgery: PRc (TCA x 1)-Ommaya - RT	H/A, left hemiparesis, behavior changes	dabrafenib 150 mg BID-trametinib 2 mg orally UID	7	PR (80%)	Yes	no	no	intermittent fever	7
Rostami et al, 2017 (26)	M,65	Surgery: STRc (EEAx1)	VS	dabrafenib 150 mg BID After 3 weeks trametinib 2 mg UID was added	3.5	NCR (91%)*	Yes	no	no	Pyrexia needing treatments interruption	2
Juratli et al, 2019 (28)	M,21	Surgery: PR(TCA)	H/A, ICHT, PI	dabrafenib 150 mg BID -trametinib 2 mg UID	6	PR (80%-90%)	Yes	no	no	NR	18
Himes et al, 2019 (22)	M,47	Surgery: STRc -RT	VS, DI	Dabrafenib 150 mg BID, after 150 mg UID, finally 225 mg BID	9	CR (>95%)	Yes	Yes (Cystic), 2 months	Medical treatment **	NR	24
Rao et al, 2019 (25)	M,35	Surgery: STRc (TCA x1)	Hy-Cognitive dysfunction	Dabrafenib 150 mg BID	24	PR (-)	Yes	Yes	NO	NR	28
Bernstein et al, 2019 (19)	M,60	Surgery : STRc x4 -RT	_	dabrafenib 150 mg BID-trametinib 2 mg UID	_	CR (-)	Yes	No	NO	Widespread verrucal keratoses	28
Distefano et al., 2020 (27)	F, 55	Surgery: STRc (EEA x1)	VS, PI	dabrafenib 150 mg BID trametinib 2 mg UID	5	NCR (95%)	Yes	Yes, (13% cystic increasing volume)	PBRT (52.2Gy/ 29Frz)	grade 1 fatigue (CTCAE v4.0), coughing, and peripheral edema	4.5
Khaddour, 2020 (23)	F,39	Surgery: STRc (EEA x 2)	H/A, VS	dabrafenib 150 mg BID trametinib 2 mg UID	9	PR (70%)	yes	No	SRS-GK (25Gy isodose 50%/5frz) ***	Grade I pyrexia	9
Sabeehur Rehman Butt et al., 2021 (16)	F,32	Surgery (x1)-SRS-GK-Surgery (EEA)	–	dabrafenib 150 mg BID trametinib 2 mg UID	3	–	–	no	no	–	3
Present Case 1	M,	Surgery: NCRc (EEA x1)	VS, H/A	dabrafenib 150 mg BID trametinib 2 mg UID	5	NCR, 90	Yes	no	RT	No	24
Present Case 2	M,	No definitive treatments (Biopsy)	VS, Psychiatric disorders	dabrafenib 150 mg BID trametinib 2 mg UID	4	NCR, 90	Yes	no	RT	No	6

Note that the only case treated in pure neoadjuvant manner with medical therapy is our case 2. The reviewed results are treated in the discussion.

EEA, Endoscopic endonasal approach; STRc, subtotal resection; PRc, Partial resection; NCRc, near complete resection; NCR, Near complete response (85-95%); PR, Partial response (<80%); CR, complete response (>95%); VS, Visual symptoms or deterioration; H/A, Headache; PI, panhypopituitarism; DI, diabetes insipidus; Hy, Hydrocephalus; ICHT, symptoms of intracranial hypertension; UID, once daily; BID, twice daily.

**The rate and the magnitude of tumor volume reduction (from 11% VS 91%) significatively improved after joint administration of MEK inhibitor (trametinib).*

***Probably pseudoprogression phenomenon after 3 year of radiation therapy.*

****CR after SRS-GK.*

inhibitor (17, 22, 25, 26), or combined BRAF/MEK inhibitor therapy (19, 23, 24, 26–29), in PCPs harboring the BRAF V600E mutation. The results of all previously published cases are summarized in **Table 1**. Our literature review identified 11 previous case reports. The mean reduction in tumor volume after targeted therapy was 89.2% (range 70-95%) with a minimal treatment period of 5 months (range 1.25-24 months). The most frequent adverse effect reported was low grade fever, which required brief discontinuation of treatment (17, 28). Although all of the patients in previously published reports responded to treatment, it could be argued that there was a selection bias because cases of non-responders may not have been published. Combined therapy using BRAF and MEK inhibitor seems to show a greater efficacy in the magnitude of reduction in tumor volume and in terms of rapidity of action compared to single-agent treatment (5, 16, 18, 19, 23, 26, 27). Moreover, in comparison to single-agent administration, a reduction in recurrence rate has also been described after combined therapy (19, 23, 27, 28). At the molecular level, the combination of BRAF inhibitors with MEK inhibitors could have an additive effect, augmenting the blockade of the downstream pathway of mitogen-activated protein kinase signaling (18, 23). Bernstein et al. (19) have also noted both mitigation of cutaneous toxicity and a reduction in development of resistance in those patients treated with combined therapy. Many questions remain unresolved including how long patients can be treated, how long treatment will control the tumor volume when targeted therapy is used at the time of recurrence as the only alternative treatment, as well as the long-term tolerance of such treatment (15, 16).

Although the clinical efficacy of BRAF/MEK inhibitor agents has been shown in treatment of PCPs, all previously published reports described its administration in settings of tumor recurrence or as adjuvant therapy (16). Recently, DiStefano et al. (27) and Khaddour et al. (23) reported a near complete response or a reduction of tumor volume, in 94% and 70% respectively after combined treatment with drabafenib and trametinib, followed by adjuvant radiosurgery and radiotherapy, in two patients that had rapid recurrence after partial endoscopic transsphenoidal resection. This approach is similar to that described in the present CASE 1 patient, and confirm the efficacy, rapid action and safety of combined BRAF/MEK inhibitor therapy for tumor debulking at the time of recurrence before repeat surgery or radiotherapy. Juratli et al. (28), reported using the same adjuvant approach after a partial tumor removal with severe complications (ischemia of anterior choroid artery territory and pan-hypopituitarism). Their results confirm the utility of targeted therapy in an adjuvant setting, in the case of a tumor growing after partial resection.

In view of the results achieved in case 1 in our study and the surgical risks of morbidity in giant infundibulotuberal tumors, neoadjuvant treatment was decided in our second case with a goal of minimizing hypothalamic damage. We performed a simple surgical procedure *via* a trans-ventricular neuroendoscopic approach with the sole aim of obtaining a tissue sample for histopathological and molecular analysis. Combined therapy with BRAF/MEK inhibitors administered thereafter showed rapid results, with a dramatic reduction in tumor volume of 90% at 4 months, associated with symptom relief. These results suggest its potential indication as first line treatment before surgery or radiation therapy (16, 19, 23, 27, 28). Recently, results from the ongoing phase-2 Alliance clinical trial (30), started in 2017 (NCT03224767), confirmed the high rate of volumetric response (i.e. the primary endpoint), in 15 of 16 newly patients with pathology-confirmed papillary CPs that received 1 or more cycles of combined therapy with vemurafenib and cometinib after surgery. The responders were maintained on this treatment with minimal side effects and without any additional therapy. Three patients progressed when the treatment was discontinued. This approach is different from our final proposed approach.

Despite the clinical and radiological algorithm to identify BRAF-mutated PCP that has been proposed by Fujito et al. (7), taking a tissue sample for immunohistochemistry (using the VE1 antibody) and allele-specific genetic testing remain the gold standard for identification of BRAF V600E as well as for the exclusion of the adamantinomatous subtype (1, 3, 5, 16, 31–34). Brastianos et al. also reported the presence of detectable circulating cells carrying the BRAF V600E mutation in their patient samples, but only after surgery (24). Future studies are required to confirm the validity of looking for BRAF V600E mutation in peripheral blood (liquid biopsy) prior to surgery (which may mobilize tumor cells into the general circulation). Currently, a tissue biopsy for definitive diagnosis is mandatory and can be safely performed using stereotaxic or trans-ventricular neuroendoscopic techniques, as well as *via* trans-sphenoidal endoscopic techniques (21, 31–36). Regardless of the technique used, a simple biopsy is definitely less aggressive than extended surgical resection.

In view of our experience and the above-mentioned preliminary data, a new treatment paradigm for giant and invasive craniopharyngiomas could be proposed in the hope of improving long-term patient outcomes (**Figure 3**). In these cases, a tissue biopsy should be the first option prior to making clinical decisions, even in the case of visual impairment, considering the rapid and impressive results in reducing tumor volume that are offered by medical treatment in papillary subtype tumors. In such tumors, neoadjuvant combined therapy should be applied for a few months in order to shrink the tumor before then considering a curative approach (surgery or radiotherapy/radiosurgery). Moreover, in case of rare ''Purely'' intraventicular tumors not only hypotalamic but also pituitary function could be preserved.

The tumor biopsy could be performed using stereotactic or neuroendoscopic transventricular techniques or using an endonasal route according to tumor anatomy. In all cases, an intraoperative pathological evaluation of the tissue sample on frozen section may provide guidance for surgical decisions. In case of PCP or unconclusive result, the surgery may be discontinued waiting for definitive conclusions. In case of ACP, the procedure continues avoiding a second surgery or anesthesia for the patients. However, considering the morbidity of

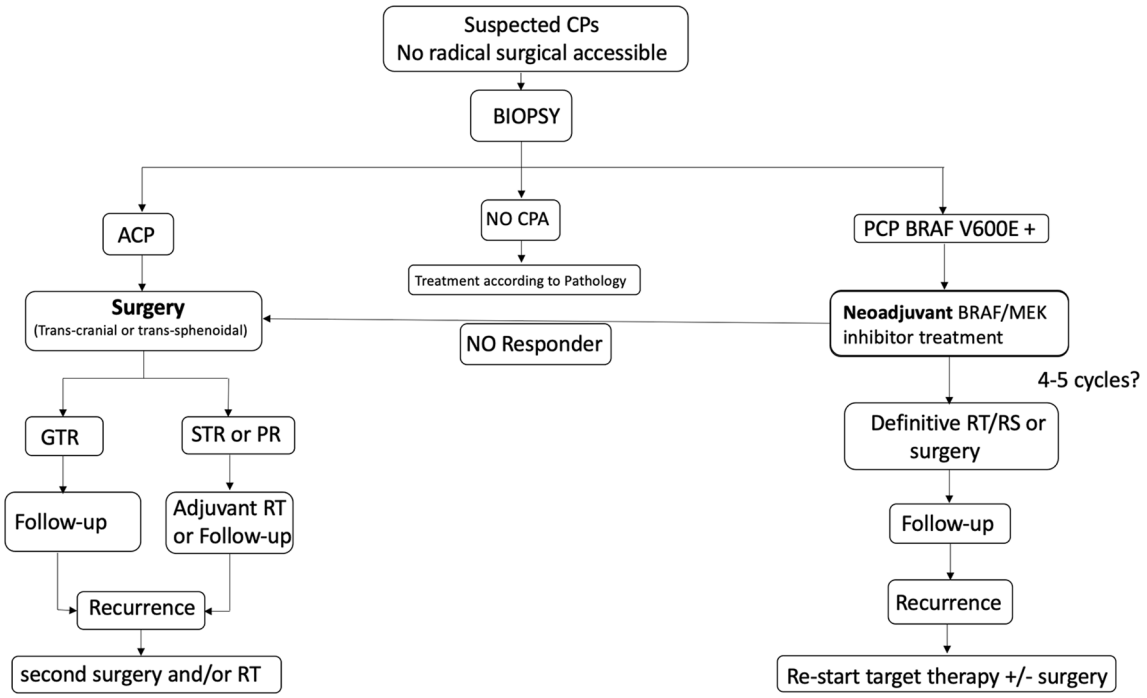

FIGURE 3 | Proposed management algorithm in case of Ventricular and Infundibulo-tuberal CPA which are not good candidate for a safe radical resection. CPs, Craniopharyngioma; ACP, Adamantinomatous CPA; PCP, Papillary CPs; RT, radiotherapy; RS, radiosurgery.

hypothalamic surgery, even a two-step surgery may be arguable in very huge CPs. Molecular detection of BRAF V600E mutation cannot yet be achieved in the prescribed time for intraoperative consultation (20-30 minutes). Rapid direct immunohistochemical methods are feasible but no study has tested the BRAF V600E antibody in the setting of craniopharyngioma intraoperative diagnosis (37–39). **Figure 4** reports an algorithm proposed for intraoperative decision making.

Although successfully treated BRAF-mutated CPs have similarly been described in children (40, 41), ACPs still account for the vast majority of CPs in the pediatric population. However as PCPs may exceptionally be encountered in children, the same attitude as in adult should be applied for pediatric giant CPs. Several studies are ongoing looking for possible drug targets in the adamantinomatous subtype (1, 16).

"Wait and see" management after tumor shrinkage and symptom relief can be supported by deferring radiotherapy if the lesion recurs. However, discontinuation of medical treatment after a partial or near-complete response in PCPs could be associated with a risk of early and long-term relapse due to the absence of a proven curative effect (15, 17, 18, 22, 25, 30). At the same time, long-term administration of BRAF/MEK inhibitors may increase the risk of epidermal cancer and have other side effects (18, 30). Himes et al. and Aylwin et al. reported early tumor recurrence 1-2 month after cessation of treatment (17, 22). Conversely, other authors have reported long-term tumor control after administration of radiotherapy (24, 27) or radiosurgery (23) immediately after responding to targeted therapy. Therefore, it seems reasonable to assign such treated patients to early definitive treatment to achieve long-term tumor control and to avoid tumor relapse and its hypothalamic and visual morbidity, as well as the need to resume medical therapy with unpredictable success. Moreover, tumor debulking could drastically reduce morbidity associated with surgery and radiotherapy. Although the total radiation dose is the same due to the intrinsic radiosensitivity of the tumor, the radiation field after tumor shrinkage is smaller thereby reducing the marginal dose to nearby critical structures. Likewise, shrinking tumor volume may allow radiosurgery to be used on small tumor remnants. Finally, in our opinion, definitive treatment should be provided early after a partial or near complete response to BRAF/MEK inhibitors and adapted to the anatomical location and volume of the tumor remnants as well as their surgical accessibility.

Obviously, larger prospective multicenter randomized studies are now warranted to confirm the safety and efficacy of this strategy.

CONCLUSION

Changes in the algorithm for the management of craniopharyngiomas should be considered in light of progress made in molecular biology and targeted therapies. Surgery and

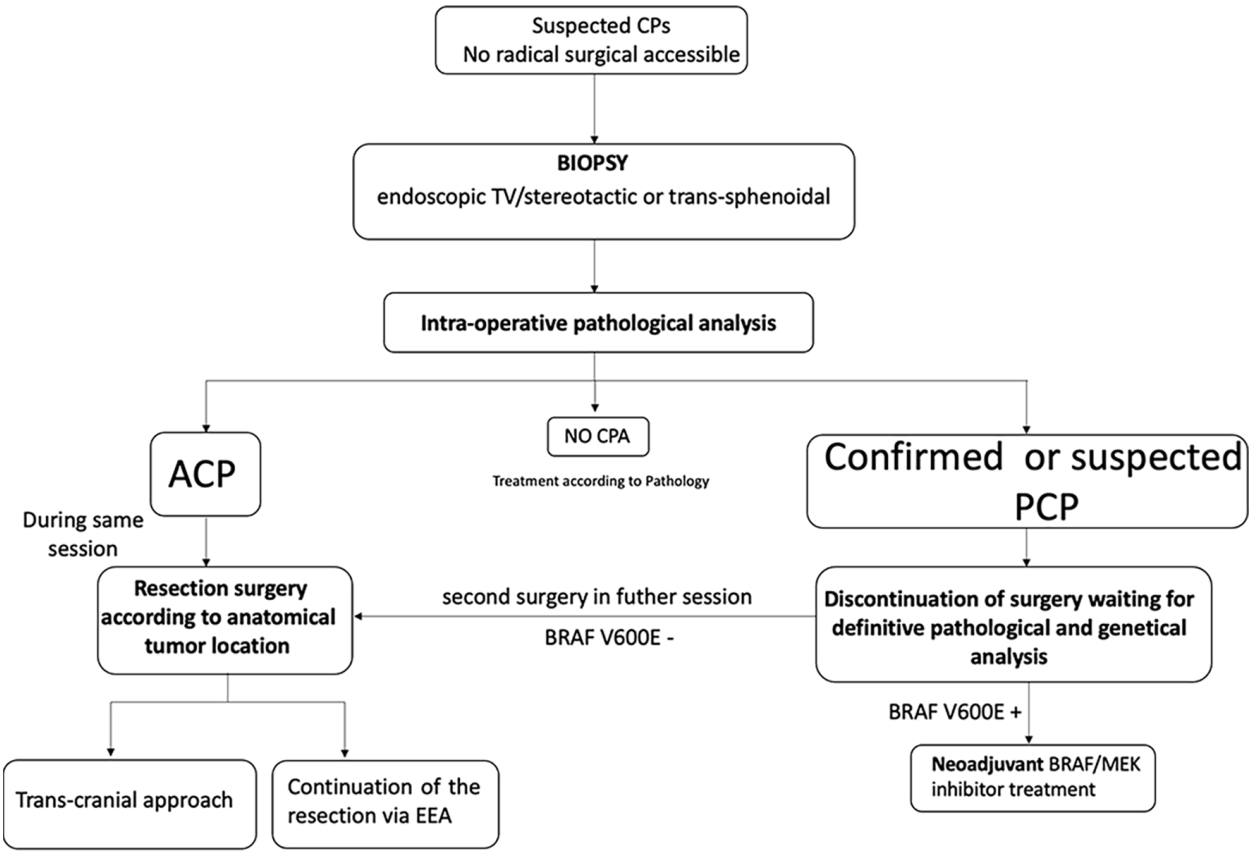

FIGURE 4 | Proposed management algorithm for intraoperative decision making using pathological analysis on frozen section. Depending on tumor anatomical location, the biopsy can be performed either by stereotactic and neuroendoscopic transventricular techniques or using an endonasal route. In the first case, there will be two surgeries (i.e. biopsy followed by craniotomy for resection if needed) that can be done during the same anesthesia. Conversely, using endoscopic endonasal approach the biopsy could be the first step of the same procedure. See text for more details. CPs, Craniopharyngioma; ACP, Adamantinomatous CPA; PCP, Papillary CPs; EEA, endonasal endoscopic approach; TV, trans-ventricular.

radiotherapy remain the definitive treatments to obtain tumor control. However, a simple biopsy prior to submitting the patient to a high-risk procedure should be considered to identify a subset of patients with papillary craniopharyngiomas with BRAF mutation. This may lead to the use of a neoadjuvant targeted therapy before considering curative treatments on the smaller target. Obviously, a large cohort study is now mandatory to validate the efficacy of this new protocol. It is hoped that these drugs may decrease morbidity and improve outcomes and quality of life in patients with these tumors that have historically been surgically difficult.

DATA AVAILABILITY STATEMENT

The original contributions presented in the study are included in the article/supplementary material. Further inquiries can be directed to the corresponding author.

ETHICS STATEMENT

Ethical review and approval was not required for the study on human participants in accordance with the local legislation and institutional requirements. The patients/participants provided their written informed consent to participate in this study. Written informed consent was obtained from the individual(s) for the publication of any potentially identifiable images or data included in this article.

AUTHOR CONTRIBUTIONS

Concept and design: EJ, GR, and FC. Acquisition of data: FC. Analysis and interpretation of data: All authors. Drafting the article: FC and EJ. Critically revising the article: All Authors. All authors contributed to the article and approved the submitted version.

REFERENCES

1. Müller HL, Merchant TE, Warmuth-Metz M, Martinez-Barbera JP, Puget S. Craniopharyngioma. *Nat Rev Dis Primers* (2019) 5(1):75. doi: 10.1038/s41572-019-0125-9
2. Martinez-Barbera JP, Andoniadou CL. Biological Behaviour of Craniopharyngiomas. *Neuroendocrinology* (2020) 110(9-10):797–804. doi: 10.1159/000506904
3. Martinez-Gutierrez JC, D'Andrea MR, Cahill DP, Santagata S, Barker FG 2nd, Brastianos PK. Diagnosis and Management of Craniopharyngiomas in the Era of Genomics and Targeted Therapy. *Neurosurg Focus* (2016) 41(6):E2. doi: 10.3171/2016.9.FOCUS16325
4. Almeida JP, Workewych A, Takami H, Velasquez C, Oswari S, Asha M, et al. Surgical Anatomy Applied to the Resection of Craniopharyngiomas: Anatomic Compartments and Surgical Classifications. *World Neurosurg* (2020) 142:611–25. doi: 10.1016/j.wneu.2020.05.171
5. Tritos NA. Is There a Role for Targeted Medical Therapies in Patients With Craniopharyngiomas? *Future Oncol* (2015) 11(24):3221–3. doi: 10.2217/fon.15.233
6. Asha MJ, Oswari S, Takami H, Velasquez C, Almeida JP, Gentili F. Craniopharyngiomas: Challenges and Controversies. *World Neurosurg* (2020) 142:593–600. doi: 10.1016/j.wneu.2020.05.172
7. Fujio S, Juratli TA, Arita K, Hirano H, Nagano Y, Brastianos PK, et al. A Clinical Rule for Preoperative Prediction of BRAF Mutation Status in Craniopharyngiomas. *Neurosurgery* (2019) 185(2):204–10. doi: 10.1093/neuros/nyy569
8. Pascual JM, González-Llanos F, Barrios L, Roda JM. Intraventricular Craniopharyngiomas: Topographical Classification and Surgical Approach Selection Based on an Extensive Overview. *Acta Neurochir (Wien)* (2004) 146 (8):785–802. doi: 10.1007/s00701-004-0295-3
9. Prieto R, Pascual JM, Hofecker V, Winter E, Castro-Dufourny I, Carrasco R, et al. Craniopharyngioma Adherence: A Reappraisal of the Evidence. *Neurosurg Rev* (2020) 43(2):453–72. doi: 10.1007/s10143-018-1010-9
10. Apra C, Enachescu C, Lapras V, Raverot G, Jouanneau E. Is Gross Total Resection Reasonable in Adults With Craniopharyngiomas With Hypothalamic Involvement? *World Neurosurg* (2019) 129:e803–e811. doi: 10.1016/j.wneu.2019.06.037
11. Iannalfi A, Fragkandrea I, Brock J, Saran F. Radiotherapy in Craniopharyngiomas. *Clin Oncol (R Coll Radiol)* (2013) 25(11):654–67. doi: 10.1016/j.clon.2013.07.005
12. Pascual JM, Prieto R, Carrasco R, Barrios L. Displacement of Mammillary Bodies by Craniopharyngiomas Involving the Third Ventricle: Surgical-MRI Correlation and Use in Topographical Diagnosis. *J Neurosurg* (2013) 119 (2):381–405. doi: 10.3171/2013.1.JNS111722
13. Pascual JM, Prieto R, Carrasco R. Infundibulo-Tuberal or Not Strictly Intraventricular Craniopharyngioma: Evidence for a Major Topographical Category. *Acta Neurochir (Wien)* (2011) 153(12):2403–25. doi: 10.1007/s00701-011-1149-4
14. Pascual JM, Prieto R, Castro-Dufourny I, Mongardi L, Rosdolsky M, Strauss S, et al. Craniopharyngiomas Primarily Involving the Hypothalamus: A Model of Neurosurgical Lesions to Elucidate the Neurobiological Basis of Psychiatric Disorders. *World Neurosurg* (2018) 120:e1245–78. doi: 10.1016/j.wneu.2018.09.053
15. Martinez NL, Khanna O, Farrell CJ. A Narrative Review of Targeted Therapy in Meningioma, Pituitary Adenoma, and Craniopharyngioma of the Skull Base. *Chin Clin Oncol* (2020) 9(6):75. doi: 10.21037/cco-20-168
16. Alexandraki KI, Kaltsas GA, Karavitaki N, Grossman AB. The Medical Therapy of Craniopharyngiomas: The Way Ahead. *J Clin Endocrinol Metab* (2019) 104(12):5751–64. doi: 10.1210/jc.2019-01299
17. Aylwin SJ, Bodi I, Beaney R. Pronounced Response of Papillary Craniopharyngioma to Treatment With Vemurafenib, a BRAF Inhibitor. *Pituitary* (2016) 19(5):544–6. doi: 10.1007/s11102-015-0663-4
18. Long GV, Stroyakovskiy D, Gogas H, Levchenko E, de Braud F, Larkin J, et al. Dabrafenib and Trametinib Versus Dabrafenib and Placebo for Val600 BRAF-Mutant Melanoma: A Multicentre, Double-Blind, Phase 3 Randomised Controlled Trial. *Lancet* (2015) 386:444–51. doi: 10.1016/S0140-6736(15)60898-4
19. Bernstein A, Mrowczynski OD, Greene A, Ryan S, Chung C, Zacharia BE, et al. Dual BRAF/MEK Therapy in BRAF V600E-Mutated Primary Brain Tumors: A Case Series Showing Dramatic Clinical and Radiographic Responses and a Reduction in Cutaneous Toxicity. *J Neurosurg* (2019) 1:1–6. doi: 10.3171/2019.8.JNS19643
20. Brastianos PK, Taylor-Weiner A, Manley PE, Jones RT, Dias-Santagata D, Thorner AR, et al. Exome Sequencing Identifies BRAF Mutations in Papillary Craniopharyngiomas. *Nat Genet* (2014) 46(2):161–5. doi: 10.1038/ng.2868
21. Steiert C, Grauvogel J, Roelz R, Demerath T, Schnell D, Beck J, et al. Stereotactic Cysto-Ventricular Catheters in Craniopharyngiomas: An Effective Minimally Invasive Method to Improve Visual Impairment and Achieve Long-Term Cyst Volume Reduction. *Neurosurg Rev* (2021) 44 (6):3411–20. doi: 10.1007/s10143-021-01510-8
22. Himes BT, Ruff MW, Van Gompel JJ, Park SS, Galanis E, Kaufmann TJ, et al. Recurrent Papillary Craniopharyngioma With BRAF V600E Mutation Treated With Dabrafenib: Case Report. *J Neurosurg* (2018) 1:1–5. doi: 10.3171/2017.11.JNS172373
23. Khaddour K, Chicoine MR, Huang J, Dahiya S, Ansstas G. Successful Use of BRAF/MEK Inhibitors as a Neoadjuvant Approach in the Definitive Treatment of Papillary Craniopharyngioma. *J Natl Compr Canc Netw* (2020) 18(12):1590–5. doi: 10.6004/jnccn.2020.7624
24. Priscilla K, Brastianos PK, Ganesh M, Shankar GM, Corey M, Gill CM, et al. Dramatic Response of BRAF V600E Mutant Papillary Craniopharyngioma to Targeted Therapy. *JNCI: J Nat Cancer Institute*(2016) 108(2):djv310. doi: 10.1093/jnci/djv310
25. Rao M, Bhattacharjee M, Shepard S, Hsu S. Newly Diagnosed Papillary Craniopharyngioma With BRAF V600E Mutation Treated With Single-Agent Selective BRAF Inhibitor Dabrafenib: A Case Report. *Oncotarget* (2019) 10(57):6038–42. doi: 10.18632/oncotarget.27203
26. Rostami E, Witt Nyström P, Libard S, Wikström J, Casar-Borota O, Gudjonsson O. Recurrent Papillary Craniopharyngioma With BRAFV600E Mutation Treated With Neoadjuvant-Targeted Therapy. *Acta Neurochir (Wien)* (2017) 159(11):2217–21. doi: 10.1007/s00701-017-3311-0
27. Di Stefano AL, Guyon D, Sejean K, Feuvret L, Villa C, Berzero G, et al. Medical Debulking With BRAF/MEK Inhibitors in Aggressive BRAF-Mutant Craniopharyngioma. *Neurooncol Adv* (2020) 2(1):vdaa141. doi: 10.1093/noajnl/vdaa141
28. Juratli TA, Jones PS, Wang N, Subramanian M, Aylwin SJB, Odia Y, et al. Targeted Treatment of Papillary Craniopharyngiomas Harboring BRAF V600E Mutations. *Cancer* (2019) 125(17):2910–4. doi: 10.1002/cncr.32197
29. Roque A, Odia Y. BRAF-V600E Mutant Papillary Craniopharyngioma Dramatically Responds to Combination BRAF and MEK Inhibitors. *CNS Oncol* (2017) 6(2):95–9. doi: 10.2217/cns-2016-0034
30. Brastianos PK, Twohy E, Geyer SM, Gerstner ER, Kaufmann TJ, Ruff M, et al. Alliance A071601: Phase II Trial of BRAF/MEK Inhibition in Newly Diagnosed Papillary Craniopharyngiomas. *J Clin Oncol* (2021) 39 (15_suppl):2000. doi: 10.1200/JCO.2021.39.15_suppl.2000
31. La Corte E, Younus I, Pivari F, Selimi A, Ottenhausen M, Forbes JA, et al. BRAF V600E Mutant Papillary Craniopharyngiomas: A Single-Institutional Case Series. *Pituitary* (2018) 21(6):571–83. doi: 10.1007/s11102-018-0909-z
32. Moreno-Torres B, Campos-Martín Y, Meléndez B, Garcia Martin RM, Vicente A, Rodríguez de Lope Á, et al. Craniopharyngiomas: A Clinicopathological and Molecular Study of 52 Cases - Experience in the Complejo Hospitalario De Toledo and Hospital Universitario 12 De Octubre (Madrid). *Clin Neuropathol* (2021) 40(1):26–35. doi: 10.5414/NP301268
33. Lauretti L, Legninda Sop FY, Pallini R, Pallini R, Fernandez E, D'Alessandris QG, et al. Neuroendoscopic Treatment of Cystic Craniopharyngiomas: A Case Series With Systematic Review of the Literature. *World Neurosurg* (2018) 110: e367–73. doi: 10.1016/j.wneu.2017.11.004
34. Müller HL. The Diagnosis and Treatment of Craniopharyngioma. *Neuroendocrinology* (2020) 110(9-10):753–66. doi: 10.1159/000504512
35. Tang B, Xie S, Huang G, Wang Z, Yang L, Yang X, et al. Clinical Features and Operative Technique of Transinfundibular Craniopharyngioma. *J Neurosurg* (2019) 14:1–10. doi: 10.3171/2019.3.JNS181953
36. Frio F, Raverot G, Jouanneau E. Ommaya Reservoir System for the Treatment of Cystic Craniopharyngiomas: Surgical Results in a Series of 11 Adult Patients and Review of the Literature. *World Neurosurg* (2019) 132:e869–77. doi: 10.1016/j.wneu.2019.07.217
37. Fukuhara N, Iwata T, Inoshita N, Yoshimoto K, Kitagawa M, Fukuhara H, et al. Immunohistochemistry or Molecular Analysis: Which Method Is Better for Subtyping Craniopharyngioma? *Endocr Pathol* (2021) 32(2):262–8. doi: 10.1007/s12022-020-09644-z

38. Yoshimoto K, Hatae R, Suzuki SO, Hata N, Kuga D, Akagi Y, et al. High-Resolution Melting and Immunohistochemical Analysis Efficiently Detects Mutually Exclusive Genetic Alterations of Adamantinomatous and Papillary Craniopharyngiomas. *Neuropathology* (2018) 38(1):3–10. doi: 10.1111/neup.12408
39. De Paoli-Iseppi R, Johansson PA, Menzies AM, Dias KR, Pupo GM, Kakavand H, et al. Comparison of Whole-Exome Sequencing of Matched Fresh and Formalin Fixed Paraffin Embedded Melanoma Tumours: Implications for Clinical Decision Making. *Pathology* (2016) 48(3):261–6. doi: 10.1016/j.pathol.2016.01.001
40. Chik CL, van Landeghem FKH, Easaw JC, Mehta V. Aggressive Childhood-Onset Papillary Craniopharyngioma Managed With Vemurafenib, a BRAF Inhibitor. *J Endocr Soc* (2021) 5(5):bvab043. doi: 10.1210/jendso/bvab043
41. Borrill R, Cheesman E, Stivaros S, Kamaly-Asl ID, Gnanalingham K, Kilday JP. Papillary Craniopharyngioma in a 4-Year-Old Girl With BRAF V600E Mutation: A Case Report and Review of the Literature. *Childs Nerv Syst* (2019) 35(1):169–73. doi: 10.1007/s00381-018-3925-4

Conflict of Interest: The authors declare that the research was conducted in the absence of any commercial or financial relationships that could be construed as a potential conflict of interest.

Publisher's Note: All claims expressed in this article are solely those of the authors and do not necessarily represent those of their affiliated organizations, or those of the publisher, the editors and the reviewers. Any product that may be evaluated in this article, or claim that may be made by its manufacturer, is not guaranteed or endorsed by the publisher.

Advantages of publishing in Frontiers

OPEN ACCESS
Articles are free to read for greatest visibility and readership

FAST PUBLICATION
Around 90 days from submission to decision

HIGH QUALITY PEER-REVIEW
Rigorous, collaborative, and constructive peer-review

TRANSPARENT PEER-REVIEW
Editors and reviewers acknowledged by name on published articles

Frontiers
Avenue du Tribunal-Fédéral 34
1005 Lausanne | Switzerland

Visit us: www.frontiersin.org
Contact us: frontiersin.org/about/contact

REPRODUCIBILITY OF RESEARCH
Support open data and methods to enhance research reproducibility

DIGITAL PUBLISHING
Articles designed for optimal readership across devices

FOLLOW US
@frontiersin

IMPACT METRICS
Advanced article metrics track visibility across digital media

EXTENSIVE PROMOTION
Marketing and promotion of impactful research

LOOP RESEARCH NETWORK
Our network increases your article's readership